frontiers | Research Topics

Neuronal identity from fate specification to function

Edited by
Nikolaos Konstantinides, Filipe Pinto-Teixeira, Simon Hippenmeyer, Luisa Cochella and Marisa Karow

Published in
Frontiers in Neuroscience

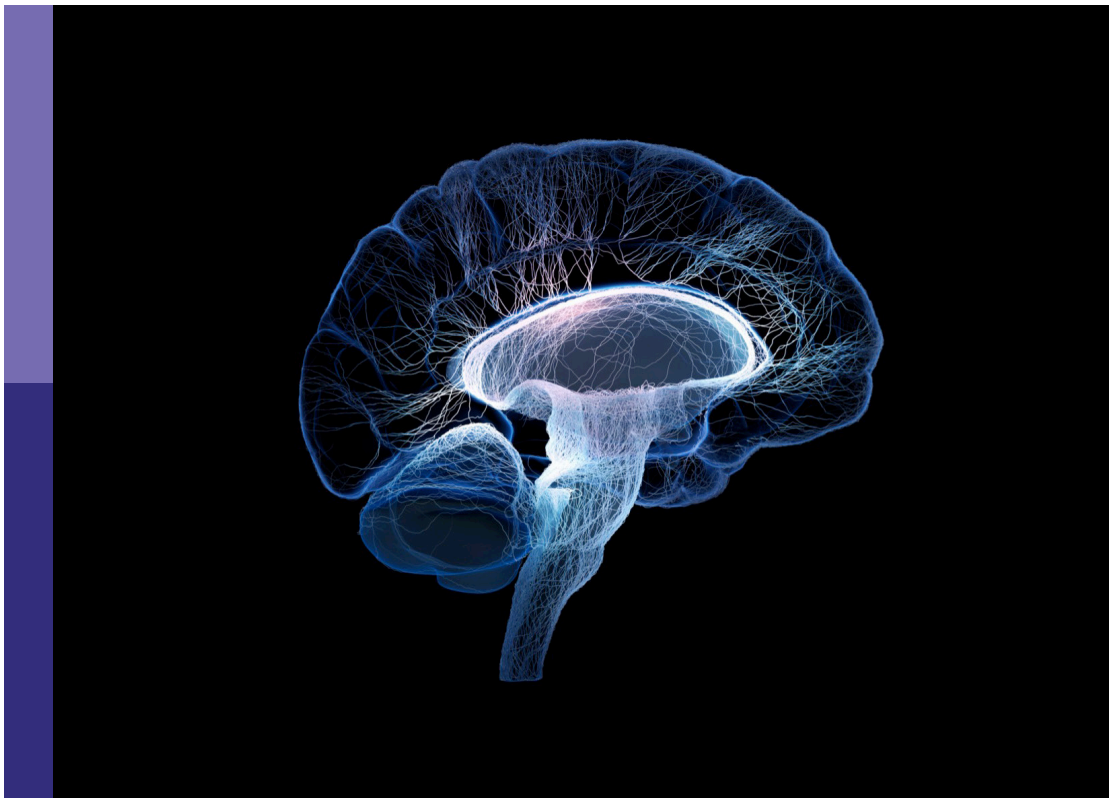

ISSN 1664-8714
ISBN 978-2-83251-323-1
DOI 10.3389/978-2-83251-323-1

About Frontiers

Frontiers is more than just an open access publisher of scholarly articles: it is a pioneering approach to the world of academia, radically improving the way scholarly research is managed. The grand vision of Frontiers is a world where all people have an equal opportunity to seek, share and generate knowledge. Frontiers provides immediate and permanent online open access to all its publications, but this alone is not enough to realize our grand goals.

Frontiers journal series

The Frontiers journal series is a multi-tier and interdisciplinary set of open-access, online journals, promising a paradigm shift from the current review, selection and dissemination processes in academic publishing. All Frontiers journals are driven by researchers for researchers; therefore, they constitute a service to the scholarly community. At the same time, the *Frontiers journal series* operates on a revolutionary invention, the tiered publishing system, initially addressing specific communities of scholars, and gradually climbing up to broader public understanding, thus serving the interests of the lay society, too.

Dedication to quality

Each Frontiers article is a landmark of the highest quality, thanks to genuinely collaborative interactions between authors and review editors, who include some of the world's best academicians. Research must be certified by peers before entering a stream of knowledge that may eventually reach the public - and shape society; therefore, Frontiers only applies the most rigorous and unbiased reviews. Frontiers revolutionizes research publishing by freely delivering the most outstanding research, evaluated with no bias from both the academic and social point of view. By applying the most advanced information technologies, Frontiers is catapulting scholarly publishing into a new generation.

What are Frontiers Research Topics?

Frontiers Research Topics are very popular trademarks of the *Frontiers journals series*: they are collections of at least ten articles, all centered on a particular subject. With their unique mix of varied contributions from Original Research to Review Articles, Frontiers Research Topics unify the most influential researchers, the latest key findings and historical advances in a hot research area.

Find out more on how to host your own Frontiers Research Topic or contribute to one as an author by contacting the Frontiers editorial office: frontiersin.org/about/contact

Neuronal identity from fate specification to function

Topic editors

Nikolaos Konstantinides — UMR7592 Institut Jacques Monod (IJM), France
Filipe Pinto-Teixeira — FR3743 Centre de Biologie Intégrative (CBI), France
Simon Hippenmeyer — Institute of Science and Technology Austria (IST Austria), Austria
Luisa Cochella — Research Institute of Molecular Pathology (IMP), Austria
Marisa Karow — University of Erlangen Nuremberg, Germany

Citation

Konstantinides, N., Pinto-Teixeira, F., Hippenmeyer, S., Cochella, L., Karow, M., eds. (2023). *Neuronal identity from fate specification to function*. Lausanne: Frontiers Media SA. doi: 10.3389/978-2-83251-323-1

Table of contents

frontiers in Neuroscience

MINI REVIEW
published: 16 September 2021
doi: 10.3389/fnins.2021.738088

Olfactory Receptor Gene Regulation in Insects: Multiple Mechanisms for Singular Expression

*Kaan Mika and Richard Benton**

Center for Integrative Genomics, Faculty of Biology and Medicine, University of Lausanne, Lausanne, Switzerland

The singular expression of insect olfactory receptors in specific populations of olfactory sensory neurons is fundamental to the encoding of odors in patterns of neuronal activity in the brain. How a receptor gene is selected, from among a large repertoire in the genome, to be expressed in a particular neuron is an outstanding question. Focusing on *Drosophila melanogaster*, where most investigations have been performed, but incorporating recent insights from other insect species, we review the multilevel regulatory mechanisms of olfactory receptor expression. We discuss how *cis*-regulatory elements, *trans*-acting factors, chromatin modifications, and feedback pathways collaborate to activate and maintain expression of the chosen receptor (and to suppress others), highlighting similarities and differences with the mechanisms underlying singular receptor expression in mammals. We also consider the plasticity of receptor regulation in response to environmental cues and internal state during the lifetime of an individual, as well as the evolution of novel expression patterns over longer timescales. Finally, we describe the mechanisms and potential significance of examples of receptor co-expression.

Keywords: olfactory receptor, sensory neuron, gene expression, neurodevelopment, evolution, feedback, *Drosophila*, insects

OPEN ACCESS

Edited by:
Nikolaos Konstantinides, UMR 7592 Institut Jacques Monod (IJM), France

Reviewed by:
Mattias Alenius, Umeå University, Sweden
Hua Yan, University of Florida, United States
Hongjie Li, Baylor College of Medicine, United States

***Correspondence:**
Richard Benton
Richard.Benton@unil.ch

Specialty section:
This article was submitted to Neurogenesis, a section of the journal Frontiers in Neuroscience

Received: *08 July 2021*
Accepted: *24 August 2021*
Published: *16 September 2021*

Citation:
Mika K and Benton R (2021) Olfactory Receptor Gene Regulation in Insects: Multiple Mechanisms for Singular Expression. Front. Neurosci. 15:738088. doi: 10.3389/fnins.2021.738088

INTRODUCTION

Most animals possess large families of olfactory receptors, which enable detection of diverse chemical signals in their environment. In insects, as in vertebrates, the majority of individual receptors are expressed in unique populations of olfactory sensory neurons (OSNs), a property critical for the representation of odor-evoked neural activity in the brain. How the specificity of insect receptor expression is defined has been an unresolved problem for two decades.

Early work, mainly in adult *Drosophila melanogaster*, focused on identifying *cis*-regulatory sequences of olfactory receptor genes as well as transcription factors (TFs) required to promote their correct expression [reviewed in Fuss and Ray (2009) and Barish and Volkan (2015)]. Here we discuss recent advances, in which new experimental approaches in *D. melanogaster* and other insect models reveal multiple levels by which selective olfactory receptor expression is achieved and the plasticity of these processes over short and long timescales. We also make select comparisons with receptor choice in mammals, which relies on a combination of stochastic and deterministic mechanisms (Dalton and Lomvardas, 2015; Monahan and Lomvardas, 2015), to illustrate convergent or divergent strategies to achieve singular receptor expression.

INSECT OLFACTORY SYSTEM BASICS

Insects have two main olfactory receptor families: odorant receptors (Ors) and ionotropic receptors (Irs) (**Figure 1A**). Both function as heteromeric odor-gated ion channels composed of subunits of a ligand-specific ("tuning") receptor, which is expressed in a unique population of OSNs, and a broadly expressed, family-specific co-receptor (Orco for Ors; Ir8a or Ir25a for Irs) (Clyne et al., 1999b; Vosshall et al., 2000; Larsson et al., 2004; Couto et al., 2005; Nakagawa et al., 2005; Benton et al., 2006, 2009; Sato et al., 2008; Abuin et al., 2011; Butterwick et al., 2018; Del Marmol et al., 2021). *Or* and *Ir* genes are dispersed throughout insect genomes, but many occur in tandem arrays (Robertson et al., 2003; Gomez-Diaz et al., 2018), presumably reflecting their genesis by non-allelic homologous recombination.

Olfactory sensory neurons are housed in two olfactory organs in *D. melanogaster* (and other insects), the antenna and maxillary palp (**Figure 1B**). Each OSN extends a ciliated dendrite, where receptor proteins localize, into porous cuticular hairs on the organ surface (Schmidt and Benton, 2020; Gonzales et al., 2021). OSN axons project to the antennal lobe in the brain (**Figure 1B**). Neurons expressing the same olfactory receptor converge onto specific glomeruli, where they synapse with projection neurons that carry sensory information to higher brain centers (Grabe and Sachse, 2018; Schlegel et al., 2021). Each hair houses the dendrites of 1–4 OSNs, flanked by four support cells, which together comprise a sensillum. There are several distinct morphological classes of sensilla (**Figure 1B**), each of which has multiple subtypes characterized by a stereotyped number of OSNs and receptor expression profile.

Adult *D. melanogaster* has ∼2200 OSNs (within the two antennae and maxillary palps), encompassing ∼30 Or-expressing and ∼10 Ir-expressing classes (Couto et al., 2005; Benton et al., 2009; Grabe et al., 2016). This complexity is roughly one-to-several orders of magnitude lower than presumed OSN types in mammals, based upon receptor numbers (Hughes et al., 2018). Some other insect species, notably ants, have several hundred *Or*s (Yan et al., 2020).

INSECT OLFACTORY SYSTEM DEVELOPMENT

Olfactory receptor expression must be appreciated in the context of OSN development. Sensilla arise from sensory organ precursors (SOPs), which are specified within a set of concentric arcs in the larval antennal imaginal disc (Rodrigues and Hummel, 2008; Barish and Volkan, 2015; Yan et al., 2020; **Figure 1C**). During early pupal stages, each SOP gives rise to a short lineage of three rounds of cell division, to produce four support cells and, potentially, four OSNs. However, up to three of these neuron precursors (depending upon the sensillum class) are removed by precisely patterned programmed cell death, yielding the final set of OSNs (Endo et al., 2007, 2011; Barish and Volkan, 2015; Chai et al., 2019; Prieto-Godino et al., 2020; **Figure 1C**).

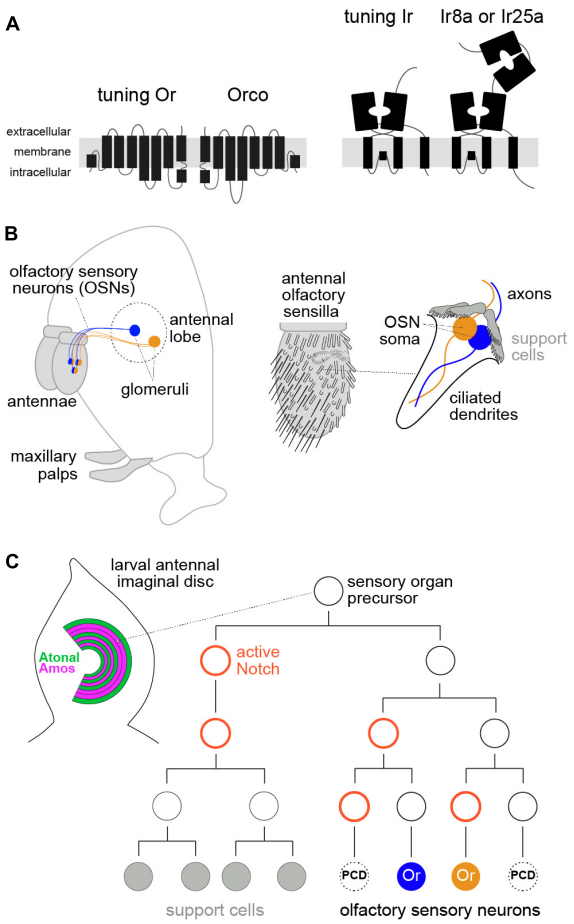

FIGURE 1 | Molecular, anatomical, and developmental properties of the peripheral olfactory system in *D. melanogaster*. **(A)** Schematic of the two main insect olfactory receptor families. Odorant receptors (Ors) are seven transmembrane domain proteins that form heteromeric odor-gated ion channels composed of subunits of a ligand-specific ("tuning") receptor and a co-receptor, Orco. Ionotropic receptors (Irs) are distantly related to ionotropic glutamate receptors, and function as odor-gated channel complexes composed of tuning Ir subunits and co-receptors (Ir8a or Ir25a). **(B)** Left: schematic of the *D. melanogaster* head (facing left) illustrating the main olfactory organs (antennae and maxillary palps, gray shading) and connectivity of two populations of olfactory sensory neurons (OSNs) to the antennal lobe in the brain. Right: schematic of the antenna, which is covered with diverse classes of sensory sensilla; the cellular organization of one sensillum, housing two OSNs, is shown on the far right (see text). **(C)** Left: schematic of the larval antennal imaginal disc, showing the concentric arcs of cells where different sensory organ precursors (SOP) are born. Amos- and Atonal-positive arcs give rise to OSN lineages expressing Ors and Irs, respectively, while other patterning determinants (not shown) are thought to specify SOP identity for different sensilla subtypes. Right: a simplified developmental lineage of an SOP producing a sensillum class with two OSNs. Two other potential neurons are removed by programmed cell death (PCD). Delta/Notch signaling determines the asymmetry of cell divisions, while many other patterning factors (not shown) are involved in specifying cell identity, encompassing both receptor expression and glomerular targeting of different OSNs (see text).

The sensillum class a given SOP will produce is determined in the antennal disc by spatially restricted TFs, including Amos and Atonal, which demarcate Or and Ir OSN precursors, respectively

(**Figure 1C**), and Dachshund and Rotund; these proteins all exhibit zonally restricted expression (or form gradients) across the rings where olfactory SOPs are specified (Rodrigues and Hummel, 2008; Barish and Volkan, 2015; Chai et al., 2019; Yan et al., 2020). Individual SOP classes therefore likely have a unique molecular identity before initiating cell division, though this has not been characterized. Each division is asymmetric, determined by Notch/Delta signaling (**Figure 1C**), to give rise to daughter cells of unique identity (Endo et al., 2007, 2011). The terminal cells of the neuronal sub-lineage are presumed to have a distinct set of fate determinants that specify the expression of receptors (Endo et al., 2007, 2011; Li et al., 2013; Barish and Volkan, 2015; Chai et al., 2019), but the molecular profile of these early developmental stages is still incompletely understood.

OLFACTORY RECEPTOR SPATIO-TEMPORAL EXPRESSION

Knowledge of the timing of olfactory receptor expression is critical to distinguish if developmental regulators have direct or indirect roles in inducing receptor gene transcription. Recent antennal bulk and single-cell/nuclear OSN RNA-sequencing at multiple timepoints indicates that transcripts for a subset of receptors are first detected from ∼24 h after puparium formation (Pan et al., 2017; Li et al., 2020; McLaughlin et al., 2021), at most a few hours after the terminal division of these lineages (Endo et al., 2011; Chai et al., 2019). Other receptors initiate expression over the subsequent ∼24–48 h, potentially reflecting asynchrony in SOP lineage development and/or differences in the mechanisms/levels of transcriptional induction. Most importantly, the single-OSN transcriptomes indicate the vast majority of individual OSNs express only one receptor gene from the earliest stages of the process. This contrasts with *OR* expression in mice, where immature OSNs transiently express low levels of multiple receptors before a single gene is chosen for high-level transcription (Hanchate et al., 2015; Tan et al., 2015). Furthermore, unlike the monoallelic *OR* expression observed in mammals (Monahan and Lomvardas, 2015), endogenous gene-tagging indicates that both receptor alleles are expressed in insect OSNs (Kurtovic et al., 2007; Grosjean et al., 2011; Auer et al., 2020).

The onset of receptor expression occurs in parallel with, or after, OSN axons converge on glomeruli in the antennal lobe (Jefferis et al., 2004; Jefferis and Hummel, 2006; Li et al., 2021). This timing is consistent with the lack of contributions of receptors to neuronal guidance (Dobritsa et al., 2003), in contrast to mammalian ORs, which have an important, though indirect, role in regulating glomerular convergence of OSNs (Sakano, 2010). However, antennal developmental transcriptomics in the clonal raider ant, *Ooceraea biroi*, revealed that receptors are expressed prior to glomerulus formation (Ryba et al., 2020), with genetic evidence hinting that Orco (at least) contributes during development to formation or maintenance of these structures (Trible et al., 2017; Yan et al., 2017; Ryba et al., 2020). In adult *D. melanogaster*, receptor transcripts continue to accumulate several days after eclosion before levels plateau (Jafari et al., 2021), indicating the continuity and/or maturation of mechanisms inducing their expression.

CIS-REGULATORY ELEMENTS

The genetically hardwired and stable choice of receptor transcription in OSNs has promoted extensive efforts to define *cis*-regulatory elements (CREs) of receptor genes through bioinformatic identification of DNA motifs (e.g., by phylogenetic footprinting) and experimental "enhancer bashing" (Ray et al., 2007, 2008; Miller and Carlson, 2010; Silbering et al., 2011; Prieto-Godino et al., 2017). These efforts – reviewed extensively elsewhere (Fuss and Ray, 2009; Barish and Volkan, 2015; Yan et al., 2020) – have revealed that CREs defining correct OSN expression are generally encompassed within a few 100–1000 base pairs upstream of coding sequences, although 3′ and intronic regions are important for certain genes. Some CREs are necessary to promote expression, while others prevent expression in inappropriate cell types. There is no evidence for distantly acting regulatory elements of insect receptor genes – as identified in some tandem arrays of mammalian receptor genes (Monahan and Lomvardas, 2015) – although clustered insect genes might share common regulatory sequences (Prieto-Godino et al., 2017). Detailed dissection of specific *Or* promoters further illustrates how the order, number, and overlap of individual CREs are critical for defining robust and selective receptor expression (Jafari and Alenius, 2015; Gonzalez et al., 2019). These advances support a model in which unique combinations of locally acting CREs ensure the correct transcriptional activation in (and only in) a given class of OSNs (**Figure 2A**). However, our global understanding of *cis*-regulation remains fragmentary: only a subset of CREs within larger genomic fragments have been identified for a few receptors and only a subset of these CREs have known binding proteins.

TRANS-ACTING FACTORS

Several TFs required for the correct expression of receptor genes in specific populations of neurons have been identified in *D. melanogaster* through loss-of-function genetic screens (Jafari et al., 2012; Chai et al., 2019; Mika et al., 2021), candidate approaches (Tichy et al., 2008; Li et al., 2013), and expression screens (Li et al., 2020) [reviewed in Fuss and Ray (2009); Barish and Volkan (2015), and Yan et al. (2020)]. Analogous to contributions of CREs, TFs can promote or repress receptor expression (and can have different roles for different genes), and unique combinations of these factors are required for individual receptors (**Figure 2A**). The convergence of several genetic screens on the same TFs (e.g., Pdm3 and E93) (Jafari et al., 2012; Chai et al., 2019; Mika et al., 2021) suggests that a majority of the core *trans*-acting regulatory proteins have been identified. These TFs contain diverse types of DNA binding domains and while some orthologous proteins might have similar roles in other insects (e.g., Acj6) (Clyne et al., 1999a; Fujii et al., 2011), they are not obviously related to key TFs functioning in *OR* expression in

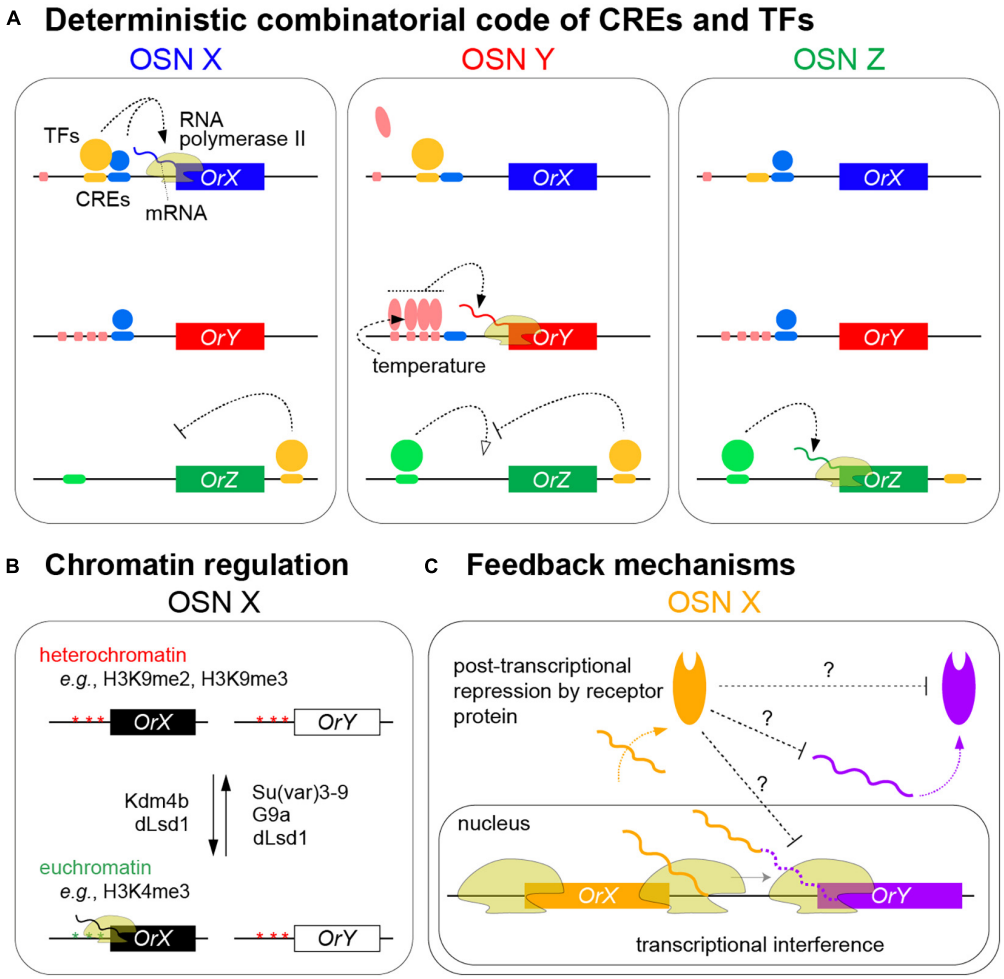

FIGURE 2 | Models of olfactory receptor expression in insects. **(A)** Summary of the mechanisms ensuring the neuron-specific transcription of olfactory receptors through the combinatorial action of CREs and TFs to promote RNA polymerase II transcription of a specific receptor gene in an olfactory sensory neuron (OSN) (only the neuronal nuclei are shown). In these hypothetical examples, *OrX* requires binding of both yellow and blue TFs to corresponding CREs to be expressed; either alone is insufficient. *OrY* requires the cooperative binding of the red TF to clustered CREs for expression; this cooperation can ensure robust expression in the face of environmental temperature changes; by contrast, the red TF does not bind to the single corresponding CRE upstream of *OrX* in these neurons. *OrZ* transcription is promoted by the green TF but suppressed by the yellow TF that binds 3′ of the gene. Other external factors might influence levels, though not spatial patterning, of receptor expression (see text). **(B)** Chromatin marks and histone-modifying enzymes contributing to the selective expression of olfactory receptors. Different enzymes display differences in their temporal expression and requirement; among these, dLsd1 – which is normally associated with removing H3K4 methylation – appears to have roles in OSNs in both promoting and repressing *Or* expression (see text). Although schematized separately for clarity, chromatin regulation is intimately related to the combinatorial binding of TFs to receptor loci. **(C)** Feedback mechanisms contributing to the refinement and/or stability of receptor expression. Transcriptional interference by *OrX* of *OrY* might occur when inefficient transcriptional termination at the 3′ end of the former gene leads to the RNA polymerase II impeding transcription initiation at *OrY* (solid wavy orange and purple lines represent protein coding transcripts from *OrX* and *OrY*, respectively; the dashed purple line represents the 3′UTR of *OrX* transcripts that incorporate sequences encoded by *OrY* that are not translated into OrY) (Mika et al., 2021). Receptor protein-dependent feedback on transcript or protein levels of other (not necessarily closely linked) receptors occurs through unknown mechanisms (Maguire et al., 2020; Jafari et al., 2021; Mika et al., 2021).

mice (Dalton and Lomvardas, 2015; Monahan and Lomvardas, 2015). In *D. melanogaster*, this core set is theoretically more than adequate in number (∼15–20) to contribute combinatorially to a unique gene regulatory network within each OSN class.

Despite this conceptual framework, many issues remain unresolved. Only a subset of TFs have defined binding motifs, and even fewer have been shown to associate physically with receptor gene regulatory sequences (typically in *in vitro* assays) (Bai et al., 2009; Jafari et al., 2012). Moreover, the presence of a motif in a CRE for a given gene does not necessarily mean that the corresponding TF is required (and vice versa) (Jafari et al., 2012; **Figure 2A**). While some TFs have lineage-specific expression and function (Li et al., 2020; Arguello et al., 2021), many have broad expression in OSNs despite very selective requirements in receptor regulation (Jafari et al., 2012; Li et al., 2020). The lack of correlation between the presence of a TF binding motif in a CRE and TF requirement for a given receptor might reflect differences in *in vitro* and *in vivo*

binding specificities for TFs and/or an indirect requirement for *trans*-acting factors in controlling receptor expression. Indeed, temporal manipulation of TF function indicates that several of these proteins have multiple roles in OSN development, for example, during SOP lineage specification (Bai and Carlson, 2010; Jafari et al., 2012; Chai et al., 2019; Arguello et al., 2021; Mika et al., 2021). Moreover, many TFs are expressed and required in late pupal/adult stages implying roles in both initiation and maintenance of correct receptor expression (Bai and Carlson, 2010; Jafari et al., 2012; Arguello et al., 2021; Mika et al., 2021). The biochemical properties of TF/CRE interactions that promote stable receptor expression in a given OSN type remain, however, largely elusive.

CHROMATIN MARKS AND CHROMOSOMAL INTERACTIONS

Recent genetic screens and candidate analyses have also identified roles for various chromatin modifiers (e.g., histone methyltransferases and deacetylases or their regulators) in the correct activation and/or repression of receptor genes (Sim et al., 2012; Alkhori et al., 2014; Jafari and Alenius, 2015; Chai et al., 2019; Gonzalez et al., 2019; Jafari et al., 2021; **Figure 2B**). Conserved epigenetic modifications, such as H3K4me3 and H3K9me2 – normally associated with active and repressed promoters, respectively – have been detected at individual receptor genes by chromatin immunoprecipitation (ChIP)-quantitative RT-PCR (Sim et al., 2012; Alkhori et al., 2014; Jafari and Alenius, 2015; Gonzalez et al., 2019; Jafari et al., 2021). Temporal analyses of the expression and requirement for some of these enzymes have begun to reveal different phases in how chromatin modifications may impact receptor expression, focusing on an *Or59b* promoter transgenic reporter (Jafari and Alenius, 2015; Gonzalez et al., 2019; Jafari et al., 2021). The H3K9me3 demethylase Kdm4B participates in the initiation of reporter expression, while Su(var)3–9 – which promotes H3K9me3 and heterochromatin formation – helps prevent ectopic expression. The activity of Su(var)3–9 appears to be antagonized by dLsd1, which contributes to reporter expression throughout OSN development. The activating role of dLsd1 in OSNs is intriguing as in other *D. melanogaster* tissues this enzyme erases H3K4 methylation to induce heterochromatin formation; this olfactory function highlights a potential parallel with mammalian Lsd1 function in facilitating *OR* expression (**Figure 2B**; Dalton and Lomvardas, 2015; Monahan and Lomvardas, 2015). Su(var)3–9 and dLsd1 expression increases after hatching and have been proposed to contribute to the termination of a "critical period" of receptor expression in young adults when the mature pattern is stabilized (Jafari et al., 2021).

Despite these insights, a global time course of chromatin state at active and silenced endogenous receptor loci in specific neuron populations is lacking, constrained by the ability to obtain enough cells of a given class for ChIP-sequencing-based methods. A low-resolution assessment of chromatin structure in several individual mature *Ir*-expressing OSN populations has been made using Chromatin Accessibility Targeted DamID (CATaDa) (Arguello et al., 2021), which exploits cell-type specific expression of the *E. coli* Dam methylase to avoid a need for cell sorting (Aughey et al., 2018). This analysis revealed that access to the DNA at different receptor genes is globally similar between neuron populations, suggesting that the specificity of transcriptional activation in a given neuron is not reliant upon uniquely accessible enhancers (at least in the analyzed *Ir* populations) (Arguello et al., 2021). Although direct comparison is currently hard, this situation might contrast with that in mammals, where all but the chosen receptor gene are maintained in a heterochromatic, silenced state (Dalton and Lomvardas, 2015; Monahan and Lomvardas, 2015). In mice, higher-level structural properties of DNA, notably interchromosomal interactions and nuclear compartmentalization of olfactory receptor genes, are important for the expression of one receptor allele and silencing of all others (Bashkirova and Lomvardas, 2019; Monahan et al., 2019), but whether such phenomena are important in insect OSNs is unknown.

FEEDBACK MECHANISMS

A central mechanism ensuring singular receptor expression in mammals is a feedback signal from the chosen receptor (Dalton and Lomvardas, 2015; Monahan and Lomvardas, 2015). Intriguingly, this feedback pathway has co-opted the unfolded protein response, through which the expressed OR induces translational homeostasis in OSNs to, ultimately, stabilize *OR* choice and prevent activation of other receptor genes (Dalton et al., 2013). In insects, feedback mechanisms were thought not to exist, as receptor genes can be ectopically expressed in other OSNs without affecting endogenous receptor gene expression (e.g., Ray et al., 2007), and neurons lacking their own receptors (through mutation) do not appear to activate expression of other receptor loci (e.g., Dobritsa et al., 2003; Grosjean et al., 2011).

Recent evidence, however, supports the existence of regulatory relationships between some receptor genes that might help to reinforce the singular expression of receptors defined by OSN-specific TF combinations (**Figure 2C**). In a tandem array of *D. melanogaster* genes (*Ir75c*, *Ir75b*, and *Ir75a*), transcription from the upstream genes was found to run through the downstream genes, blocking their expression in *cis*, potentially through transcriptional interference (Mika et al., 2021). Ir75c can also prevent accumulation of the other receptor proteins in *trans*, through a protein-dependent, post-transcriptional (but unknown) mechanism (Mika et al., 2021; **Figure 2C**). Whether similar interactions occur between other clustered genes is unclear, but such phenomena might help explain how recent receptor duplicates initially acquire exclusive expression patterns. In the mosquito, *Anopheles gambiae*, broad transgenic overexpression of one *Or* led to reduced transcription of most other *Or*s, but not the vast majority of other OSN-expressed genes (Maguire et al., 2020). This suppression mechanism is also unknown, but appears to depend upon the ectopically expressed Or protein (**Figure 2C**). Similar transcriptional suppression of *Or*s upon widespread misexpression of one receptor was also reported in *D. melanogaster* (Jafari et al., 2021). In either species,

it is unclear whether this type of repression uses a similar or different pathway to mammalian OR feedback, and if such a pathway operates downstream of endogenously expressed, and not only transgenically expressed, receptors.

ENVIRONMENTAL AND INTERNAL STATE INFLUENCES

Although the precise spatial patterning of receptor expression is under the control of hard-wired genetic programs, growing evidence indicates that an animal's internal state and environmental cues can impact the level of receptor expression, facilitated by the ease of performing RNA-sequencing in diverse species under different conditions. For example, the mating status of *Drosophila suzukii* and the pine caterpillar moth, *Dendrolimus punctatus*, are linked to changes in expression of some *Or*s (Zhang et al., 2017; Crava et al., 2019). Blood-feeding in mosquitoes leads to transcriptional down- or up-regulation of certain olfactory receptors (Rinker et al., 2013; Matthews et al., 2016). Odor exposure itself can lead to changes in receptor expression in *D. melanogaster* (Zhou et al., 2009; von der Weid et al., 2015; Koerte et al., 2018) although the affected receptors are not necessarily those that respond to the odor stimulus (Koerte et al., 2018). Similarly, in the honeybee, *Apis mellifera*, olfactory conditioning can cause alterations in receptor expression (Claudianos et al., 2014).

In most of these examples, we know little about the physiological and ecological significance of such changes or how external factors influence receptor expression. However, analysis of the impact of temperature stress and starvation upon the transcription of endogenous receptors and transgenic reporters in *D. melanogaster* has revealed the importance of cooperation between clustered CREs to buffer against environment fluctuations, hinting at a biochemical basis ensuring robust receptor expression (Jafari and Alenius, 2015; Gonzalez et al., 2019; Jafari et al., 2021). Temperature stress also affects the expression of chromatin modifying enzymes, which might contribute to the stabilization of ectopic reporter expression (Jafari et al., 2021). Further study of such short-term plasticity of receptor expression might help reveal new insights into the mechanisms that promote their selective neuronal expression.

EVOLVABILITY

The overall precision of olfactory receptor expression within a species belies the flexibility of this sensory system over evolutionary timescales (Ramdya and Benton, 2010). Comparative antennal transcriptomic studies (using bulk RNA-sequencing) in closely related species have revealed differences in expression level of many receptors (McBride et al., 2014; Shiao et al., 2015; Crowley-Gall et al., 2016; Pan et al., 2017), although these datasets cannot distinguish changes in receptor expression level within an OSN population from changes in numbers of neurons expressing a particular gene. More strikingly, enormous variation exists in the size of olfactory receptor repertoires (from <10 to >500) – and, presumably, corresponding number of neuron types – between species (Robertson, 2019; Yan et al., 2020).

How new olfactory receptor expression patterns evolve to define a distinct neuron class is largely obscure. Even relatively recently duplicated receptor genes can have quite different *cis*- and *trans*-regulatory mechanisms (Prieto-Godino et al., 2017; Mika et al., 2021), prohibiting easy identification of the responsible genetic changes that drove the divergence in their spatial expression. The evolution of new receptor expression patterns is of course intimately linked with the evolution of novel neuron types. One potential way new OSN classes can be created is through changes in the genetically patterned programmed cell death that normally removes many populations during development (Sen et al., 2004; Endo et al., 2007; Chai et al., 2019; **Figure 1C**). Artificial blockage of programmed cell death in the developing sensory lineages in *D. melanogaster* is sufficient to generate "undead" neurons that express olfactory receptors (Prieto-Godino et al., 2020). Intriguingly, the subset of receptor genes transcribed in undead neurons is enriched for those that are found in tandem arrays, and which are (exceptionally) co-expressed in "normal" OSNs (see below). The reason for this phenomenon is unknown but hints at a molecular property of these tandem arrays (e.g., chromatin state) that makes one or more of the constituent receptor genes permissive for expression in OSN precursors that are normally condemned to die.

RECEPTOR CO-EXPRESSION

While we have emphasized mechanisms underlying the discrete expression of olfactory receptors, there are cases of receptor co-expression. The most obvious examples are co-expression of tuning receptors with co-receptor subunits (Larsson et al., 2004; Nakagawa et al., 2005; Benton et al., 2006; Sato et al., 2008; Abuin et al., 2011; **Figure 1A**). The mechanisms specifying the broad expression of co-receptors are mostly unknown (Mika et al., 2021) and these genes might use different gene regulatory networks to those of tuning receptors. Analysis in *D. melanogaster* and the mosquito *Aedes aegypti* showed that different co-receptors are not mutually exclusive, and can often be detected in OSN classes where they do not have a (known) partner tuning receptor (Abuin et al., 2011; Task et al., 2020; Younger et al., 2020). These observations raise the interesting possibility that some neurons have two types of receptors contributing to their response profile (Younger et al., 2020) and/or that co-receptors alone modulate the responses of other receptor classes (Task et al., 2020; Vulpe et al., 2021). Alternatively, overlapping co-receptor expression might simply reflect a lack of regulatory pathways to constrain their broad expression to neurons in which they function.

Several examples of co-expressed tuning receptors have been described in various insect species. In some cases, two receptors arise from alternative splicing of transcripts expressed from a common locus (Robertson et al., 2003; Ray et al., 2007; Lebreton et al., 2017). Other examples of co-expression appear to be due to di/polycistronic transcripts encoded by clustered receptor genes

(Ray et al., 2007; Koutroumpa et al., 2014; Karner et al., 2015). However, caution is necessary in interpretation of such "co-expression" based upon RNA *in situ* hybridization data alone, because this can be confounded by the existence of read-through transcription, where exons of downstream genes in tandem arrays are incorporated into the transcripts of upstream genes, but not encode the corresponding receptor protein (Prieto-Godino et al., 2017; Mika et al., 2021). Notably, in *A. aegypti*, the number of tuning receptors expressed in olfactory organs (determined by bulk RNA-sequencing) is in large excess of the number of glomeruli, suggesting that co-expression of tuning receptors is widespread in this insect (Younger et al., 2020).

There are still only a few clear examples of co-expressed tuning receptor genes that encode functionally distinct proteins. Some of these genes are adjacent in the genome, consistent with conservation of CREs upon gene duplication (Dobritsa et al., 2003), while others are unlinked (Goldman et al., 2005), suggesting convergence in their *cis*-regulatory landscape. Tuning receptor co-expression can expand the response profile of a neuron class (Lebreton et al., 2017), although in many cases it might reflect a "transient" evolutionary state where duplicated receptor genes have not yet acquired distinct expression patterns (Ramdya and Benton, 2010).

DISCUSSION

The exquisite specificity of insect olfactory receptor expression is widely viewed as resulting from a deterministic process relying on sets of TFs acting through receptor-gene specific combinations of CREs (Ray et al., 2007). While this model remains largely valid, two issues require further investigation.

First, our knowledge of the molecular biology of receptor choice is still superficial: we do not have a complete picture of the CREs, the chromatin state, and the associated TFs for any receptor gene. Such properties are extraordinarily hard to characterize in insect OSNs, given their rarity, small size, and difficulty to extract them from (or image them within) cuticle-covered tissues, as well as the relatively rapid development from SOP to mature neuron. However, new *in vivo* cell-type specific RNA/chromatin profiling and transgenesis-based approaches in *D. melanogaster* (and, in theory, in other genetically manipulatable species) (van den Ameele et al., 2019; Li, 2020) might aid in better understanding these mechanistic details. The relatively compact size of most receptor gene regulatory elements – in comparison to many other neural gene enhancers – suggests that the problem is tractable, and further study could offer general insights into how genes exhibit highly selective expression patterns in the nervous system.

Second, it is increasingly unclear to what extent receptor expression relies solely on a combinatorial code of CREs and TFs in all insects. This model was developed principally from studies in *D. melanogaster*, where the receptor repertoires might be sufficiently small to be regulated by deterministic processes. However, there is growing evidence for feedback mechanisms and dynamic chromatin regulation in this insect, as well as hints that species with larger receptor repertoires use additional/alternative regulatory mechanisms. These advances raise the possibility that greater mechanistic similarities – or at least analogies – exist with the process of olfactory receptor choice in mammals than currently appreciated.

AUTHOR CONTRIBUTIONS

KM and RB wrote the manuscript. Both authors contributed to the article and approved the submitted version.

FUNDING

Research in RB's Laboratory was supported by the University of Lausanne, ERC Consolidator and Advanced Grants (615094 and 833548, respectively), and the Swiss National Science Foundation (310030B_18537).

ACKNOWLEDGMENTS

We thank Nadine Vastenhouw, Meg Younger, and members of the Benton Laboratory for discussions and comments on the manuscript.

REFERENCES

Abuin, L., Bargeton, B., Ulbrich, M. H., Isacoff, E. Y., Kellenberger, S., and Benton, R. (2011). Functional architecture of olfactory ionotropic glutamate receptors. *Neuron* 69, 44–60. doi: 10.1016/j.neuron.2010.11.042

Alkhori, L., Ost, A., and Alenius, M. (2014). The corepressor Atrophin specifies odorant receptor expression in *Drosophila*. *FASEB J.* 28, 1355–1364. doi: 10.1096/fj.13-240325

Arguello, J. R., Abuin, L., Armida, J., Mika, K., Chai, P. C., and Benton, R. (2021). Targeted molecular profiling of rare olfactory sensory neurons identifies fate, wiring, and functional determinants. *Elife* 10:e63036. doi: 10.7554/eLife.63036

Auer, T. O., Khallaf, M. A., Silbering, A. F., Zappia, G., Ellis, K., Alvarez-Ocana, R., et al. (2020). Olfactory receptor and circuit evolution promote host specialization. *Nature* 579, 402–408. doi: 10.1038/s41586-020-2073-7

Aughey, G. N., Estacio Gomez, A., Thomson, J., Yin, H., and Southall, T. D. (2018). CATaDa reveals global remodelling of chromatin accessibility during stem cell differentiation in vivo. *Elife* 7:e32341. doi: 10.7554/eLife.32341

Bai, L., and Carlson, J. R. (2010). Distinct functions of *acj6* splice forms in odor receptor gene choice. *J. Neurosci.* 30, 5028–5036. doi: 10.1523/JNEUROSCI.6292-09.2010

Bai, L., Goldman, A. L., and Carlson, J. R. (2009). Positive and negative regulation of odor receptor gene choice in *Drosophila* by *acj6*. *J. Neurosci.* 29, 12940–12947. doi: 10.1523/JNEUROSCI.3525-09.2009

Barish, S., and Volkan, P. C. (2015). Mechanisms of olfactory receptor neuron specification in *Drosophila*. *Wiley Interdiscip. Rev. Dev. Biol.* 4, 609–621. doi: 10.1002/wdev.197

Bashkirova, E., and Lomvardas, S. (2019). Olfactory receptor genes make the case for inter-chromosomal interactions. *Curr. Opin. Genet. Dev.* 55, 106–113. doi: 10.1016/j.gde.2019.07.004

Benton, R., Sachse, S., Michnick, S. W., and Vosshall, L. B. (2006). Atypical membrane topology and heteromeric function of *Drosophila* odorant receptors *in vivo*. *PLoS Biol.* 4:e20. doi: 10.1371/journal.pbio.0040020

Benton, R., Vannice, K. S., Gomez-Diaz, C., and Vosshall, L. B. (2009). Variant ionotropic glutamate receptors as chemosensory receptors in *Drosophila*. *Cell* 136, 149–162.

Butterwick, J. A., Del Marmol, J., Kim, K. H., Kahlson, M. A., Rogow, J. A., Walz, T., et al. (2018). Cryo-EM structure of the insect olfactory receptor Orco. *Nature* 560, 447–452. doi: 10.1038/s41586-018-0420-8

Chai, P. C., Cruchet, S., Wigger, L., and Benton, R. (2019). Sensory neuron lineage mapping and manipulation in the *Drosophila* olfactory system. *Nat. Commun.* 10:643. doi: 10.1038/s41467-019-08345-4

Claudianos, C., Lim, J., Young, M., Yan, S., Cristino, A. S., Newcomb, R. D., et al. (2014). Odor memories regulate olfactory receptor expression in the sensory periphery. *Eur. J. Neurosci.* 39, 1642–1654. doi: 10.1111/ejn.12539

Clyne, P. J., Certel, S. J., de Bruyne, M., Zaslavsky, L., Johnson, W. A., and Carlson, J. R. (1999a). The odor specificities of a subset of olfactory receptor neurons are governed by Acj6, a POU-domain transcription factor. *Neuron* 22, 339–347.

Clyne, P. J., Warr, C. G., Freeman, M. R., Lessing, D., Kim, J., and Carlson, J. R. (1999b). A novel family of divergent seven-transmembrane proteins: candidate odorant receptors in *Drosophila*. *Neuron* 22, 327–338.

Couto, A., Alenius, M., and Dickson, B. J. (2005). Molecular, anatomical, and functional organization of the *Drosophila* olfactory system. *Curr. Biol.* 15, 1535–1547.

Crava, C. M., Sassu, F., Tait, G., Becher, P. G., and Anfora, G. (2019). Functional transcriptome analyses of *Drosophila suzukii* antennae reveal mating-dependent olfaction plasticity in females. *Insect Biochem. Mol. Biol.* 105, 51–59. doi: 10.1016/j.ibmb.2018.12.012

Crowley-Gall, A., Date, P., Han, C., Rhodes, N., Andolfatto, P., Layne, J. E., et al. (2016). Population differences in olfaction accompany host shift in *Drosophila mojavensis*. *Proc. Biol. Sci.* 283:20161562. doi: 10.1098/rspb.2016.1562

Dalton, R. P., and Lomvardas, S. (2015). Chemosensory Receptor Specificity and Regulation. *Annu. Rev. Neurosci.* 38, 331–349. doi: 10.1146/annurev-neuro-071714-034145

Dalton, R. P., Lyons, D. B., and Lomvardas, S. (2013). Co-opting the unfolded protein response to elicit olfactory receptor feedback. *Cell* 155, 321–332. doi: 10.1016/j.cell.2013.09.033

Del Marmol, J., Yedlin, M. A., and Ruta, V. (2021). The structural basis of odorant recognition in insect olfactory receptors. *Nature* doi: 10.1038/s41586-021-03794-8 [Online ahead of print]

Dobritsa, A. A., van der Goes van Naters, W., Warr, C. G., Steinbrecht, R. A., and Carlson, J. R. (2003). Integrating the molecular and cellular basis of odor coding in the *Drosophila* antenna. *Neuron* 37, 827–841.

Endo, K., Aoki, T., Yoda, Y., Kimura, K., and Hama, C. (2007). Notch signal organizes the *Drosophila* olfactory circuitry by diversifying the sensory neuronal lineages. *Nat. Neurosci.* 10, 153–160. doi: 10.1038/nn1832

Endo, K., Karim, M. R., Taniguchi, H., Krejci, A., Kinameri, E., Siebert, M., et al. (2011). Chromatin modification of Notch targets in olfactory receptor neuron diversification. *Nat. Neurosci.* 15, 224–233. doi: 10.1038/nn.2998

Fujii, T., Namiki, S., Abe, H., Sakurai, T., Ohnuma, A., Kanzaki, R., et al. (2011). Sex-linked transcription factor involved in a shift of sex-pheromone preference in the silkmoth *Bombyx mori*. *Proc. Natl. Acad. Sci. U. S. A.* 108, 18038–18043. doi: 10.1073/pnas.1107282108

Fuss, S. H., and Ray, A. (2009). Mechanisms of odorant receptor gene choice in *Drosophila* and vertebrates. *Mol. Cell Neurosci.* 41, 101–112. doi: 10.1016/j.mcn.2009.02.014

Goldman, A. L., Van der Goes van Naters, W., Lessing, D., Warr, C. G., and Carlson, J. R. (2005). Coexpression of two functional odor receptors in one neuron. *Neuron* 45, 661–666.

Gomez-Diaz, C., Martin, F., Garcia-Fernandez, J. M., and Alcorta, E. (2018). The Two Main Olfactory Receptor Families in *Drosophila*, ORs and IRs: A Comparative Approach. *Front. Cell Neurosci.* 12:253. doi: 10.3389/fncel.2018.00253

Gonzales, C. N., McKaughan, Q., Bushong, E. A., Cauwenberghs, K., Ng, R., Madany, M., et al. (2021). Systematic morphological and morphometric analysis of identified olfactory receptor neurons in *Drosophila melanogaster*. *eLife*. doi: 10.7554/eLife.69896 [Online ahead of print]

Gonzalez, A., Jafari, S., Zenere, A., Alenius, M., and Altafini, C. (2019). Thermodynamic model of gene regulation for the Or59b olfactory receptor in *Drosophila*. *PLoS Comput. Biol.* 15:e1006709. doi: 10.1371/journal.pcbi.1006709

Grabe, V., Baschwitz, A., Dweck, H. K. M., Lavista-Llanos, S., Hansson, B. S., and Sachse, S. (2016). Elucidating the Neuronal Architecture of Olfactory Glomeruli in the *Drosophila* Antennal Lobe. *Cell Rep.* 16, 3401–3413. doi: 10.1016/j.celrep.2016.08.063

Grabe, V., and Sachse, S. (2018). Fundamental principles of the olfactory code. *BioSystems* 164, 94–101. doi: 10.1016/j.biosystems.2017.10.010

Grosjean, Y., Rytz, R., Farine, J. P., Abuin, L., Cortot, J., Jefferis, G. S., et al. (2011). An olfactory receptor for food-derived odours promotes male courtship in *Drosophila*. *Nature* 478, 236–240. doi: 10.1038/nature10428

Hanchate, N. K., Kondoh, K., Lu, Z., Kuang, D., Ye, X., Qiu, X., et al. (2015). Single-cell transcriptomics reveals receptor transformations during olfactory neurogenesis. *Science* 350, 1251–1255. doi: 10.1126/science.aad2456

Hughes, G. M., Boston, E. S. M., Finarelli, J. A., Murphy, W. J., Higgins, D. G., and Teeling, E. C. (2018). The Birth and Death of Olfactory Receptor Gene Families in Mammalian Niche Adaptation. *Mol. Biol. Evol.* 35, 1390–1406. doi: 10.1093/molbev/msy028

Jafari, S., and Alenius, M. (2015). Cis-Regulatory Mechanisms for Robust Olfactory Sensory Neuron Class-restricted Odorant Receptor Gene Expression in *Drosophila*. *PLoS Genet.* 11:e1005051. doi: 10.1371/journal.pgen.1005051

Jafari, S., Alkhori, L., Schleiffer, A., Brochtrup, A., Hummel, T., and Alenius, M. (2012). Combinatorial activation and repression by seven transcription factors specify *Drosophila* odorant receptor expression. *PLoS Biol.* 10:e1001280. doi: 10.1371/journal.pbio.1001280

Jafari, S., Henriksson, J., Yan, H., and Alenius, M. (2021). Stress and odorant receptor feedback during a critical period after hatching regulates olfactory sensory neuron differentiation in *Drosophila*. *PLoS Biol.* 19:e3001101. doi: 10.1371/journal.pbio.3001101

Jefferis, G. S., and Hummel, T. (2006). Wiring specificity in the olfactory system. *Semin. Cell Dev. Biol.* 17, 50–65. doi: 10.1016/j.semcdb.2005.12.002

Jefferis, G. S., Vyas, R. M., Berdnik, D., Ramaekers, A., Stocker, R. F., Tanaka, N. K., et al. (2004). Developmental origin of wiring specificity in the olfactory system of *Drosophila*. *Development* 131, 117–130.

Karner, T., Kellner, I., Schultze, A., Breer, H., and Krieger, J. (2015). Co-expression of six tightly clustered odorant receptor genes in the antenna of the malaria mosquito *Anopheles gambiae*. *Front. Ecol. Evol.* 3:26. doi: 10.3389/fevo.2015.00026

Koerte, S., Keesey, I. W., Khallaf, M. A., Cortes Llorca, L., Grosse-Wilde, E., Hansson, B. S., et al. (2018). Evaluation of the DREAM Technique for a High-Throughput Deorphanization of Chemosensory Receptors in *Drosophila*. *Front. Mol. Neurosci.* 11:366. doi: 10.3389/fnmol.2018.00366

Koutroumpa, F. A., Karpati, Z., Monsempes, C., Hill, S. R., Hansson, B. S., Jacquin-Joly, E., et al. (2014). Shifts in sensory neuron identity parallel differences in pheromone preference in the European corn borer. *Front. Ecol. Evol.* 2:65. doi: 10.3389/fevo.2014.00065

Kurtovic, A., Widmer, A., and Dickson, B. J. (2007). A single class of olfactory neurons mediates behavioural responses to a *Drosophila* sex pheromone. *Nature* 446, 542–546.

Larsson, M. C., Domingos, A. I., Jones, W. D., Chiappe, M. E., Amrein, H., and Vosshall, L. B. (2004). *Or83b* encodes a broadly expressed odorant receptor essential for *Drosophila* olfaction. *Neuron* 43, 703–714.

Lebreton, S., Borrero-Echeverry, F., Gonzalez, F., Solum, M., Wallin, E. A., Hedenstrom, E., et al. (2017). A *Drosophila* female pheromone elicits species-specific long-range attraction via an olfactory channel with dual

specificity for sex and food. *BMC Biol.* 15:88. doi: 10.1186/s12915-017-0427-x

Li, H. (2020). Single-cell RNA sequencing in *Drosophila:* technologies and applications. *Wiley Interdiscip. Rev. Dev. Biol.* 10:e396. doi: 10.1002/wdev.396

Li, H., Li, T., Horns, F., Li, J., Xie, Q., Xu, C., et al. (2020). Single-Cell Transcriptomes Reveal Diverse Regulatory Strategies for Olfactory Receptor Expression and Axon Targeting. *Curr. Biol.* 30, 1189–1198.e5. doi: 10.1016/j.cub.2020.01.049

Li, Q., Ha, T. S., Okuwa, S., Wang, Y., Wang, Q., Millard, S. S., et al. (2013). Combinatorial Rules of Precursor Specification Underlying Olfactory Neuron Diversity. *Curr. Biol.* 23, 2481–2490. doi: 10.1016/j.cub.2013.10.053

Li, T., Fu, T.-M., Li, H., Xie, Q., Luginbuhl, D. J., Betzig, E., et al. (2021). Cellular Bases of Olfactory Circuit Assembly Revealed by Systematic Time-lapse Imaging. *bioRxiv* [Preprint]. doi: 10.1101/2021.05.04.442682

Maguire, S. E., Afify, A., Goff, L. A., and Potter, C. J. (2020). A Feedback Mechanism Regulates Odorant Receptor Expression in the Malaria Mosquito, *Anopheles gambiae*. *bioRxiv* [Preprint]. doi: 10.1101/2020.07.23.218586

Matthews, B. J., McBride, C. S., DeGennaro, M., Despo, O., and Vosshall, L. B. (2016). The neurotranscriptome of the *Aedes aegypti* mosquito. *BMC Genomics* 17:32. doi: 10.1186/s12864-015-2239-0

McBride, C. S., Baier, F., Omondi, A. B., Spitzer, S. A., Lutomiah, J., Sang, R., et al. (2014). Evolution of mosquito preference for humans linked to an odorant receptor. *Nature* 515, 222–227. doi: 10.1038/nature13964

McLaughlin, C. N., Brbic, M., Xie, Q., Li, T., Horns, F., Kolluru, S. S., et al. (2021). Single-cell transcriptomes of developing and adult olfactory receptor neurons in *Drosophila*. *Elife* 10:e63856. doi: 10.7554/eLife.63856

Mika, K., Cruchet, S., Chai, P. C., Prieto-Godino, L. L., Auer, T. O., Pradervand, S., et al. (2021). Olfactory receptor-dependent receptor repression in *Drosophila*. *Sci. Adv.* 7:eabe3745. doi: 10.1126/sciadv.abe3745

Miller, C. J., and Carlson, J. R. (2010). Regulation of odor receptor genes in trichoid sensilla of the *Drosophila* antenna. *Genetics* 186, 79–95. doi: 10.1534/genetics.110.117622

Monahan, K., Horta, A., and Lomvardas, S. (2019). LHX2- and LDB1-mediated trans interactions regulate olfactory receptor choice. *Nature* 565, 448–453. doi: 10.1038/s41586-018-0845-0

Monahan, K., and Lomvardas, S. (2015). Monoallelic expression of olfactory receptors. *Annu. Rev. Cell Dev. Biol.* 31, 721–740. doi: 10.1146/annurev-cellbio-100814-125308

Nakagawa, T., Sakurai, T., Nishioka, T., and Touhara, K. (2005). Insect sex-pheromone signals mediated by specific combinations of olfactory receptors. *Science* 307, 1638–1642.

Pan, J. W., Li, Q., Barish, S., Okuwa, S., Zhao, S., Soeder, C., et al. (2017). Patterns of transcriptional parallelism and variation in the developing olfactory system of *Drosophila* species. *Sci. Rep.* 7:8804. doi: 10.1038/s41598-017-08563-0

Prieto-Godino, L. L., Rytz, R., Cruchet, S., Bargeton, B., Abuin, L., Silbering, A. F., et al. (2017). Evolution of acid-sensing olfactory circuits in drosophilids. *Neuron* 93, 661–676.e6. doi: 10.1016/j.neuron.2016.12.024

Prieto-Godino, L. L., Silbering, A. F., Khallaf, M. A., Cruchet, S., Bojkowska, K., Pradervand, S., et al. (2020). Functional integration of "undead" neurons in the olfactory system. *Sci. Adv.* 6:eaaz7238. doi: 10.1126/sciadv.aaz7238

Ramdya, P., and Benton, R. (2010). Evolving olfactory systems on the fly. *Trends Genet.* 26, 307–316. doi: 10.1016/j.tig.2010.04.004

Ray, A., van der Goes, van Naters, W., and Carlson, J. (2008). A Regulatory Code for Neuron-Specific Odor Receptor Expression. *PLoS Biol.* 6:e125. doi: 10.1371/journal.pbio.0060125

Ray, A., van der Goes, van Naters, W., Shiraiwa, T., and Carlson, J. R. (2007). Mechanisms of odor receptor gene choice in *Drosophila*. *Neuron* 53, 353–369.

Rinker, D. C., Pitts, R. J., Zhou, X., Suh, E., Rokas, A., and Zwiebel, L. J. (2013). Blood meal-induced changes to antennal transcriptome profiles reveal shifts in odor sensitivities in *Anopheles gambiae*. *Proc. Natl. Acad. Sci. U. S. A.* 110, 8260–8265. doi: 10.1073/pnas.1302562110

Robertson, H. M. (2019). Molecular Evolution of the Major Arthropod Chemoreceptor Gene Families. *Annu. Rev. Entomol.* 64, 227–242. doi: 10.1146/annurev-ento-020117-043322

Robertson, H. M., Warr, C. G., and Carlson, J. R. (2003). Molecular evolution of the insect chemoreceptor gene superfamily in *Drosophila melanogaster*. *Proc. Natl. Acad. Sci. U. S. A.* 100, 14537–14542.

Rodrigues, V., and Hummel, T. (2008). Development of the *Drosophila* olfactory system. *Adv. Exp. Med. Biol.* 628, 82–101. doi: 10.1007/978-0-387-78261-4_6

Ryba, A. R., McKenzie, S. K., Olivos-Cisneros, L., Clowney, E. J., Pires, P. M., and Kronauer, D. J. C. (2020). Comparative Development of the Ant Chemosensory System. *Curr. Biol.* 30, 3223–3230.e4. doi: 10.1016/j.cub.2020.05.072

Sakano, H. (2010). Neural map formation in the mouse olfactory system. *Neuron* 67, 530–542. doi: 10.1016/j.neuron.2010.07.003

Sato, K., Pellegrino, M., Nakagawa, T., Nakagawa, T., Vosshall, L. B., and Touhara, K. (2008). Insect olfactory receptors are heteromeric ligand-gated ion channels. *Nature* 452, 1002–1006.

Schlegel, P., Bates, A. S., Sturner, T., Jagannathan, S. R., Drummond, N., Hsu, J., et al. (2021). Information flow, cell types and stereotypy in a full olfactory connectome. *Elife* 10:e66018. doi: 10.7554/eLife.66018

Schmidt, H. R., and Benton, R. (2020). Molecular mechanisms of olfactory detection in insects: beyond receptors. *Open Biol.* 10:200252. doi: 10.1098/rsob.200252

Sen, A., Kuruvilla, D., Pinto, L., Sarin, A., and Rodrigues, V. (2004). Programmed cell death and context dependent activation of the EGF pathway regulate gliogenesis in the *Drosophila* olfactory system. *Mech. Dev.* 121, 65–78.

Shiao, M. S., Chang, J. M., Fan, W. L., Lu, M. Y., Notredame, C., Fang, S., et al. (2015). Expression Divergence of Chemosensory Genes between *Drosophila sechellia* and Its Sibling Species and Its Implications for Host Shift. *Genome Biol. Evol.* 7, 2843–2858. doi: 10.1093/gbe/evv183

Silbering, A. F., Rytz, R., Grosjean, Y., Abuin, L., Ramdya, P., Jefferis, G. S., et al. (2011). Complementary Function and Integrated Wiring of the Evolutionarily Distinct *Drosophila* Olfactory Subsystems. *J. Neurosci.* 31, 13357–13375. doi: 10.1523/JNEUROSCI.2360-11.2011

Sim, C. K., Perry, S., Tharadra, S. K., Lipsick, J. S., and Ray, A. (2012). Epigenetic regulation of olfactory receptor gene expression by the Myb-MuvB/dREAM complex. *Genes Dev.* 26, 2483–2498. doi: 10.1101/gad.201665.112

Tan, L., Li, Q., and Xie, X. S. (2015). Olfactory sensory neurons transiently express multiple olfactory receptors during development. *Mol. Syst. Biol.* 11:844. doi: 10.15252/msb.20156639

Task, D., Lin, C.-C., Afify, A., Li, H., Vulpe, A., Menuz, K., et al. (2020). Widespread Polymodal Chemosensory Receptor Expression in *Drosophila* Olfactory Neurons. *bioRxiv* [Preprint]. doi: 10.1101/2020.11.07.355651

Tichy, A. L., Ray, A., and Carlson, J. R. (2008). A new *Drosophila* POU gene, *pdm3*, acts in odor receptor expression and axon targeting of olfactory neurons. *J. Neurosci.* 28, 7121–7129. doi: 10.1523/JNEUROSCI.2063-08.2008

Trible, W., Olivos-Cisneros, L., McKenzie, S. K., Saragosti, J., Chang, N. C., Matthews, B. J., et al. (2017). *orco* Mutagenesis Causes Loss of Antennal Lobe Glomeruli and Impaired Social Behavior in Ants. *Cell* 170, 727–735.e10. doi: 10.1016/j.cell.2017.07.001

van den Ameele, J., Krautz, R., and Brand, A. H. (2019). TaDa! Analysing cell type-specific chromatin in vivo with Targeted DamID. *Curr. Opin. Neurobiol.* 56, 160–166. doi: 10.1016/j.conb.2019.01.021

von der Weid, B., Rossier, D., Lindup, M., Tuberosa, J., Widmer, A., et al. (2015). Large-scale transcriptional profiling of chemosensory neurons identifies receptor-ligand pairs in vivo. *Nat. Neurosci.* 18, 1455–1463. doi: 10.1038/nn.4100

Vosshall, L. B., Wong, A. M., and Axel, R. (2000). An olfactory sensory map in the fly brain. *Cell* 102, 147–159.

Vulpe, A., Mohapatra, P., and Menuz, K. (2021). Functional characterization of odor responses and gene expression changes in olfactory co-receptor mutants in *Drosophila*. *bioRxiv* [Preprint]. doi: 10.1101/2021.06.18.449017

Yan, H., Jafari, S., Pask, G., Zhou, X., Reinberg, D., and Desplan, C. (2020). Evolution, developmental expression and function of odorant

receptors in insects. *J. Exp. Biol.* 223:jeb208215. doi: 10.1242/jeb.208215

Yan, H., Opachaloemphan, C., Mancini, G., Yang, H., Gallitto, M., Mlejnek, J., et al. (2017). An Engineered *orco* Mutation Produces Aberrant Social Behavior and Defective Neural Development in Ants. *Cell* 170, 736–747.e9. doi: 10.1016/j.cell.2017.06.051

Younger, M. A., Herre, M., Ehrlich, A. R., Gong, Z., Gilbert, Z. N., Rahiel, S., et al. (2020). Non-canonical odor coding ensures unbreakable mosquito attraction to humans. *bioRxiv* [Preprint]. doi: 10.1101/2020.11.07.368720

Zhang, S. F., Zhang, Z., Kong, X. B., Wang, H. B., and Liu, F. (2017). Dynamic Changes in Chemosensory Gene Expression during the *Dendrolimus punctatus* Mating Process. *Front. Physiol.* 8:1127. doi: 10.3389/fphys.2017.01127

Zhou, S., Stone, E. A., Mackay, T. F., and Anholt, R. R. (2009). Plasticity of the chemoreceptor repertoire in *Drosophila melanogaster*. *PLoS Genet.* 5:e1000681. doi: 10.1371/journal.pgen.1000681

Conflict of Interest: The authors declare that the research was conducted in the absence of any commercial or financial relationships that could be construed as a potential conflict of interest.

frontiers in Neuroscience

REVIEW
published: 03 December 2021
doi: 10.3389/fnins.2021.771687

Induced Neurons From Germ Cells in *Caenorhabditis elegans*

Iris Marchal[1,2]* *and Baris Tursun*[1,2,3]*

[1] Berlin Institute for Medical Systems Biology, Berlin, Germany, [2] Max Delbrück Center for Molecular Medicine in the Helmholtz Association, Berlin, Germany, [3] Department of Biology, Institute of Zoology, University of Hamburg, Hamburg, Germany

Cell fate conversion by the forced overexpression of transcription factors (TFs) is a process known as reprogramming. It leads to de-differentiation or *trans*-differentiation of mature cells, which could then be used for regenerative medicine applications to replenish patients suffering from, e.g., neurodegenerative diseases, with healthy neurons. However, TF-induced reprogramming is often restricted due to cell fate safeguarding mechanisms, which require a better understanding to increase reprogramming efficiency and achieve higher fidelity. The germline of the nematode *Caenorhabditis elegans* has been a powerful model to investigate the impediments of generating neurons from germ cells by reprogramming. A number of conserved factors have been identified that act as a barrier for TF-induced direct reprogramming of germ cells to neurons. In this review, we will first summarize our current knowledge regarding cell fate safeguarding mechanisms in the germline. Then, we will focus on the molecular mechanisms underlying neuronal induction from germ cells upon TF-mediated reprogramming. We will shortly discuss the specific characteristics that might make germ cells especially fit to change cellular fate and become neurons. For future perspectives, we will look at the potential of *C. elegans* research in advancing our knowledge of the mechanisms that regulate cellular identity, and what implications this has for therapeutic approaches such as regenerative medicine.

Keywords: germline, neuron, reprogramming, epigenetics, chromatin, safeguarding, *C. elegans*

OPEN ACCESS

Edited by:
Filipe Pinto-Teixeira, Centre de Biologie Intégrative (CBI), France

Reviewed by:
Moritz Mall, German Cancer Research Center (DKFZ), Germany
Esteban Mazzoni, New York University, United States

***Correspondence:**
Iris Marchal
Iris.Marchal@mdc-berlin.de
Baris Tursun
Baris.Tursun@mdc-berlin.de

Specialty section:
This article was submitted to Neurogenesis, a section of the journal Frontiers in Neuroscience

Received: *06 September 2021*
Accepted: *08 November 2021*
Published: *03 December 2021*

Citation:
Marchal I and Tursun B (2021) Induced Neurons From Germ Cells in Caenorhabditis elegans. Front. Neurosci. 15:771687. doi: 10.3389/fnins.2021.771687

INTRODUCTION

Transcription Factor-Induced Reprogramming of Cell Fates

Forced overexpression of transcription factors (TFs) can induce reprogramming to dedifferentiate or *trans*-differentiate mature cells. Thereby, either induced pluripotent stem cells, or other specific types by direct conversion can be generated, respectively (Yamanaka, 2012; Wang et al., 2021). The prospect that reprogrammed cells could be used for tissue replacement therapies to repair diseased or injured tissues in patients demands for efficient reprogramming procedures. Yet, TF-induced reprogramming is often restricted and depends on the context of tissue types (Brumbaugh et al., 2019; Haridhasapavalan et al., 2020). As a consequence, TF expression that can induce ectopic fates in highly plastic cells, such as in early embryos, usually fail to reprogram mature cells in a complex adult multicellular organism (Yuzyuk et al., 2009; Tursun et al., 2012). The limitation of TFs to convert cell fates is caused by factors that safeguard cellular identity and prevent perturbations of their state. Understanding the molecular mechanisms that are involved

in cellular fate safeguarding provides insight into what defines cell types at the molecular level and illustrates which factors are crucial in the correct transition from one type to the other (Rothman and Jarriault, 2019). The germline of *C. elegans* helped identifying a number of evolutionarily conserved factors that act as barriers for TF-induced reprogramming of germ cells to neurons, which will be summarized in this review.

The *Caenorhabditis elegans* Germline: Specification, Proliferation and Differentiation

During *C. elegans* development, the germline is set apart from the soma by the 16–24 cell stage of embryogenesis (Sulston et al., 1983). At that stage, germline potential is appointed to the P blastomeres which ultimately give rise the first primordial germ cell (PGC) P4. By the time the nematode has reached the adult stage, PGC P4 has proliferated and given rise to an adult germline of over a thousand cells in the hermaphrodite (Hirsh et al., 1976). An adult *C. elegans* hermaphrodite germline consists of two gonadal arms, with each arm containing mitotic stem cells, meiotic cells, oocytes and sperm cells (**Figure 1**). The somatic distal tip cells (DTCs) are located at the distal most end of the adult gonad where they control germline mitosis and thereby provide the niche for adult germ line stem cells (GSC) (Byrd et al., 2014). As germ cells move away from the DTC and reach the transition zone, they enter and proceed through the different stages of meiotic prophase I (Hirsh et al., 1976). After the transition zone, cells move through the pachytene where they gradually grow until they enter the proximal arm as oocytes. As *C. elegans* is a hermaphrodite, oocyte maturation is triggered by sperm-derived major sperm protein (MSP) and happens to the oocyte closest to the spermatheca (Miller et al., 2001). Subsequently, the oocyte enters the spermatheca at ovulation and is then fertilized, giving rise to a whole new organism (McCarter et al., 1999).

SAFEGUARDING GERMLINE IDENTITY BY REPRESSING UNSOLICITED INDUCTION OF NEURONAL FATES

With its property of giving rise to meiotic cells, the *C. elegans* gonad provides a unique possibility to study molecular mechanisms that maintain totipotency and that protect the germ cell fate. The totipotency and immortality of the germline is protected by preventing differentiation toward somatic fates. This safeguarding is controlled at multiple levels from translational modifications to post-transcriptional regulation and through extensive chromatin regulation.

Safeguarding Germline Identity by Regulating Protein Translation

At the protein translation level, two conserved translational regulators, MEX-3 and GLD-1, are essential for maintaining totipotency. Ciosk et al. (2006) showed that in a *mex-3 gld-1* double mutant germ cells spontaneously differentiated into somatic cell types, including two types of muscle (pharynx and body), unspecific neurons and intestinal cells. The induction of the mixed somatic fates is accompanied by tissue type-specific characteristics. These include filaments and adhesive structures resembling those found in normal muscles, pan-neuronal *unc-119:GFP* reporter expression typical for neurons and auto-fluorescent granules similar to those of wild-type intestinal cells (Ciosk et al., 2006). The somatic differentiation as observed in the *mex-3 gld-1* double mutants is reminiscent of human germ cell tumors called teratomas consisting of mixed tissue types (Ciosk et al., 2006). Moreover, *mex-3 gld-1* double mutants show a significant reduction in size and number of germ cell-specific P-granules in the central regions of the germline. P-granules are specialized ribonucleoprotein structures and their reduction is likely to be a hallmark of germ cells that undergo differentiation toward somatic fates.

Safeguarding Germline Identity by P Granules

Interestingly, it was later shown that P granules provide another level of germline protection, as loss of P granules by itself may cause differentiation of germ cell into somatic lineages (Updike et al., 2014). Germline specific P-granules, also known as germline granules, are composed of two main classes of RNA-binding proteins belonging to the RGG domain-containing proteins: PGL-1 and PGL-2, and the DEAD-box proteins GLH1-4 (Jennifer and Wang, 2014; Strome and Updike, 2015). The role of P-granules in cell fate regulation was revealed when simultaneous depletion of PGL-1 and PGL3 in combination with GLH-1 and GLH-4 induced expression of the body wall muscle myosin (MYO-3) and the pan-neuronal reporters *unc-119:GFP* and *unc-33:GFP* (Updike et al., 2014). The GFP-expressing germ cells had extended neurite-like projections suggesting differentiation into specific neuronal subtypes. However, expression of neuronal markers that report terminally differentiated neurons was not observed. Interestingly, promoting the terminal differentiation of neurons toward the glutamatergic taste neuron identity through additional ectopic expression of the fate-inducing Zn-finger TF CHE-1 (Tursun et al., 2012) did result in the expression of the terminal ASE neuron fate marker *gcy-5:GFP* (Updike et al., 2014). Overall, these results show that P-granules act as a barrier for differentiation of germ cell to somatic cell types through their role in small RNA biogenesis and post-transcriptional regulation, thereby maintaining the totipotency of germ cells.

Preventing Unsolicited Induction of Neuronal Fates at the Epigenetic Level

Another level of protection of germline totipotency is located at the level of epigenetics. Suppression of the evolutionary conserved chromatin regulators SPR-5 and LET-418 (the worm homologs of Lysine-specific histone demethylase (LSD-1) and Mi2 respectively) causes *C. elegans* germ cells to display teratoma-like characteristics (Käser-Pébernard et al., 2014). Germ cells express pan-neuronal genes such as *unc-119*, obtain neuron-like projections or express muscle markers such as MYO-3 (myosin) in *spr-5 let-418* double mutants (Käser-Pébernard et al., 2014).

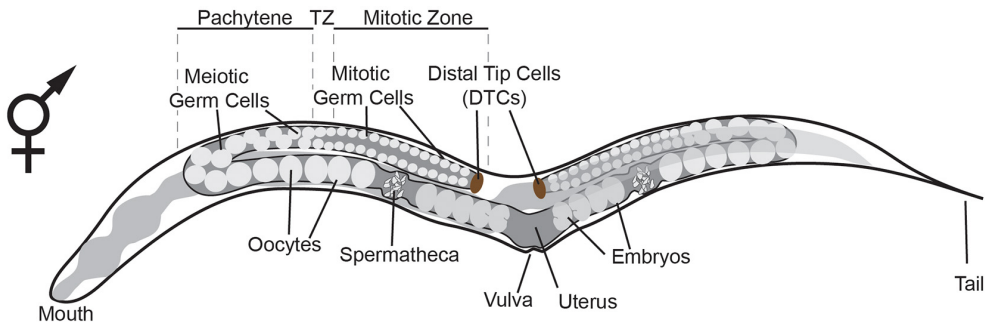

FIGURE 1 | Schematic representation of the adult hermaphrodite germline. The germline consists of two gonadal arms, with each arm containing mitotic germ cells, meiotic germ cells, oocytes and spermatheca. The somatic distal tip cells (DTCs) are located at the distal most end of the gonad where they control germline mitosis (Byrd et al., 2014). As germ cells move away from the DTC and reach the transition zone (TZ), they enter and proceed through meiosis. After the TZ, cells move through the pachytene where they grow until they enter the proximal arm as oocytes. Oocyte maturation is triggered by the spermatheca (Miller et al., 2001). The oocyte enters the spermatheca at ovulation and is fertilized giving rise to an embryo.

The demethylase SPR-5 interacts with LET-418 in two complexes, the nucleosome remodeling and deacetylase (NuRD) complex and the MEC complex. Hence, the absence of SPR-5 allows increased H3K4 methylation, indicating increased chromatin activation (Käser-Pébernard et al., 2014). Moreover, another study showed that knock-out of the H3K4 methyltransferase SET domain-containing 2 (SET-2) or its cofactor, WD-repeat 5.1 (WDR-5.1), also leads to expression of somatic markers in the germline and causes soma-like differentiation of germ cells (Robert et al., 2014). Again, this somatic differentiation was characterized by expression of neuronal genes such as *ceh-2* and *ceh-20* and muscle genes such as *unc-120*. These findings illustrate that loss of epigenetic regulators and altered chromatin regulation affect the epigenetic landscape of the germline and provide a permissive context for spontaneous germ cell transdifferentiation into somatic cell lineages (**Figure 2**).

OVERCOMING BARRIERS OF TRANSCRIPTION-FACTOR MEDIATED GERM-CELL-TO-NEURON REPROGRAMMING

The Histone Chaperone LIN-53 Prevents Transcription-Factor Mediated Germ-Cell-to-Neuron Reprogramming

Cellular transdifferentiation by the forced overexpression of cell-fate inducing TFs is limited due to cell fate safeguard mechanisms. As described above, these protective mechanisms often rely on epigenetic regulation. As a result, TFs that can induce ectopic fates in highly plastic cells such as developing embryos, usually fail to induce conversion of germ cells to somatic identities (Tursun et al., 2012). One factor that has been identified as a barrier for neuronal induction in germ cells is the histone chaperone LIN-53 (Harrison et al., 2006). LIN-53 prevents direct reprogramming of germ cells into ASE neurons upon heat-shock induced overexpression of the zinc finger TF CHE-1 (Tursun et al., 2012). While overexpression of CHE-1 alone in embryos resulted in the ectopic expression of the ASE fate marker *gcy-5:GFP* in most embryonic cells, broad CHE-1 mis-expression in adult worms allowed marker expression only in a small number of head sensory neurons but nowhere else in the animal.

RNAi mediated knock-down of *lin-53* in combination with CHE-1 overexpression in adult animals allowed induction of *gcy-5:GFP* in mitotic germ cells. The converted germ cells expressed markers for the pan-neuronal fate (e.g., *rab-3*, *unc-119*, *snb-1*, *unc-33* and *unc-10*) as well as for the specific neuron sub-type (*gcy-5*, *ceh-36* and *eat-4*), while expression of markers for other neuron sub-types were not observed. Moreover, the converted cells underwent drastic morphological changes adopting neuron-like nuclear morphology and growing axonal projections (Tursun et al., 2012). These morphological changes were accompanied by loss of P-granules and of PGL-1, illustrating a complete conversion of germ cells into neuron-like cells. *lin-53* removal also permitted conversion of germ cells into other neuron sub-types. Upon overexpression of the EBF-like TF UNC-3 or the Pitx type homeodomain TF UNC-30 germ cells were converted to cholinergic or GABAergic motor neurons respectively. Like CHE-1 induction, UNC-3 or UNC-30 induction resulted in germ cells losing their characteristic morphology, adopting neuron-like morphology and growing axonal projections. Interestingly, converted germ cells displayed neuronal identity markers that are corresponding to the specific fate that is induced by the overexpressed TF. For example, in the case of UNC-3 induced reprogramming converted cells only express a marker for cholinergic ventral cord motor neurons (*acr-2*) but none of the ASE neuronal fate markers. These observations indicate that this conversion is different from undirected differentiation of germ cells into mixed somatic cell types as observed during teratoma formation. Instead, the TF-induced conversion upon depletion of LIN-53 is specific and directed toward distinct neuron sub-types depending on the overexpressed TF. Notably, although the mis-expression of the cell fate inducing TFs (CHE-1, UNC-3 and UNC-30) and the RNAi mediated depletion of *lin-53* were both in the entire adult body, neuronal induction occurs in the germline only. Hence, removal of LIN-53 allows direct conversion into

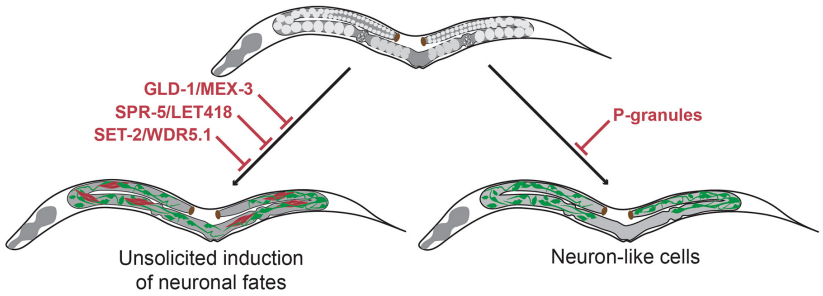

FIGURE 2 | Molecular mechanisms that maintain germline totipotency and prevent unsolicited induction of somatic fates. Upon loss of the translational regulators GLD-1 and MEX-3 germ cells spontaneously differentiate to somatic cells thereby forming germline teratomas that contain multiple cell types at once including neurons (Ciosk et al., 2006). Loss of the chromatin regulators SPR-5/LET-418 (Käser-Pébernard et al., 2014) and SET-2/WDR-5.1 (Robert et al., 2014) also result in germline teratomas. Loss of germline P-granules leads to differentiation of germ cells to neuron-like cells, which do no acquire characteristics of terminally differentiated neurons (Updike et al., 2014). Green cells indicate neuron-like cells, red cells indicate muscle-like cells.

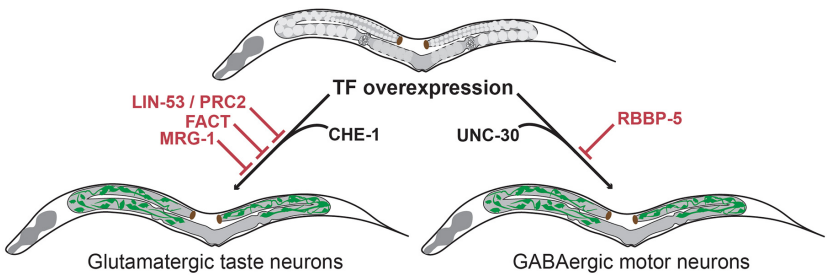

FIGURE 3 | Transcription factor-induced germ cell reprogramming to neuronal fates. The histone chaperone LIN-53 prevents reprogramming of germ cells into glutamatergic taste neurons (known as ASE) upon overexpression of the Zn-finger TF CHE-1 (Tursun et al., 2012). LIN-53 cooperates with the Poly Comb Repressive Complex 2 (PRC2) to prevent neuronal induction in the germline (Patel et al., 2012). The heterodimeric histone chaperone FACT (Kolundzic et al., 2018) and the chromodomain protein MRG-1 block germ cell conversion to glutamatergic neurons (Hajduskova et al., 2019). The methyltransferase complex member RBBP-5 blocks germ cell reprogramming to GABAergic neurons upon UNC-30 TF-induction (Kazmierczak et al., 2020).

distinct neuronal subtypes in what seems to be a germline-specific manner (**Figure 3**).

Interestingly, the CAF-1 histone chaperone complex (containing the mouse ortholog of LIN-53) was later identified as a strong cellular safeguard of somatic cell identity during reprogramming to neurons and induced pluripotent stem cells (iPSCs) (Cheloufi and Hochedlinger, 2017), indicating that the role of LIN-53 as a reprogramming barrier is conserved.

LIN-53 Cooperates With PRC2 to Prevent Neuronal Induction in the Germline

LIN-53 is a component of many distinct multiprotein complexes (e.g., NuRD, CAF, HAT1 and PRC2 complex) (Loyola and Almouzni, 2004; Harrison et al., 2006) with various functions in chromatin biology. Further study showed that the effect of *lin-53* depletion in germ-cell-to-neuron reprogramming is phenocopied by the removal of other components of the Polycomb repressive complex 2 (PRC2) (Patel et al., 2012; **Figure 3**). PRC2 is a highly conserved epigenetic regulator that represses chromatin through the deposition of H3K27 di- and trimethylation marks, which are associated with developmentally regulated genes (Kelly and Fire, 1998; Xu et al., 2001). This observation suggests that PRC2 defines a chromatin state that protect the genome from aberrant regulatory inputs. Disruption of this chromatin state in germ cells renders them susceptible to direct reprogramming into neurons. Interestingly, this protective chromatin state may differ among cell types as the loss of PRC2 only allows induction of neuronal and muscle fate in germ cells, but no other somatic cell types (Patel et al., 2012).

The Methyltransferase Complex Member RBBP-5 Blocks Transcription Factor-Induced Conversion of Germ Cells to GABAergic Neurons

The methyltransferase complex member RBBP-5 was recently identified as a novel germ cell reprogramming barrier in a screen to identify factors that increase LIN-53 depletion mediated reprogramming efficiency into GABAergic neurons (Kazmierczak et al., 2020). Although LIN-53 depletion alone allows germ cell to GABAergic neuron reprogramming upon UNC-30 overexpression, the conversion efficiency is rather limited when compared to conversion to glutamatergic ASE neurons upon CHE-1 overexpression. To test whether GABAergic neuron induction could be enhanced, additional chromatin regulators were tested in co-depletion with LIN-53. This led to the identification of RBBP-5 as a novel reprogramming barrier that blocks conversion of germ cells specifically into GABAergic neurons (**Figure 3**).

The mechanisms by which RBBP-5 operates as a barrier to reprogramming remains to be determined. However, these results illustrate the high specificity of the molecular programs that define cellular sates and antagonize the induction of neuronal cell fates.

The FACT Complex Member HMG-3 Is a Conserved Reprogramming Barrier in the Germline

To reveal other factors that are barriers to neuronal reprogramming in *C. elegans*, Kolundzic et al. (2018) performed a whole-genome RNAi screen using overexpression of the fate inducing TF CHE-1 and identified around 119 target genes that allow ectopic *gcy-5:GFP* induction in the germline upon depletion (out of 171 total targets identified as reprogramming barriers, other tissues tested were intestine, muscle and epidermis). These factors are implicated in a number of biological processes such as proteostasis, cell shape, mitochondrial function, aging and nuclear factors (Kolundzic et al., 2018).

Among the candidates identified as barriers to neuronal reprogramming were the three subunits of the histone chaperone FACT (Facilitates Chromatin Transcription) namely HMG-3, HMG-4 and SPT-16 (Kolundzic et al., 2018). The study showed that FACT has two tissue-specific isoforms in *C. elegans*. HMG-3 is exclusively expressed in the germline, where it forms a complex with the ubiquitously expressed SPT-16. In contrast, HMG-4 is predominantly expressed in the soma and thereby forms the somatic isoform of FACT together with SPT-16.

As a result, RNAi-mediated depletion of *hmg-4* and *spt-16* allowed partial intestine-to neuron reprogramming, whereas depletion of *hmg-3* allows germ-cell-to-neuron conversion. Interestingly, single-molecule fluorescence *in situ* hybridization (smFISH) revealed that intestinal cells switch to a stable neuron-like gene expression profile upon *hmg-4* and *spt-16* depletion-mediated reprogramming. However, the converted cells do not obtain a neuron-like morphology. Yet, depletion of *hmg-3* allows extended conversion into neurons as illustrated by changes in nuclear morphology and the expression of multiple pan-neuronal and neuron-specific reporter genes (pan-neuronal: *rab-3*, *unc-119*; ciliated neurons: *ift-20*, ASE-expressed neuronal genes (*gcy-5*, *ceh-36*, *rab-3*, *unc-10*, and *unc-119*). Notably, depletion of germline-specific FACT without CHE-1 induction led to an impairment of cell fate maintenance of the germline. Depletion of *hmg-3* decreased the expression of germ-cell specific markers such as PIE-1, and P-Granule levels indicating that the permissiveness for germ cell to neuron reprogramming upon *hmg-3* RNAi is created by weakening the starting cell fate.

The same study also demonstrated that FACT's function as a reprogramming barrier is conserved, as siRNA mediated depletion of the human FACT homologs SSRP1 and SUPTH16 enhanced reprogramming efficiency of human fibroblasts into iPSCs and induced neurons (Kolundzic et al., 2018). Chromatin and transcriptome analysis upon FACT knockdown revealed a general decrease in expression of factors previously described as reprogramming inhibitors such as CAF-1 (Cheloufi and Hochedlinger, 2017) and an increase in reprogramming promoting factors such as SALL4 (Buganim et al., 2013). Taken together, FACT is an evolutionary conserved reprogramming barrier that safeguards cellular identity by maintaining appropriate gene expression profiles (**Figure 3**).

The Chromodomain Protein MRG-1 Blocks Transcription Factor Mediated Neuronal Induction in Germ Cells

MRG-1 is a component of the NuA4 histone acetyl transferase complex and is orthologous to the mammalian chromodomain-containing MRG15 (Chen et al., 2009). It has been shown to regulate the proliferation and differentiation of *C. elegans* germ cells during development (Fujita et al., 2002; Gupta et al., 2015). MRG-1 was recently identified as another novel factor that counteracts germ cell reprogramming into neurons upon neuron-fate inducing TF overexpression (Hajduskova et al., 2019). RNAi mediated depletion of *mrg-1* in combination with CHE-1 expression allowed germ-cell-to neuron conversion. As described before for LIN-53 and FACT, the converted neurons obtained molecular and morphological characteristics resembling the specific neuronal fate. Neuronal expression was confirmed by both transgenic reporter expression and smFISH. Moreover, the reprogrammed germ cells lost their P-granules and PIE-1 expression indicating a faithful conversion of germ cells into neurons.

The function of MRG-1 as a reprogramming barrier in the germline is independent from that of LIN-53 and PRC2. Whereas depletion of *lin-53* and other members of the PRC2 complex leads to global loss of H3K27me3, there were no changes in this chromatin mark observed in *mrg-1*-depleted animals. In fact, ChIP-seq analysis of MRG-1 showed very limited colocalization with LIN-53 and instead showed that it primarily binds loci that carry the active chromatin marks H3K36me3, H3K9ac and H3K4me3 (Hajduskova et al., 2019). This finding suggests that MRG-1 might protect the germline from converting into neurons by maintaining the expression of germline-specific genes (**Figure 3**).

Interestingly, immunoprecipitation of MRG-1 followed by mass-spectrometry (IP-MS) identified SIN-3, SET-26 and OGT-1 as novel interacting partners. This finding indicates that MRG-1 might also be involved in repressive chromatin regulating complexes. Since these interaction partners all mediate chromatin regulation, they might contribute to MRG-1's function as cellular safeguard of the germline. Indeed, *sin-3*, *set-26* and *ogt-1* mutants increase reprogramming efficiency upon *mrg-1* depletion, indicating that these factors cooperate with MRG-1 in preventing neuronal induction in the germline (Hajduskova et al., 2019). Overall, MRG-1 seems to act as a safeguard of active chromatin signature to maintain germ cell identity—at the same time it cooperates with repressive chromatin regulators to prevent ectopic gene expression.

A more recent study performing in-depth CoIP-MS additionally detected a strong interaction of MRG-1 with the Small Ubiquitin-like Modifier (SUMO) (Baytek et al., 2021). It was shown that MRG-1 is post-translationally modified by SUMO, and that this modification affects the chromatin binding

profile of MRG-1. SUMO has been implicated in stabilizing cell identity in the context of reprogramming somatic cells to iPSCs (Cossec et al., 2018). Moreover, SUMOylation of the TF Gatad2a, a component of the nucleosome remodeling and deacetylase (NuRD) complex, disrupts the assembly and stability of NuRD thereby inhibiting iPSCs formation (Mor et al., 2018). However, it is not yet known whether this extra layer of regulation through the SUMOylation of MRG-1 has an effect on its function as a barrier of germ cell to neuron reprogramming.

Mammalian Germ Cell to Neuron Reprogramming

Recent studies in mammals have investigated the use of germline stem cells (GSCs) as a potential source of neuronal tissues for clinical therapy (Chen et al., 2020). For example, it was shown that functional neurons and glia cells can be generated from adult mouse spermatogonial stem cells (SSCs) (Glaser et al., 2008; Streckfuss-Bömeke et al., 2009). Established protocols for neural differentiation of murine embryonic stem cells (ESCs) using fibroblast growth factor (FGF) and sonic hedgehoc (shh) expression as initiation for differentiation were adapted to differentiate GSCs into neurons and glia cells (Glaser et al., 2008; Streckfuss-Bömeke et al., 2009). The GSC-derived neuron populations contain specific subtypes (including GABAergic, glutamatergic and dopaminergic) and show membrane potential properties and postsynaptic currents resembling fully functional matured neurons *in vitro* (Glaser et al., 2008; Streckfuss-Bömeke et al., 2009).

More recently, Yang et al. (2019) generated functional dopaminergic (DA) neurons from human spermatogonial stem cells (hSSCs). To convert hSSCs to neurons they were exposed to olfactory ensheathing cell conditioned culture medium (OECCM) containing FGF and shh and additional small molecules such as forskolin, valproic acid and SB431542 (Yang et al., 2019). The exposure to these small molecules has previously been used to differentiate mouse embryonic fibroblasts (MEFs) to neural crest like precursors (Takayama et al., 2017) and was shown to be of critical importance to achieve hSSCs to DA neuron conversion (Yang et al., 2019). SSC-derived DA neurons obtained gene-expression profiles similar to wild type DA neurons and acquired neuronal morphological features. Moreover, they obtained sophisticated functional properties typical for DA neurons including synapse formation, dopamine release, spontaneous action potentials and neuron-specific calcium flux. When the SSC-derived DA neurons were implanted in the striatum of a mouse model of Parkinson disease (PD) they survived, migrated, and further converted into DA neurons without causing tumor formation. Strikingly, transplantation of the SSC-derived DA neurons into the PD mouse model improved sensorimotor function (Yang et al., 2019). This observation supports the therapeutic potential of germline-derived neurons in treating neurogenerative diseases.

Generally, clinical application of GSCs is beneficial when compared to embryonic stem cells as it bypasses ethical concerns, risk of teratoma formation and immune rejection (Yamanaka, 2020). Studies in mammalian systems illustrates the relevance of fundamental research into cellular reprogramming in *C. elegans,* as mechanisms are conserved and analogous across species and findings can provide new avenues for future regenerative medicine applications.

FUTURE PERSPECTIVES

In this review, we have discussed our current knowledge regarding cell fate safeguard mechanisms and the molecular mechanisms underlying TF-mediated reprogramming of *C. elegans* germ cells into neurons. Detailed molecular and morphological analyses have shown an ability to reprogramming germ cells into multiple specific neuronal subtypes upon depletion of reprogramming barriers. The studies described here, mainly focus on factors involved in chromatin regulation. At the level of chromatin regulation, numerous factors have been identified as reprogramming barriers that seem to act in separate pathways. This indicates the multiple independent levels of protection of cells to safeguard their identities. Moreover, the whole-genome RNAi screen by which FACT was identified as a cellular safeguard revealed other candidates implicated in multiple biological processes such as proteostasis, cell shape, mitochondrial function, and aging (Kolundzic et al., 2018). It will be fascinating to reveal the molecular mechanisms by which these factors regulate cell fate and whether their role in blocking reprogramming into neurons is evolutionary conserved. Also, better understanding the molecular mechanisms of cell fate protection and reprogramming blocking may explain why some barriers appear to be tissue or context-specific. It is important to determine which barrier factors are expressed in which cell types—and importantly—at which transcript and protein levels. The levels and availability of required partnering factors may also vary in different tissues. It is conceivable that varying expression levels in different cell types and availability of required complex members (for LIN-53 e.g., subunits of PRC2, NuRD, CAF, or SIN3) (Loyola and Almouzni, 2004; Harrison et al., 2006) may influence the strength of a factor as a reprogramming barrier. Future studies in combination with single-cell transcriptome and genome analyses will provide more insight to which degree safeguarding factors and barriers are restricted to protecting certain tissue types at the functional level or simply due to limited availability.

As shown by the depletion of the FACT complex members *hmg-4* and *spt-16*, stable changes in gene expression profiles toward the new fate is not always sufficient to obtain fully induced neurons to an extent where they possess neuron-like morphology. Interestingly, germ cell reprogramming does not seem to suffer from this issue. Additionally, most reprogramming barriers are expressed in multiple tissues and their depletion in combination with fate-inducing TF expression was performed in the whole organism. However, primarily germ cells appear to be the tissue that allows full neuronal induction. This raises the question whether reprogramming mechanisms differ between cell types, and whether germ cells possess any cell type-specific characteristics that make them particularly suited to change cellular fate.

One aspect that influences reprogramming with regard to final identity, specifically toward neurons, might be the very specific morphology changes needed. For example, some tissues, like the intestine, might be unfit for full conversion because of structural constraints. Moreover, we could speculate that the initial function of the germline could influence the ability to reprogram. The unique feature of totipotency in the germline might provide protection strategies that are distinct from somatic tissues, which need to maintain a specific differentiated state. Alternatively, the intrinsic cellular context, mode of metabolism, and the micro- and macro-environment of the starting cell type might make specific cell types particularly amenable for reprogramming (Rothman and Jarriault, 2019; Lambert et al., 2021).

So far, studying the extend of reprogramming of induced neurons from germ cells has mainly focused on molecular and morphological features. Future analyses could be extended with functional assays such as electrophysiology to study whether they are capable of action potentials and network formation. Moreover, recent technological advancements at the single cell level (such as transcriptome and chromatin accessibility analyses) will allow us to study direct reprogramming more dynamically. Applying single cell technologies such as scRNA-seq and scATAC-seq for *C. elegans* will advance our knowledge of germline totipotency and mechanisms of germ cell safeguarding. Understanding these mechanisms will also improve techniques for generating neuronal tissues for clinical applications and might shed light on why some germ cells are well suited to become neurons while other cell types are not.

AUTHOR CONTRIBUTIONS

IM conceptualized and wrote the manuscript together with BT. BT helped to conceptualize the manuscript, advised and supported the manuscript writing. Both authors contributed to the article and approved the submitted version.

FUNDING

This work was supported by the Max Delbrück Center for Molecular Medicine in the Helmholtz Association.

ACKNOWLEDGMENTS

We would like to thank the members of the Tursun lab for critical reading.

REFERENCES

Baytek, G., Blume, A., Demirel, F. G., and Bulut, S. (2021). SUMOylation of the chromodomain factor MRG-1 in C . Elegans affects chromatin-regulatory dynamics. *bioRxiv*[Preprint] 1–21. doi: 10.1101/2021.02.14.431134

Brumbaugh, J., Di Stefano, B., and Hochedlinger, K. (2019). Reprogramming: identifying the mechanisms that safeguard cell identity. *Development* 146:23.

Buganim, Y., Faddah, D. A., and Jaenisch, R. (2013). Mechanisms and models of somatic cell reprogramming. *Nat. Rev. Genet.* 14, 427–439.

Byrd, D. T., Knobel, K., Affeldt, K., Crittenden, S. L., and Kimble, J. (2014). A DTC niche plexus surrounds the germline stem cell pool in *Caenorhabditis elegans*. *PLoS One* 9:e88372. doi: 10.1371/journal.pone.0088372

Cheloufi, S., and Hochedlinger, K. (2017). Emerging roles of the histone chaperone CAF-1 in cellular plasticity. *Curr. Opin. Genet. Dev.* 46, 83–94. doi: 10.1016/j.gde.2017.06.004

Chen, T. K., Tkano-Maruyama, M., Pereira-Smith, O. M., and Gaufo, G. O. (2009). MRG15, a component of HAT and HDAC complexes, is essential for proliferation and differentiation of neural precursor cells. *J. Neurosci. Res.* 87, 1522–1531. doi: 10.1002/jnr.21976

Chen, Z., Hong, F., Wang, Z., Hao, D., and Yang, H. (2020). Spermatogonial stem cells are a promising and pluripotent cell source for regenerative medicine. *Am. J. Transl. Res.* 12, 7048–7059.

Ciosk, R., DePalma, M., and Priess, J. R. (2006). Translational regulators maintain totipotency in the *Caenorhabditis elegans* germline. *Science* 311, 851–853. doi: 10.1126/science.1122491

Cossec, J. C., Theurillat, I., Chica, C., Búa Aguín, S., Gaume, X., Andrieux, A., et al. (2018). SUMO safeguards somatic and pluripotent cell identities by enforcing distinct chromatin states. *Cell Stem Cell* 23, 742–757. doi: 10.1016/j.stem.2018.10.001

Fujita, M., Takasaki, T., Nakajima, N., Kawano, T., Shimura, Y., and Sakamoto, H. (2002). MRG-1, a mortality factor-related chromodomain protein, is required maternally for primordial germ cells to initiate mitotic proliferation in C. elegans. *Mech. Dev.* 114, 61–69. doi: 10.1016/s0925-4773(02)00058-8

Glaser, T., Opitz, T., Kischlat, T., Konang, R., Sasse, P., Fleischmann, B. K., et al. (2008). Adult germ line stem cells as a source of functional neurons and glia. *Stem Cells* 26, 2434–2443.

Gupta, P., Leahul, L., Wang, X., Wang, C., Bakos, B., Jasper, K., et al. (2015). Proteasome regulation of the chromodomain protein MRG-1 controls the balance between proliferative fate and differentiation in the C. elegans germ line. *Development* 142, 291–302. doi: 10.1242/dev.115147

Hajduskova, M., Baytek, G., Kolundzic, E., Gosdschan, A., Kazmierczak, M., Ofenbauer, A., et al. (2019). MRG-1/MRG15 is a barrier for germ cell to neuron reprogramming in *Caenorhabditis elegans*. *Genetics* 211, 121–139. doi: 10.1534/genetics.118.301674

Haridhasapavalan, K. K., Raina, K., Dey, C., Adhikari, P., and Thummer, R. P. (2020). An insight into reprogramming barriers to iPSC Generation. *Stem Cell Rev. Rep.* 16, 56–81. doi: 10.1007/s12015-019-09931-1

Harrison, M. M., Ceol, C. J., Lu, X., and Horvitz, H. R. (2006). Some *C. elegans* class B synthetic multivulva proteins encode a conserved LIN-35 Rb-containing complex distinct from a NuRD-like complex. *Proc. Natl. Acad. Sci. U.S.A.* 103, 16782–16787. doi: 10.1073/pnas.0608461103

Hirsh, D., Oppenheim, D., and Klass, M. (1976). Development of the reproductive system of *Caenorhabditis elegans*. *Dev. Biol.* 49, 200–219. doi: 10.1016/0012-1606(76)90267-0

Jennifer, G. S., and Wang, T. (2014). P granules. *Curr. Biol.* 24, 637–638.

Käser-Pébernard, S., Müller, F., and Wicky, C. (2014). LET-418/Mi2 and SPR-5/LSD1 cooperatively prevent somatic reprogramming of *C. elegans* germline stem cells. *Stem Cell Rep.* 2, 547–559. doi: 10.1016/j.stemcr.2014.02.007

Kazmierczak, M., Farré, C., Díaz, I., Ofenbauer, A., and Tursun, B. (2020). The CONDOR pipeline for simultaneous knockdown of multiple genes identifies RBBP-5 as a germ cell reprogramming barrier in C. elegans. *bioRxiv*[Preprint] doi: 10.1101/2020.09.01.276972

Kelly, W. G., and Fire, A. (1998). Chromatin silencing and the maintenance of a functional germline in *Caenorhabditis elegans*. *Development* 125, 2451–2456. doi: 10.1242/dev.125.13.2451

Kolundzic, E., Ofenbauer, A., Bulut, S. I., Uyar, B., Baytek, G., Sommermeier, A., et al. (2018). FACT Sets a barrier for cell fate reprogramming in *Caenorhabditis elegans* and human cells. *Dev. Cell* 46, 611–626.e12. doi: 10.1016/j.devcel.2018.07.006

Lambert, J., Lloret-Fernández, C., Laplane, L., Poole, R. J., and Jarriault, S. (2021). On the origins and conceptual frameworks of natural plasticity—Lessons from single-cell models in *C. elegans*. *Curr. Top. Dev. Biol.* 144, 111–159. doi: 10.1016/bs.ctdb.2021.03.004

Loyola, A., and Almouzni, G. (2004). Histone chaperones, a supporting role in the limelight. *Biochim. Biophys. Acta Gene Struct. Expr.* 1677, 3–11. doi: 10.1016/j.bbaexp.2003.09.012

McCarter, J., Bartlett, B., Dang, T., and Schedl, T. (1999). On the control of oocyte meiotic maturation and ovulation in *Caenorhabditis elegans*. *Dev. Biol.* 205, 111–128. doi: 10.1006/dbio.1998.9109

Miller, M. A., Nguyen, V. Q., Lee, M. H., Kosinski, M., Schedl, T., Caprioli, R. M., et al. (2001). A sperm cytoskeletal protein that signals oocyte meiotic maturation and ovulation. *Science* 291, 2144–2147. doi: 10.1126/science.1057586

Mor, N., Rais, Y., Sheban, D., Peles, S., Aguilera-Castrejon, A., Zviran, A., et al. (2018). Neutralizing Gatad2a-Chd4-Mbd3/NuRD complex facilitates deterministic induction of naive pluripotency. *Cell Stem Cell* 23, 412–425. doi: 10.1016/j.stem.2018.07.004

Patel, T., Tursun, B., Rahe, D. P., and Hobert, O. (2012). Removal of polycomb repressive complex 2 makes *C. elegans* germ cells susceptible to direct conversion into specific somatic cell types. *Cell Rep.* 2, 1178–1186. doi: 10.1016/j.celrep.2012.09.020

Robert, V. J., Mercier, M. G., Bedet, C., Janczarski, S., Merlet, J., Garvis, S., et al. (2014). The SET-2/SET1 histone H3K4 methyltransferase maintains pluripotency in the *Caenorhabditis elegans* germline. *Cell Rep.* 9, 443–450. doi: 10.1016/j.celrep.2014.09.018

Rothman, J., and Jarriault, S. (2019). Developmental plasticity and cellular reprogramming in *Caenorhabditis elegans*. *Genetics* 213, 723–757. doi: 10.1534/genetics.119.302333

Streckfuss-Bömeke, K., Vlasov, A., Hülsmann, S., Yin, D., Nayernia, K., Engel, W., et al. (2009). Generation of functional neurons and glia from multipotent adult mouse germ-line stem cells. *Stem Cell Res.* 2, 139–154. doi: 10.1016/j.scr.2008.09.001

Strome, S., and Updike, D. (2015). Specifying and protecting germ cell fate. *Nat. Rev. Mol. Cell Biol.* 16, 406–416. doi: 10.1038/nrm4009

Sulston, J. E., Schierenberg, E., White, J. G., and Thomson, J. N. (1983). The embryonic cell lineage of the nematode *Caenorhabditis elegans*. *Dev. Biol.* 100, 64–119. doi: 10.1016/0012-1606(83)90201-4

Takayama, Y., Wakabayashi, T., Kushige, H., Saito, Y., Shibuya, Y., Shibata, S., et al. (2017). Brief exposure to small molecules allows induction of mouse embryonic fibroblasts into neural crest-like precursors. *FEBS Lett.* 591, 590–602. doi: 10.1002/1873-3468.12572

Tursun, B., Patel, T., Kratsios, P., and Hobert, O. (2012). Direct conversion of *C. elegans* germ cells into specific neuron types. *Science* 331, 304–308. doi: 10.1126/science.1199082

Updike, D. L., Knutson, A. K. A., Egelhofer, T. A., Campbell, A. C., and Strome, S. (2014). Germ-granule components prevent somatic development in the *C. elegans* germline. *Curr. Biol.* 24, 970–975. doi: 10.1016/j.cub.2014.03.015

Wang, H., Yang, Y., Liu, J., and Qian, L. (2021). Direct cell reprogramming: approaches, mechanisms and progress. *Nat. Rev. Mol. Cell Biol.* 22, 410–424. doi: 10.1038/s41580-021-00335-z

Xu, L., Fong, Y., and Strome, S. (2001). The *Caenorhabditis elegans* maternal-effect sterile proteins, MES-2, MES-3, and MES-6, are associated in a complex in embryos. *Proc. Natl. Acad. Sci. U.S.A.* 98, 5061–5066. doi: 10.1073/pnas.081016198

Yamanaka, S. (2012). Induced pluripotent stem cells: past, present, and future. *Cell Stem Cell* 10, 678–684. doi: 10.1016/j.stem.2012.05.005

Yamanaka, S. (2020). Pluripotent stem cell-based cell therapy—promise and challenges. *Cell Stem Cell* 27, 523–531. doi: 10.1016/j.stem.2020.09.014

Yang, H., Hao, D., Liu, C., Huang, D., Chen, B., Fan, H., et al. (2019). Generation of functional dopaminergic neurons from human spermatogonial stem cells to rescue parkinsonian phenotypes. *Stem Cell Res. Ther.* 10, 1–19. doi: 10.1186/s13287-019-1294-x

Yuzyuk, T., Fakhouri, T. H. I., Kiefer, J., and Mango, S. E. (2009). The polycomb complex protein mes-2/E(z) promotes the transition from developmental plasticity to differentiation in *C. elegans* embryos. *Dev. Cell* 16, 699–710. doi: 10.1016/j.devcel.2009.03.008

Conflict of Interest: The authors declare that the research was conducted in the absence of any commercial or financial relationships that could be construed as a potential conflict of interest.

Publisher's Note: All claims expressed in this article are solely those of the authors and do not necessarily represent those of their affiliated organizations, or those of the publisher, the editors and the reviewers. Any product that may be evaluated in this article, or claim that may be made by its manufacturer, is not guaranteed or endorsed by the publisher.

frontiers in Neuroscience

BRIEF RESEARCH REPORT
published: 17 December 2021
doi: 10.3389/fnins.2021.784649

Ebf Activates Expression of a Cholinergic Locus in a Multipolar Motor Ganglion Interneuron Subtype in *Ciona*

*Sydney Popsuj and Alberto Stolfi**

School of Biological Sciences, Georgia Institute of Technology, Atlanta, GA, United States

Conserved transcription factors termed "terminal selectors" regulate neuronal subtype specification and differentiation through combinatorial transcriptional regulation of terminal differentiation genes. The unique combinations of terminal differentiation gene products in turn contribute to the functional identities of each neuron. One well-characterized terminal selector is COE (Collier/Olf/Ebf), which has been shown to activate cholinergic gene batteries in *C. elegans* motor neurons. However, its functions in other metazoans, particularly chordates, is less clear. Here we show that the sole COE ortholog in the non-vertebrate chordate *Ciona robusta*, Ebf, controls the expression of the cholinergic locus *VAChT/ChAT* in a single dorsal interneuron of the larval Motor Ganglion, which is presumed to be homologous to the vertebrate spinal cord. We propose that, while the function of Ebf as a regulator of cholinergic neuron identity conserved across bilaterians, its exact role may have diverged in different cholinergic neuron subtypes (e.g., interneurons vs. motor neurons) in chordate-specific motor circuits.

Keywords: Ebf, COE, cholinergic, *Ciona*, tunicates, motor ganglion, acetylcholine

OPEN ACCESS

Edited by:
Luisa Cochella,
Research Institute of Molecular Pathology (IMP), Austria

Reviewed by:
Takehiro Kusakabe,
Konan University, Japan
Paschalis Kratsios,
University of Chicago, United States

***Correspondence:**
Alberto Stolfi
alberto.stolfi@biosci.gatech.edu

Specialty section:
This article was submitted to Neurogenesis, a section of the journal Frontiers in Neuroscience

Received: *28 September 2021*
Accepted: *30 November 2021*
Published: *17 December 2021*

Citation:
Popsuj S and Stolfi A (2021) Ebf Activates Expression of a Cholinergic Locus in a Multipolar Motor Ganglion Interneuron Subtype in Ciona. Front. Neurosci. 15:784649. doi: 10.3389/fnins.2021.784649

INTRODUCTION

The myriad functions of nervous systems are made possible by the rich functional diversity of neuronal types and subtypes that are generated and connected to one another. Each terminally differentiated neuron in a neural circuit differs in their morphological, biochemical, and electrical properties. These properties in turn are often defined by coordinated gene expression changes regulated by transcription factors termed "terminal selectors" (Etchberger et al., 2007; Allan and Thor, 2015; Hobert and Kratsios, 2019). Terminal selectors can act alone or in combination to regulate the transcription of genes encoding rate-limiting effectors of terminal differentiation features. However, transcription factors that act as terminal selectors in one context might not function as such in other contexts.

Many terminal selectors have been shown to be evolutionarily conserved throughout animals, like Pou4/Brn3-family homeodomain factors expressed in various bilaterian and cnidarian neuron

types (Finney et al., 1988; Eng et al., 2007; Serrano-Saiz et al., 2013, 2018; Zhang et al., 2014; Tournière et al., 2020). Another example comes from the COE (Collier/Olf/Ebf) family of transcription factors. A COE ortholog, UNC-3 in *C. elegans,* was shown to initiate and maintain the transcription of cholinergic genes, encoding essential components required for synthesis, transport, and reuptake of the major neurotransmitter acetylcholine (Kratsios et al., 2012) in motor neurons. Similarly, UNC-3 was found to control cholinergic gene expression in premotor interneurons as well, suggesting a broader function in regulating the development of cholinergic neurotransmission (Pereira et al., 2015). The COE ortholog Ebf was also found to be important for cholinergic motor neuron development in the invertebrate chordate *Ciona,* suggesting its role as a cholinergic motor neuron terminal selector is conserved from nematodes to chordates (Kratsios et al., 2012). However, subsequent studies on COE orthologs in vertebrates found a more nuanced role in motor neuron differentiation: different *EBF* paralogs are expressed in distinct spinal cord motor neurons innervating different axial muscles in mouse (Catela et al., 2019). Furthermore, Ebf2 is required for differentiation of a subset of motor neurons innervating epaxial (back) muscles, but not for their expression of cholinergic genes like *Vesicular acetylcholine transporter (VAChT)* (Catela et al., 2019). Thus, the regulation of cholinergic gene expression in vertebrate motor neurons may have shifted away from Ebf to another transcription factor, Islet (Cho et al., 2014; Catela et al., 2019).

Given the emerging differences between cholinergic gene regulation in vertebrate and invertebrate motor neurons, we decided to further investigate the role of Ebf in the regulation of cholinergic neuron identity in *Ciona.* With recent advances in tissue-specific CRISPR/Cas9-mediated mutagenesis (Stolfi et al., 2014) and the mapping of the *Ciona* larval connectome (Ryan et al., 2016), we were able to expand on this work with greater resolution than before. Based on these new tools and insights, we show here that Ebf activates cholinergic gene expression in a single neuron in the dorsal motor ganglion (MG) identified by the connectome as the Ascending Motor Ganglion Neuron 5 (AMG5) (Ryan et al., 2018; Kourakis et al., 2019). Although AMG5 is a cholinergic neuron situated in the major motor control center of the larva, it does not synapse directly onto muscles but rather onto other neurons of the MG, including

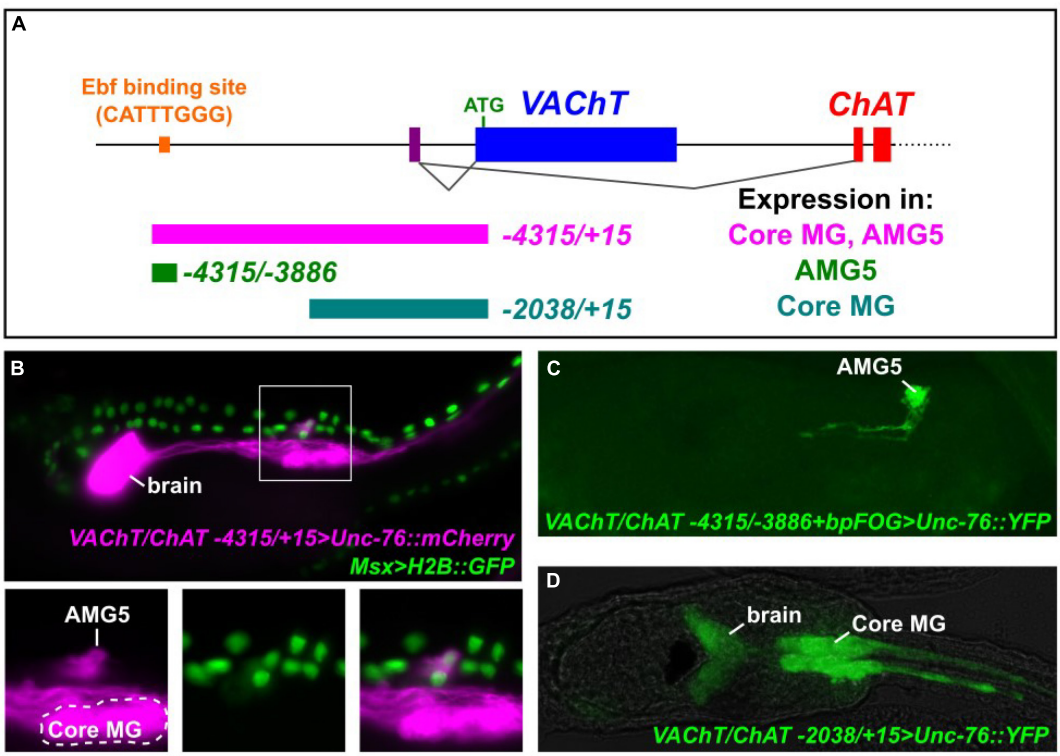

FIGURE 1 | Expression of *VAChT/ChAT* cholinergic locus in the AMG5 neuron. **(A)** Cartoon schematic of the *VAChT/ChAT* locus encoding VAChT and ChAT from two mutually exclusive, alternatively spliced transcript variants sharing the same non-coding exon 1 (purple bar). Dotted line indicates additional exons encoding ChAT not shown. Colored bars underneath locus indicate *cis*-regulatory sequences tested, numbers reflect distance from the start codon (+ 1) of *VAChT*. Expression in "core" motor ganglion (MG) and Ascending Motor Ganglion neuron 5 (AMG5) was assessed qualitatively. An Ebf binding site previously reported (Kratsios et al., 2012) is situated -4111 bp upstream of *VAChT.* **(B)** Co-electroporation of *VAChT/ChAT -4315/ + 15 > Unc-76:mCherry* and *Msx > H2B:GFP* revealed co-expression in AMG5 at 19 h post-fertilization (hpf) at 20°C, a cholinergic interneuron of the dorsal MG, derived from the dorsal cells of the neural tube. **(C)** A minimal fragment surrounding the Ebf binding site is sufficient to drive AMG5-specific reporter expression at 18 hpf, 20°C. Image is a confocal Z stack projection. **(D)** A smaller proximal fragment from *VAChT/ChAT (-2083/ + 15)* lacking the Ebf binding site is sufficient to drive expression in other cholinergic neurons including those of the core MG, but not in AMG5, at 19 hpf, 18°C.

primary motor neurons. We discuss these findings in the context of different scenarios for the evolution of cholinergic gene regulation in chordate motor circuits.

METHODS

Ciona robusta (*intestinalis* Type A) adults were collected in the San Diego, CA region (M-REP Consulting). Gametes were isolated and prepared for *in vitro* fertilization as previously described (Christiaen et al., 2009b). Dechorionated zygotes were transfected by electroporation as previously described (Christiaen et al., 2009a). All relevant sequences are described in **Supplementary Sequence File 1**. Embryos were raised at 20°C (unless otherwise stated) and fixed in MEMFA fixative (3.7% formaldehyde, 0.1 M MOPS pH7.4, 0.5 M NaCl, 1 mM EGTA, 2 mM MgSO4, 0.1% Triton-X100) for 15 min, rinsed once in PBS/0.4% Triton-X100/50 mM NH4Cl and once in PBS/0.1% Triton-X100, then finally mounted in 1X PBS/50% Glycerol/2% DABCO mounting solution. Images were acquired on inverted epifluorescence (Leica DMIL LED or DMi8) or scanning point confocal microscopes (Zeiss LSM 700). Confocal images were processed as maximum intensity Z projections using Zeiss LSM or ImageJ software. CRISPR/Cas9-mediated knockout of Ebf was performed using 30 μg *FOG > Cas9 (Gandhi et al., 2017)*, 40 μg *U6 > Ebf.C (Gandhi et al., 2017)* or *U6 > Control (Stolfi et al., 2014)*, 15 μg *FOG > H2B:mCherry (Rothbächer et al., 2007; Gline et al., 2009)*, and 90 μg *VAChT/ChAT -4315/-3886 + bpFOG > Unc-76:GFP*. The Unc-76 tag has been previously used for efficient labeling of neurons especially their axons (Dynes and Ngai, 1998; Imai et al., 2009).

RESULTS

We previously identified a predicted binding site for Ebf (CATTTGGG) approximately 4.1 kb upstream of the translation start codon of *Ciona VAChT,* based on the consensus sequence

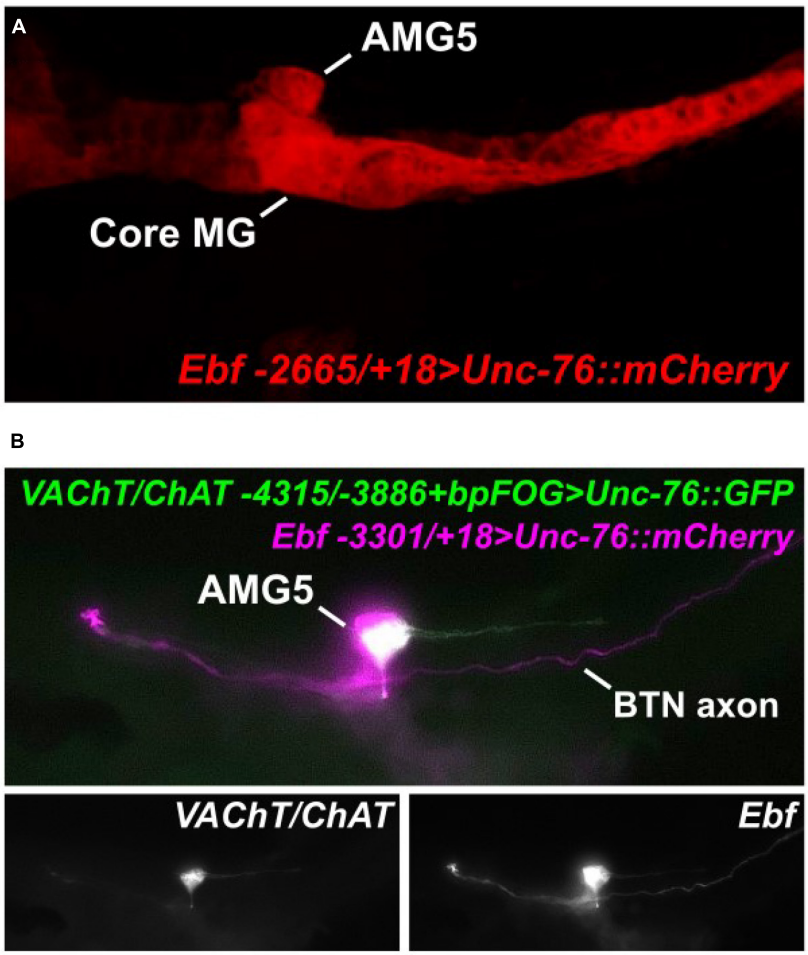

FIGURE 2 | AMG5 co-expresses *VAChT/ChAT* and *Ebf*. **(A)** An *Ebf* reporter plasmid labels various CNS neurons including AMG5 at 18 h post-fertilization (hpf) at 20°C. Image is a confocal Z stack projection. **(B)** Co-electroporation of the *Ebf* reporter and the minimal AMG5-specific *VAChT/ChAT* reporter revealed co-expression in AMG5 at 17 hpf, 20°C. In this example, the larva shows mosaic incorporation of the plasmids only in the animal pole-derived lineages, which give rise to AMG5 and the Bipolar Tail Neuron (BTN) that also expresses Ebf (Stolfi et al., 2015), but not the core MG.

CCCNNGGG (**Figure 1A**; Kratsios et al., 2012). *VAChT* and *Choline acetyltransferase (ChAT)* form a cholinergic locus (henceforth referred to as *VAChT/ChAT*) in which alternative splicing of a shared transcript results in two distinct mRNAs coding for different effectors of cholinergic neurotransmission: VAChT (also known as Slc18a3) and ChAT. This peculiar arrangement is conserved from nematodes to chordates (Alfonso et al., 1993). A fluorescent reporter plasmid spanning -4315 bp upstream of the VAChT translation start that includes this predicted Ebf site was previously shown to drive expression in all cholinergic neurons of the larva (**Figure 1B**; Kratsios et al., 2012). This includes cholinergic neurons of the brain, MG, and in bipolar tail neurons.

While the "core" MG comprises bilateral pairs of neurons derived from the lateral rows of the neural tube which includes the two pairs of major primary, or lower motor neurons (Cole and Meinertzhagen, 2004; Ryan et al., 2016), a set of ascending motor ganglion (AMG) neurons is situated dorsal to the MG, relaying peripheral inputs to neurons of the core MG (Ryan et al., 2016, 2018). These have been shown to comprise a mix of cholinergic and GABAergic neurons and (previously called dvCNs and dvGNs, respectively) (Takamura et al., 2010). More recently, it was shown that AMG neurons 1–4, 6, and 7 are GABAergic, while AMG neuron 5 (AMG5) represents the sole cholinergic neuron in this cluster (Kourakis et al., 2019). Indeed, we found that the full-length (-4315/ + 15) *VAChT/ChAT* reporter labels a single cell just dorsal to the anterior half of the core MG, in the exact spot where we expect AMG5 to be (**Figure 1B**). Co-electroporation with the reporter *Msx > H2B:GFP*, which labels animal pole-derived lateral neural plate border cells that give rise to the dorsal row of the neural tube (Cole and Meinertzhagen, 2004; Russo et al., 2004; Stolfi et al., 2015; **Figure 1B**). This suggests the AMG5 neuron comes from one of the b8.19 blastomeres on either side of the embryo prior to neural tube closure (Cole and Meinertzhagen, 2004; Pasini et al., 2006). To our knowledge, this is the first evidence for the developmental origins of AMG5 from the Msx + dorsal row of the neural tube, although we could not ascertain whether this cell is invariantly derived from the left or right side of the embryo.

When we tested a smaller fragment surrounding the predicted Ebf site (-4315/-3886) in conjunction with a heterologous basal promoter (bpFOG) (Rothbächer et al., 2007), we found that this was sufficient to drive expression of fluorescent reporter solely in AMG5, but not any other cholinergic neuron (**Figure 1C**). This revealed the characteristic morphology of AMG5 as originally determined by the serial-section electron micrographs of the connectome study (Ryan et al., 2016, 2018; Ryan and Meinertzhagen, 2019), including unusual left and right ascending neurites (**Figure 1C**). Therefore we conclude that this region around the previously identified Ebf site corresponds to a *cis*-regulatory element that is sufficient to drive *VAChT/ChAT* in the cholinergic AMG5 neuron. In contrast, a shorter proximal fragment spanning -2083 bp upstream of *VAChT* (not encompassing the AMG5-specific element) was sufficient to drive expression in other cholinergic neurons, including the motor neurons and other "core" MG neurons (**Figure 1D**).

Because of the predicted Ebf binding site in this AMG5-specific *VAChT/ChAT cis*-regulatory element (-4315/-3886), we hypothesized that Ebf might be directly activating *VAChT/ChAT* expression (and thus cholinergic identity) specifically in AMG5. Consistent with this hypothesis, we found that fluorescent protein expression driven by *Ebf cis*-regulatory sequences (Stolfi and Levine, 2011; Razy-Krajka et al., 2014) also labeled AMG5 and other cholinergic neurons, but not other surrounding (GABAergic) AMG neurons (**Figure 2A**). Co-expression with *VAChT/ChAT* reporter was confirmed by co-electroporation of *Ebf* and AMG5-specific *VAChT/ChAT* reporter plasmids (**Figure 2B**). Further, mutating the predicted Ebf site from

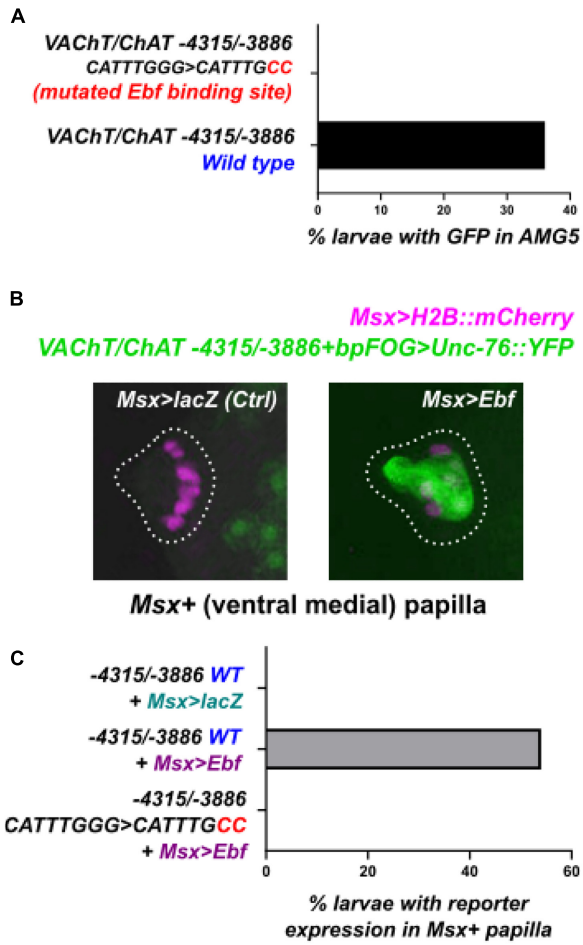

FIGURE 3 | An Ebf binding site is necessary for *VAChT/ChAT* reporter activity. **(A)** Mutating the Ebf binding site in the minimal AMG5-specific *VAChT/ChAT cis*-regulatory element was sufficient to abolish its activity in AMG5. Mutated reporter $n = 50$, wild-type reporter $n = 44$. **(B)** The AMG5-specific *VAChT/ChAT* reporter can be ectopically activated in ventral papilla cells at 15.5 h post-fertilization (hpf) at 20°C, by overexpressing Ebf there (using *Msx > Ebf*). No expression is seen in the negative control electroporated with the neutral construct *Msx > lacZ* instead. Images are confocal Z stack projections. **(C)** Yet Ebf overexpression in the ventral papilla does not cause ectopic expression of the mutated *VAChT/ChAT* reporter, suggesting the Ebf binding site is indispensable for Ebf-mediated activation of this element. For each of the three conditions, $n = 50$.

CATTTGGG to CATTGCC in the context of the -4315/-3886 *cis*-regulatory element completely abolished reporter activity in AMG5 (**Figure 3A**). To test if Ebf can activate this AMG5-specific element, we overexpressed it in the ventral sensory papilla of the larva using the *Msx* promoter (Russo et al., 2004; **Figure 3B**). This strategy had previously been used to test ectopic expression of the full-length *VAChT/ChAT* reporter plasmid in response to Ebf overexpression (Kratsios et al., 2012). As expected, Ebf overexpression activated the *VAChT/ChAT* -4315/-3886 reporter in the papilla 54% of larvae, compared to 0% of larvae upon overexpression of a negative control *lacZ* sequence instead (**Figures 3B,C**). Furthermore, Ebf overexpression did not activate the expression of the *VAChT/ChAT* -4315/-3886 reporter carrying the mutated Ebf site (CATTTGGG to CATTGCC, **Figure 3C**). Taken together, these data suggest that Ebf directly activates an AMG5-specific *cis*-regulatory element for *VAChT/ChAT* expression.

To verify that Ebf acts in *trans* to activate this minimal AMG5-specific *VAChT/ChAT* *cis*-regulatory element, we performed tissue-specific CRISPR/Cas9-mediated knockout of *Ebf* in *Ciona* embryos. We co-electroporated a highly efficient, previously validated single-chain guide RNA (sgRNA) vector targeting *Ebf* (Gandhi et al., 2017) together with *FOG > Cas9,* which drives Cas9 specifically in the animal pole-derived blastomeres at the 8-cell stage (Rothbächer et al., 2007; Gandhi et al., 2017). This combination was sufficient to abolish expression of *VAChT/ChAT -4315/-3886* reporter in AMG5 (**Figure 4**). Taking these manipulations in *cis* and *trans* together, we conclude that Ebf binds to and activates a distal *cis*-regulatory element of *VAChT/ChAT* that is activated only in AMG5, the sole cholinergic neuron in this region immediately dorsal to the "core" MG.

As for a possible earlier role for Ebf that could explain the loss of *VAChT/ChAT* reporter expression in AMG5, *Ebf* is not expressed zygotically in the lineage that gives rise to AMG5, before that cell is born. This is known thanks to detailed *in situ* hybridization screens (Imai et al., 2004, 2006, 2009). *Ebf* expression in the early embryo is non-existent until the late gastrula stage, when it comes up in the A9.32 pair of blastomeres and a pair of tail tip cells (none of which give rise to the AMG neurons). Therefore, we find it highly unlikely that CRISPR knockout of *Ebf* in the animal pole using *FOG > Cas9* is abrogating AMG5 specification prior to its birth.

DISCUSSION

We show here that *VAChT/ChAT* reporter gene expression in the dorsal motor ganglion region of *Ciona* requires the transcription factor Ebf. Since *Ebf* and *VAChT/ChAT* are co-expressed in a single neuron (recently identified as AMG5) in this region, we suspect that it may act as a classically defined terminal selector (Etchberger et al., 2007; Allan and Thor, 2015; Hobert and Kratsios, 2019) of cholinergic identity in this cell. The AMG neurons are a synaptically interconnected cluster of 7 ascending interneurons that receive synaptic connections from a variety of neurons processing diverse sensory inputs including light, gravity, touch, and possibly chemosensation. Their synaptic targets include neurons of the core MG and neurons of the brain (Ryan et al., 2016). It was recently shown that *VAChT/ChAT* is expressed in a single AMG neuron (AMG5), while the remaining 6 AMG neurons express *Vesicular GABA transporter (VGAT)* instead, indicating a GABAergic identity (Kourakis et al., 2019). AMG5 is a single multipolar neuron

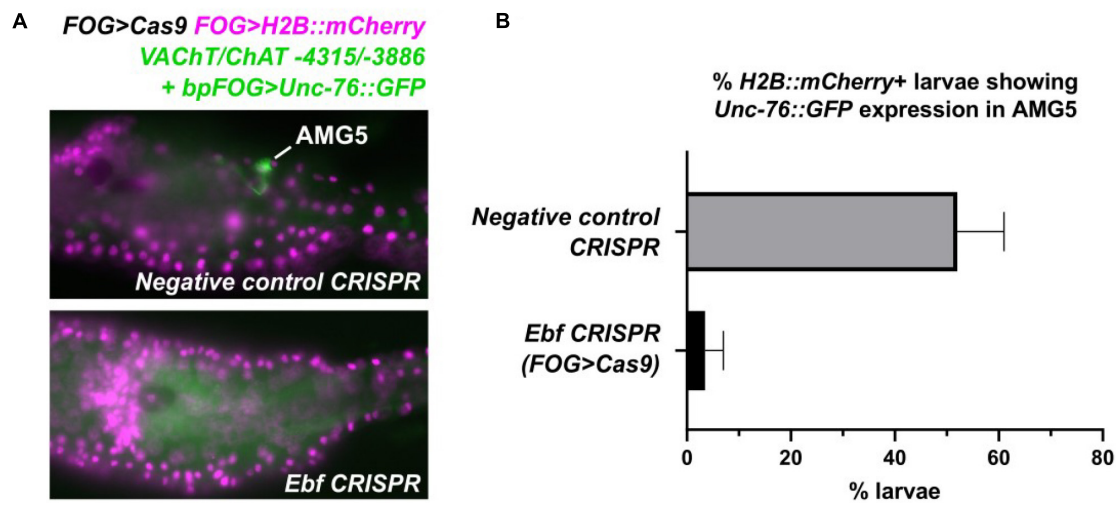

FIGURE 4 | Tissue-specific CRISPR/Cas9-mediated knockout of *Ebf* abolishes *VAChT/ChAT* expression in AMG5. **(A)** F0 larvae co-electroporated with *FOG > Cas9, FOG > H2B:mCherry,* and the AMG5-specific *VAChT/ChAT* reporter (*-4315/-3886 + bpFOG > Unc-76:GFP),* and either a negative control guide RNA or an *Ebf*-targeting guide RNA (Gandhi et al., 2017) were scored for GFP signal in AMG5 at 17 h post-fertilization at 20°C. *FOG > Cas9* restricts CRISPR activity to the animal pole-derived cells from which AMG5 is born. **(B)** Scoring results of negative control and *Ebf* CRISPR larvae, averaged over two replicates. Negative control: replicate 1 $n = 54$, replicate 2 $n = 49$. *Ebf* CRISPR: replicate 1 $n = 58$, replicate 2 $n = 43$. Error bars indicate range between replicates. These results indicate that knocking out *Ebf* in the animal pole mostly abolishes *VAChT/ChAT* reporter expression in AMG5.

situated right on the midline surrounded by the remaining AMG neurons, with left and right axon branches projecting anteriorly. It receives heavy inputs from glutamatergic posterior apical trunk epidermal neurons (pATENs) and is presynaptic to prominent cholinergic neurons of the core MG including Motor Neuron 1 (MN1) and the Descending Decussating Neuron (ddN) (Ryan et al., 2016). Given its cholinergic identity and unique position and connectivity in the connectome, its function may be to trigger swimming behavior though cholinergic excitation of primary motor neurons, relaying an as-of-yet unidentified sensory stimulus transduced by the pATENs.

In *C. elegans,* the Ebf ortholog UNC-3 is a terminal selector for cholinergic neuron fate (Kratsios et al., 2012), suggesting a deep evolutionary history of this transcription factor as a determinant of cholinergic neuron fate. While the most abundant and prominent cholinergic neuron type in *C. elegans* is the motor neuron, UNC-3 does regulate cholinergic gene expression in cholinergic interneurons as well (Pereira et al., 2015). Similarly, expression of Ebf2 and other Ebf paralogs is seen in various neuronal precursors of the developing mammalian spinal cord, including those in the dorsal horn (Catela et al., 2019), where sparse expression of cholinergic genes has been observed (Mesnage et al., 2011). Given the role of dorsal horn interneurons in sensory integration, and the developmental origin of AMG neurons from the dorsal row of cells of the *Ciona* neural tube, AMG5 might be a homolog of these rare cholinergic interneurons of the mammalian spinal cord dorsal horn.

Although we previously used a dominant-repressor form of Ebf to suggest its role in specifying *Ciona* cholinergic motor neurons (Kratsios et al., 2012), we show here that a shorter *VAChT/ChAT cis*-regulatory fragment lacking a key Ebf binding site is sufficient to drive expression in motor neurons, but not AMG5. Therefore, it is likely that Ebf directly activates *VAChT/ChAT* in AMG5 but not necessarily in the neurons of the "core" MG that includes the primary motor neurons of the larva. This does not rule out a role for Ebf in regulating the activation and/or maintenance of other cholinergic effectors or more generic terminal differentiation genes in primary motor neurons. Additionally, there are cholinergic neurons, including primary motor neurons, in the post-metamorphic adults (Hozumi et al., 2015; Jokura et al., 2020), and it remains entirely unknown if these depend on Ebf for their specification and/or cholinergic fate.

Taken together, our results may help bridge the seemingly divergent roles of Ebf/UNC-3 in regulating motor neuron differentiation in *C. elegans* and mammals. While in *C. elegans* UNC-3 regulates cholinergic gene expression in primary motor neurons (Kratsios et al., 2012), Ebf factors in mouse regulate other aspects of motor neuron differentiation independently of their cholinergic identity (Catela et al., 2019). In the *Ciona* larva, we see a possible evolutionary intermediate between these two extremes. While Ebf directly regulates *VAChT/ChAT* expression in a cholinergic neuron of the motor ganglion that is immediately presynaptic to the primary motor neurons of the larva, its role in the primary motor neurons may reflect a more vertebrate-like function. Alternatively, there may be greater genetic redundancy in regulation of cholinergic gene expression in chordate motor neurons. A broader phylogenetic sampling may answer whether any of these (nematode, tunicate, vertebrate) closely resemble the ancestral condition in the last bilaterian common ancestor.

DATA AVAILABILITY STATEMENT

The raw data supporting the conclusions of this article will be made available by the authors, without undue reservation.

AUTHOR CONTRIBUTIONS

SP and AS designed, performed, and interpreted the experiments. AS wrote the manuscript, with edits and suggestions by SP. Both authors contributed to the article and approved the submitted version.

FUNDING

This work was funded by the NSF grant 1940743 (IOS) and NIH grant GM143326 to AS, and an ARCS Foundation fellowship to SP.

ACKNOWLEDGMENTS

We would like to thank Susanne Gibboney, Florian Razy-Krajka, and all members of the laboratory for advice and technical assistance. We thank Paschalis Kratsios, Oliver Hobert, and Mike Levine for their advice and support.

SUPPLEMENTARY MATERIAL

The Supplementary Material for this article can be found online at: https://www.frontiersin.org/articles/10.3389/fnins.2021.784649/full#supplementary-material

REFERENCES

Alfonso, A., Grundahl, K., Duerr, J. S., Han, H.-P., and Rand, J. B. (1993). The Caenorhabditis elegans unc-17 gene: a putative vesicular acetylcholine transporter. *Science* 261, 617–619. doi: 10.1126/science.8342028

Allan, D. W., and Thor, S. (2015). Transcriptional selectors, masters, and combinatorial codes: regulatory principles of neural subtype specification. *Wiley Interdiscip. Rev. Dev. Biol.* 4, 505–528. doi: 10.1002/wdev.191

Catela, C., Correa, E., Wen, K., Aburas, J., Croci, L., Consalez, G. G., et al. (2019). An ancient role for collier/Olf/Ebf (COE)-type transcription factors in axial motor neuron development. *Neural Dev.* 14:2. doi: 10.1186/s13064-018-0125-6

Cho, H.-H., Cargnin, F., Kim, Y., Lee, B., Kwon, R.-J., Nam, H., et al. (2014). Isl1 directly controls a cholinergic neuronal identity in the developing forebrain and

spinal cord by forming cell type-specific complexes. *PLoS Genet.* 10:e1004280. doi: 10.1371/journal.pgen.1004280

Christiaen, L., Wagner, E., Shi, W., and Levine, M. (2009b). Isolation of sea squirt (Ciona) gametes, fertilization, dechorionation, and development. *Cold Spring Harb. Protoc.* 2009:pdb.prot5344. doi: 10.1101/pdb.prot5344

Christiaen, L., Wagner, E., Shi, W., and Levine, M. (2009a). Electroporation of transgenic DNAs in the sea squirt Ciona. *Cold Spring Harb. Protoc.* 2009:pdb.prot5345. doi: 10.1101/pdb.prot5345

Cole, A. G., and Meinertzhagen, I. A. (2004). The central nervous system of the ascidian larva: mitotic history of cells forming the neural tube in late embryonic *Ciona intestinalis*. *Dev. Biol.* 271, 239–262. doi: 10.1016/j.ydbio.2004.04.001

Dynes, J. L., and Ngai, J. (1998). Pathfinding of olfactory neuron axons to stereotyped glomerular targets revealed by dynamic imaging in living zebrafish embryos. *Neuron* 20, 1081–1091. doi: 10.1016/s0896-6273(00)80490-0

Eng, S. R., Dykes, I. M., Lanier, J., Fedtsova, N., and Turner, E. E. (2007). POU-domain factor Brn3a regulates both distinct and common programs of gene expression in the spinal and trigeminal sensory ganglia. *Neural Dev.* 2, 1–17. doi: 10.1186/1749-8104-2-3

Etchberger, J. F., Lorch, A., Sleumer, M. C., Zapf, R., Jones, S. J., Marra, M. A., et al. (2007). The molecular signature and cis-regulatory architecture of a C. elegans gustatory neuron. *Genes Dev.* 21, 1653–1674. doi: 10.1101/gad.1560107

Finney, M., Ruvkun, G., and Horvitz, H. R. (1988). The C. elegans cell lineage and differentiation gene unc-86 encodes a protein with a homeodomain and extended similarity to transcription factors. *Cell* 55, 757–769. doi: 10.1016/0092-8674(88)90132-8

Gandhi, S., Haeussler, M., Razy-Krajka, F., Christiaen, L., and Stolfi, A. (2017). Evaluation and rational design of guide RNAs for efficient CRISPR/Cas9-mediated mutagenesis in Ciona. *Dev. Biol.* 425, 8–20. doi: 10.1016/j.ydbio.2017.03.003

Gline, S. E., Kuo, D. H., Stolfi, A., and Weisblat, D. A. (2009). High resolution cell lineage tracing reveals developmental variability in leech. *Dev. Dyn.* 238, 3139–3151. doi: 10.1002/dvdy.22158

Hobert, O., and Kratsios, P. (2019). Neuronal identity control by terminal selectors in worms, flies, and chordates. *Curr. Opin. Neurobiol.* 56, 97–105. doi: 10.1016/j.conb.2018.12.006

Hozumi, A., Horie, T., and Sasakura, Y. (2015). Neuronal map reveals the highly regionalized pattern of the juvenile central nervous system of the ascidian *Ciona intestinalis*. *Dev. Dyn.* 244, 1375–1393. doi: 10.1002/dvdy.24317

Imai, K. S., Hino, K., Yagi, K., Satoh, N., and Satou, Y. (2004). Gene expression profiles of transcription factors and signaling molecules in the ascidian embryo: towards a comprehensive understanding of gene networks. *Development* 131, 4047–4058. doi: 10.1242/dev.01270

Imai, K. S., Levine, M., Satoh, N., and Satou, Y. (2006). Regulatory blueprint for a chordate embryo. *Science* 312, 1183–1187. doi: 10.1126/science.1123404

Imai, K. S., Stolfi, A., Levine, M., and Satou, Y. (2009). Gene regulatory networks underlying the compartmentalization of the Ciona central nervous system. *Development* 136, 285–293. doi: 10.1242/dev.026419

Jokura, K., Nishino, J. M., Ogasawara, M., and Nishino, A. (2020). An α7-related nicotinic acetylcholine receptor mediates the ciliary arrest response in pharyngeal gill slits of Ciona. *J. Exp. Biol.* 223:jeb209320.

Kourakis, M. J., Borba, C., Zhang, A., Newman-Smith, E., Salas, P., Manjunath, B., et al. (2019). Parallel visual circuitry in a basal chordate. *eLife* 8:e44753. doi: 10.7554/eLife.44753

Kratsios, P., Stolfi, A., Levine, M., and Hobert, O. (2012). Coordinated regulation of cholinergic motor neuron traits through a conserved terminal selector gene. *Nat. Neurosci.* 15, 205–214. doi: 10.1038/nn.2989

Mesnage, B., Gaillard, S., Godin, A. G., Rodeau, J.-L., Hammer, M., Von Engelhardt, J., et al. (2011). Morphological and functional characterization of cholinergic interneurons in the dorsal horn of the mouse spinal cord. *J. Comp. Neurol.* 519, 3139–3158. doi: 10.1002/cne.22668

Pasini, A., Amiel, A., Rothbächer, U., Roure, A., Lemaire, P., and Darras, S. (2006). Formation of the ascidian epidermal sensory neurons: insights into the origin of the chordate peripheral nervous system. *PLoS Biol.* 4:e225. doi: 10.1371/journal.pbio.0040225

Pereira, L., Kratsios, P., Serrano-Saiz, E., Sheftel, H., Mayo, A. E., Hall, D. H., et al. (2015). A cellular and regulatory map of the cholinergic nervous system of C. elegans. *eLife* 4:e12432. doi: 10.7554/eLife.12432

Razy-Krajka, F., Lam, K., Wang, W., Stolfi, A., Joly, M., Bonneau, R., et al. (2014). Collier/OLF/EBF-dependent transcriptional dynamics control pharyngeal muscle specification from primed cardiopharyngeal progenitors. *Dev. Cell* 29, 263–276. doi: 10.1016/j.devcel.2014.04.001

Rothbächer, U., Bertrand, V., Lamy, C., and Lemaire, P. (2007). A combinatorial code of maternal GATA, Ets and β-catenin-TCF transcription factors specifies and patterns the early ascidian ectoderm. *Development* 134, 4023–4032. doi: 10.1242/dev.010850

Russo, M. T., Donizetti, A., Locascio, A., D'Aniello, S., Amoroso, A., Aniello, F., et al. (2004). Regulatory elements controlling Ci-msxb tissue-specific expression during *Ciona intestinalis* embryonic development. *Dev. Biol.* 267, 517–528. doi: 10.1016/j.ydbio.2003.11.005

Ryan, K., Lu, Z., and Meinertzhagen, I. A. (2016). The CNS connectome of a tadpole larva of *Ciona intestinalis* (L.) highlights sidedness in the brain of a chordate sibling. *Elife* 5:e16962. doi: 10.7554/eLife.16962

Ryan, K., Lu, Z., and Meinertzhagen, I. A. (2018). The peripheral nervous system of the ascidian tadpole larva: types of neurons and their synaptic networks. *J. Comp. Neurol.* 526, 583–608. doi: 10.1002/cne.24353

Ryan, K., and Meinertzhagen, I. A. (2019). Neuronal identity: the neuron types of a simple chordate sibling, the tadpole larva of *Ciona intestinalis*. *Curr. Opin. Neurobiol.* 56, 47–60. doi: 10.1016/j.conb.2018.10.015

Serrano-Saiz, E., Leyva-Díaz, E., De La Cruz, E., and Hobert, O. (2018). BRN3-type POU Homeobox Genes Maintain the Identity of Mature Postmitotic Neurons in Nematodes and Mice. *Curr. Biol.* 28, 2813–2823.e2.

Serrano-Saiz, E., Poole, R. J., Felton, T., Zhang, F., De La Cruz, E. D., and Hobert, O. (2013). Modular control of glutamatergic neuronal identity in C. elegans by distinct homeodomain proteins. *Cell* 155, 659–673. doi: 10.1016/j.cell.2013.09.052

Stolfi, A., Gandhi, S., Salek, F., and Christiaen, L. (2014). Tissue-specific genome editing in Ciona embryos by CRISPR/Cas9. *Development* 141, 4115–4120. doi: 10.1242/dev.114488

Stolfi, A., and Levine, M. (2011). Neuronal subtype specification in the spinal cord of a protovertebrate. *Development* 138, 995–1004. doi: 10.1242/dev.061507

Stolfi, A., Ryan, K., Meinertzhagen, I. A., and Christiaen, L. (2015). Migratory neuronal progenitors arise from the neural plate borders in tunicates. *Nature* 527, 371–374. doi: 10.1038/nature15758

Takamura, K., Minamida, N., and Okabe, S. (2010). Neural map of the larval central nervous system in the ascidian *Ciona intestinalis*. *Zoolog. Sci.* 27, 191–203.

Tournière, O., Dolan, D., Richards, G. S., Sunagar, K., Columbus-Shenkar, Y. Y., Moran, Y., et al. (2020). NvPOU4/Brain3 Functions as a Terminal Selector Gene in the Nervous System of the Cnidarian *Nematostella vectensis*. *Cell Rep.* 30, 4473–4489.e5.

Zhang, F., Bhattacharya, A., Nelson, J. C., Abe, N., Gordon, P., Lloret-Fernandez, C., et al. (2014). The LIM and POU homeobox genes ttx-3 and unc-86 act as terminal selectors in distinct cholinergic and serotonergic neuron types. *Development* 141, 422–435. doi: 10.1242/dev.099721

Conflict of Interest: The authors declare that the research was conducted in the absence of any commercial or financial relationships that could be construed as a potential conflict of interest.

Publisher's Note: All claims expressed in this article are solely those of the authors and do not necessarily represent those of their affiliated organizations, or those of the publisher, the editors and the reviewers. Any product that may be evaluated in this article, or claim that may be made by its manufacturer, is not guaranteed or endorsed by the publisher.

frontiers in Neuroscience

REVIEW
published: 03 January 2022
doi: 10.3389/fnins.2021.781160

From Cell States to Cell Fates: How Cell Proliferation and Neuronal Differentiation Are Coordinated During Embryonic Development

*Carla Belmonte-Mateos and Cristina Pujades**

Department of Experimental and Health Sciences, Universitat Pompeu Fabra, Barcelona, Spain

OPEN ACCESS

Edited by:
Filipe Pinto-Teixeira, FR3743 Centre de Biologie Intégrative (CBI), France

Reviewed by:
Patricia Jusuf, The University of Melbourne, Australia
Fabienne Pituello, FR3743 Centre de Biologie Intégrative (CBI), France
Eric Agius, Centre de Biologie Intégrative, France, in collaboration with reviewer FP
Ryota L. Matsuoka, Lerner Research Institute, Cleveland Clinic, United States

***Correspondence:**
Cristina Pujades
cristina.pujades@upf.edu
orcid.org/0000-0001-6423-7451

Specialty section:
This article was submitted to Neurogenesis, a section of the journal Frontiers in Neuroscience

Received: *22 September 2021*
Accepted: *29 November 2021*
Published: *03 January 2022*

Citation:
Belmonte-Mateos C and Pujades C (2022) From Cell States to Cell Fates: How Cell Proliferation and Neuronal Differentiation Are Coordinated During Embryonic Development. Front. Neurosci. 15:781160. doi: 10.3389/fnins.2021.781160

The central nervous system (CNS) exhibits an extraordinary diversity of neurons, with the right cell types and proportions at the appropriate sites. Thus, to produce brains with specific size and cell composition, the rates of proliferation and differentiation must be tightly coordinated and balanced during development. Early on, proliferation dominates; later on, the growth rate almost ceases as more cells differentiate and exit the cell cycle. Generation of cell diversity and morphogenesis takes place concomitantly. In the vertebrate brain, this results in dramatic changes in the position of progenitor cells and their neuronal derivatives, whereas in the spinal cord morphogenetic changes are not so important because the structure mainly grows by increasing its volume. Morphogenesis is under control of specific genetic programs that coordinately unfold over time; however, little is known about how they operate and impact in the pools of progenitor cells in the CNS. Thus, the spatiotemporal coordination of these processes is fundamental for generating functional neuronal networks. Some key aims in developmental neurobiology are to determine how cell diversity arises from pluripotent progenitor cells, and how the progenitor potential changes upon time. In this review, we will share our view on how the advance of new technologies provides novel data that challenge some of the current hypothesis. We will cover some of the latest studies on cell lineage tracing and clonal analyses addressing the role of distinct progenitor cell division modes in balancing the rate of proliferation and differentiation during brain morphogenesis. We will discuss different hypothesis proposed to explain how progenitor cell diversity is generated and how they challenged prevailing concepts and raised new questions.

Keywords: neural stem cells (NSC), neurogenesis, neuronal differentiation, morphogenesis, cell fate, cell state

A SHORT HISTORIC GLANCE AT CELL FATE

The making of an embryo entails the production of billions of specialized cells from a single pluripotent cell, the zygote, and their organization into tissues and organs. During embryonic development, stem cells must balance self-renewal, commitment to specific fates and differentiation to generate the wide diversity of cells in the correct numbers and proportions to construct functional organs. The embryo undergoes morphogenesis, which consists of specific tissue changes occurring orderly in time. This results in a multitude of tissue and organism shapes, which

are controlled by fundamental processes involving cell mechanics. The high reproducibility of embryonic development argues that these events are tightly spatiotemporally regulated and that embryonic cells interpret specific information that organizes their behavior. Thus, to learn how to construct functional organs we need to elucidate the mechanisms that regulate how cell proliferation, specification and differentiation occur alongside morphogenesis. Or in other words, how gene regulatory networks (GRN) encode tissue shape.

These questions, such as how cells acquire their fate, have fascinated scientists for centuries. Experiments from the 1890s led to the emergence of the hypothesis that developmental mechanisms regulate the differentiation of different cell types occurring on a developmental landscape sculpted by genes (Waddington, 1957; for reviews covering this topic see Slack, 2002; Takahashi and Yamanaka, 2016; Collinet and Lecuit, 2021). This deterministic view considered that genes defined all developmental cell trajectories and gave rise to the *mosaic theory of development* in which the fate of each cell in an embryo was specified very early and followed fixed developmental trajectories. This implied a crucial role for cell-autonomous factors and that cells –once committed– could not change their fate. The publication of the stereotyped cell lineages trees of *Caenorhabditis elegans* in 1983 (Sulston et al., 1983), showing that the segregation of genetic determinants at each cellular division defined the different cell populations in the progeny, consolidated this view. The identification of *morphogens*, secreted molecules whose concentration conferred positional information within a field of cells, and the discovery of the *master genes*, which were able to drive the entire genetic cascade to form an organ, reinforced the idea of a genetic program controlling development. In spite of it, several observations from experimental embryologists in the early XX century suggested that development resulted from more than deterministic rules (Rogers and Schier, 2011). Experimental embryology manipulations mainly in amphibians indicated that during development cell–cell and cell–environment interactions led cells to adopt a particular fate in a not predetermined manner. The discovery, by Brown in hydra and Spemann and Mangold in amphibians, that groups of cells –inductors– could change the fate of neighboring competent cells challenged again the *mosaic theory*. Development could proceed by selection of a few viable dynamical cellular states, which resulted from local cell–cell interactions occurring within the embryo in a self-organized manner. This led to the idea that non–cell-autonomous factors were needed for cells to acquire different functions. This has been called the *regulative view of development* (for reviews see Robertis, 2006; Rogers and Schier, 2011). Now, we know that both deterministic and self-organization programs play important roles.

In this review, we will focus on how cell behaviors and neuronal fates are deployed during the development of the vertebrate Central Nervous System (CNS). Specifically, we will cover some examples of how neural progenitor cells transition through different proliferation modes to finally differentiate, and the implications for the overall growth and morphogenesis of the CNS. Due to the vast and unattainable literature, attention will be paid to some of the latest cell lineage and clonal studies, since they inform us about the role that **time** plays in the deployment of the different cell fates –a crucial factor not very much addressed up to now. We will focus on two of the paradigm models for tissue growth in the vertebrate CNS: the brain cortex, which undergoes dramatic morphogenetic changes, and the spinal cord that mainly grows by increase of volume. We will also cover the differences between cell states and cell fates, a current debate boosted with the latest large-scale molecular profiling studies. And finally, we will close discussing different hypotheses proposed to explain how progenitor cell diversity is generated and how they challenge prevailing concepts and raise new questions.

FRAMING THE QUESTION: PROGENITOR CELLS VERSUS DIFFERENTIATED NEURONS

The complex structure of our brain relies on the production and proper organization of diverse pools of neurons and glia from a relatively small number of neural progenitors during embryonic development. Despite the impressive progress in neurobiology over the last years, our understanding of how these multiple cell types are generated and maintained in highly organized spatial patterns, and how changes in this ground plan can result in pathologies, is still limited. We learnt that spatial patterning cues can produce different types of neural progenitors, and hence different types of neurons and glia along the anteroposterior (AP) or dorsoventral (DV) axes of the CNS (see section "The two paradigm models for tissue growth in the central nervous system: the spinal cord and the brain cortex"; Jessell, 2000). It is also known that neuronal production is asynchronous along the CNS, and work specially from Drosophila helped to unveil the molecular mechanisms by which individual progenitors sequentially generate the different cell types —a process called temporal cell specification (for review see Kohwi and Doe, 2013)—. Moreover, stem cells operate in a noisy and dynamic environment, as their gene expression levels fluctuate in response to intrinsic factors and/or environmental cues. Currently, big data approaches producing large amounts of measurements have the potential to help us to decipher how spatial and temporal cues are integrated to generate specific neuronal types and how aging progenitors change competence to produce different cell types over time.

The embryonic CNS is initially subdivided into regions along the body axes, where there is a progressive refinement of pattern. Each region has a distinct identity that underlies the generation of a specific set of cell types, each of which must be generated at the right time and place and in the correct proportions for normal development and proper function (Kiecker and Lumsden, 2005). The various neuronal populations found in the CNS arise from progenitor cells in specific locations of the embryonic neural tube. Moreover, cell diversity is generated at the same time that the brain undergoes a dramatic transformation from a simple tubular structure —the neural tube— to a highly convoluted structure —the brain, resulting in changes in the

position of neuronal progenitors and their derivatives over time. In the developing CNS, the neural tube undergoes a segmentation process along the AP axis. This results in the formation of three embryonic brain vesicles —the forebrain, midbrain and hindbrain— and the elongated spinal cord (for review see Kiecker and Lumsden, 2005). At early stages of embryonic development, neuroepithelial cells (NEC) intensively proliferate by repeated symmetric cell divisions. NEC extend from the apical (ventricular) to the basal epithelial surfaces of the neural tube, and display interkinetic nuclear migration (IKNM) with the corresponding translocation of the nucleus according to the cell cycle phase –a beautiful orchestration between epithelial morphogenesis and cell proliferation. Although NEC are characterized by the expression of Sox2 and Nestin, and apical markers like Occludin and Zona Occludens 1 (ZO-1) (Götz and Huttner, 2005), there is no specific "molecular code" to define them. In spite of these common features, not all progenitors allocated in distinct CNS territories are equal. For instance, in the cortex, NEC gradually elongate and can become radial glial cells (RGC), with the cell bodies in the ventricular zone (VZ) and long radial fibers projecting to the basal surface. RGC undergo asymmetric cell divisions, giving rise to one RGC and either one immature neuron (IN) or an intermediate progenitor (IP). IP can further divide to give rise to neurons. Both NEC and RGC are considered as neural stem cells and are retained in the ventricular zone, close to the neural tube lumen (Alvarez-Buylla et al., 2001; Malatesta and Götz, 2013). They share the expression of several molecular markers and both cell types undergo IKNM (Than-Trong and Bally-Cuif, 2015). On the other hand, apical progenitors within the spinal cord retain NEC features and might proliferate symmetrically or asymmetrically, and this is ultimately governed by long-range morphogen gradients across the DV axis (Ulloa and Briscoe, 2007; Saade et al., 2013; Le Dréau et al., 2014). Thus, neural stem cells change their competency as development proceeds, and the generation of neuronal heterogeneity relies on the adscription of distinct progenitor/neurogenic competence (Beattie and Hippenmeyer, 2017). To acquire organs of a specific robust size and cell composition during development requires tight coordination between the maintenance of neural stem cells and the acquisition of neurogenic capacity. The rates of cell differentiation and proliferation must be tightly coordinated and balanced: early on, extensive cell proliferation dominates to allow the tissues to grow; later on, the growth rate ceases (or almost ceases, depending on the tissue) as more cells differentiate and exit the cell cycle (for review see Blanpain and Simons, 2013). Furthermore, and remarkably, stereotyped tissue growth must occur despite large variability in proliferation rates (He et al., 2012). If we consider tissues such as the CNS, in which differentiated neurons have no proliferation capacity, it implies that coordinating cell division modalities is crucial for regulating the growth of the tissue. Thus, symmetric self-renewing divisions for expanding the stem cell niche, asymmetric divisions for maintaining the progenitor pool —through this process stem cells are continually lost and replaced—, and finally either symmetric neurogenic divisions or direct cell differentiation need to be properly balanced to generate the right final number of differentiated neurons (for recent review see Zechner et al., 2020). This is accompanied with changes in the relative spatial distribution of both progenitors and differentiated neurons during morphogenesis. Clonal analyses, which describe the derivatives of a single cell, provide insight into the mode of tissue growth and its regionalization. They reveal the diversity of cell behaviors that underlies progression along a lineage tree, which has led to the elaboration of conceptual frameworks for cell lineage analysis (Buckingham and Meilhac, 2011). Thus, if we want to elucidate how the CNS is built up, we need to strengthen our knowledge about (i) the dynamics of the different cell populations (e.g., how progenitor cell populations spatiotemporally allocate, what the division rates are, and in what proportions), (ii) the transitions and switches between different division modes, and (iii) the sequential transition from the progenitor recruitment to the final functional neuronal populations.

During development, neural stem cells actively proliferate and give rise first to neurons, and then to glial cells. Neurogenesis is initiated by proneural genes, which encode basic helix-loop-helix (bHLH) transcription factors that form homodimers or heterodimers through the HLH domain and bind to DNA targets through the basic region (Bertrand et al., 2002). They trigger the specification of neuronal lineages and commit progenitors to neuronal differentiation by promoting cell cycle exit and activating a downstream cascade of differentiation genes (Castro et al., 2011; for review see Guillemot, 2007). The first step toward achieving the cell diversity observed in adults occurs with the organization of neuronal progenitor cells into distinct domains in response to morphogen signals. Such patterning signals drive the expression of specific sets of transcription factors and subdivide the developing nervous system into discrete progenitor domains (Ribes and Briscoe, 2009; Cohen et al., 2013) assigning spatial and molecular identity to them. The assigned identity depends on the location of the progenitors in the neural tube, and the interpretation of the two-dimensional grid, along the AP and DV axes. The transcription factors expressed in response to patterning signals will control the final neuronal fate. Once neuronal progenitors are committed, they undergo neuronal differentiation, migrating away from the ventricular zone, and giving rise to differentiated neurons. Thus, the spatiotemporal control of this process is fundamental for generating functional neuronal networks, and to ensure progenitor availability for later stages it is crucial to regulate their division mode, their quiescent state, and the timing at which distinct pools of progenitors engage in neurogenesis.

Addressing how spatiotemporally controlled cell proliferation, specification, and differentiation occur alongside morphogenesis in the CNS has been technically challenging to date; no *in vitro* system can recapitulate this *in vivo* process, which involves an extraordinary well-orchestrated migration of differentiated neurons from their birth site as well as complex tissue morphogenetic movements. Thus, reconstructing cell lineages has proved to be central to comprehend how the wide diversity of cell types is generated. Now, we have a wide palette of novel imaging and large-scale transcriptomic technologies to address

this question. Next, we will briefly summarize them and discuss their advantages.

From Cell Lineage to Cell Diversity: Genetically Encoded Lineage Tools

Intertwined with the concept of cell lineage is that of cell commitment. Cell lineage follows the normal fate of a cell and its daughters, leading to the formulation of genealogical trees of cells with increasingly restricted cell fate choices as development proceeds. For many years, comprehensive lineage reconstructions had been possible only in lower invertebrates, such as the nematode *Caenorhabditis elegans* (Sulston et al., 1983), or in basic chordates as *Ciona intestinalis* (Tassy et al., 2006). However, recent technological developments have proved to be valuable to address the lineages of organisms with non-stereotypic development. By reconstructing different cell lineages, we can now determine the functional cell transitions that distinct cell populations undergo, the impact of morphogenesis in the spatial distribution of progenitor cells, and the dynamics of the whole cell population. In other words, they provide the cellular data to complement the well-described GRNs involved in cell specification and differentiation. Multiple efforts have been deployed to developing tools for cell lineage analysis. These tools can be classified into: (i) cell birth-dating, aimed to identify when cells are born; (ii) cell fate mapping, to reveal the developmental potential of progenitor cells at later developmental stages; (iii) clonal analysis, to decipher the derivatives from a progenitor cell; and (iv) cell lineage tracing, to describe the mitotic connections between two or more genealogically related cells, allowing the assessment of cell lineages and cell behaviors in the whole organ context. They can be applied either to single cells in a mosaic manner or to an entire cell population (Garcia-Marques et al., 2021).

Imaging-based strategies provide an excellent spatial resolution, allowing to determine genetic clonal relationships based on the mitotic history, such as twin-spot Mosaic Analysis with a Repressible Cell Marker (twin-spot MARCM) in the nervous system of Drosophila (Yu et al., 2009), or Mosaic Analysis with Double Markers (MADM) in mice (Zong et al., 2005; Gao et al., 2014). The first enables the visualization of sister-paired clones from the same progenitor in two different colors, while the latest, permits to identify different recombination events by single or combined segregation of two fluorescent proteins (GFP and RFP) in daughter cells, therefore enabling the tracing of such derivatives in a total of three colors (green, red, and yellow). To improve their limited clonal resolution, multicolor labeling tools such as Confetti (Snippert et al., 2010), Brainbow (Livet et al., 2007; Weissman et al., 2011; Cai et al., 2013), StarTrack (García-Marqués and López-Mascaraque, 2013; Figueres-Oñate et al., 2016) or MAGIC (Loulier et al., 2014), rely on a stochastic and combinatorial expression of different fluorescent reporter genes induced by recombinases, which results in the generation of multiple color hues that label clonally related cells in the same color palette (for detailed reviews on cell lineage tools, both imaging and sequencing-based, see Espinosa-Medina et al., 2019; Figueres-Oñate et al., 2020; Garcia-Marques et al., 2021). Although the development of such multicolor strategies has been a major step forward in the cell lineage tracing field, they are not scalable, and in many cases they do not provide temporal resolution.

Noteworthy, the development of high-resolution 4D imaging paired with Light Sheet Fluorescence Microscopy (LSFM) using zebrafish transgenic embryos set up the path for understanding early embryonic development and assess cell lineages and behaviors at high spatiotemporal coverage and resolution (Keller et al., 2008; Olivier et al., 2010; Luengo-Oroz et al., 2011; Keller and Ahrens, 2015; Dyballa et al., 2017). This was accompanied with the development of cell-tracking tools, instrumental to reconstruct cell lineages and cell rearrangements upon time (Amat et al., 2014; Faure et al., 2016; Wolff et al., 2018; Wan et al., 2019). Although this approach provides valuable temporal information about cell lineages —and therefore cell hierarchies— in the context of the whole cell population, they are not scalable and need high computing power and specific *know-how* for the tracking analyses.

In addition to these imaging-based cell lineage tools, the development of CRISPR/Cas and the high-throughput and highspeed sequencing revolution have pushed forward the emergence of sequencing-based lineage strategies, which enable the establishment of cell connections upon unique genomic landmarks, also known as barcodes. Whether it is by Cas9/sgRNA induced genomic mutations (Cotterell et al., 2020; CARLIN, Bowling et al., 2020; ScarTrace, Alemany et al., 2018; LINNAEUS, Spanjaard et al., 2018) or by the insertion of exogenous arrays of DNA with multiple and inducible CRISPR/Cas target sites such as scGestalt (McKenna et al., 2016; Raj et al., 2018), barcoding tools label individual cells with a unique combination of scarred sequences. This cumulative stochastic barcode editing provides a unique DNA scar combinatory that will prevail in derivative cells, while adding up new generated ones. This enables the "tracing" of such derivatives after a transcriptomic analysis, using pseudo-time scales to generate cell trajectories and infer relationships between progenitor cells and their progeny. Similarly, other methods such as MEMOIR by engineered Mutagenesis with Optical *In situ* Readout, asses trajectories by combining barcoding elements and sequential rounds of multiplexed *in situ* hybridization (Frieda et al., 2017). Its improved version intMEMOIR goes further allowing the differentiation between cellular states due to the higher number of integrated barcode combinations as the result of the array's inversion after genomic recombination (Chow et al., 2021). Although these strategies provide valuable single-cell transcriptional signature maps and atlases, the barcoding and omics combination still fails to represent cell behavior at the tissue level, neither provides cell division rates nor kinetics. Moreover, no functional relationships (circuits) are obtained.

To overcome such limitations, there is an urgent need for 4D tools that allow cell lineage relationships and temporality within the morphological context to be scalable. A few strategies have recently emerged that comply with the requirements of such need. One of these is CLADES (Cell Lineage Access Driven by an Edition Sequence), a genetic tool in Drosophila that enables cell lineage tracing coupled with birth-dating information. It

is based on the sequential activation of a cascade of different reporters in progenitor cells by CRISPR/Cas9 induction, which are inherited by their differentiated progeny. This enables the cell lineage tracing without losing the temporal input, since early born and late-born cells will be labeled in different colors of the reporter cascade (Garcia-Marques et al., 2020). However, while clonal resolution is not an issue in Drosophila with a few and highly stereotypic lineages, cell lineages in vertebrates remain incompletely characterized due to the higher tissue complexity and the larger size of embryos. Therefore, there is still the demand to incorporate new strategies that couple temporal and clonal information preserving the anatomical context to fill the remaining gap between cell biology and genetic determinism. To strengthen the importance of such factors in a tissue context, in the next section we discuss how time and space shape differently two paradigmatic structures of the CNS, the brain cortex and the spinal cord.

THE TWO PARADIGM MODELS FOR TISSUE GROWTH IN THE CENTRAL NERVOUS SYSTEM: THE SPINAL CORD AND THE BRAIN CORTEX

The CNS is comprised by morphologically different regions that become adult functional structures distinct in cell type composition and shape. Such structures are 4D developmental landscapes in which both the spatial coordinates and the temporal component are determining factors for the proper acquisition of cell types and numbers. Despite the impressive progress over the past decades, the comprehension of how billions of neurons come together to form the nervous system and enable function and behavior is still largely unknown. Two well-studied examples of intrinsically different structures of the CNS are the brain cortex and the spinal cord. While the first evolves from a relatively simple-layered neural tube to a complex structure with bulges and grooves, the oval embryonic spinal cord undergoes a volume scale-up with no dramatic change of form. Thus, the requirements for coordinating cell specification and morphogenesis are expected to differ. In this section, we contrast the biology of both paradigms and discuss several studies that demonstrated the role of cell position and time on cell specification, cell fate, and tissue growth.

Position (and Time) Determines Neural Identity and Growth in the Spinal Cord

The characterization of the adult spinal cord according to morphology, molecular markers, neuronal connectivity and axonal projections revealed a modular organization with stereotypical position of specific neurons (Sagner and Briscoe, 2019). During spinal cord formation, long-range morphogen signals emanating from the roof and floor plates pattern the tissue along the DV axis by regulating cell fate through transcription factor expression. This transcription factor code defines 11 molecularly distinct neural progenitor domains –six dorsal and five ventral–, each of which gives rise to one or more different neuronal subtypes (Alaynick et al., 2011; Lu et al., 2015). As development proceeds, progenitors in each domain specify in a spatiotemporally ordered manner and either amplify, or give rise to the corresponding type of post-mitotic neurons (Jessell, 2000; Dessaud et al., 2008; Le Dréau and Martí, 2013). Thus, the stereotypical position of cells –and the spatial regulation of gene expression– is crucial in the formation of neuronal circuits. However, several large-scale molecular profiling studies provided catalogs of gene expression, revealing a higher complexity of cell types (Delile et al., 2019; Rayon and Briscoe, 2021). For instance, single-cell RNA-sequencing experiments in mice embryonic and adult spinal cord suggest the existence of at least several dozen of molecularly different neuronal subtypes (Delile et al., 2019). This reveals the sequential upregulation or induction of sets of transcriptions factors that underpin the identity of the derivative arising neurons, generating a temporal stratification of neuronal subtypes from each domain. Thus, complementary to the positioning, time also plays a role in neuronal identity acquisition and in the generation of neuronal diversity (Sagner and Briscoe, 2019).

In the spinal cord, distance from the DV poles seems to dictate progenitor competence since neural progenitors acquire distinct identities in response to opposing morphogen gradients (Jessell, 2000; Ribes and Briscoe, 2009; Le Dréau and Martí, 2013). These morphogens, Sonic hedgehog (Shh) ventrally and Bone Morphogenetic Proteins (BMP) and Wnts dorsally, induce the expression of several homeodomain and bHLH transcription factors in discrete domains along the DV axis (Kutejova et al., 2016). Since their combinatorial expression confers neuronal identity to progenitors, they are exquisitely regulated. They cross-regulate forming a well-defined GRN accountable for the response to morphogen gradients by modular enhancers (Peterson et al., 2012; Oosterveen et al., 2013). During neurogenesis, the spinal cord continues to grow along its DV axis and expand the mantle zone with the differentiated neurons, raising the questions of how discrete progenitor domains and specific gene expression territories remain stable and scalable upon being challenged by cell proliferation and how DV patterning and neurogenesis are intertwined. Lately, a two-phase model has been proposed for explaining the growth and patterning of the spinal cord (Kicheva and Briscoe, 2015). The pattern of neuronal progenitor domains would be established at early developmental stages, when the position of a cell within the morphogen gradients grid can be precisely decoded (Sagner and Briscoe, 2019). These progenitors would maintain certain cell plasticity such as they could switch identities (Dessaud et al., 2007, 2010), facilitating the transition along different progenitor states. Upon tissue growth, the pattern of progenitor domains would be maintained by GRN cross-repressive interactions and unequal neuronal differentiation rates would determine domain sizes (Kicheva et al., 2014). However, how the neuronal differentiation dynamics of different progenitor populations is regulated has not been revealed. Interestingly, the regulatory programs and neuronal cell types are highly similar in different vertebrates, despite the distinct developmental time scales across species. Differences in protein turnover play a role in interspecies differences in the tempo

of motoneuron differentiation (Rayon et al., 2020); however, whether similar mechanisms may operate to specifically regulate the differentiation rate of the distinct progenitor domains is not known yet.

Dynamics of morphogen signaling and cell division mode have been linked in the spinal cord, since the onset of neurogenesis in dorsal interneurons and ventral motoneurons is controlled by BMP/SMAD- and Shh-signaling, respectively (Saade et al., 2013; Le Dréau et al., 2014). As example, in motoneuron progenitors (MNp) Shh maintains self-expanding symmetric proliferative divisions, while preventing progenitors from switching to neurogenic divisions. A reduction in Shh activity results in reduction of symmetric proliferative cell divisions, coinciding with the developmental time of motoneuron generation (Saade et al., 2013, 2017). While clones of the MNp domain grow equally in both axes, the rest of the domains show more elongated cell clones in DV, resulting in an inferior net growth rate DV/AP (Kicheva et al., 2014). A 3D computational simulation of the spinal cord DV growth shows that the differences in the spread and shape of MNp clones, and the isotropic growth, can be explained by the higher differentiation rate of these progenitors (Kicheva et al., 2014; Guerrero et al., 2019). Overall, these studies demonstrate that DV progenitor position influences proliferative capacity, cell fate and growth in the spinal cord. However, they do not explain why MNp differentiate at a higher rate than progenitors in adjacent domains. As neurons differentiate, they delaminate toward the mantle zone. This active displacement of neurons shapes the spinal cord in such a manner that progenitor cells are kept in the ventricular zone and differentiated neurons allocate in the adjacent medial domain, and the tissue grows without dramatic morphogenetic changes.

In several systems temporal cues regulate neuroblast competence –and therefore expansion of neural diversity– by specifying distinct neuronal fates using combinatorial temporal patterning (Bayraktar and Doe, 2013). In the spinal cord, the birth order of neurons also underlies specificity in neuronal connectivity and circuit formation (McArthur and Fetcho, 2017; Pujala and Koyama, 2019; Wan et al., 2019). As previously mentioned, several works have stressed the importance of the temporal transcription factor code for subdividing neurons through the DV axis (Delile et al., 2019). Although these results suggest that the temporal transcriptional factor code is functionally important, it seems that temporal cues would work within a given neuronal population to help to expand its diversity. Thus in the spinal cord, the precise position of neural progenitors serves as a functional ground for neuronal subtype determination.

Similar to other regions of the CNS, neural progenitors in the spinal cord give rise first to neurons and later to glial cells. This temporal switch relies on the sequential induction of SoxE and NFI factors and is regulated by several signaling pathways (Deneen et al., 2006; Kang et al., 2012). As an example, studies in zebrafish embryos demonstrate that motoneurons and oligodendrocytes emerge from the same ventral progenitor domain, the MNp (Zannino and Appel, 2009; Esain et al., 2010). In mice, most of the oligodendrocytes are generated after motoneurons in a Shh-dependent manner (Soula et al., 2001; Fogarty et al., 2005). However, 5% of the total population arises in a Shh-independent manner from a dorsal Dbx1-expressing region at early postnatal stages and distribute to the lateral white matter, radially opposite to their site of origin. In contrast, pMN-derived oligodendrocyte cells usually distribute in the gray matter (Fogarty et al., 2005). Similarly, DV position also determines the astrocytic subtype since the expression of *Pax6* and *Nkx6.1* confers positional identity defining three distinct astrocyte subpopulations. Each of these progenitor domains displays a specific code for Reelin and Slit guidance molecules, resulting in a correlation between the origin of astrocyte subtype and their final position within the neural tube (Hochstim et al., 2008). Thus, in oligodendrocytes and astrocytes, both birth-dating and DV position within the spinal cord influence their final location within the adult structure.

Time Determines Neural Identity and Growth in the Brain Cortex

Since Cajal's descriptions of the brain cortex cytoarchitecture and laminar distribution, the development of clonal analysis and cell lineage tools has fastened and accurately unveiled its organization and composition. The cerebral cortex evolves from a dense and packed single cell sheet composed solely by progenitors –the embryonic forebrain– to a stratified tissue remarkably conserved across most mammals. The neocortex is organized into six distinct layers, each of them with neuronal heterogeneity that emerges from sequentially born progenitors. The ventricular zone (VZ) harbors the soma of progenitor cells, followed by the subventricular zone (SVZ) as the main area of cell amplification. The cortical plate consists of several cell layers that sequentially accumulate on top (LI-LVI, being LI the uppermost and LVI the deepest layer), in an 'inside-out' manner, where early born neurons locate in deep layers, whereas newly born neurons migrate and position in upper layers (Angevine and Sidman, 1961; Rakic, 1974; Takahashi et al., 1999). In contrast, their glial counterparts organize in a stochastic manner along the apicobasal extent of the cortical plate (Zhang X. et al., 2020).

Neuroepithelial cells are the early progenitors populating the VZ, which divide in a symmetric proliferative manner prior to neurogenesis (Subramanian et al., 2017). As neurogenesis starts, NEC transition to RGC that are classically defined by the combination of several features: (i) an elongated morphology with contacts in the apical and basal surfaces of the neuroepithelium; (ii) the maintenance of the apicobasal polarity, (iii) the expression of astroglial markers such as glutamate transporter (GLAST) (Hartfuss et al., 2001), glial fibrillary acidic protein (GFAP), glutamine synthase (GS), and brain-lipid-binding protein (BLBP) (Feng et al., 1994; Arellano et al., 2021). Nascent RGC may undergo symmetric proliferative cell divisions to expand the progenitor pool, and later they transition into the neurogenic state and asymmetrically divide, thereby producing a self-renewed RGC and a differentiated cortical neuron (Noctor et al., 2004). Ventricular RGC might as well give rise to one RGC and either an IP or to another progenitor type, the basal radial glial cell (bRGC) (Miyata et al., 2001; Haubensak et al., 2004;

Noctor et al., 2004) that migrates to the SVZ becoming the major contributor to neuronal diversification (for reviews see Huttner and Kosodo, 2005; Penisson et al., 2019). These bRGC differ from apical RGC in their retraction of the ventricular processes before their division (Miyata et al., 2001), and in their division mode, since they usually generate either two bRGC by symmetric proliferative division or two daughter neurons by symmetric differentiative division (Haubensak et al., 2004; Noctor et al., 2004).

By consecutive waves of neurogenesis, distinct cortical layers are formed in the 'inside-out' fashion (for reviews see Rakic, 2009; Taverna et al., 2014; Hansen et al., 2017). Despite its pluripotency, cortical RGC undergo a progressive fate restriction over time (Desai and Mcconnell, 2000), since they lose the capacity to generate deep cortical layer neurons, limiting their derivatives to upper layers (McConnell and Kaznowski, 1991; Frantz and McConnell, 1996). Most clonal analysis studies suggest that the RGC behavior can be predictable across all developmental stages. RGC in the neurogenic phase do not undergo terminal differentiation in a stochastic manner but rather follow a defined non-random program of cell cycle exit resulting in eight to nine neurons produced by one RGC (Gao et al., 2014). In the same line, MADM clones induced in RGC at later developmental stages, right before the onset of gliogenesis, show more neurons in the upper layers (Zhang X. et al., 2020). Similarly, other studies demonstrate that as more fate restricted the cortex progenitor cells are, less neuronal cell types they are able to generate. For instance, when IP are early targeted, the derived neurons locate mainly in deeper layers instead of covering the entire translaminar area (Mihalas and Hevner, 2018); when they are targeted even later in development, they mainly produce neurons that locate in upper layers instead (Tarabykin et al., 2001). These results indicate that RGC constitute a pretty homogeneous cell population. However, a recent report shows that a limited number of progenitors display a stochastic neuronal output to account for the diverse clone types (Llorca et al., 2019). When they map the lineage of genetically labeled progenitor cells focusing on progenitors that start generating neurons early during development, they observe that early born neurons locate in deep layers as expected, and that a substantial group of neurons are confined either to the deep or superficial layers. They propose that heterogeneous lineage configurations can arise directly from neurogenesis and contribute to diverse neuronal types (Llorca et al., 2019). Overall, these observations suggest that the laminar position allows a crude classification of projection neurons and dictates their connectivity, although the progenitor population might not be so homogeneous.

Radial glial cells can also produce glial cells, both astrocytes and oligodendrocytes, which organize dispersedly along the apicobasal extent of the cortical plate. Once the neurogenic capacity of the remaining progenitors decreases, intrinsic and extrinsic signals set the start of gliogenesis (for review see Kessaris et al., 2008). However, the mechanisms of lineage progression from neurogenesis to gliogenesis remain largely unexplored. Astrocytes arise few days later than neurons as the result of remaining RGC detaching from apicobasal poles and retracting their projections (Noctor et al., 2004). Although astrocytes show some layer-specific features (Lanjakornsiripan et al., 2018; Batiuk et al., 2020), a clonal analysis study using MAGIC Markers combinatorial labeling, demonstrates that astrocytes do not follow an 'inside-out' pattern; instead, they distribute along the cortical area and acquire their fate in a stochastic manner (Clavreul et al., 2019; Zhang X. et al., 2020). It is well known that oligodendrocytes arise from both NG2-positive (Mo and Zecevic, 2009) and NG2-negative (Gensert and Goldman, 2001) oligodendrocyte progenitor cells; however their birth-date is still unclear. There are several reasons for this such as (i) oligodendrocytes found in the cortex are a result of competing waves emanating both locally and from other brain areas (Spassky et al., 1998; He et al., 2001; Tekki-Kessaris et al., 2001; Gorski et al., 2002; Kessaris et al., 2006), and (ii) fully differentiated and functional myelinating oligodendrocytes maturate during postnatal stages (for reviews on intrinsic and extrinsic factors driving oligodendrocyte development and maturation see Meijer et al., 2012; Baydyuk et al., 2020). Neuronal layer inversion studies suggest oligodendrocytes indeed need the correct sequential positioning of neurons to acquire their characteristic asymmetric distribution along the cortical area (Tan et al., 2009). Thus, temporal cues regulate the successive generation of layered postmitotic neurons and glial cells. Although we have a framework for RGC lineage progression, there are still open questions such as (i) how heterogenous the pool of RGC is, (ii) whether deterministic and stochastic modes of neuronal production coexist, and (iii) how cortex morphogenesis and cell fate acquisition are coordinated.

Recent advances have challenged that time and spatial location are the main determining factors for cell specification and cell fate acquisition for the generation of cell diversity in the CNS. High-throughput transcriptional profiling studies have allowed the envisioning of new horizons for cell characterization based on their individual RNA profile and challenged the "cell fate" concept proposing cellular state as the accurate terminology (**Figure 1A**). This brings on the table an open debate that goes beyond nomenclature: cell fate or cell state?

CELL FATE VERSUS CELL STATE: THE NEVER-ENDING DEBATE

In recent years, new powerful and high-resolution methods such as single-cell transcriptomics and single-cell barcoding lineage tracing have challenged the classical lineage tree view, where stem cells have unlimited potential and each of the multiple progenitor populations have a predetermined fate. It is becoming increasingly apparent that cells have the bias toward a certain fate, while progenitor populations display certain plasticity. Therefore, the idea of a differentiation tree in which the stem and progenitor populations are separated and differentiation occurs as discrete steps along the tree is changing to a model where differentiation is a continuous process, with stem and progenitor cells being biased toward a certain fate. Currently, this is extensively debated in the hematopoietic system, which has long served as a model for stem-cell research (Laurenti and Göttgens, 2018), and it is suggested that this scenario could be

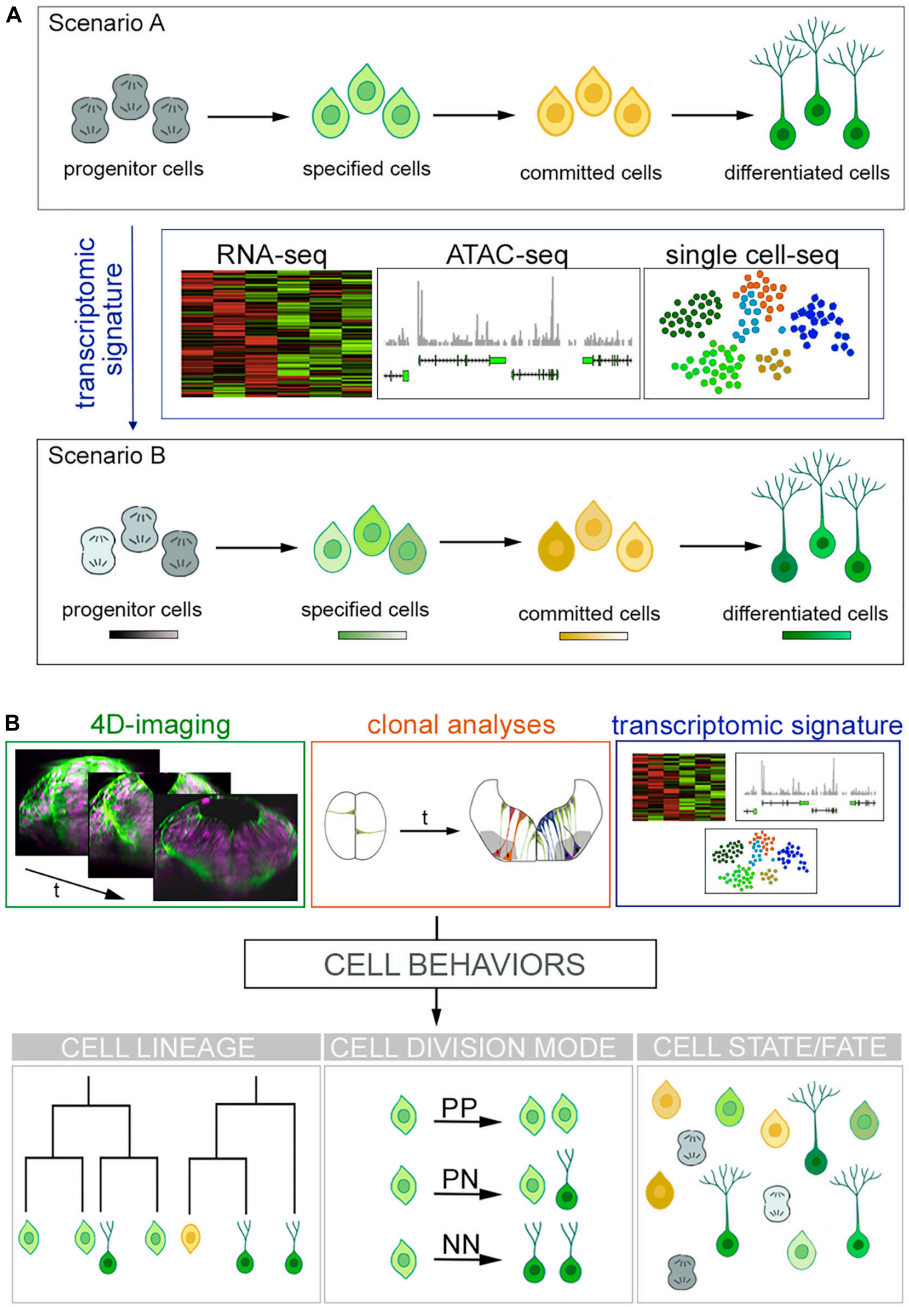

FIGURE 1 | Cell fates vs. cell states and new approaches for cell lineage reconstruction. **(A)** Overview of the current scenarios for cells progressing toward differentiation. Scenario A shows progenitor cells transitioning toward specification and commitment to finally differentiate. New high-throughput sequencing technologies (RNA-seq, ATAC-seq, and single cell sequencing) produce large volumes of data providing transcriptomic signatures. This unveils the emergence of different cell states within a cell fate depicted as color hues in Scenario B. **(B)** Future challenges to comprehend how cells acquire their fate. Next generation tools might blend big data provided by (i) 4D imaging that informs us about cell hierarchies and behaviors (see transverse views of zebrafish hindbrain over time; cell nuclei are in magenta and plasma membranes in green), (ii) clonal analyses, which informs about tissue growth; and (iii) transcriptomic signatures telling us about GRN in order to fill the gap between genetic determinism, cell behavior and cell fate while keeping the morphological context. The best scenario would be to blend such amount information in order to understand cell behaviors and to generate full cell lineages.

shared in the CNS. Indeed, broad sampling of different CNS territories using single-cell transcriptional profiling allows us to monitor global gene expression in thousands of individual cells. This enables the identification of wider progenitor cell types than previously recognized, and provides an extraordinary molecular characterization. The use of these big data approaches and the ability of integrating them with the cellular and genomic data, are the challenges to overcome in order to transform the biological

knowledge into useful insights for treating the neurological disorders (Briscoe and Marín, 2020).

Cell Fate Versus Cell State of Neural Cells

As previously stated, new technological approaches mainly based in single-cell molecular profiling elicit new arguments about what a cell type is. Cell types are the basic building blocks of multicellular organisms, determined and maintained by gene regulatory programs; however, cell type classification schemes remain ambiguous (Arendt et al., 2016). A classic discrete cell type categorization from progenitor cells to their differentiated derivates has been challenged lately as such description considers that cells follow discrete steps in a linear path to acquire their fate. Instead, it has been suggested cells navigate through different states toward differentiation (**Figure 1A**). Conceptually, cell fate comprises the future identity of a cell and it is determined by multiple factors such as gene expression, cell–cell interactions and external cues –both mechanical and biochemical. Therefore, cell fate would be the discrete and final step that defines the type of a cell. In contrast, the state of a cell implies a temporary feature, as it undergoes transitions over time from a starting point in space to the next one in a continuum of a dynamic system. Such scenario is usually envisioned as a space of states (Trapnell, 2015) and has recently become one of the most fervent debates in biology (see Clevers et al., 2017 for disparate views on cell identity, cell fate and cell state concepts).

Although a cell type is characterized by morphology, function, position and gene expression, even homogeneous cell type populations display high heterogeneity in their transcriptional profile. The current challenges biology faces are the untangling and the interpretation of this heterogeneity at the individual cell level, and for this, many genetic and transcriptomic profiles are carried out to characterize individual cell signatures. Posterior cell clustering and mapping of such libraries identify intermediate cell states, as single cells with a similar transcriptomic profile are likely to be closely related. However, the question poses: can we predict from the transcriptome of a progenitor cell, the identity, connectivity and function of their derivatives?

Several studies have reported the existence of transitory cell states within the CNS using these approaches. For instance, single-cell RNA-sequencing analysis of FACS sorted cortical apical progenitors identifies different transcriptional states according to the pseudo-developmental stage (Telley et al., 2019). While at early mice embryonic stages apical progenitors are characterized by the expression of genes related with cell intrinsic transcriptional programs, at later stages they progress to a more environmental-sensing transcriptomic signature, which already suggests that environmental cues may play a key role in refining the neuronal heterogeneity arising from cortical apical progenitors (Telley et al., 2019). In the zebrafish hindbrain, a single-cell RNA-sequencing study at different embryonic patterning stages identified discrete cellular states that differ on their transcription factor expression, and recapitulate the transition of progenitors to neuronal differentiation (Tambalo et al., 2020). This can suggest that cells display different competence states, and/or the existence of a heterogeneous progenitor pool. Barcoding systems have contributed exponentially to the untangling of new cellular states in the CNS by generating cell trajectories (Raj et al., 2018), although in none of the cases cell hierarchies could be established. As we discussed in Section "Framing the question: progenitor cells vs. differentiated neurons" of this review, the impact of single-cell transcriptomics on the characterization of gene programs for neuronal diversification is undeniable; however, these tools are based solely on transcriptomic signatures with neither spatial organization nor cell–cell contact inputs since they require tissue dissociation. Moreover, since they rely on pseudo-time parameters they lack the developmental history of cells, raising the question of whether cell identity can be defined by a single signature pattern of gene expression. Although the integration of imaging approaches that maintain the 3D tissue conformation might solve the first issue, such as MERFISH (Chen et al., 2015; Zhang M. et al., 2020) or STARmap (Wang et al., 2018), these trajectory-based assays alone are not sufficient to capture the intricacy of such dynamic systems.

These high-resolution data approaches provide an unprecedented level of detail and are indeed revolutionizing the study of CNS development. They demonstrate (again) that complexity is build up during embryonic development, and suggest that once "crude cell fates" are established, the final cell identities are refined upon time with cells transitioning through different cell states. In other epithelial systems, stem cells constitute a heterogeneous compartment in which cells transit reversibly between different states of competence (Blanpain and Simons, 2013). The big leap forward would be to combine cell lineage, developmental cell trajectories, and molecular mechanisms, to comprehend how neuronal diversity arises. Most importantly perhaps, if dynamic cellular features are predictable at a population rather than single-cell level, understanding the emergent properties of cell populations instead of by the detailed account of their individual components should be considered to address the emergence of functional circuits during embryogenesis.

Pools of Progenitors and Quiescent Stem Cells

If this scenario was not complex enough, the CNS harbors groups of cells that display a different progenitor behavior, such as (i) progenitor pools that engage into neurogenesis at different times, and (ii) quiescent progenitor cells, which are out of the cell cycle progression and more commonly found in adult stages. Their presence and long-term maintenance are crucial for the acquisition of tissue cell diversity, survival and regeneration after injury (for reviews on quiescence see Cheung and Rando, 2013; Cho et al., 2019; van Velthoven and Rando, 2019). Interestingly, such differences between progenitors are not always evident at a molecular level, thus, the transcriptional signature becomes a powerful distinction tool to assess state differences. Although usually considered dormant, quiescent cells require an active and complex regulation, thus, considering quiescent or active neural stem cells as binary fates or binary cell states is incorrect. In fact, there is a gray scale of states in which the so called primed neural stem cells –in a less deep quiescent state– are able to revert their

"dormancy" to activate and contribute to adult neurogenesis, being able to return to quiescence after their contribution (Sueda et al., 2019; Urbán and Cheung, 2021).

In the mouse forebrain, for instance, barcoding studies revealed that progenitors in a dormant state upregulate genes related with their ability to keep in their adult quiescent niche, which differentiate them from their active counterparts. Also, although quiescent progenitors from different forebrain regions maintain the transcriptional hallmarks of their specific embryonic ancestor cells, once they reacquire an active state they cluster together showing a similar transcriptomic signature and favoring the same neuronal type production (Borrett et al., 2020). This illustrates that different cellular transitory states might result in the same final fate. Such transcriptional hallmarks acquired during embryogenesis and shared at later developmental stages, have also been reported in the zebrafish brain (Raj et al., 2018). On a similar note, a clonal analysis approach demonstrates that adult neural stem cells of the mouse cortex arise from progenitors already specified at early embryonic stages (Fuentealba et al., 2015; Furutachi et al., 2015). These results raise some inevitable questions: is there such thing as a progenitor fate? If we understand fate as the final state of a cell, and considering quiescent cells might eventually reactivate upon environmental requirements, one could argue that in this case there is no such thing as a progenitor fate and the terminology "steady-state" might be more accurate. On top of that, the previously mentioned evidences on cell trajectories and cell lineage tracing, linking progenitor cells with adult quiescent neural stem cells at a transcriptomic and molecular levels, denote a putative cell fate or "steady-state" determination from birth. What brings another question for open discussion: is cell fate determined, or is this a stochastic process?

Cell Fate Decisions: Stochasticity Versus Determinism

A long-standing question in developmental neurobiology is to determine how cell diversity arises from groups of "equivalent" progenitor cells. Understanding how cell fate choices are made is crucial to comprehend the spatiotemporal dynamics of tissue and organ formation and to predict cell behaviors. Waddington's analogy of cells represented as bowls rolling down valleys in a downhill landscape is one of the most well-known examples of cell fate decision-making in a dynamic system (Waddington, 1957). The path to two different states or fates is illustrated as branching valleys and it represents fate choices in a cell's endeavor, not mitotic events. This model, referred as well as *the epigenetic landscape*, proposes that a cell's potential for development, meaning the down-path it takes, is marked by groups of genes or biochemical interactions, already speculating about the GRN control of cell fate decision (for reviews see Enver et al., 2009; Fagan, 2012). Waddington's landscape model is general, qualitative, and although portraits the concept of cell competence, it does not provide the 3D-positional input within the tissue, or it considers intermediate cell states between one decision and the next. It implies bowls (cells) that go down chosen valleys (fate decision) cannot go back to the previous position once they are committed. It does not resolve if the decision of choosing a developmental path (to go through the different valleys) is stochastic or already determined. Since Waddington's theory, several genetic fate mapping studies in combination with mathematical models have tried to tackle this issue in specific structures (for review see Zechner et al., 2020). While there is no debate around the vast heterogeneity harbored in the CNS, there is not a single view in the generation and acquisition of such cell type variety. While some lines of research suggest it must correlate with progenitor subtype diversity –implicating fate is determined before differentiation–, other studies suggest that the brain may harbor multipotent progenitors whose decision of generating different fates is merely stochastic.

One of the best studied cases is the brain cortex (see section "The two paradigm models for tissue growth in the central nervous system: the spinal cord and the brain cortex"). In the recent years the technological advances in single-cell transcriptomes led to revisit the knowledge on cortical projection neuron heterogeneity and its ontogeny (Briscoe and Marín, 2020). A genetic fate mapping study on a subset of RGC demonstrates that the murine cerebral cortex contains RGC sub-lineages with distinct fate potentials. Using *in vivo* genetic fate mapping and *in vitro* clonal analysis, they identify a Cux2-positive RGC lineage intrinsically specified to generate only upper-layer neurons, independently of niche and birthdate. Interestingly, when forced to exit earlier the cell cycle, the outcome is also specific for upper layer neurons, indicating these RGC progenitors already specified to generate upper layer neurons regardless of birthdate were intrinsically programmed to generate neurons predominantly later than their lower layer counterparts (Franco et al., 2012). Thus, this study indicates that molecular fate specification ensures proper birth order, rather than vice versa. In this same line, a MADM clonal analysis on RGC progenitors revealed that all progenitors give rise to eight to nine neurons in a reproducible way, and that after this stereotyped neuronal generation, glial cells are produced. Such behavior was interpreted as a deterministic neural fate acquisition pattern (Gao et al., 2014). However, Guo et al. (2013) demonstrated the existence of multipotent neocortical progenitors. Genetic fate mapping of Cux2-positive RGC shows that they sequentially generate both deep- and upper-layer projection neuron subtypes and glia. More recently, clonal analysis studies combined with mathematical models favored the existence of a stochastic acquisition of neuronal fates, challenging again the deterministic view. They developed mathematical models that could emulate their biological observations in mice cortex using MADM-induced clonal analysis, and the best fitting models suggested that indeed neurogenic fate decisions could be stochastic (Llorca et al., 2019). They proposed that the heterogeneity of neuronal fates in the cortex might be explained by the existence of two distinct progenitor cell populations, which would randomly generate the translaminar cell diversity across the cortical plate. These observations raise further questions such as (i) can the two progenitor subtypes be molecularly identified, (ii) do the stochastic events occur within progenitors or in the progeny, and (iii) what is the relative

final contribution of stochastic and deterministic processes (Klingler and Jabaudon, 2020).

The stochasticity in neurogenic fate decisions has also been shown in other CNS structures such as the adult zebrafish telencephalon (Than-Trong et al., 2020) and both zebrafish and *Drosophila*'s retina (Bell et al., 2007; He et al., 2012). Intriguingly, both cell fate decision mechanisms operate in the retina. Retinal progenitor cells have the same competence; however, extrinsic and intrinsic cues induce cell fate in a reproducible deterministic manner during embryonic development (for review see Cepko, 2014). Stochastic cell fate decisions are most abundant at early stages of retinal neurogenesis (He et al., 2012). By contrast, more deterministic division patterns become prominent late in embryonic development, probably because they often arise from a committed precursor, which gives rise to later born neurons. For instance, in zebrafish the assignment of Müller glial fate, a retina-specific RGC, has been shown to follow a deterministic pattern instead (Rulands et al., 2018). This is a clear illustration of how two distinct neural fates can be acquired following a different pattern within the same structure. Overall, these data suggest that generation of cell diversity cannot be explained by one model solely but instead might be better represented by a synergistic cooperation of stochastic and deterministic features.

FUTURE CHALLENGES

New technologies and large datasets are providing new perspectives on long-standing questions about the ontogeny, the composition, and the function of the cellular components of the CNS. However, the progress will depend not only on the improvement of acquisition and analytical capacity to process big amounts of data, but on their successful application to build up intellectual frameworks (**Figure 1B**). For the question of cell types/cell identities and cell fates/cell states, the prevailing view is that each type of neurons uses a specific set of features such as gene expression, morphology, position, neuronal activity, . . . to define cell identity, which are regulated by specific transcriptional signatures. This would be consistent with the idea that cell identity is defined by the specific gene expression programs executed by GRN (Davidson and Erwin, 2006). But is the knowledge of a neuron transcriptome sufficient to define its identity and predict the functional features? Probably not if we consider the role of cell hierarchies, and that morphologically different neurons located in either distinct or similar regions of the CNS can be transcriptomically similar. For instance, motoneurons from the hindbrain and the spinal cord are quite similar in terms of gene expression, but their ontology is different. Thus, cell lineage –and therefore the temporal component– is also likely to be an important feature to comprehend what cell type identity means. Can we reconstruct neurogenesis from birth to entire circuit at cell type and functional levels? Can we monitor the emergence of coordinated neuronal activity at single-cell level and see how circuits are build up upon development? Can we apply this knowledge to brain organoids derived from human iPS to mimic the spatial and temporal developmental landscapes for easier manipulation? And finally, can we create organs upon demand to substitute parts of the old ones?

AUTHOR CONTRIBUTIONS

CB-M and CP contributed to the concept, design, and writing of the review. Both authors contributed to the article and approved the submitted version.

FUNDING

This work was funded by grant PGC2018-095663-B-I00 from Ministry of Science and Innovation (MICIN), Agencia Estatal de Investigación (AEI) and Fondo Europeo de Desarrollo Regional (FEDER) to CP. DCEXS-UPF is a Unidad de Excelencia María de Maeztu funded by the AEI (CEX2018-000792-M). CB-M is a recipient of a predoctoral FPI fellowship from the MICIN. CP is a recipient of ICREA Academia award (Generalitat de Catalunya).

ACKNOWLEDGMENTS

The authors would like to thank the members of the lab for critical discussions and insight.

REFERENCES

Alaynick, W. A., Jessell, T. M., and Pfaff, S. L. (2011). SnapShot: spinal cord development. *Cell* 146, 1–7. doi: 10.1016/j.cell.2011.06.038

Alemany, A., Florescu, M., Baron, C. S., Peterson-Maduro, J., and Van Oudenaarden, A. (2018). Whole-organism clone tracing using single-cell sequencing. *Nature* 556, 108–112. doi: 10.1038/nature25969

Alvarez-Buylla, A., García-Verdugo, J. M., and Tramontin, A. D. (2001). A unified hypothesis on the lineage of neural stem cells. *Nat. Rev. Neurosci.* 2, 287–293. doi: 10.1038/35067582

Amat, F., Lemon, W., Mossing, D. P., McDole, K., Wan, Y., Branson, K., et al. (2014). Fast, accurate reconstruction of cell lineages from large-scale fluorescence microscopy data. *Nat. Methods* 11, 951–958. doi: 10.1038/nmeth.3036

Angevine, J. B., and Sidman, R. L. (1961). Autoradiographic study of cell migration during histogenesis of cerebral cortex in the mouse. *Nature* 192, 766–768. doi: 10.1038/192766b0

Arellano, J. I., Morozov, Y. M., Micali, N., and Rakic, P. (2021). Radial glial cells: new views on old questions. *Neurochem. Res.* 46, 2512–2524. doi: 10.1007/s11064-021-03296-z

Arendt, D., Musser, J. M., Baker, C. V. H., Bergman, A., Cepko, C., Erwin, D. H., et al. (2016). The origin and evolution of cell types. *Nat. Rev. Genet.* 17, 744–757. doi: 10.1038/nrg.2016.127

Batiuk, M. Y., Martirosyan, A., Wahis, J., de Vin, F., Marneffe, C., Kusserow, C., et al. (2020). Identification of region-specific astrocyte subtypes at single cell resolution. *Nat. Commun.* 11, 1–15. doi: 10.1038/s41467-019-14198-8

Baydyuk, M., Morrison, V. E., Gross, P. S., and Huang, J. K. (2020). Extrinsic factors driving oligodendrocyte lineage cell progression in CNS development and injury. *Neurochem. Res.* 45, 630–642. doi: 10.1007/s11064-020-02967-7

Bayraktar, O. A., and Doe, C. Q. (2013). Combinatorial temporal patterning in progenitors expands neural diversity. *Nature* 498, 449–455. doi: 10.1038/nature12266

Beattie, R., and Hippenmeyer, S. (2017). Mechanisms of radial glia progenitor cell lineage progression. *FEBS Lett.* 591, 3993–4008. doi: 10.1002/1873-3468.12906

Bell, M. L., Earl, J. B., and Britt, S. G. (2007). Two types of *Drosophila* R7 photoreceptor cells are arranged randomly: a model for stochastic cell-fate determination. *J. Comp. Neurol.* 502, 75–85. doi: 10.1002/cne.21298

Bertrand, N., Castro, D. S., and Guillemot, F. (2002). Proneural genes and the specification of neural cell types. *Nat. Rev. Neurosci.* 3, 517–530. doi: 10.1038/nrn874

Blanpain, C., and Simons, B. D. (2013). Unravelling stem cell dynamics by lineage tracing. *Nat. Rev. Mol. Cell Biol.* 14, 489–502. doi: 10.1038/nrm3625

Borrett, M. J., Innes, B. T., Jeong, D., Tahmasian, N., Storer, M. A., Bader, G. D., et al. (2020). Single-cell profiling shows murine forebrain neural stem cells reacquire a developmental state when activated for adult neurogenesis. *Cell Rep.* 32:108022. doi: 10.1016/j.celrep.2020.108022

Bowling, S., Sritharan, D., Osorio, F. G., Nguyen, M., Cheung, P., Rodriguez-Fraticelli, A., et al. (2020). An engineered CRISPR-Cas9 mouse line for simultaneous readout of lineage histories and gene expression profiles in single cells. *Cell* 181, 1693–1694. doi: 10.1016/j.cell.2020.06.018

Briscoe, J., and Marín, O. (2020). Looking at neurodevelopment through a big data lens. *Science* 369:eaaz8627. doi: 10.1126/SCIENCE.AAZ8627

Buckingham, M. E., and Meilhac, S. M. (2011). Tracing cells for tracking cell lineage and clonal behavior. *Dev. Cell* 21, 394–409. doi: 10.1016/j.devcel.2011.07.019

Cai, D., Cohen, K. B., Luo, T., Lichtman, J. W., and Sanes, J. R. (2013). Improved tools for the brainbow toolbox. *Nat. Methods* 10, 540–547. doi: 10.1038/nmeth.2450

Castro, D. S., Martynoga, B., Parras, C., Ramesh, V., Pacary, E., Johnston, C., et al. (2011). A novel function of the proneural factor Ascl1 in progenitor proliferation identified by genome-wide characterization of its targets. *Genes Dev.* 25, 930–945. doi: 10.1101/gad.627811

Cepko, C. (2014). Intrinsically different retinal progenitor cells produce specific types of progeny. *Nat. Rev. Neurosci.* 15, 615–627. doi: 10.1038/nrn3767

Chen, K. H., Boettiger, A. N., Moffitt, J. R., Wang, S., and Zhuang, X. (2015). Spatially resolved, highly multiplexed RNA profiling in single cells. *Science* 348:aaa6090. doi: 10.1126/science.aaa6090

Cheung, T. H., and Rando, T. A. (2013). Molecular regulation of stem cell quiescence. *Nat. Rev. Mol. Cell Biol.* 14, 329–340. doi: 10.1038/nrm3591. Molecular

Cho, I. J., Lui, P. P. W., Obajdin, J., Riccio, F., Stroukov, W., Willis, T. L., et al. (2019). Mechanisms, hallmarks, and implications of stem cell quiescence. *Stem Cell Rep.* 12, 1190–1200. doi: 10.1016/j.stemcr.2019.05.012

Chow, K.-H. K., Budde, M. W., Granados, A. A., Cabrera, M., Yoon, S., Cho, S., et al. (2021). Imaging cell lineage with a synthetic digital recording. *Science* 372:eabb3099. doi: 10.1126/science.abb3099

Clavreul, S., Abdeladim, L., Hernández-Garzón, E., Niculescu, D., Durand, J., Ieng, S. H., et al. (2019). Cortical astrocytes develop in a plastic manner at both clonal and cellular levels. *Nat. Commun.* 10, 1–14. doi: 10.1038/s41467-019-12791-5

Clevers, H., Rafelski, S., Elowitz, M., and Lein, E. (2017). What is your conceptual definition of "Cell Type" in the context of a mature organism? *Cell Syst.* 4, 255–259. doi: 10.1016/j.cels.2017.03.006

Cohen, M., Briscoe, J., and Blassberg, R. (2013). Morphogen interpretation: the transcriptional logic of neural tube patterning. *Curr. Opin. Genet. Dev.* 23, 423–428. doi: 10.1016/j.gde.2013.04.003

Collinet, C., and Lecuit, T. (2021). Programmed and self-organized flow of information during morphogenesis. *Nat. Rev. Mol. Cell Biol.* 22, 245–265. doi: 10.1038/s41580-020-00318-6

Cotterell, J., Vila-Cejudo, M., Batlle-Morera, L., and Sharpe, J. (2020). Endogenous CRISPR/Cas9 arrays for scalable whole-organism lineage tracing. *Development* 147:dev184481. doi: 10.1242/dev.184481

Davidson, E. H., and Erwin, D. H. (2006). Gene regulatory networks and the evolution of animal body plans. *Science* 311, 796–801. doi: 10.1126/science.1126454

Delile, J., Rayon, T., Melchionda, M., Edwards, A., Briscoe, J., and Sagner, A. (2019). Single cell transcriptomics reveals spatial and temporal dynamics of gene expression in the developing mouse spinal cord. *Development* 146:dev173807. doi: 10.1242/dev.173807

Deneen, B., Ho, R., Lukaszewicz, A., Hochstim, C. J., Gronostajski, R. M., and Anderson, D. J. (2006). The Transcription factor NFIA controls the onset of gliogenesis in the developing spinal cord. *Neuron* 52, 953–968. doi: 10.1016/j.neuron.2006.11.019

Desai, A. R., and Mcconnell, S. K. (2000). Progressive restriction in fate potential by neural progenitors during cerebral cortical development. *Development* 127, 2863–2872.

Dessaud, E., McMahon, A. P., and Briscoe, J. (2008). Pattern formation in the vertebrate neural tube: a sonic hedgehog morphogen-regulated transcriptional network. *Development* 135, 2489–2503. doi: 10.1242/dev.009324

Dessaud, E., Ribes, V., Balaskas, N., Yang, L. L., Pierani, A., Kicheva, A., et al. (2010). Dynamic assignment and maintenance of positional identity in the ventral neural tube by the morphogen sonic hedgehog. *PLoS Biol.* 8:e1000382. doi: 10.1371/journal.pbio.1000382

Dessaud, E., Yang, L. L., Hill, K., Cox, B., Ulloa, F., Ribeiro, A., et al. (2007). Interpretation of the sonic hedgehog morphogen gradient by a temporal adaptation mechanism. *Nature* 450, 717–720. doi: 10.1038/nature06347

Dyballa, S., Savy, T., Germann, P., Mikula, K., Remesikova, M., Špir, R., et al. (2017). Distribution of neurosensory progenitor pools during inner ear morphogenesis unveiled by cell lineage reconstruction. *eLife* 6:e22268. doi: 10.7554/eLife.22268

Enver, T., Pera, M., Peterson, C., and Andrews, P. W. (2009). Stem cell states, fates, and the rules of attraction. *Cell Stem Cell* 4, 387–397. doi: 10.1016/j.stem.2009.04.011

Esain, V., Postlethwait, J. H., Charnay, P., and Ghislain, J. (2010). FGF-receptor signalling controls neural cell diversity in the zebrafish hindbrain by regulating olig2 and sox9. *Development* 137, 33–42. doi: 10.1242/dev.038026

Espinosa-Medina, I., Garcia-Marques, J., Cepko, C., and Lee, T. (2019). High-throughput dense reconstruction of cell lineages. *Open Biol.* 9:190229. doi: 10.1098/rsob.190229

Fagan, M. B. (2012). Waddington redux: models and explanation in stem cell and systems biology. *Biol. Philos.* 27, 179–213. doi: 10.1007/s10539-011-9294-y

Faure, E., Savy, T., Rizzi, B., Melani, C., Stašová, O., Fabrèges, D., et al. (2016). A workflow to process 3D+time microscopy images of developing organisms and reconstruct their cell lineage. *Nat. Commun.* 7, 1–10. doi: 10.1038/ncomms9674

Feng, L., Hatten, M. E., and Heintz, N. (1994). Brain lipid-binding protein (BLBP): a novel signaling system in the developing mammalian CNS. *Neuron* 12, 895–908. doi: 10.1016/0896-6273(94)90341-7

Figueres-Oñate, M., García-Marqués, J., and López-Mascaraque, L. (2016). UbC-StarTrack, a clonal method to target the entire progeny of individual progenitors. *Sci. Rep.* 6:33896. doi: 10.1038/srep33896

Figueres-Oñate, M., Sánchez-González, R., and López-Mascaraque, L. (2020). Deciphering neural heterogeneity through cell lineage tracing. *Cell. Mol. Life Sci.* 78, 1971–1982. doi: 10.1007/s00018-020-03689-3

Fogarty, M., Richardson, W. D., and Kessaris, N. (2005). A subset of oligodendrocytes generated from radial glia in the dorsal spinal cord. *Development* 132, 1951–1959. doi: 10.1242/dev.01777

Franco, S. J., Gil-Sanz, C., Martinez-Garay, I., Espinosa, A., Harkins-Perry, S. R., Ramos, C., et al. (2012). Fate-restricted neural progenitors in the mammalian cerebral cortex. *Science* 337, 746–749. doi: 10.1126/science.1223616

Frantz, G. D., and McConnell, S. K. (1996). Restrictions of late cerebral corticl progenitor cells to an upper-layer fate. *Neuron* 17, 55–61. doi: 10.1016/s0896-6273(00)80280-9

Frieda, K. L., Linton, J. M., Hormoz, S., Choi, J., Chow, K. H. K., Singer, Z. S., et al. (2017). Synthetic recording and in situ readout of lineage information in single cells. *Nature* 541, 107–111. doi: 10.1038/nature20777

Fuentealba, L. C., Rompani, S. B., Parraguez, J. I., Obernier, K., Romero, R., Cepko, C. L., et al. (2015). Embryonic origin of postnatal neural stem cells. *Cell* 161, 1644–1655. doi: 10.1016/j.cell.2015.05.041

Furutachi, S., Miya, H., Watanabe, T., Kawai, H., Yamasaki, N., Harada, Y., et al. (2015). Slowly dividing neural progenitors are an embryonic origin of adult neural stem cells. *Nat. Neurosci.* 18, 657–665. doi: 10.1038/nn.3989

Gao, P., Postiglione, M. P., Krieger, T. G., Hernandez, L., Wang, C., Han, Z., et al. (2014). Deterministic progenitor behavior and unitary production of neurons in the neocortex. *Cell* 159, 775–788. doi: 10.1016/j.cell.2014.10.027

Garcia-Marques, J., Espinosa-Medina, I., Ku, K. Y., Yang, C. P., Koyama, M., Yu, H. H., et al. (2020). A programmable sequence of reporters for lineage analysis. *Nat. Neurosci.* 23, 1618–1628. doi: 10.1038/s41593-020-0676-9

Garcia-Marques, J., Espinosa-Medina, I., and Lee, T. (2021). The art of lineage tracing: from worm to human. *Prog. Neurobiol.* 199:101966. doi: 10.1016/j.pneurobio.2020.101966

García-Marqués, J., and López-Mascaraque, L. (2013). Clonal identity determines astrocyte cortical heterogeneity. *Cereb. Cortex* 23, 1463–1472. doi: 10.1093/cercor/bhs134

Gensert, J. M., and Goldman, J. E. (2001). Heterogeneity of cycling glial progenitors in the adult mammalian cortex and white matter. *J. Neurobiol.* 48, 75–86. doi: 10.1002/neu.1043

Gorski, J. A., Talley, T., Qiu, M., Puelles, L., Rubenstein, J. L. R., and Jones, K. R. (2002). Cortical excitatory neurons and glia, but not GABAergic neurons, are produced in the Emx1-expressing lineage. *J. Neurosci.* 22, 6309–6314. doi: 10.1523/jneurosci.22-15-06309.2002

Götz, M., and Huttner, W. B. (2005). The cell biology of neurogenesis. *Nat. Rev. Mol. Cell Biol.* 6, 777–788. doi: 10.1038/nrm1739

Guerrero, P., Perez-Carrasco, R., Zagorski, M., Page, D., Kicheva, A., Briscoe, J., et al. (2019). Neuronal differentiation influences progenitor arrangement in the vertebrate neuroepithelium. *Development* 146:dev176297. doi: 10.1242/dev.176297

Guillemot, F. (2007). Spatial and temporal specification of neural fates by transcription factor codes. *Development* 134, 3771–3780. doi: 10.1242/dev.006379

Guo, C., Eckler, M. J., McKenna, W. L., McKinsey, G. L., Rubenstein, J. L. R., and Chen, B. (2013). Fezf2 expression identifies a multipotent progenitor for neocortical projection neurons, astrocytes and oligodendrocytes. *Neuron* 80, 1–7. doi: 10.1016/j.neuron.2013.09.037.Fezf2

Hansen, A. H., Duellberg, C., Mieck, C., Loose, M., and Hippenmeyer, S. (2017). Cell polarity in cerebral cortex development—cellular architecture shaped by biochemical networks. *Front. Cell. Neurosci.* 11:176. doi: 10.3389/fncel.2017.00176

Hartfuss, E., Galli, R., Heins, N., and Götz, M. (2001). Characterization of CNS precursor subtypes and radial glia. *Dev. Biol.* 229, 15–30. doi: 10.1006/dbio.2000.9962

Haubensak, W., Attardo, A., Denk, W., and Huttner, W. B. (2004). Neurons arise in the basal neuroepithelium of the early mammalian telencephalon: a major site of neurogenesis. *Proc. Natl. Acad. Sci. U.S.A.* 101, 3196–3201. doi: 10.1073/pnas.0308600100

He, J., Zhang, G., Almeida, A. D., Cayouette, M., Simons, B. D., and Harris, W. A. (2012). How variable clones build an invariant retina. *Neuron* 75, 786–798. doi: 10.1016/j.neuron.2012.06.033

He, W., Ingraham, C., Rising, L., Goderie, S., and Temple, S. (2001). Multipotent stem cells from the mouse basal forebrain contribute GABAergic neurons and oligodendrocytes to the cerebral cortex during embryogenesis. *J. Neurosci.* 21, 8854–8862. doi: 10.1523/jneurosci.21-22-08854.2001

Hochstim, C., Deneen, B., Lukaszewicz, A., Zhou, Q., and David, J. (2008). The spinal cord contains positionally distinct astrocyte subtypes whose identities are specified by a homeodomain transcriptional code. *Cell* 133, 510–522. doi: 10.1016/j.cell.2008.02.046

Huttner, W. B., and Kosodo, Y. (2005). Symmetric versus asymmetric cell division during neurogenesis in the developing vertebrate central nervous system. *Curr. Opin. Cell Biol.* 17, 648–657. doi: 10.1016/j.ceb.2005.10.005

Jessell, T. M. (2000). Neuronal specification in the spinal cord: inductive signals and transcriptional codes. *Nat. Rev. Genet.* 1, 20–29. doi: 10.1038/35049541

Kang, P., Lee, H. K., Glasgow, S. M., Finley, M., Donti, T., Gaber, Z. B., et al. (2012). Sox9 and NFIA coordinate a transcriptional regulatory cascade during the initiation of gliogenesis. *Neuron* 74, 79–94. doi: 10.1016/j.neuron.2012.01.024.Sox9

Keller, P. J., and Ahrens, M. B. (2015). Visualizing whole-brain activity and development at the single-cell level using light-sheet microscopy. *Neuron* 85, 462–483. doi: 10.1016/j.neuron.2014.12.039

Keller, P. J., Schmidt, A. D., Wittbrodt, J., and Stelzer, E. H. K. (2008). Reconstruction of zebrafish early embryonic development by scanned light sheet microscopy. *Science* 322, 1065–1069. doi: 10.1126/science.1162493

Kessaris, N., Fogarty, M., Iannarelli, P., Grist, M., Wegner, M., and Richardson, W. D. (2006). Competing waves of oligodendrocytes in the forebrain and postnatal elimination of an embryonic lineage. *Nat. Neurosci.* 9, 173–179. doi: 10.1038/nn1620

Kessaris, N., Pringle, N., and Richardson, W. D. (2008). Specification of CNS glia from neural stem cells in the embryonic neuroepithelium. *Philos. Trans. R. Soc. B Biol. Sci.* 363, 71–85. doi: 10.1098/rstb.2006.2013

Kicheva, A., Bollenbach, T., Ribeiro, A., Valle, H. P., and Lovell-, R. (2014). Coordination of progenitor specification and growth in the mouse and chick spinal cord. *Sciecne* 345, 1–24. doi: 10.1126/science.1254927.Coordination

Kicheva, A., and Briscoe, J. (2015). Developmental pattern formation in phases. *Trends Cell Biol.* 25, 579–591. doi: 10.1016/j.tcb.2015.07.006

Kiecker, C., and Lumsden, A. (2005). Compartments and their boundaries in vertebrate brain development. *Nat. Rev. Neurosci.* 6, 553–564. doi: 10.1038/nrn1702

Klingler, E., and Jabaudon, D. (2020). Do progenitors play dice? *eLife* 8:e51381. doi: 10.7554/eLife.51381

Kohwi, M., and Doe, C. Q. (2013). Temporal fate specification and neural progenitor competence during development. *Nat. Rev. Neurosci.* 14, 823–838. doi: 10.1038/nrn3618

Kutejova, E., Sasai, N., Shah, A., Gouti, M., and Briscoe, J. (2016). Neural progenitors adopt specific identities by directly repressing all alternative progenitor transcriptional programs. *Dev. Cell* 36, 639–653. doi: 10.1016/j.devcel.2016.02.013

Lanjakornsiripan, D., Pior, B. J., Kawaguchi, D., Furutachi, S., Tahara, T., Katsuyama, Y., et al. (2018). Layer-specific morphological and molecular differences in neocortical astrocytes and their dependence on neuronal layers. *Nat. Commun.* 9:1623. doi: 10.1038/s41467-018-03940-3

Laurenti, E., and Göttgens, B. (2018). From haematopoietic stem cells to complex differentiation landscapes. *Nature* 553, 418–426. doi: 10.1038/nature25022

Le Dréau, G., and Martí, E. (2013). The multiple activities of BMPs during spinal cord development. *Cell. Mol. Life Sci.* 70, 4293–4305. doi: 10.1007/s00018-013-1354-9

Le Dréau, G., Saade, M., Gutiérrez-Vallejo, I., and Martí, E. (2014). The strength of SMAD1/5 activity determines the mode of stem cell division in the developing spinal cord. *J. Cell Biol.* 204, 591–605. doi: 10.1083/jcb.201307031

Livet, J., Weissman, T. A., Kang, H., Draft, R. W., Lu, J., Bennis, R. A., et al. (2007). Transgenic strategies for combinatorial expression of fluorescent proteins in the nervous system. *Nature* 450, 56–62. doi: 10.1038/nature06293

Llorca, A., Ciceri, G., Beattie, R., Wong, F. K., Diana, G., Serafeimidou-Pouliou, E., et al. (2019). A stochastic framework of neurogenesis underlies the assembly of neocortical cytoarchitecture. *eLife* 8:51381.

Loulier, K., Barry, R., Mahou, P., Franc, Y. L., Supatto, W., Matho, K. S., et al. (2014). multiplex cell and lineage tracking with combinatorial labels. *Neuron* 81, 505–520. doi: 10.1016/j.neuron.2013.12.016

Lu, D. C., Niu, T., and Alaynick, W. A. (2015). Molecular and cellular development of spinal cord locomotor circuitry. *Front. Mol. Neurosci.* 8:25. doi: 10.3389/fnmol.2015.00025

Luengo-Oroz, M. A., Ledesma-Carbayo, M. J., Peyriéras, N., and Santos, A. (2011). Image analysis for understanding embryo development: a bridge from microscopy to biological insights. *Curr. Opin. Genet. Dev.* 21, 630–637. doi: 10.1016/j.gde.2011.08.001

Malatesta, P., and Götz, M. (2013). Radial glia - from boring cables to stem cell stars. *Development* 140, 483–486. doi: 10.1242/dev.085852

McArthur, K. L., and Fetcho, J. R. (2017). Key features of structural and functional organization of *Zebrafish* facial motor neurons are resilient to disruption of neuronal migration. *Curr. Biol.* 27, 1746–1756. doi: 10.1016/j.cub.2017.05.033

McConnell, S. K., and Kaznowski, C. E. (1991). Cell cycle dependence of laminar determination in developing neocortex. *Science* 254, 282–285. doi: 10.1126/science.1925583

McKenna, A., Findlay, G. M., Gagnon, J. A., Horwitz, M. S., Schier, A. F., and Shendure, J. (2016). Whole-organism lineage tracing bycombinatorial and cumulativegenome editing. *Science* 353, 1–13.

Meijer, D. H., Kane, M. F., Mehta, S., Liu, H., Harrington, E., Taylor, C. M., et al. (2012). Separated at birth? the functional and molecular divergence of OLIG1 and OLIG2. *Nat. Rev. Neurosci.* 13, 819–831. doi: 10.1038/nrn3386

Mihalas, A. B., and Hevner, R. F. (2018). Clonal analysis reveals laminar fate multipotency and daughter cell apoptosis of mouse cortical intermediate progenitors. *Development* 145:e164335. doi: 10.1242/dev.164335

Miyata, T., Kawaguchi, A., Okano, H., and Ogawa, M. (2001). Asymmetric inheritance of radial glial fibers by cortical neurons. *Neuron* 31, 727–741. doi: 10.1016/S0896-6273(01)00420-2

Mo, Z., and Zecevic, N. (2009). Human fetal radial glia cells generate oligodendrocytes in vitro. *Glia* 57, 490–498. doi: 10.1002/glia.20775

Noctor, S. C., Martinez-Cerdeño, V., Ivic, L., and Kriegstein, A. R. (2004). Cortical neurons arise in symmetric and asymmetric division zones and migrate through specific phases. *Nat. Neurosci.* 7, 136–144. doi: 10.1038/nn1172

Olivier, N., Luengo-Oroz, M. A., Duloquin, L., Faure, E., Savy, T., Veilleux, I., et al. (2010). Cell lineage reconstruction of early *Zebrafish embryos* using label-free nonlinear microscopy. *Science* 329, 967–971. doi: 10.1126/science.1189428

Oosterveen, T., Kurdija, S., Enstero, M., Uhde, C. W., Bergsland, M., Sandberg, M., et al. (2013). SoxB1-driven transcriptional network underlies neural-specific interpretation of morphogen signals. *Proc. Natl. Acad. Sci. U.S.A.* 110, 7330–7335. doi: 10.1073/pnas.1220010110

Penisson, M., Ladewig, J., Belvindrah, R., and Francis, F. (2019). Genes and mechanisms involved in the generation and amplification of basal radial glial cells. *Front. Cell. Neurosci.* 13:381. doi: 10.3389/fncel.2019.00381

Peterson, K. A., Nishi, Y., Ma, W., Vedenko, A., Shokri, L., Zhang, X., et al. (2012). Neural-specific Sox2 input and differential Gli-binding affinity provide context and positional information in Shh-directed neural patterning. *Genes Dev.* 26, 2802–2816. doi: 10.1101/gad.207142.112

Pujala, A., and Koyama, M. (2019). Chronology-based architecture of descending circuits that underlie the development of locomotor repertoire after birth. *eLife* 8:e42135. doi: 10.7554/eLife.42135

Raj, B., Wagner, D. E., McKenna, A., Pandey, S., Klein, A. M., Shendure, J., et al. (2018). Simultaneous single-cell profiling of lineages and cell types in the vertebrate brain. *Nat. Biotechnol.* 36, 442–450. doi: 10.1038/nbt.4103

Rakic, P. (1974). Neurons in rhesus monkey visual cortex: sustematic relation between time of origin and eventual disposition. *Science* 183, 425–427. doi: 10.1126/science.183.4123.425

Rakic, P. (2009). Evolution of the neocortex: a perspective from developmental biology. *Nat. Rev. Neurosci.* 10, 724–735. doi: 10.1038/nrn2719

Rayon, T., and Briscoe, J. (2021). Cross-species comparisons and in vitro models to study tempo in development and homeostasis. *Interface Focus* 11:20200069. doi: 10.1098/rsfs.2020.0069

Rayon, T., Stamataki, D., Perez-Carrasco, R., Garcia-Perez, L., Barrington, C., Melchionda, M., et al. (2020). Species-specific pace of development is associated with differences in protein stability. *Science* 369:eaba7667. doi: 10.1126/science.aba7667

Ribes, V., and Briscoe, J. (2009). Establishing and interpreting graded Sonic Hedgehog signaling during vertebrate neural tube patterning: the role of negative feedback. *Cold Spring Harb. Perspect. Biol.* 1, 1–16. doi: 10.1101/cshperspect.a002014

Robertis, E. M. D. (2006). Spemann's organizer and self- regulation in amphibian embryos. *Nat. Rev. Mol. Cell Biol.* 7, 296–302. doi: 10.1038/nrm1855

Rogers, K. W., and Schier, A. F. (2011). Morphogen gradients: from generation to interpretation. *Annu. Rev. Cell Dev. Biol.* 27, 377–407. doi: 10.1146/annurev-cellbio-092910-154148

Rulands, S., Iglesias-Gonzalez, A. B., and Boije, H. (2018). Deterministic fate assignment of *Müller glia* cells in the *Zebrafish retina* suggests a clonal backbone during development. *Eur. J. Neurosci.* 48, 3597–3605. doi: 10.1111/ejn.14257

Saade, M., Gonzalez-Gobartt, E., Escalona, R., Usieto, S., and Martí, E. (2017). Shh-mediated centrosomal recruitment of PKA promotes symmetric proliferative neuroepithelial cell division. *Nat. Cell Biol.* 19, 493–503. doi: 10.1038/ncb3512

Saade, M., Gutiérrez-Vallejo, I., LeDréau, G., Rabadán, M. A., Miguez, D. G., Buceta, J., et al. (2013). Sonic hedgehog signaling switches the mode of division in the developing nervous system. *Cell Rep.* 4, 492–503. doi: 10.1016/j.celrep.2013.06.038

Sagner, A., and Briscoe, J. (2019). Establishing neuronal diversity in the spinal cord: a time and a place. *Development* 146:e182154. doi: 10.1242/dev.182154

Slack, J. M. W. (2002). Conrad hal waddington: the last renaissance biologist? *Nat. Rev. Genet.* 3, 889–895. doi: 10.1038/nrg933

Snippert, H. J., van der Flier, L. G., Sato, T., van Es, J. H., van den Born, M., Kroon-Veenboer, C., et al. (2010). Intestinal crypt homeostasis results from neutral competition between symmetrically dividing Lgr5 stem cells. *Cell* 143, 134–144. doi: 10.1016/j.cell.2010.09.016

Soula, C., Danesin, C., Kan, P., Grob, M., Poncet, C., and Cochard, P. (2001). Distinct sites of origin of oligodendrocytes and somatic motoneurons in the chick spinal cord: oligodendrocytes arise from Nkx2.2-expressing progenitors by a Shh-dependent mechanism. *Development* 128, 1369–1379. doi: 10.1242/dev.128.8.1369

Spanjaard, B., Hu, B., Mitic, N., Olivares-Chauvet, P., Janjuha, S., Ninov, N., et al. (2018). Simultaneous lineage tracing and cell-type identification using CrIsPr-Cas9-induced genetic scars. *Nat. Biotechnol.* 36, 469–473. doi: 10.1038/nbt.4124

Spassky, N., Goujet-Zalc, C., Parmantier, E., Olivier, C., Martinez, S., Ivanova, A., et al. (1998). Multiple restricted origin of oligodendrocytes. *J. Neurosci.* 18, 8331–8343. doi: 10.1523/jneurosci.18-20-08331.1998

Subramanian, L., Bershteyn, M., Paredes, M. F., and Kriegstein, A. R. (2017). Dynamic behaviour of human neuroepithelial cells in the developing forebrain. *Nat. Commun.* 8:14167. doi: 10.1038/ncomms14167

Sueda, R., Imayoshi, I., Harima, Y., and Kageyama, R. (2019). High Hes1 expression and resultant Ascl1 suppression regulate quiescent vs. active neural stem cells in the adult mouse brain. *Genes Dev.* 33, 511–523. doi: 10.1101/gad.323196.118

Sulston, J. E., Schierenberg, E., White, J. G., and Thomson, J. N. (1983). The embryonic cell lineage of the nematode *Caenorhabditis elegans*. *Dev. Biol.* 100, 64–119. doi: 10.1016/0012-1606(83)90201-4

Takahashi, K., and Yamanaka, S. (2016). A decade of transcription factor-mediated reprogramming to pluripotency. *Nat. Rev. Mol. Cell Biol.* 17, 183–193. doi: 10.1038/nrm.2016.8

Takahashi, T., Goto, T., Miyama, S., Nowakowski, R. S., and Caviness, V. S. (1999). Sequence of neuron origin and neocortical laminar fate: relation to cell cycle of origin in the developing murine cerebral wall. *J. Neurosci.* 19, 10357–10371. doi: 10.1523/jneurosci.19-23-10357.1999

Tambalo, M., Mitter, R., and Wilkinson, D. G. (2020). A single cell transcriptome atlas of the developing zebrafish hindbrain. *Development* 147:e184143. doi: 10.1242/dev.184143

Tan, S. S., Kalloniatis, M., Truong, H. T., Binder, M. D., Cate, H. S., Kilpatrick, T. J., et al. (2009). Oligodendrocyte positioning in cerebral cortex is independent of projection neuron layering. *Glia* 57, 1024–1030. doi: 10.1002/glia.20826

Tarabykin, V., Stoykova, A., Usman, N., and Gruss, P. (2001). Cortical upper layer neurons derive from the subventricular zone as indicated by Svet1 gene expression. *Development* 128, 1983–1993. doi: 10.1242/dev.128.11.1983

Tassy, O., Daian, F., Hudson, C., Bertrand, V., and Lemaire, P. (2006). A quantitative approach to the study of cell shapes and interactions during early chordate embryogenesis. *Curr. Biol.* 16, 345–358. doi: 10.1016/j.cub.2005.12.044

Taverna, E., Götz, M., and Huttner, W. B. (2014). The cell biology of neurogenesis: toward an understanding of the development and evolution of the neocortex. *Annu. Rev. Cell Dev. Biol.* 30, 465–502. doi: 10.1146/annurev-cellbio-101011-155801

Tekki-Kessaris, N., Woodruff, R., Hall, A. C., Gaffield, W., Kimura, S., Stiles, C. D., et al. (2001). Hedgehog-dependent oligodendrocyte lineage specification in the telencephalon. *Development* 128, 2545–2554. doi: 10.1242/dev.128.13.2545

Telley, L., Agirman, G., Prados, J., Amberg, N., Fièvre, S., Oberst, P., et al. (2019). Temporal patterning of apical progenitors and their daughter neurons in the developing neocortex. *Science* 364:eaav2522. doi: 10.1126/science.aav2522

Than-Trong, E., and Bally-Cuif, L. (2015). Radial glia and neural progenitors in the adult zebrafish central nervous system. *Glia* 63, 1406–1428. doi: 10.1002/glia.22856

Than-Trong, E., Kiani, B., Dray, N., Ortica, S., Simons, B., Rulands, S., et al. (2020). Lineage hierarchies and stochasticity ensure the long-term maintenance of adult neural stem cells. *Sci. Adv.* 6, 26–29. doi: 10.1126/sciadv.aaz5424

Trapnell, C. (2015). Defining cell types and states with single-cell genomics. *Genome Res.* 25, 1491–1498. doi: 10.1101/gr.190595.115

Ulloa, F., and Briscoe, J. (2007). Morphogens and the control of cell proliferation and patterning in the spinal cord. *Cell Cycle* 6, 2640–2649. doi: 10.4161/cc.6.21.4822

Urbán, N., and Cheung, T. H. (2021). Stem cell quiescence: the challenging path to activation. *Development* 148:dev165084. doi: 10.1242/dev.165084

van Velthoven, C. T. J., and Rando, T. A. (2019). Stem cell quiescence: dynamism, restraint, and cellular idling. *Cell Stem Cell* 24, 213–225. doi: 10.1016/j.stem.2019.01.001

Waddington, C. H. (1957). *The Strategy of the Genes: A Discussion of Some Aspects of Theoretical Biology. George*. London: Allen and Unwin.

Wan, Y., Wei, Z., Looger, L. L., Koyama, M., Druckmann, S., and Keller, P. J. (2019). Single-cell reconstruction of emerging population activity in an entire developing circuit. *Cell* 179, 355–372. doi: 10.1016/j.cell.2019.08.039

Wang, X., Allen, W. E., Wright, M. A., Sylwestrak, E. L., Samusik, N., Vesuna, S., et al. (2018). Three-dimensional intact-tissue sequencing of single-cell transcriptional states. *Science* 361:eaat5691. doi: 10.1126/science.aat5691

Weissman, T. A., Sanes, J. R., Lichtman, J. W., and Livet, J. (2011). Generating and imaging multicolor brainbow mice. *Cold Spring Harb. Protoc.* 6, 763–769. doi: 10.1101/pdb.top114

Wolff, C., Tinevez, J. Y., Pietzsch, T., Stamataki, E., Harich, B., Guignard, L., et al. (2018). Multi-view light-sheet imaging and tracking with the MaMuT software reveals the cell lineage of a direct developing arthropod limb. *eLife* 7:34410. doi: 10.7554/eLife.34410

Yu, H. H., Chen, C. H., Shi, L., Huang, Y., and Lee, T. (2009). Twin-spot MARCM to reveal the developmental origin and identity of neurons. *Nat. Neurosci.* 12, 947–953. doi: 10.1038/nn.2345

Zannino, D. A., and Appel, B. (2009). Olig2 + precursors produce abducens motor neurons and oligodendrocytes in the zebrafish hindbrain. *J. Neurosci.* 29, 2322–2333. doi: 10.1523/JNEUROSCI.3755-08.2009

Zechner, C., Nerli, E., and Norden, C. (2020). Stochasticity and determinism in cell fate decisions. *Development* 147, 1–8. doi: 10.1242/dev.181495

Zhang, M., Eichhorn, S. W., Zingg, B., Yao, Z., Zeng, H., Hongwei, D., et al. (2020). Molecular, spatial and projection diversity of neurons in primary motor cortex revealed by in situ single-cell transcriptomics. *bioRxiv* [Preprint]. doi: 10.1101/2020.06.04.105700

Zhang, X., Mennicke, C. V., Xiao, G., Beattie, R., Haider, M. A., Hippenmeyer, S., et al. (2020). Clonal analysis of gliogenesis in the cerebral cortex reveals stochastic expansion of glia and cell autonomous responses to egfr dosage. *Cells* 9:2662. doi: 10.3390/cells9122662

Zong, H., Espinosa, J. S., Su, H. H., Muzumdar, M. D., and Luo, L. (2005). Mosaic analysis with double markers in mice. *Cell* 121, 479–492. doi: 10.1016/j.cell.2005.02.012

Conflict of Interest: The authors declare that the research was conducted in the absence of any commercial or financial relationships that could be construed as a potential conflict of interest.

Publisher's Note: All claims expressed in this article are solely those of the authors and do not necessarily represent those of their affiliated organizations, or those of the publisher, the editors and the reviewers. Any product that may be evaluated in this article, or claim that may be made by its manufacturer, is not guaranteed or endorsed by the publisher.

frontiers in Neuroscience

REVIEW
published: 04 February 2022
doi: 10.3389/fnins.2021.801791

Emerging Roles for Hox Proteins in the Last Steps of Neuronal Development in Worms, Flies, and Mice

Weidong Feng[1,2,3†], *Yinan Li*[1,2,4†] *and Paschalis Kratsios*[1,2*]

[1] *Department of Neurobiology, University of Chicago, Chicago, IL, United States,* [2] *University of Chicago Neuroscience Institute, Chicago, IL, United States,* [3] *Committee on Development, Regeneration, and Stem Cell Biology, University of Chicago, Chicago, IL, United States,* [4] *Committee on Neurobiology, University of Chicago, Chicago, IL, United States*

OPEN ACCESS

Edited by:
Filipe Pinto-Teixeira, FR3743 Centre de Biologie Intégrative (CBI), France

Reviewed by:
Marie Kmita, Institut de Recherches Cliniques de Montréal (IRCM), Canada
Polyxeni Philippidou, Case Western Reserve University, United States
Françoise Gofflot, Catholic University of Louvain, Belgium

***Correspondence:**
Paschalis Kratsios
pkratsios@uchicago.edu

† These authors have contributed equally to this work

Specialty section:
This article was submitted to Neurogenesis, a section of the journal Frontiers in Neuroscience

Received: *25 October 2021*
Accepted: *31 December 2021*
Published: *04 February 2022*

Citation:
Feng W, Li Y and Kratsios P (2022) Emerging Roles for Hox Proteins in the Last Steps of Neuronal Development in Worms, Flies, and Mice. Front. Neurosci. 15:801791. doi: 10.3389/fnins.2021.801791

A remarkable diversity of cell types characterizes every animal nervous system. Previous studies provided important insights into how neurons commit to a particular fate, migrate to the right place and form precise axodendritic patterns. However, the mechanisms controlling later steps of neuronal development remain poorly understood. Hox proteins represent a conserved family of homeodomain transcription factors with well-established roles in anterior-posterior (A-P) patterning and the early steps of nervous system development, including progenitor cell specification, neuronal migration, cell survival, axon guidance and dendrite morphogenesis. This review highlights recent studies in *Caenorhabditis elegans*, *Drosophila melanogaster* and mice that suggest new roles for Hox proteins in processes occurring during later steps of neuronal development, such as synapse formation and acquisition of neuronal terminal identity features (e.g., expression of ion channels, neurotransmitter receptors, and neuropeptides). Moreover, we focus on exciting findings suggesting Hox proteins are required to maintain synaptic structures and neuronal terminal identity during post-embryonic life. Altogether, these studies, in three model systems, support the hypothesis that certain Hox proteins are continuously required, from early development throughout post-embryonic life, to build and maintain a functional nervous system, significantly expanding their functional repertoire beyond the control of early A-P patterning.

Keywords: neuronal development, terminal identity, Hox genes, transcription factors, terminal selectors, synapse formation, synapse maturation

INTRODUCTION

Nervous system development is a multi-step process that generates a multitude of cell types. Dividing progenitor cells, or neural stem cells, will ultimately give rise to distinct types of neurons and glia. Newly born, post-mitotic neurons face a number of early challenges before participating into a functional neural circuit. They need to be molecularly specified, migrate to the right place, and acquire distinct axo-dendritic morphologies. Studies in all major model organisms suggest

that these early steps of nervous system development are often controlled by Hox proteins, a conserved family of homeodomain transcription factors critical for anterior-posterior (A-P) patterning and formation of the animal body plan. The roles of Hox proteins during the early steps of nervous system development have been summarized in excellent reviews (Di Bonito et al., 2013a; Philippidou and Dasen, 2013; Parker and Krumlauf, 2020). Here, we highlight recent studies in *Caenorhabditis elegans*, *Drosophila melanogaster*, and mice that uncovered new roles for Hox in the last steps of neuronal development. We define as "last steps" the processes of synapse formation and acquisition of neuronal terminal identity features (e.g., expression of neurotransmitter [NT] receptors, neuropeptides, ion channels) because such processes represent the final events that lead to the establishment of a functional neural circuit. Perhaps more strikingly, a number of Hox proteins are continuously expressed in post-mitotic neurons of invertebrate and vertebrate nervous systems (discussed herein). Depletion of Hox gene activity at later stages of development and post-embryonic life supports the emerging hypothesis that Hox proteins are required not only to establish, but also maintain synaptic structures and terminal identity features. This review will focus on these exciting studies, offering new insights into the function of Hox proteins in the final steps of neuronal development.

THE ROLE OF HOX GENES IN LATE STAGES OF *Caenorhabditis elegans* NERVOUS SYSTEM DEVELOPMENT

The *C. elegans* genome contains six Hox genes. The anterior Hox (*ceh-13/Lab/Hox1)* together with the mid-body Hox *(lin-39/Scr/Dfd/Hox3-5 and mab-5/Antp/Hox6-8)* and posterior Hox *(egl-5/AbdB/Hox9-13)* genes were identified 30 years ago (Costa et al., 1988; Clark et al., 1993; Van Auken et al., 2000), whereas two additional posterior Hox genes *(nob-1*, *php-3)* were discovered in 2000 (Van Auken et al., 2000). *C. elegans* Hox genes are organized in three different sub-clusters located on Chromosome III (**Figure 1A**). Previous work revealed that *C. elegans* Hox genes control A-P patterning and the development of lateral epidermis and ventral ectoderm (Kenyon, 1986; Costa et al., 1988; Chisholm, 1991; Cowing and Kenyon, 1992; Clark et al., 1993; Wang et al., 1993; Wittmann et al., 1997; Brunschwig et al., 1999). Critical roles for Hox genes have also been described during the early steps of *C. elegans* nervous system development, that is, in the specification and survival of neuronal progenitors (Fixsen et al., 1985; Kenyon, 1986; Clark et al., 1993; Salser et al., 1993; Wang et al., 1993; Kalis et al., 2014), cell migration (Chisholm, 1991; Salser and Kenyon, 1992; Harris et al., 1996; Sym et al., 1999; Tihanyi et al., 2010; Wang et al., 2013), and neurite/axonal growth (Jia and Emmons, 2006; Zheng et al., 2015a). Below, we focus on recent studies uncovering functions for *C. elegans* Hox genes in processes occurring during later stages of neuronal development, such as synapse formation and acquisition of terminal identity.

Control of Synapse Formation/Maturation in *Caenorhabditis elegans*

The posterior Hox gene *egl-5* is necessary for migration of the hermaphrodite-specific motor neuron (HSN) from the tail to the vulva, where it stimulates vulva muscle contraction resulting in egg laying (Baum et al., 1999). In posteriorly located sensory neurons, *egl-5* controls neurite outgrowth (Zheng et al., 2015a). Besides its involvement in cell migration and neurite outgrowth, *egl-5* also controls the wiring of the posteriorly located cholinergic motor neuron DA9 (Kratsios et al., 2017). In wild-type animals, the DA9 axon extends circumferentially to reach the dorsal body wall muscle and form *en passant* neuromuscular synapses. In *egl-5* mutants, these DA9 synapses are generated at the "wrong" place; they are found more anteriorly when compared to wild-type animals, suggesting a synaptic specificity defect. Interestingly, split GFP reporter technology (GRASP) also revealed that the DA9 synaptic input (received by the AVG interneuron) fails to be maintained in adult *egl-5* mutants, despite being properly established at earlier larval stages, indicating a critical role for *egl-5* in synapse maintenance. Together, these findings suggest that the posterior Hox gene *egl-5* controls both synaptic input and output of a posterior cholinergic motor neuron (DA9) in *C. elegans*.

Control of Neuronal Terminal Identity by *Caenorhabditis elegans* Hox Genes

Once post-mitotic neurons have established synapses, the function of every neuronal circuit critically relies on the ability of its constituent neurons to communicate with each other via neurotransmitters and/or neuropeptides, as well as to display neuron type-specific electrophysiological signatures. These function-defining features are determined by the expression of neurotransmitter (NT) biosynthesis proteins, ion channels, neuropeptides, NT receptors, and cell adhesion molecules. Genes coding for such proteins have been termed "terminal identity" genes (Hobert, 2008; Hobert and Kratsios, 2019), and are expressed continuously – from late developmental stages through adulthood – to determine the final (mature) identity and function of each neuron type. Recent studies on two different neuron types in *C. elegans*, namely the touch receptors and nerve cord motor neurons, revealed a new role for Hox genes in the control of neuronal terminal identity (**Table 1**). We highlight these studies below.

Hox Genes Control Terminal Identity Features of *Caenorhabditis elegans* Touch Receptor Neurons

In *C. elegans,* there are six touch receptor neurons (TRNs) mediating sensory responses to light touch. TRNs are classified into four subtypes: (a) bilaterally symmetrical pairs of ALM and PLM neurons are located at the midbody and tail region, respectively and (b) single AVM and PVM neurons are located in the midbody (**Figure 1B**). ALM and PLM are born embryonically, while AVM and PVM are generated post-embryonically. TRNs synapse onto and provide input to command interneurons (PVC, AVB, AVD, AVA), which

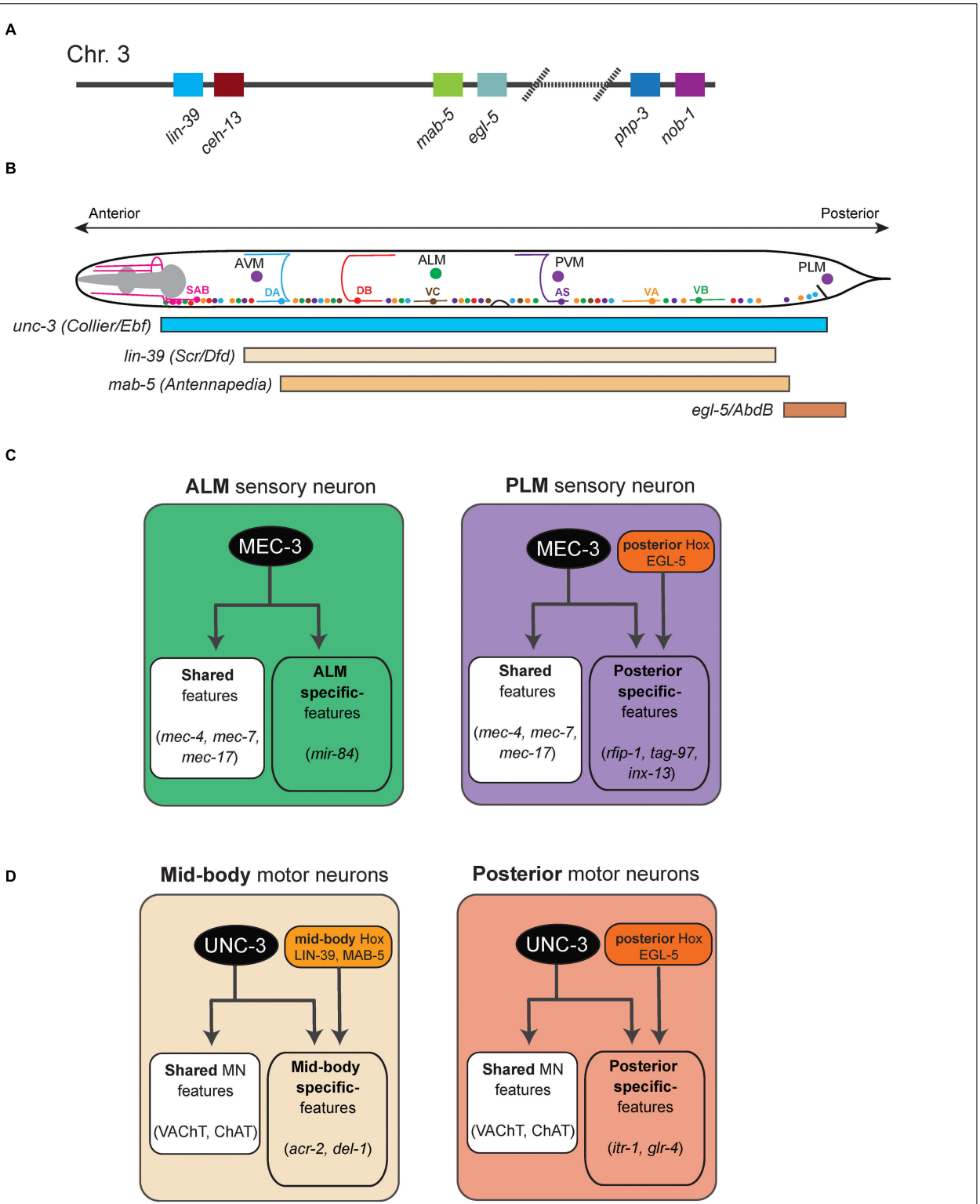

FIGURE 1 | Hox gene functions in mechanosensory and motor neurons in *C. elegans*. **(A)** Schematic of the *C. elegans* Hox gene cluster. **(B)** Schematic showing the cell body location of mechanosensory neurons (AVM, ALM, PVM, PLM) and cholinergic MNs in the ventral nerve cord (SAB, DA, DB, VA, VB, VC, AS). The GABAergic MNs are not shown. **(C)** The terminal selector MEC-3 controls ALM and PLM terminal identity. The activity of the posterior Hox gene *egl-5* diversifies PLM from ALM. Examples of terminal identity genes are shown in italics. **(D)** An intersectional strategy for the control of terminal identity of midbody (UNC-3, LIN-39, MAB-5) and posterior (UNC-3, EGL-5) MNs along the A-P axis of the *C. elegans* ventral nerve cord. See text for details.

TABLE 1 | Hox gene studies focused on late steps of nervous system development.

Species	Gene	Description	References
C. elegans	*egl-5*	*egl-5* regulates terminal differentiation of PLM	Toker et al., 2003
C. elegans	*egl-5*	EGL-5 is required for subtype-specific circuit formation by acting in both the sensory neuron and downstream interneuron to promote functional connectivity in touch receptor neurons.	Zheng et al., 2015a
C. elegans	*ceh-13*	CEH-13 functions cell non-autonomously to guide ALM migration and axonal outgrowth	Zheng et al., 2015a
C. elegans	*php-3*	PHP-3 makes PLM neurons morphologically distinct from ALM neurons independently with egl-5	Zheng et al., 2015a
C. elegans	*nob-1*	*nob-1* is needed to generate the cells that become the PLM neurons	Zheng et al., 2015b
C. elegans	*ceh-13, egl-5*	CEH-13 and EGL-5 act as transcriptional guarantors to ensure reliable and robust *mec-3* expression during terminal neuronal differentiation of touch receptor neurons	Zheng et al., 2015b
C. elegans	*lin-39, mab-5, egl-5*	Hox genes function as *unc-3* co-factors to specify cholinergic motor neuron sub-class terminal identities	Kratsios et al., 2017
C. elegans	*lin-39, mab-5*	*lin-39* and *mab-5* regulates and maintains subtype specific terminal identities of both cholinergic and GABAergic motor neurons	Feng et al., 2020
C. elegans	*lin-39 mab-5*	Hox genes regulates *cfi-1* to regulate ventral cord motor neuron terminal identity	Li et al., 2020
C. elegans	*egl-5*	*egl-5* is crucial for HSN to adopt the serotonergic identity	Chisholm, 1991
C. elegans	*egl-5*	*egl-5* regulates HSN terminal identity through regulating UNC-86	Baum et al., 1999
C. elegans	*egl-5*	*egl-5* is required for the adoption of dopaminergic identity for ray cells through regulation of dbl-1	Lints and Emmons, 1999
C. elegans	*ceh-13*	*ceh-13* specifies the terminal identity of two GABAergic motor neurons DD1 and DD2	Aquino-Nunez et al., 2020
Drosophila	*Ubx*	*Ubx* acts in both muscles and motoneurons to orchestrate formation of specific neuromuscular connections	Hessinger et al., 2017
Drosophila	*Abd-B*	Temporal control of neuronal differentiation by *Abd-B* in the context of CCAP peptidergic neurons	Moris-Sanz et al., 2015
Drosophila	*Ubx, abd-A*	Segmentally homologous neurons acquire two different terminal neuropeptidergic fates in the Drosophila nervous system	Gabilondo et al., 2018
Drosophila	*Ubx, abd-A*	*Ubx* and *abd-A* are required to maintain the expression of the neuropeptide *Lk* in larval stages	Estacio-Gomez et al., 2013
Drosophila	*Dfd*	*Dfd* is continuously required to maintain the expression of Ankyrin2 extra large (Ank2-XL) and thus synaptic stability in head motor neurons (MNs) that innervate the mouth hood elevator (MHE) and depressor (MHD) muscles	Friedrich et al., 2016
Mouse	*Hoxa2*	Hoxa2-dependent development of the mouse facial somatosensory map	Oury et al., 2006
Mouse	*Hoxa2*	Hoxa2 selects barrelette neuron identity and connectivity in the mouse somatosensory brainstem.	Bechara et al., 2015
Mouse	*Hox2*	Hox2 genes are required for tonotopic map precision and sound discrimination in the mouse auditory brainstem	Karmakar et al., 2017
Mouse	*Hoxa5*	Hoxa5 functions early after birth to impact expression of genes with synaptic function	Lizen et al., 2017b
Mouse	*Hoxa5*	Hoxa5 specifies pontine neuron positional identity and input connectivity	Maheshwari et al., 2020
Mouse	*Hoxc8*	*Hoxc8* is required for the maintenance of terminal identity genes *Nrg1, Mcam*, and *Pappa* in spinal motor neurons.	Catela et al., 2021
Mouse	*Hox5*	Late removal of *Hox5* genes depletes PMC motor neuron number and branches, suggesting it is continuously required for the survival of these neurons.	Philippidou et al., 2012

stimulate downstream motor neurons, thus generating touch reflex responses. Early specification and differentiation of TRNs have been well investigated (Bounoutas and Chalfie, 2007), but how each TRN subtype acquires its unique terminal identity remains poorly understood.

At the behavioral level, animals lacking *egl-5* (posterior Hox) gene activity are touch-insensitive at the tail, suggesting defects in the development of the posteriorly located PLM neuron (Chisholm, 1991). Later studies indeed demonstrated that *egl-5* is necessary for PLM terminal identity (Toker et al., 2003; Zheng et al., 2015a; **Figure 1C**). In addition to *egl-5*, two other poster Hox genes (*nob-1*, *php-3*) control PLM development; *nob-1* is necessary for the generation of PLM precursors, whereas *php-3* together with *egl-5* diversifies PLM from its more anteriorly located counterpart, the ALM neuron. Lastly, *egl-5* controls PLM morphological characteristics, such as neurite length, by repressing anterior Hox genes (*lin-39, mab-5)* and TALE cofactors (Zheng et al., 2015a). The case of *egl-5* highlights a recurring theme of Hox gene action across model systems, that is, Hox genes are required for various facets of development of a specific neuron type.

In the more anteriorly located ALM neurons, the anterior Hox gene *ceh-13* regulates ALM terminal identity, as evidenced by reduced expression of a handful of terminal identity genes

(*mec-4, mec-7, mec-17, mec-18*) in *ceh-13* mutant animals. Mechanistically, these studies proposed that CEH-13 and EGL-5 function as transcriptional guarantors by controlling the levels of expression of the terminal selector gene *mec-3*, which in turn is required for terminal identity of both ALM and PLM neurons (**Figure 1C**; Zheng et al., 2015a,b). CEH-13 and EGL-5 increase the probability of *mec-3* transcriptional activation by the POU-homeodomain transcription factor UNC-86 via the same Hox/Pbx binding site in ALM and PLM neurons respectively. This molecular mechanism ensures robustness of TRN terminal differentiation.

A multifaceted role of Hox genes is evident during the development of the *C. elegans* touch-reflex circuit: (a) Hox genes are involved in both early (e.g., generation of TRN precursor cells) and late steps of TRN development (e.g., terminal identity). (b) All six *C. elegans* Hox genes affect TRN development in various ways: *ceh-13* regulates ALM terminal identity; *lin-39 and mab-5* regulate the migration of AVM/PVM precursor; *egl-5* and *php-3* regulate PLM terminal identity; *nob-1* is necessary for the generation of PLM precursors. (c) Although it remains mechanistically unclear how they control TRN-specific terminal identity genes (e.g., NT receptors, ion channels, neuropeptides), two Hox proteins (CEH-13, EGL-5) appear to act directly as transcriptional guarantors of *mec-3*, the terminal selector for all *C. elegans* TRNs. (d) Intriguingly, Hox genes control the development of neurons at different layers (sensory, interneuron) of the touch-reflex circuit. That is, sensory TRN terminal identity requires Hox gene function, whereas the identity of the PVC command interneurons (which receive sensory input from the PLM touch receptors) requires *egl-5* gene activity (Chisholm, 1991; Zheng et al., 2015a).

Hox Genes Control Terminal Identity Features of Ventral Nerve Cord Motor Neurons

Similar to the touch receptor studies described above, the availability of terminal identity markers for ventral nerve cord motor neurons (MNs) in *C. elegans* has critically advanced our mechanistic understanding of Hox gene function in the nervous system. Nine distinct classes of MNs are found in the nerve cord of *C. elegans* hermaphrodite animals. Based on neurotransmitter usage, they can be classified into two categories: cholinergic (SAB, DA, DB, VA, VB, AS, VC) and GABAergic (DD, VD) MNs (**Figure 1B**). The SAB, DA, DB, and DD classes are generated embryonically, whereas the VA, VB, VC, VD, and AS neurons are generated post-embryonically (Von Stetina et al., 2006). The terminal identity of most cholinergic MN classes in the nerve cord (SAB, DA, DB, VA, VB, AS) critically depends on the terminal selector UNC-3, member of the conserved family of Collier/Olf/Ebf(COE) family of TFs (Prasad et al., 1998, 2008; Kratsios et al., 2011, 2015). Mechanistically, UNC-3 binds directly to the *cis*-regulatory region of terminal identity genes (e.g., acetylcholine [ACh] biosynthesis proteins, ion channels, neuropeptides) and activates their transcription. The homeodomain TF UNC-30 (PITX) acts in an analogous manner in GABAergic (DD, VD) MNs (Jin et al., 1994; Eastman et al., 1999).

In the context of both cholinergic and GABAergic MNs, recent work demonstrated that Hox genes act as cofactors of terminal selectors (Kratsios et al., 2017; Feng et al., 2020). In GABAergic MNs, the mid-body Hox genes *lin-39* and *mab-5* collaborate with *unc-30* to control terminal identity gene expression. In cholinergic MNs, *lin-39* and *mab-5* collaborate with *unc-3* to activate expression of several terminal identity genes (*unc-129, del-1, acr-2, dbl-1, unc-77, slo-2*) (**Figure 1D**). Like UNC-3, chromatin immunoprecipitation experiments suggest that LIN-39 and MAB-5 act directly (Kratsios et al., 2017; Feng et al., 2020). Apart from this UNC-3 co-factor role, *lin-39* is also the rate-limiting factor for ensuring cholinergic MN identity. In the absence of *unc-3*, LIN-39 no longer binds to the *cis*-regulatory region of cholinergic MN genes. Instead, it relocates and switches targets, resulting in ectopic activation of alternative identity genes (Feng et al., 2020). Hence, the terminal selector UNC-3 prevents a Hox transcriptional switch to safeguard cholinergic MN identity.

Are Hox genes required during adulthood to maintain terminal identity features and thereby ensure continuous functionality of individual neuron types? Inducible, protein depletion experiments using the auxin inducible degradation (AID) system demonstrated that the midbody Hox protein LIN-39 is required in adult life to maintain MN terminal identity features (Feng et al., 2020; Li et al., 2020). This finding was somewhat unexpected because Hox genes are mostly thought to act early during animal development. Additional work on Hox is needed in *C. elegans* and other model systems to rigorously test whether maintenance of neuronal terminal identity is a key feature of Hox gene function in the nervous system.

The organization of cholinergic MNs into distinct subtypes along the A-P axis also offers an opportunity to dissect the molecular mechanisms underlying neuronal subtype identity. For example, the DA class of nine MNs can be subdivided into four subtypes based on cell boy position: DA1 is located at the anterior ganglion (retrovesicular ganglion [RVG]), DA2–7 are located at the VNC, and DA8–9 are found at the posterior ganglion (preanal ganglion [PAG]). In addition to their position, cholinergic MN subtypes do show distinct connectivity features and expression profiles of terminal identity genes (Kratsios et al., 2017). Hox genes control cholinergic MN subtype identity along the A-P axis of the *C. elegans* nervous system via an intersectional strategy that involves the terminal selector UNC-3 (Kratsios et al., 2017). For example, UNC-3 is expressed in all 9 DA neurons, but collaborates with the mid-body Hox genes *lin-39* and *mab-5* in mid-body DA2-7 neurons to control their terminal identity (**Figure 1D**). Similarly, UNC-3 and the posterior Hox gene *egl-5* determine posterior MN (DA9) terminal identity (**Figure 1D**). Although the molecular mechanism of *egl-5* activity in posterior MNs is unknown, biochemical evidence suggests that LIN-39 – like UNC-3 – acts directly by binding on the *cis*-regulatory region of terminal identity genes. This direct mode of regulation further extends to intermediary TFs (*cfi-1/Arid3a, bnc-1/Bnc1/2*) responsible for MN subtype identity (Kerk et al., 2017; Li et al., 2020).

The role of the anterior Hox gene *ceh-13* during *C. elegans* neuronal terminal differentiation is largely elusive, partly due to the early larval lethality of *ceh-13* mutants

(Brunschwig et al., 1999). A recent study suggested *ceh-13* controls terminal identity features of GABAergic motor neurons (DD1, DD2) located in the anterior ganglion, but the underlying mechanisms remain unknown (Aquino-Nunez et al., 2020).

Posterior Hox Gene *egl-5* Controls the Identity of Serotonergic and Dopaminergic Neurons

In addition to its role on posterior MNs, the posterior Hox gene *egl-5* controls the terminal identity of two other neuron types. The hermaphrodite specific neurons (HSNs) partially lose their ability to produce serotonin in *egl-5* mutants (Chisholm, 1991). Moreover, *egl-5* acts in tail sensory neurons of the *C. elegans* male. Upon *egl-5* genetic removal, these neurons do not adopt dopaminergic fate and cannot be induced to express dopamine (Lints and Emmons, 1999).

THE ROLE OF HOX GENES IN LATE STAGES OF *Drosophila* NERVOUS SYSTEM DEVELOPMENT

Eight Hox genes are embedded in the genome of the fruit fly *Drosophila melanogaster*: *labial (lab), proboscipedia (pb), Deformed (Dfd), Sex combs reduced (Scr), Antennapedia (Antp), Ultrabithorax (Ubx), abdominal-A (abd-A)* and *Abdominal-B (Abd-B)* (**Figure 2A**). Hox genes were first discovered in *Drosophila* during the 20th century; genetic experiments identified mutants with dramatic phenotypes caused by homeotic transformations (e.g., legs instead of antennae in *Antp* mutants, duplication of thoracic segments in *Ubx* mutants) (Nusslein-Volhard and Wieschaus, 1980). Subsequent studies showed that the principles of Hox gene function and their role in establishing the body plan along the A-P axis are conserved across species.

Based on their chromosomal location, *Drosophila* Hox genes are organized in two gene complexes. The Antennapedia complex or Antp-C (consisting of *lab, pb, Dfd, Scr,* and *Antp*) specifies the anterior body plan from the head to the anterior thorax, while the Bithorax complex or Bx-C (consisting of *Ubx, abd-A*, and *Abd-B*) specifies the segments in posterior thorax and abdomen (**Figure 2B**). An important characteristic of Hox gene expression is their "temporal and spatial collinearity," that is, the genes located at the 3′ end of a complex/cluster are expressed earlier and more rostrally than those residing at the 5′ end (Kmita and Duboule, 2003; Gaunt, 2015). This appears to be a highly conserved property of Hox genes and has been found in *Drosophila* and many other species (Gaunt, 2015).

During development, neurons in *Drosophila* arise from neuroblasts (NBs) located in three thoracic (T1–T3) and eight abdominal (A1–A8) segments of the ventral nerve cord (VNC) (**Figures 2C,D**). These NBs possess the potency to generate any neuron type, but they give rise to unique types of neuronal progenies depending on their location along the A-P axis. This spatial pattern of distinct neuronal types correlates with the combinatorial expression pattern of Hox genes along the A-P axis of the *Drosophila* body. During neurogenesis, Hox gene activity guides NBs to exit the cell cycle and promotes (or blocks) apoptosis, eventually leading to a spatial map of unique neuron types (Estacio-Gomez and Diaz-Benjumea, 2014; Gummalla et al., 2014). Moreover, *Drosophila* Hox genes control additional steps during early nervous system development, such as neuronal specification and axo-dendritic morphogenesis (Reichert and Bello, 2010; Baek et al., 2013; Estacio-Gomez and Diaz-Benjumea, 2014). We will discuss below recent studies suggesting Hox genes also control later steps of *Drosophila* nervous system development, such as synapse formation and neuronal terminal identity (**Table 1**).

Control of Synapse Formation/Maturation by *Drosophila* Hox Genes

Compelling evidence suggests that the *Drosophila* Hox gene *Ubx* controls neuromuscular synapse formation in the embryo (Hessinger et al., 2017). Interestingly, it does so by acting both in muscles and motor neurons. In abdominal segments A1–A7 of wild-type embryos, RP motor neurons innervate the ventrolateral muscles VL1-4. However, these motor neurons fail to make correct contacts with muscle VL1 in *Ubx* mutant embryos. Mechanistically, this study provides an intriguing link between Hox and Wnt signaling pathway – Wnt is instrumental for neuromuscular synapse formation across species (Klassen and Shen, 2007; Strochlic et al., 2012; Kerr et al., 2014). The authors proposed a model in which Ubx controls, in VL2 muscles, *Wnt4* expression. Upon its secretion, Wnt4 is sensed by motor neurons (destined to innervate the VL1 muscles) via the Wnt receptor Fz-2. The Ubx-dependent Wnt4 signal from VL2 muscles triggers the repulsion of arriving growth cones belonging to motor neurons, hence these neurons innervate different muscles (VL1). Although the precise mechanism of Ubx function in these motor neurons remains obscure, rescue experiments clearly demonstrated that *Ubx* orchestrates the interaction between two cell types, muscles and motor neurons, to regulate the establishment of neuromuscular synapses in the fly embryo.

A second example of Hox gene involvement in *Drosophila* synapse formation comes from head motor neurons (MNs) that innervate the mouth hook elevator (MHE) and depressor (MHD) muscles, which coordinate the elevation and depression of the mouth hook (MH). The anterior Hox gene *Dfd* is expressed in a subset of MNs that specifically innervate the MHE (Friedrich et al., 2016). These *Dfd*-expressing MNs play a critical role in controlling the MH-dependent motor behaviors, including hatching at the end of embryogenesis and feeding in larval stages. In *Dfd* mutants, while the number of these MNs remains unchanged, they fail to extend axonal projections to their muscle targets, resulting in failure to hatch. Intriguingly, removing *Dfd* after the establishment of synaptic connections also results in impaired MH movements in larvae, suggesting *Dfd* is continuously required for the normal functions of these MNs (Friedrich et al., 2016). Genetically, *Dfd acts* upstream of a microtubule-organizing complex which is important for synapse stability even after their establishment. *Dfd* is continuously required to maintain the expression of Ankyrin2 extra large (Ank2-XL), which is known to be involved in determining the physical properties of synapses. Importantly, synaptic specificity

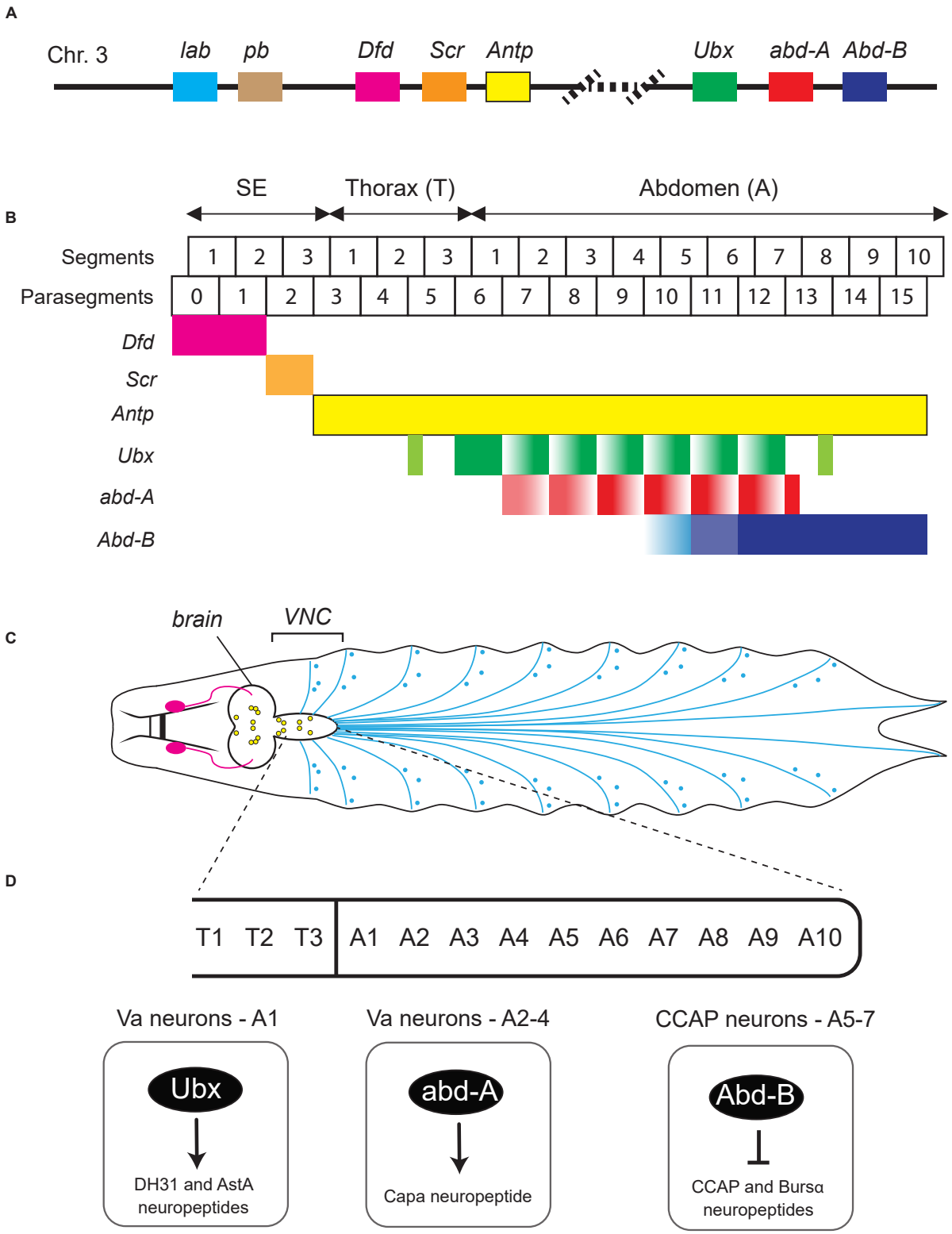

FIGURE 2 | Hox gene expression in the *Drosophila* nerve cord. **(A)** Schematic of the *Drosophila* Hox gene cluster. **(B)** Six Hox genes (*Dfd, Scr, Antp, Ubx, abd-A, Abd-B*) are expressed in the *Drosophila* ventral nerve cord (VNC). Their expression pattern along the A-P axis is color-coded. SE, subesophagus; Th, thorax; Ab, abdomen. Adapted from Estacio-Gomez and Diaz-Benjumea (2014). **(C)** Schematic of the nervous system in *Drosophila* larvae showing the brain, VNC, and the peripheral nervous system at the late 3rd instar stage. Adapted from Sokabe et al. (2016). **(D)** Examples of *Drosophila* Hox genes that control terminal identity features of VNC neurons. See text for details.

is dependent on actions of *Dfd* both in motor neurons and muscles, reminiscent of the Ubx case discussed above (Hessinger et al., 2017). Altogether, the above studies on *Drosophila Ubx* and *Dfd* support the hypothesis that Hox genes, in addition to their well-documented roles in motor neuron specification, survival and axonal pathfinding (Baek et al., 2013; Philippidou and Dasen, 2013), also control the establishment and maintenance of neuromuscular synapses.

Control of Neuronal Terminal Identity by *Drosophila* Hox Genes

Much of our current understanding of Hox gene function in the *Drosophila* nervous system derives from studies on the abdominal leucokinergic neurons (ABLKs), which express the neuropeptide *Leucokinin* (*Lk*) and are often used as a model system to study both embryonic and post-embryonic neurogenesis (Estacio-Gomez and Diaz-Benjumea, 2014). During embryonic neurogenesis, the NB5-5 progenitor gives rise to 7 pairs of embryonic ABLKs (eABLKs), one in each of the first 7 abdominal segments (A1–7) of the VNC (**Figures 2B,C**). *Lk* is not initially expressed in the eABLKs when they are born but becomes detectable at later developmental stages (first instar larva). Later, additional post-embryonic ABLKs (pABLKs) are generated (third instar larva), and express *Lk* in pupal stages. The cell type-specific expression of the terminal identity gene encoding *Lk* is critically dependent on Bx-C (*Ubx, abd-A, Abd-B*) gene activity (Estacio-Gomez et al., 2013). Although *Lk* is a single Hox-dependent terminal identity gene, this study does suggest a later role for Hox in *Drosophila* neurons.

Hox genes are also expressed in the neuroectoderm at early development, but then become silenced when NBs delaminate and are reactivated at later stages in specific neurons. The posterior abdominal Hox genes, *Ubx* and *abd-a*, are expressed in post-mitotic eABLKs in the first instar larvae, where they are redundantly required for the expression of *Lk*. Moreover, when both *Ubx* and *abd-A* are knocked down specifically from early second instar larvae, it results in loss of *Lk* expression in late third instar larvae (Estacio-Gomez et al., 2013), suggesting maintenance of *Lk* in eABLKs relies on continuous expression of *Ubx* and *abd-A*. On the other hand, the other posterior Hox gene *Abd-B* represses *Lk* expression in non-ABLK cells during both embryonic and larval neurogenesis. Similarly, *Abd-B* is continuously required to maintain the repression of *Lk*, as removing *Abd-B* from first instar larvae results in de-repression of *Lk* and increased number of ABLKs in third star larvae and adults. Another study on *Abd-B* yielded similar results in the context of the crustacean cardioactive peptide (CCAP)-expressing neurons, which control ecdysis (Moris-Sanz et al., 2015). In A5–7 segments, the CCAP efferent neurons are defined by the expression of two terminal identity markers – the neuropeptides CCAP and Bursicon α (Bursα). Using a hypomorphic allele, the authors found that Abd-B represses CCAP/Bursα in early larvae. Hence, the precise onset of CCAP/Bursα expression critically relies on Abd-B-mediated repression (**Figure 2D**). Moreover, RNAi-induced knocked down of *Abd-B* in the first instar larve results in expression of the CCAP/Bursα neuropeptides, suggesting Abd-B is continuously required to maintain repression of CCAP/Bursα (Moris-Sanz et al., 2015).

The Hox genes *Ubx* and *abd-A* are also necessary to diversify the terminal identity of distinct neuropeptidergic neurons in the first four abdominal (A1–A4) segments of the fly VNC (Gabilondo et al., 2018). In A1, *Ubx* controls the identity of ventral abdominal (Va) neurons expressing the neuropeptides DH31 and AstA (**Figure 2D**). In A2–A4, *abd-A* controls the identity of distinct Va neurons expressing the neuropeptide Capa (**Figure 2D**). The diversification of these neuropeptidergic neurons is a product of regionalized, segment-specific Hox gene expression. For example, *abd-A* is not expressed in A1, whereas *Ubx* is expressed in all abdominal segments. Regionalized expression in the nervous system is a common feature between invertebrate and vertebrate Hox genes. In particular, the case of Va neuropeptidergic neurons where segment-specific Hox genes control segment-specific Va neuron terminal identity is reminiscent of a Hox-based strategy used by *C. elegans* MNs. In that case, mid-body (*lin-39, mab-5*) and posterior (*egl-5*) Hox genes control the terminal identity of mid-body and posterior MNs, respectively (**Figure 1D**; Kratsios et al., 2017).

Although the underlying mechanisms remain unknown, these studies strongly suggest that Hox genes can establish and maintain terminal identity features of post-mitotic neurons in *Drosophila*.

THE ROLE OF HOX GENES IN LATE STAGES OF MOUSE NERVOUS SYSTEM DEVELOPMENT

During early vertebrate evolution, the single Hox gene cluster of vertebrate ancestors was duplicated twice, eventually giving rise to four clusters – *HoxA, HoxB, HoxC*, and *HoxD* in mammals (Soshnikova et al., 2013). In mice, these four clusters contain 39 Hox genes, which are further categorized into 13 paralog groups (PG) based on their relative position within the clusters and gene sequence (**Figure 3A**). The majority of these Hox genes are expressed in the mouse central nervous system (CNS) during development (Krumlauf et al., 1993; Briscoe and Wilkinson, 2004; Philippidou and Dasen, 2013).

A large body of work in the mouse hindbrain and spinal cord has uncovered critical roles for Hox genes in defining segment identity and establishing spatial gene expression patterns necessary for neuronal differentiation during early embryogenesis (Narita and Rijli, 2009; Di Bonito et al., 2013a; Philippidou and Dasen, 2013; Parker and Krumlauf, 2020). These early Hox roles appear conserved in the zebrafish nervous system as well (Ghosh and Sagerstrom, 2018). The expression of Hox genes in the mouse hindbrain between embryonic day 7.5 (E7.5) to E9.5 appears strictly restricted within territories defined by rhombomere (transiently divided segments of the developing neural tube) boundaries (**Figure 3B**). Rhombomere boundaries create a series of anterior limits for Hox gene expression along the A-P axis. In the hindbrain, *Hox1-2* genes have more anterior boundaries compared to *Hox3-4* genes. On

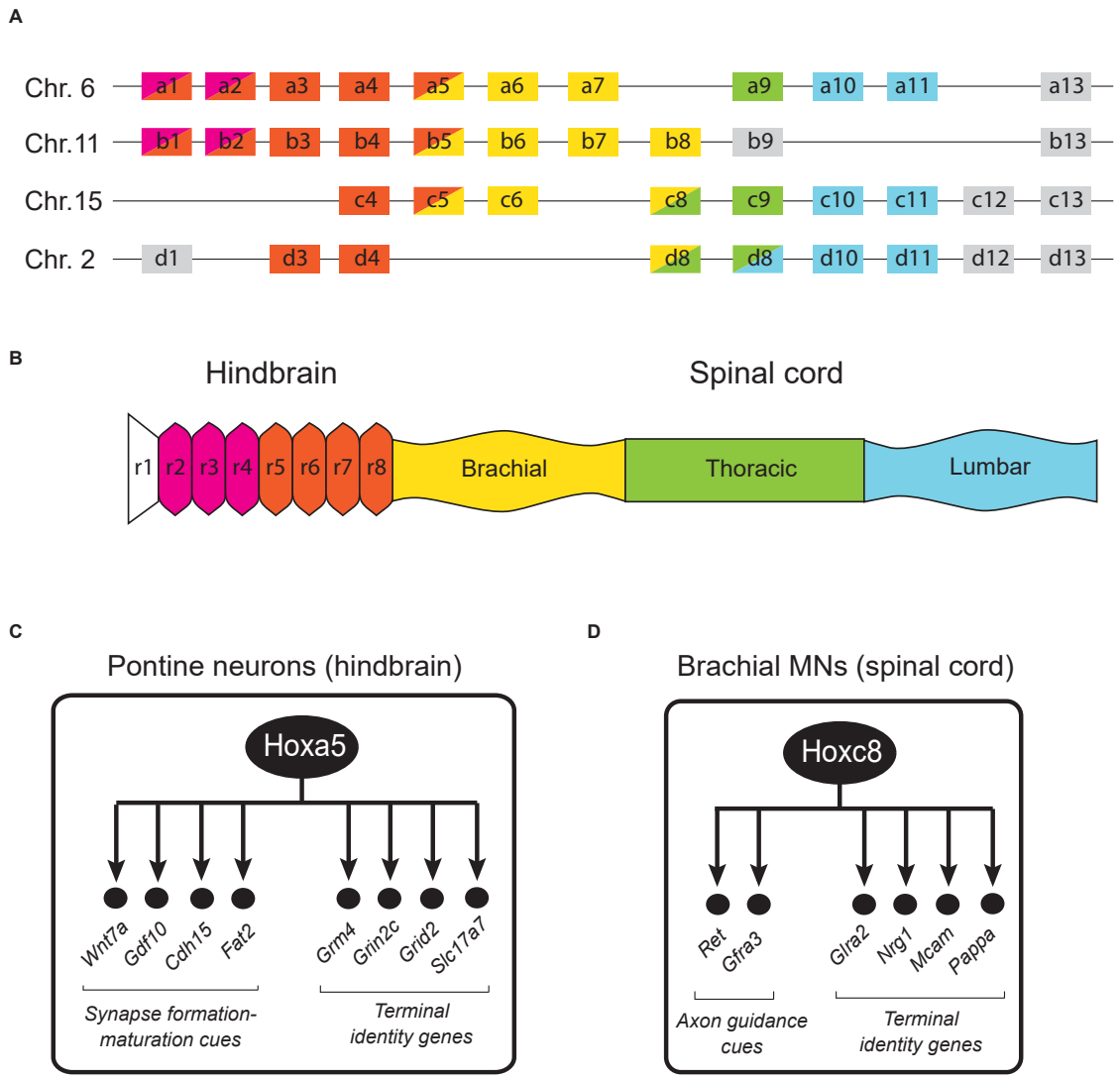

FIGURE 3 | Hox gene expression in the mouse hindbrain and spinal cord. **(A)** The 39 Hox genes in mice are distributed in four clusters (a, b, c, d). **(B)** Region-specific Hox gene expression is shown along the rostrocaudal axis of the embryonic nervous system. Adapted from Philippidou and Dasen (2013). The dynamic nature of Hox gene expression is not illustrated for simplicity. **(C)** Schematic summary of putative Hoxa5 target genes in pontine neurons. See text for details. **(D)** Schematic summary of Hoxc8 target genes in brachial MNs. See text for details.

the other hand, *Hox5-13* genes are mainly expressed in the spinal cord, which is posterior to the hindbrain. The overall map of Hox gene expression along the A-P axis therefore displays spatial collinearity (**Figures 3A,B**). With a number of exceptions (discussed below), most Hox studies in the mouse hindbrain and spinal cord have focused on early steps of neuronal development, and thereby uncovered crucial roles for Hox in progenitor and neuronal cell fate specification, cell migration, neuronal survival, as well as axo-dendritic growth and pathfinding (Narita and Rijli, 2009; Di Bonito et al., 2013a; Philippidou and Dasen, 2013; Parker and Krumlauf, 2020).

Although Hox gene expression is well documented in early embryonic stages, their expression in late embryonic and postnatal stages is poorly characterized. Interestingly, a number of studies in the mouse hindbrain showed that the segmental Hox gene expression pattern in postmitotic neurons is also maintained in late embryonic and early postnatal stages (Pasqualetti et al., 2007; Geisen et al., 2008; Di Bonito et al., 2013b; Karmakar et al., 2017; Lizen et al., 2017a). Two systematic expression studies on the 39 mouse Hox genes revealed that the majority of Hox genes remain expressed in the hindbrain after birth and until adulthood (Hutlet et al., 2016; Tomas-Roca et al., 2016). Hutlet et al. (2016) found that the 24 Hox genes that are normally active during early development of the hindbrain continue to be expressed during adulthood. Neuroanatomical localization analysis revealed that these Hox genes are still expressed in adult post-mitotic neurons derived from rhombomeres, with visible anterior boundaries restricting individual Hox genes along

the A-P axis. This indicates that the spatial collinearity rule is also maintained in adult hindbrain. Intriguingly, transcripts of some Hox genes were also identified in more anterior regions (forebrain) where they are not expressed during embryogenesis, suggesting Hox gene neo-expression in the adult CNS. More specifically, *Hoxb1, Hoxb3, Hoxb4, Hoxd3*, and *Hoxa5* transcripts were detected in both neocortex and the thalamus. Temporal analysis showed that their expression starts as early as the second postnatal week but becomes more robust only in the third postnatal week. In a separate study, Coughlan et al. have reported that the expression of *Hox9-11* genes is maintained and remains robust in spinocerebellar neurons until P7 (Coughlan et al., 2019), that is weeks after neuronal progenitor specification occurs. Of note, analysis of HOX expression in human samples showed that 15 genes are expressed in the adult brain (Takahashi et al., 2004). As in the hindbrain, Hox gene expression in the mouse embryonic spinal cord has been detected in progenitor cells and postmitotic neurons (Dasen et al., 2003, 2005; Dasen, 2009; Sweeney et al., 2018; Baek et al., 2019). A recent study focused on the brachial domain of the spinal cord found that *Hox4-8* expression is maintained in postmitotic neurons during early postnatal stages (Catela et al., 2021).

The maintained Hox expression in the mouse hindbrain and spinal cord prompts the question of what are the biological functions of mouse Hox genes in post-mitotic neurons during late developmental and postnatal stages? Below, we highlight studies on the role of mouse Hox genes in synapse formation/maturation and neuronal terminal identity; these late-occurring processes critically determine the functionality of neural circuits located in the hindbrain and spinal cord (**Table 1**).

Control of Synapse Formation/Maturation by Mouse Hox Genes

The expression of Hox genes in neuronal progenitors and postmitotic neurons necessitates the employment of conditional and temporally controlled gene inactivation strategies to discriminate between early and late Hox gene functions.

The first temporally controlled Hox gene inactivation study was conducted in the trigeminal system, which relays somatosensory stimuli (e.g., touch, pain) from the face to the cortex. A key structure for such relay is the principal trigeminal nucleus in the hindbrain. Oury et al. (2006) used a tamoxifen-inducible Cre/loxP strategy to inactivate *Hoxa2* at different developmental stages in postmitotic neurons of the principal trigeminal nucleus. The authors found that late removal of *Hoxa2* leads to topographic connectivity defects of these neurons. Consistently, *Hoxa2* ectopic expression experiments suggested that maintained *Hoxa2* expression is sufficient to direct topographic axon targeting and synaptic specificity defects, potentially implicating *Hoxa2* in the regulation of molecules acting at the presynapse (Bechara et al., 2015; Gofflot and Lizen, 2018).

Apart from its role in the trigeminal system, *Hoxa2* is involved in synaptic refinement of connectivity within the brainstem auditory circuit (Karmakar et al., 2017). *Hoxa2* and *Hoxb2* are expressed throughout embryonic and postnatal life (at least up to 2 months of age) in neurons of the anterior ventral cochlear nucleus (AVCN) (Narita and Rijli, 2009). In wild-type mice, glutamatergic neurons in the AVCN, called "Bushy cells," receive a single axonal input from one spiral ganglion neuron that forms a unique and large synapse, the endbulb of Held (Gofflot and Lizen, 2018). In mice lacking *Hoxa2* and *Hoxb2* gene activity specifically in postmitotic AVCN Bushy cells, multiple receiving inputs were observed, suggesting an involvement for these Hox genes in synapse (endbulb of Held) elimination/maturation (Karmakar et al., 2017). Importantly, these connectivity defects resulted in behavioral defects (failure to discriminate two close pure-tone frequencies) (Karmakar et al., 2017). At the molecular level, a comparative transcriptomic analysis revealed *Wnt3a* and multiple cadherins (*Cdh4, Cdh11, Cdh13, Cdh7*) as downstream targets of HOXA2/HOXB2 in AVNC Bushy cells. Given the prominent role of WNT signaling and cadherins in synapse formation and maintenance (Dickins and Salinas, 2013; Basu et al., 2015), these downstream targets could at least partially explain the connectivity defects observed in Bushy cells of mice lacking *Hoxa2* and *Hoxb2*.

In the mouse brainstem, *Hoxa5* is continuously expressed from embryonic to adult stages (Lizen et al., 2017a), suggesting its involvement at different stages of neuronal development. To test whether *Hoxa5* is functionally required in brainstem neurons, Lizen et al. (2017b) used an inducible Cre/loxP approach to inactivate *Hoxa5* at postnatal days 1–4 (P1–4) and then conducted an unbiased transcriptomic (RNA-Seq) analysis. Because *Hoxa5* expression is enriched in brainstem neurons that belong to the precerebellar system, called "pontine neurons," it is likely this RNA-Seq approach primarily uncovered changes in RNA expression in these neurons. This study identified several genes with known roles in synapse formation and maturation as Hoxa5 targets, such as the secreted molecules *Wnt7a* and GDF10 (member of TGFβ superfamily) and the cell adhesion molecules *Cdh15* and *Fat2* (Gofflot and Lizen, 2018; **Figure 3C**). Consistent with these observations, a more recent study found that postmitotic *Hoxa5* expression specifies pontine neuron connectivity (Maheshwari et al., 2020).

Similar to their roles in the *C. elegans* and *Drosophila* nervous systems, mouse Hox genes can affect neural circuit formation in various ways by acting at different stages. Besides controlling synapse formation and specificity, they can also regulate axonal pathfinding which eventually leads to a failure to establish a functional neural circuit. Supporting this possibility, several mouse studies have shown that correct expression of guidance cue receptors is often co-regulated by Hox genes (Oury et al., 2006; Geisen et al., 2008; Di Bonito et al., 2013a; Maheshwari et al., 2020). For example, in the precerebellar anterior extramural migrating stream, *Hox5* genes repress the repulsive Netrin receptor *Unc5b*, while *Hox2* genes positively regulate it (Di Meglio et al., 2013). Moreover, *Hoxa2* is required for the expression of Slit receptor *Robo3* in commissural neurons in the hindbrain and *Robo2* in precerebellar pontine neurons (Di Bonito et al., 2013a).

In spinal cord circuits, several studies revealed connectivity defects upon Hox gene inactivation (Dasen et al., 2005, 2008; Catela et al., 2015, 2016; Baek et al., 2019). For example, *Hox5* genes are required for proper connectivity of phrenic motor neurons to premotor interneurons and the diaphragm muscle (Philippidou et al., 2012; Vagnozzi et al., 2020). The phrenic motor neurons express a unique combination *Hox5*-dependent cell adhesion molecules of the Cadherin (Cdh) family (Vagnozzi et al., 2020), which is known to control neuronal connectivity across model systems. Importantly, early or late genetic removal of *Hox5* in mice affects diaphragm innervation, suggesting a continuous Hox requirement for establishment and maintenance of neuronal wiring (Philippidou et al., 2012).

Conditional inactivation studies of *Hoxc8* also revealed striking connectivity defects in spinal neurons. That is, *Hoxc8* removal specifically in sensory neurons affects sensory-motor connectivity (Shin et al., 2020), whereas motor neuron-specific depletion of *Hoxc8* affects forelimb muscle innervation (Catela et al., 2016). Mechanistically, *Hoxc8* controls expression of axon molecules *Ret* and Gfrα to establish proper muscle innervation (**Figure 3D**). Besides their role in axon guidance, many of the aforementioned axon guidance molecules are also required for synapse formation and plasticity. This leads to the possibility that Hox genes may also maintain synaptic plasticity at post-natal stages, as suggested by the aforementioned Hoxa5 study in pontine neurons (Lizen et al., 2017b).

Control of Neuronal Terminal Identity by Mouse Hox Genes

Recent work suggests that mouse Hox genes, similar to their *C. elegans* and *Drosophila* counterparts, control terminal identity features (e.g., NT biosynthesis components, NT receptors, ion channels) of post-mitotic neurons. In the context of pontine neurons in the brainstem, *Hoxa5* appears necessary for the maintained expression of genes encoding several glutamate receptor subunits (*Grm4, Grin2c, Grid2*), which are required for glutamatergic input by pyramidal cells (Lizen et al., 2017b). Moreover, *Hoxa5* also ensures the maintained expression of *Slc17a7* (VGLUT1), which is crucial for loading synaptic vesicles with glutamate – a key step for the synaptic output of pontine neurons onto granule cells of the cerebellum (Lizen et al., 2017b; Gofflot and Lizen, 2018; **Figure 3C**). In the mouse spinal cord, *Hoxc8* is required for the induction and maintenance of several terminal identity genes (*Nrg1, Mcam*, *Pappa*) in motor neurons of the brachial region (Catela et al., 2021; **Figure 3D**). Interestingly, while these terminal differentiation genes require Hoxc8 for both initiation and maintenance of their expression, not all Hoxc8 target genes behave in the same way. In fact, the suite of Hoxc8 targets in brachial MNs is dynamic across different life stages. For example, the glycine receptor subunit alpha-2 (*Glra2*) appears significantly downregulated upon conditional knockout of *Hoxc8* at postnatal day 8 (p8) but is unaffected upon *Hoxc8* knockout at embryonic day 12 (e12). One possible explanation for this phenomenon is that *Glra2* is redundantly regulated by additional transcription factors at early stages, whose expression fades away later on and *Hoxc8*-mediated regulation becomes necessary for maintenance. Although the underlying mechanisms remain elusive, these findings suggest that Hox genes are continuously required in the mouse nervous system to establish and maintain neuronal terminal identity features.

CONCLUSION

A large body of work has uncovered critical roles for Hox genes in the early steps of nervous system development, such as progenitor cell specification, neuronal migration, cell survival and axo-dendritic growth. This review highlights recent studies in *C. elegans, Drosophila*, and mice that identified later functions for Hox genes in post-mitotic neurons, such as the control of synapse formation/maturation and neuronal terminal identity. These studies strongly suggest that Hox proteins multitask over time within a neuronal lineage by acting at the level of progenitors and/or post-mitotic neurons. Precisely controlled, temporal inactivation of Hox gene activity is necessary to continue uncovering the breadth of Hox gene functions in the nervous system. The realization of this ambitious goal critically relies on inducible genetic approaches coupled with powerful transcriptomic, biochemical, and behavioral methods.

AUTHOR CONTRIBUTIONS

WF and YL: literature search, writing — original draft, and review and editing. PK: supervision, literature search, writing — original draft, and review and editing. All authors contributed to the article and approved the submitted version.

FUNDING

This work was supported by grants from National Institute of Neurological Disorders and Stroke (NINDS) of the NIH (Award Numbers R01NS116365 and R21NS108505) to PK.

ACKNOWLEDGMENTS

We thank the reviewers for their constructive comments. We apologize to colleagues for not including their work herein due to space constraints.

REFERENCES

Aquino-Nunez, W., Mielko, Z. E., Dunn, T., Santorella, E. M., Hosea, C., Leitner, L., et al. (2020). cnd-1/NeuroD1 functions with the homeobox gene ceh-5/Vax2 and hox gene ceh-13/labial to specify aspects of RME and DD neuron fate in *Caenorhabditis elegans*. *G3* 10, 3071–3085. doi: 10.1534/g3.120.401515

Baek, M., Enriquez, J., and Mann, R. S. (2013). Dual role for Hox genes and Hox co-factors in conferring leg motoneuron survival and identity in *Drosophila*. *Development* 140, 2027–2038. doi: 10.1242/dev.090902

Baek, M., Menon, V., Jessell, T. M., Hantman, A. W., and Dasen, J. S. (2019). Molecular logic of spinocerebellar tract neuron diversity and connectivity. *Cell Rep.* 27, 2620.e4–2635.e4. doi: 10.1016/j.celrep.2019.04.113

Basu, R., Taylor, M. R., and Williams, M. E. (2015). The classic cadherins in synaptic specificity. *Cell Adh. Migr.* 9, 193–201. doi: 10.1080/19336918.2014.1000072

Baum, P. D., Guenther, C., Frank, C. A., Pham, B. V., and Garriga, G. (1999). The *Caenorhabditis elegans* gene ham-2 links Hox patterning to migration of the Hsn motor neuron. *Genes Dev.* 13, 472–483. doi: 10.1101/gad.13.4.472

Bechara, A., Laumonnerie, C., Vilain, N., Kratochwil, C. F., Cankovic, V., Maiorano, N. A., et al. (2015). Hoxa2 selects barrelette neuron identity and connectivity in the mouse somatosensory brainstem. *Cell Rep.* 13, 783–797. doi: 10.1016/j.celrep.2015.09.031

Bounoutas, A., and Chalfie, M. (2007). Touch sensitivity in *Caenorhabditis elegans*. *Pflugers. Arch.* 454, 691–702. doi: 10.1007/s00424-006-0187-x

Briscoe, J., and Wilkinson, D. G. (2004). Establishing neuronal circuitry: Hox genes make the connection. *Genes Dev.* 18, 1643–1648. doi: 10.1101/gad.1227004

Brunschwig, K., Wittmann, C., Schnabel, R., Burglin, T. R., Tobler, H., and Muller, F. (1999). Anterior organization of the *Caenorhabditis elegans* embryo by the labial-like Hox gene ceh-13. *Development* 126, 1537–1546. doi: 10.1242/dev.126.7.1537

Catela, C., Shin, M. M., and Dasen, J. S. (2015). Assembly and function of spinal circuits for motor control. *Annu. Rev. Cell Dev. Biol.* 31, 669–698. doi: 10.1146/annurev-cellbio-100814-125155

Catela, C., Shin, M. M., Lee, D. H., Liu, J. P., and Dasen, J. S. (2016). Hox proteins coordinate motor neuron differentiation and connectivity programs through Ret/Gfralpha genes. *Cell Rep.* 14, 1901–1915. doi: 10.1016/j.celrep.2016.01.067

Catela, C., Weng, Y., Wen, K., Feng, W., and Kratsios, P. (2021). Control of spinal motor neuron terminal differentiation through sustained Hoxc8 gene activity. *bioRxiv* [Preprint]. doi: 10.1101/2021.05.26.445841v1

Chisholm, A. (1991). Control of cell fate in the tail region of *C. elegans* by the gene egl-5. *Development* 111, 921–932. doi: 10.1242/dev.111.4.921

Clark, S. G., Chisholm, A. D., and Horvitz, H. R. (1993). Control of cell fates in the central body region of *C. elegans* by the homeobox gene lin-39. *Cell* 74, 43–55. doi: 10.1016/0092-8674(93)90293-y

Costa, M., Weir, M., Coulson, A., Sulston, J., and Kenyon, C. (1988). Posterior pattern formation in *C. elegans* involves position-specific expression of a gene containing a homeobox. *Cell* 55, 747–756. doi: 10.1016/0092-8674(88)90131-6

Coughlan, E., Garside, V. C., Wong, S. F. L., Liang, H., Kraus, D., Karmakar, K., et al. (2019). A hox code defines spinocerebellar neuron subtype regionalization. *Cell Rep.* 29, 2408.e4–2421.e4. doi: 10.1016/j.celrep.2019.10.048

Cowing, D. W., and Kenyon, C. (1992). Expression of the homeotic gene mab-5 during *Caenorhabditis elegans* embryogenesis. *Development* 116, 481–490. doi: 10.1242/dev.116.2.481

Dasen, J. S. (2009). Transcriptional networks in the early development of sensory-motor circuits. *Curr. Top. Dev. Biol.* 87, 119–148. doi: 10.1016/S0070-2153(09)01204-6

Dasen, J. S., De Camilli, A., Wang, B., Tucker, P. W., and Jessell, T. M. (2008). Hox repertoires for motor neuron diversity and connectivity gated by a single accessory factor, FoxP1. *Cell* 134, 304–316. doi: 10.1016/j.cell.2008.06.019

Dasen, J. S., Liu, J. P., and Jessell, T. M. (2003). Motor neuron columnar fate imposed by sequential phases of Hox-c activity. *Nature* 425, 926–933. doi: 10.1038/nature02051

Dasen, J. S., Tice, B. C., Brenner-Morton, S., and Jessell, T. M. (2005). A Hox regulatory network establishes motor neuron pool identity and target-muscle connectivity. *Cell* 123, 477–491. doi: 10.1016/j.cell.2005.09.009

Di Bonito, M., Glover, J. C., and Studer, M. (2013a). Hox genes and region-specific sensorimotor circuit formation in the hindbrain and spinal cord. *Dev. Dyn.* 242, 1348–1368. doi: 10.1002/dvdy.24055

Di Bonito, M., Narita, Y., Avallone, B., Sequino, L., Mancuso, M., Andolfi, G., et al. (2013b). Assembly of the auditory circuitry by a Hox genetic network in the mouse brainstem. *PLoS Genet.* 9:e1003249. doi: 10.1371/journal.pgen.1003249

Di Meglio, T., Kratochwil, C. F., Vilain, N., Loche, A., Vitobello, A., Yonehara, K., et al. (2013). Ezh2 orchestrates topographic migration and connectivity of mouse precerebellar neurons. *Science* 339, 204–207. doi: 10.1126/science.1229326

Dickins, E. M., and Salinas, P. C. (2013). Wnts in action: from synapse formation to synaptic maintenance. *Front. Cell Neurosci.* 7:162. doi: 10.3389/fncel.2013.00162

Eastman, C., Horvitz, H. R., and Jin, Y. (1999). Coordinated transcriptional regulation of the unc-25 glutamic acid decarboxylase and the unc-47 GABA vesicular transporter by the *Caenorhabditis elegans* UNC-30 homeodomain protein. *J. Neurosci.* 19, 6225–6234. doi: 10.1523/JNEUROSCI.19-15-06225.1999

Estacio-Gomez, A., and Diaz-Benjumea, F. J. (2014). Roles of Hox genes in the patterning of the central nervous system of *Drosophila*. *Fly* 8, 26–32. doi: 10.4161/fly.27424

Estacio-Gomez, A., Moris-Sanz, M., Schafer, A. K., Perea, D., Herrero, P., and Diaz-Benjumea, F. J. (2013). Bithorax-complex genes sculpt the pattern of leucokinergic neurons in the *Drosophila* central nervous system. *Development* 140, 2139–2148. doi: 10.1242/dev.090423

Feng, W., Li, Y., Dao, P., Aburas, J., Islam, P., Elbaz, B., et al. (2020). A terminal selector prevents a Hox transcriptional switch to safeguard motor neuron identity throughout life. *eLife* 9:e50065. doi: 10.7554/eLife.50065

Fixsen, W., Sternberg, P., Ellis, H., and Horvitz, R. (1985). Genes that affect cell fates during the development of *Caenorhabditis elegans*. *Cold. Spring Harb. Symp. Quant. Biol.* 50, 99–104. doi: 10.1101/sqb.1985.050.01.014

Friedrich, J., Sorge, S., Bujupi, F., Eichenlaub, M. P., Schulz, N. G., Wittbrodt, J., et al. (2016). Hox function is required for the development and maintenance of the drosophila feeding motor unit. *Cell Rep.* 14, 850–860. doi: 10.1016/j.celrep.2015.12.077

Gabilondo, H., Rubio-Ferrera, I., Losada-Perez, M., Del Saz, D., Leon, Y., Molina, I., et al. (2018). Segmentally homologous neurons acquire two different terminal neuropeptidergic fates in the *Drosophila* nervous system. *PLoS One* 13:e0194281. doi: 10.1371/journal.pone.0194281

Gaunt, S. J. (2015). The significance of Hox gene collinearity. *Int. J. Dev. Biol.* 59, 159–170. doi: 10.1387/ijdb.150223sg

Geisen, M. J., Di Meglio, T., Pasqualetti, M., Ducret, S., Brunet, J. F., Chedotal, A., et al. (2008). Hox paralog group 2 genes control the migration of mouse pontine neurons through slit-robo signaling. *PLoS Biol.* 6:e142. doi: 10.1371/journal.pbio.0060142

Ghosh, P., and Sagerstrom, C. G. (2018). Developing roles for Hox proteins in hindbrain gene regulatory networks. *Int. J. Dev. Biol.* 62, 767–774. doi: 10.1387/ijdb.180141cs

Gofflot, F., and Lizen, B. (2018). Emerging roles for HOX proteins in synaptogenesis. *Int. J. Dev. Biol.* 62, 807–818. doi: 10.1387/ijdb.180299fg

Gummalla, M., Galetti, S., Maeda, R. K., and Karch, F. (2014). Hox gene regulation in the central nervous system of *Drosophila*. *Front. Cell Neurosci.* 8:96. doi: 10.3389/fncel.2014.00096

Harris, J., Honigberg, L., Robinson, N., and Kenyon, C. (1996). Neuronal cell migration in *C. elegans*: regulation of Hox gene expression and cell position. *Development* 122, 3117–3131. doi: 10.1242/dev.122.10.3117

Hessinger, C., Technau, G. M., and Rogulja-Ortmann, A. (2017). The *Drosophila* Hox gene Ultrabithorax acts in both muscles and motoneurons to orchestrate formation of specific neuromuscular connections. *Development* 144, 139–150. doi: 10.1242/dev.143875

Hobert, O. (2008). Regulatory logic of neuronal diversity: terminal selector genes and selector motifs. *Proc. Natl. Acad. Sci. U.S.A.* 105, 20067–20071. doi: 10.1073/pnas.0806070105

Hobert, O., and Kratsios, P. (2019). Neuronal identity control by terminal selectors in worms, flies, and chordates. *Curr. Opin. Neurobiol* 56, 97–105. doi: 10.1016/j.conb.2018.12.006

Hutlet, B., Theys, N., Coste, C., Ahn, M. T., Doshishti-Agolli, K., Lizen, B., et al. (2016). Systematic expression analysis of Hox genes at adulthood reveals novel patterns in the central nervous system. *Brain Struct. Funct.* 221, 1223–1243. doi: 10.1007/s00429-014-0965-8

Jia, L., and Emmons, S. W. (2006). Genes that control ray sensory neuron axon development in the *Caenorhabditis elegans* male. *Genetics* 173, 1241–1258. doi: 10.1534/genetics.106.057000

Jin, Y., Hoskins, R., and Horvitz, H. R. (1994). Control of type-D GABAERGIC neuron differentiation by *C. elegans* UNC-30 homeodomain protein. *Nature* 372, 780–783. doi: 10.1038/372780a0

Kalis, A. K., Kissiov, D. U., Kolenbrander, E. S., Palchick, Z., Raghavan, S., Tetreault, B. J., et al. (2014). Patterning of sexually dimorphic neurogenesis in the *Caenorhabditis elegans* ventral cord by Hox and Tale homeodomain transcription factors. *Dev. Dyn.* 243, 159–171. doi: 10.1002/dvdy.24064

Karmakar, K., Narita, Y., Fadok, J., Ducret, S., Loche, A., Kitazawa, T., et al. (2017). Hox2 genes are required for tonotopic map precision and sound discrimination

in the mouse auditory brainstem. *Cell Rep.* 18, 185–197. doi: 10.1016/j.celrep.2016.12.021

Kenyon, C. (1986). A gene involved in the development of the posterior body region of *C. elegans*. *Cell* 46, 477–487. doi: 10.1016/0092-8674(86)90668-9

Kerk, S. Y., Kratsios, P., Hart, M., Mourao, R., and Hobert, O. (2017). Diversification of *C. elegans* motor neuron identity via selective effector gene repression. *Neuron* 93, 80–98. doi: 10.1016/j.neuron.2016.11.036

Kerr, K. S., Fuentes-Medel, Y., Brewer, C., Barria, R., Ashley, J., Abruzzi, K. C., et al. (2014). Glial wingless/Wnt regulates glutamate receptor clustering and synaptic physiology at the *Drosophila* neuromuscular junction. *J. Neurosci.* 34, 2910–2920. doi: 10.1523/JNEUROSCI.3714-13.2014

Klassen, M. P., and Shen, K. (2007). Wnt signaling positions neuromuscular connectivity by inhibiting synapse formation in *C. elegans*. *Cell* 130, 704–716. doi: 10.1016/j.cell.2007.06.046

Kmita, M., and Duboule, D. (2003). Organizing axes in time and space; 25 years of colinear tinkering. *Science* 301, 331–333. doi: 10.1126/science.1085753

Kratsios, P., Kerk, S. Y., Catela, C., Liang, J., Vidal, B., Bayer, E. A., et al. (2017). An intersectional gene regulatory strategy defines subclass diversity of *C. elegans* motor neurons. *eLife* 6:e25751. doi: 10.7554/eLife.25751

Kratsios, P., Pinan-Lucarre, B., Kerk, S. Y., Weinreb, A., Bessereau, J. L., and Hobert, O. (2015). Transcriptional coordination of synaptogenesis and neurotransmitter signaling. *Curr. Biol.* 25, 1282–1295. doi: 10.1016/j.cub.2015.03.028

Kratsios, P., Stolfi, A., Levine, M., and Hobert, O. (2011). Coordinated regulation of cholinergic motor neuron traits through a conserved terminal selector gene. *Nat. Neurosci.* 15, 205–14. doi: 10.1038/nn.2989

Krumlauf, R., Marshall, H., Studer, M., Nonchev, S., Sham, M. H., and Lumsden, A. (1993). Hox homeobox genes and regionalisation of the nervous system. *J. Neurobiol.* 24, 1328–1340. doi: 10.1002/neu.480241006

Li, Y., Osuma, A., Correa, E., Okebalama, M. A., Dao, P., Gaylord, O., et al. (2020). Establishment and maintenance of motor neuron identity via temporal modularity in terminal selector function. *eLife* 9:e59464. doi: 10.7554/eLife.59464

Lints, R., and Emmons, S. W. (1999). Patterning of dopaminergic neurotransmitter identity among *Caenorhabditis elegans* ray sensory neurons by a TGFbeta family signaling pathway and a Hox gene. *Development* 126, 5819–5831. doi: 10.1242/dev.126.24.5819

Lizen, B., Hutlet, B., Bissen, D., Sauvegarde, D., Hermant, M., Ahn, M. T., et al. (2017a). HOXA5 localization in postnatal and adult mouse brain is suggestive of regulatory roles in postmitotic neurons. *J. Comp. Neurol.* 525, 1155–1175. doi: 10.1002/cne.24123

Lizen, B., Moens, C., Mouheiche, J., Sacre, T., Ahn, M. T., Jeannotte, L., et al. (2017b). Conditional loss of Hoxa5 function early after birth impacts on expression of genes with synaptic function. *Front. Mol. Neurosci.* 10:369. doi: 10.3389/fnmol.2017.00369

Maheshwari, U., Kraus, D., Vilain, N., Holwerda, S. J. B., Cankovic, V., Maiorano, N. A., et al. (2020). Postmitotic Hoxa5 expression specifies pontine neuron positional identity and input connectivity of cortical afferent subsets. *Cell Rep.* 31:107767. doi: 10.1016/j.celrep.2020.107767

Moris-Sanz, M., Estacio-Gomez, A., Sanchez-Herrero, E., and Diaz-Benjumea, F. J. (2015). The study of the Bithorax-complex genes in patterning CCAP neurons reveals a temporal control of neuronal differentiation by Abd-B. *Biol. Open* 4, 1132–1142. doi: 10.1242/bio.012872

Narita, Y., and Rijli, F. M. (2009). Hox genes in neural patterning and circuit formation in the mouse hindbrain. *Curr. Top. Dev. Biol.* 88, 139–167. doi: 10.1016/S0070-2153(09)88005-8

Nusslein-Volhard, C., and Wieschaus, E. (1980). Mutations affecting segment number and polarity in *Drosophila*. *Nature* 287, 795–801. doi: 10.1038/287795a0

Oury, F., Murakami, Y., Renaud, J. S., Pasqualetti, M., Charnay, P., Ren, S. Y., et al. (2006). Hoxa2- and rhombomere-dependent development of the mouse facial somatosensory map. *Science* 313, 1408–1413. doi: 10.1126/science.1130042

Parker, H. J., and Krumlauf, R. (2020). A Hox gene regulatory network for hindbrain segmentation. *Curr. Top. Dev. Biol.* 139, 169–203. doi: 10.1016/bs.ctdb.2020.03.001

Pasqualetti, M., Diaz, C., Renaud, J. S., Rijli, F. M., and Glover, J. C. (2007). Fate-mapping the mammalian hindbrain: segmental origins of vestibular projection neurons assessed using rhombomere-specific Hoxa2 enhancer elements in the mouse embryo. *J. Neurosci.* 27, 9670–9681. doi: 10.1523/JNEUROSCI.2189-07.2007

Philippidou, P., and Dasen, J. S. (2013). Hox genes: choreographers in neural development, architects of circuit organization. *Neuron* 80, 12–34. doi: 10.1016/j.neuron.2013.09.020

Philippidou, P., Walsh, C. M., Aubin, J., Jeannotte, L., and Dasen, J. S. (2012). Sustained Hox5 gene activity is required for respiratory motor neuron development. *Nat. Neurosci.* 15, 1636–1644. doi: 10.1038/nn.3242

Prasad, B., Karakuzu, O., Reed, R. R., and Cameron, S. (2008). unc-3-dependent repression of specific motor neuron fates in *Caenorhabditis elegans*. *Dev. Biol.* 323, 207–215. doi: 10.1016/j.ydbio.2008.08.029

Prasad, B. C., Ye, B., Zackhary, R., Schrader, K., Seydoux, G., and Reed, R. R. (1998). unc-3, a gene required for axonal guidance in *Caenorhabditis elegans*, encodes a member of the O/E family of transcription factors. *Development* 125, 1561–1568. doi: 10.1242/dev.125.8.1561

Reichert, H., and Bello, B. (2010). Hox genes and brain development in *Drosophila*. *Adv. Exp. Med. Biol.* 689, 145–153.

Salser, S. J., and Kenyon, C. (1992). Activation of a *C. elegans* Antennapedia homologue in migrating cells controls their direction of migration. *Nature* 355, 255–258. doi: 10.1038/355255a0

Salser, S. J., Loer, C. M., and Kenyon, C. (1993). Multiple HOM-C gene interactions specify cell fates in the nematode central nervous system. *Genes Dev.* 7, 1714–1724. doi: 10.1101/gad.7.9.1714

Shin, M. M., Catela, C., and Dasen, J. (2020). Intrinsic control of neuronal diversity and synaptic specificity in a proprioceptive circuit. *eLife* 9:e56374. doi: 10.7554/eLife.56374

Sokabe, T., Chen, H. C., Luo, J., and Montell, C. (2016). A switch in thermal preference in *Drosophila* larvae depends on multiple rhodopsins. *Cell Rep.* 17, 336–344. doi: 10.1016/j.celrep.2016.09.028

Soshnikova, N., Dewaele, R., Janvier, P., Krumlauf, R., and Duboule, D. (2013). Duplications of hox gene clusters and the emergence of vertebrates. *Dev. Biol.* 378, 194–199. doi: 10.1016/j.ydbio.2013.03.004

Strochlic, L., Falk, J., Goillot, E., Sigoillot, S., Bourgeois, F., Delers, P., et al. (2012). Wnt4 participates in the formation of vertebrate neuromuscular junction. *PLoS One* 7:e29976. doi: 10.1371/journal.pone.0029976

Sweeney, L. B., Bikoff, J. B., Gabitto, M. I., Brenner-Morton, S., Baek, M., Yang, J. H., et al. (2018). Origin and segmental diversity of spinal inhibitory interneurons. *Neuron* 97, 341.e3–355.e3. doi: 10.1016/j.neuron.2017.12.029

Sym, M., Robinson, N., and Kenyon, C. (1999). MIG-13 positions migrating cells along the anteroposterior body axis of *C. elegans*. *Cell* 98, 25–36. doi: 10.1016/S0092-8674(00)80603-0

Takahashi, Y., Hamada, J., Murakawa, K., Takada, M., Tada, M., Nogami, I., et al. (2004). Expression profiles of 39 Hox genes in normal human adult organs and anaplastic thyroid cancer cell lines by quantitative real-time RT-PCR system. *Exp. Cell Res.* 293, 144–153. doi: 10.1016/j.yexcr.2003.09.024

Tihanyi, B., Vellai, T., Regos, A., Ari, E., Muller, F., and Takacs-Vellai, K. (2010). The *C. elegans* Hox gene ceh-13 regulates cell migration and fusion in a non-colinear way. Implications for the early evolution of Hox clusters. *BMC Dev. Biol.* 10:78. doi: 10.1186/1471-213X-10-78

Toker, A. S., Teng, Y., Ferreira, H. B., Emmons, S. W., and Chalfie, M. (2003). The *Caenorhabditis elegans* spalt-like gene sem-4 restricts touch cell fate by repressing the selector Hox gene egl-5 and the effector gene mec-3. *Development* 130, 3831–3840. doi: 10.1242/dev.00398

Tomas-Roca, L., Corral-San-Miguel, R., Aroca, P., Puelles, L., and Marin, F. (2016). Crypto-rhombomeres of the mouse medulla oblongata, defined by molecular and morphological features. *Brain Struct. Funct.* 221, 815–838. doi: 10.1007/s00429-014-0938-y

Vagnozzi, A. N., Garg, K., Dewitz, C., Moore, M. T., Cregg, J. M., Jeannotte, L., et al. (2020). Phrenic-specific transcriptional programs shape respiratory motor output. *eLife* 9:e52859. doi: 10.7554/eLife.52859

Van Auken, K., Weaver, D. C., Edgar, L. G., and Wood, W. B. (2000). *Caenorhabditis elegans* embryonic axial patterning requires two recently discovered posterior-group Hox genes. *Proc. Natl. Acad. Sci. U.S.A.* 97, 4499–4503. doi: 10.1073/pnas.97.9.4499

Von Stetina, S. E., Treinin, M., and Miller, D. M. III (2006). The motor circuit. *Int. Rev. Neurobiol.* 69, 125–167.

Wang, B. B., Muller-Immergluck, M. M., Austin, J., Robinson, N. T., Chisholm, A., and Kenyon, C. (1993). A homeotic gene cluster patterns the anteroposterior body axis of *C. elegans*. *Cell* 74, 29–42. doi: 10.1016/0092-8674(93)90292-x

Wang, X., Zhou, F., Lv, S., Yi, P., Zhu, Z., Yang, Y., et al. (2013). Transmembrane protein MIG-13 links the Wnt signaling and Hox genes to the cell polarity in neuronal migration. *Proc. Natl. Acad. Sci. U.S.A.* 110, 11175–11180. doi: 10.1073/pnas.1301849110

Wittmann, C., Bossinger, O., Goldstein, B., Fleischmann, M., Kohler, R., Brunschwig, K., et al. (1997). The expression of the *C. elegans* labial-like Hox gene ceh-13 during early embryogenesis relies on cell fate and on anteroposterior cell polarity. *Development* 124, 4193–4200.

Zheng, C., Diaz-Cuadros, M., and Chalfie, M. (2015a). Hox genes promote neuronal subtype diversification through posterior induction in *Caenorhabditis elegans*. *Neuron* 88, 514–527. doi: 10.1016/j.neuron.2015.09.049

Zheng, C., Jin, F. Q., and Chalfie, M. (2015b). Hox proteins act as transcriptional guarantors to ensure terminal differentiation. *Cell Rep.* 13, 1343–1352. doi: 10.1016/j.celrep.2015.10.044

Conflict of Interest: The authors declare that the research was conducted in the absence of any commercial or financial relationships that could be construed as a potential conflict of interest.

frontiers in Neuroscience

REVIEW
published: 07 March 2022
doi: 10.3389/fnins.2021.787753

Open Frontiers in Neural Cell Type Investigations; Lessons From *Caenorhabditis elegans* and Beyond, Toward a Multimodal Integration

*Georgia Rapti**

Developmental Biology Unit, European Molecular Biology Laboratory, Heidelberg, Germany

Nervous system cells, the building blocks of circuits, have been studied with ever-progressing resolution, yet neural circuits appear still resistant to schemes of reductionist classification. Due to their sheer numbers, complexity and diversity, their systematic study requires concrete classifications that can serve reduced dimensionality, reproducibility, and information integration. Conventional hierarchical schemes transformed through the history of neuroscience by prioritizing criteria of morphology, (electro)physiological activity, molecular content, and circuit function, influenced by prevailing methodologies of the time. Since the molecular biology revolution and the recent advents in transcriptomics, molecular profiling gains ground toward the classification of neurons and glial cell types. Yet, transcriptomics entails technical challenges and more importantly uncovers unforeseen spatiotemporal heterogeneity, in complex and simpler nervous systems. Cells change states dynamically in space and time, in response to stimuli or throughout their developmental trajectory. Mapping cell type and state heterogeneity uncovers uncharted terrains in neurons and especially in glial cell biology, that remains understudied in many aspects. Examining neurons and glial cells from the perspectives of molecular neuroscience, physiology, development and evolution highlights the advantage of multifaceted classification schemes. Among the amalgam of models contributing to neuroscience research, *Caenorhabditis elegans* combines nervous system anatomy, lineage, connectivity and molecular content, all mapped at single-cell resolution, and can provide valuable insights for the workflow and challenges of the multimodal integration of cell type features. This review reflects on concepts and practices of neuron and glial cells classification and how research, in *C. elegans* and beyond, guides nervous system experimentation through integrated multidimensional schemes. It highlights underlying principles, emerging themes, and open frontiers in the study of nervous system development, regulatory logic and evolution. It proposes unified platforms to allow

OPEN ACCESS

Edited by:
Luisa Cochella,
Research Institute of Molecular Pathology (IMP), Austria

Reviewed by:
Oliver Hobert,
Columbia University, United States
Simon Hippenmeyer,
Institute of Science and Technology Austria (IST Austria), Austria

***Correspondence:**
Georgia Rapti
grapti@embl.de

Specialty section:
This article was submitted to Neurogenesis, a section of the journal Frontiers in Neuroscience

Received: *01 October 2021*
Accepted: *30 December 2021*
Published: *07 March 2022*

Citation:
Rapti G (2022) Open Frontiers in Neural Cell Type Investigations; Lessons From Caenorhabditis elegans and Beyond, Toward a Multimodal Integration. Front. Neurosci. 15:787753. doi: 10.3389/fnins.2021.787753

integrated annotation of large-scale datasets, gene-function studies, published or unpublished findings and community feedback. Neuroscience is moving fast toward interdisciplinary, high-throughput approaches for combined mapping of the morphology, physiology, connectivity, molecular function, and the integration of information in multifaceted schemes. A closer look in mapped neural circuits and understudied terrains offers insights for the best implementation of these approaches.

Keywords: neurons, glia, development, evolution, transcriptomics, genetics, databases, integration

INTRODUCTION: NERVOUS SYSTEM COMPLEXITY AND THE DEMAND FOR CELL CLASSIFICATION

Neural circuits have long appeared resistant to a coherent reductionist understanding, partly due to their structural and functional complexity. Neuron numbers are high across species, from billions in human brains to millions in mouse and zebrafish brains, hundred thousand in *Drosophila melanogaster* and hundreds in *Caenorhabditis elegans*. Numbers of macroglia, neurons' ectoderm-derived sister cells, rise from thousands to millions across vertebrates and dozens to thousands in invertebrate models. Neural cells have diverse properties delineating complementary perspectives; morphology (pattern of membrane projections), molecular features (neurotransmitter receptors, transporters, effector proteins), circuit function (chemosensory/mechanosensory/interneurons, myelinating/non-myelinating glia, etc.) (Zeng and Sanes, 2017; Allen and Lyons, 2018; Singhvi and Shaham, 2019; Bittern et al., 2020). It is well accepted that neural cell types serve as building blocks of circuits and dissecting their diversity and connectivity is key to investigate nervous system function.

Due to their diversity and sheer numbers, analyzing neural cells systematically requires categorizing them molecularly and functionally. Such classification serves various purposes. First, it allows experimental reproducibility; understanding nervous system biology requires consistent accessibility of defined cells across time and space, to allow coupling of their developmental programs to their functional roles. The resulting reduced dimensionality serves the need to interpolate information, assess known and unknowns, highlight emerging concepts, regulatory programs, functional mechanisms and evolutionary relations. As discussed below, in *C. elegans*, reliable identification of nervous system cells at single-cell resolution allows mapping of their connectivity and mechanistic understanding of their development and interactions. Gene-function discovery in cells with similar functions and molecular content dissects the disease mechanisms altering specific cells or genes across cell types (Takano, 2015; Ponroy Bally and Murai, 2021). Classification by criteria shared across organisms allows to evaluate knowledge in different models and to proceed in testable hypotheses. By investigating cell behavior and function across species, organisms may be understood in light of the cell types they present or lack (Marioni and Arendt, 2017).

Cell classification previously hampered by laborious approaches lacking quantitative reproducibility is fast becoming an issue of the past, resolved by recent high-throughput methods. Nevertheless, classifications are arbitrary man-made concepts; we compose categories while natural selection may be working toward continuums of diversity. Each cell type exists in a single state at a time, transitions between states in time and space, and can be thought of as a subset of cell states in a multidimensional space (Trapnell, 2015). Classification in the nervous system meets conceptual challenges; how fine or firm are the distinctions of cell types is difficult to define. Everyone agrees on broad classes of motorneurons and interneurons, astrocytes and oligodendrocytes, yet such coarse distinctions bear little use for the above-mentioned purposes. If each neural cell type differs from another in molecular, morphological, and functional properties combined, the conceptual challenge persists beyond the growing large-scale approaches that enable in-depth characterization of individual cells. Can we devise classification schemes or information arrangements that fairly balance overarching distinctions of cell types and within-cell-type variability? Cell types are defined by the possible space of their states, arising from an array of experimental descriptions recounting a cell's content, development, and function. The aim of a classification in a given system (developmental, molecular, evolutionary neuroscience) should be clear, while if it is meant to serve multiple purposes, a multi-faceted and dynamic classification is key. A closer look at *C. elegans*, the first metazoan with nervous system anatomy, connectivity and molecular content mapped with single-cell resolution, highlights aspects of multi-faceted classification, providing lessons for workflows and challenges of such integration.

This review reflects on neural cell type classification and how recent research, in *C. elegans* and beyond, can guide nervous system study through integrated classification schemes. It does not intend to comprehensively summarize the *C. elegans* nervous system regulatory mechanisms or functions, reviewed elsewhere comprehensively (Hobert, 2016a). I discuss how gene-function analysis and recent advances in molecular atlases highlight unforeseen cell heterogeneity and classification challenges. I suggest integrated classification schemes in unified platforms to allow equal annotation of large-scale datasets with published or unpublished findings and community feedback. Altogether, using examples in and outside *C. elegans* research, I discuss how reconciling morphological, molecular, functional knowledge and classification approaches enables comprehensive nervous system study.

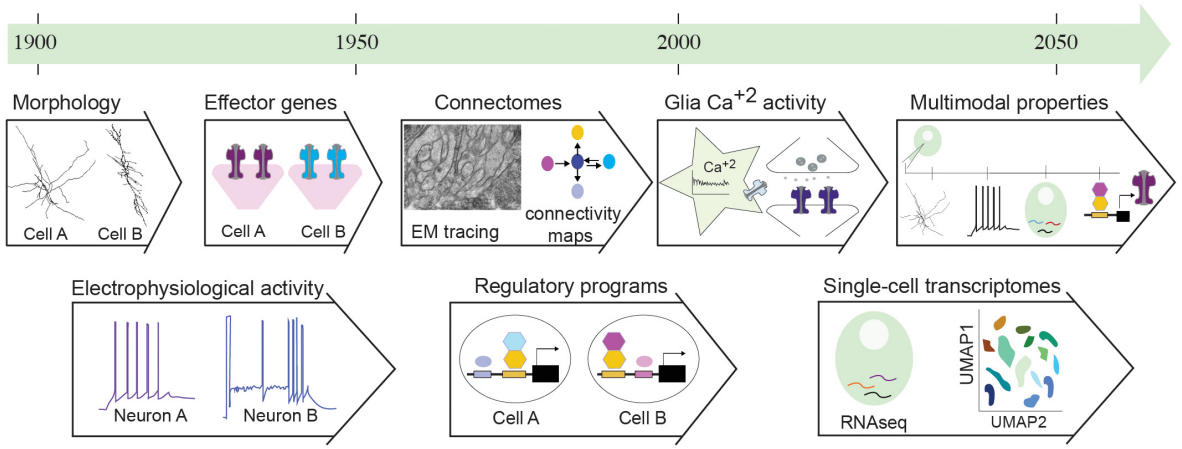

FIGURE 1 | Nervous system properties serving cell classification criteria throughout time. This historical timeline presents properties of nervous system cells that served as classification criteria throughout the 20th and 21st centuries. Initial classifications followed morphological features. These were paired with electrophysiological recordings of neurons, but not glia. Soon, the revolution of molecular biology and genetics in model organisms uncovered effector genes of functional modules and regulatory programs of neural cells. Electron microscopy (EM) tracing enabled mapping synaptic connections, providing circuit connectomes. Recently, calcium activity was described in glial cells, implicated in regulating neuronal function. In the last two decades, transcriptomics and specifically single-cell transcriptomics enables classification of transcriptomic cell clusters through dimensionality reduction analysis (UMAP). Combination of these approaches pave the way to multimodal analysis of properties for integrated classifications. Details and relevant citations are found in the text. EM figure kindly provided by G. Rapti, Y. Lu, S. Shaham (unpublished data).

INVESTIGATING NERVOUS SYSTEM CELLS ACROSS DIFFERENT ERAS AND CLASSIFICATIONS

Navigating From Cell Morphology to Activity

Cell type descriptions transform alongside our ever-progressing knowledge, within the nervous system and beyond. The first cell description was based on form; Hooke referred to "pores, or cells...", due to the rigid wall of plant cells (Hooke, 1665). Two centuries later, Schultze casts aside this previous definition to define cells by their content and not their boundary; a "naked speck of protoplasm with a nucleus"(Kutschera, 2011). In 1896, Wilson described cells as "the basis of the life of all organisms"(Hyman and Simons, 2011). Similarly, nervous system cells were initially defined by morphology and architecture, and later functionally and molecularly (**Figure 1**). Ramoìn y Cajal provided one of the founding nervous system descriptions and the first extensive neuron classification based on morphology, the principal criteria available at the time (Ramón Y Cajal, 1911). Early drawings by Virchow and Deiter described the cells known today as (macro)glia, which were grouped morphologically by Lenhossek, Andriezen, and Koelliker in a classification largely adopted and developed by Cajal (García-Marín et al., 2007). Neurons and glia are now recognized cell components of all bilaterian nervous systems, composing peripheral sensory structures and centralized ganglia. Interestingly, increased brain complexity appears correlated to increased glial numbers (glia compose 15% of *C. elegans* or *Drosophila* nervous systems and 50–90% of mammalian brain areas) (Freeman and Rowitch, 2013). Yet neuron and glial cell types were ill-defined by morphological criteria alone. For example, astrocytes were grouped in fibrous (stellate-shaped, with long, thin processes, predominant in white matter) and protoplasmic (with short, ramified processes, predominant in gray matter). Yet, protoplasmic astrocytes are now known to transform into fibrous astrocytes upon specific environmental or signaling cues (Sun et al., 2010). Morphological criteria alone can hamper cell classifications.

In parallel with the first morphological descriptions of neural cells, studies on nerve excitability, by Du Bois Reymond among others, pioneered early electrophysiological approaches. These provided the conceptual framework to envision circuit function as a result of electrical signals (Finkelstein, 2015). Since then, traditional electrophysiological stimulations alongside anatomical methodologies remained dominant for a half−century, extensively employed to reveal functional architecture of brain regions (Hubel and Wiesel, 1962; O'Keefe and Nadel, 1979). While focusing on electrophysiology, glial cells (from the Greek word for glue, *γλοία*) were described as electrically non-excitable, passive material, providing insulation and trophic support to neurons. With functions lying beyond early electrophysiological operations, glial cells were often overlooked (Varoqueaux and Fasshauer, 2017), yet they contain voltage-sensitive ion channels and neurotransmitter receptors and may exert electrical activity (Gallo and Ghiani, 2000a,b). Astrocytes and other glia interacting with axons and synapses, display a complex repertoire of Ca^{2+} signaling. The evolving field of glia neuroscience is advancing techniques for recording and studying Ca^{2+} activity, its spatiotemporal dynamics in single astrocytes and across networks (Semyanov et al., 2020; **Figure 1**). Today, measuring neuron and glial activities remains prominent for functional cell investigation.

From Cell's Molecular Content to Transcript Profiling

In the 90's, the "decade of the brain," electrophysiology gave ground to molecular investigations (Bargmann, 1998; Südhof and Malenka, 2008; Changeux, 2020). Hypothesis−driven experimentation steered research away from "descriptive" approaches, while the preeminent molecular biology revolution and advanced genetics in model organisms allowed for uncovering mechanisms of nervous system cell physiology and interactions (St Johnston, 2002; Rapti, 2020). Studies in invertebrates and vertebrates -spearheaded by *C. elegans*, *Drosophila,* and mice- identified conserved molecules shaping intricate cell morphologies, synaptic neurotransmission, and connectivity (Leung-Hagesteijn et al., 1992; DiAntonio et al., 1993; Nonet et al., 1993; Zallen et al., 1998). Conventionally, neurons were distinguished from glia in the basis of synaptic neurotransmission. Yet, the recently uncovered molecular signaling pathways of glia have much in common with those of neurons (Fields and Stevens-Graham, 2002; Allen and Lyons, 2018). Interestingly, work in non-Bilateria highlights that molecular components of synapses exist in animals devoid of nervous systems, such as Placozoa and Porifera, raising discussion about the exact relation between the evolutionary origins of neurons and synapses (Moroz and Kohn, 2016; Arendt, 2020). This raises the question: can synaptic molecules sufficiently define neural cell types? Challenges of early molecular classifications are more obvious in glial cells, that are transcriptionally diverse with no known universal glial markers (Zhang et al., 2014). Glial cells are recognized by immunoreactivity of the intermediate filament protein GFAP, transporters, and metabolic enzymes such as glutamine synthetase, all of them also expressed in non-neural cells (Yang and Wang, 2015).

In the last decades, the advent of transcriptomics revolutionized the molecular description of cells by high-throughput measuring of gene expression, moving away from single-gene analysis (Trapnell, 2015; Marioni and Arendt, 2017; Tasic et al., 2018). Recent transcriptomics describe the organization of cell-type landscapes in circuits of mouse, Drosophila and *C. elegans*, while whole-organism single-cell transcriptomics, first in *C. elegans* and then in the annelid *Platynereis dumerilii* and cnidarian *Nematostella vectensis*, provide pioneer insights into the molecular content of nervous system cells in Bilateria and non-Bilateria species (Cao et al., 2017; Achim et al., 2018; Loo et al., 2019; Packer et al., 2019; Taylor et al., 2021). Aside from historical classifications and alongside large-scale molecular approaches, transcript profiling was suggested as the objective approach to determining a cell's "ground state," the unique basis that determines the cell's capabilities (Fishell and Heintz, 2013). Nevertheless, transcriptomics entails challenges. Neural cells are challenging to dissociate, presenting elongated processes with concomitant RNA subcellular localization, which may lead to false-negative results if disrupted during dissociation (Ho et al., 2018; Perez et al., 2021). Analyzing single-cell RNA-sequencing datasets using unsupervised clustering faces computational challenges, including difficulty to report under-represented cells (Kiselev et al., 2019). The resolution of single-cell transcriptomics distinguishes similar cell clusters, that may be states of the same "cell type." It was suggested that no two cells are transcriptionally the same while the number of possible cell types appears proportional to the number of cells analyzed (Svensson et al., 2020). These observations emphasize the notion of cell state. Transcript variation within cell types reflects stochastic expression or responses to the environment, introducing questions of whether previously unrecognized cell states are distinct types or whether recognized types represent points in a continuum of states. Similarly to carving out research into manageable subdomains (neurodevelopment, neurophysiology), there seem to be no easy dividing lines for cell types as the organism is a continuum of spatiotemporal cell interactions.

Following Hierarchy or Integration?

Integrating genomics with functional knowledge *in vivo* is vital for linking molecular repertoires with cell development and function. The challenge lies in defining meaningful ways to do this. Transcriptome fingerprints of cells represent genes with equal weight, but expression level is not indicative of functional impact in key cell characteristics, as discussed below. Gene-function studies distinguish cell properties that define functional identity or others that portray intrinsic variability. Some suggest that classifications should follow principal choices on "the most relevant functions" of studied cell types, but such subjective decisions may hinder discovery. Recent studies and methodologies focus on multifaceted characterization of distinct modalities of neural cell types toward integration for future multimodal classification schemes (**Figure 1**). The *C. elegans* neuroscience community proceeded for long in a seemingly unbiased "cataloging" of cell features (morphological, molecular, functional), which may have been a driver of continuous discovery of new cellular functions.

CELL CLASSIFICATIONS IN THE MAPPED NERVOUS SYSTEM OF *Caenorhabditis elegans*

Today's understanding of nervous systems is an amalgam of contributions of studies in invertebrate and vertebrate models. Among the most comprehensively studied nervous systems is that of *C. elegans*, the first metazoan combining organism-wide cell atlas, lineage, connectome, fully sequenced genome, whole-organism and embryo single-cell transcriptomes (Sulston and Horvitz, 1977; Sulston et al., 1983; White et al., 1986; Cao et al., 2017; Molina-García et al., 2019; Packer et al., 2019; Satterstrom et al., 2020; Taylor et al., 2021). The need for curation of a rich amount of data was met by information integration and facilitated by the limited number of *C. elegans* cells. A closer look at the multifaceted description of this system provides insights for classification schemes in more complex circuits.

The *C. elegans* nervous system consists of 302 neurons and 50 ectoderm-derived glia in hermaphrodites and 387 neurons and 90 glia in males, described morphologically by pioneer studies

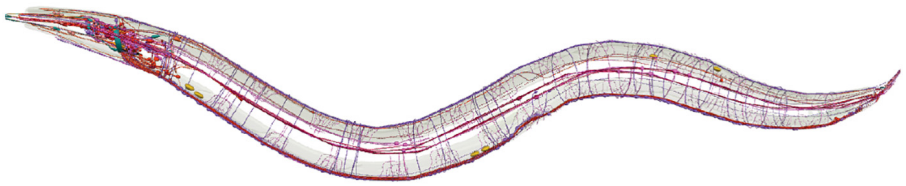

Neurotransmitter / Neuron type	ACh	Amine	GABA	Glu	Unknown
Sensory	9	3	1	22	3
Interneuron	19	2	2	11	9
Motorneuron	17	1	5	1	1

Symmetry / Glial cell type	bilateral	4-radial	6-radial
Sheath (on axons)	0	1	0
Sheath (on dendrites)	5	1	1
Socket	4	3	1

FIGURE 2 | Summary of neurons (red, purple) and glial cell types (blue, cyan) in the *C. elegans* nervous system. Illustration of nervous system with neurons, glial cells and fascicles is kindly provided by Openworm.org (Sarma et al., 2018). Tables present the *C. elegans* nervous system cell types, listed based on their characterized symmetry, terminal neurotransmitter identities (for neurons), morphology (for glial cells). Sheath on axons/dendrites refers to glia with membranes that ensheath axons or dendritic tips, respectively. Details and relevant citations are provided in the text.

of the first lineaging and ultrastructural analysis of an entire nervous system (Albertson and Thomson, 1976; Sulston et al., 1983; White et al., 1986; Cook et al., 2019). While its small neuron size hindered the prevalence of electrophysiology, early studies concentrated on a comprehensive mapping of neuron morphology, anatomy and connectivity at single-cell resolution and *C. elegans* neuronal cells are categorized using all these criteria combined. The *C. elegans* hermaphrodite neurons are functionally grouped into 37 sensory neurons, 44 interneurons and 23 motorneurons (**Figure 2**). They represent 118 neuronal classes, based on their anatomical features: 26 classes of single unilateral neurons, 70 classes of 35 bilaterally symmetrical neuron pairs, 10 classes presenting 4 radially symmetrical members, 3 classes of 6 radially-symmetrical members, 1 class with 3 head motor neuron and 8 distinct classes of nerve cord motor neurons (White et al., 1986; Hobert et al., 2016). All classes, except for the last two, include neurons of different functional modalities. Interestingly, 2 of the 70 bilaterally-symmetrical neuron pairs (AWCR/AWCL and ASER/ASEL) consist of neurons that can be further subclassified into different types due to their specific molecular diversification, as discussed below. Aside anatomy, neurotransmitter identities of all neurons are now mapped: 38 classes (78 neurons) are glutamatergic with expression of vesicular glutamate transporter EAT-4/VGLUT, 52 classes (159 neurons) are cholinergic with expression of vesicular acetylcholine transporter VAChT/UNC-17, 6 classes (26 neurons) are GABAergic expressing the biosynthetic enzyme glutamic acid decarboxylase (GAD/UNC-25), 7 classes (11 neurons) appear to be GABA-uptaking neurons expressing the vesicular GABA transporter (VGAT/UNC-47) – and 13 classes (26 neurons) are aminergic (i.e., dopaminergic, serotonergic, etc.) (Serrano-Saiz et al., 2013; Pereira et al., 2015; Gendrel et al., 2016). To date, a plethora of studies investigate these neuronal types in exquisite detail, examining mechanistically their development, specification, functions, and different states while interacting with the environment.

The *C. elegans* hermaphrodite ectoderm-derived glia, initially termed "support cells," can be similarly classified based on anatomical features: there are 9 classes of bilaterally symmetrical pairs (ADEsh, ADEso, AMsh, AMso, OLLsh, OLLso, PDEsh, PDEso, PHsh), 5 classes of 4 radially symmetrical members (CEPsh, CEPso, OLQsh, OLQso, PHso) and 2 classes presenting 6 radially symmetrical members (ILsh, ILso) (**Figure 2**). Based on their anatomical relation to neurons, glia can be "sheath" glia ("sh") or "socket" glia (so) (Ward et al., 1975; Sulston et al., 1983; White et al., 1986; Altun and Hall, 2011). "Sheath" glia present membrane processes that envelop neuronal processes, either ensheathing brain axons and synapses (CEPsh), or wrapping around dendritic endings, in sensory organs (AMsh, ILsh, OLQsh, OLLsh, PHsh). "Socket" glia in sensory organs form pores for neuronal dendritic endings to access the environment (ADEso, AMso, CEPso, ILo, OLLso, OLQso, PDEso, PHso). Several glial cells are implicated in aspects of nervous system development and function, including axon and dendrite morphogenesis, synapse positioning and neurotransmission, male-specific neurogenesis, animal longevity, locomotion, and sleep (Bacaj et al., 2008; Sammut et al., 2015; Singhvi et al., 2016; Rapti et al., 2017; Katz et al., 2018; Frakes et al., 2020). Key recognized roles of *C. elegans* glial cells are analogous to those of fly and mammalian glial cells, yet *C. elegans* glial cells remain understudied. Many of these glial cell types are not functionally characterized and how their fates are determined or compared is unknown. Whether each glial cell defines one type or multiple glia comprise the same cell type remains unknown. Notably, even for well-studied neurons, the terms "class" and "type" are used rather interchangeably, without universally sharp defining criteria. These definitions are sometimes elusive in vertebrate cell types too, and may affect cell classifications as discussed below (Tasic et al., 2018; Zhang et al., 2021).

CELL IDENTITY, A MULTIDIMENSIONAL PROCESS FROM REGULATORY PROGRAMS TO EFFECTOR MODULES

Mapping the *C. elegans* nervous system anatomy and connectivity at single-cell resolution guides closely our studies of neurodevelopment and fate diversification. Regulatory

programs underlying diversification suggest specific criteria for cell classification in developmental and evolutionary studies. Pioneer work in *C. elegans*, defined *terminal selectors* as master-regulator transcription factors that are continuously expressed in postmitotic cells and instruct terminal cell identity by regulating expression of cell type-specific effector genes (Hobert, 2008; Hobert and Kratsios, 2019). To date, a remarkable number of terminal selectors is identified across neuron types, highlighting a theme of combinatorial functionality (Hobert, 2016a). Strikingly, four conserved factors specify almost half of *C. elegans* neuron types while several terminal selectors are repeatedly used in distinct types (Hobert and Kratsios, 2019). For example, PROP1/UNC-42 acts as terminal selector in neurons SMD, RMD, AIB, RIV, which do not share the same neurotransmitter identity, morphology or function (SMD, RMD are motorneurons; AIB, RIV interneurons; RIV, SMD and RMD are cholinergic; AIB is glutamatergic). This is surprising at first but PROP1/UNC-42 acts with other terminal selectors in different combinations to regulate distinct fates (Berghoff et al., 2021). Remarkably, recent studies present a unique combination of homeodomain proteins expressed in each *C. elegans* neuron class, and suggest that cell type diversity can be delineated by the presence of molecular descriptors (Reilly et al., 2020). Intriguingly, terminal selectors can have different requirements across cells. Some bind DNA cooperatively, such as LHX9/TTX-3 and VSX2/CEH-10 in AIY neurons, others in an additive way like ERG/FLI1/AST-1, DLX1/CEH-43 and PBX2/CEH-20 in dopamine neurons (Altun-Gultekin et al., 2001; Wenick and Hobert, 2004; Doitsidou et al., 2013; Berghoff et al., 2021). Considering a comprehensive array of regulatory factors and their functional interactions serves better to delineate neuronal cell types than single terminal selectors alone, while experimental validation is key to define functional roles of factors in distinct cell types.

Alongside terminal selectors, additional mechanisms instruct neuronal and glial cell identity, including transiently expressed transcription factors (**Figure 3A**). Hmx/Nkx/MLS-2 regulates cell-specific expression of the terminal selector Otx/CEH-36 to control fate of AWC neurons while together with Pax6/VAB-3 it controls glial expression of the transcription factor Olig2/HLH-17 and cell development of CEPsh glia. Hmx/Nkx/MLS-2 appears only transiently expressed in embryonic AWC and CEPsh and their precursors (Yoshimura et al., 2008; Kim et al., 2010; Taylor et al., 2021). Transcriptional repressors also affect differentiation by type-specific repression of terminal selectors' target genes (Hobert and Kratsios, 2019). Aside transcription factors, microRNAs can drive repression to define functional identity; *lsy-6* introduces asymmetry between bilateral neurons ASEL/ASER, through cell-specific repression of transcription factor NKX6.3/COG-1 while miR-791 regulates the CO2-sensing function of BAG neurons by repressing house-keeping genes (Cochella and Hobert, 2012; Drexel et al., 2016). Thus, a comprehensive repertoire of terminal selectors together with other regulatory programs compile the full array of mechanisms that control cell-specific use of genomic information, a cell type's 'regulatory signature' (Arendt et al., 2016; **Figure 3B**).

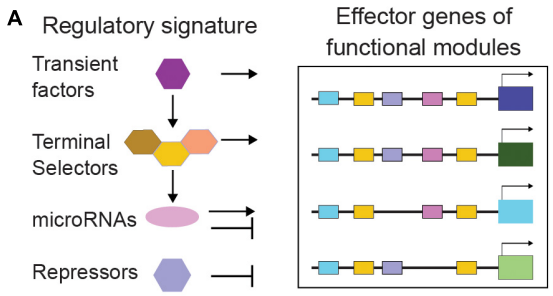

B

Molecular factors	Cell type 1	Cell type 2	Cell type 1
TF1			
TF2			
TF3			
TF4			
E.G.1			
E.G.2			
E.G.3			
E.G.4			

FIGURE 3 | Regulatory signatures and functional modules can describe cell types by combinatorial codes. **(A)** The combination of regulatory signatures and functional modules describes cell types comprehensively. Transient factors, terminal selectors, and other activator and repressor mechanisms combined define a cell type's 'regulatory signature.' **(B)** Combinatorial codes of regulatory factors direct effector genes to encode distinct functional modules in different cell types. TF, transcription factor; E.G., effector gene. Specific examples and references are provided in the text.

However tempting and fruitful is to classify neural cells strictly by their regulatory signature, studying effector genes remains of paramount importance. Some transcription factors driving identity acquisition are subject to signaling by effector genes. The olfactory neurons AWCL and AWCR acquire a strikingly antisymmetric, anti-correlated fate, when correct contact of their axons triggers gap junction signaling, calcium flux, and kinase activity that feed back onto homeobox factors and microRNAs driving asymmetric gene expression and function (Hsieh et al., 2012). Thus, effector genes engage in feedback loops affecting regulatory programs. Additionally, cell-type-specific batteries of effector genes are key for identifying regulatory factors. Genetic screens for altered expression of neurotransmission effector genes uncovered the regulatory logic differentiating distinct neurotransmitter identities (Flames and Hobert, 2009; Serrano-Saiz et al., 2013; Pereira et al., 2015; Gendrel et al., 2016). Moreover, combinatorial roles of type-specific transcriptional repressors, were uncovered by following the unique expression patterns of effector genes in distinct motorneurons (Kerk et al., 2017). Delineating cell types comprehensively leans on the combination of their regulatory signature and core molecular modules of effector genes. Consequently, identifying functional genes of neural cells through *in vivo* studies remains key in nervous system investigations and classifications.

UNCHARTED TERRAINS IN CELL TYPES AND CELL HETEROGENEITY

Newly Discovered Cells Across Model Organisms

A century of cell biology and physiology would suggest that morphological and electrophysiological maps of neural cells are comprehensive in laboratory models. Yet, new cell types are still discovered in understudied and well-studied contexts. "Rosehip" GABAergic neurons, that locally control dendritic computation in pyramidal neurons, were recently discovered in layer 1 of the human neocortex (Boldog et al., 2018). In adult mouse ventricular-subventricular zones, new oligodendrocyte precursors and astrocytic cells "gorditas" were discovered upon activation of quiescent stem cells (Delgado et al., 2021). Zebrafish was thought to lack astrocytes while postembryonic radial glia were considered analogous to mammalian astrocytes in terms of gene expression and functional contribution to glutamate-dependent epileptic seizures (Lyons and Talbot, 2015; Niklaus et al., 2017). Yet, recent studies describe zebrafish cells with properties of mammalian astrocytes, such as expression of glutamate aspartate transporter, membrane tiling and association with synapses (Chen et al., 2020). Research in Drosophila discovered neurons that partition dorsal and ventral visual circuits and transient neuronal populations wrapping neuropils during development and dying before adulthood (Özel et al., 2021). Studies in *C. elegans* also present newly discovered neuron and glial cells; interneurons MCM and ciliated neurons PHD driving sexually dimorphic behavior, are generated in males by sex-shared glia AMso and PHso1 (Sammut et al., 2015; Molina-García et al., 2020). Identification of these cells was enabled by recent mapping of the nervous system anatomy and connectivity in *C. elegans* males, in contrast to the connectome of hermaphrodites already mapped for more than 3 decades (White et al., 1986; Cook et al., 2019). Besides, *C. elegans* glial cells were early mapped but only named "neuronal support cells," yet recent in-depth functional studies uncover their glial features and analogies with vertebrate counterparts. For example, CEPsh glia are suggested to be analogous to astrocytes by molecular content and functions (Colón-Ramos et al., 2007; Yoshimura et al., 2008; Rapti et al., 2017; Katz et al., 2019). Thus, cell discovery lies in uncharted terrains of nervous systems in various, more and less complex models. As resolution in transcriptomics and functional studies increases, cell discovery continues, adding to an ongoing mapping of cell heterogeneity.

Heterogeneity and Shared Factors Across Cell Types

Neural circuit cell types were historically regarded as homogeneous cell populations, yet it becomes increasingly evident that they exhibit significant functional and molecular heterogeneity (Chaboub and Deneen, 2013; Foerster et al., 2019). A key frontline in mapping cell type heterogeneity is the biology of glial cells, their regulatory logic and divergency. Master regulators and regulatory programs of glia-specific identities often remain elusive. Early studies in Drosophila suggested that the gene *glial cells missing* (gcm) is necessary and sufficient for specification of glial cell fate (Hosoya et al., 1995; Jones et al., 1995), while later studies identified that gcm1 and gcm2 gliogenic factors also drive neurodevelopment (Chotard et al., 2005). Mammalian orthologs *Gcm1* and *Gcm2* functionally substitute for fly *gcm* but present no expression nor function in mammalian glia (Günther et al., 2000). Even in the well-studied nervous system of *C. elegans,* the regulatory logic of glial cell development is understudied, contrary to the detailed documentation of factors driving neuronal, pansensory or panneuronal identity (Swoboda et al., 2000; Stefanakis et al., 2015). Few transient transcription factors affecting glial cell identity are described. Hmx/Nkx/MLS-2 and Pax6/VAB-3 drive Olig2/HLH-17 expression in CEPsh glia, similarly to their homologs driving Olig2 expression in mouse glia, Aristaless/ALR-1 regulates the functional structure of AMso glia, FOXD4/UNC-130 instructs specification of ILsoD, Atoh1/LIN-32 instructs diversification of AMsh glia, while Prox1/PROS-1 regulates the secretome of AMsh glia and OTX/OTD/TTX-1 their stressed-induced remodeling (Tucker et al., 2005; Yoshimura et al., 2008; Procko et al., 2011; Wallace et al., 2016; Zhang et al., 2020; Mizeracka et al., 2021). Strikingly, these transcription factors regulating *C. elegans* glial fate also affect neuronal fates, alongside their glial functions (**Figure 4A**). MLS-2 and VAB-3 specify functional identity of AWC and BAG neurons respectively, ALR-1 ensures differentiation of touch receptor neurons, FOXD4/UNC-130 diversifies neurons AWA and ASG, TTX-1 specifies AFD neurons, while CND-1, NGN-1, and LIN-32 suppress glial fate and promote neuronal fate (Sarafi-Reinach and Sengupta, 2000; Satterlee et al., 2001; Kim et al., 2010; Topalidou et al., 2011; Brandt et al., 2019; Zhang et al., 2020). These examples of regulators shared between neurons and glial cells are often not lineage-specific (in contrast to examples of lineage convergence discussed below). In vertebrates, regulators specifying glial fates without affecting neuronal development are also sparse or lacking. Olig1 and Olig2 factors in neural progenitors drive both oligodendrocyte fate and motorneuron generation and their abolishment results in generation of interneurons and astrocytes (Anderson et al., 2002; Lu et al., 2002). Vertebrate Sox9 may promote astrogenesis by regulating the nuclear factor NFIA to maintain multipotent progenitors, while transcription factors controlling astrocyte-specific fate are unknown (Poskanzer and Molofsky, 2018). Unlike the highly methylated differentiated neurons, the mammalian glial methylome resembles the fetal methylome suggesting that glial transcriptional flexibility and heterogeneity is instructed by the environment (Poskanzer and Molofsky, 2018). Indeed, Sonic hedgehog by Purkinje neurons, drives molecular and functional diversification of Bergman glia and stellate astrocytes (Farmer et al., 2016). The quest for cell-type identifiers is ongoing even for recognised, distinct cell types.

Sparsity of Molecular Identifiers

The sparsity of known regulators of specific fates may result from understudied functional heterogeneity (**Figure 4B**). Effector genes, often used as a proxy to uncover fate regulatory factors, are hardly described in glia. Besides the enzymatic apparatus

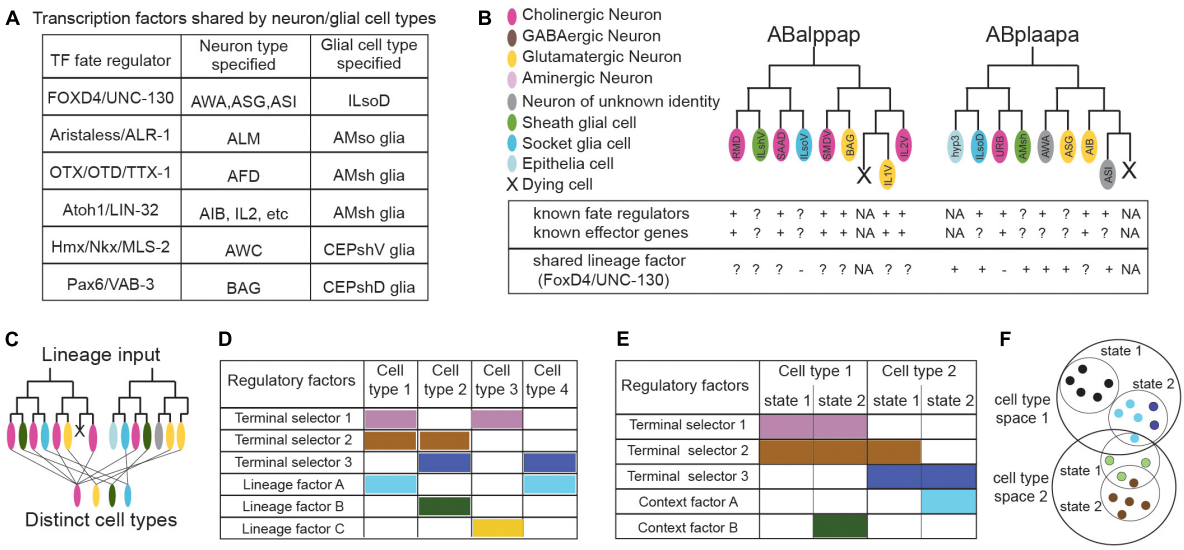

FIGURE 4 | Frontiers in cell classification: regulators shared across cell types **(A)**, sparsity of known factors **(B)**, lineage convergence **(B,C)**, combinatorial profiles **(D,E)**, and the dynamics of cell states **(F)**. **(A)** Some *C. elegans* transcription factors specify both glial and neuronal cell types, while glial-specific factors are largely unknown (proteins appear as "vertebrate/*C. elegans* homolog"). **(B)** Schematics representing part of the *C. elegans* lineage and our knowledge on transcriptional regulators and effector genes of the featured cell types, that may be used as identifiers of cell identity. Known regulatory factors of identity are sometimes unknown for certain cell types, especially glial cells. The UNC-130 transcription factor regulates fate of different cell types within one sub-lineage but not similar types from convergent lineages (ILsoV, ILso). The unknowns of lineage convergence and the sparsity of known factors regulating identity can affect cell classification. Cells color-coded as indicated, gray; neurons of unknown neurotransmitter identity. Factors with functional importance; "+", dispensable; "–", or uncharacterized "?", NA, non-applicable. **(C)** Schematics summarizing lineage convergence, with distinct cells arising from the same lineage and similar cell types from distant lineages. **(D)** Transcription factors have combinatorial actions for cell specification. Terminal selectors and lineage-related factors work toward diversification by lineage convergence. **(E)** Terminal selectors in conjunction with context-specific factors regulate state transitions in the same cell type. **(F)** Effector genes (encoding neurotransmitter machinery, etc.)- here in colored dots- may be shared or divergent across different states of a cell type. Single molecular identifiers may be shared between cell types, thus appearing insufficient to define them. Relevant examples and citations are provided in the text.

driving metabolic support, glial genes driving morphogenesis and modulation of neurons are understudied, but these may have conserved roles in evolution (Heiman and Shaham, 2007). Studies dissecting *in vivo* glia development and function should provide valuable insight into their molecular repertoire of regulatory and effector genes, to guide faithful classification and cross-species study of glial cell types (Singhvi et al., 2016; Wallace et al., 2016; Rapti et al., 2017; Lee I. H. et al., 2021). Lessons from *C. elegans* studies of a modular logic for pan-neuronal fate specification suggest that pan-glial fate may also be regulated in a peace-mile manner with distinct glia types using distinct combinations of transcription factors (Stefanakis et al., 2015). Future focus on the molecular convergence and divergence of neurons and glial cells can illuminate mechanisms of neural circuit cell heterogeneity. Such challenges in uncharted terrains of cell heterogeneity across space, time, development and evolution should be taken into account when considering future schemes of investigation.

EXPLORING CELL TYPES THROUGHOUT NERVOUS SYSTEM DEVELOPMENT

Current cell classifications follow the terminal neurotransmitter identity, often without involving the developmental factors that establish cell appositions underlying connectivity. This is inadvertently influenced by the prevalence of gene expression studies in postembryonic cells with defined identities. Nevertheless, should we consider regulators of development in the quest for cell type identifiers? Cell morphogenesis allows cell targeting necessary for synaptic and functional connectivity. The underlying cell-type-specific genes encoding morphogenesis factors are key features of cell physiology and undergo pressure of natural selection. Thus, morphogenesis effectors and their regulatory programs can contribute valuable information to cell type classification.

How developmental history, morphogenesis and terminal cell type function is coordinated remains elusive. During *C. elegans* brain assembly, many sister neurons present different axon paths and navigation times while some lineage-distant neurons bundle closely together (Rapti et al., 2017; Moyle et al., 2021). There are few examples of fate regulators affecting cell-type-specific morphogenesis, like the transiently expressed NKX-/MLS-2 which regulates formation of CEPsh glia and AWC neurons (Yoshimura et al., 2008; Kim et al., 2010). Recently it was demonstrated that certain connectivity features of neurons wiring together are regulated by terminal selectors (Berghoff et al., 2021). How cell-specific regulatory programs affect effector genes of morphogenesis, such as adhesion and guidance receptors, remains understudied. Mapping lineage relations, cell identities, morphogenesis and circuit functions can provide links between

developmental programs and functional cell classification. This is key for a comprehensive investigation of cell types through the lens of development.

In *C. elegans,* the lineage history is invariant, was first mapped 4 decades ago (Sulston and Horvitz, 1977; Sulston et al., 1983) and can now be analyzed by automated lineage tracing (Bao et al., 2006; Boyle et al., 2006; Murray et al., 2006). Today it is extensively annotated with functional information, offering an opportunity to assess how much developmental data (lineage, state transitions, regulatory programs) are needed to meaningfully classify terminally differentiated cells and study factors of cell development in relation to cell identity. An invariant cell lineage doesn't mean that cell fates are determined by the lineage pattern. Intriguingly, early lineaging indicated that cells with similar morphology and connectivity can be produced by distinct lineages (Sulston and Horvitz, 1977; Sulston et al., 1983). Similar lineage history appears neither necessary nor sufficient for two cells to belong to the same neuron class (Hobert, 2016b). Lineage patterns do not readily correlate with transcription factor expression, cell terminal fate, form and function. For example, the fates of six lineage-distant IL1 neurons and six lineally distant RMD neurons are specified by transcription factors SOX14/SOX-2 and PROP1/UNC-42 respectively. Multiple lineages produce highly similar neural cell types, a phenomenon termed *convergent differentiation* (**Figures 4B,C**). This may be explained by local inductive interactions instructing fate or shared transcription factors able to integrate distinct lineage histories (Hobert and Kratsios, 2019).

Cell type specification during development was early described in the powerful metaphor of "Waddington landscape"; cells depicted as balls traverse a hill of "epigenetic landscape" and encounter ridges or furrows that restrict their path, ultimately forcing them to stop and acquire a stable mature identity (Waddington, 1957). Conventionally, cell types were considered as monolithic points in the Waddington landscape, fixed entities with specific characteristics and features or from a systems perspective, stable fixed points in transcriptomic space. Recent transcriptomics reveals that *C. elegans* glia and neurons often become transcriptionally distinguished only in the final cell division of progenitors producing terminally differentiated cells, in contrast to non-neural tissues (muscle, dermis, intestine) which arise by lineage clades presenting within-clade transcriptomic similarity (Packer et al., 2019). Thus, neural cell types undergo a shift from lineage-correlated to fate-correlated gene expression with cells of distant lineages converging transcriptionally to adopt the same terminal fate, while diverging from their close lineage-relatives. This sudden transcriptomic shift during embryonic fate commitment of neural cells is in contrast to predictions of a smooth Waddington's landscape. The phenomenon of convergence is not *C. elegans* specific but also prevalent elsewhere, like in mouse excitatory and inhibitory neurons (Cao et al., 2019). Overall, such dynamics of nervous system regulatory states through cell generations during development is a key challenge in developmental neuroscience.

Recent *C. elegans* studies delineating transcription factor roles in convergent differentiation in neurons or glia may provide molecular insights in other species. FOXD4/UNC-130 is expressed in and required for the diversification of different cell types (neurons AWA, ASG, ASI and glia ILsoD) arising from the same sublineage but not the diversification of similar types arising from other sub-lineages (Sarafi-Reinach and Sengupta, 2000; Mizeracka et al., 2021). On the other hand, Atoh1/LIN-32 is expressed in and required for the specification of related, left/right or radially symmetrical, neural cell types generated from distinct sublineages (Masoudi et al., 2021). The later transcription factor may control expression of terminal selectors in the specified cell types. Thus, it appears that a combination of cell type-related terminal selectors together with timely transient factors and lineage-related transcription factors underly lineage convergence and direct cell type specification (**Figures 4C,D**).

Combining *in vivo* studies of lineage, developmental mechanisms, molecular repertoire through transcriptomics and computational analysis will enable testable hypotheses to predict and identify links between regulatory programs of fate, morphogenesis, terminal identity, and functional connectivity. Intriguingly, cell fate specification can proceed through different pathways during natural generation of cell types or *in vitro* cell transformation induced in the laboratory (Treutlein et al., 2016). Cells derived through these different pathways are considered of the same type based on restricted molecular and morphological characteristics. Yet, how their complete repertoire of regulatory and effector genes resembles is unclear. Deciding on accepted criteria for cell-type distinctions in relation to their developmental path is important for a mechanistic understanding of cell development and function, including cell fate transformations often aiming to treat disease.

CONSIDERING CELL STATES IN SPACE AND TIME

Alongside cell-type heterogeneity, neural cells present spatiotemporally dynamic states, after their initial fate commitment both in complex and contained circuits. Previous studies suggest that cell states are defined by gene expression reversibly regulated by extracellular cues or transitory stimuli (Poulin et al., 2016). Well-defined criteria distinguishing cell types and states will enable to chart complex circuits lacking *in vivo* single-cell-resolution maps. Considering experimental observations in the light of current definitions can examine which sharp boundaries are delineated between cell types and states.

Several *C. elegans* neural cell types, arising from invariant cell lineages, display transcriptional changes that may underline dynamic cell states in space or time, some dependent on activity or the environment. Neural cells can undergo state changes under stress conditions. Upon starvation, the AIB interneurons change gap junction composition in response to concerted function of terminal selector PROP1/UNC-42 and the dauer-specific transcriptional regulator FoxO/DAF-16 (Bhattacharya et al., 2019). The sensory neurons IL2 remodel their dendritic architecture in response to adverse environmental conditions,

also under regulation of FoxO/DAF-16 (Androwski et al., 2020). Under high temperature or starvation, the glia AMsh change morphology and undergo fusion while maintaining known fate markers. This is instructed by the GPCR/REMO-1, the transcription factor Otx1/TTX-1 and its direct target VEGFR-related tyrosine kinase FLT1/VER-1 (Procko et al., 2011; Lee I. H. et al., 2021). Then, the glia-ensheathed dendritic endings of AWC neurons also expand together with the AMsh glial membranes.

Developmental transitions also entail time-dependent cell state changes. The embryonically born DD motorneurons synaptically connect to and innervate ventral muscles, only to undergo extensive rewiring at the end of the animal's first larval stage. In a striking example of plasticity, they eliminate early synapses and form new input and output synapses innervating dorsal muscles. Then, ventral muscles get innervated by newly born ventral VD motorneurons (White et al., 1986; Howell and Hobert, 2016; Philbrook et al., 2018). While changing circuit partners, DD motorneurons maintain their morphology and GABAergic neurotransmitter identity. This remodeling is dependent on neuronal activity, is instructed by transcription factors acting cell-autonomously and the heterochronic pathway (Hallam and Jin, 1998; Thompson-Peer et al., 2012; Miller-Fleming et al., 2016).

Cell states also occur via sex dimorphism, another context that introduces complexity in cell heterogeneity. Sexually dimorphic neurons with shared lineage and morphology present distinct gene expression, connectivity and neurotransmitter identity. During sexual maturation of males but not hermaphrodites, sex-shared interneurons AIM change neurotransmitter identity from glutamatergic to cholinergic, through a combined action of terminal selector POU4F/UNC-86 and the male-specific transcription factor LIN-29 (Pereira et al., 2015). Otherwise, the sex-shared PHB neurons undergo synaptic pruning of their juvenile synapses in interneurons AVA and AVG to maintain wiring on AVA in hermaphrodites and on AVG in males (White et al., 1986; Oren-Suissa et al., 2016; Cook et al., 2019). *C. elegans* cell state transitions may be more widespread, since gene expression is dynamic in cells across larval stages (Sun and Hobert, 2021) and appears different between embryonic and postembryonic stages of the same cells (Cao et al., 2017; Packer et al., 2019).

External signals inducing spatially or temporally distinct state transitions and their reversibility often remain elusive. Such states may have been classified as different cell types in other circuits lacking complete single-cell resolution maps. In *C. elegans* they are recognized as states of the same cell type in light of the mapped, invariant lineage and nervous system anatomy. Under the same light, bilaterally symmetric neurons AWCL/AWCR and ASEL/ASER are classified as distinct subtypes, despite sharing key regulatory factors and morphology while diverging in some effector genes and function (Hobert et al., 2016). AWCR/AWCL neurons present asymmetric expression of chemoreceptors (STR-*2* and SRSX-3 respectively*)* and sense different odorants (butanone and 2,3-pentanedione respectively*)*. AWCL is considered transcriptionally the "default state," while the alternative AWCR is generated, after induction by a transient calcium influx through voltage-gated channels and gap junctions, and downstream signaling of regulatory factors to maintain asymmetry (Alqadah et al., 2016). Similarly, bilateral neurons ASER/ASEL express distinct chemoreceptors (GCY-1,-3,-, 4-,5,-22 TRP-2 and GCY-6,-7,-14,-20, respectively) in addition to their shared receptors, and regulate different circuit outputs. Increases in NaCl concentration activate ASEL and inactivate ASER, that generate opposite intracellular Ca^{2+} transients and promote forward locomotion or reversals respectively (Suzuki et al., 2008). Each pair of AWCL/AWCR and ASEL/ASER share neurotransmitter identity and terminal selectors (OTX-1/CEH-36 or C2H2/CHE-1 respectively) but respond differently to stimuli, and this is mediated transcriptionally (Cochella and Hobert, 2012). Calcium influx acts as transient external stimuli for divergence of AWCL/AWCR, while Notch signals induce ASEL/ASER divergence (Sagasti et al., 2001; Bertrand et al., 2011; Alqadah et al., 2016). Moreover, homeotic transformations between bilateral neurons of each pair are described for both pairs (Arlotta and Hobert, 2015). Nevertheless, AWCL/AWCR and ASEL/ASER are accepted distinct types, not cell states. External cues, suggested to induce cell state changes, can often regulate divergence of cell types with distinct morphology, connectivity, regulatory and effector genes. For example, Wnt signaling through a TCF/POP-1-cascade restricts Vsx/CEH-10 expression to one of two sister cells to diversify cholinergic interneuron AIY and motorneuron SMDD (Bertrand and Hobert, 2009). Besides, fate transformations also occur elsewhere, resulting in switches between non-bilateral neuron types with distinct morphology, connectivity, neurotransmitter identity and function, like between interneurons BDU and sensory neurons ALM (Arlotta and Hobert, 2015). Consequently, cell state transitions are underlined by combined action of terminal selectors and context-specific factors and result in changing some cell-type effector genes or connectivity (**Figures 4E,F**). Defined stimuli or transformations alone appear insufficient to define boundaries between cell types and states; comprehensive analysis of cell properties and programs is key.

Developmental remodeling and state transitions of neural cells are observed in many circuits beyond *C. elegans*, including Drosophila photoreceptors and mammalian olfactory neurons (Sprecher and Desplan, 2008; Cheetham et al., 2016). Different neurons and glial cells in the mammalian brain exhibit graded transcriptomic differences, portraying within-cell-type heterogeneity for which neither technical nor biological noise is a likely explanation (Cembrowski et al., 2018; Tasic et al., 2018). Considering state transitions raises the question: how do regulatory mechanisms of plasticity intersect with the function of terminal selectors? The above *C. elegans* examples of context-specific cell remodeling during sexual maturation or stress, highlight an emerging theme: terminal selectors act in conjunction with condition-specific factors to induce condition-specific effector genes. Comparative single-cell transcriptomics is challenged to elucidate the extent of transient variation in a regulatory program, for example, the environmentally induced variations in cells with shared terminal selectors. Meeting this challenge is harder in complex tissues and can benefit from *in vivo* experimentation in model organisms.

VIEWING NERVOUS SYSTEM CELL TYPES THROUGH THE LENS OF EVOLUTION

Incorporating evolutionary logic in the classification of neural cells is crucial in order to investigate open questions on their origins, cross-species relations and the transition from decentralized nerve nets to centralized nervous systems (Perry et al., 2017; Arendt et al., 2019; Rey et al., 2021). Differential expression of transcription factors is primarily used to build evolutionary cell-type trees. Hierarchical evolutionary classifications depict a scheme of cell diversification through genetic individuation, where a new cell type presents a new Core Regulatory Complex with at least one new transcription factor and the resulting molecular interactions (Arendt et al., 2019). Interestingly, each mature *C. elegans* neuron type expresses a unique combination of homeodomain proteins, portraying neuron type diversity, and combinatorial homeobox gene expression is also identified beyond *C. elegans* (Allen et al., 2020; Reilly et al., 2020). As discussed above, cell type specification is established by regulatory factors reused across cell types and other transient transcription factors and regulatory mechanisms. Moreover, transcript levels alone cannot always predict function of regulatory programs, as discussed below. Cell classifications serving both lenses of development and evolution would ideally incorporate known regulatory programs and functional knowledge rather than follow individual transcription factors or transcriptomic data alone. On the other hand, current neural cell classifications follow functional genes; neurons are often classified by their interneuron/sensory/motorneuron function and neurotransmitter identity (Hobert et al., 2016; Zeng and Sanes, 2017). Since natural selection acts on the fitness of animal behavior driven by effector molecules and their regulatory programs in congruence, comprehensive maps of effector genes may facilitate cell comparisons across species and mechanistic understanding of molecular diversity. Comparing entire cell transcriptomes and relative transcript enrichments is also used to delineate cell analogies across species. Relative transcript enrichment in molecular profiles of *C. elegans* glia and mouse brain cells delineates a close relationship of postembryonic CEPsh glia and mouse astrocytes (Katz et al., 2019). Such comparisons require to incorporate homologs with different number of paralogs across species, facilitated by investigating the functional importance of expressed genes.

A combined knowledge of regulatory programs and effector modules enables to trace evolution of cell types across species through the lens of both these molecular signatures combined (Arendt et al., 2016; Hobert et al., 2016; Arendt, 2020). This may allow to assess possible co-regulation of neural cell-type-specific functional modules. Evolution studies suggest that the principle neuronal characteristics, the functional molecular factors of synapses, pre-exist the origin of neurons. Modules of pre-synapse and post-synapse are separately present as modules of vesicle release, signaling and filopodia outgrowth, in non-neuronal cells of non-Bilateria organisms. Neurons may have evolved through the innovation of integration of different modules (Arendt, 2020). Whether innovation of the neuron's origin involved a co-regulation of different neuronal modules requires further investigation. Likewise, defining the evolutionary history of glial cell types requires building a consensus for their essential functional machineries and their regulatory programs. Overall, cell type classifications incorporating definitions that enable cross-species investigations facilitate future evolutionary studies of neural cells.

MAPPING NEURAL CELL TYPES: FROM SINGLE CRITERIA TOWARD A MULTIFACETED CLASSIFICATION

Multifaceted Descriptions of Cell Types

Charting the remarkable heterogeneity and cooperative roles of neural cells will pave ways toward the full picture of circuit assembly and function. Neuroscience research is moving fast toward interdisciplinary approaches to increase resolution in cell investigation. *C. elegans* is the first model with available genome sequence, lineaging, connectome and whole-organism single-cell transcriptomics. This enables nervous system mapping by molecular, anatomical and functional criteria combined, from single-cell to single-gene resolution (**Figure 5**). Recent breakthroughs in areas of imaging, sequencing, proteomics, and automatization enable advanced cell-type descriptions in more complex circuits as well (**Figure 1**). Gene profiling and electrophysiology combined, map the molecular taxonomy of mouse forebrain neurons (Sugino et al., 2006). Paired transcriptomics and proteomics investigate the molecular content of cortical neurons (Poulopoulos et al., 2019). Recent approaches allow combined electrophysiological, morphological, and transcriptomic characterization of individual neurons (Gouwens et al., 2020; Kalmbach et al., 2021; Lee B. R. et al., 2021). While early morphological classifications were considered outdated, cell morphology defines circuit function; axon appositions influence wiring and elaborate glia ramifications drive synapse ensheathment and function (Chung et al., 2015). A constantly advancing toolbox and visualization techniques highlights a come-back of morphological criteria into the picture. Light and electron microscopy reconstructions are greatly exploited for circuit mapping (Lichtman et al., 2008; Saleeba et al., 2019). Morphological reconstructions paired with high throughput electrophysiological recordings decode a wealth of morpho-electric properties (Gouwens et al., 2019). Combined expression studies and electron microscopy reconstructions in new model organisms, map tissue morphological and molecular characteristics to identify neural cell types (Vergara et al., 2021). Additionally, CRISPR/Cas9-mediated genome editing delineates neural gene function in high resolution (Nishizono et al., 2020; Fang et al., 2021). Individual researcher groups and consortia deliver large-scale profiling data and cell biology experimentalists are key to functionally dissect them. These approaches provide unparalleled resolution of a cell's molecular content, allowing to distinguish cell clusters, hierarchical arrangement of cell populations, and transitions between states (Lähnemann et al., 2020).

Integration of Cell Type Features

With high-throughput combinatorial approaches at hand, interpolating the anatomical, physiological, molecular and functional cell properties at single-cell-type resolution remains challenging in complex circuits. Pragmatic cell definitions following explicit, acknowledged criteria can enable investigating cell-type-specific development, function, position within taxa and ontological relations to other cells. Are single classification criteria adequate for such multifaceted investigations? Early *C. elegans* nervous system cell classifications that remain valid to date were guided by combined knowledge of the invariant cell lineage, anatomy and connectivity (Sulston and Horvitz, 1977; Sulston et al., 1983; White et al., 1986; Hobert et al., 2016). Despite its smaller cell numbers and simpler morphologies than vertebrate counterparts, *C. elegans* anatomy alone could provide sufficient resolution to distinguish most but not all recognized neural cell types. For example, neurons ASI and ASK could comprise one type based on similar axon and dendrite morphology alone but clearly constitute different types by criteria of distinct connectivity, or molecular content and functions (White et al., 1986; Taylor et al., 2021). Another primary criterion of classification is the cell's molecular content, often represented by its transcriptome (Zeng and Sanes, 2017; Yuste et al., 2020). Yet, classifications by transcriptomics alone can present limitations. In vertebrates, cross-modal correspondence between transcriptomics and anatomy is largely strong, yet finer transcriptomic cell clusters present sometimes overlapping anatomy (Tasic et al., 2018; Yuste et al., 2020). A closer look at *C. elegans* studies suggests that transcriptomics alone cannot speak to proteins' functional roles. LHX9/TTX-3 and LHX3/CEH-14 regulate fate of neurons AIY, ASK and neurons ALA respectively, but present different transcript levels in these neurons, sometimes not enriched (Altun-Gultekin et al., 2001; Van Buskirk and Sternberg, 2010; Serrano-Saiz et al., 2013; Taylor et al., 2021). These factors have no detected transcripts in the lineage sisters of AIY and ALA (Cengen[1]), suggesting that their relative transcript enrichment between sister cells may be more predictive of function than absolute transcript levels in a given cell. Importantly, *in vivo* expression corresponds largely well with transcriptomics. Most transcription factors specifying neuronal fates show transcripts in the neurons they specify (Hobert, 2016a; Cao et al., 2017; Packer et al., 2019; Reilly et al., 2020; Taylor et al., 2021). Yet, in few cases, factors are not clearly detected in transcriptomes of neurons that they are known to regulate. For example, LHX3/CEH-14, and Vsx2/CEH-10 specify the fate of neurons AFD and RME respectively, and are detected in these neurons by *in vivo* expression studies (Forrester et al., 1998; Serrano-Saiz et al., 2013; Kagoshima and Kohara, 2015; Gendrel et al., 2016; Taylor et al., 2021). Yet their transcripts are not clearly detected by large-scale transcriptomics probably due to incomplete profiling depth, an issue faced in single-cell-transcriptomics across organisms (Cao et al., 2017; Packer et al., 2019; Taylor et al., 2021). These comprehensive studies highlight that while "transcriptional phenotypes" show "potential" for translation, transcriptomics alone may be insufficient to predict function and expression levels adequate for protein activity vary in a given cell and process. Possible differing correlations between transcript levels and functions of cell-type molecular identifiers should be considered if classifying cell types by transcriptomics. Moreover, graded transcriptomic heterogeneity in vertebrates is widespread and functionally relevant (Cembrowski and Menon, 2018). Whether it results from within-cell-type variability or partial knowledge of cell identifiers is under investigation. *in vivo* experimentation is key to intersect trajectories of low-dimensional transcriptomic data with cell types. This does not disprove the value of anatomy and transcriptomics for classification. It highlights that finer classification is achieved when integrating them, like in *C. elegans* studies.

Mapping uncharted circuits requires a conceptual leap linking cells' regulatory signature and molecular make-up to functional physiology. If single criteria appear inadequate in complex circuits, hybrid approaches that consider all available information can be adapted. A useful way to classify neural circuit cells could be an integrated, multifaceted database with "cell-type spaces" presenting all features employed for classification: cell architecture, function, connectivity, lineage, regulatory and effector genes (**Figures 5**, **6**). This inclusive cell taxonomy can depict cells as genetically encoded circuit elements, an elegant perspective to describe the brain as an organ and circuit. Early *C. elegans* nervous system classification, guided by anatomy, connectivity and mapped lineage, is in remarkable agreement with recent gene expression studies (Sulston et al., 1983; White et al., 1986; Hobert et al., 2016; Packer et al., 2019; Taylor et al., 2021). The mouse retina is another example where grouping cells by different criteria leads coherently to the same discrete neuron types (Shekhar et al., 2016). Certain features of these circuits facilitate classifications: *C. elegans* cell lineage is invariant and mapped, the retina's laminar pattern is stereotypical and enables positional cell identification, and both have developmental patterning is seemingly 'hard−wired' (activity-independent). Whether such rewarding correspondence of diverse criteria will occur in other less "hard−wired" circuits with numerous cells comprising each cell type remains under investigation (Zeng and Sanes, 2017; BRAIN Initiative Cell Census Network [BICCN], 2021).

In partly mapped circuits, integrating information that feeds into morphological, molecular, wiring criteria enables harmonized cell classifications, applicable across disciplines. Like strategies in taxonomic systematics, using multiple criteria serves hierarchical classification schemes (Zeng and Sanes, 2017). Developmental and evolutionary classification emphasize regulatory programs (Arendt et al., 2019). Transcription factor combinations describing distinct cells can be identified by *in vivo* expression analysis (Reilly et al., 2020) or by computationally filtering transcriptomic cell clusters for transcription factor transcripts (Özel et al., 2021). Effector genes supporting functional modalities, like neurotransmission, also serve as primary criteria for classifications in *C. elegans*, Drosophila, mouse, and emerging-model systems (Hobert et al., 2016; Perry et al., 2017; Zeng and Sanes, 2017; Bates et al., 2019; Williams and Jékely, 2019; Özel et al., 2021). Multimodal platforms that incorporate both transcription factors and functional effectors

[1]https://cengen.shinyapps.io/CengenApp/

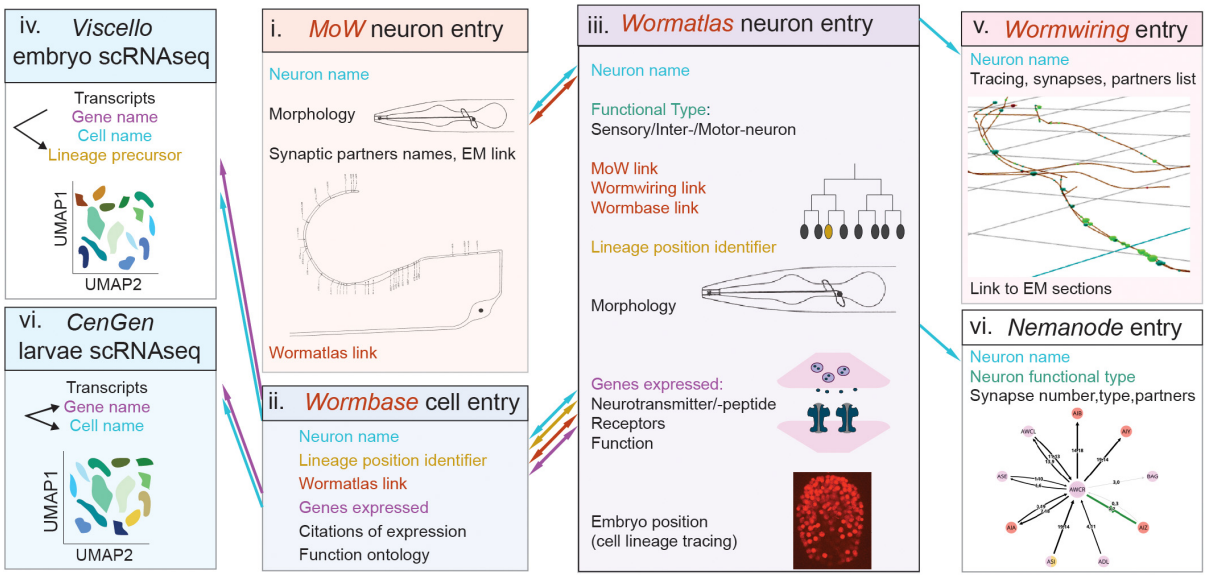

FIGURE 5 | *Caenorhabditis elegans* databases allow navigation across neural cell modalities and facilitate cell classifications. Simultaneous navigation across these databases with cell entries and modalities enables certain extent of information integration, as described in the text. The schematics represents databases displaying features of cell anatomy, connectivity, molecular content. Boxes denote distinct databases. Nomenclature shared across databases, which helps integration is color-coded in blue (neuron name), orange (lineage position) or purple (gene name). Links embedded in one database, leading to another database, are color-coded in brown. Flow of navigation between databases is indicated with arrows, color-coded as described above. Morphology schematics in (i, iii) and connectivity schemes in (i, v, vii) are adapted from the named databases. Names of databases are in italics, i-vii denotes studies and databases in chronoligal sequence. Webpage links of the databases, and citations of relevant publications, are provided in the text and footnotes.

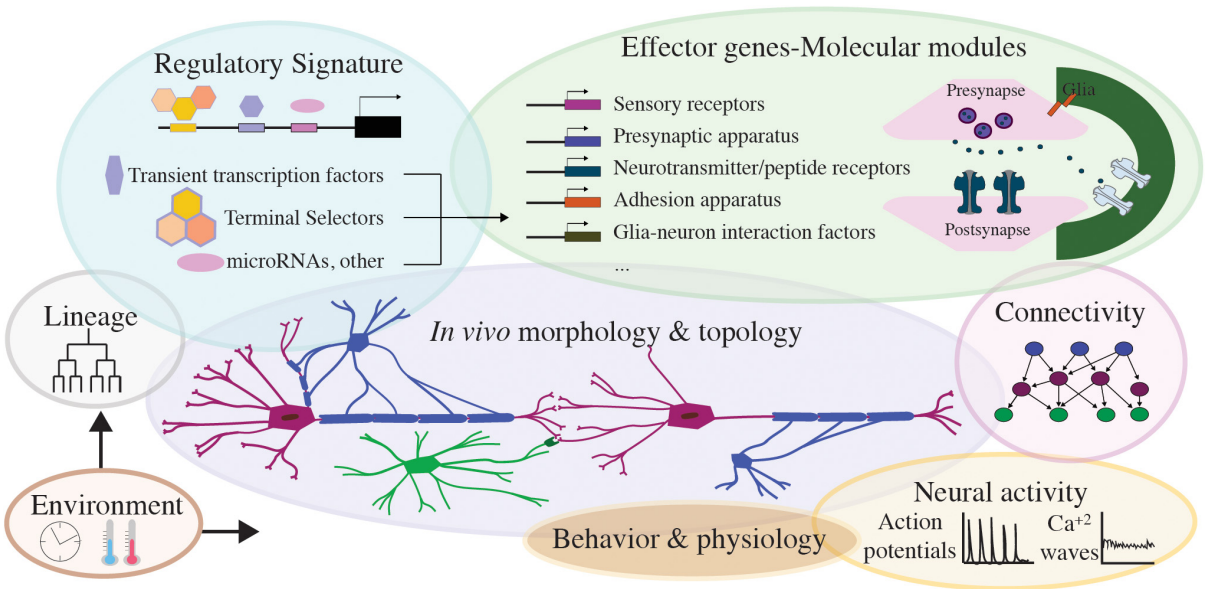

FIGURE 6 | Features of nervous system cell types, toward integrated, multimodal cell classification. Schematics presenting different modalities of nervous system cell types: regulatory signature factors and core effector genes of each cell's molecular modules, the lineage and environmental inputs influencing them, and the resulting neural cell morphology, behavior, connectivity. Activity in nervous system cells manifests as neuronal action potential or glial calcium waves and drives nervous system cell physiology and circuit function. Integrating these modalities will prove valuable toward multifaceted cell classifications across nervous systems.

as molecular identifiers, would enable to examine different hierarchical schemes. Understanding similarities or differences of cells depends on the information on their properties available at a given time. Each morphological, electrical, molecular or functional experimental approach detects complementary attributes. Until circuits are fully mapped, such multipurpose

frameworks enable crosstalk between studies of development, function and evolution, toward a more complete image of cell types. Eventually, in well-mapped circuits, classifications by distinct criteria may greatly co-vary, like in *C. elegans* and mouse retina (Hobert et al., 2016; Zeng and Sanes, 2017).

FEEDBACK LOOPS AND MULTIMODAL INTEGRATION: LESSONS FROM ATLASES IN *Caenorhabditis elegans* AND BEYOND

Multifaceted Databases in *Caenorhabditis elegans*

C. elegans atlases provide paradigmatic platforms for cell classification. For decades, *C. elegans* cell classifications integrate morphology, connectivity and genetics in concert, and-in-hand with published and unpublished community's knowledge. Providing ample 'phenotypic space' to interpolate identity and function, they afford the stereotypical map of neuron and glial cells described above. Recent transcriptomics clusters are annotated to physical cell identities by exploiting more than 868 *in vivo* expression reporters of fate and effector genes, many arising from community's studies (Cao et al., 2017; Packer et al., 2019; Taylor et al., 2021). Matching transcriptomics to embryonic cells also utilized embryonic lineage tracing of 251 reporters (Packer et al., 2019). Transcriptomics clusters match adequately to well-studied cells, except of certain neurons (DD and VD), embryonic cells and glial cells (OLQsh, OLQso, ILsh, ILso, CEPso), understudied at single-cell resolution. Thus, community knowledge and its integration are crucial to our multimodal view of *C. elegans* neural cell types.

C. elegans nervous system cell classifications are organized largely in multifaceted databases, including *Wormbase*[2], *Wormatlas*[3], *Wormwiring*[4], *Nemanode*[5]. These feature information on cell nomenclature, morphology, physiology, gene expression, wiring and display some extent of integration (**Figure 5**). *Wormbase* features gene entries, presenting genome location, homologies, cellular expression and function, related publications and sometimes conference proceedings. It features entries dedicated to each individual cell, recording its lineage position, reporters' expression, citations and links to *Wormatlas*. In *Wormatlas,* webpages dedicated to each neuron present lineage identity, morphology, effector gene expression and cell function. These cell entries include links to the first connectome, the "Mind of the Worm," (White et al., 1986; Altun and Hall, 2011) and to *Wormwiring*. *Wormwiring* presents recent matrices of process adjacencies and synaptic connections of each neural cell of both sexes (Cook et al., 2019). *Nemanode* is a recent resource of single-cell-resolution connectomes throughout *C. elegans* postembryonic development (Witvliet et al., 2021). *C. elegans* single-cell transcriptomics datasets are available in *CellAtlas*[6], *Viscello*[7], *Cengen*[8]. These browsers provide lists of cells presenting a specific transcript. CenGEN also provides transcript content of most nervous system cells at single-cell resolution. These platforms highlight remarkable community efforts to map nervous system cells comprehensively and dynamically. Comprehensive cell studies involve simultaneous navigation across these platforms, a feasible task owing to consistent nomenclature and limited *C. elegans* cell numbers.

These resources can be considered as graspable phases evolving toward an integrated navigable map. *Wormbase* and *Wormatlas* are scalable, continuously updated with upcoming information on cell functions and gene expression. Future curations building up on integration could enable easier navigation across different cell-specific modalities. Cell entries could integrate developmental aspects, fate regulators and embryonic physiology. They can include information on cell type/state heterogeneity, i.e., features of gene expression, process adjacencies and synaptic connectivity matrices in sex dimorphic or nutrition-deprived states (Cook et al., 2019; Witvliet et al., 2021). Including links to *Nemanode* would highlight each cell's developmentally plastic wiring. Integrating transcriptomic profiles in *Wormatlas* or *Wormbase* entries of individual cells could enable visualizing cell-type transcripts. As glial cell studies gain considerable ground, *Wormatlas* could include entries dedicated to individual glial cells, currently missing. Embryonic cell physiology is another future frontier to tackle.

Integration of Cell Features Beyond *Caenorhabditis elegans*

Beyond *C. elegans*, integrated platforms of multimodal "cell spaces" in different species is the current path forward to study nervous system biology in high resolution. An accumulating number of datasets, community efforts and collaborations across institutes converge toward the future picture of cell classifications. The *Fruit Fly Brain Observatory*[9] presents fly brain neurons, their location, morphology, connectivity and biophysical properties, integrating structural and genetic data (Lazar et al., 2021). The *Allen Cell Type Database*[10] features morphological, electrophysiological features and microarray gene expression data of specific brain cells (Sunkin et al., 2013). The A*llen Mouse Brain Common Coordinate Framework i*ntegrates 3D multimodal and multiscale datasets in mouse cortical areas of 10-μm voxels (Wang et al., 2020). The *Tabula Muris*[11] compiles a compendium of transcriptomic data of mouse organs (Schaum et al., 2018). The *BRAIN Initiative Cell Census Network* (BICCN)[12], aiming to catalog mouse, monkey and human brain cells, reported a multimodal cell census atlas of the mammalian primary motor cortex with a cross-modal analysis

[2]https://wormbase.org//#012-34-5

[3]https://www.wormatlas.org/neurons/Individual%20Neurons/Neuronframeset.html

[4]https://wormwiring.org/

[5]https://nemanode.org/

[6]https://atlas.gs.washington.edu/worm-rna/

[7]https://cello.shinyapps.io/celegans/

[8]https://cengen.shinyapps.io/CengenApp/

[9]https://www.fruitflybrain.org/#/

[10]http://celltypes.brain-map.org/

[11]https://tabula-muris.ds.czbiohub.org/

[12]https://biccn.org/

of transcriptomics, epigenomics, physiological and anatomical properties (BRAIN Initiative Cell Census Network [BICCN], 2021). It also provided genetic toolsets to link molecular, developmental and functional cell identities of glutamatergic projection neurons. *Hippocampome* [13] is a comprehensive knowledge base, of 122 neuron types of the rodent hippocampus identified by literature mining based on neurotransmitter, axonal and dendritic patterns, synaptic specificity, electrophysiology, and molecular biomarkers (Sanchez-Aguilera et al., 2021). The *Human Cell Atlas*[14] aims to map all human cells with -omics technologies (Rozenblatt-Rosen et al., 2017). Besides these multimodal sources, recent individual platforms provide data delineating mouse spatial transcriptomics of the whole brain or specific brain areas (Di Bella et al., 2021; La Manno et al., 2021). These remarkable efforts combined will enable future studies of cell type development and evolution.

The Future of Multimodal Integration

Overall, future integrated databases can comprise cell spaces that incorporate information on lineage, physiology, morphological, electrophysiological and functional features, transcriptomics, gene-function (**Figure 6**). Alongside integration and mapping uncharted territories, adaptability will facilitate the dynamic improvement of these platforms. Open-access, user-accessible sources can enable personalized searches of cells based on top–down criteria, with flexibility to examine hierarchical schemes by different criteria. This would allow for testable hypothesis throughout development, across circuits, eventually across species. These platforms would involve extensive curation of information resources, and technology development for harmonizing multiple studies. They can also grow their interdisciplinarity by embracing community annotations. Early *C. elegans* transcriptomes adopted some of the first community annotation strategies, by hosting transcript cell matrices and vignettes for working with the data (Cao et al., 2017)[6]. Multimodal platforms could feature user-friendly interactive ways for experts to share feedback on the entries. They could greatly benefit from feedback-loops across disciplines, with input from experimentalists and experts in data generation and interpretation. Such feedback is critical to build up-to-date databases and refers to concepts, technologies and standardizing methods, arising from integrating multiple avenues of study. Incorporating unpublished knowledge whenever possible could accelerate the pace of scientific progress and innovation. Along the road, as the number of species with cell atlases increase, creating links between atlases of different organisms could facilitate cross-species investigations. Whether such links would follow gene homologs or specific cell modalities should be defined across communities. Integrating community atlases, -omics sources, *in vivo* experimental data and users' feedback in a multifaceted database is the next step for comprehensive, multimodal investigations of cell types within and across species.

[13] Hippocampome.org

[14] https://www.humancellatlas.org/

AUTHOR CONTRIBUTIONS

GR conceived the idea and composed the manuscript.

FUNDING

GR is supported by the European Molecular Biology Laboratory.

ACKNOWLEDGMENTS

I thank members of the Rapti group, colleagues at the Developmental Biology Unit and Epigenetics and Neurobiology Unit at EMBL and at the Interdisciplinary Center for Neurosciences for insightful discussions. I thank Scott Emmons, David Hall, Stephen Larson, and Mei Zhen for permitting use of images from open-source websites. I apologize to those whose work was not cited unintentionally due to oversight or space considerations. I thank the reviewers for helpful comments on the manuscript.

REFERENCES

Achim, K., Eling, N., Vergara, H. M., Bertucci, P. Y., Musser, J., Vopalensky, P., et al. (2018). Whole-body single-cell sequencing reveals transcriptional domains in the annelid larval body. *Mol. Biol. Evol.* 35, 1047–1062. doi: 10.1093/molbev/msx336

Albertson, D. G., and Thomson, J. N. (1976). The pharynx of Caenorhabditis elegans. *Philos. Trans. R. Soc. Lond. B Biol. Sci.* 275, 299–325. doi: 10.1098/rstb.1976.0085

Allen, A. M., Neville, M. C., Birtles, S., Croset, V., Treiber, C. D., Waddell, S., et al. (2020). A single-cell transcriptomic atlas of the adult Drosophila ventral nerve cord. *Elife* 9:e54074. doi: 10.7554/eLife.54074

Allen, N. J., and Lyons, D. A. (2018). Glia as architects of central nervous system formation and function. *Science* 362, 181–185. doi: 10.1126/science.aat0473

Alqadah, A., Hsieh, Y. W., Schumacher, J. A., Wang, X., Merrill, S. A., Millington, G., et al. (2016). SLO BK Potassium Channels Couple Gap Junctions to Inhibition of Calcium Signaling in Olfactory Neuron Diversification. *PLoS Genet.* 12:e1005654. doi: 10.1371/journal.pgen.1005654

Altun, Z., and Hall, D. (2011). *Handbook - Nervous System General Description*. Available Online at: Wormatlas.Org.

Altun-Gultekin, Z., Andachi, Y., Tsalik, E. L., Pilgrim, D., Kohara, Y., and Hobert, O. (2001). A regulatory cascade of three homeobox genes, ceh-10, ttx-3 and ceh-23, controls cell fate specification of a defined interneuron class in C. elegans. *Development* 128, 1951–1969.

Anderson, D. J., Choi, G., and Zhou, Q. (2002). Olig genes and the genetic logic of CNS neural cell fate determination. *Clin. Neurosci. Res.* 2, 17–28. doi: 10.1016/S1566-2772(02)00014-2

Androwski, R. J., Asad, N., Wood, J. G., Hofer, A., Locke, S., Smith, C. M., et al. (2020). Mutually exclusive dendritic arbors in C. elegans neurons share a common architecture and convergent molecular cues. *PLoS Genet.* 16:e1009029. doi: 10.1371/journal.pgen.1009029

Arendt, D. (2020). The Evolutionary Assembly of Neuronal Machinery. *Curr. Biol.* 30, R603–R616. doi: 10.1016/j.cub.2020.04.008

Arendt, D., Bertucci, P. Y., Achim, K., and Musser, J. M. (2019). Evolution of neuronal types and families. *Curr. Opin. Neurobiol.* 56, 144–152. doi: 10.1016/j.conb.2019.01.022

Arendt, D., Musser, J. M., Baker, C. V. H., Bergman, A., Cepko, C., Erwin, D. H., et al. (2016). The origin and evolution of cell types. *Nat. Rev. Genet.* 17, 744–757. doi: 10.1038/nrg.2016.127

Arlotta, P., and Hobert, O. (2015). Homeotic Transformations of Neuronal Cell Identities. *Trends Neurosci.* 38, 751–762. doi: 10.1016/j.tins.2015.10.005

Bacaj, T., Tevlin, M., Lu, Y., and Shaham, S. (2008). Glia are essential for sensory organ function in C. elegans. *Science* 322, 744–747. doi: 10.1126/science.1163074

Bao, Z., Murray, J. I., Boyle, T., Ooi, S. L., Sandel, M. J., and Waterston, R. H. (2006). Automated cell lineage tracing in Caenorhabditis elegans. *Proc. Natl. Acad. Sci. U. S. A.* 103, 2707–2712. doi: 10.1073/pnas.0511111103

Bargmann, C. I. (1998). Neurobiology of the Caenorhabditis elegans genome. *Science* 282, 2028–2033. doi: 10.1126/science.282.5396.2028

Bates, A. S., Janssens, J., Jefferis, G. S., and Aerts, S. (2019). Neuronal cell types in the fly: single-cell anatomy meets single-cell genomics. *Curr. Opin. Neurobiol.* 56, 125–134. doi: 10.1016/j.conb.2018.12.012

Berghoff, E. G., Glenwinkel, L., Bhattacharya, A., Sun, H., Varol, E., Mohammadi, N., et al. (2021). The prop1-like homeobox gene unc-42 specifies the identity of synaptically connected neurons. *Elife* 10:e64903. doi: 10.7554/eLife.64903

Bertrand, V., Bisso, P., Poole, R. J., and Hobert, O. (2011). Notch-dependent induction of left/right asymmetry in C. elegans interneurons and motorneurons. *Curr. Biol.* 21, 1225–1231. doi: 10.1016/j.cub.2011.06.016

Bertrand, V., and Hobert, O. (2009). Linking Asymmetric Cell Division to the Terminal Differentiation Program of Postmitotic Neurons in C. elegans. *Dev. Cell* 16, 563–575. doi: 10.1016/j.devcel.2009.02.011

Bhattacharya, A., Aghayeva, U., Berghoff, E. G., and Hobert, O. (2019). Plasticity of the Electrical Connectome of C. elegans. *Cell* 176, 1174–1189. doi: 10.1016/j.cell.2018.12.024

Bittern, J., Pogodalla, N., Ohm, H., Brüser, L., Kottmeier, R., Schirmeier, S., et al. (2020). Neuron–glia interaction in the Drosophila nervous system. *Dev. Neurobiol.* 81, 1–15. doi: 10.1002/dneu.22737

Boldog, E., Bakken, T. E., Hodge, R. D., Novotny, M., Aevermann, B. D., Baka, J., et al. (2018). Transcriptomic and morphophysiological evidence for a specialized human cortical GABAergic cell type. *Nat. Neurosci.* 21, 1185–1195. doi: 10.1038/s41593-018-0205-2

Boyle, T. J., Bao, Z., Murray, J. I., Araya, C. L., and Waterston, R. H. (2006). AceTree: a tool for visual analysis of Caenorhabditis elegans embryogenesis. *BMC Bioinformatics* 7:275. doi: 10.1186/1471-2105-7-275

BRAIN Initiative Cell Census Network [BICCN] (2021). A multimodal cell census and atlas of the mammalian primary motor cortex. *Nature* 598, 86–102. doi: 10.1038/s41586-021-03950-0

Brandt, J. P., Rossillo, M., Du, Z., Ichikawa, D., Barnes, K., Chen, A., et al. (2019). Lineage context switches the function of a C. elegans Pax6 homolog in determining a neuronal fate. *Development* 146:dev168153. doi: 10.1242/dev.168153

Cao, J., Packer, J. S., Ramani, V., Cusanovich, D. A., Huynh, C., Daza, R., et al. (2017). Comprehensive single-cell transcriptional profiling of a multicellular organism. *Science* 357, 661–667. doi: 10.1126/science.aam8940

Cao, J., Spielmann, M., Qiu, X., Huang, X., Ibrahim, D. M., Hill, A. J., et al. (2019). The single-cell transcriptional landscape of mammalian organogenesis. *Nature* 566, 496–502. doi: 10.1038/s41586-019-0969-x

Cembrowski, M. S., and Menon, V. (2018). Continuous Variation within Cell Types of the Nervous System. *Trends Neurosci.* 41, 337–348. doi: 10.1016/j.tins.2018.02.010

Cembrowski, M. S., Phillips, M. G., DiLisio, S. F., Shields, B. C., Winnubst, J., Chandrashekar, J., et al. (2018). Dissociable Structural and Functional Hippocampal Outputs via Distinct Subiculum Cell Classes. *Cell* 173, 1280–1292.e18. doi: 10.1016/j.cell.2018.03.031

Chaboub, L. S., and Deneen, B. (2013). Developmental origins of astrocyte heterogeneity: the final frontier of CNS development. *Dev. Neurosci.* 34, 379–388. doi: 10.1159/000343723

Changeux, J. P. (2020). Discovery of the first neurotransmitter receptor: the acetylcholine nicotinic receptor. *Biomolecules* 10:547. doi: 10.3390/biom10040547

Cheetham, C. E. J., Park, U., and Belluscio, L. (2016). Rapid and continuous activity-dependent plasticity of olfactory sensory input. *Nat. Commun.* 7:10729. doi: 10.1038/ncomms10729

Chen, J., Poskanzer, K. E., Freeman, M. R., and Monk, K. R. (2020). Live-imaging of astrocyte morphogenesis and function in zebrafish neural circuits. *Nat. Neurosci.* 23, 1297–1306. doi: 10.1038/s41593-020-0703-x

Chotard, C., Leung, W., and Salecker, I. (2005). glial cells missing and gcm2 cell autonomously regulate both glial and neuronal development in the visual system of Drosophila. *Neuron* 48, 237–251. doi: 10.1016/j.neuron.2005.09.019

Chung, W. S., Allen, N. J., and Eroglu, C. (2015). Astrocytes control synapse formation, function, and elimination. *Cold Spring Harb. Perspect. Biol.* 7:a020370. doi: 10.1101/cshperspect.a020370

Cochella, L., and Hobert, O. (2012). Embryonic Priming of a miRNA Locus Predetermines Postmitotic Neuronal Left/Right Asymmetry in C. elegans. *Cell* 151, 1229–1242. doi: 10.1016/j.cell.2012.10.049

Colón-Ramos, D. A., Margeta, M. A., and Shen, K. (2007). Glia promote local synaptogenesis through UNC-6 (netrin) signaling in C. elegans. *Science* 318, 103–106. doi: 10.1126/science.1143762

Cook, S. J., Jarrell, T. A., Brittin, C. A., Wang, Y., Bloniarz, A. E., Yakovlev, M. A., et al. (2019). Whole-animal connectomes of both Caenorhabditis elegans sexes. *Nature* 571, 63–71. doi: 10.1038/s41586-019-1352-7

Delgado, A. C., Maldonado-Soto, A. R., Silva-Vargas, V., Mizrak, D., Von Känel, T., Tan, K. R., et al. (2021). Release of stem cells from quiescence reveals gliogenic domains in the adult mouse brain. *Science* 372, 1205–1209. doi: 10.1126/science.abg8467

Di Bella, D. J., Habibi, E., Stickels, R. R., Scalia, G., Brown, J., Yadollahpour, P., et al. (2021). Molecular logic of cellular diversification in the mouse cerebral cortex. *Nature* 595, 554–559. doi: 10.1038/s41586-021-03670-5

DiAntonio, A., Parfitt, K. D., and Schwarz, T. L. (1993). Synaptic transmission persists in synaptotagmin mutants of Drosophila. *Cell* 73, 1281–1290. doi: 10.1016/0092-8674(93)90356-U

Doitsidou, M., Flames, N., Topalidou, I., Abe, N., Felton, T., Remesal, L., et al. (2013). A combinatorial regulatory signature controls terminal differentiation of the dopaminergic nervous system in C. elegans. *Genes Dev.* 27, 1391–1405. doi: 10.1101/gad.217224.113

Drexel, T., Mahofsky, K., Latham, R., Zimmer, M., and Cochella, L. (2016). Neuron type-specific miRNA represses two broadly expressed genes to modulate an avoidance behavior in C. elegans. *Genes Dev.* 30, 2042–2047. doi: 10.1101/gad.287904.116

Fang, H., Bygrave, A. M., Roth, R. H., Johnson, R. C., and Huganir, R. L. (2021). An optimized crispr/cas9 approach for precise genome editing in neurons. *Elife* 10, 1–25. doi: 10.7554/eLife.65202

Farmer, W. T., Abrahamsson, T., Chierzi, S., Lui, C., Zaelzer, C., Jones, E. V., et al. (2016). Neurons diversify astrocytes in the adult brain through sonic hedgehog signaling. *Science* 351, 849–854. doi: 10.1126/science.aab3103

Fields, R. D., and Stevens-Graham, B. (2002). New Insights into Neuron-Glia Communication. *Science* 298, 556–562. doi: 10.1126/science.298.5593.556

Finkelstein, G. (2015). Mechanical neuroscience: Emil du Bois-Reymond's innovations in theory and practice. *Front. Syst. Neurosci.* 9:133. doi: 10.3389/fnsys.2015.00133

Fishell, G., and Heintz, N. (2013). The neuron identity problem: form meets function. *Neuron* 80, 602–612. doi: 10.1016/j.neuron.2013.10.035

Flames, N., and Hobert, O. (2009). Gene regulatory logic of dopamine neuron differentiation. *Nature* 458, 885–889. doi: 10.1038/nature07929

Foerster, S., Hill, M. F. E., and Franklin, R. J. M. (2019). Diversity in the oligodendrocyte lineage: plasticity or heterogeneity? *Glia* 67, 1797–1805. doi: 10.1002/glia.23607

Forrester, W. C., Perens, E., Zallen, J. A., and Garriga, G. (1998). Identification of Caenorhabditis elegans genes required for neuronal differentiation and migration. *Genetics* 148, 151–165. doi: 10.1093/genetics/148.1.151

Frakes, A. E., Metcalf, M. G., Tronnes, S. U., Bar-Ziv, R., Durieux, J., Gildea, H. K., et al. (2020). Four glial cells regulate ER stress resistance and longevity via neuropeptide signaling in C. Elegans. *Science* 367, 436–440. doi: 10.1126/science.aaz6896

Freeman, M. R., and Rowitch, D. H. (2013). Evolving concepts of gliogenesis: a look way back and ahead to the next 25 years. *Neuron* 80, 613–623. doi: 10.1016/j.neuron.2013.10.034

Gallo, V., and Ghiani, C. A. (2000a). Glutamate receptors in glia: new cells, new inputs and new functions. *Trends Pharmacol. Sci.* 21, 252–258. doi: 10.1016/S0165-6147(00)01494-2

Gallo, V., and Ghiani, C. A. (2000b). Reply: glia and neurons continue to talk. *Trends Pharmacol. Sci.* 21:375. doi: 10.1016/s0165-6147(00)01544-3

García-Marín, V., García-López, P., and Freire, M. (2007). Cajal's contributions to glia research. *Trends Neurosci.* 30, 479–487. doi: 10.1016/j.tins.2007.06.008

Gendrel, M., Atlas, E. G., and Hobert, O. (2016). A cellular and regulatory map of the GABAergic nervous system of C. elegans. *Elife* 5:e17686. doi: 10.7554/eLife.17686

Gouwens, N. W., Sorensen, S. A., Baftizadeh, F., Budzillo, A., Lee, B. R., Jarsky, T., et al. (2020). Integrated Morphoelectric and Transcriptomic Classification of Cortical GABAergic Cells. *Cell* 183, 935–953.e19. doi: 10.1016/j.cell.2020.09.057

Gouwens, N. W., Sorensen, S. A., Berg, J., Lee, C., Jarsky, T., Ting, J., et al. (2019). Classification of electrophysiological and morphological neuron types in the mouse visual cortex. *Nat. Neurosci.* 22, 1182–1195. doi: 10.1038/s41593-019-0417-0

Günther, T., Chen, Z. F., Kim, J., Priemel, M., Rueger, J. M., Amling, M., et al. (2000). Genetic ablation of parathyroid glands reveals another source of parathyroid hormone. *Nature* 406, 199–203. doi: 10.1038/35018111

Hallam, S. J., and Jin, Y. (1998). lin-14 regulates the timing of synaptic remodelling in Caenorhabditis elegans. *Nature* 395, 78–82. doi: 10.1038/25757

Heiman, M. G., and Shaham, S. (2007). Ancestral roles of glia suggested by the nervous system of Caenorhabditis elegans. *Neuron Glia Biol.* 3, 55–61. doi: 10.1017/S1740925X07000609

Ho, H., De Both, M., Siniard, A., Sharma, S., Notwell, J. H., Wallace, M., et al. (2018). A guide to single-cell transcriptomics in adult rodent brain: the medium spiny neuron transcriptome revisited. *Front. Cell. Neurosci.* 12:159. doi: 10.3389/fncel.2018.00159

Hobert, O. (2008). Regulatory logic of neuronal diversity: terminal selector genes and selector motifs. *Proc. Natl. Acad. Sci. U. S. A.* 105, 20067–20071. doi: 10.1073/pnas.0806070105

Hobert, O. (2016a). A map of terminal regulators of neuronal identity in Caenorhabditis elegans. *Wiley Interdiscip. Rev. Dev. Biol.* 5, 474–498. doi: 10.1002/wdev.233

Hobert, O. (2016b). Terminal Selectors of Neuronal Identity. *Curr. Top. Dev. Biol.* 116, 455–475. doi: 10.1016/bs.ctdb.2015.12.007

Hobert, O., Glenwinkel, L., and White, J. (2016). Revisiting Neuronal Cell Type Classification in Caenorhabditis elegans. *Curr. Biol.* 26, R1197–R1203. doi: 10.1016/j.cub.2016.10.027

Hobert, O., and Kratsios, P. (2019). Neuronal identity control by terminal selectors in worms, flies, and chordates. *Curr. Opin. Neurobiol.* 56, 97–105. doi: 10.1016/j.conb.2018.12.006

Hooke, R. (1665). *Micrographia: or, some physiological descriptions of minute bodies made by magnifying glasses*. London: Royal Society.

Hosoya, T., Takizawa, K., Nitta, K., and Hotta, Y. (1995). Glial cells missing: a binary switch between neuronal and glial determination in drosophila. *Cell* 82, 1025–1036. doi: 10.1016/0092-8674(95)90281-3

Howell, K., and Hobert, O. (2016). Small Immunoglobulin Domain Proteins at Synapses and the Maintenance of Neuronal Features. *Neuron* 89, 239–241. doi: 10.1016/j.neuron.2016.01.005

Hsieh, Y. W., Chang, C., and Chuang, C. F. (2012). The MicroRNA mir-71 Inhibits Calcium Signaling by Targeting the TIR-1/Sarm1 Adaptor Protein to Control Stochastic L/R Neuronal Asymmetry in C. elegans. *PLoS Genet.* 8:e1002864. doi: 10.1371/journal.pgen.1002864

Hubel, D. H., and Wiesel, T. N. (1962). Receptive fields, binocular interaction and functional architecture in the cat's visual cortex. *J. Physiol.* 160, 106–154. doi: 10.1113/jphysiol.1962.sp006837

Hyman, A. H., and Simons, K. (2011). Beyond HeLa cells. *Nature* 480, 34–34. doi: 10.1038/480034a

Jones, B. W., Fetter, R. D., Tear, G., and Goodman, C. S. (1995). glial cells missing: a genetic switch that controls glial versus neuronal fate. *Cell* 82, 1013–1023. doi: 10.1016/0092-8674(95)90280-5

Kagoshima, H., and Kohara, Y. (2015). Co-expression of the transcription factors CEH-14 and TTX-1 regulates AFD neuron-specific genes gcy-8 and gcy-18 in C. elegans. *Dev. Biol.* 399, 325–336. doi: 10.1016/j.ydbio.2015.01.010

Kalmbach, B. E., Hodge, R. D., Jorstad, N. L., Owen, S., de Frates, R., Yanny, A. M., et al. (2021). Signature morpho-electric, transcriptomic, and dendritic properties of human layer 5 neocortical pyramidal neurons. *Neuron* 109, 2914–2927.e5. doi: 10.1016/j.neuron.2021.08.030

Katz, M., Corson, F., Iwanir, S., Biron, D., and Shaham, S. (2018). Glia Modulate a Neuronal Circuit for Locomotion Suppression during Sleep in C. elegans. *Cell Rep.* 22, 2601–2614. doi: 10.1016/j.celrep.2018.02.036

Katz, M., Corson, F., Keil, W., Singhal, A., Bae, A., Lu, Y., et al. (2019). Glutamate spillover in C. elegans triggers repetitive behavior through presynaptic activation of MGL-2/mGluR5. *Nat. Commun.* 10:1882. doi: 10.1038/s41467-019-09581-4

Kerk, S. Y., Kratsios, P., Hart, M., Mourao, R., and Hobert, O. (2017). Diversification of C. elegans Motor Neuron Identity via Selective Effector Gene Repression. *Neuron* 93, 80–98. doi: 10.1016/j.neuron.2016.11.036

Kim, K., Kim, R., and Sengupta, P. (2010). The HMX/NKX homeodomain protein MLS-2 specifies the identity of the AWC sensory neuron type via regulation of the ceh-36 Otx gene in C. elegans. *Development* 137, 963–974. doi: 10.1242/dev.044719

Kiselev, V. Y., Andrews, T. S., and Hemberg, M. (2019). Challenges in unsupervised clustering of single-cell RNA-seq data. *Nat. Rev. Genet.* 20, 273–282. doi: 10.1038/s41576-018-0088-9

Kutschera, U. (2011). The cell was defined 150 years ago. *Nature* 480:457. doi: 10.1038/480457c

La Manno, G., Siletti, K., Furlan, A., Gyllborg, D., Vinsland, E., Mossi Albiach, A., et al. (2021). Molecular architecture of the developing mouse brain. *Nature* 596, 92–96. doi: 10.1038/s41586-021-03775-x

Lähnemann, D., Köster, J., Szczurek, E., McCarthy, D. J., Hicks, S. C., Robinson, M. D., et al. (2020). Eleven grand challenges in single-cell data science. *Genome Biol.* 21:31. doi: 10.1186/s13059-020-1926-6

Lazar, A. A., Liu, T., Turkcan, M. K., and Zhou, Y. (2021). Accelerating with flybrainlab the discovery of the functional logic of the drosophila brain in the connectomic and synaptomic era. *Elife* 10, 1–65. doi: 10.7554/eLife.62362

Lee, B. R., Budzillo, A., Hadley, K., Miller, J. A., Jarsky, T., Baker, K., et al. (2021). Scaled, high fidelity electrophysiological, morphological, and transcriptomic cell characterization. *Elife* 10, 1–30. doi: 10.7554/eLife.65482

Lee, I. H., Procko, C., Lu, Y., and Shaham, S. (2021). Stress-Induced Neural Plasticity Mediated by Glial GPCR REMO-1 Promotes C. elegans Adaptive Behavior. *Cell Rep.* 34:108607. doi: 10.1016/j.celrep.2020.108607

Leung-Hagesteijn, C., Spence, A. M., Stern, B. D., Zhou, Y., Su, M. W., Hedgecock, E. M., et al. (1992). UNC-5, a transmembrane protein with immunoglobulin and thrombospondin type 1 domains, guides cell and pioneer axon migrations in C. elegans. *Cell* 71, 289–299. doi: 10.1016/0092-8674(92)90357-I

Lichtman, J. W., Livet, J., and Sanes, J. R. (2008). A technicolour approach to the connectome. *Nat. Rev. Neurosci.* 9, 417–422. doi: 10.1038/nrn2391

Loo, L., Simon, J. M., Xing, L., McCoy, E. S., Niehaus, J. K., Guo, J., et al. (2019). Single-cell transcriptomic analysis of mouse neocortical development. *Nat. Commun.* 10:134. doi: 10.1038/s41467-018-08079-9

Lu, Q. R., Sun, T., Zhu, Z., Ma, N., Garcia, M., Stiles, C. D., et al. (2002). Common developmental requirement for Olig function indicates a motor neuron/oligodendrocyte connection. *Cell* 109, 75–86. doi: 10.1016/S0092-8674(02)00678-5

Lyons, D. A., and Talbot, W. S. (2015). Glial Cell Development and Function in Zebrafish. *Cold Spring Harb. Perspect. Biol.* 7:a020586. doi: 10.1101/cshperspect.a020586

Marioni, J. C., and Arendt, D. (2017). How single-cell genomics is changing evolutionary and developmental biology. *Annu. Rev. Cell Dev. Biol.* 33, 537–553. doi: 10.1146/annurev-cellbio-100616-060818

Masoudi, N., Yemini, E., Schnabel, R., and Hobert, O. (2021). Piecemeal regulation of convergent neuronal lineages by bHLH transcription factors in Caenorhabditis elegans. *Development* 148:dev199224. doi: 10.1242/DEV.199224

Miller-Fleming, T. W., Petersen, S. C., Manning, L., Matthewman, C., Gornet, M., Beers, A., et al. (2016). The DEG/ENaC cation channel protein UNC-8 drives activity-dependent synapse removal in remodeling GABAergic neurons. *Elife* 5, 1–28. doi: 10.7554/eLife.14599

Mizeracka, K., Rogers, J. M., Rumley, J. D., Shaham, S., Bulyk, M. L., Murray, J. I., et al. (2021). Lineage-specific control of convergent differentiation by a Forkhead repressor. *Development* 148:dev199493. doi: 10.1242/dev.199493

Molina-García, L., Cook, S., Kim, B., Bonnington, R., Sammut, M., O'Shea, J., et al. (2019). A direct glia-to-neuron natural transdifferentiation ensures nimble sensory-motor coordination of male mating behaviour. *bioRxiv* [preprint]. doi: 10.1101/285320

Molina-García, L., Lloret-Fernández, C., Cook, S. J., Kim, B., Bonnington, R. C., Sammut, M., et al. (2020). Direct glia-to-neuron transdifferentiation gives rise to a pair of male-specific neurons that ensure nimble male mating. *Elife* 9:e48361. doi: 10.7554/eLife.48361

Moroz, L. L., and Kohn, A. B. (2016). Independent origins of neurons and synapses: insights from ctenophores. *Philos. Trans. R. Soc. B Biol. Sci.* 371:20150041. doi: 10.1098/rstb.2015.0041

Moyle, M. W., Barnes, K. M., Kuchroo, M., Gonopolskiy, A., Duncan, L. H., Sengupta, T., et al. (2021). Structural and developmental principles of neuropil assembly in C. elegans. *Nature* 591, 99–104. doi: 10.1038/s41586-020-03169-5

Murray, J. I., Bao, Z., Boyle, T. J., and Waterston, R. H. (2006). The lineaging of fluorescently-labeled Caenorhabditis elegans embryos with StarryNite and AceTree. *Nat. Protoc.* 1, 1468–1476. doi: 10.1038/nprot.2006.222

Niklaus, S., Cadetti, L., Vom Berg-Maurer, C. M., Lehnherr, A., Hotz, A. L., Forster, I. C., et al. (2017). Shaping of signal transmission at the photoreceptor synapse by EAAT2 glutamate transporters. *eNeuro* 4, ENEURO.339–ENEURO.316. doi: 10.1523/ENEURO.0339-16.2017

Nishizono, H., Yasuda, R., and Laviv, T. (2020). Methodologies and Challenges for CRISPR/Cas9 Mediated Genome Editing of the Mammalian Brain. *Front. Genome Ed.* 2:602970. doi: 10.3389/fgeed.2020.602970

Nonet, M. L., Grundahl, K., Meyer, B. J., and Rand, J. B. (1993). Synaptic function is impaired but not eliminated in C. elegans mutants lacking synaptotagmin. *Cell* 73, 1291–1305. doi: 10.1016/0092-8674(93)90357-V

O'Keefe, J., and Nadel, L. (1979). *Hippocampus as cognitive map*. Oxford: Oxford University Press.

Oren-Suissa, M., Bayer, E. A., and Hobert, O. (2016). Sex-specific pruning of neuronal synapses in Caenorhabditis elegans. *Nature* 533, 206–211. doi: 10.1038/nature17977

Özel, M. N., Simon, F., Jafari, S., Holguera, I., Chen, Y. C., Benhra, N., et al. (2021). Neuronal diversity and convergence in a visual system developmental atlas. *Nature* 589, 88–95. doi: 10.1038/s41586-020-2879-3

Packer, J. S., Zhu, Q., Huynh, C., Sivaramakrishnan, P., Preston, E., Dueck, H., et al. (2019). A lineage-resolved molecular atlas of C. Elegans embryogenesis at single-cell resolution. *Science* 365:eaax1971. doi: 10.1126/science.aax1971

Pereira, L., Kratsios, P., Serrano-Saiz, E., Sheftel, H., Mayo, A. E., Hall, D. H., et al. (2015). A cellular and regulatory map of the cholinergic nervous system of C. Elegans. *Elife* 4:e12432. doi: 10.7554/eLife.12432

Perez, J. D., Tom Dieck, S., Alvarez-Castelao, B., Tushev, G., Chan, I. C. W., and Schuman, E. M. (2021). Subcellular sequencing of single neurons reveals the dendritic transcriptome of gabaergic interneurons. *Elife* 10:e63092. doi: 10.7554/eLife.63092

Perry, M., Konstantinides, N., Pinto-Teixeira, F., and Desplan, C. (2017). Generation and Evolution of Neural Cell Types and Circuits: insights from the Drosophila Visual System. *Annu. Rev. Genet.* 51, 501–527. doi: 10.1146/annurev-genet-120215-035312

Philbrook, A., Ramachandran, S., Lambert, C. M., Oliver, D., Florman, J., Alkema, M. J., et al. (2018). Neurexin directs partner-specific synaptic connectivity in C. Elegans. *Elife* 7:e35692. doi: 10.7554/eLife.35692

Ponroy Bally, B., and Murai, K. K. (2021). Astrocytes in Down Syndrome Across the Lifespan. *Front. Cell. Neurosci.* 15:702685. doi: 10.3389/fncel.2021.702685

Poskanzer, K. E., and Molofsky, A. V. (2018). Dynamism of an Astrocyte in Vivo: perspectives on Identity and Function. *Annu. Rev. Physiol.* 80, 143–157. doi: 10.1146/annurev-physiol-021317-121125

Poulin, J. F., Tasic, B., Hjerling-Leffler, J., Trimarchi, J. M., and Awatramani, R. (2016). Disentangling neural cell diversity using single-cell transcriptomics. *Nat. Neurosci.* 19, 1131–1141. doi: 10.1038/nn.4366

Poulopoulos, A., Murphy, A. J., Ozkan, A., Davis, P., Hatch, J., Kirchner, R., et al. (2019). Subcellular transcriptomes and proteomes of developing axon projections in the cerebral cortex. *Nature* 565, 356–360. doi: 10.1038/s41586-018-0847-y

Procko, C., Lu, Y., and Shaham, S. (2011). Glia delimit shape changes of sensory neuron receptive endings in C. elegans. *Development* 138, 1371–1381. doi: 10.1242/dev.058305

Ramón Y Cajal, S. (1911). *Histologie du systeme nerveux de l'homme et des vertebres*. France: Hachette Livre.

Rapti, G. (2020). A perspective on C. elegans neurodevelopment: from early visionaries to a booming neuroscience research. *J. Neurogenet.* 34, 259–272. doi: 10.1080/01677063.2020.1837799

Rapti, G., Li, C., Shan, A., Lu, Y., and Shaham, S. (2017). Glia initiate brain assembly through noncanonical Chimaerin-Furin axon guidance in C. elegans. *Nat. Neurosci.* 20, 1350–1360. doi: 10.1038/nn.4630

Reilly, M. B., Cros, C., Varol, E., Yemini, E., and Hobert, O. (2020). Unique homeobox codes delineate all the neuron classes of C. elegans. *Nature* 584, 595–601. doi: 10.1038/s41586-020-2618-9

Rey, S., Zalc, B., and Klämbt, C. (2021). Evolution of glial wrapping: a new hypothesis. *Dev. Neurobiol.* 81, 453–463. doi: 10.1002/dneu.22739

Rozenblatt-Rosen, O., Stubbington, M. J. T., Regev, A., and Teichmann, S. A. (2017). The Human Cell Atlas: from vision to reality. *Nature* 550, 451–453. doi: 10.1038/550451a

Sagasti, A., Hisamoto, N., Hyodo, J., Tanaka-Hino, M., Matsumoto, K., and Bargmann, C. I. (2001). The CaMKII UNC-43 activates the MAPKKK NSY-1 to execute a lateral signaling decision required for asymmetric olfactory neuron fates. *Cell* 105, 221–232. doi: 10.1016/S0092-8674(01)00313-0

Saleeba, C., Dempsey, B., Le, S., Goodchild, A., and McMullan, S. (2019). A student's guide to neural circuit tracing. *Front. Neurosci.* 13:897. doi: 10.3389/fnins.2019.00897

Sammut, M., Cook, S. J., Nguyen, K. C. Q., Felton, T., Hall, D. H., Emmons, S. W., et al. (2015). Glia-derived neurons are required for sex-specific learning in C. Elegans. *Nature* 526, 385–390. doi: 10.1038/nature15700

Sanchez-Aguilera, A., Wheeler, D. W., Jurado-Parras, T., Valero, M., Nokia, M. S., Cid, E., et al. (2021). An update to Hippocampome.org by integrating single-cell phenotypes with circuit function in vivo. *PLoS Biol.* 19:e3001213. doi: 10.1371/journal.pbio.3001213

Sarafi-Reinach, T. R., and Sengupta, P. (2000). The forkhead domain gene unc-130 generates chemosensory neuron diversity in C. elegans. *Genes Dev.* 14, 2472–2485. doi: 10.1101/gad.832300

Sarma, G. P., Lee, C. W., Portegys, T., Ghayoomie, V., Jacobs, T., Alicea, B., et al. (2018). OpenWorm: overview and recent advances in integrative biological simulation of *Caenorhabditis elegans*. *Philos. Trans. R. Soc. B Biol. Sci.* 373. doi: 10.1098/rstb.2017.0382

Satterlee, J. S., Sasakura, H., Kuhara, A., Berkeley, M., Mori, I., and Sengupta, P. (2001). Specification of thermosensory neuron fate in C. elegans requires ttx-1, a homolog of otd/Otx. *Neuron* 31, 943–956. doi: 10.1016/S0896-6273(01)00431-7

Satterstrom, F. K., Kosmicki, J. A., Wang, J., Breen, M. S., De Rubeis, S., An, J. Y., et al. (2020). Large-Scale Exome Sequencing Study Implicates Both Developmental and Functional Changes in the Neurobiology of Autism. *Cell* 180, 568–584.e23. doi: 10.1016/j.cell.2019.12.036

Schaum, N., Karkanias, J., Neff, N. F., May, A. P., Quake, S. R., Wyss-Coray, T., et al. (2018). Single-cell transcriptomics of 20 mouse organs creates a Tabula Muris. *Nature* 562, 367–372. doi: 10.1038/s41586-018-0590-4

Semyanov, A., Henneberger, C., and Agarwal, A. (2020). Making sense of astrocytic calcium signals — from acquisition to interpretation. *Nat. Rev. Neurosci.* 21, 551–564. doi: 10.1038/s41583-020-0361-8

Serrano-Saiz, E., Poole, R. J., Felton, T., Zhang, F., De La Cruz, E. D., and Hobert, O. (2013). Modular control of glutamatergic neuronal identity in C. elegans by distinct homeodomain proteins. *Cell* 155, 659–673. doi: 10.1016/j.cell.2013.09.052

Shekhar, K., Lapan, S. W., Whitney, I. E., Tran, N. M., Evan, Z., Kowalczyk, M., et al. (2016). Comprehensive classification of retinal bipolar neurons by single-cell transcriptomics. *Cell* 166, 1308–1323. doi: 10.1016/j.cell.2016.07.054

Singhvi, A., Liu, B., Friedman, C. J., Fong, J., Lu, Y., Huang, X.-Y., et al. (2016). A Glial K/Cl Transporter Controls Neuronal Receptive Ending Shape by Chloride Inhibition of an rGC. *Cell* 165, 936–948. doi: 10.1016/j.cell.2016.03.026

Singhvi, A., and Shaham, S. (2019). Glia-Neuron Interactions in Caenorhabditis elegans. *Annu. Rev. Neurosci.* 42, 149–168. doi: 10.1146/annurev-neuro-070918-050314

Sprecher, S. G., and Desplan, C. (2008). Switch of rhodopsin expression in terminally differentiated Drosophila sensory neurons. *Nature* 454, 533–537. doi: 10.1038/nature07062

St Johnston, D. (2002). The art and design of genetic screens: drosophila melanogaster. *Nat. Rev. Genet.* 3, 176–188. doi: 10.1038/nrg751

Stefanakis, N., Carrera, I., and Hobert, O. (2015). Regulatory Logic of Pan-Neuronal Gene Expression in C. elegans. *Neuron* 87, 733–750. doi: 10.1016/j.neuron.2015.07.031

Südhof, T. C., and Malenka, R. C. (2008). Understanding Synapses: past, Present, and Future. *Neuron* 60, 469–476. doi: 10.1016/j.neuron.2008.10.011

Sugino, K., Hempel, C. M., Miller, M. N., Hattox, A. M., Shapiro, P., Wu, C., et al. (2006). Molecular taxonomy of major neuronal classes in the adult mouse forebrain. *Nat. Neurosci.* 9, 99–107. doi: 10.1038/nn1618

Sulston, J. E., and Horvitz, H. R. (1977). Post-embryonic cell lineages of the nematode, Caenorhabditis elegans. *Dev. Biol.* 56, 110–156. doi: 10.1016/0012-1606(77)90158-0

Sulston, J. E., Schierenberg, E., White, J. G., and Thomson, J. N. (1983). The embryonic cell lineage of the nematode Caenorhabditis elegans. *Dev. Biol.* 100, 64–119. doi: 10.1016/0012-1606(83)90201-4

Sun, D., Lye-Barthel, M., Masland, R. H., and Jakobs, T. C. (2010). Structural remodeling of fibrous astrocytes after axonal injury. *J. Neurosci.* 30, 14008–14019. doi: 10.1523/JNEUROSCI.3605-10.2010

Sun, H., and Hobert, O. (2021). Temporal transitions in the post-mitotic nervous system of Caenorhabditis elegans. *Nature* 600, 93–99. doi: 10.1038/s41586-021-04071-4

Sunkin, S. M., Ng, L., Lau, C., Dolbeare, T., Gilbert, T. L., Thompson, C. L., et al. (2013). Allen Brain Atlas: an integrated spatio-temporal portal for exploring the central nervous system. *Nucleic Acids Res.* 41, D996–D1008. doi: 10.1093/nar/gks1042

Suzuki, H., Thiele, T. R., Faumont, S., Ezcurra, M., Lockery, S. R., and Schafer, W. R. (2008). Functional asymmetry in Caenorhabditis elegans taste neurons and its computational role in chemotaxis. *Nature* 454, 114–117. doi: 10.1038/nature06927

Svensson, V., da Veiga Beltrame, E., and Pachter, L. (2020). A curated database reveals trends in single-cell transcriptomics. *Database* 2020:baaa073. doi: 10.1093/DATABASE/BAAA073

Swoboda, P., Adler, H. T., and Thomas, J. H. (2000). The RFX-type transcription factor DAF-19 regulates sensory neuron cilium formation in C. Elegans. *Mol. Cell* 5, 411–421. doi: 10.1016/S1097-2765(00)80436-0

Takano, T. (2015). Interneuron dysfunction in syndromic autism: recent advances. *Dev. Neurosci.* 37, 467–475. doi: 10.1159/000434638

Tasic, B., Yao, Z., Graybuck, L. T., Smith, K. A., Nguyen, T. N., Bertagnolli, D., et al. (2018). Shared and distinct transcriptomic cell types across neocortical areas. *Nature* 563, 72–78. doi: 10.1038/s41586-018-0654-5

Taylor, S. R., Santpere, G., Weinreb, A., Barrett, A., Reilly, M. B., Xu, C., et al. (2021). Molecular topography of an entire nervous system. *Cell* 184, 4329–4347.e23. doi: 10.1016/j.cell.2021.06.023

Thompson-Peer, K. L., Bai, J., Hu, Z., and Kaplan, J. M. (2012). HBL-1 patterns synaptic remodeling in C.elegans. *Neuron* 73, 453–465. doi: 10.1016/j.neuron.2011.11.025

Topalidou, I., Van Oudenaarden, A., and Chalfie, M. (2011). Caenorhabditis elegans aristaless/Arx gene alr-1 restricts variable gene expression. *Proc. Natl. Acad. Sci. U. S. A.* 108, 4063–4068. doi: 10.1073/pnas.1101329108

Trapnell, C. (2015). Defining cell types and states with single-cell genomics. *Genome Res.* 25, 1491–1498. doi: 10.1101/gr.190595.115

Treutlein, B., Lee, Q. Y., Camp, J. G., Mall, M., Koh, W., Shariati, S. A. M., et al. (2016). Dissecting direct reprogramming from fibroblast to neuron using single-cell RNA-seq. *Nature* 534, 391–395. doi: 10.1038/nature18323

Tucker, M., Sieber, M., Morphew, M., and Han, M. (2005). The Caenorhabditis elegans aristaless Orthologue, alr-1, Is Required for Maintaining the Functional and Structural Integrity of the Amphid Sensory Organs. *Mol. Biol. Cell* 16, 4695–4704. doi: 10.1091/mbc.e05-03-0205

Van Buskirk, C., and Sternberg, P. W. (2010). Paired and LIM class homeodomain proteins coordinate differentiation of the C. elegans ALA neuron. *Development* 137, 2065–2074. doi: 10.1242/dev.040881

Varoqueaux, F., and Fasshauer, D. (2017). Getting Nervous: an Evolutionary Overhaul for Communication. *Annu. Rev. Genet.* 51, 455–476. doi: 10.1146/annurev-genet-120116-024648

Vergara, H. M., Pape, C., Meechan, K. I., Zinchenko, V., Genoud, C., Wanner, A. A., et al. (2021). Whole-body integration of gene expression and single-cell morphology. *Cell* 184, 4819–4837.e22. doi: 10.1016/j.cell.2021.07.017

Waddington, C. H. (1957). *The strategy of the genes. A discussion of some aspects of theoretical biology*. Crows Nest, New South Wales: Allen & Unwin

Wallace, S. W., Singhvi, A., Liang, Y., Lu, Y., and Shaham, S. (2016). PROS-1/Prospero Is a Major Regulator of the Glia-Specific Secretome Controlling Sensory-Neuron Shape and Function in C. elegans. *Cell Rep.* 15, 550–562. doi: 10.1016/j.celrep.2016.03.051

Wang, Q., Ding, S. L., Li, Y., Royall, J., Feng, D., Lesnar, P., et al. (2020). The Allen Mouse Brain Common Coordinate Framework: a 3D Reference Atlas. *Cell* 181, 936–953.e20. doi: 10.1016/j.cell.2020.04.007

Ward, S., Thomson, N., White, J. G., and Brenner, S. (1975). Electron microscopical reconstruction of the anterior sensory anatomy of the nematode Caenorhabditis elegans. *J. Comp. Neurol.* 160, 313–337. doi: 10.1002/cne.901600305

Wenick, A. S., and Hobert, O. (2004). Genomic cis-regulatory architecture and trans-acting regulators of a single interneuron-specific gene battery in C. elegans. *Dev. Cell* 6, 757–770. doi: 10.1016/j.devcel.2004.05.004

White, J. G., Southgate, E., Thomson, J. N., and Brenner, S. (1986). The Structure of the Nervous System of the Nematode Caenorhabditis elegans. *Philos. Trans. R. Soc. Lond. B Biol. Sci.* 314, 1–340. doi: 10.1098/rstb.1986.0056

Williams, E. A., and Jékely, G. (2019). Neuronal cell types in the annelid Platynereis dumerilii. *Curr. Opin. Neurobiol.* 56, 106–116. doi: 10.1016/j.conb.2018.12.008

Witvliet, D., Mulcahy, B., Mitchell, J. K., Meirovitch, Y., Berger, D. R., Wu, Y., et al. (2021). Connectomes across development reveal principles of brain maturation. *Nature* 596, 257–261. doi: 10.1038/s41586-021-03778-8

Yang, Z., and Wang, K. K. W. (2015). Glial fibrillary acidic protein: from intermediate filament assembly and gliosis to neurobiomarker. *Trends Neurosci.* 38, 364–374. doi: 10.1016/j.tins.2015.04.003

Yoshimura, S., Murray, J. I., Lu, Y., Waterston, R. H., and Shaham, S. (2008). mls-2 and vab-3 Control glia development, hlh-17/Olig expression and glia-dependent neurite extension in C. elegans. *Development* 135, 2263–2275. doi: 10.1242/dev.019547

Yuste, R., Hawrylycz, M., Aalling, N., Aguilar-Valles, A., Arendt, D., Arnedillo, R. A., et al. (2020). A community-based transcriptomics classification and nomenclature of neocortical cell types. *Nat. Neurosci.* 23, 1456–1468. doi: 10.1038/s41593-020-0685-8

Zallen, J. A., Yi, B. A., and Bargmann, C. I. (1998). The conserved immunoglobulin superfamily member SAX-3/Robo directs multiple aspects of axon guidance in C. elegans. *Cell* 92, 217–227. doi: 10.1016/s0092-8674(00)80916-2

Zeng, H., and Sanes, J. R. (2017). Neuronal cell-type classification: challenges, opportunities and the path forward. *Nat. Rev. Neurosci.* 18, 530–546. doi: 10.1038/nrn.2017.85

Zhang, A., Noma, K., and Yan, D. (2020). Regulation of Gliogenesis by lin-32 /Atoh1 in Caenorhabditis elegans. *G3* 10, 3271–3278. doi: 10.1534/g3.120.401547

Zhang, T., Zeng, Y., Zhang, Y., Zhang, X., Shi, M., Tang, L., et al. (2021). Neuron type classification in rat brain based on integrative convolutional and tree-based recurrent neural networks. *Sci. Rep.* 11:7291. doi: 10.1038/s41598-021-86780-4

Zhang, Y., Chen, K., Sloan, S. A., Bennett, M. L., Scholze, A. R., O'Keeffe, S., et al. (2014). An RNA-sequencing transcriptome and splicing database of glia, neurons, and vascular cells of the cerebral cortex. *J. Neurosci.* 34, 11929–11947. doi: 10.1523/JNEUROSCI.1860-14.2014

Conflict of Interest: The author declares that the research was conducted in the absence of any commercial or financial relationships that could be construed as a potential conflict of interest.

frontiers | Frontiers in Neuroscience

REVIEW
published: 24 May 2022
doi: 10.3389/fnins.2022.909400

Neural Cell Type Diversity in Cnidaria

*Simon G. Sprecher**

Department of Biology, University of Fribourg, Fribourg, Switzerland

Neurons are the fundamental building blocks of nervous systems. It appears intuitive that the human brain is made up of hundreds, if not thousands different types of neurons. Conversely, the seemingly diffuse nerve net of Cnidaria is often assumed to be simple. However, evidence that the Cnidaria nervous system is indeed simple is sparse. Recent technical advances make it possible to assess the diversity and function of neurons with unprecedented resolution. Transgenic animals expressing genetically encoded Calcium sensors allow direct physiological assessments of neural responses within the nerve net and provide insight into the spatial organization of the nervous system. Moreover, response and activity patterns allow the characterization of cell types on a functional level. Molecular and genetic identities on the other hand can be assessed combining single-cell transcriptomic analysis with correlations of gene expression in defined neurons. Here I review recent advances on these two experimental strategies focusing on *Hydra*, *Nematostella,* and *Clytia*.

Keywords: nervous system, evolution, neurotransmitter, Cnidaria, *Nematostella*, *Hydra*, *Clytia*

OPEN ACCESS

Edited by:
Nikolaos Konstantinides, UMR 7592 Institut Jacques Monod (IJM), France

Reviewed by:
Océane Tournière, University of Nice Sophia Antipolis, France
Chiara Sinigaglia, UMR 7232 Biologie Intégrative des Organismes Marins (BIOM), France

***Correspondence:**
Simon G. Sprecher
simon.sprecher@unifr.ch

Specialty section:
This article was submitted to Neurogenesis, a section of the journal Frontiers in Neuroscience

Received: *31 March 2022*
Accepted: *05 May 2022*
Published: *24 May 2022*

Citation:
Sprecher SG (2022) Neural Cell Type Diversity in Cnidaria. Front. Neurosci. 16:909400. doi: 10.3389/fnins.2022.909400

INTRODUCTION

The nervous system provides various critical functions throughout the life of animals. Sensory neurons allow us to perceive information about the environment, while motoneurons innervate muscles and control movements. Depending on the complexity of a nervous system there may be numerous interneurons linked in-between input and output neurons, which in turn are at the core of various types of computations that occur in neural circuits, such as the integration of information or the formation of memories. However, not all animals have neurons. Two early branching metazoan phyla, Sponges and Placozoans, do not have *bona fide* neurons, even though the molecular machinery, which is required for a functioning nervous system is largely present. Ctenophores on the other hand do have a nervous system (Whelan et al., 2017; Sachkova et al., 2021). The phylogenetic position of these early branching metazoans remains heavily debated and thereby also to some degree the origin of neurons. However, there is wide consensus that Cnidaria are the sister group of Bilateria (Moroz et al., 2014; Moroz, 2015; Whelan et al., 2015; Burkhardt and Sprecher, 2017; Feuda et al., 2017; Simion et al., 2017; Turner, 2021). Importantly, Cnidaria do have a nervous system. While the cnidarian nervous system is often termed a "simple nerve net" there is currently little evidence that the cnidarian nervous system is indeed simple. Cnidaria are typically radially symmetrical and therefore only contain an oral-aboral axis, defined by the single opening to the gastric cavity, often referred to as mouth opening. However, several species—including *Nematostella*, display an additional axis, termed directive axis and are therefore bilateral symmetrical (Saina et al., 2009). Cnidaria do not show a higher degree of nervous system centralization and do not possess a ganglia in a classical sense (Sarnat and Netsky, 2002; Hombria et al., 2021). However, the lack of ganglia should not directly imply that the body is covered with a

uniform, diffuse nerve net. Depending on the species there may be different degree of complexity and condensation of neurons. Many species contain typically a prominent nerve ring surrounding the mouth opening, they may also have radial nerves and even ganglion-like aggregation of neurons. One of the best studied, complex neural organs of Cnidaria are the rhopalia, a sensory structure found in cubozoans. The rhopalium contains two lens eyes, as well as two pairs of simpler pit eyes and a statocyst (Nilsson et al., 2005). Anatomical studies in *Tripedalia cystophora* showed that the rhopalial nervous system contains over 1,000 neurons, which can be further divided into several morphologically different cell types, some defined by the expression of neuropeptides (Nielsen et al., 2021). While architecture of the neural circuits remains still largely unknown it has been shown that *Tripedalia cystophora* use visual cues from the surrounding world to alter its swimming behavior and thereby navigates in mangrove areas by using terrestrial cues seen through the water surface (Petie et al., 2011; Garm et al., 2012). The example of the rhopalial nervous system of cubozoans shows that in certain cnidaria species the nervous system may have evolved structures that are much more complex than the widely assumed simple nerve net (Petie et al., 2011; Garm et al., 2012; Nielsen et al., 2021). While one may argue that medusae have an overall more complex lifestyle since they are freely swimming, also the behavioral capacity of polyps may be more complicated than naively expected. The freshwater polyp *Hydra* has been studied particularly for its regenerative capacity for over a century (Galliot, 2012). *Hydra* has been shown to display an array of different behaviors, including rather complex behaviors, such as somersaulting, during which the animal detaches its foot and "stands" on its head, while moving the foot to become attached somewhere else (Passano and McCullough, 1962; Lenhoff, 1968; Han et al., 2018). Such types of behaviors require coordination of certain behavioral motives, which are most likely associated with the transition of the use of different neural networks. However, whether there are commonalities in circuit organization between different clades or between medusae and polyp remains largely unexplored. Similarly, the molecular nature and functional impact of different neuron types is not well understood. A first line of exploration in cell-type diversity in the nervous system comes from single-cell transcriptomics studies. The approach allows to analyze the molecular fingerprint of different cell types and to virtually investigate gene expression profiles. By linking single-cell sequencing data with reporter gene expression or *in situ* hybridization techniques it is possible to connect cell types and their identities. While such an approach requires the availability of genomic or transcriptomic data, the decrease in costs to establish a reference genome or transcriptome opens the approach for various species. The phylum Cnidaria contains several clades, that differ substantially in their life cycle and body plan (**Figure 1**). Much of the knowledge on the cnidarian nervous system stems from a few experimental species for which molecular and genetic techniques are established or emerging (Kelava et al., 2015; Bosch et al., 2017; Rentzsch et al., 2017; Helm, 2018; Rentzsch et al., 2019; Frank et al., 2020; Vogg et al., 2021; Houliston et al., 2022). Apart from *Hydra*, which was already mentioned these lab bread species include the starlet sea anemone *Nematostella vectensis*, the moon jellyfish *Aurelia aurita*, the jellyfish *Clytia hemisphaerica*, species of the hydrozoan genus *Hydractinia* (**Figure 1**; Houliston et al., 2010; Albert, 2011; Rosengarten and Nicotra, 2011; Technau and Steele, 2011; Matveev et al., 2012; Plickert et al., 2012; Layden et al., 2016; Rentzsch and Technau, 2016; Bosch et al., 2017; Frank et al., 2020; Rottinger, 2021; Nicotra, 2022). Substantial work has identified core developmental pathways in early neurogenesis, which appear to make use of a similar set of transcription factors as in bilaterians including members of the atonal and SoxB families (Layden et al., 2012; Kanska and Frank, 2013; Richards and Rentzsch, 2015; Flici et al., 2017; Gahan et al., 2017; Rentzsch et al., 2017). Much less is known regarding the processes involved in terminal differentiation, circuit assembly as well as the genetic diversity of neurons and their precise functions. In the current review I will focus on recent insights into the cell type diversity on a genetic level and links to functional roles.

ORGANIZATION OF THE CNIDARIAN NERVOUS SYSTEM

At larval stages the nervous system has been used to study development studies for instance in *Nematostella, Clytia* as well as in *Hydractinia* (Leclere et al., 2012; Flici et al., 2017; Gahan et al., 2017; Rentzsch et al., 2017). However, the organization of the life cycle differs between distinct cnidarian clades. Mature animals may either have the form of either medusa or polyp (Technau and Steele, 2011). While the homology between the two body plans remains debated the gross organization of the nervous systems displays similarities (Rentzsch et al., 2019). In both cases there is typically a nerve ring surrounding the mouth opening and a more diffuse nerve net covering most parts of the body (Rentzsch et al., 2019). An intriguing feature of cnidarian synapses is that they are not necessarily unidirectional meaning that in in these cases neuronal signals may spread in both directions. Apart from the superficially diffuse nerve net there may be organized nerves running along the mesenteries in *Nematostella*, an endodermal structure containing muscles as well as gonads (Tucker et al., 2011). However, it remains largely unknown how diverse the neurons in the nerve net in fact are. Some insight into the organization and potentially diversity stems from studies using behavioral experiments in combination with genetically encoded Calcium sensors in *Hydra* and *Clytia*.

Hydra displays a series of different behaviors including contracting or bending and tentacle swaying. A recent machine learning based approach allowed a deeper characterization of six different basic behaviors: silent, elongation, tentacle swaying, body swaying, bending, contracting, and feeding (Han et al., 2018). Some more ground pattern behaviors appear more uniform such as bending, contracting, or extending. Somersaulting and feeding are more complex behaviors and consist of a series of individual behavioral motives. Such more complex behaviors require the animal to undergo a specific series of behavioral motives in a specific order, which in turn requires transition of different pre-motor and motor-programs in the nervous system. While they may be seen as not particularly

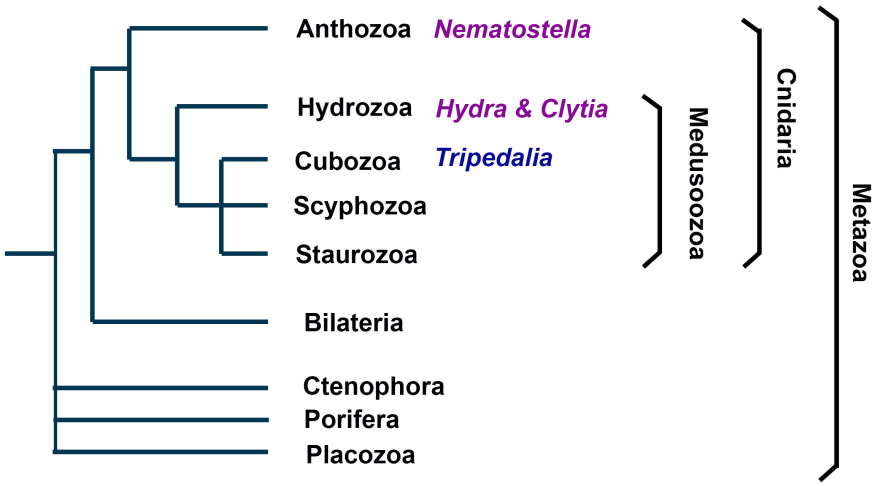

FIGURE 1 | Phylogenetic position and main clades of Cnidaria. As metazoans Cnidaria are the sister group of bilaterians. They comprise the subphylums Anthozoa and Medusozoa, each consisting of several clades. Anthozoa are thought to be the earliest branch among Cnidaria and do not have a medusoid life stage. *Nematostella vectensis* belongs to Anthozoa. *Hydra* and *Clytia* belong to Hydrozoan, which belong to the Medusozoa.

challenging on a computational level, it nevertheless means that the neural circuits or circuits elements have to be able to execute the motor-programs in consecutive fashion and have to be stereotypic in a way to achieve the required outcome, but flexible to adapt for variation of the outcome. Interestingly in the case of *Hydra* semi-independent neural circuits have been identified based on activity patterns using the genetically encoded Gcamp sensor (Dupre and Yuste, 2017). Activity recording showed that different ensembles of neurons are active during different types of behaviors. For instance, an ensemble of neurons is active during elongations, termed Rp1 (Rp for rhythmic potentials), while another ensemble is active during radial contractions, termed Rp2. Such findings show that the nerve net in polyps is made up of different circuits which are required during different behaviors.

In medusae the umbrella contains both a nerve net as well as different types of muscles, thereby controlled deformations of the umbrella can be directly used for different types of behaviors including swimming and feeding. *Clytia* medusa show a folding behavior of the umbrella, which thereby facilitates the transfer of caught plankton from the tentacle to the mouth. Neurons expressing the Fmrfamide peptide are involved in this behavior (Weissbourd et al., 2021). Using transgenic animals expressing the nitroreductase gene, bi-cistronically with Rfp, allowed to specifically kill Fmrfamide neurons when providing the drug metronidazole, while monitoring the removal of cells using Rfp. In animals lacking Fmrfamide neurons the folding behavior is completely lost. Using another transgenic line that expresses the genetically encoded Calcium sensor Gcamp in Fmrfamide expressing neurons shows that these cells are indeed active during the folding behavior. Interestingly, by monitoring the Gcamp activity patterns in more detail it became evident that there are different, discrete ensembles of neurons that appear to make up the entire Fmrfamide population in the umbrella (Weissbourd et al., 2021). Thus, also in medusae different neural subcircuits exist, that are critical for specific aspects of behavior.

These examples show that the nerve net is not uniform, and that certain neuron types and certain ensembles of neurons are required for distinct motoprograms driving behavior. It furthermore demonstrates that there is a spatial organization and subdivision of a certain, molecularly defined neuron type. On a technical level these approaches highlight the impact of two comparably simple and widely used neurogenetic tools in many model organisms: genetic cell-ablation and optic activity monitoring.

MOLECULAR IDENTITIES OF CNIDARIAN NEURONS

Functional features of neurons, such as propagation of membrane currents, transport of and packaging of neurotransmitter or the release of neurotransmitters at the synapse depend on a molecular level on series specific proteins. The expression of these genes encoding for these proteins may in turn be used as defining molecular markers. Such markers typically include synaptic proteins, enzymes in neurotransmitter synthesis, neuronal cell adhesion proteins, but also other pan-neuronal markers, for which the function is less well understood. The Rna binding protein Elav belongs to the latter group. Initially identified in the fruit fly, Elav family proteins have been shown to be expressed in neurons of vertebrates, but also in Cnidaria (Marlow et al., 2009; Nakanishi et al., 2012). The conserved expression in neurons further suggests a common function of these proteins in the nervous system. In *Nematostella vectensis* a transgenic Elav-mOrange reporter is widely expressed in the nervous system, but the line appears to not express pan-neuronally since other neuronal reporter lines are not completely overlapping with the Elav-mOrange reporter (Nakanishi et al., 2012). Single-cell transcriptomics also identified Elav as neuronal marker in *Clytia* (Chari et al., 2021). The pan-neuronal *Hydra* Gcamp line

described above made use of an *actin*-promotor, a gene family that is not exclusively expressed in the nervous system, but cytoskeletal genes are often strongly enriched in the nervous system and some genes may contain nervous system specific enhancers (Dupre and Yuste, 2017). Widely used antibodies for the nervous system include for instance anti acetylated-tubulin or anti tyrosinated tubulin antibodies. Other typical markers that are either specific or highly enriched in many neuron types includes certain proteins for synaptic transmission, such as Synaptobrevin, Synaptotagmin, Synapsin, Homer, or Synaptophysin.

Such common neural markers genes are important features in single-cell transcriptomic studies and help identify neural cell clusters. Recent single-cell transcriptomic analyses were performed on *Nematostella*, *Hydra,* and *Clytia*, investigations more species are very likely underway. The characterization of clusters identified by single-cell transcriptomic approaches and how they may be linked to cell-fates or cellular identities resulted in a broad, rather vivid discussion in the community on what cell types indeed are, how—or even if- clear boundaries cell-types can be drawn, how developmental transitions should be assessed and how in a broader sense the cell-state should be defined. It is important in this context to note that cell clusters in single cell analyses may comprise more than one cell type and that the boundaries ultimately largely depend on sampling depth and to some degree also on conscious decisions when analyzing the data. Nevertheless, the findings of single-cell studies are powerful and extremely informative. In *Nematostella* 32 cell clusters were identified by restricted expression or enrichment of specific genes comprising both larval and adult tissues (Sebe-Pedros et al., 2018). These genes include several transcription factors such as *Pou4*, *Rx*, *FoxD*, *FoxL2*, *SoxC,* or Six1/2. Identification of marker genes in single-cell transcriptomic analyses can indeed be powerful approach for addressing neural identity a transgenic reporter for *FoxL2* shows expression in neurons and cnidocytes and a reporter for *otxC* in neurons. While molecular or functional features of these neural types and a putative role for the behavior of the animals remains currently unexplored these examples show that combining single-cell analysis with subsequent enhancer analysis of marker genes provides a powerful technical approach for neurogenetic studies. Other neural cluster markers in *Nematostella* include G-protein coupled receptors, ion channels and candidate neuropeptide precursors genes. In a *Hydra* single-cell transcriptomic experiment 15 nervous system associated clusters were identified, three containing neural progenitors and 12 consisting of differentiated neuron subtypes (Siebert et al., 2019). Markers specific or enriched in defined clusters include *Lwamide*, *Cnot*, *Innexin2*, *Ndf1,* and *Alpha-Ltx-Lhe1a-like*. To determine differential expression of genes in endodermal and or ectodermal nerve net a TagSeq based experiment allowed to differentiate clusters that belong to the two domains. Gfp reporter transgenes for Ndf1 and Alpha-Ltx-Lhe1a-like indeed allowed a differentiation and showed that *Ndf1*-Gfp is expressed in endodermal neurons, while *Alpha-Ltx-Lhe1a-like*-Gfp is expressed in ectodermal neurons. This example elegantly shows that a further assignment of clusters within defined spatial domains of the nervous system can be achieved. Single cell transcriptomic analysis of *Clytia* identified 14 neural clusters as well as a cluster of neural progenitors defined by the expression of the bhlh transcription factor *Neurogenin (Chari et al., 2021)*. As in *Nematostella* and *Hydra* the expression of specific or enriched markers include transcription factors such as *Six-like*, *Sox10,* and *Hlh6* as well as G-protein coupled receptors *agpcr3* and *agpcr2*. Interestingly, the neuropeptide precursor genes *Pp11* and *Pp5* also belong to these markers. *In situ* hybridization of six neuropeptide precursor (Pp11, Pp5, Pp25, Pp17, Pp20, and Pp7) show marked expression in different subpopulations of neurons, which correlates with data from the scrnaseq study. Interestingly also in *Hydra* a series of highly specific regionalized neuropetides, and thereby likely neural subtypes, were described using *in situ* hybridization (Noro et al., 2019).

While single-cell analyses directly provide insight into the molecular fingerprint of neurons and thereby open direct avenues for future genetic studies, it is important to note that these approaches can also immediately be used to go beyond mapping genes to cells *in silico*. An intriguing example are findings on developmental trajectories of different cell types. Whole animal or whole organ single-cell transcriptomics often contain progenitor cells, differentiated cells and mature cells. Developmental transitions are typically transient and different degrees between immature and mature cells can be observed. Several approaches have been developed to investigate these including Monocle, Rna velocity and Slingshot (La Manno, et al., 2018; Street et al., 2018; Cao et al., 2019). In *Hydra* well studied multipotent interstitial stem cells (Iscs) have been shown to be at the center of developmental and regenerative processes. Interestingly, single-cell transcriptomic analysis shows different intermediate progenitor cell types and allowed to reconstruct two putative trajectories originating from a *Hy-icell1* expressing stem cell population into first two types of *HvSoxC* expressing cells (Siebert et al., 2019). These different lineages appear to be ectoderm and endodermal pathways. It is interesting to note that in either lineage go through a Myb-expressing progenitor, suggesting that the neurogenic program is comparable. Another interesting finding is that these analyses corroborate that nematocytes, gland cells, and neurons are closely related in their linage origin. This core developmental relationship was found in *Clytia*, *Nematostella,* and *Hydra*. There are a few interesting points that can be drawn from this notion. First, some features of nematocytes display similarities with sensory cells. They are a highly derived and cnidaria-specific cell type they are activated only touch. Moreover, nematocytes firing is not a purely mechanical reflex as it not elicited if for instance two tentacles touch each other. Interestingly gene expression analysis of isolated nematocytes of *Nematostella* showed that *Cnido-Jun* and *Cnido-Fos1* are enriched in these cells, two genes which are widely used in neurosciences as immediate early genes depicting neuronal activity (Sunagar et al., 2018). The actual stinging process is an ultrafast exocytosis of the extrusive organelle, which is Calcium-dependent, similarly to synaptic exocytosis. However, if and how nematocytes use neuron-like molecular mechanisms in their cellular function and how they are connected to the nervous system remains still largely unexplored. Second, also gland cells display molecular similarities with neurons, including the

fact that they can use controlled exocytosis to release certain vesicles.

While the use of neuropeptides is an important and global feature of neural communication, the main form of chemical synaptic communication is thought to depend on small molecule neurotransmitters. These neurotransmitters include Glutamate, Acetylcholine, and Gaba. Markers for a specific neurotransmitter identity are either the detection of the neurotransmitter molecule itself as well as the genes or proteins for are enzymes that are involved in the biosynthesis of the neurotransmitter or vesicular neurotransmitter transporters. While most enzymes required for the synthesis of neurotransmitters are present in Cnidaria their function is not well studied. Single-cell analysis in *Clytia* shows that the closest homologs of the vesicular Glutamate transporters are either expressed in nematocysts or non-neuronal cells. Interestingly *vGlut* genes of *Clytia* lack a conserved and critical arginine residue suggesting that vesicular release of Glutamate may not be occurring. Moreover, glutamate decarboxylase (Gad), which is critical in Gaba biosynthesis appears to be restricted to gastrodermal cells (Chari et al., 2021). Interestingly *in situ* hybridization studies in *Nematostella* showed that the core enzymes involved in the biosynthesis of Glutamate, Acetylcholine and Gaba also appear to be predominantly expressed in non-neuronal tissues (Oren et al., 2014). Application of the Gaba receptor agonist baclofen during development in *Nematostella* appears to have inhibitory effects on neurogenesis further suggesting a non-neuronal, but rather a developmental role of Gaba receptor signaling (Levy et al., 2021). In *Nematostella* anti-Gaba immunostaining showed expression in neurons associated with the pharynx and putatively sensory neurons. Taken together these findings raise the question of what in fact common and widely used neurotransmitters in Cnidaria are.

STRUCTURE OF CNIDARIAN NEURONS

The cellular morphology of neurons is diverse. Thus, while features are shared between neurons, there is no clear neural prototype. A core feature of neurons is the existence of neurites, which in many cases can be divided into dendrites and axons. Dendrites typically are shorter and may loosely be regarded as input regions, while axons are long and provide output. However, this input-output relationship of dendrites and axons is clearly too simplistic to consider the diverse pre- and post-synaptic interactions between neurons. Depending on the number of neurites which originate from the soma different cellular morphologies can be defined such as monopolar neurons (one neurite), bipolar neurons (two neurites), tripolar neurons (three neurites), and quadripolar neurons (four neurites). Typically, invertebrate and vertebrate neurons differ substantially in their gross cellular morphology (Smarandache-Wellmann, 2016). The prototype vertebrate neuron has one long, unbranched axon and several short, branching dendritic arbors. Physiologically the synaptic integration occurs in dendrites and soma and the action potential is thought to be initiated from the axon hillock and propagating away from the soma. In invertebrate ganglia the cell bodies are often removed from the neuropil in a fashion that a single neurite extends from the soma, which then branches into axons and dendrites (**Figure 2**). A prototypic neuron would have a bifurcation of the primary neurite into a single, unbranched axon and a dendritic arbor, which can further branch out (Smarandache-Wellmann, 2016). This rather simplistic depiction provides some morphological framework to assess cnidarian neurons. As mentioned above a quite unusual feature of cnidarian synapses is that they may be bidirectional in their organization. This of course complicates conceptually how flow of information in a network is coordinated. Currently

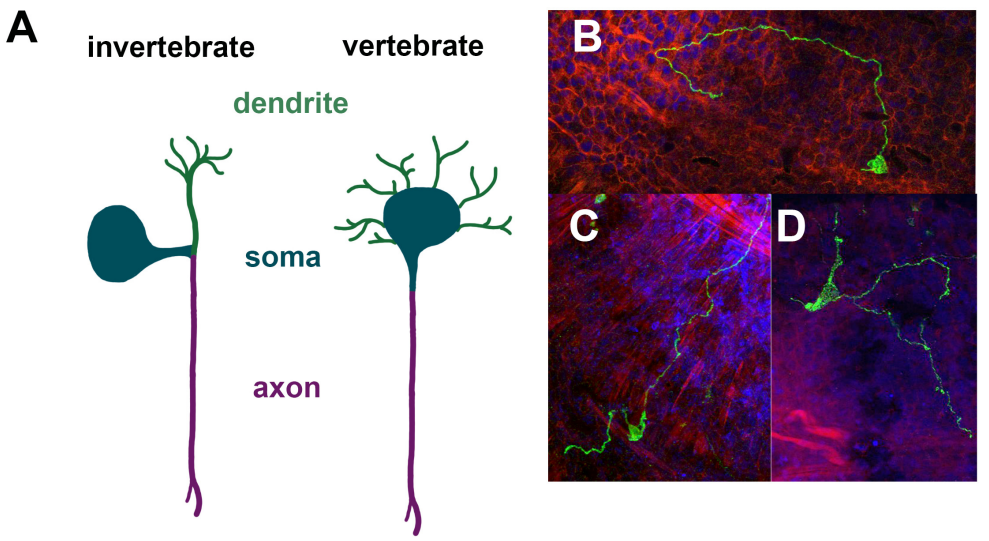

FIGURE 2 | Morphological properties of cnidarian neurons. Prototype invertebrate neuron with a unique primary neurite compared to the prototype vertebrate neuron with a single axon and multiple dendritic arbors **(A)**. Unipolar, bipolar and tripolar neurons in *Nematostella* expressing Elav-mOrange in mosaic animals **(B–D)**.

there is little information about the precise make up and wiring of neurons in cnidarian nerve nets. Moreover, how general this notion is in *Hydra*, *Nematostella* and *Clytia* or which types of neurons show non-polar synapses remains unknown.

In the past morphological features have been used to assign a certain type to some neurons (**Figure 2**). In *Nematostella*, typically the location of a neuron was noted and if it is associated with a specific organ as well as the number of neurite extensions. For instance, neurons expressing the neuropeptide Lwamide have been characterized using a Lwamide-mCherry reporter line (Havrilak et al., 2017). There are five morphologically distinct neuron types: longitudinal neurons, tripolar neurons, mesentery neurons, pharyngeal neurons and tentacular neurons. Different branching patterns have also been defined as type 1 ganglion cells for bipolar neurons, type 2 ganglion cell for tripolar neurons and type 3 ganglion cells for quadripolar neurons (Marlow et al., 2009). However, it is worth noting that the branching pattern is currently defined by the branching from the soma and possible branching of longer axons have not been further assigned.

PERSPECTIVE

Cnidaria are a diverse group of animals, which have adapted to various different aquatic environments including the deep sea, polar regions, tropical, and temperate seas as well as freshwater ecosystems. They can be colonial or solitary and propagate sexually or asexually. From a neurobiological perspective we know surprisingly little about this animal clade, even though they are placed at a particularly relevant phylogenetic position as sister group to bilaterians. Much of our general knowledge about nervous systems stems from vertebrates and a few invertebrate clades. The comparison between canonical models, such as mouse, zebrafish, *Drosophila,* and *C. elegans* highlight commonalities and differences between nervous systems. However, despite the use of different bilaterian models, much about the fundamental features and origin of nervous systems remains unknown. Cnidaria are here in the unique position to provide answers. The advent of high-throughput sequencing and emergence of genomes of different Cnidaria species has already provided critical information of the genomic make-up of the nervous system on a molecular level. Adding single-cell transcriptomic data has provided a much-needed additional degree of resolution, thus allowing us to peek into the diversity of neuron types and providing ample opportunity for hypothesis driven research. In particular the possibility for transgenesis and genome editing in several species further opens up avenues for detailed genetic and mechanistic studies. Many of our general assumption on neurons function get corroborated, but there are also many areas that bring surprises. Until today most molecular and genetic studies focus on neurogenesis and nervous system development. The tools to assess gene function of behavior and to move toward neurogenetics are there in several species. While I here focus on *Hydra*, *Nematostella* and *Cyltia* it is worth mentioning that transgenesis and Crispr genome editing has also been achieved in *Hydractinia* (Kunzel et al., 2010; Gahan et al., 2017; Sanders et al., 2018; Chrysostomou et al., 2022). It is fair to assume that in the coming years studies, such as the ones discussed here on *Hydra*, *Nematostella*, *Cyltia, Hydractinia, Aurelia,* and possibly other species will provide important insights into the function of nervous systems in Cnidaria, but also much broader into nervous system evolution.

AUTHOR CONTRIBUTIONS

The author confirms being the sole contributor of this work and has approved it for publication.

FUNDING

This work was supported by the Swiss National Science Foundation grant IZCOZ0_182957.

REFERENCES

Albert, D. J. (2011). What's on the mind of a jellyfish?. *Neurosci. Biobehav. Rev.* 35, 474–482.

Bosch, T. C. G., Klimovich, A., Domazet-Loso, T., Grunder, S., Holstein, T. W., Jékely, G., et al. (2017). Back to the Basics: cnidarians Start to Fire. *Trends Neurosci.* 40, 92–105. doi: 10.1016/j.tins.2016.11.005

Burkhardt, P., and Sprecher, S. G. (2017). Evolutionary origin of synapses and neurons - Bridging the gap. *Bioessays* 39, 1–10.

Cao, J., Spielmann, M., Qiu, X., Huang, X., and Ibrahim, D. M. (2019). The single-cell transcriptional landscape of mammalian organogenesis. *Nature* 566, 496–502. doi: 10.1038/s41586-019-0969-x

Chari, T., Weissbourd, B., Gehring, J., Ferraioli, A., Leclere, L., Herl, M., et al. (2021). Whole-animal multiplexed single-cell RNA-seq reveals transcriptional shifts across Clytia medusa cell types. *Sci. Adv.* 7:eabh1683. doi: 10.1126/sciadv.abh1683

Chrysostomou, E., Febrimarsa, DuBuc, T., and Frank, U. (2022). Gene Manipulation in Hydractinia. *Methods Mol. Biol.* 2450, 419–436. doi: 10.1007/978-1-0716-2172-1_22

Dupre, C., and Yuste, R. (2017). Non-overlapping Neural Networks in Hydra vulgaris. *Curr. Biol.* 27, 1085–1097. doi: 10.1016/j.cub.2017.02.049

Feuda, R., Dohrmann, M., Pett, W., Philippe, H., Rota-Stabelli, O., Lartillot, N., et al. (2017). Improved Modeling of Compositional Heterogeneity Supports Sponges as Sister to All Other Animals. *Curr. Biol.* 27, 3864–3870.e4. doi: 10.1016/j.cub.2017.11.008

Flici, H., Schnitzler, C. E., Millane, R. C., Govinden, G., Houlihan, A., and Boomkamp, S. D. (2017). An Evolutionarily Conserved SoxB-Hdac2 Crosstalk Regulates Neurogenesis in a Cnidarian. *Cell Rep.* 18, 1395–1409. doi: 10.1016/j.celrep.2017.01.019

Frank, U., Nicotra, M. L., and Schnitzler, C. E. (2020). The colonial cnidarian Hydractinia. *Evodevo* 11:7.

Gahan, J. M., Schnitzler, C. E., DuBuc, T. Q., Doonan, L. B., Kanska, J., Gornik, S. G., et al. (2017). Functional studies on the role of Notch signaling in Hydractinia development. *Dev. Biol.* 428, 224–231. doi: 10.1016/j.ydbio.2017.06.006

Galliot, B. (2012). Hydra, a fruitful model system for 270 years. *Int. J. Dev. Biol.* 56, 411–423. doi: 10.1387/ijdb.120086bg

Garm, A., Bielecki, J., Petie, R., and Nilsson, D. E. (2012). Opposite patterns of diurnal activity in the box jellyfish Tripedalia cystophora and Copula sivickisi. *Biol. Bull* 222, 35–45. doi: 10.1086/BBLv222n1p35

Han, S., Taralova, E., Dupre, C., and Yuste, R. (2018). Comprehensive machine learning analysis of Hydra behavior reveals a stable basal behavioral repertoire. *Elife* 7:e32605. doi: 10.7554/eLife.32605

Havrilak, J. A., Faltine-Gonzalez, D., Wen, Y., Fodera, D., Simpson, A. C., Magie, C. R., et al. (2017). Characterization of NvLWamide-like neurons reveals stereotypy in Nematostella nerve net development. *Dev. Biol.* 431, 336–346. doi: 10.1016/j.ydbio.2017.08.028

Helm, R. R. (2018). Evolution and development of scyphozoan jellyfish. *Biol. Rev. Camb. Philos. Soc.* 93, 1228–1250. doi: 10.1111/brv.12393

Hombria, J. C., Garcia-Ferres, M., and Sanchez-Higueras, C. (2021). Anterior Hox Genes and the Process of Cephalization. *Front. Cell Dev. Biol.* 9:718175. doi: 10.3389/fcell.2021.718175

Houliston, E., Leclere, L., Munro, C., Copley, R. R., and Momose, T. (2022). Past, present and future of Clytia hemisphaerica as a laboratory jellyfish. *Curr. Top. Dev. Biol.* 147, 121–151.

Houliston, E., Momose, T., and Manuel, M. (2010). Clytia hemisphaerica: a jellyfish cousin joins the laboratory. *Trends Genet.* 26, 159–167. doi: 10.1016/j.tig.2010.01.008

Kanska, J., and Frank, U. (2013). New roles for Nanos in neural cell fate determination revealed by studies in a cnidarian. *J. Cell Sci.* 126, 3192–3203. doi: 10.1242/jcs.127233

Kelava, I., Rentzsch, F., and Technau, U. (2015). Evolution of eumetazoan nervous systems: insights from cnidarians. *Philos. Trans. R. Soc. Lond B. Biol. Sci.* 370:20150065. doi: 10.1098/rstb.2015.0065

Kunzel, T., Heiermann, R., Frank, U., Muller, W., Tilmann, W., Tilmann, w, et al. (2010). Migration and differentiation potential of stem cells in the cnidarian Hydractinia analysed in eGFP-transgenic animals and chimeras. *Dev. Biol.* 348, 120–129. doi: 10.1016/j.ydbio.2010.08.017

La Manno, , G., Soldatov, R., Zeisel, A., Braun, E., Hochgerner , H., Lönnerberg, P. et al (2018). RNA velocity of single cells. *Nature* 560, 494–498.

Layden, M. J., Boekhout, M., and Martindale, M. Q. (2012). Nematostella vectensis achaete-scute homolog NvashA regulates embryonic ectodermal neurogenesis and represents an ancient component of the metazoan neural specification pathway. *Development* 139, 1013–1022. doi: 10.1242/dev.073221

Layden, M. J., Rentzsch, F., and Rottinger, E. (2016). The rise of the starlet sea anemone Nematostella vectensis as a model system to investigate development and regeneration. *Wiley Interdisc. Rev. Dev. Biol.* 5, 408–428. doi: 10.1002/wdev.222

Leclere, L., Jager, M., Barreau, C., Chang, P., Le Guyader, H., Manuel, M,et al. (2012). Maternally localized germ plasm mRNAs and germ cell/stem cell formation in the cnidarian Clytia. *Dev. Biol.* 364, 236–248. doi: 10.1016/j.ydbio.2012.01.018

Lenhoff, H. M. (1968). Behavior, hormones, and Hydra. *Science* 161, 434–442. doi: 10.1126/science.161.3840.434

Levy, S., Brekhman, V., Bakhman, A., Malik, A., Sebe-Pedros, A., Kosloff, Met al. (2021). Ectopic activation of GABAB receptors inhibits neurogenesis and metamorphosis in the cnidarian Nematostella vectensis. *Nat. Ecol. Evol.* 5, 111–121. doi: 10.1038/s41559-020-01338-3

Marlow, H. Q., Srivastava, M., Matus, D. Q., Rokhsar, D., and Martindale, M. Q. (2009). Anatomy and development of the nervous system of Nematostella vectensis, an anthozoan cnidarian. *Dev. Neurobiol.* 69, 235–254. doi: 10.1002/dneu.20698

Matveev, I. V., Adonin, L. S., Shaposhnikova, T. G., and Podgornaya, O. I. (2012). Aurelia aurita-Cnidarian with a prominent medusiod stage. *J. Exp. Zool. B. Mol. Dev. Evol.* 318, 1–12. doi: 10.1002/jez.b.21440

Moroz, L. L. (2015). Convergent evolution of neural systems in ctenophores. *J. Exp. Biol.* 218, 598–611. doi: 10.1242/jeb.110692

Moroz, L. L., Kocot, K. M., Citarella, M. R., Dosung, S., Norekian, T. P.,Povolotskaya, IS et al. (2014). The ctenophore genome and the evolutionary origins of neural systems. *Nature* 510, 109–114. doi: 10.1038/nature13400

Nakanishi, N., Renfer, E., Technau, U., and Rentzsch, F. (2012). Nervous systems of the sea anemone Nematostella vectensis are generated by ectoderm and endoderm and shaped by distinct mechanisms. *Development* 139, 347–357. doi: 10.1242/dev.071902

Nicotra, M. L. (2022). The Hydractinia allorecognition system. *Immunogenetics* 74, 27–34. doi: 10.1007/s00251-021-01233-6

Nielsen, S. K. D., Koch, T. L., Wiisbye, S. H., Grimmelikhuijzen, C. J. P., and Garm, A. (2021). Neuropeptide expression in the box jellyfish Tripedalia cystophora-New insights into the complexity of a "simple" nervous system. *J. Comp. Neurol.* 529, 2865–2882. doi: 10.1002/cne.25133

Nilsson, D. E., Gislen, L., Coates, M. M., Skogh, C., and Garm, A. (2005). Advanced optics in a jellyfish eye. *Nature* 435, 201–205. doi: 10.1038/nature03484

Noro, Y., Yum, S., Nishimiya-Fujisawa, C., Busse, C., Shimizu, H.,Mineta, K et al. (2019). Regionalized nervous system in Hydra and the mechanism of its development. *Gene. Expr. Patterns* 31, 42–59. doi: 10.1016/j.gep.2019.01.003

Oren, M., Brickner, I., Appelbaum, L., and Levy, O. (2014). Fast neurotransmission related genes are expressed in non nervous endoderm in the sea anemone Nematostella vectensis. *PLoS One* 9:e93832. doi: 10.1371/journal.pone.0093832

Passano, L. M., and McCullough, C. B. (1962). The Light Response and the Rhythmic Potentials of Hydra. *Proc. Natl. Acad. Sci. U. S. A.* 48, 1376–1382. doi: 10.1073/pnas.48.8.1376

Petie, R., Garm, A., and Nilsson, D. E. (2011). Visual control of steering in the box jellyfish Tripedalia cystophora. *J. Exp. Biol.* 214, 2809–2815. doi: 10.1242/jeb.057190

Plickert, G., Frank, U., and Muller, W. A. (2012). Hydractinia, a pioneering model for stem cell biology and reprogramming somatic cells to pluripotency. *Int. J. Dev. Biol.* 56, 519–534. doi: 10.1387/ijdb.123502gp

Rentzsch, F., Juliano, C., and Galliot, B. (2019). Modern genomic tools reveal the structural and cellular diversity of cnidarian nervous systems. *Curr. Opin. Neurobiol.* 56, 87–96. doi: 10.1016/j.conb.2018.12.004

Rentzsch, F., Layden, M., and Manuel, M. (2017). The cellular and molecular basis of cnidarian neurogenesis. *Wiley Interdisc. Rev. Dev. Biol.* 6:e257. doi: 10.1002/wdev.257

Rentzsch, F., and Technau, U. (2016). Genomics and development of Nematostella vectensis and other anthozoans. *Curr. Opin. Genet. Dev.* 39, 63–70. doi: 10.1016/j.gde.2016.05.024

Richards, G. S., and Rentzsch, F. (2015). Regulation of Nematostella neural progenitors by SoxB. Notch and bHLH genes. *Development* 142, 3332–3342. doi: 10.1242/dev.123745

Rosengarten, R. D., and Nicotra, M. L. (2011). Model systems of invertebrate allorecognition. *Curr. Biol.* 21, R82–R92. doi: 10.1016/j.cub.2010.11.061

Rottinger, E. (2021). Nematostella vectensis, an Emerging Model for Deciphering the Molecular and Cellular Mechanisms Underlying Whole-Body Regeneration. *Cells* 10:2692. doi: 10.3390/cells10102692

Sachkova, M. Y., Nordmann, E. L., Soto-Angel, J. J., Meeda, Y., Gorski, B., Naumann, B et al. (2021). Neuropeptide repertoire and 3D anatomy of the ctenophore nervous system. *Curr. Biol.* 31, 5274–5285.e6. doi: 10.1016/j.cub.2021.09.005

Saina, M., Genikhovich, G., Renfer, E., and Technau, U. (2009). BMPs and chordin regulate patterning of the directive axis in a sea anemone. *Proc. Natl. Acad. Sci. U. S. A.* 106, 18592–18597. doi: 10.1073/pnas.0900151106

Sanders, S. M., Ma, Z., Hughes, J. M., Riscoe, B. M., Gibson, G. A.,Watson, A. M et al. (2018). CRISPR/Cas9-mediated gene knockin in the hydroid Hydractinia symbiolongicarpus. *BMC Genomics* 19:649. doi: 10.1186/s12864-018-5032-z

Sarnat, H. B., and Netsky, M. G. (2002). When does a ganglion become a brain?. *Semin. Pediatr. Neurol.* 9, 240–253. doi: 10.1053/spen.2002.32502

Sebe-Pedros, A., Saudemont, B., Chomsky, E., Plessier, F., Mailhe, M. P., Renno, J et al. (2018). Cnidarian Cell Type Diversity and Regulation Revealed by Whole-Organism Single-Cell RNA-Seq. *Cell* 173, 1520–1534. doi: 10.1016/j.cell.2018.05.019

Siebert, S., Farrell, J. A., Cazet, J. F., Abeykoon, Y., Primack, A. S., Schnitzler, C. E et al. (2019). Stem cell differentiation trajectories in Hydra resolved at single-cell resolution. *Science* 365:eaav9314. doi: 10.1126/science.aav9314

Simion, P., Philippe, H., Baurain, D., Jager, M., Richter, D. J., Di Franco, A. et al. (2017). A Large and Consistent Phylogenomic Dataset Supports Sponges as the Sister Group to All Other Animals. *Curr. Biol.* 27, 958–967. doi: 10.1016/j.cub.2017.02.031

Smarandache-Wellmann, C. R. (2016). Arthropod neurons and nervous system. *Curr. Biol.* 26, R960–R965.

Street, K., Risso, D., Fletcher, R. B., Das, D., Ngai, J., Yosef, N et al. (2018). Slingshot: cell lineage and pseudotime inference for single-cell transcriptomics. *BMC Genomics* 19:477. doi: 10.1186/s12864-018-4772-0

Sunagar, K., Columbus-Shenkar, Y. Y., Fridrich, A., Gutkovich, N., Aharoni, R.,Yehu, M et al. (2018). Cell type-specific expression profiling unravels the development and evolution of stinging cells in sea anemone. *BMC Biol.* 16:108. doi: 10.1186/s12915-018-0578-4

Technau, U., and Steele, R. E. (2011). Evolutionary crossroads in developmental biology: cnidaria. *Development* 138, 1447–1458. doi: 10.1242/dev.048959

Tucker, R. P., Shibata, B., and Blankenship, T. N. (2011). Ultrastructure of the mesoglea of the sea anemone Nematostella vectensis (Edwardsiidae). *Invertebr. Biol.* 130, 11–24.

Turner, E. C. (2021). Possible poriferan body fossils in early Neoproterozoic microbial reefs. *Nature* 596, 87–91. doi: 10.1038/s41586-021-03773-z

Vogg, M. C., Buzgariu, W., Suknovic, N. S., and Galliot, B. (2021). Cellular, Metabolic, and Developmental Dimensions of Whole-Body Regeneration in Hydra. *Cold Spring Harb. Perspect. Biol.* 13, 1–15.

Weissbourd, B., Momose, T., Nair, A., Kennedy, A., Hunt, B., Anderson, D, J et al. (2021). A genetically tractable jellyfish model for systems and evolutionary neuroscience. *Cell* 184, 5854–5868.e20. doi: 10.1016/j.cell.2021.10.021

Whelan, N. V., Kocot, K. M., Moroz, L. L., and Halanych, K. M. (2015). Error, signal, and the placement of Ctenophora sister to all other animals. *Proc. Natl. Acad. Sci. U. S. A.* 112, 5773–5778. doi: 10.1073/pnas.1503453112

Whelan, N. V., Kocot, K. M., Moroz, T. P., Mukherjee, K., Williams, P.,Paulay, G et al. (2017). Ctenophore relationships and their placement as the sister group to all other animals. *Nat. Ecol. Evol.* 1, 1737–1746.

Conflict of Interest: The author declares that the research was conducted in the absence of any commercial or financial relationships that could be construed as a potential conflict of interest.

Publisher's Note: All claims expressed in this article are solely those of the authors and do not necessarily represent those of their affiliated organizations, or those of the publisher, the editors and the reviewers. Any product that may be evaluated in this article, or claim that may be made by its manufacturer, is not guaranteed or endorsed by the publisher.

frontiers | Frontiers in Neuroscience

ORIGINAL RESEARCH
published: 20 June 2022
doi: 10.3389/fnins.2022.903881

Foxa2 and Pet1 Direct and Indirect Synergy Drive Serotonergic Neuronal Differentiation

Begüm Aydin[1†], Michael Sierk[2], Mireia Moreno-Estelles[1,3], Link Tejavibulya[1†], Nikathan Kumar[1†], Nuria Flames[3], Shaun Mahony[4*] and Esteban O. Mazzoni[1*]*

[1] Department of Biology, New York University, New York City, NY, United States, [2] Interdisciplinary Sciences Department, Saint Vincent College, Latrobe, PA, United States, [3] Developmental Neurobiology Unit, Instituto de Biomedicina de Valencia IIBV-CSIC, Valencia, Spain, [4] Center for Eukaryotic Gene Regulation, Department of Biochemistry and Molecular Biology, The Pennsylvania State University, University Park, PA, United States

Neuronal programming by forced expression of transcription factors (TFs) holds promise for clinical applications of regenerative medicine. However, the mechanisms by which TFs coordinate their activities on the genome and control distinct neuronal fates remain obscure. Using direct neuronal programming of embryonic stem cells, we dissected the contribution of a series of TFs to specific neuronal regulatory programs. We deconstructed the Ascl1-Lmx1b-Foxa2-Pet1 TF combination that has been shown to generate serotonergic neurons and found that stepwise addition of TFs to Ascl1 canalizes the neuronal fate into a diffuse monoaminergic fate. The addition of pioneer factor Foxa2 represses Phox2b to induce serotonergic fate, similar to *in vivo* regulatory networks. Foxa2 and Pet1 appear to act synergistically to upregulate serotonergic fate. Foxa2 and Pet1 co-bind to a small fraction of genomic regions but mostly bind to different regulatory sites. In contrast to the combinatorial binding activities of other programming TFs, Pet1 does not strictly follow the Foxa2 pioneer. These findings highlight the challenges in formulating generalizable rules for describing the behavior of TF combinations that program distinct neuronal subtypes.

Keywords: neuronal differentiation, direct programming methods, Pet1, Foxa2, stem cell differentiation, transcription factor

OPEN ACCESS

Edited by:
Nikolaos Konstantinides, UMR 7592 Institut Jacques Monod, France

Reviewed by:
Evan Deneris, Case Western Reserve University, United States
Elisabetta Furlanis, Harvard Medical School, United States

***Correspondence:**
Nuria Flames
nflames@ibv.csic.es
Shaun Mahony
sam77@psu.edu
Esteban O. Mazzoni
eom204@nyu.edu

[†]***Present addresses:***
Begüm Aydin, Laboratory of Mucosal Immunology, The Rockefeller University, New York City, NY, United States
Link Tejavibulya, Interdepartmental Neuroscience Program, Yale School of Medicine, New Haven, CT, United States
Nikathan Kumar, Department of Surgery, UCSF East Bay, Oakland, CA, United States

Specialty section:
This article was submitted to Neurogenesis, a section of the journal Frontiers in Neuroscience

Received: *24 March 2022*
Accepted: *24 May 2022*
Published: *20 June 2022*

Citation:
Aydin B, Sierk M, Moreno-Estelles M, Tejavibulya L, Kumar N, Flames N, Mahony S and Mazzoni EO (2022) Foxa2 and Pet1 Direct and Indirect Synergy Drive Serotonergic Neuronal Differentiation. Front. Neurosci. 16:903881. doi: 10.3389/fnins.2022.903881

INTRODUCTION

The complex functions of the nervous system require an exquisite repertoire of specialized neuron types primarily defined by their transcriptome. Effector genes contributing to neuronal terminal features are the components of the transcriptome that define the functionality of the neuron, from functions common to all neurons (cell polarity, excitability, etc.) to those specific for neuronal types (neurotransmitter receptors, transporters, biosynthetic enzymes, etc.). With the growing collection of induced pluripotent and embryonic stem cells carrying neurodegenerative genotypes – for example the iPSC Neurodegeneration Initiative (iNDI) project – there is a need to establish rules that govern transcription factor-induced neuronal programming to differentiate them into diverse neuronal types with high accuracy and efficiency (Wapinski et al., 2013).

Transcription factors (TFs) are the main players controlling transcriptional activity during cell-type specification. In recent years, reprogramming, direct programming, and transdifferentiation

experiments have taken advantage of this principle to impose cell type-specific gene regulatory programs (Morris, 2016; Aydin and Mazzoni, 2019). TF-induced direct programming into neurons has gained popularity due to its efficiency and scalability. Direct neural programming can be rationalized as a two-module process, consisting of inducing a "generic" neuronal fate (axonal growth, synaptic machinery, etc.) and specifying neuronal type-specific gene expression controlling features such as neurotransmitter biosynthesis. The expression of the pro-neuronal TFs Ascl1 and Neurog2 induce neuronal fate from pluripotent stem cells (Busskamp et al., 2014; Aydin et al., 2019). Although Ascl1 and Neurog2 induce their own neuronal subtype bias, combining the pro-neuronal TF with other neuronal fate-specific TF combinations refines the transcriptome and accelerates terminal neuron-type specific fate conversion (Aydin et al., 2019; Lin et al., 2021). For example, pairing Neurog2 with Isl1 and Lhx3 drives spinal motor neuron fate from pluripotent stem cells (Hester et al., 2011; Mazzoni et al., 2013). On the other hand, combining Ascl1 with Lmx1a and Nurr1 induces midbrain dopaminergic fate (Caiazzo et al., 2011).

Because it provides a well-controlled cellular environment amenable for precise time series and experimental perturbations, direct programming has become a favored strategy to investigate how TFs control cell fate. The proneural Ascl1 or Neurog2 behave as pioneer TFs (Castro et al., 2006; Wapinski et al., 2013; Soufi et al., 2015; Smith et al., 2016; Aydin et al., 2019). Thus, they can access sites on the genome even when they are occluded by nucleosomes and are therefore able to induce neuronal fate from both pluripotent and terminally differentiated cells (Farah et al., 2000; Parras et al., 2002; Castro et al., 2006). The binding of other neuronally expressed TFs can be affected by the accessibility landscape established by Ascl1 or Neurog2. For example, the broadly expressed Ebf2 and Brn2 bias their binding targets toward regions made accessible by pro-neuronal TFs (Castro et al., 2006; Wapinski et al., 2013; Aydin et al., 2019). However, neuron type-selecting TFs do not always bind to regions bound by proneural TFs. The Isl1 and Lhx3 TF pair dimerize during motor neuron direct programming and do not follow the Neurog2-established TF accessibility (Velasco et al., 2017). In turn, in a feed-forward transcriptional logic, Isl1-Lhx3 binding changes as differentiation progresses following the changing accessibility created by the Onecut TFs (which also have pioneer activity) induced by Neurog2 (Rhee et al., 2016; Velasco et al., 2017; van der Raadt et al., 2019). Expression of non-pioneer TFs can also modify the binding landscape of a given TF and its direct targets. For example, swapping Lhx3 with Phox2a allows Isl1 to target a new set of regulatory elements and program a different motor neuron type (Mazzoni et al., 2013). Thus, Isl1-Lhx3 and Isl1-Phox2a target enhancers to induce neuronal type-specific gene expression in two related neuronal types. These examples show the wide range of strategies used to implement specific neuron fates and the importance of both direct and indirect interactions between TFs. Thus, much work remains to be done to elucidate which rules apply to various TF combinations, including possible conflicts when coexpressing multiple pioneer TFs.

Monoamine neurotransmitters contain one amino group connected to an aromatic ring by a two-carbon chain. In vertebrates, they include mainly catecholamines (dopamine, noradrenaline, adrenaline) and serotonin. Each monoaminergic neuron type is classified by coordinated expression of a set of genes that control the synthesis and transport of specific monoamines, and some of these genes are shared among all monoaminergic neurons (Flames and Hobert, 2011). However, how these sets of genes are regulated during monoaminergic neuron differentiation is unclear. Ascl1 is prominently expressed in the monoaminergic central and peripheral neural progenitors, and it is both necessary and sufficient to promote neurogenesis (Pattyn et al., 2004; Vasconcelos and Castro, 2014). Another pioneer TF, the Forkhead family TF Foxa2 is expressed in midbrain dopaminergic neurons and ventral hindbrain serotonergic progenitor domains (Vasconcelos and Castro, 2014). Reciprocal repression between homeodomain protein Phox2b and Foxa2 mediates the progenitor switches from visceral motor neuron fate into serotonergic fate (Pattyn et al., 2000). In this region, prolonged Foxa2 expression in progenitors is required for the activation of serotonergic TFs such as Gata2, Lmx1b, and Pet1 (also known as Fev) (Jacob et al., 2007). The LIM homeodomain TF Lmx1b is expressed along the ventral midbrain and hindbrain, and it is also important for the development of both dopaminergic and serotonergic neurons. In Lmx1b homozygous mutants, serotonergic neuron precursors fail to activate the expression of Tph2/tryptophan hydroxylase, Sert/serotonin reuptaker, and Vmat2/vesicular monoamine transporter and fail in the synthesis of serotonin (5-HT) even though the number of serotonergic precursors does not change (Ding et al., 2003). Moreover, Lmx1b is also required for correct midbrain dopaminergic neuron specification (Smidt et al., 2000; Lin et al., 2009; Yan et al., 2011). Finally, Pet1 is an ETS transcription factor expressed in central nervous system postmitotic serotonergic neurons and is required for normal serotonergic neuron differentiation, function, and fate maintenance (Hendricks et al., 2003; Maurer et al., 2004). Thus Ascl1, Foxa2, and Lmx1b are required for both dopaminergic and serotonergic specification, while Pet1 is exclusively involved in serotonergic induction. *In vivo,* this set of TFs acts at different stages in the differentiation process. Ascl1 and Foxa2 are pioneer factors acting mainly in progenitors, while Lmx1b and Pet1 act in postmitotic cells to directly induce neuron-type specific features (Hendricks et al., 1999; Cheng et al., 2003; Pattyn et al., 2004; Jacob et al., 2007). In addition, expression of both Lmx1b and Pet1 is sustained throughout the life of the animal and is required to maintain neuron fate (Liu et al., 2010; Donovan et al., 2019). Considering their postmitotic, direct and terminal actions, Lmx1b and Pet1 can be classified as terminal selectors for serotonergic fate.

We deconstructed a monoaminergic TF combination to interrogate how adding TFs shapes their activity and neuronal programming. The Ascl1 + Lmx1b + Foxa2 + Pet1 (ALFP) TF combination transdifferentiates human fibroblasts toward serotonergic neuron fate (Xu et al., 2016). This study focuses on a simple system programming neuronal fate from mouse pluripotent stem cells by increasing the TF number from induced

(i) Ascl1 only (iA) to iALFP. As expected, all combinations generated neurons efficiently due to the inclusion of the proneural Ascl1. Based on typical dopaminergic and serotonergic marker immunocytochemistry, iALFP induces serotoninergic fate at higher percentages than do differentiating cells expressing iA, iAL, iALP, or iALF. The fact that iALFP expression differs from a simple superposition of iALF and iALP suggests Pet1 and Foxa2 act synergistically. Thus, we investigated how the induction of different TF combinations affects neuronal gene expression, TF binding, and chromatin accessibility. We find that each TF combination shows a specific gene expression profile. iALFP is the most different from naive embryoid bodies (EB) and the best inducer of serotonergic effector gene expression. As expected for a pioneer TF, Foxa2 does not change its binding location when expressed with Pet1. On the other hand, Pet1 binds to different sites in the presence of Foxa2. Although the few Foxa2-Pet1 co-bound sites seem to be biologically relevant, Foxa2 and Pet1 bind mostly independently to different genomic locations.

RESULTS

Foxa2 and Pet1 Act in Concert With Ascl1 and Lmx1b to Induce Serotonergic Identity

To study how TF combinations induce neuronal and serotoninergic differentiation, we constructed a series of mouse isogenic inducible embryonic stem cell lines (iESCs), inserting each TF combination at the HPRT locus (Iacovino et al., 2011; Mazzoni et al., 2011). Self-cleaving 2A peptides between coding sequences allowed for simultaneous and equimolar induction of TFs in each inducible cell line (Mazzoni et al., 2013). In total we built the following inducible lines: Ascl1 (iA), Ascl1 + Lmx1b (iAL), Ascl1 + Lmx1b + Foxa2 (iALF), Ascl1 + Lmx1b + Pet1 (iALP), and Ascl1 + Lmx1b + Foxa2 + Pet1 (iALFP) (**Figure 1A**). The last TF in each combination was tagged with V5. iESCs were detached and allowed to form EB and 2 days later, TFs were induced by adding 3ug/ml of Doxycycline (Dox) to initiate differentiation (**Figure 1B**). All cell lines induced TF expression at high percentages after 2 days of Dox and efficient cleavage of the multicistronic constructs (**Figure 1C**, **Supplementary Figure 1A**, and **Supplementary Table 1**). As evidenced by efficient neuronal differentiation (TUJ1, **Figure 1C** and **Supplementary Table 1**), adding multiple TFs in a polycistronic construct did not inhibit Ascl1 pro-neuronal activity. We note that as the inducible construct became larger and more complex, there was a slight decrease in TF induction (**Figure 1C** and **Supplementary Table 1**). However, all combinations were very effective at inducing neuronal fate, with more than 95% of the cells expressing the construct becoming neurons in all lines (**Supplementary Table 1**).

Two days after Dox treatment, we dissociated the EBs into single-cell suspension and plated them as a monolayer to measure neuronal conversion and induction of monoaminergic fate (**Figure 1B**). TUJ1 staining revealed once more that each iESC line differentiates to a neuronal fate efficiently and maintains neuronal fate after 7 days in culture (**Figure 1D** and **Supplementary Table 1**). We then stained these neurons with antibodies against serotonin (5HT), Tryptophan hydroxylase (TPH), and tyrosine hydroxylase (TH) to quantify serotonergic (5HT and TPH) and catecholaminergic fate (TH is expressed in dopaminergic, adrenergic and noradrenergic neurons) (**Figure 1D** and **Supplementary Table 1**). None of the TF combinations induced TH in a sizable fraction of the cells. However, there was an increase in markers for serotoninergic fate as the TF combination became more complex, from iA to iALFP (**Figure 1D** and **Supplementary Table 1**). Neither Ascl1 alone (iA), nor in combination with Lmx1b (iAL), induced 5HT or TPH. The addition of Pet1 or Foxa2 to iAL (iALP and iALF, respectively) was sufficient to induce serotonergic staining and TPH expression (**Figure 1D** and **Supplementary Table 1**). Interestingly, the full TF set (iALFP) induced serotoninergic markers at higher levels than the simple addition of iALP + iALF effects (**Figure 1E** and **Supplementary Table 1**). Thus, we conclude that iALFP induces neurons expressing serotonergic fate when differentiating ESCs. Moreover, Pet1 and Foxa2 are required and seem to act synergistically to induce this specific neuron-type fate.

Foxa2 and Pet1 Make Both Independent and Synergistic Contributions to Gene Expression

To characterize the contributions that Foxa2 and Pet1 make to the serotonergic expression program, we performed bulk RNA-seq experiments in EBs and in each of the five cell lines after inducing expression of the various TF combinations 2 and 9 days after Dox treatment to measure the initial transcriptional response and the terminal neuronal fate. **Figures 2A,B** show the numbers of up- and down-regulated genes ($\log_2$ fold change $\geq$ 1.0, adjusted p-value $<$ 0.05) for all pairwise comparisons at 48 h and 9 days post-induction, respectively.

As expected, all TF inductions produce substantial numbers of differentially expressed genes compared with EBs, with the full TF set (iALFP) inducing the largest transcriptional difference vs. EBs (**Figures 2A,B**). However, each TF combination generates unique patterns of gene expression. The iAL line displays relatively little change in expression compared with iA (834 genes upregulated, 452 down-regulated at 48 h), suggesting that Lmx1b does not substantially modulate the broad proneural expression program initiated by Ascl1. However, we noticed high levels of endogenous Lmx1b expression in the iA line (**Figure 2C**), which might partly explain their transcriptional similarities. The addition of Pet1 (iALP) causes modest increases in the number of genes differentially expressed at either day 2 (113 up, 57 down from iAL) or day 9 (144 up, 370 down from iAL) (**Figures 2A,B**). The expression impact of the exogenous Pet1 may also be reduced since the iAL line induced some levels of endogenous Pet1 (**Figure 2C**).

Endogenous Foxa2 expression levels are low in iA, iAL, and iALP. The addition of exogenous Foxa2 had a substantial impact on gene expression. The iALF line has a relatively large number

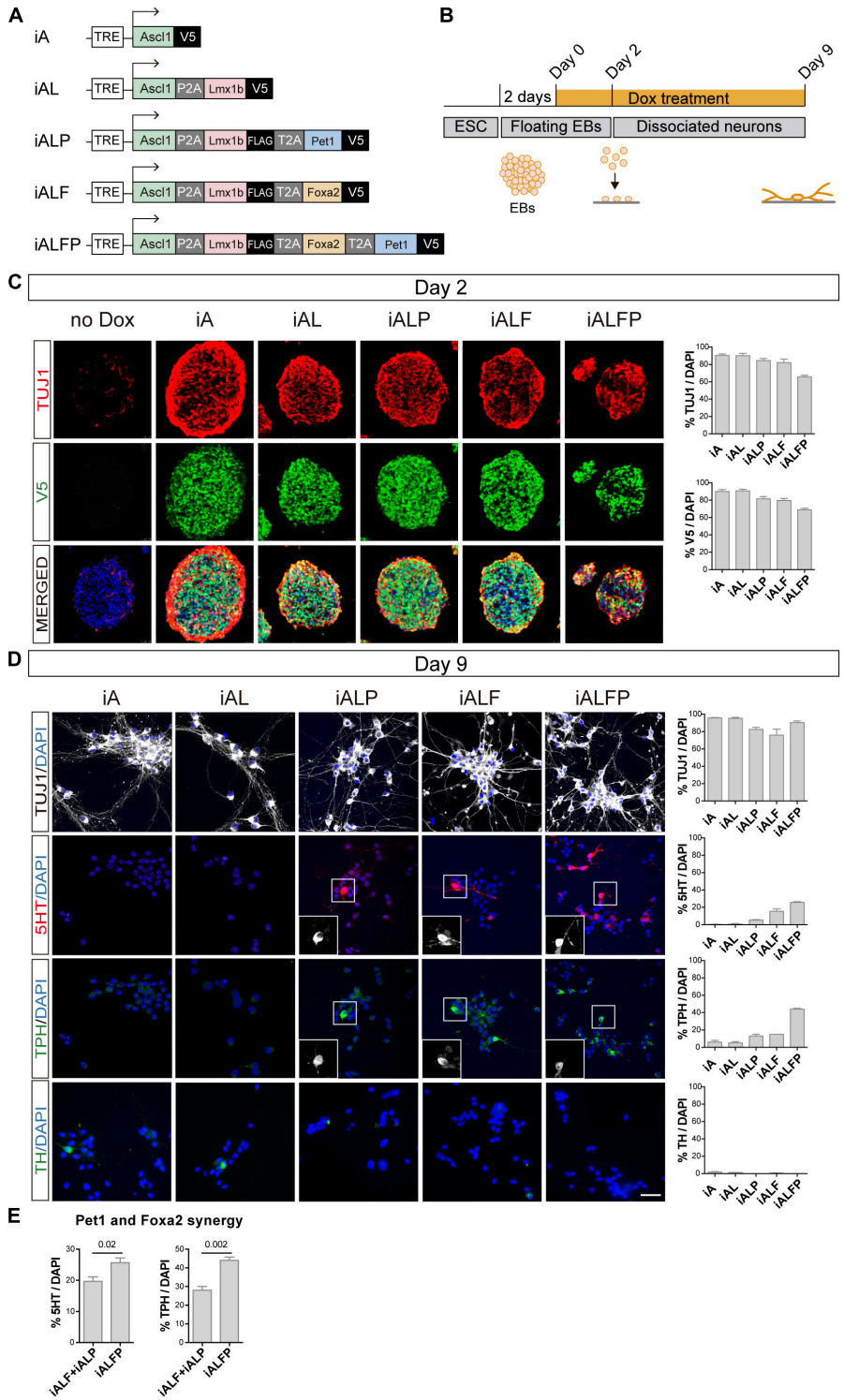

FIGURE 1 | Dissection of the combinatorial action of serotonergic TFs. **(A)** TF combinations induced in ESC. **(B)** TF induction, differentiation, and analysis outline. Doxycycline treatment is started 2 days after floating EB preparation. EBs are dissociated and plated 2 days later (Day 2) and cultured in the presence of doxycycline for 7 more days (Day 9 analysis). **(C)** Micrographs and quantification of TF induction (monitored by V5 expression) and neuronal fate (monitored by beta tubulin 3,TUJ1 staining) in EBs 2 days after doxycycline treatment. Broad iTF and neuronal differentiation induction in all cell lines. **(D)** Micrographs and quantification of neuronal (TUJ1), serotonergic (5HT and TPH) and catecholaminergic (TH) fate after 7 days of neuronal differentiation. Catecholaminergic expression is absent in all lines, while serotonergic markers are highest in iALFP. **(E)** Measurement of synergistic effects in iAFLP line. The addition of iALF + iALP serotonergic or TPH expression is significantly lower than values found in iALFP, suggesting synergistic effects between Pet1 and Foxa2. Scale bar: 50 μm.

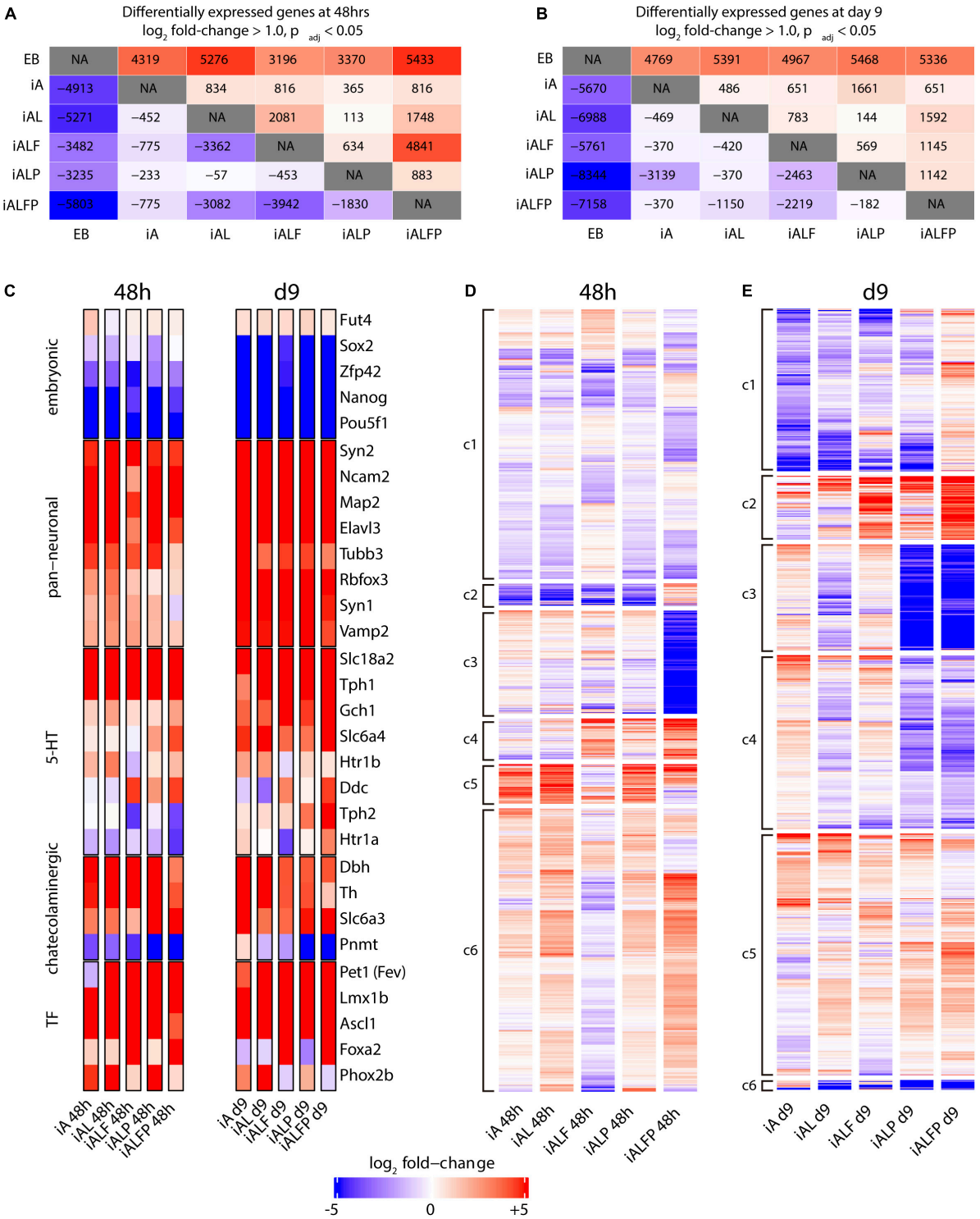

FIGURE 2 | Transcription profile of induced neurons at differentiation days 2 and 9. A, B. Counts of up- and downregulated genes under different exogenous transcription factor constructs at 48 h **(A)** and 9 days **(B)** post-induction. Conditions were compared in a pairwise fashion using DESeq2. The upper half of the diagonal is upregulated genes, the lower half is downregulated genes. **(C)** Heatmap of diagnostic gene expression at 48 h and 9 days post TF induction. Slc18a2 a.k.a. Vmat2; Slc6a4 a.k.a. Sert; Slc6a3 a.k.a. Dat. **(D,E)** Bulk RNA-seq heatmaps under different exogenous transcription factor constructs at 48 h **(D)** and 9 days **(E)** post-induction. At each timepoint, genes that were either upregulated or downregulated in all five conditions were removed, and genes that did not have a log fold change of at least 1.0 with an adjusted *p*-Value of 0.05 according to DESeq2 in at least one of the five transcription factor conditions were also removed, leaving 6393 genes at 48 h and 3970 genes at day 9. These remaining genes were clustered using K-means clustering using the R kmeans function. Transcripts were assigned to six clusters (c1 to c6) based on the expression pattern across all conditions.

of expression differences compared with iAL (2,081 up, 3,362 down at 2 days, **Figure 2A**). Surprisingly, while Pet1 does not significantly affect expression when expressed alongside Ascl1 and Lmx1b, it strongly modulates the gene expression program induced by iALF. The induction of all four TFs together (iALFP) produces an expression pattern that is different from iALF at both day 2 (4,841 up, 3,942 down) and day 9 of differentiation (1,145 up, 2,219 down) (**Figures 2A,B**). These results resonate with the hypothesis that Pet1 and Foxa2 act synergistically. We also noticed that although cell-line specific gene expression profiles are found both at day 2 and day 9 of differentiation (**Figures 2A,B**), differences are exacerbated at earlier time points suggesting convergence toward more similar neuron fates.

Next, we focused on the expression of diagnostic genes for pluripotency, pan-neuronal or monoaminergic cell fate. As expected, pluripotency genes were downregulated upon TF induction (**Figure 2C**). Concomitantly pan-neuronal gene expression was activated in all cell lines at 2 days and at higher levels and broadly at 9 days (**Figure 2C**). In addition, catecholaminergic effector gene expression [tyrosine hydroxylase (Th), dopamine transporter (Slc6a3) and dopamine beta hydroxylase (Dbh)] is observed in all cell lines at both differentiation times. At two days, core genes coding for 5HT biosynthesis was higher but incomplete in the iALFP line. However, this marker set increased in iALFP by 9 days of differentiation (**Figure 2C**). In mammals, the Tph1 and Tph2 genes code for the tryptophan hydroxylase, regulating the rate-limiting step for 5HT biosynthesis. *In vivo*, Tph2 but not Tph1 is expressed in hindbrain serotonergic neurons. We find high Tph1 expression in all cell lines at both differentiation time points, however, Tph2 expression is only induced by iALFP at 9 days of differentiation (**Figure 2C**). Thus, the serotonergic signature settles in iALFP as neurons mature in culture.

We noted that Th is slightly repressed in iALFP at longer differentiation times. The presence of Th transcript contrasts with the lack of TH staining (**Figure 1D**) and might indicate additional layers of posttranscriptional control, as has been described *in vivo* (Xu et al., 2007). Expression of noradrenergic specific enzyme Phenylethanolamine-N-methyltransferase (Pnmt) is slightly induced in iA line but highly repressed in iALP and iALFP at 9 days of differentiation (**Figure 2C**). Foxa2 is critical for serotoninergic development in the hindbrain by suppressing Phox2b TFs (Jacob et al., 2007). Recapitulating this regulation, iALF and iALFP cells do not express Phox2b induced by iA, iAL, and iALP. Foxa2 repression of Phox2b is seen at 2 and 9 days of doxycycline treatment but is stronger at later time points (**Figure 2C**). In summary, all cell lines equally repress pluripotency and induce generic neuronal gene expression. Although alternative monoaminergic fates are not entirely silenced, the ALFP TF combination is the one that more closely reproduces serotonergic effector gene expression, particularly at longer differentiation times.

To further explore the differences in expression programs more broadly, we performed K-means clustering on all genes with a $\log_2$ fold change of at least $\pm$ 1.0 in at least one of the 5 cell lines compared to EB (**Supplementary Figure 1**). The five cell lines have broadly similar transcription regulation patterns from EBs, consistent with the notion that neuronal differentiation drives most transcriptional changes. To separate the neuronal component from a possible neuronal subtype signature, we removed all either upregulated or downregulated genes in all five cell lines and re-clustered the remaining genes. The resulting heatmaps at day 2 (**Figure 2D**) and day 9 (**Figure 2E**) illustrate the unique impacts on expression caused by each TF combination. A list of GO terms for each cluster can be found in **Supplementary Tables 3, 4**.

We first focused on the analysis of day 2 as it better reflects the direct actions of TF combinations. The expression clusters found at day 2 include several expression patterns that are present in the iALFP line, but not in either the iALF or the iALP lines (**Supplementary Tables 2–4** for clusters' GO terms at day 2 and day 9 respectively). For example, cluster 2 shows a group of 186 genes that are generally downregulated in all cell lines except for iALFP. Cluster 3, in contrast, contains genes that are strongly downregulated only in the context of iALFP and contains genes associated with GABA transporter activity according to Enrichr (Xie et al., 2021), many pseudogenes, and several Hox genes expressed in the most posterior rhombomeres (Hoxb2, Hoxb5, and Hoxa3). These two gene clusters suggest that Pet1 and Foxa2 synergistically create a unique expression program when expressed alongside Lmx1b and Ascl1. Other expression clusters suggest somewhat independent roles for Foxa2 and Pet1 in activating subsets of genes. Cluster 5 contains genes whose expression is inverted by the addition of Pet1, that is genes upregulated in iALF that are downregulated in iALFP and vice versa genes downregulated in iALF that are upregulated in iALFP. This cluster is enriched for genes associated with neuronal differentiation. Several of them, including Cnr1, Cyfip2, Fgf13, Col25a1, and Slc17a8, are downregulated in serotonergic neurons in the Lmx1b mutant mice (of note, Lmx1b is also upstream of Pet1 expression) (Donovan et al., 2019). Cluster 4 contains upregulated genes in both iALF and iALFP, suggesting that they are downstream of Foxa2. This cluster is enriched for genes associated with dopaminergic and serotonergic neurogenesis (Ddc, Shh, Lmx1a, En1, Gli1, Nkx2.2) and genes associated with axon guidance in serotoninergic neurons (Donovan et al., 2019). Many Cluster 6 genes are downregulated in iALF, but upregulated in iALP and iALFP, suggesting that Pet1 overexpression overrides an apparent repressive effect of Foxa2 to activate these genes.

The expression clusters found at day 9 also reflect differences in each cell line, including patterns present in the iALFP line, but not in either the iALF or the iALP lines (**Figure 2E**). However, enriched GO terms did not reach statistical significance. We found that many of the genes from Cluster 4 at 48h (those upregulated in both iALF and iALFP) are also present in differential expression clusters at day 9, particularly in clusters 1 and 2 corresponding to genes with higher expression in ALFP than in ALF or ALP. This gene set is enriched for cadherin-mediated cell adhesion. Ddc, the effector gene required for serotonin biosynthesis, is also present in this group of genes along with additional genes expressed in mouse brain serotonergic neurons (Zeisel et al., 2018), such as Renbp, Naip6, Macc1, Iqcf5, Il1r1, Hsd367, Foxa1, Cthrc1, Crybg3, Col7a1 and Clps. Finally, FPKM values for Th, Tph1 and Tph2 expression confirms

synergistic actions of Foxa2 and Pet1 in Th repression and Tph activation (**Supplementary Figure 1**).

In total, transcriptomic analysis suggests that adding serotonergic TFs to Ascl1 induced gene expression patterns associated with serotonergic fate. We note that Pet1 and Foxa2 are required to independently and synergistically control different gene expression modules.

Single-Cell RNA-Seq Confirms Mixed Monoaminergic Fate Induction at Early Differentiation Time Points

The bulk RNA-seq results show that TF induction generated a mixture of different monoaminergic fates. To dissect if heterogeneity of bulk gene expression corresponds to different cell populations or to mixed neuron-type fate induction in single cells and to try to deconvolve the effects of Pet1-Foxa2 synergy, we performed single-cell RNA-seq experiments (scRNA-seq) 2 days after Dox induction in iALF and iALFP. To avoid possible artifacts induced by inefficient 2A peptide cleavage producing unprocessed Foxa2-Pet1 TF proteins, we created a new line where Pet1 is driven by an independent Dox-inducible promoter (iALFiP). Neuronal and serotonergic staining at 9 days of doxycycline treatment is similar to iALFP (**Supplementary Table 1**). To measure the difference with neurons induced by Ascl1 only, we spiked iALF and iALFiP single-cell suspensions with a fluorescently labeled iA line immediately before scRNA-seq encapsulation (**Figures 3A,B**). Confirming the strong effect of adding TFs to Ascl1, the iALF and iALFiP cells labeled by the Foxa2-V5 transgene clustered away from iA cells labeled by Tubb3:GFP in a dimensional reduction representation (**Figure 3C**).

iALF and iALFiP combinations contained cells in different states of neuronal differentiation, as seen by a range of endogenous Tubb3 and Map2 transcript levels (**Figure 3D**). Expression of most serotonin and catecholamine biosynthesis pathway genes are not or almost not detectable at this early stage of differentiation, including serotonin exclusive Tph2 and Slc6a4 (a.k.a. Sert) genes, catecholaminergic exclusive Slc6a3 (a.k.a Dat), and Dbh or shared Gch, and Slc18a2 (a.k.a. Vmat2). However, scRNA-seq reveals expression for Ddc (commonly expressed by serotonergic and catecholaminergic genes) and Th (not expressed by serotonergic neurons) (**Figures 3E,F**). Ddc expression is present in iALF and iALFiP cells with high Tubb3 and Map2 expression levels but absent from iA cells. Th expression also coincides with high levels of Tubb3 and Map2, although its expression seems lower and in fewer cells than Ddc expression, particularly in iALFiP.

As expected from bulk RNA-seq, iALF and iALFiP cells repress Phox2b expression (**Figure 3F**). Next, we analyzed scRNA-seq expression for genes classified in cluster 4 in our bulk RNA-seq experiments. This gene set contains upregulated genes in both iALF and iALFiP, suggesting that they are downstream of Foxa2 and are enriched for dopaminergic and serotonergic neurogenesis genes. We selected some genes with detectable expression in serotonergic neurons *in vivo* (Zeisel et al., 2018). These genes are expressed in iALF and iALFiP but not induced in iA. Some of them show higher or broader expression in iALFiP compared to iALF (such as Cthrc1, Cps1 and Macc1) (**Figure 3G**), while others (such as Crybg3, Iqcf5 or Foxa1) seem more similarly expressed in iALF and iALFP (**Figure 3G**).

In total, the scRNA-seq experiments showed that both TF combinations induce a collection of cells with varying states of maturation 48 h after Dox induction. As expected, neurons further along the differentiation pathway express genes associated with terminal neurotransmitter fate (Th and Ddc) supporting maturation as a key factor to induce the terminal serotoninergic markers. Thus, most of the effector genes are still undetectable at this early differentiation stage. Broad Th expression suggest mixed monoaminergic fate induction at early time points. Although iALF and iALFiP cells induce similar neuronal fates overall, iALFiP generates a higher percentage of cells with genes associated with serotonergic fate, such as Cthrc1, Cps1 and Macc1.

Foxa2 and Pet1 Bind Mostly Independently to the Genome

Since Pet1 and Foxa2 appear to synergistically regulate some sets of genes after only 2 days of differentiation (**Figure 2D**), we asked whether they interact with each other at their DNA-binding targets. We thus performed ChIP-seq on Foxa2 in the iALF and iALFiP cell lines and Pet1 in the iALP and iALFiP cell lines, where all experiments were performed after 2 days of TF combination induction. Although Foxa2 tends not to bind proximal to transcription start sites, Pet1 has a more evenly distributed binding (**Supplementary Figure 2**). All sets of binding sites are enriched for appropriate cognate DNA-binding motifs. MEME-ChIP motif discovery analysis finds Foxa2's cognate binding motif enriched at Foxa2's binding sites and the expected ETS family motif enriched in all three Pet1 binding site categories (**Figure 4**).

We first asked if the differences between iALF and iALFP (and iALFiP) transcriptional output are explained by Pet1 modifying Foxa2's genomic binding. Foxa2 binding locations appear to be unaffected by the presence of Pet1, as the vast majority of Foxa2 sites display similar levels of ChIP enrichment in the iALF and iALFiP lines (**Figure 4A**). In contrast, over 60% of Pet1 sites display significant differential enrichment between the iALP and iALFiP conditions (23% are preferred in iALP while 39% are preferred in iALFiP and 38% are shared) (**Figure 4B**). While this suggests that Pet1's binding targets are modified by Foxa2 expression, only a fraction of Pet1's differential binding locations are directly attributable to a shift toward Foxa2's binding sites. Specifically, of the 9,340 sites preferentially bound by Pet1 in iALFiP vs. iALP, only 1891 (20%) overlap Foxa2 binding locations. Thus, at most, only 20% of Pet1 differential binding could be directly affected by Foxa2 binding in cis. And considering all Pet1 and Foxa2 binding sites in ALFP only 3% are shared between the two TFs (**Figure 4C**).

To find sequence features that may explain the shift in Pet1 binding sites across cell lines, we divided all Pet1 bound sites into iALP > iALFiP, iALP = iALFiP and iALP < iALFiP and turned to the SeqUnwinder discriminative motif-finding

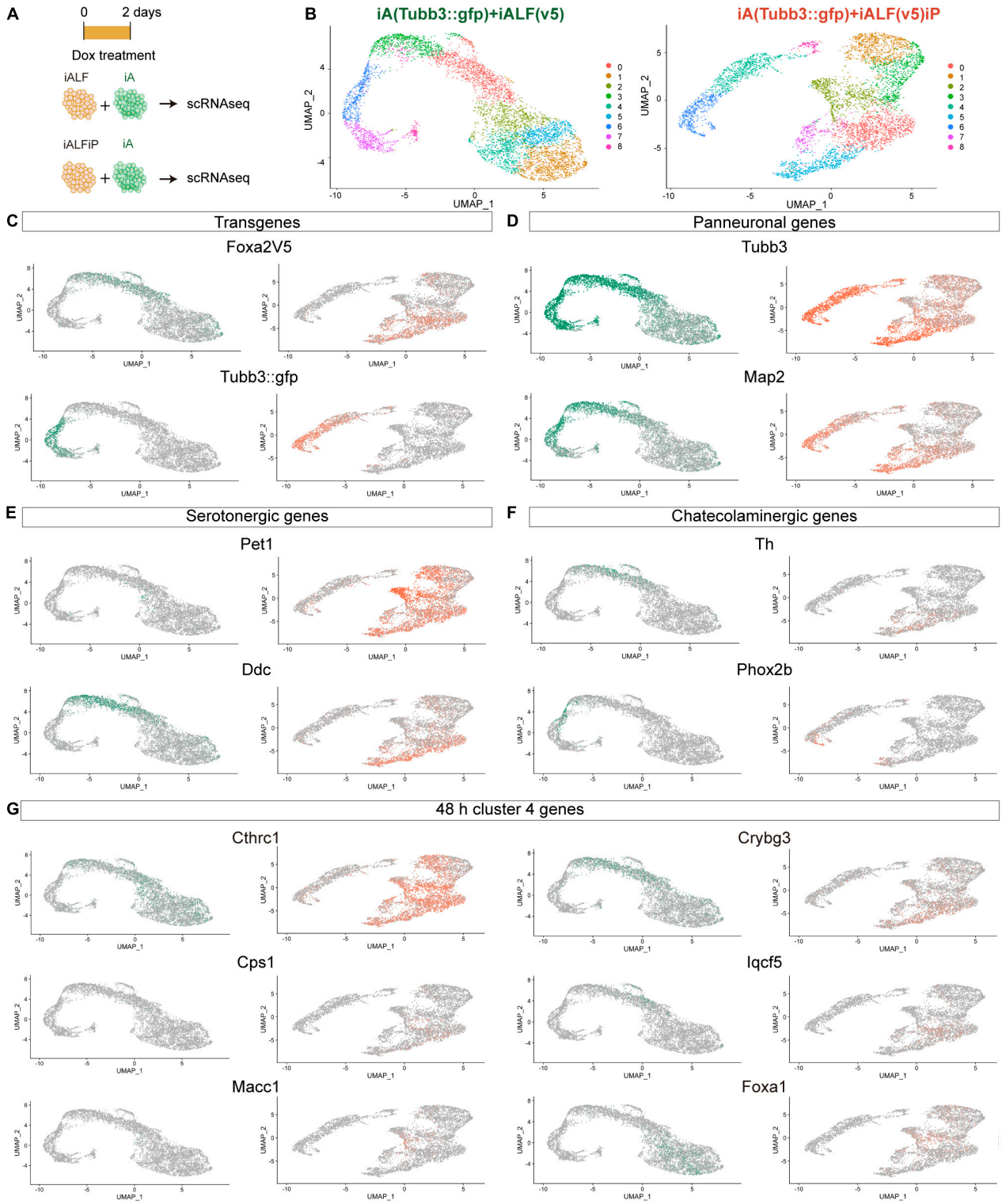

FIGURE 3 | Single-cell RNA-seq of iALF and iALFiP neurons at differentiation day 2. **(A)** Experimental outline. iALF and iALFiP cells were mixed with Tubb3:GFP-expressing iA cells for comparison. **(B)** UMAP visualization of iALF and iALFiP clustering. Clusters are shown in colors and numbered from 1 to 8. **(C–G)** Projection of specific genes in panel **(B)**. **(C)** Transgene expression clearly separates iA (Tubb3:GFP+) from iALF and iALFiP. **(D)** The transgene expression levels corelate with neural differentiation states suggesting a differentiation cline across cells. **(E,F)** Both lines contain cells expressing serotoninergic genes but iALFiP represses Phox2b. **(G)** Projection of representative Cluster 4 (**Figure 2D**) on the single cell clusters. **(C–G)** Green = expression in iALF + Tubb3:GFP, Orange = iALFP + Tubb3:GFP.

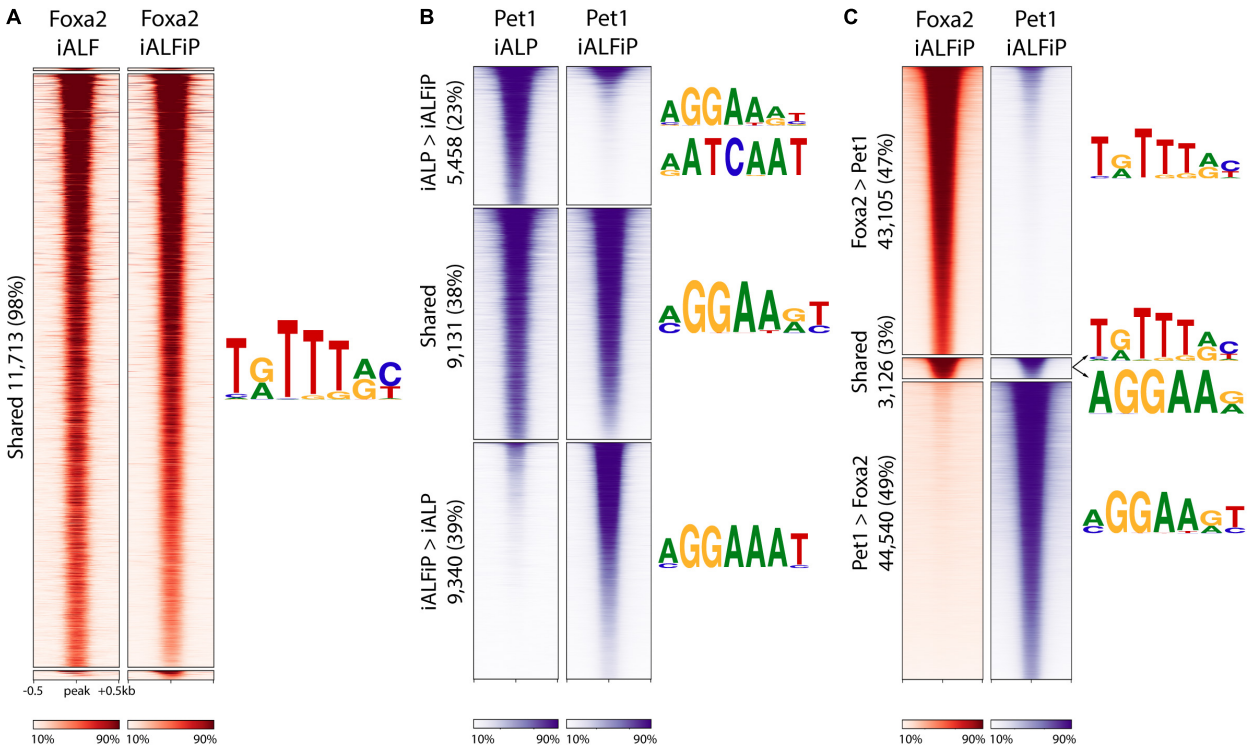

FIGURE 4 | The presence of Foxa2 affects the location of Pet1 binding. **(A)** Heatmap of ChIP-seq reads at Foxa2 binding sites in ALF and ALFiP induction backgrounds after 12 h. A 1 kb window around the peak center is plotted. The plots are divided top-to-bottom based on the preferential binding patterns ALF > ALFiP, shared, and ALFiP > ALF, according to MultiGPS. The sequence logos of the motifs detected by MEME-ChIP are shown to the right of the region. **(B)** Heatmap of ChIP-seq reads of Pet1 binding sites in ALP and ALFP background. **(C)** Heatmap of ChIP-seq reads at Foxa2 (red) and Pet1 (blue) binding sites in ALFP background. The color scaling in all heatmaps vary between the read counts observed in the 10th and 90th percentiles of bin.

platform (Kakumanu et al., 2017). SeqUnwinder identifies two Forkhead-like motifs that distinguish the iALFiP-preferred Pet1 sites from the other categories (**Supplementary Figure 2**). This is consistent with the 20% overlap of those Pet1 binding sites with Foxa2 binding, as noted above. In contrast, the iALP-preferred Pet1 sites contain discriminative motifs that match Homeodomain TFs, including a motif preferred by Onecut TFs (**Supplementary Figure 2**). Of note, when we compared Pet1 binding sites with our previously characterized Onecut2 binding sites (measured in iA cells after 48 h of induction, Aydin et al., 2019), we found a substantially higher overlap with iALP-preferred Pet1 sites (27%) compared with iALFiP-preferred sites (<1%). We further measured the binding of Lmx1b in iAL cells, finding 5,151 binding sites in total (**Supplementary Figure 3**), and again found a higher overlap with iALP-preferred Pet1 sites (12%) compared with iALFP-preferred sites (<1%).

Consistent with it being a pioneer TF, the ChIP-seq analyses support a model in which Foxa2 binds directly to cognate sites and is largely unaffected by the over-expression of Pet1. On the other hand, Foxa2 heavily perturbs Pet1's binding targets. Surprisingly, only a small fraction of Pet1 binding changes could be explained by Foxa2 pioneer activity in cis. This fraction of shifted binding sites could be explained by Pet1 moving away from binding alongside other pioneer TFs expressed in neurons, like Onecut, toward binding alongside Foxa2. Nevertheless, most Pet1 sites preferentially bound in iALFiP are occupied independently of Foxa2 binding, likely interacting with additional unidentified TFs downstream of Foxa2.

Both Foxa2 and Pet1 Bind to Relatively Inaccessible Regions on the Genome

The previously described Fox TF pioneer activity motivated us to ask if Foxa2 behaves similarly in this context and if Pet1 acts as a pioneer or not. To that end, we performed ATAC-seq experiments in the EB, iA (48 h), iALF (48 h), iALFiP (48 h), and iALFiP (day 9) conditions. A large majority (89%) of Foxa2 binding sites are inaccessible in the preexisting EB cells (**Figure 5**). Consistent with Foxa2's known pioneering activity, Foxa2 binding increases chromatin accessibility at many sites in both iALF and iALFiP cell lines, and this accessibility is maintained and strengthened in day 9 iALFiP neurons (**Figure 5**).

Pet1 displays a more complex association with accessibility. Over half of Pet1 binding sites in iALFiP cells are devoid of accessibility signatures in the preexisting EB cells, suggesting that Pet1 can bind to inaccessible chromatin (**Figure 6**). Intriguingly, and in contrast to the stereotypical behavior of a pioneer TF, Pet1 binding sites do not gain accessibility following Pet1 binding. Of the Pet1 binding sites that have preexisting accessibility in EB cells, most are bound by Pet1 in both iALP and iALFiP cell lines

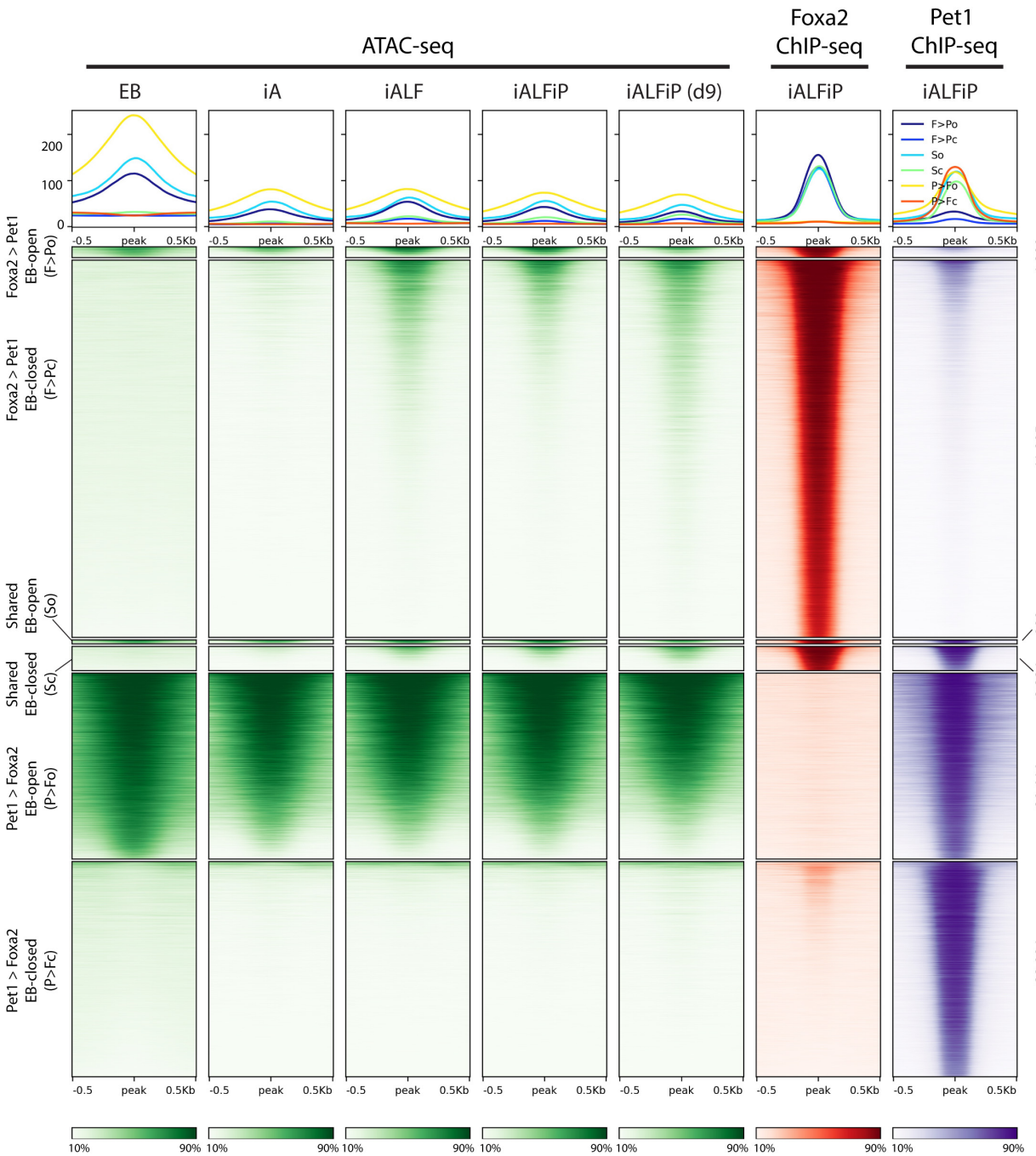

FIGURE 5 | Comparison of ATAC-seq profiles with iALFiP Foxa2 and Pet1 binding categories. ATAC-seq heatmaps plot EB, iA (48 h), iALF (48 h), iALFiP (48 h), and iALFiP (d9) ATAC-seq signals over the Foxa2 and Pet1 binding categories displayed in **Figure 4C**. Each Foxa2 and Pet1 binding category is first split into two groups according to overlap with ATAC-seq domains in the preexisting EB cell state. Thus, six categories of sites are plotted. Panels above heatmaps display average ATAC-seq or ChIP-seq signals in each of the six categories. The color scaling in all heatmaps vary between the read counts observed in the 10th and 90th percentiles of bin.

and thus fall under the "shared" or "iALP = iALFiP" category of Pet1 binding (**Figure 6**). Most iALP-preferred Pet1 sites are inaccessible in EB, and while some of these sites display increased accessibility in iA (48 h) and iALFiP (9 days) cells, most do not in iALF and iALFiP at 48h.

In summary, Foxa2 mainly binds to inaccessible chromatin regions and increases accessibility. We cannot rule out that Pet1 plays a pioneering role at a subset of its binding sites, but it is unlikely given the overall trend that the ATAC-seq signal does not increase at Pet1 bound sites.

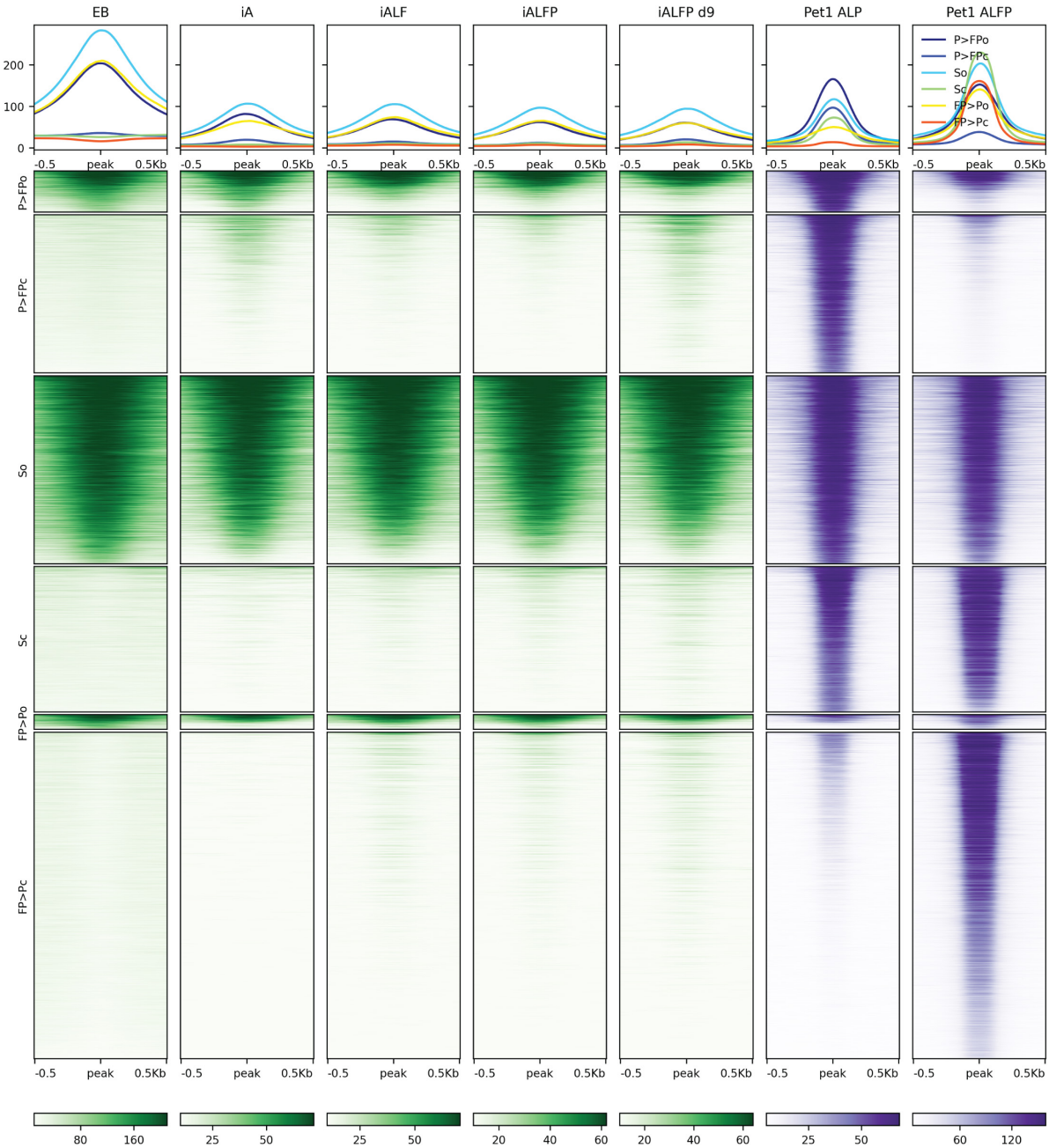

FIGURE 6 | Comparison of ATAC-seq profiles with iALFiP Foxa2 and Pet1 binding categories. ATAC-seq heatmaps plot EB, iA (48 h), iALF (48 h), iALFiP (48 h), and iALFiP (d9) ATAC-seq signals over the iALP and iALFiP Pet1 binding categories displayed in **Figure 4B**. Each Pet1 binding category is first split into two groups according to overlap with ATAC-seq domains in the preexisting EB cell state. Thus, six categories of sites are plotted. Panels above heatmaps display average ATAC-seq or ChIP-seq signals in each of the six categories. The color scaling in all heatmaps vary between the read counts observed in the 10th and 90th percentiles of bin.

Foxa2 and Pet1 Binding Sites Are Associated With Neuronal Subtype Specification

To assess whether the binding patterns of Foxa2 and Pet1 are associated with the expression patterns unique to iALFiP, we analyzed their gene associations using GREAT (McLean et al., 2010). As shown in **Figure 7A**, Foxa2's binding sites are highly associated with genes that are specifically upregulated at 48 h by TF combinations that include Foxa2 (**Figure 2D**; cluster 4). These genes display upregulation in both iALF and iALFiP and are significantly associated with dopaminergic neurogenesis pathway genes according to Enrichr (**Figure 7B**). Other categories of

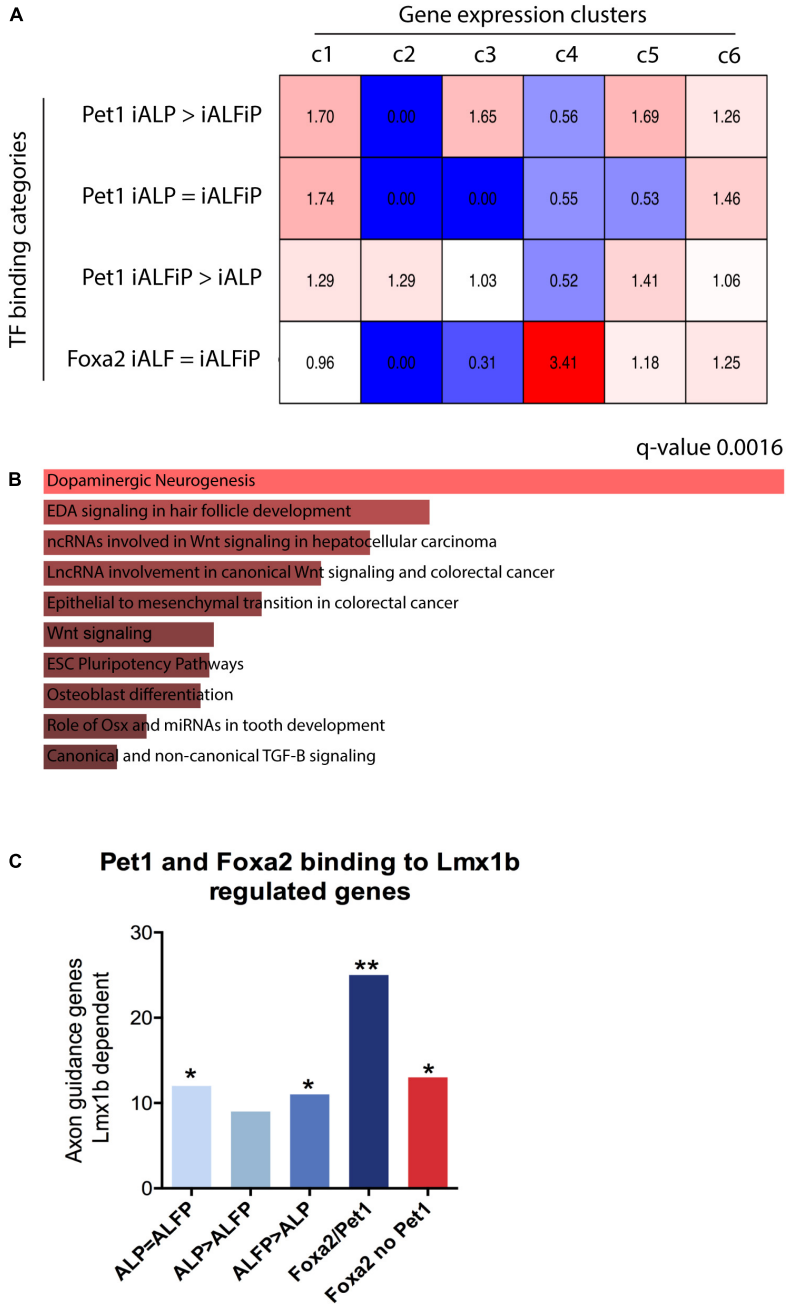

FIGURE 7 | (A) Overlap between bulk RNA-seq clusters from **Figure 2** 48 h and transcription factor binding sites from ChIP-seq experiments. Numbers represent over- and under-representation factors compared with randomly selected regions. **(B)** Gene Ontology analysis for genes bound by Foxa2 in cluster 4 shows enrichment for dopaminergic neurogenesis. **(C)** Overlap between specific binding categories and known serotonergic targets of Lmx1b shows that genes associated to Foxa1/Pet1 co-bound sites are highly enriched for serotonergic functions. *$p < 0.5$, **$p < 0.05$.

binding sites show relatively weaker associations with gene expression categories.

Finally, we directly analyzed the binding patterns of Foxa2 and Pet1 in genes with axonal functions that are known downstream targets of Lmx1b serotonergic terminal selector (Donovan et al., 2019). We selected the top 500 genes associated to each class of binding sites: (1) Pet1 binding ALP = ALFiP; (2) Pet1 binding ALP > ALFiP; (3) Pet1 binding ALP < ALFiP, (4) Pet1/Foxa2 shared sites and (5) Foxa2 binding not co-bound with Pet1. All binding categories are enriched for Lmx1b downstream targets, however the Foxa2/Pet1 bound genes show higher enrichment than considering Pet1 or Foxa2 binding alone (**Figure 7C**). These results suggest both dependent and independent binding of Pet1 and Foxa2 are

important for correct serotonergic differentiation at early differentiation stages.

CONCLUSION AND LIMITATIONS

Transcription factors are potent inducers of gene expression and are thus popularly used to control cell fate for research and clinical applications. This work aimed to understand how TF combinations control specific neuronal fates. To that end, we took advantage of a TF set that contains TFs associated with monoaminergic neuronal fate and proposed to induce serotonergic neuronal fate (Xu et al., 2016). By dissecting the Ascl1 + Lmx1b + Foxa2 + Pet1 (iALFP) combination at the transcriptional output level, combined with how the Pet1 and Foxa2 TFs bind to the genome, we concluded that Pet1 and Foxa2 synergize to induce serotonergic gene expression by binding to some common but mostly distinct sites in the genome. While Foxa2 behaves as a pioneer TF, binds to the same targets in both combinations and increases chromatin accessibility, Pet1 binding is variable. Moreover, Pet1 does not seem to increase chromatin accessibility upon binding. In mouse serotonergic neurons the majority of Pet1 bound regions decrease their accessibility in Pet1 mutants (Zhang et al., 2022). Our data suggests Pet1 could be required in accessibility maintenance rather than acting as a pioneer factor.

Forced TF expression is a standard tool used to investigate TF activity in gain-of-function experiments and laboratory attempts to control cell fate. It is not surprising that Ascl1 induces neuronal fate from pluripotent cells since it has been shown to be sufficient to differentiate stem cells, glia and fibroblast into neurons (Vierbuchen et al., 2010; Raposo et al., 2015; Aydin et al., 2019). With different degrees of success, pro-neuronal TFs such as Ascl1 and Neurog2 were combined with other TFs to canalize differentiation into specific neuronal types (reviewed in Aydin and Mazzoni, 2019). For example, Neurog2 expression alone drives mouse stem cells into a set of possible cortical neuronal identities (Aydin et al., 2019), and pairing Neurog2 with Isl1 and Lhx3 forces most differentiating neurons to become spinal motor neurons (Hester et al., 2011; Mazzoni et al., 2013). While iALFP increases the levels of serotonergic neurons, no combination we tested was able to produce a homogenous culture of 5HT positive neurons. Allowing cultures to mature was enough to canalize the originally dispersed Neurog2-induced neurons into a specific fate (Lu et al., 2019). Similarly, we find better serotonin effector gene expression after 9 days compared to 48 h. Long-term culture might enable iALFP cells to coalesce into a stronger serotonergic fate. Another common limitation of direct programming strategies rests on the TF combination. Here we focused on deconvolving the action of 4 different TFs. However, dozens of TFs are coexpressed in each neuronal type. Further work in basic serotoninergic differentiation mechanisms might produce a new TF set with robust induction capabilities.

We should also consider that induced programming does not reproduce the temporal TF cascade during embryonic differentiation. *In vivo*, TF temporal progression is tightly regulated along the developmental history of a neuron, and this temporal axis might be critical in selecting specific target genes. Indeed, *in vivo*, Ascl1 and Foxa2 are expressed in progenitors, while Lmx1b and Pet1 are expressed and maintained in postmitotic neurons. Thus, Pet1 and Foxa2 are only ephemerally coexpressed in serotonergic neurons *in vivo* while constantly coexpressed during direct programming. Our *in vitro* results show limited Foxa2 and Pet1 direct co-binding, which might reflect *in vivo* gene regulatory networks. Nevertheless, Foxa2 strongly modifies the Pet1 binding landscape during programming, probably through induction of additional downstream TFs. Pet1 controls the expression of different sets of genes during serotoninergic neuron maturation, from axon elongation to axonal branching or neuronal maturation (Wyler et al., 2016; Donovan et al., 2019). Thus, Foxa2 indirect Pet1 relocation could guide Pet1 transitions between stage-specific functions during neuronal maturation. We also want to highlight that despite the low number of Pet1 and Foxa2 co-bound targets, they seem to be biologically relevant as they are highly enriched for genes coding for axonal components that are downstream of the Lmx1b serotonergic terminal selector (which is also known to regulate Pet1 expression itself) (Donovan et al., 2019).

Foxa2 is a well-known pioneer TF, so it makes sense that its binding does not depend on the presence of Pet1. Before the studies presented here, we hypothesized that Pet1 binding would gravitate toward Foxa2 accessible sites. However, our results suggest that Pet1 and Foxa2 synergize to induce serotoninergic fate mostly by binding to different regulatory elements. This implies that establishing general rules that predict the programming abilities of different TF combinations may be challenging. Unlike the clear differences in sequence preference when Isl1 partners with Lhx3 vs. Phox2a (Mazzoni et al., 2013), we did not detect rules that predict Pet1 binding when expressed with Foxa2. As stated above, unknown TFs may co-bind with Pet1 and play a role in producing the transcriptional output generated by Foxa2 + Pet1. Together, this work suggests that each TF combination has its own nuances. Analyzing more examples will produce generalizable rules governing TF binding, leading to the production of specific neuronal subtypes.

MATERIALS AND METHODS

Experimental Procedures

Cell Line Generation and Cell Differentiation

Inducible cell lines were generated using a previously described inducible cassette exchange (ICE) method (Iacovino et al., 2011). Resulting transgenic lines contain a single-copy insertion of the transgenes into the HPRT locus that is expression competent. p2Lox-Ascl1 (iAscl1) plasmid was generated by cloning mouse Ascl1 cDNA into p2Lox-V5 plasmid. Likewise, the additional transcription factors were cloned by amplifying open reading frames with p2a or t2a linker peptides as shown in **Figure 1**. Lmx1b sequence was V5-tagged in iAL and FLAG-tagged at the C-terminal in iALF, iALP, and iALFP, and iALFiP combinations to facilitate immunoprecipitation for ChIP experiments and asses induction efficiency by antibody staining. Pet1 was also V5-tagged for ChIP experiments. Second tetracycline response

element (TRE) containing inducible line was generated by inserting TRE-Pet1-HA construct into p2Lox-ALF plasmid which allows two separate TRE elements to control expression of ALF vs Pet1 constructs. HA-tag was added to second TRE Pet1 construct to facilitate ChIP experiments.

Tubb3:T2A-GFPnls ESC knock-in cell line used in sc-RNA-seq experiment was made as described previously (Aydin et al., 2019). The p2Lox-Ascl1 plasmid was nucleofected to Tubb3:T2A-GFPnls ESC line to generate iAscl1 Tubb3:GFP stable line.

The inducible mESCs were grown in 2i (2-inhibitors) based medium Advanced DMEM/F12: Neurobasal (1:1) Medium (Gibco), supplemented with 2.5% mESC-grade fetal bovine serum (vol/vol, Corning), N2 (Gibco), B27 (Gibco), 2 mM L-glutamine (Gibco), 0.1 mM ß-mercaptoethanol (Gibco), 1,000 U ml–1 leukemia inhibitory factor (Millipore), 3 mM CHIR (BioVision) and 1 mM PD0325901 (Sigma) on 0.1% gelatin (Milipore) coated plates at 37 °C, 8% CO2. To generate embryoid bodies (EBs), mESCs were dissociated using TrpLE (Gibco) and plated in AK medium Advanced DMEM/F12: Neurobasal (1:1) Medium, 10% Knockout SR (vol/vol) (Gibco), penicillin–streptomycin (Gibco), 2 mM L-glutamine and 0.1 mM (ß-mercaptoethanol) on untreated plates for 2 days (day –2) at 37 °C, 8% CO2. After 2 days, the expression of the transgenes was induced by adding 3 μg ml–1 doxycycline (Sigma, D9891) to the AK medium. For differentiating mESC (EB) antibody stainings, RNA-seq, sc-RNA-seq, and ATAC-seq experiments, 2–3 × 105 cells were plated in each 100-mm untreated dishes (Corning). For ChIP-seq experiments, the same conditions were used, but the seeded cell number was scaled up to 3–3.5 × 106 cells in 245mm × 245mm square dishes (Corning). For day 9 attached neuron antibody stainings, bulk RNA-seq, ATAC-seq experiments, EBs induced with doxycycline for 2 days (48h + doxycycline) were dissociated with 0.05% Trypsin-EDTA (Gibco) and plated on poly-D-lysine (Sigma, P0899) on coated 4-well plates. The dissociated neurons were grown in neuronal medium with supplements [Neurobasal Medium supplemented with 2% fetal bovine serum, B27, 0.5mM L-glutamine, 0.01mM β-mercaptoethanol, 3 μgml–1 doxycycline, 10 ngml–1 GDNF (PeproTech, 450–10), 10ngml–1 BDNF (PeproTech, 450–02), 10ngml–1 CNTF (PeproTech 450–13), 10 μM Forskolin (Fisher, BP2520–5), and 100 μM IBMX (Tocris, 2845)] at 37Co, 5%CO2. Antimitotic reagents [4 μM 5-fluoro-2'-deoxyuridine (Sigma, F0503) and 4 μM uridine (Sigma, U3003)] were added to eliminate residual proliferating cells.

Immunocytochemistry

Embryoid bodies were fixed in 4% paraformaldehyde (vol/vol) in PBS. Fixed EBs were cryoprotected in 30% sucrose and were embedded in OCT (Tissue-Tek) and sectioned for staining. Primary antibody stainings were done by overnight incubation at 4°C, and secondary antibody stainings were incubated for 1 h at room temperature. Day 9 neuronal stainings were done on coverslips coated with poly-D-lysine with the primary and secondary antibody incubation times as described above. Samples were mounted with Fluoroshield with 4,6-diamidino-2phenylindole (DAPI; Sigma) and images were acquired using a SP5 Leica confocal microscope. The following primary and secondary antibodies were used: V5 (Ms): ThermoFisher #R960-25; Tuj1 (MS): Covance #mms-435p; Tuj1 (Rb): Sigma #T2200;5-HT (Rb): Sigma #S5545; 5-HT (Gt): Abcam # Ab66047; TH (Rb): Peel-Freez #P40101-0; TH (Ms): Chemicon #MAB318; TPH1/2 (Sheep): Millipore #AB1541. Alexa 555 anti-mouse: Invitrogen # A31570; Alexa 488 anti-mouse: Invitrogen # A21202; Alexa 633 anti-mouse: Invitrogen # A21052; Alexa 555 anti-rabbit: Invitrogen # A31572; Alexa 555 anti-goat: Invitrogen # A21432; Alexa 488 anti-rabbit: Invitrogen # A21206; Alexa 488 anti-sheep: Invitrogen # A11015.

RNA-Seq

Cells were collected in duplicates at 48 h and 9 days after doxycycline induction. We combined new iA RNA-seq with those published (Aydin et al., 2019) to make an n of 5. TRIzol (Invitrogen, 15596026) reagent was used to isolate RNA. Isolated RNA was purified with RNeasy mini kit (Qiagen, 74106). RNA integrity was measured using Agilent High Sensitivity RNA Screentape (Agilent Tech, 5067–5080). 500 ng RNA was spiked (1:100) with ERCC Exfold Spike-in mixes (Thermo Fisher Scientific, 4456739) for accurate comparison across samples. RNA-seq libraries were prepared with Illumina TruSeq LS kit v2 (RS-122–2001; RS-122–2002). KAPA library amplification kit was used for the final quantification of the library before pooling (Roche Lightcycler 480). The libraries were sequenced on an Illumina Next-Seq 500 using V2 and V2.5 chemistry for 50 cycles (single-end) at NYU Genomics Core facility.

Single-Cell RNA-Seq

Cells were collected 48 h after doxycycline induction, and washes were done in 1 × PBS with 0.04 mg ml–1 BSA (Thermo Fisher Scientific, AM2616). Clumps were removed by using a 30 μM CellTrics filter (cat. no. 04-004-2326). 25% iA (Tubb3:GFP) and 75% iALF or 25% iA (Tubb3:GFP) and 75% iALFiP were pooled as to separate libraries having 1,000 cells per μl. 10X Genomics Chromium Single Cell 3' library kit was used to generate a single-cell library for a targeted cell recovery rate of 10,000 cells (Chromium i7 Multiplex Kit, Chromium Single Cell B Chip Kit v3, Chromium Single Cell 3' GEM, Library and Gel Bead Kit v3). The libraries were sequenced on an Illumina Next-Seq 500 High Output using V2.5 chemistry with 26 × 98 bp – 150 cycles run confirmation at NYU Genomics Core facility.

ChIP-Seq

Cells were collected and fixed with 1 mM DSG (ProtoChem) followed by 1% FA (vol/vol) each for 15 min at room temperature. Pellets containing 25–30 × 10^6 cells were aliquoted and flash-frozen at –80°C. Cells were lysed in lysis buffer containing 50 mM HEPES-KOH (pH 7.5), 140 mM NaCl, 1 mM EDTA, 10% glycerol (vol/vol), 0.5% Igepal (vol/vol), 0.25% Triton X-100 (vol/vol) with 1 × protease inhibitors (Roche, 11697498001) at 4°C for 10 min. Cells were resuspended in 50 mM HEPES-KOH (pH 7.5), 140 mM NaCl, 1 mM EDTA, 10% glycerol (vol/vol), 0.5% Igepal (vol/vol), 0.25% Triton X-100 (vol/vol), and incubated 10 min at 4°C. Nuclear extracts were resuspended in cold sonication buffer [50 mM HEPES (pH 7.5), 140 mM NaCl, 1 mM EDTA, 1 mM EGTA, 1% Triton X-100, 0.1% sodium deoxycholate (wt/vol),

0.1% SDS (wt/vol)]. Sonication was performed with Bioruptor Pico sonicator device (Diagenode) with 30 sec ON/30 sec OFF, 18 cycles, with Bioruptor sonication beads (0.45 mg beads per 1 ml sample). Immunoprecipitation was done overnight at 4°C on a rotator with Dynabeads protein-G (Thermo Fisher Scientific) conjugated antibodies. 5 μg of the following antibodies were used for immunoprecipitation: anti-Ascl1 (Abcam, ab74065); anti-HA (Abcam, ab9110); anti-V5 (Abcam, ab15828). Subsequent washes were done in 1X sonication buffer (cold) first, sonication buffer with 500 nM NaCl (cold), LiCl wash buffer [20 mM Tris−HCl (pH 8.0)] (cold), 1 mM EDTA, 250 mM LiCl, 0.5% NP-40, 0.5% sodium deoxycholate (cold), and TE buffer [10 mM Tris, 1 mM EDTA, (pH 8)] (cold). Samples were eluted in elution buffer [50 mM Tris−HCl (pH 8.0), 10 mM EDTA (pH 8.0), 1% SDS] by incubating for 45 min at 65°C. Eluted sample and input (sonicated only) were incubated overnight at 65°C to reverse the crosslink. RNA was digested by the addition of 0.2 mg ml^{-1} RNase A (Sigma) and incubating for 2 h at 37°C. Protein digestion was performed by adding 0.2 mg ml^{-1} Proteinase K (Invitrogen) for 30 min at 55°C. DNA extraction was done with Phenol:chloroform:isoamyl alcohol (25:24:1; vol/vol) (Invitrogen) followed by ethanol precipitation. 1/3 of ChIP DNA (1:100 dilution of input DNA) was used to prepare lllumina DNA sequencing libraries. Bioo Scientific multiplexed adapters were ligated after end repair and A-tailing, and unligated adapters were removed with Agencourt AmpureXP beads (Beckman Coulter) purification. Adapter-ligated DNA was amplified by PCR using TruSeq primers (Sigma). DNA libraries between 300 and 500bp in size were purified from agarose gel using a Qiagen minElute column, and the final quantification of the library before pooling was done using a KAPA library amplification kit (Roche Lightcycler 480). The libraries were sequenced on an Illumina Next-Seq 500 using V2 chemistry for 50 cycles (single-end) at NYU Genomics Core facility. The experiments were done in duplicate.

ATAC-Seq

The 50,000 cells were harvested and washed twice in cold 1X PBS. Cells were resuspended in 10 mM Tris (pH 7.4), 10 mM NaCl, 3 mM MgCl2, and 0.1% NP-40, and centrifuged immediately at 4°C for 10 min. Day 9 attached neuron samples were lyzed in 0.01% NP-40 instead. The pellet was resuspended in 25 μl of 2 × TD buffer, 2.5 μl TDE1 (Nextera DNA sample preparation kit, FC-121– 1030) followed by incubation for 30 min at 37°C. The reaction was cleaned up with Min-elute PCR purification kit (Qiagen, 28004). The optimal number of PCR cycles were determined to be the one-third of the maximum fluorescence measured by quantitative PCR reaction with 1 × SYBR Green (Invitrogen), custom-designed primers (Buenrostro et al., 2013) and 2 × NEB MasterMix (New England Labs, M0541). The library was cleaned up with Min-elute PCR kit and quantified using Qubit (Life Technologies, Q32854). The fragment length distribution of the library was determined using an Agilent High Sensitivity DNA D1000 Screentape (5067–5585) system, and the final quantification of the library before pooling was done using a KAPA library amplification kit (Roche Lightcycler 480). The libraries were sequenced on an Illumina Next-Seq 500 using V2 chemistry for 150 cycles (paired-end 75 bp) at NYU Genomics Core facility. The experiments were done in duplicate.

Quantification and Statistical Analysis

RNA-Seq Data Analysis

All RNA-seq fastq files were aligned to the mouse genome (version mm10) using STAR (Dobin et al., 2013) version 2.7.7a with options: `--outFilterMultimapNmax 10 --alignSJoverhangMin 8 --alignSJDBoverhangMin 1 --outFilterMismatchNmax 999 --outFilterMismatchNoverReadLmax 0.2 --alignIntronMin 20 --alignIntronMax 1000000 --alignMatesGapMax 1000000`. Read assignment to genes was performed by the Rsubread (Liao et al., 2019) featureCounts (v2.0.2) command using the GENCODE M20 annotation. DESeq2 (Love et al., 2014) was used to define differentially expressed genes using a *q*-Value cutoff of less than 0.05. K-means clustering was performed using the kmeans package in R. Values of K between 4 and 10 were tested, with 6 offering the best qualitative balance between cluster size and interpretability. Enrichr (Xie et al., 2021) was used to perform gene enrichment analysis. Heatmaps were generated using the ComplexHeatmap (Gu et al., 2016) package in R.

Single-Cell RNA-Seq Data Analysis

Fastq files were generated by using CellRanger (v.2.1.0) from 10x Genomics with default settings[1]. A custom reference genome was generated using the CellRanger mkref function by passing the modified FastA and GTF files as described (Aydin et al., 2019) to distinguish the pooled cell lines by adding exogenous sequences to the mm10 reference genome. CellRanger count function was used to generate single cell feature counts for the library. CellRanger merge function was used to merge datasets. Downstream analyses and graph visualizations were performed in Seurat R package (Butler et al., 2018) (v3). Briefly, we removed the cells that have unique gene counts greater than 6,800 (potential doublets) and less than 200. After removing the unwanted cells, we normalized the data by a global-scaling normalization method (logNormalize) with the default scale factor (10,000). Linear dimensional reduction was performed by PCA, and the clustering was performed by using the statistically significant principal components (identified using the jackStraw method and by the standard deviation of principle components). Seurat objects were integrated by FindIntegrationAnchors and IntegrateData functions as described in this tutorial[2]. The results were visualized using UMAP plots.

ChIP-Seq Data Analysis

All ChIP-seq fastq files were aligned to the mouse genome (version mm10) using Bowtie (Langmead et al., 2009), with only uniquely mapped reads used for analysis. MultiGPS

[1]https://support.10xgenomics.com/single-cell-gene-expression/software/pipelines/latest/what-is-cell-ranger

[2]https://satijalab.org/seurat/v3.0/immune_alignment.html

(Mahony et al., 2014) (version 0.75) was used to define transcription factor DNA binding events, with a cutoff of q-Value < 0.01 (using binomial tests and Benjamini-Hochberg multiple hypothesis correction) for designating statistically significant events. Differential binding analysis between different conditions was also performed with MultiGPS, which uses EdgeR (Robinson et al., 2010) internally. Heatmaps were generated using the Deeptools package (Ramirez et al., 2016). Motifs were identified using MEME-ChIP (version 5.3.3) (Machanick and Bailey, 2011) using default parameters.

Discriminative Motif Analysis

SeqUnwinder (version 0.1.5) (Kakumanu et al., 2017) was used to find motifs that discriminate between Pet1 binding site categories, using parameters: `--threads 4 --win 200 --mink 4 --maxk 5 --r 10 --x 3 --a 400 --hillsthresh 0.1 --memesearchwin 16`, and using MEME version 5.3.3 internally.

ATAC-Seq Data Analysis

All ATAC-seq fastq files were aligned to the mouse genome (version mm10) using Bowtie (Langmead et al., 2009), with only uniquely mapped reads used for analysis. Heatmaps were plotted using Deeptools (Ramirez et al., 2016).

Associations Between Differentially Expressed Genes and Differentially Bound Transcription Factor Binding Sites

The GREAT (McLean et al., 2010) command-line tools were used to define regulatory domains and to assess the associations between ChIP-seq binding locations and differentially expressed genes. The GREAT regulatory domains were defined using the GREAT "basal plus extension" model using settings: basalUpstream = 5000, basalDownstream = 1000, maxExtension = 100000. Overrepresentation was calculated compared to the average & standard deviation of ten sets of randomly selected locations as described previously (Aydin et al., 2019).

DATA AVAILABILITY STATEMENT

The datasets presented in this study can be found in online repositories. The names of the repository/repositories and accession number(s) can be found below: https://www.ncbi.nlm.nih.gov/geo/query/acc.cgi?acc=GSE199315.

AUTHOR CONTRIBUTIONS

BA performed most of the experiments. MS and BA analyzed the data. MM-E and BA made and validated the cell lines with the help of LT and NK. NF, SM, and EM formulated the project and supervised the research. BA, MS, NF, SM, and EM wrote the manuscript. All authors contributed to the article and approved the submitted version.

FUNDING

The research in the Mahony lab was supported by the NIH grant R35GM144135. The research in the Flames lab was supported by ERC-StG- 2011-281920; ERC-Co- 2020-101002203; and PID2020-115635RB-I00. The research in the Mazzoni lab was supported by the NIH/NIA grant 5R21AG067174.

SUPPLEMENTARY MATERIAL

The Supplementary Material for this article can be found online at: https://www.frontiersin.org/articles/10.3389/fnins.2022.903881/full#supplementary-material

Supplementary Figure 1 | (A) Western bot of all inducible lines 48 h after induction revealed with anti-V5 antibody for the last TF in each combination. **(B)** AFPKMs of selected markers. **(C)** Volcano plots of gene expression under various exogenous transcription factor constructs at 48 h and 9 days post-induction. All plots are differential expression compared to embryonic bodies. Dashed lines show the p-Value cutoff (<0.05) and log fold change cutoff (≥ 1.0). Red points pass both cutoffs, blue points pass the p-Value cutoff, green points pass the log fold change cutoff, and gray points pass neither cutoff. Some specific diagnostic genes are labeled and are plotted as a triangle. Plot was made with the R EnhancedVolcano package. **(D,E)** Bulk RNA-seq heatmaps under different exogenous transcription factor constructs at 48 h **(D)** and 9 days **(E)** post-induction. In contrast to the filtered sets of genes shown in **Figure 2**, these plots display a K-means clustering (using the R kmeans function) of all genes that are significantly differentially expressed in one or more conditions. **(F)** Venn diagrams comparing the differential expression of the lines. Red: Genes upregulated, Blue: Genes downregulated.

Supplementary Figure 2 | (A) Motif enrichment at Pet1 binding sites. **(B)** Foxa2 and Pet1 binding distribution.

Supplementary Figure 3 | Lmx1b ChiP-seq analysis.

Supplementary Table 1 | Raw scoring data for **Figure 1**.

Supplementary Table 2 | Genes names for clusters in **Figure 2**.

Supplementary Table 3 | GO terms associated with clusters in **Figure 2** 48 hs.

Supplementary Table 4 | GO terms associated with clusters in **Figure 2** Day 9.

REFERENCES

Aydin, B., Kakumanu, A., Rossillo, M., Moreno-Estelles, M., Garipler, G., Ringstad, N., et al. (2019). Proneural factors Ascl1 and Neurog2 contribute to neuronal subtype identities by establishing distinct chromatin landscapes. *Nat. Neurosci.* 22, 897–908. doi: 10.1038/s41593-019-0399-y

Aydin, B., and Mazzoni, E. O. (2019). Cell reprogramming: the many roads to success. *Annu. Rev. Cell Dev. Biol.* 35, 433–452. doi: 10.1146/annurev-cellbio-100818-125127

Buenrostro, J. D., Giresi, P. G., Zaba, L. C., Chang, H. Y., and Greenleaf, W. J. (2013). Transposition of native chromatin for fast and sensitive epigenomic profiling of open chromatin, DNA-binding proteins and nucleosome position. *Nat. Methods* 10, 1213–1218. doi: 10.1038/nmeth.2688

Busskamp, V., Lewis, N. E., Guye, P., Ng, A. H., Shipman, S. L., Byrne, S. M., et al. (2014). Rapid neurogenesis through transcriptional activation in human stem cells. *Mol. Syst. Biol.* 10:760. doi: 10.15252/msb.20145508

Butler, A., Hoffman, P., Smibert, P., Papalexi, E., and Satija, R. (2018). Integrating single-cell transcriptomic data across different conditions,

technologies, and species. *Nat. Biotechnol.* 36, 411–420. doi: 10.1038/nbt.4096

Caiazzo, M., Dell'Anno, M. T., Dvoretskova, E., Lazarevic, D., Taverna, S., Leo, D., et al. (2011). Direct generation of functional dopaminergic neurons from mouse and human fibroblasts. *Nature* 476, 224–227. doi: 10.1038/nature10284

Castro, D. S., Skowronska-Krawczyk, D., Armant, O., Donaldson, I. J., Parras, C., Hunt, C., et al. (2006). Proneural bHLH and Brn proteins coregulate a neurogenic program through cooperative binding to a conserved DNA motif. *Dev. Cell* 11, 831–844. doi: 10.1016/j.devcel.2006.10.006

Cheng, L., Chen, C. L., Luo, P., Tan, M., Qiu, M., Johnson, R., et al. (2003). Lmx1b, Pet-1, and Nkx2.2 coordinately specify serotonergic neurotransmitter phenotype. *J. Neurosci.* 23, 9961–9967. doi: 10.1523/JNEUROSCI.23-31-09961.2003

Ding, Y. Q., Marklund, U., Yuan, W., Yin, J., Wegman, L., Ericson, J., et al. (2003). Lmx1b is essential for the development of serotonergic neurons. *Nat. Neurosci.* 6, 933–938. doi: 10.1038/nn1104

Dobin, A., Davis, C. A., Schlesinger, F., Drenkow, J., Zaleski, C., Jha, S., et al. (2013). STAR: ultrafast universal RNA-seq aligner. *Bioinformatics* 29, 15–21. doi: 10.1093/bioinformatics/bts635

Donovan, L. J., Spencer, W. C., Kitt, M. M., Eastman, B. A., Lobur, K. J., Jiao, K., et al. (2019). Lmx1b is required at multiple stages to build expansive serotonergic axon architectures. *eLife* 8:e48788. doi: 10.7554/eLife.48788

Farah, M. H., Olson, J. M., Sucic, H. B., Hume, R. I., Tapscott, S. J., and Turner, D. L. (2000). Generation of neurons by transient expression of neural bHLH proteins in mammalian cells. *Development* 127, 693–702. doi: 10.1242/dev.127.4.693

Flames, N., and Hobert, O. (2011). Transcriptional control of the terminal fate of monoaminergic neurons. *Annu. Rev. Neurosci.* 34, 153–184. doi: 10.1146/annurev-neuro-061010-113824

Gu, Z., Eils, R., and Schlesner, M. (2016). Complex heatmaps reveal patterns and correlations in multidimensional genomic data. *Bioinformatics* 32, 2847–2849. doi: 10.1093/bioinformatics/btw313

Hendricks, T., Francis, N., Fyodorov, D., and Deneris, E. S. (1999). The ETS domain factor Pet-1 is an early and precise marker of central serotonin neurons and interacts with a conserved element in serotonergic genes. *J. Neurosci.* 19, 10348–10356. doi: 10.1523/JNEUROSCI.19-23-10348.1999

Hendricks, T. J., Fyodorov, D. V., Wegman, L. J., Lelutiu, N. B., Pehek, E. A., Yamamoto, B., et al. (2003). Pet-1 ETS gene plays a critical role in 5-HT neuron development and is required for normal anxiety-like and aggressive behavior. *Neuron* 37, 233–247. doi: 10.1016/s0896-6273(02)01167-4

Hester, M. E., Murtha, M. J., Song, S., Rao, M., Miranda, C. J., Meyer, K., et al. (2011). Rapid and efficient generation of functional motor neurons from human pluripotent stem cells using gene delivered transcription factor codes. *Mol. Ther.* 19, 1905–1912. doi: 10.1038/mt.2011.135

Iacovino, M., Bosnakovski, D., Fey, H., Rux, D., Bajwa, G., Mahen, E., et al. (2011). Inducible cassette exchange: a rapid and efficient system enabling conditional gene expression in embryonic stem and primary cells. *Stem Cells* 29, 1580–1588. doi: 10.1002/stem.715

Jacob, J., Ferri, A. L., Milton, C., Prin, F., Pla, P., Lin, W., et al. (2007). Transcriptional repression coordinates the temporal switch from motor to serotonergic neurogenesis. *Nat. Neurosci.* 10, 1433–1439. doi: 10.1038/nn1985

Kakumanu, A., Velasco, S., Mazzoni, E., and Mahony, S. (2017). Deconvolving sequence features that discriminate between overlapping regulatory annotations. *PLoS Comput. Biol.* 13:e1005795. doi: 10.1371/journal.pcbi.1005795

Langmead, B., Trapnell, C., Pop, M., and Salzberg, S. L. (2009). Ultrafast and memory-efficient alignment of short DNA sequences to the human genome. *Genome Biol.* 10:R25. doi: 10.1186/gb-2009-10-3-r25

Liao, Y., Smyth, G. K., and Shi, W. (2019). The R package Rsubread is easier, faster, cheaper and better for alignment and quantification of RNA sequencing reads. *Nucleic Acids Res.* 47:e47. doi: 10.1093/nar/gkz114

Lin, H. C., He, Z., Ebert, S., Schornig, M., Santel, M., Nikolova, M. T., et al. (2021). NGN2 induces diverse neuron types from human pluripotency. *Stem Cell Rep.* 16, 2118–2127. doi: 10.1016/j.stemcr.2021.07.006

Lin, W., Metzakopian, E., Mavromatakis, Y. E., Gao, N., Balaskas, N., Sasaki, H., et al. (2009). Foxa1 and Foxa2 function both upstream of and cooperatively with Lmx1a and Lmx1b in a feedforward loop promoting mesodiencephalic dopaminergic neuron development. *Dev. Biol.* 333, 386–396. doi: 10.1016/j.ydbio.2009.07.006

Liu, C., Maejima, T., Wyler, S. C., Casadesus, G., Herlitze, S., and Deneris, E. S. (2010). Pet-1 is required across different stages of life to regulate serotonergic function. *Nat. Neurosci.* 13, 1190–1198. doi: 10.1038/nn.2623

Love, M. I., Huber, W., and Anders, S. (2014). Moderated estimation of fold change and dispersion for RNA-seq data with DESeq2. *Genome Biol.* 15:550. doi: 10.1186/s13059-014-0550-8

Lu, C., Shi, X., Allen, A., Baez-Nieto, D., Nikish, A., Sanjana, N. E., et al. (2019). Overexpression of NEUROG2 and NEUROG1 in human embryonic stem cells produces a network of excitatory and inhibitory neurons. *FASEB J.* 33, 5287–5299. doi: 10.1096/fj.201801110RR

Machanick, P., and Bailey, T. L. (2011). MEME-ChIP: motif analysis of large DNA datasets. *Bioinformatics* 27, 1696–1697. doi: 10.1093/bioinformatics/btr189

Mahony, S., Edwards, M. D., Mazzoni, E. O., Sherwood, R. I., Kakumanu, A., Morrison, C. A., et al. (2014). An integrated model of multiple-condition ChIP-Seq data reveals predeterminants of Cdx2 binding. *PLoS Comput. Biol.* 10:e1003501. doi: 10.1371/journal.pcbi.1003501

Maurer, P., Rorive, S., de Kerchove d'Exaerde, A., Schiffmann, S. N., Salmon, I., and de Launoit, Y. (2004). The Ets transcription factor Fev is specifically expressed in the human central serotonergic neurons. *Neurosci. Lett.* 357, 215–218. doi: 10.1016/j.neulet.2003.12.086

Mazzoni, E. O., Mahony, S., Closser, M., Morrison, C. A., Nedelec, S., Williams, D. J., et al. (2013). Synergistic binding of transcription factors to cell-specific enhancers programs motor neuron identity. *Nat. Neurosci.* 16, 1219–1227. doi: 10.1038/nn.3467

Mazzoni, E. O., Mahony, S., Iacovino, M., Morrison, C. A., Mountoufaris, G., Closser, M., et al. (2011). Embryonic stem cell-based mapping of developmental transcriptional programs. *Nat. Methods* 8, 1056–1058. doi: 10.1038/nmeth.1775

McLean, C. Y., Bristor, D., Hiller, M., Clarke, S. L., Schaar, B. T., Lowe, C. B., et al. (2010). GREAT improves functional interpretation of cis-regulatory regions. *Nat. Biotechnol.* 28, 495–501. doi: 10.1038/nbt.1630

Morris, S. A. (2016). Direct lineage reprogramming via pioneer factors; a detour through developmental gene regulatory networks. *Development* 143, 2696–2705. doi: 10.1242/dev.138263

Parras, C. M., Schuurmans, C., Scardigli, R., Kim, J., Anderson, D. J., and Guillemot, F. (2002). Divergent functions of the proneural genes Mash1 and Ngn2 in the specification of neuronal subtype identity. *Genes Dev.* 16, 324–338. doi: 10.1101/gad.940902

Pattyn, A., Goridis, C., and Brunet, J. F. (2000). Specification of the central noradrenergic phenotype by the homeobox gene Phox2b. *Mol. Cell Neurosci.* 15, 235–243. doi: 10.1006/mcne.1999.0826

Pattyn, A., Simplicio, N., van Doorninck, J. H., Goridis, C., Guillemot, F., and Brunet, J. F. (2004). Ascl1/Mash1 is required for the development of central serotonergic neurons. *Nat. Neurosci.* 7, 589–595. doi: 10.1038/nn1247

Ramirez, F., Ryan, D. P., Gruning, B., Bhardwaj, V., Kilpert, F., Richter, A. S., et al. (2016). deepTools2: a next generation web server for deep-sequencing data analysis. *Nucleic Acids Res.* 44, W160–W165. doi: 10.1093/nar/gkw257

Raposo, A. A., Vasconcelos, F. F., Drechsel, D., Marie, C., Johnston, C., Dolle, D., et al. (2015). Ascl1 coordinately regulates gene expression and the chromatin landscape during neurogenesis. *Cell Rep.* 10, 1544–1556. doi: 10.1016/j.celrep.2015.02.025

Rhee, H. S., Closser, M., Guo, Y., Bashkirova, E. V., Tan, G. C., Gifford, D. K., et al. (2016). Expression of terminal effector genes in mammalian neurons is maintained by a dynamic relay of transient enhancers. *Neuron* 92, 1252–1265. doi: 10.1016/j.neuron.2016.11.037

Robinson, M. D., McCarthy, D. J., and Smyth, G. K. (2010). edgeR: a bioconductor package for differential expression analysis of digital gene expression data. *Bioinformatics* 26, 139–140. doi: 10.1093/bioinformatics/btp616

Smidt, M. P., Asbreuk, C. H., Cox, J. J., Chen, H., Johnson, R. L., and Burbach, J. P. (2000). A second independent pathway for development of mesencephalic dopaminergic neurons requires Lmx1b. *Nat. Neurosci.* 3, 337–341. doi: 10.1038/73902

Smith, D. K., Yang, J., Liu, M. L., and Zhang, C. L. (2016). Small molecules modulate chromatin accessibility to promote NEUROG2-mediated fibroblast-to-neuron reprogramming. *Stem Cell Rep.* 7, 955–969. doi: 10.1016/j.stemcr.2016.09.013

Soufi, A., Garcia, M. F., Jaroszewicz, A., Osman, N., Pellegrini, M., and Zaret, K. S. (2015). Pioneer transcription factors target partial DNA motifs on nucleosomes to initiate reprogramming. *Cell* 161, 555–568. doi: 10.1016/j.cell.2015.03.017

van der Raadt, J., van Gestel, S. H. C., Nadif Kasri, N., and Albers, C. A. (2019). ONECUT transcription factors induce neuronal characteristics and remodel chromatin accessibility. *Nucleic Acids Res.* 47, 5587–5602. doi: 10.1093/nar/gkz273

Vasconcelos, F. F., and Castro, D. S. (2014). Transcriptional control of vertebrate neurogenesis by the proneural factor Ascl1. *Front. Cell Neurosci.* 8:412. doi: 10.3389/fncel.2014.00412

Velasco, S., Ibrahim, M. M., Kakumanu, A., Garipler, G., Aydin, B., Al-Sayegh, M. A., et al. (2017). A multi-step transcriptional and chromatin state cascade underlies motor neuron programming from embryonic stem cells. *Cell Stem Cell* 20, 205.e8–217.e8. doi: 10.1016/j.stem.2016.11.006

Vierbuchen, T., Ostermeier, A., Pang, Z. P., Kokubu, Y., Sudhof, T. C., and Wernig, M. (2010). Direct conversion of fibroblasts to functional neurons by defined factors. *Nature* 463, 1035–1041. doi: 10.1038/nature08797

Wapinski, O. L., Vierbuchen, T., Qu, K., Lee, Q. Y., Chanda, S., Fuentes, D. R., et al. (2013). Hierarchical mechanisms for direct reprogramming of fibroblasts to neurons. *Cell* 155, 621–635. doi: 10.1016/j.cell.2013.09.028

Wyler, S. C., Spencer, W. C., Green, N. H., Rood, B. D., Crawford, L., Craige, C., et al. (2016). Pet-1 switches transcriptional targets postnatally to regulate maturation of serotonin neuron excitability. *J. Neurosci.* 36, 1758–1774. doi: 10.1523/JNEUROSCI.3798-15.2016

Xie, Z., Bailey, A., Kuleshov, M. V., Clarke, D. J. B., Evangelista, J. E., Jenkins, S. L., et al. (2021). Gene set knowledge discovery with enrichr. *Curr. Protoc.* 1:e90. doi: 10.1002/cpz1.90

Xu, L., Chen, X., Sun, B., Sterling, C., and Tank, A. W. (2007). Evidence for regulation of tyrosine hydroxylase mRNA translation by stress in rat adrenal medulla. *Brain Res.* 1158, 1–10. doi: 10.1016/j.brainres.2007.04.080

Xu, Z., Jiang, H., Zhong, P., Yan, Z., Chen, S., and Feng, J. (2016). Direct conversion of human fibroblasts to induced serotonergic neurons. *Mol. Psychiatry* 21, 62–70. doi: 10.1038/mp.2015.101

Yan, C. H., Levesque, M., Claxton, S., Johnson, R. L., and Ang, S. L. (2011). Lmx1a and lmx1b function cooperatively to regulate proliferation, specification, and differentiation of midbrain dopaminergic progenitors. *J. Neurosci.* 31, 12413–12425. doi: 10.1523/JNEUROSCI.1077-11.2011

Zeisel, A., Hochgerner, H., Lonnerberg, P., Johnsson, A., Memic, F., van der Zwan, J., et al. (2018). Molecular architecture of the mouse nervous system. *Cell* 174, 999.e22–1014.e22. doi: 10.1016/j.cell.2018.06.021

Zhang, X. L., Spencer, W. C., Tabuchi, N., Kitt, M. M., and Deneris, E. S. (2022). Reorganization of postmitotic neuronal chromatin accessibility for maturation of serotonergic identity. *eLife* 11:e75970. doi: 10.7554/eLife.75970

Conflict of Interest: The authors declare that the research was conducted in the absence of any commercial or financial relationships that could be construed as a potential conflict of interest.

Publisher's Note: All claims expressed in this article are solely those of the authors and do not necessarily represent those of their affiliated organizations, or those of the publisher, the editors and the reviewers. Any product that may be evaluated in this article, or claim that may be made by its manufacturer, is not guaranteed or endorsed by the publisher.

frontiers | Frontiers in Neuroscience

BRIEF RESEARCH REPORT
published: 21 June 2022
doi: 10.3389/fnins.2022.908719

The E3 Ubiquitin Ligase CRL5 Regulates Dentate Gyrus Morphogenesis, Adult Neurogenesis, and Animal Behavior

*Raenier V. Reyes[1‡], Keiko Hino[1‡], Cesar Patricio Canales[1†], Eamonn James Dickson[2], Anna La Torre[1] and Sergi Simó[1]**

[1] Department of Cell Biology and Human Anatomy, University of California, Davis, Davis, CA, United States, [2] Department of Physiology and Membrane Biology, University of California, Davis, Davis, CA, United States

OPEN ACCESS

Edited by:
Simon Hippenmeyer, Institute of Science and Technology Austria (IST Austria), Austria

Reviewed by:
Isabel Martinez Garay, Cardiff University, United Kingdom
Yves Jossin, Catholic University of Louvain, Belgium

***Correspondence:**
Sergi Simó
ssimo@ucdavis.edu

†Present addresses:
Cesar Patricio Canales, Department of Psychiatry and Behavioral Sciences, University of California, Davis, Davis, CA, United States;
Department of Neurobiology, Physiology and Behavior, University of California, Davis, Davis, CA, United States

‡These authors share first authorship

Specialty section:
This article was submitted to Neurogenesis, a section of the journal Frontiers in Neuroscience

Received: 30 March 2022
Accepted: 19 May 2022
Published: 21 June 2022

Citation:
Reyes RV, Hino K, Canales CP, Dickson EJ, La Torre A and Simó S (2022) The E3 Ubiquitin Ligase CRL5 Regulates Dentate Gyrus Morphogenesis, Adult Neurogenesis, and Animal Behavior. Front. Neurosci. 16:908719. doi: 10.3389/fnins.2022.908719

The dentate gyrus (DG) is an essential part of the hippocampal formation and participates in the majority of hippocampal functions. The DG is also one of the few structures in the mammalian central nervous system that produces adult-born neurons and, in humans, alterations in adult neurogenesis are associated with stress and depression. Given the importance of DG in hippocampal function, it is imperative to understand the molecular mechanisms driving DG development and homeostasis. The E3 ubiquitin ligase Cullin-5/RBX2 (CRL5) is a multiprotein complex involved in neuron migration and localization in the nervous system, but its role during development and in the adult DG remain elusive. Here, we show that CRL5 participates in mossy fiber pruning, DG layering, adult neurogenesis, and overall physical activity in mice. During DG development, RBX2 depletion causes an overextension of the DG mossy fiber infrapyramidal bundle (IPB). We further demonstrate that the increased activity in Reelin/DAB1 or ARF6 signaling, observed in RBX2 knockout mice, is not responsible for the lack of IPB pruning. Knocking out RBX2 also affects granule cell and neural progenitor localization and these defects were rescued by downregulating the Reelin/DAB1 signaling. Finally, we show that absence of RBX2 increases the number neural progenitors and adult neurogenesis. Importantly, RBX2 knockout mice exhibit higher levels of physical activity, uncovering a potential mechanism responsible for the increased adult neurogenesis in the RBX2 mutant DG. Overall, we present evidence of CRL5 regulating mossy fiber pruning and layering during development and opposing adult neurogenesis in the adult DG.

Keywords: CRL5, RBX2, adult neurogenesis, mossy fibers, dentate gyrus development

INTRODUCTION

Dentate gyrus (DG) morphogenesis is a complex process that requires the coordination of neural stem cell (NSC) and intermediate progenitor (IP) proliferation, neurogenesis, and cell migration to form the well-known arrowhead, laminated structure within the hippocampus (Khalaf-Nazzal and Francis, 2013; Nelson et al., 2020). The principal neurons in the DG are granules cells (GCs),

located in the granule cell layer (GCL), and IPs and NSCs below the GCs in the subgranular zone (SGZ). Importantly, the NSCs produce adult-born GCs throughout the lifespan of many animals (Goncalves et al., 2016). In humans, defects in DG development or homeostasis cause a variety of diseases, including epilepsy and mood affective disorders (Hayashi et al., 2018; Santos et al., 2019).

The murine DG development starts at embryonic day (E) 13 by the first generation of immature GCs, IPs, and NSCs in the ventricular zone area known as dentate notch (i.e., Primary germinative matrix). This mix of post-mitotic and progenitor cells migrate, and divide, in their way to the DG primordium and migrate around the hippocampal fissure to stablish the upper blade of the DG, first, and the lower blade, afterward. Finally, a tertiary germinative matrix located in the hilar area will generate GC for the inner leaflet of the GCL and the NSCs for the SGZ (Altman and Bayer, 1990; Khalaf-Nazzal and Francis, 2013; Hayashi et al., 2015; Nelson et al., 2020).

In comparison to the cortex, fewer signaling pathways have been studied in the context of DG development. Among the few, the Reelin/DAB1 signaling pathway has been shown to be indispensable for migration directionality of GC, and likely of IPs and NSCs, at late DG migratory stages (Li et al., 2009; Wang et al., 2018). Importantly, a combination of Reelin/DAB1 and Notch signaling is necessary for radial glia scaffolding, contributing to proper cell migration and DG development (Sibbe et al., 2009; Brunne et al., 2013). Moreover, Reelin/DAB1 signaling positively correlates with adult neurogenesis in gain- and loss-of-function mouse models (Pujadas et al., 2010; Teixeira et al., 2012).

The E3 ubiquitin ligase Cullin-5/RING ligase (CRL5) is a multiprotein complex nucleated around the core proteins Cullin-5 (Cul5) and RING box protein 2 (RBX2; also known as RNF7). CRL5 uses up to 38 different substrate adaptors to recruit target proteins to the complex for ubiquitylation (Okumura et al., 2016). In the central nervous system, CRL5 contributes to neuron migration and localization, neuronal layering, and dendritogenesis (Simo and Cooper, 2013; Fairchild et al., 2018; Han et al., 2020). Two CRL5-regulated signaling pathways are mainly associated with these phenotypes, the Reelin/DAB1 and ARL4C/ARF6 signaling. Knocking out of RBX2 causes ectopic cortical layering and the accumulation of signaling effectors and among them the active, tyrosine-phosphorylated DAB1 (pY-DAB1). Reduction of DAB1 accumulation partially rescues the cortical layering phenotypes caused by RBX2 depletion. Moreover, knocking out SOCS7, a CRL5 substrate adaptor that binds and recruits pY-DAB1 for poly-ubiquitylation, causes a similar pY-DAB1 accumulation and cortical disruption as RBX2 depletion without affecting other CRL5-dependent signaling effectors (Simo and Cooper, 2013; Han et al., 2020). In the hippocampus, CRL5 also regulates neuron polarity and dendritogenesis by opposing the activity of the small GTPases ARL4C and ARF6 (Hofmann et al., 2007; Han et al., 2020). However, the role of CRL5 in DG development and adult neurogenesis remains elusive. Here, we show that CRL5 participates in developmental GC axon (i.e., mossy fibers) pruning, independently of Reelin/DAB1 or ARF6 activity. Moreover, CRL5 controls the number of NSCs and the lamination of GCs, IPs, and NSCs, in part through the downregulation of Reelin/DAB1 signaling. Finally, we show that CRL5 regulates adult neurogenesis, likely by promoting higher levels of physical activity.

METHODS

Animals

All animals were used with the approval from the University of California, Davis Institutional Animal Care and Use Committees and housed in accordance with the guidelines provided by the National Institute of Health. Control (*rbx2 fl/fl*), Rbx2cKO-Emx1 (*rbx2 fl/fl; Emx1-Cre*), *dab1* and *socs7* knockout mice were obtained as described in Simo and Cooper (2013), Fairchild et al. (2018), and Han et al. (2020). To generate the RBX2; NestinCREERT2; Ai9 mice, me crossed *rbx2 fl/fl* mice with the Cre-reporter Ai9 mice [*Gt(ROSA)26Sor*$^{TM9(CAG-tdTomato)Hze}$, The Jackson Laboratory #7909; Madisen et al., 2010] until homozygosis for both genes. We also crossed RBX2 floxed mice with *Nestin-Cre/ERT2* transgenic mice (The Jackson Laboratory #16261; Lagace et al., 2007) to obtain *rbx2 fl/+; Nestin-Cre/ERT2* mice. Finally, we intercrossed *rbx2 fl/fl; Ai9/Ai9* mice with *rbx2 fl/+; Nestin-Cre/ERT2* mice to obtain control (*rbx2 fl/+ ; Ai9/+ ; Nestin-Cre/ERT2*) and tamoxifen-induced RBX2 knockout NSCs (*rbx2 fl/fl; Ai9/+ ; Nestin-Cre/ERT2*). To generate double RBX2 and ARF6 conditional knockout mice, we obtained Arf6 floxed mice (*Arf6*$^{tm1.1Gdp}$, The Jackson Laboratory #28669; Marquer et al., 2016), and crossed it with Rbx2cKO-Emx1 mice until homozygosis of *rbx2* and *arf6* floxed alleles and heterozygosis of the Emx1-Cre allele. When embryonic samples were required, females were mated, and the morning a vaginal plug was observed was considered P0.

Histology and Immunofluorescence

Postnatal (P) 21 and P75 mice were anesthetized and transcardially perfused with phosphate-buffered saline (PBS) followed by 3.7% formalin/PBS using a peristaltic pump. Perfused brains were collected and postfixed at 4°C overnight in the same solution. Tissues were cryoprotected with 30% sucrose/PBS solution. Next, brains were embedded in Optimum Cutting Temperature (OCT) compound (Tissue-Tek) and quickly frozen using dry-ice. OCT-embedded brain blocks were cryo-sectioned on a coronal plane (30 μm). Immunostainings were performed in free-floating sections with agitation. First, sections were antigen retrieved with 10 mM sodium citrate (pH 6) at 95°C for 20'. Then, tissue was blocked with PBS, 0.5% Triton X-100, and 5% milk or 10% normal donkey serum for 1 h at room temperature. Blocking solution, but reducing Triton X-100 concentration to 0.3%, was used for primary antibody incubation (overnight, 4°C). The following primary antibodies were used for immunohistochemistry: anti-Calbindin (1/10; NeuroMab #73-452), anti-Calbindin (1/200; Sigma-Aldrich #C9848), TUJ1 (1/500; Biolengend #801201), anti-DCX (1/200; Santa Cruz Biotechnology #sc-8066, discontinued), anti-SOX2 (1/200; Santa Cruz Biotechnology #sc-17320, discontinued); anti-Ki-67 (1/200; Biolegend #151202); anti-DAB1 (1/200; Sigma-Aldrich

#HPA052033). Species-specific Alexa Fluor 488- and/or 568-conjugated immunoglobulin G (IgG) (1/200; Life Technologies) were used in blocking solution but reducing Triton X-100 concentration to 0.3% (90 min, room temperature). DAPI (Sigma-Aldrich) was used for nuclear staining. Images were taken in a Fluoview FV3000 confocal microscope (Olympus) or Axio Imager.M2 with Apotome.2 microscope system (Zeiss). All images were assembled by using FIJI and Photoshop and Illustrator (Adobe).

Infrapyramidal Bundle Length Measurement

We measured the length of the IPB and *stratum pyramidale* of 3 brain slices, 100 μm apart, per brain, normalized the IPB length to the length of the *stratum pyramidale* in each slice, and average the results to obtain the normalized IPB length per brain. For consistency, we only measure IPB length in brain slices containing dorsal (septal) hippocampi.

Dentate Gyrus Explants

DG explants were obtained from E18 control and RBX2cKO-Emx1 brains using a previously published protocol (Gil and del Rio, 2012). DG explants were co-culture with HEK293T cell aggregates expressing mock (pCAG-EGFP) or Semaphorin-3F expression plasmid in three dimension collagen (Thermo Fisher Scientific, #A1048301) matrices for 96 h. Afterward, explants were fixed and immunostained using an anti-β-III-Tubulin antibody (1/200, Biolegend #801201) and Alexa Fluor-488 secondary antibody (1:200; Life Technologies). Images were taken in a Fluoview FV3000 confocal microscope (Olympus). To quantify axonal growth each explant was divided into four quadrants and the number of axons that crossed a line placed at a distance of 100 μm from the limit of the explant was counted for the proximal and distal quadrants. The proximal/distal (P/D) ratio of axonal growth was obtained by dividing the β-III-tubulin fluorescent signal intensity in the proximal quadrant by that in the distal quadrant; yields 1 for radial growth, more than 1 for attractive effect and less than 1 for repulsive effect.

RAC1/CDC42/RHO Pull Down Assay

The hippocampal regions of control or RBX2cKO–Emx1 mice (P21) were carefully dissected and lysed in lysis buffer (50 mM HEPES, 150 mM NaCl, 1.5 $MgCl_2$, 1 mM EGTA, 10% Glycerol, 1% Triton X-100, and a protease and phosphatase inhibitors). Protein lysate were clear out of cellular debris by centrifugation. Protein supernatant were mixed with purified fusion proteins containing GST-hPAK1-PBD (RAC1 and CDC42 pull down) or GST-Rhotekin-RBD (RHO pull down) for 3 h at 4°C (de Rooij and Bos, 1997). GST-fused proteins and associated small GTPases were pull-down using Glutathione-Sepharose beads (Santa Cruz Biotechnology, #sc-2003). Beads were washed four times with cold lysis buffer and samples were resolved by SDS-polyacrylamide gels. Western blot analysis was performed as described in Han et al. (2020) using anti-RAC1, anti-CDC42, and anti-RHO antibodies (1/1,000, Santa Cruz Biotechnology, #sc-514583, #sc-390210, and #sc-418, respectively) to detect pulled down proteins and RAC1 in whole lysates. Pull down constructs were a generous gift from Dr. Jonathan Chernoff (Addgene plasmid #12217) and Dr. Martin Schwartz (Addgene plasmid #15247, Ren et al., 1999).

Protein Analysis

P10 hippocampal samples from control (RBX2 fl/fl), Rbx2cKO-Emx1, SOCS7 +/–, and SOCS7 −/− mice were lysed in lysis buffer, resolved in SDS-polyacrylamide gels, and analyzed by Western blotting, as previously described. Blots were probed with anti-phosphotyrosine 4G10 (1/5,000; Millipore #05-321), then stripped and reprobe for DAB1 protein (1/5,000; Rockland #100-401-225).

Open Fields Test

The open field test was performed and analyzed as described elsewhere (Silverman et al., 2011). Briefly, individual mice were placed in a VersaMax Animal Activity Monitoring System (AccuScan Instruments, Columbus, OH, United States) for a 30-min test session. The testing room was illuminated with overhead lighting at ∼ 30 lx. The chambers consisted of clear Plexiglas sides and floor, approximately 40 × 40 × 30.5 cm. Mice were placed in the center of the open field at the initiation of the testing session. Photocells at standard heights for recording activity were aligned 8 to a side, dividing the chamber into 64 equal squares. Each time an animal crossed a photoelectric beam it counted as an "event". Horizontal activity (events), total distance (cm), vertical activity (events), and center time (sec.) were automatically collected using the Versamax activity monitor and analyzer software system. Test chambers were cleaned with 70% ethanol between test subjects. At least 5 min between cleaning and the start of the next session was allowed for ethanol evaporation and odor dissipation.

Tamoxifen Injection and tdTomato + cells Quantification

P30 *rbx2 fl/+; Ai9/+; Nestin-Cre/ERT2* and *rbx2 fl/fl; Ai9/+; Nestin-Cre/ERT2* mice were intraperitoneally injected with 80 mg/kg body weight of Tamoxifen, dissolved in 1:20 solution of EtOH and corn oil (Feil et al., 2009), for 5 consecutive days. 30 days after the last injection, animals were transcardially perfused and processed for cryosection as described. Brains were section at 30 μm and all slices containing hippocampus were collected and mounted in stereological fashion. Brain slices were counterstained with DAPI and images of the whole DG in both hemispheres were taken with an Axio Imager.M2 with Apotome.2 microscope system (Zeiss). We quantified all *Ai9*+ cells in both DG per brain. *Ai9*+ cells outside the DG proper were not quantified.

EdU Injection and Granule Cell Survival

P21 control and Rbx2cKO-Emx1 mice were injected with 12.5 mg/kg body weight of EdU (Click-iT EdU Imaging Kit, Life Technologies). 6 months post-injection, animals were processed as described and EdU detected following the manufacturer instructions.

Statistics

Statistical analyses were performed with Prism 9 (GraphPad Software). Statistical analysis used for each experiment is described in the corresponding figure legend. For parametric sample distribution, unpaired Student's *t*-test was used for two-population comparison and one-way ANOVA with Tukey's *post-hoc* test for multiple comparisons. For the open field test result analysis, we used two-way ANOVA Tukey's *post-hoc* test for multiple comparisons, except for the total activity were an unpaired Student's *t*-test was used. For non-parametric sample distribution, Mann Whitney test was used for two-population comparison.

RESULTS

CRL5 Promotes Mossy Fiber Pruning in the Developing Dentate Gyrus

To investigate the role of CRL5 during DG development, we conditionally depleted RBX2 in the telencephalon by intercrossing *rbx2* floxed mice with an *Emx1*-Cre driver mouse (Rbx2cKO-Emx1 mice), which readily depletes RBX2 and disrupts CRL5 activity from embryonic day (E)10 (Gorski et al., 2002; Han et al., 2020). Rbx2cKO-Emx1 mice are born at expected Mendelian rations, thrive as control littermates (*rbx2 fl/fl*), and survive until adulthood. To assess gross DG morphological defects, we stained control and Rbx2cKO-Emx1 samples against calbindin (CalB), which labels mature GCs, including GC axons (i.e., mossy fibers), at postnatal day (P)21 (**Figure 1A**). As expected, control brains showed two CalB+ axon bundles departing the DG, the long suprapyramidal bundle (SPB), which forms the *stratum lucidum* in the CA3, and the short infrapyramidal bundle (IPB) that after exiting the DG rapidly crosses the *stratum pyramidale* and joins the SPB (Bagri et al., 2003; Khalaf-Nazzal and Francis, 2013). In comparison, depletion of RBX2 caused an overextension of the mossy fiber IPB, reaching the apex of the CA3 curvature (**Figures 1A,B**). During development, SPB and IPB mossy fibers initially extend above and below the *stratum pyramidale* of the CA3, respectively, and during postnatal stages the IPB prunes almost completely, cross the *stratum pyramidale*, and joins the SPB (Bagri et al., 2003). First, we tested whether the IPB extension defects observed in RBX2 mutant animals were a temporal delay in axon pruning. Control and RBX2 mutant DG were collected at P75, a stage when IPB pruning is long completed, and stained against CalB. Similar IPB overextension was present in Rbx2cKO-Emx1 brains, highlighting a novel role for CRL5 in IPB pruning (**Figure 1B** and **Supplementary Figure 1A**). We hypothesized that signaling pathways deregulated in the RBX2 mutant brain may be responsible for this phenotype. Thus, we assessed whether sustained Reelin/DAB1 or ARF6 activation were responsible for IPB overextension. To test the role of sustained Reelin/DAB1 signaling in IPB pruning, we used Rbx2cKO-Emx1; DAB1 +/– mice, which significantly reduces the accumulation of pY-DAB1, and SOCS7 knockout mice, which promotes pY-DAB1 accumulation without affecting other CRL5-regulated signaling effectors (**Supplementary Figure 2**; Simo and Cooper, 2013; Han et al., 2020). Accumulation of pY-DAB1 in the SOCS7 mutant DG was not sufficient to cause IPB overextension and reducing DAB1 levels in Rbx2cKO-Emx1 failed to rescue IPB overextension (**Supplementary Figures 1B,C**). Next, we generated a new mutant mouse conditionally targeting RBX2 and ARF6 using the Emx1-CRE driver (RBX2/ARF6cKO-Emx1) and analyzed its IPB. Depleting ARF6 did not rescue IPB overextension cause by CRL5 inactivation (**Supplementary Figure 1D**). Interestingly, in all the conditions where we observed IPB overextension, there was also a complementary thinning of the SPB, due to the absence of IPB axons bundling with the SPB.

IPB overextension was previously described in mutant animals for the Semaphorin-3F co-receptors Neuropilin-2 and Plexin-3A (Chen et al., 2000; Cheng et al., 2001). Furthermore, Bagri et al. (2003) showed that, at postnatal stages, Sempahorin-3F secretion from neuropeptide Y-expressing interneurons drives IPB mossy fiber pruning. Next, we assessed whether RBX2 mutant GC axons were able to sense and respond to Sempahorin-3F using an axon repulsion assay. DG explants were obtained from control and Rbx2cKO-Emx1 embryos at E18 and co-cultured with HEK293T cells expressing either a mock plasmid (pCAG-EGFP) or Semaphorin-3F-expressing plasmid. In comparison to mock plasmid, expression of Semaphorin-3F trigger a strong repulsion of GC axons in both control and RBX2 mutant DG explants, indicating that RBX2 mutant GC axons respond to Semophorin-3F as controls (**Figures 1C,D**). Despite we have not tested the expression of Semaphorin-3F in our mutant animals, interneurons are not targeted by the Emx1-Cre strain used in our experiments (Gorski et al., 2002) and therefore we do not expect any defects on interneuron genesis, localization, or maturation.

At the molecular level, IPB pruning depends on activation of the RAC-GAP protein β2-Chimaerin and, consequently, inactivation of the Rac small GTPase family (Riccomagno et al., 2012). Surprisingly, pull-down assays using the p21-binding domain (PBD) of PAK1 showed that in RBX2 mutant samples RAC1-GTP and Cdc42-GTP levels are lower than control, while the activity of the RHOA GTPase remain unaffected (**Figure 1E**). These data suggest that CRL5-dependent deregulation of RAC1 and/or CDC42 activity may be responsible for the lack of IPB pruning observed in the RBX2 mutant DG.

CRL5 Regulates Dentate Gyrus Lamination and Adult Neurogenesis

CalB staining also revealed dramatic layering defects in the DG of Rbx2cKO-Emx1 mice (**Figure 1A**). To further investigate this phenotype, we analyzed the distribution of mature GCs (CalB+), immature GCs/IPs (DCX+), and type-1/2a NSCs (SOX2+) in P21 control and RBX2 mutant DGs (Brown et al., 2003; Hsieh, 2012; Goncalves et al., 2016). As expected from control DGs, the majority of CalB+ somas located in the outer-half of the of granule cell layer (GCL), and the DCX+ cells and SOX2+ NSCs in the subgranular zone (SGZ) (**Figures 2A,E–G**). In comparison, knocking out RBX2 completely disrupted DG layering with CalB+ neurons located in all layers of the DG, including the

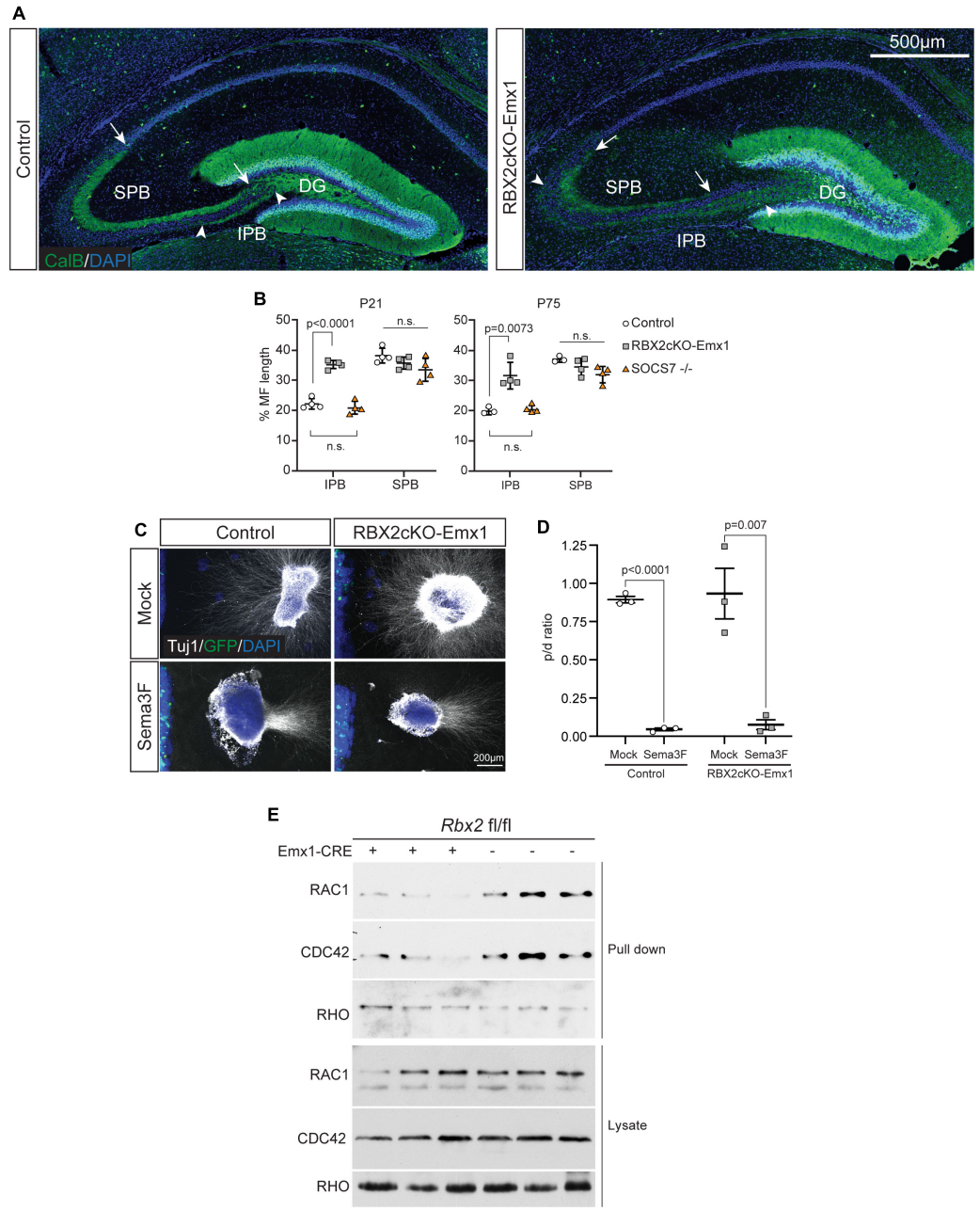

FIGURE 1 | RBX2 participates in mossy fiber IPB pruning. **(A)** IPB overextension in the RBX2cKO-Emx1 mice at P21. Stainings of control and RBX2cKO-Emx1 DG showed a similar extension of mossy fiber SPB (arrows demarcate SPB extension), whereas mossy fiber IPD was ectopically extended in the RBX2 mutant DG (arrowheads demarcate IPB extension). **(B)** Quantification of IPB extension in control, RBX2cKO-Emx1, and SOCS7 knock out (–/–) DG at P21 (left) and P75 (right). Mean ± SEM. Statistics, one-way ANOVA with Tukey's method adjusted *p*-value. **(C)** Axons from E18.5 control and RBX2 mutant DG explant were repelled when confronted with a source of Semphorin-3F (Sema3F). Notice the HEK293T cell aggregate transfected with control plasmid or Sema3F-expressing plasmid on the left hand side of the image. For quantification, DG explants were divided in four quadrants and β-III-Tubulin fluorescent signal measured in proximal (in front of the cell aggregate) and distal (opposite) quadrants. **(D)** The ratio of proximal and distal (p/d) showed that both control and Rbx2 mutant DG axons were repelled by Sema3F. Mean ± SEM. Statistics, unpaired Student's *t*-test. **(E)** Decreased RAC1-GTP and CDC42-GTP levels upon RBX2 depletion in comparison to control. RHO-GTP levels remained unaffected.

hilus, and DCX+ and SOX2+ cells displaced from the SGZ (**Figures 2B,E–G**).

Given that Reelin/DAB1 signaling is important for DG layering and reducing DAB1 levels partially rescues the layering phenotypes in the RBX2 mutant cortex (Simo and Cooper, 2013), we assessed whether sustained Reelin/DAB1 signaling was also responsible for the DG layering defects observed upon RBX2 depletion. We analyzed the DG layering in Rbx2cKO-Emx1;

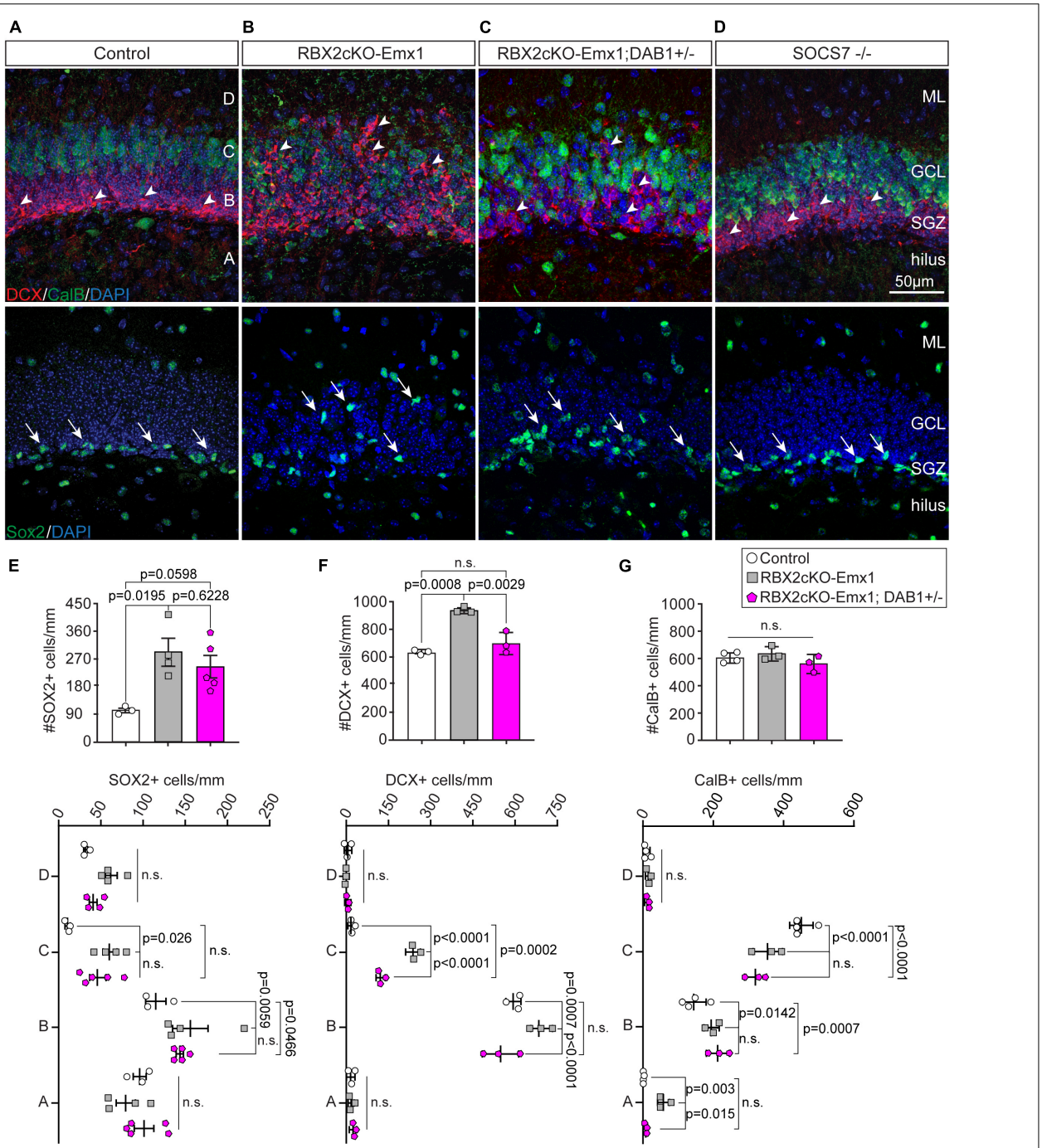

FIGURE 2 | RBX2 regulates layering during DG development and controls NSC proliferation. **(A,B)** Depletion of RBX2 disrupted the localization of Doublecortin (DCX)+ (arrowheads) and calbindin (CalB)+ cells in comparison to control DG at P21. Similarly, SOX2+ NSCs, which normally locate in the subgranular zone (SGZ), were displaced to other areas of the DG upon RBX2 depletion. **(C)** Reducing DAB1 accumulation partially rescued the localization defects of DCX+ cells caused by knocking out RBX2, whereas it had little effect in CalB+ and SOX2+ cells. **(D)** Knocking out SOCS7 did not affect the neuron localization and layering in the DG. Total number (top) and layer distribution (bottom) of SOX2+ **(E)**, DCX+ **(F)**, and CalB+ **(G)** cells in the DG. The DG was divided in four layers as shown in **(A)**. Mean ± SEM. Statistics, one-way ANOVA with Tukey's method adjusted *p*-value for total number of cell analyses and two-way ANOVA with Tukey's method adjusted *p*-value for layering analyses. ML, molecular layer; GCL, granule cell layer.

DAB1 +/– mice, in which pY-DAB1 levels are significantly reduced, and in SOCS7 –/– mice, in which pY-DAB1 accumulates (**Supplementary Figure 2**). Reducing pY-DAB1 levels partially rescued the misposition of DCX+ cells, whereas it failed to rescue ectopic SOX2+ and CalB+ cells (**Figures 2C,F,G**). Moreover, accumulation of pY-DAB1, in SOCS7 –/– mice,

was not sufficient to cause any layering defects (**Figure 2D**). Interestingly, knocking down RBX2 and ARF6 worsen the layering phenotypes with further displacement of CalB+ GCs in the molecular layer (ML) and hilus (**Supplementary Figures 1D,D'**), a phenotype previously observed in hippocampal pyramidal neurons (Han et al., 2020).

Importantly, depletion of RBX2 increased the number of SOX2+ and DCX+ cells in the hippocampus in comparison to control (**Figures 2E,F**). However, only the increment of DCX+ cells was abolished when DAB1 levels were rescued, whereas the number of SOX2+ cells failed to change between control and Rbx2cKO-Emx1; DAB1 +/– (**Figure 2F**). No differences in the amount of mature granule cells were detected in any condition (**Figure 2G**). An increased number of DCX+ cells suggests that RBX2 depletion promotes NSC proliferation in the DG. To assess this possibility, we stained control and Rbx2cKO-Emx1 brains with the cell cycle marker Ki-67 (Peissner et al., 1999). In comparison to controls, RBX2 mutant hippocampus showed a significant increase in Ki-67+ cells at P10, P21, and in adult DGs, albeit at progressively lower levels as animals aged (**Figures 3A,B,E–G**; Kuhn et al., 1996). Given that Reelin/DAB1 signaling promotes adult neurogenesis (Pujadas et al., 2010; Teixeira et al., 2012) and reduction of DAB1 levels rescued the number of DCX+ cells in the RBX2 mutant DG (**Figure 2F**), we hypothesized that sustained Reelin/DAB1 signaling was responsible for the increased cell proliferation in absence of CRL5 activity. To test this possibility, we analyzed the number of actively proliferating cells in RBX2cKO-Emx1; DAB1 +/– and SOCS7 mutant DGs. Whereas reducing DAB1 levels in the RBX2 mutant hippocampus rescues the number of proliferating cells, depletion of SOCS7 promoted a similar increase in the number of Ki-67+ cells in the DG as observed in RBX2 mutant mice (**Figures 3C,D,F,H**). Despite the increased proliferation rate, we did not observe an obvious change in DG size between control and RBX2 mutant DG. This prompted us to analyze the survival rate of adult-born GCs in absence of CRL5 activity by injecting the thymidine-analog EdU at P21 in control and RBX2cKO-Emx1 mice and counting the number of EdU+ cells present in the DG after 6 month. We found less EdU+ cells in the RBX2 mutant DG, suggesting either a decrease in GC survival or an increase in NSC proliferation without neurogenesis (e.g., NSC self-renewal) (**Supplementary Figure 3A**).

We further investigated the direct role of RBX2 promoting NSC proliferation and adult neurogenesis. We crossed our *rbx2* floxed animals with *Nestin-Cre/ERT2* mice, which express tamoxifen-inducible Cre in adult NSCs, and the Cre-reporter mice Ai9 (Lagace et al., 2007; Madisen et al., 2010). Rbx2 fl/fl; Ai9/+; Nestin-Cre/ERT2 or control (control mice had only one *rbx2* allele floxed) littermates were treated with tamoxifen at P30 and brains were collected 30 days post treatment. Surprisingly, no significant differences in the number of tdTomato+ cells were observed between control and RBX2-depleted brains (**Supplementary Figure 3B**). These data indicates that depletion of RBX2 in NSCs at juvenile stages is not sufficient to promote NSC proliferation and neurogenesis.

Increased Motor Activity in Rbx2cKO-Emx1 Mice

Among the factors that most highly correlate with increased adult neurogenesis is physical exercise (Goncalves et al., 2016; Saraulli et al., 2017). To test whether RBX2 depletion affects mouse behavior, particularly mouse physical activity, we performed open field tests with adult control and Rbx2cKO-Emx1 mice (P75). Depletion of RBX2 significantly increased overall mouse activity (**Figure 4**). Both horizontal and vertical (i.e., rearing) activity, as well as total distance travel were increased in Rbx2cKO-Emx1 females and males. No differences in the amount of time spent in the center of the field were observed between genotypes or gender (**Figure 4**), excluding anxiety-related differences. Importantly, the increased activity in RBX2 mutant mice was observed in all time bins analyzed, suggesting that changes in exploratory drive or anxiety, mostly shown during the first minutes of the test, are not the principal drivers for the phenotypes observed (Gould et al., 2009). Overall, our data indicate that CRL5 regulates mouse activity, which in turn may promote the increase in NSC proliferation observed in the adult RBX2 mutant DG.

DISCUSSION

DG morphogenesis requires the timely activation of myriad of signaling pathways and the interaction of multiple cell types in a coordinated fashion (Frotscher et al., 2003; Li and Pleasure, 2007; Cayre et al., 2009; Li et al., 2009; Sibbe et al., 2009; Wang et al., 2018; Nelson et al., 2020). Whereas much progress has been made in understanding the molecular mechanisms involved in cortical projection neuron migration and cortical layering, fewer studies address the molecular complexity underlying DG development. Moreover, the importance of signal termination for DG morphogenesis or homeostasis, including adult neurogenesis, remains for the most part unknown.

Our results show that CRL5 participates in mossy fibers IPB pruning. Genetic depletion of RBX2, which renders CRL5 complex inactive, disrupts IPB pruning causing IPB overextension. These axonal defects were not related to CRL5-dependent regulation of Reelin/DAB1 or ARF6 signaling, as reducing DAB1 levels or knocking out ARF6 in the context of RBX2 depletion failed to rescue IPB pruning. RBX2 mutant GC axons were capable to respond to Semaphorin-3Y in a common axon repulsion assay (Chen et al., 2000; Cheng et al., 2001), indicating their capability of sensing Sempahorin-3Y through Plexin-A3 and Neuropilin-2 co-receptors and triggering the appropriate signaling pathways despite CRL5 inactivation (Zhou et al., 2008). In comparison to axon repulsion where the signaling cascade is triggered by Plexin-A3, Sempahorin-3Y-dependent mossy fiber pruning initiates at Neuropilin-2 by the recruitment of the RAC GAP β2-Chimaerin and triggering the inhibition of RAC1 (Riccomagno et al., 2012). Interestingly, another molecular mechanism where Ephrin-B3 reverse signaling leads to activation of RAC1 (i.e., higher RAC1-GTP levels) prior IPB pruning has been described (Xu and Henkemeyer, 2009). Our results show that IPB pruning is blocked in absence of CRL5 activity and the levels of RAC1-GTP and CDC42-GTP are lower than

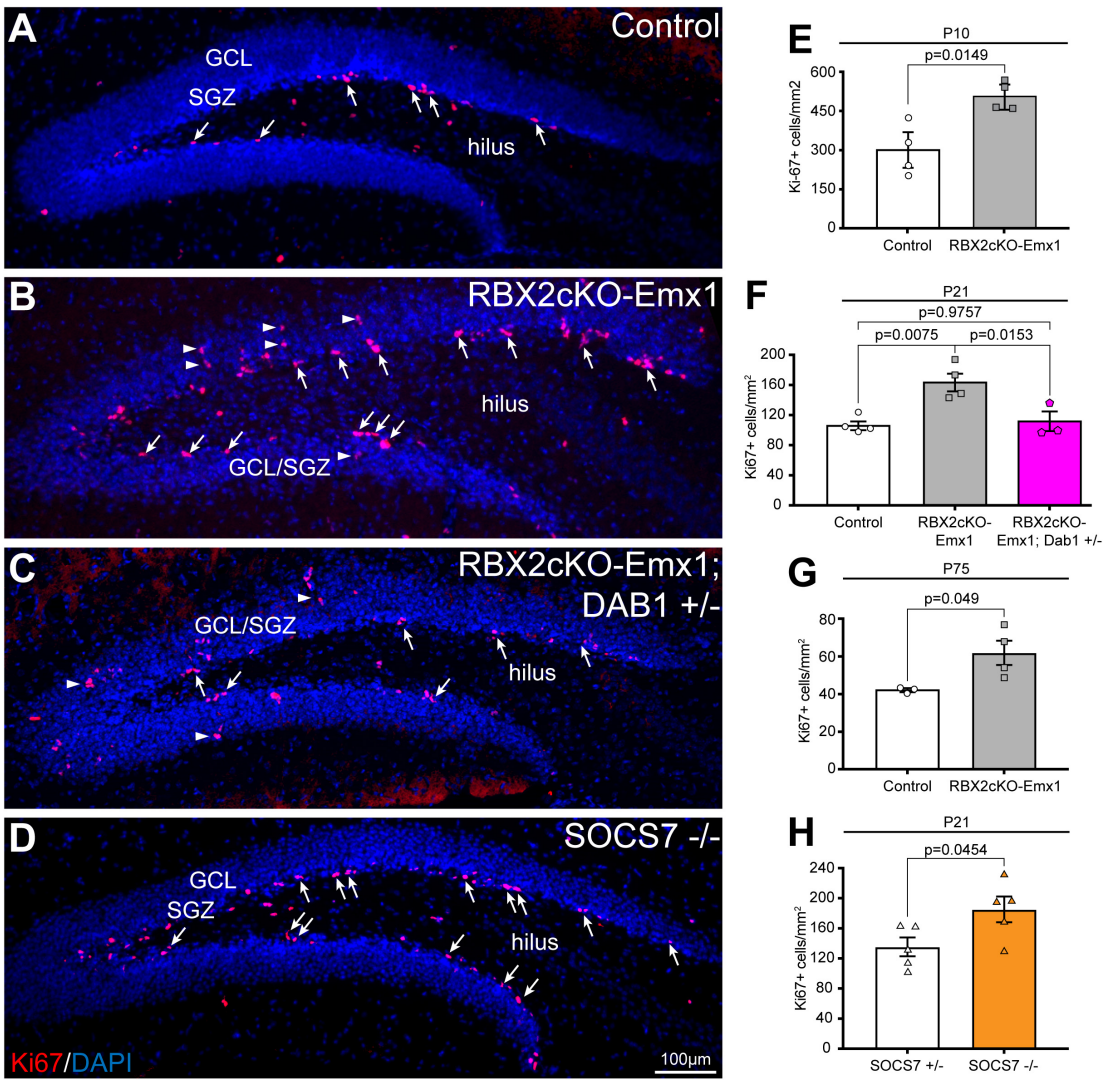

FIGURE 3 | RBX2 controls NSC proliferation in a Reelin/Dab1-dependent fashion. **(A,B)** Knocking out RBX2 promoted NSC proliferation, detected by Ki-67 staining (arrows), in comparison to control DG at P21. Arrowheads indicate Ki-67+ cells away from the innermost layer in the DG **(C)** reducing DAB1 levels in the RBX2 mutant DG rescues cell proliferation. **(D)** SOCS7 depletion showed the same levels of Ki-67+ cells (arrows). **(D–F)** Quantification of Ki-67+ cells in control (*Rbx2 fl/fl*) vs. RBX2cKO-Emx1 DG at P10 **(E)**, P21 also including RBX2cKO-Emx1; DAB1 +/– quantification **(F)**, P75 **(G)**, and of control (SOCS7+/–) and SOCS7 mutant (SOCS7–/–) DG at P21 **(H)**. Mean ± SEM. Statistics, unpaired Student's *t*-test **(E,G,H)** and one-way ANOVA with Tukey's method adjusted *p*-value **(F)**.

control. Thus, our data suggest that CRL5 may participate on IPB pruning in a similar manner as Ephrin-B3 reverse signaling. It is possible that both signaling pathways dial in on RAC1 to tightly regulate its temporal and spatial activation to control IPB pruning. Future work should address whether CRL5 directly participates in EphB/Ephrin-B3 or Semaphorin-3F signaling and determine its molecular involvement.

Similarly to other layered structures in the central nervous system (Simo and Cooper, 2013; Fairchild et al., 2018; Han et al., 2020), CRL5 regulates neuron position and lamination in the DG. Given the complex migration behaviors of the cells forming the DG (Nelson et al., 2020), it is difficult to predict when and where the layering defects observed in the RBX2 mutant DG arise. A riveting possibility is that lack of CRL5 activity impedes DG cells to hold their intended locations and disperse, as previously observed in cortical projection neurons (Simo and Cooper, 2013). On the contrary, the role of sustained Reelin/DAB1 signaling has a smaller contribution in the DG layering in comparison to cortex, given that reducing DAB1 levels mildly rescued GC ectopic layering and SOCS7 mutant DG showed no layering defects. Importantly, depletion of ARF6 exacerbated the neuron dispersion phenotype observed in absence of RBX2, suggesting that ARF6 overactivation impairs GC motility (Falace et al., 2014; Han et al., 2020).

Moreover, we showed that depletion of RBX2 promotes NSC proliferation likely through sustained Reelin/DAB1 signaling, as similar number in Ki-67+ cells are observed in RBX2 and SOCS7

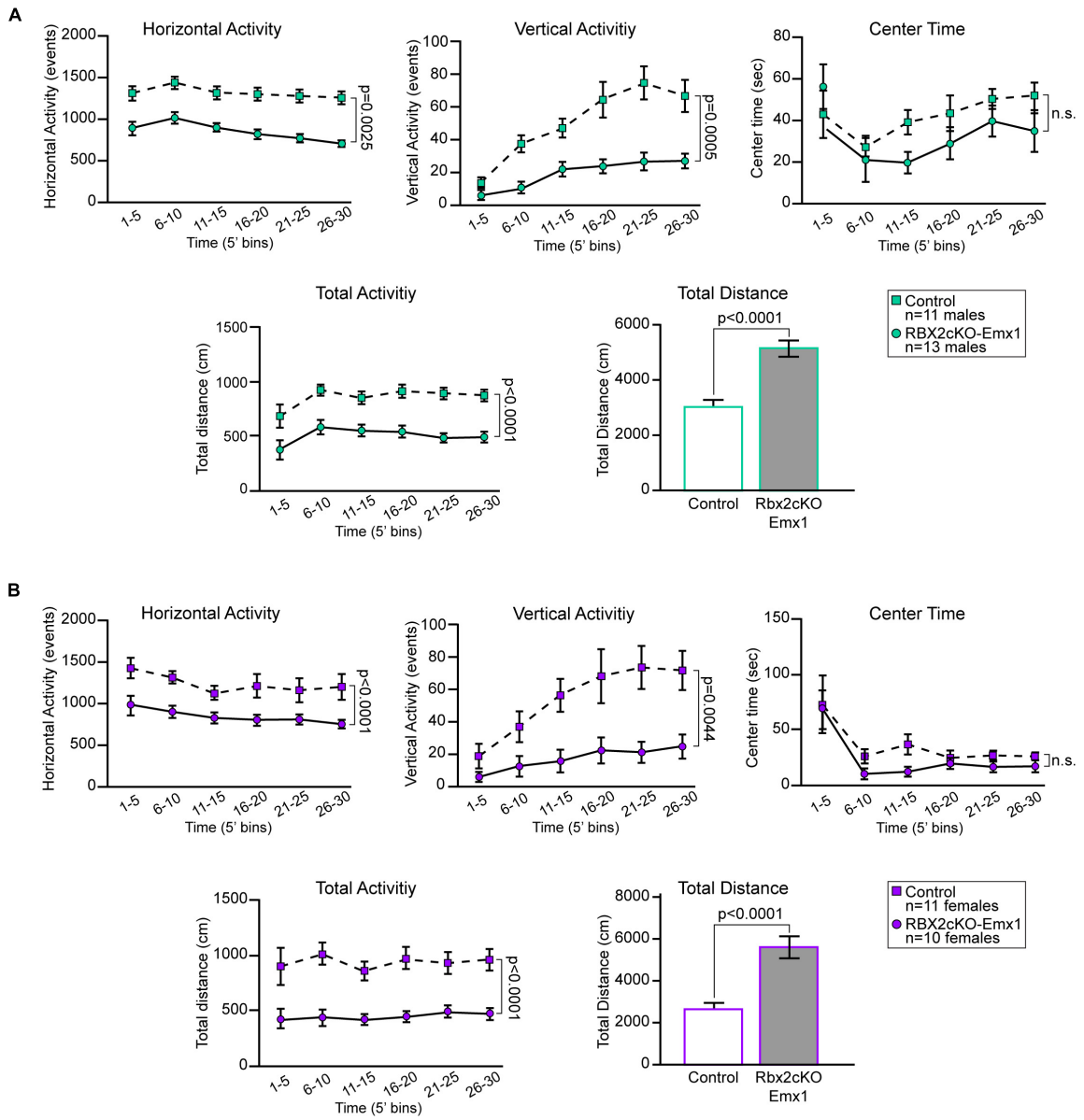

FIGURE 4 | In an open field test, both RBX2 mutant male **(A)** and female **(B)** mice (P75) showed increased horizontal (distance moved) and vertical (rearing) activity as well as higher total activity and distance moved in 30 min in comparison to control mice. On the contrary, both male and female RBX2cKO-Emx1 mice did not show changes in the amount of time spent at the center of the field. Mean ± SEM. Statistics, two-way ANOVA for all quantifications, except unpaired Student's *t*-test for total distance quantification.

mutant DG. The most likely scenario is that NSC proliferation promotes adult neurogenesis and, supporting this hypothesis, ectopic Reelin over-expression in the adult hippocampus also promotes NSC proliferation and adult neurogenesis (Pujadas et al., 2010). If this hypothesis is correct, decreased adult-born GC survival in the RBX2 mutant DGs is likely a consequence of failing integration into the existing synaptic network due to the DG layering defects observed in these animals (Doengi et al., 2016; Huckleberry and Shansky, 2021). Alternatively, increased NSC proliferation may represent an exuberant form of NSC and IP self-renewal, which would increase the numbers of SOX2+ and DCX+ cells, as observed in the RBX2 mutant DG, and consequently decreasing the number of adult-born GCs.

Surprisingly, knocking out RBX2 in adult Nestin+ cells (i.e., NSCs) did not promote an increase overall cell proliferation suggesting that non-cell autonomous mechanisms are involved to promote NSC/IP proliferation in absence of RBX2 or that RBX2 depletion at two developmental stages (e.g., embryonic -Emx1-Cre- vs. juvenile -Nestin-Cre/ERT2) had differential cellular effects.

We also demonstrate that RBX2 depletion promotes physical activity. Physical activity is well known to promote adult

neurogenesis and GC survival in the DG (Vivar et al., 2013; Goncalves et al., 2016; Saraulli et al., 2017). Thus, we hypothesize that CRL5-dependent increase in physical activity may enhance NSC proliferation in the adult DG. Future work should address how CRL5 inactivation in the telencephalon promotes higher levels of physical activity.

DATA AVAILABILITY STATEMENT

The original contributions presented in this study are included in the article/**Supplementary Material**, further inquiries can be directed to the corresponding author.

ETHICS STATEMENT

The animal study was reviewed and approved by the Institutional Animal Care and Use Committees (University of California, Davis).

AUTHOR CONTRIBUTIONS

AL, ED, and SS designed the research. RR, KH, CC, and SS performed the research. AL and ED contributed to the new reagents and analytical tools. SS wrote the manuscript with AL and ED editing. All authors contributed to the article and approved the submitted version.

FUNDING

This work was supported by NIH Grants R01 GM127513 to ED, R01 EY026942 to AL, and R01 NS109176 to SS.

ACKNOWLEDGMENTS

We would like to thank Hwai-Jong Cheng for the Sempahorin-3F expression construct. We would also like to thank Ysidra Camarena, Yasmin Haddadi, and Wenzhe Li for technical assistance. We also benefited from the use of the National Eye Institute Core Facilities (supported by NIH Grant P30 EY012576) and the UC Davis MIND Institute IDDRC Rodent Behavior Core (University of California, Davis).

SUPPLEMENTARY MATERIAL

The Supplementary Material for this article can be found online at: https://www.frontiersin.org/articles/10.3389/fnins.2022.908719/full#supplementary-material

Supplementary Figure 1 | Defects in IPB pruning in RBX2 mutant DG are independent of age and Reelin/Dab1 and ARF6 signaling. **(A)** IPB overextension in the RBX2cKO-Emx1 mice remains in adult mice (P75). Similar to P21 results, CalB stainings of control and RBX2cKO-Emx1 DG showed an ectopically IPB extension only in the RBX2 mutant DG. Arrows and arrowheads demarcate SPB and IPB extension, respectively. **(B)** SOCS7 depletion, which causes a sustained activation of Reelin/DAB1 signaling, does not affect IPB pruning. **(C)** Reducing the accumulation levels of DAB1 in the RBX2 mutant DG is not sufficient to rescue IPB pruning. **(D)** Similarly, knocking out ARF6 together with RBX2 failed to rescue IPB pruning. D', double RBX2 and ARF6 mutant DG showed an increased dispersion of CalB+ cells.

Supplementary Figure 2 | pY-DAB1 and DAB1 accumulation levels in RBX2 and SOCS7 mutant models. **(A)** DAB1 stainings in P21 control (RBX2 fl/fl), RBX2cKO-Emx1, SOCS7–/–, RBX2cKO-Emx1; DAB1+/– DG, and DAB1–/–. **(B,C)** Western blotting of P10 control and Rbx2cKO-Emx1 **(B)** and SOCS7–/– **(C)** hippocampal lysates. Red arrowhead indicates pY-Dab1.

Supplementary Figure 3 | (A) Decreased number of EdU+ cells survived in the RBX2 mutant DG in comparison to control. Mean ± SEM. Statistics, unpaired Student's *t*-test. **(B)** Representative images of control and tamoxifen-dependent depletion of RBX2 in NSCs does not promote adult neurogenesis. Mean ± SEM. Statistics, Mann Whitney test.

REFERENCES

Altman, J., and Bayer, S. A. (1990). Mosaic organization of the hippocampal neuroepithelium and the multiple germinal sources of dentate granule cells. *J. Comp. Neurol.* 301, 325–342. doi: 10.1002/cne.903010302

Bagri, A., Cheng, H. J., Yaron, A., Pleasure, S. J., and Tessier-Lavigne, M. (2003). Stereotyped pruning of long hippocampal axon branches triggered by retraction inducers of the semaphorin family. *Cell* 113, 285–299. doi: 10.1016/s0092-8674(03)00267-8

Brown, J. P., Couillard-Despres, S., Cooper-Kuhn, C. M., Winkler, J., Aigner, L., and Kuhn, H. G. (2003). Transient expression of doublecortin during adult neurogenesis. *J. Comp. Neurol.* 467, 1–10. doi: 10.1002/cne.10874

Brunne, B., Franco, S., Bouche, E., Herz, J., Howell, B. W., Pahle, J., et al. (2013). Role of the postnatal radial glial scaffold for the development of the dentate gyrus as revealed by Reelin signaling mutant mice. *Glia* 61, 1347–1363. doi: 10.1002/glia.22519

Cayre, M., Canoll, P., and Goldman, J. E. (2009). Cell migration in the normal and pathological postnatal mammalian brain. *Prog. Neurobiol.* 88, 41–63. doi: 10.1016/j.pneurobio.2009.02.001

Chen, H., Bagri, A., Zupicich, J. A., Zou, Y., Stoeckli, E., Pleasure, S. J., et al. (2000). Neuropilin-2 regulates the development of selective cranial and sensory nerves and hippocampal mossy fiber projections. *Neuron* 25, 43–56.

Cheng, H. J., Bagri, A., Yaron, A., Stein, E., Pleasure, S. J., and Tessier-Lavigne, M. (2001). Plexin-A3 mediates semaphorin signaling and regulates the development of hippocampal axonal projections. *Neuron* 32, 249–263. doi: 10.1016/s0896-6273(01)00478-0

de Rooij, J., and Bos, J. L. (1997). Minimal Ras-binding domain of Raf1 can be used as an activation-specific probe for Ras. *Oncogene* 14, 623–625. doi: 10.1038/sj.onc.1201005

Doengi, M., Krupp, A. J., Korber, N., and Stein, V. (2016). SynCAM 1 improves survival of adult-born neurons by accelerating synapse maturation. *Hippocampus* 26, 319–328. doi: 10.1002/hipo.22524

Fairchild, C. L., Hino, K., Han, J. S., Miltner, A. M., Allina, G. P., Brown, C. E., et al. (2018). RBX2 maintains final retinal cell position in a DAB1-dependent and -independent fashion. *Development* 145:dev155283. doi: 10.1242/dev.155283

Falace, A., Buhler, E., Fadda, M., Watrin, F., Lippiello, P., Pallesi-Pocachard, E., et al. (2014). TBC1D24 regulates neuronal migration and maturation through modulation of the ARF6-dependent pathway. *Proc. Natl. Acad. Sci. U.S.A.* 111, 2337–2342. doi: 10.1073/pnas.1316294111

Feil, S., Valtcheva, N., and Feil, R. (2009). Inducible Cre mice. *Methods Mol. Biol.* 530, 343–363. doi: 10.1007/978-1-59745-471-1_18

Frotscher, M., Haas, C. A., and Forster, E. (2003). Reelin controls granule cell migration in the dentate gyrus by acting on the radial glial scaffold. *Cereb. Cortex* 13, 634–640. doi: 10.1093/cercor/13.6.634

Gil, V., and del Rio, J. A. (2012). Analysis of axonal growth and cell migration in 3D hydrogel cultures of embryonic mouse CNS tissue. *Nat. Protoc.* 7, 268–280. doi: 10.1038/nprot.2011.445

Goncalves, J. T., Schafer, S. T., and Gage, F. H. (2016). Adult neurogenesis in the hippocampus: from stem cells to behavior. *Cell* 167, 897–914. doi: 10.1016/j.cell.2016.10.021

Gorski, J. A., Talley, T., Qiu, M., Puelles, L., Rubenstein, J. L., and Jones, K. R. (2002). Cortical excitatory neurons and glia, but not GABAergic neurons, are produced in the Emx1-expressing lineage. *J. Neurosci.* 22, 6309–6314. doi: 10.1523/JNEUROSCI.22-15-06309.2002

Gould, T. D., Dao, D. T., and Kovacsics, C. E. (2009). "The open field test," in *Mood and Anxiety Related Phenotypes in Mice*, ed. T. D. Gould (Totowa, NJ: Humana Press). doi: 10.9758/cpn.2020.18.3.341

Han, J. S., Hino, K., Li, W., Reyes, R. V., Canales, C. P., Miltner, A. M., et al. (2020). CRL5-dependent regulation of the small GTPases ARL4C and ARF6 controls hippocampal morphogenesis. *Proc. Natl. Acad. Sci. U.S.A.* 117, 23073–23084. doi: 10.1073/pnas.2002749117

Hayashi, K., Kubo, K., Kitazawa, A., and Nakajima, K. (2015). Cellular dynamics of neuronal migration in the hippocampus. *Front. Neurosci.* 9:135. doi: 10.3389/fnins.2015.00135

Hayashi, Y., Jinnou, H., Sawamoto, K., and Hitoshi, S. (2018). Adult neurogenesis and its role in brain injury and psychiatric diseases. *J. Neurochem.* 147, 584–594.

Hofmann, I., Thompson, A., Sanderson, C. M., and Munro, S. (2007). The Arl4 family of small G proteins can recruit the cytohesin Arf6 exchange factors to the plasma membrane. *Curr. Biol.* 17, 711–716. doi: 10.1016/j.cub.2007.03.007

Hsieh, J. (2012). Orchestrating transcriptional control of adult neurogenesis. *Genes Dev.* 26, 1010–1021. doi: 10.1101/gad.187336.112

Huckleberry, K. A., and Shansky, R. M. (2021). The unique plasticity of hippocampal adult-born neurons: contributing to a heterogeneous dentate. *Hippocampus* 31, 543–556. doi: 10.1002/hipo.23318

Khalaf-Nazzal, R., and Francis, F. (2013). Hippocampal development - old and new findings. *Neuroscience* 248, 225–242. doi: 10.1016/j.neuroscience.2013.05.061

Kuhn, H. G., Dickinson-Anson, H., and Gage, F. H. (1996). Neurogenesis in the dentate gyrus of the adult rat: age-related decrease of neuronal progenitor proliferation. *J. Neurosci.* 16, 2027–2033. doi: 10.1523/JNEUROSCI.16-06-02027.1996

Lagace, D. C., Whitman, M. C., Noonan, M. A., Ables, J. L., DeCarolis, N. A., Arguello, A. A., et al. (2007). Dynamic contribution of nestin-expressing stem cells to adult neurogenesis. *J. Neurosci.* 27, 12623–12629. doi: 10.1523/JNEUROSCI.3812-07.2007

Li, G., Kataoka, H., Coughlin, S. R., and Pleasure, S. J. (2009). Identification of a transient subpial neurogenic zone in the developing dentate gyrus and its regulation by Cxcl12 and reelin signaling. *Development* 136, 327–335. doi: 10.1242/dev.025742

Li, G., and Pleasure, S. J. (2007). Genetic regulation of dentate gyrus morphogenesis. *Prog. Brain Res.* 163, 143–152. doi: 10.1016/S0079-6123(07)63008-8

Madisen, L., Zwingman, T. A., Sunkin, S. M., Oh, S. W., Zariwala, H. A., Gu, H., et al. (2010). A robust and high-throughput Cre reporting and characterization system for the whole mouse brain. *Nat. Neurosci.* 13, 133–140.

Marquer, C., Tian, H., Yi, J., Bastien, J., Dall'Armi, C., Yang-Klingler, Y., et al. (2016). Arf6 controls retromer traffic and intracellular cholesterol distribution via a phosphoinositide-based mechanism. *Nat. Commun.* 7:11919. doi: 10.1038/ncomms11919

Nelson, B. R., Hodge, R. D., Daza, R. A., Tripathi, P. P., Arnold, S. J., Millen, K. J., et al. (2020). Intermediate progenitors support migration of neural stem cells into dentate gyrus outer neurogenic niches. *eLife* 9:e53777. doi: 10.7554/eLife.53777

Okumura, F., Joo-Okumura, A., Nakatsukasa, K., and Kamura, T. (2016). The role of cullin 5-containing ubiquitin ligases. *Cell Div.* 11:1. doi: 10.1186/s13008-016-0016-3

Peissner, W., Kocher, M., Treuer, H., and Gillardon, F. (1999). Ionizing radiation-induced apoptosis of proliferating stem cells in the dentate gyrus of the adult rat hippocampus. *Brain Res. Mol. Brain Res.* 71, 61–68. doi: 10.1016/s0169-328x(99)00170-9

Pujadas, L., Gruart, A., Bosch, C., Delgado, L., Teixeira, C. M., Rossi, D., et al. (2010). Reelin regulates postnatal neurogenesis and enhances spine hypertrophy and long-term potentiation. *J. Neurosci.* 30, 4636–4649. doi: 10.1523/JNEUROSCI.5284-09.2010

Ren, X. D., Kiosses, W. B., and Schwartz, M. A. (1999). Regulation of the small GTP-binding protein Rho by cell adhesion and the cytoskeleton. *EMBO J.* 18, 578–585. doi: 10.1093/emboj/18.3.578

Riccomagno, M. M., Hurtado, A., Wang, H., Macopson, J. G., Griner, E. M., Betz, A., et al. (2012). The RacGAP beta2-Chimaerin selectively mediates axonal pruning in the hippocampus. *Cell* 149, 1594–1606. doi: 10.1016/j.cell.2012.05.018

Santos, V. R., Melo, I. S., Pacheco, A. L. D., and Castro, O. W. (2019). Life and death in the hippocampus: What's bad? *Epilepsy Behav.* 121:106595. doi: 10.1016/j.yebeh.2019.106595

Saraulli, D., Costanzi, M., Mastrorilli, V., and Farioli-Vecchioli, S. (2017). The long run: neuroprotective effects of physical exercise on adult neurogenesis from youth to old age. *Curr. Neuropharmacol.* 15, 519–533. doi: 10.2174/1570159X14666160412150223

Sibbe, M., Forster, E., Basak, O., Taylor, V., and Frotscher, M. (2009). Reelin and Notch1 cooperate in the development of the dentate gyrus. *J. Neurosci.* 29, 8578–8585. doi: 10.1523/JNEUROSCI.0958-09.2009

Silverman, J. L., Turner, S. M., Barkan, C. L., Tolu, S. S., Saxena, R., Hung, A. Y., et al. (2011). Sociability and motor functions in Shank1 mutant mice. *Brain Res.* 1380, 120–137. doi: 10.1016/j.brainres.2010.09.026

Simo, S., and Cooper, J. A. (2013). Rbx2 regulates neuronal migration through different cullin 5-RING ligase adaptors. *Dev. Cell.* 27, 399–411. doi: 10.1016/j.devcel.2013.09.022

Teixeira, C. M., Kron, M. M., Masachs, N., Zhang, H., Lagace, D. C., Martinez, A., et al. (2012). Cell-autonomous inactivation of the reelin pathway impairs adult neurogenesis in the hippocampus. *J. Neurosci.* 32, 12051–12065. doi: 10.1523/JNEUROSCI.1857-12.2012

Vivar, C., Potter, M. C., and van Praag, H. (2013). All about running: synaptic plasticity, growth factors and adult hippocampal neurogenesis. *Curr. Top. Behav. Neurosci.* 15, 189–210. doi: 10.1007/7854_2012_220

Wang, S., Brunne, B., Zhao, S., Chai, X., Li, J., Lau, J., et al. (2018). Trajectory analysis unveils reelin's role in the directed migration of granule cells in the dentate gyrus. *J. Neurosci.* 38, 137–148. doi: 10.1523/JNEUROSCI.0988-17.2017

Xu, N. J., and Henkemeyer, M. (2009). Ephrin-B3 reverse signaling through Grb4 and cytoskeletal regulators mediates axon pruning. *Nat. Neurosci.* 12, 268–276. doi: 10.1038/nn.2254

Zhou, Y., Gunput, R. A., and Pasterkamp, R. J. (2008). Semaphorin signaling: progress made and promises ahead. *Trends Biochem. Sci.* 33, 161–170. doi: 10.1016/j.tibs.2008.01.006

Conflict of Interest: The authors declare that the research was conducted in the absence of any commercial or financial relationships that could be construed as a potential conflict of interest.

frontiers | Frontiers in Neuroscience

TYPE Original Research
PUBLISHED 18 August 2022
DOI 10.3389/fnins.2022.917071

OPEN ACCESS

EDITED BY
Simon Hippenmeyer,
Institute of Science and Technology Austria, Austria

REVIEWED BY
Marisa Karow,
University of Erlangen Nuremberg, Germany
Laurent Nguyen,
University of Liège, Belgium

*CORRESPONDENCE
Carol Schuurmans
cschuurm@sri.utoronto.ca

SPECIALTY SECTION
This article was submitted to Neurogenesis, a section of the journal Frontiers in Neuroscience

RECEIVED 10 April 2022
ACCEPTED 25 July 2022
PUBLISHED 18 August 2022

CITATION
Ghazale H, Park E, Vasan L, Mester J, Saleh F, Trevisiol A, Zinyk D, Chinchalongporn V, Liu M, Fleming T, Prokopchuk O, Klenin N, Kurrasch D, Faiz M, Stefanovic B, McLaurin J and Schuurmans C (2022) Ascl1 phospho-site mutations enhance neuronal conversion of adult cortical astrocytes *in vivo*. *Front. Neurosci.* 16:917071. doi: 10.3389/fnins.2022.917071

Ascl1 phospho-site mutations enhance neuronal conversion of adult cortical astrocytes *in vivo*

Hussein Ghazale[1,2], EunJee Park[1,2], Lakshmy Vasan[1,3], James Mester[1,4], Fermisk Saleh[1,2], Andrea Trevisiol[1,4], Dawn Zinyk[1], Vorapin Chinchalongporn[1,2], Mingzhe Liu[1,3], Taylor Fleming[1,2], Oleksandr Prokopchuk[1], Natalia Klenin[5], Deborah Kurrasch[5], Maryam Faiz[6], Bojana Stefanovic[1,4], JoAnne McLaurin[1,3] and Carol Schuurmans[1,2,3]*

[1]Sunnybrook Research Institute, Toronto, ON, Canada, [2]Department of Biochemistry, University of Toronto, Toronto, ON, Canada, [3]Department of Laboratory Medicine and Pathobiology, University of Toronto, Toronto, ON, Canada, [4]Department of Medical Biophysics, University of Toronto, Toronto, ON, Canada, [5]Department of Medical Genetics, Cumming School of Medicine, Hotchkiss Brain Institute, Alberta Children's Hospital Research Institute, University of Calgary, Calgary, AB, Canada, [6]Department of Surgery, University of Toronto, Toronto, ON, Canada

Direct neuronal reprogramming, the process whereby a terminally differentiated cell is converted into an induced neuron without traversing a pluripotent state, has tremendous therapeutic potential for a host of neurodegenerative diseases. While there is strong evidence for astrocyte-to-neuron conversion *in vitro, in vivo* studies in the adult brain are less supportive or controversial. Here, we set out to enhance the efficacy of neuronal conversion of adult astrocytes *in vivo* by optimizing the neurogenic capacity of a driver transcription factor encoded by the proneural gene Ascl1. Specifically, we mutated six serine phospho-acceptor sites in Ascl1 to alanines (Ascl1^{SA6}) to prevent phosphorylation by proline-directed serine/threonine kinases. Native Ascl1 or Ascl1^{SA6} were expressed in adult, murine cortical astrocytes under the control of a glial fibrillary acidic protein (GFAP) promoter using adeno-associated viruses (AAVs). When targeted to the cerebral cortex *in vivo*, mCherry^{+} cells transduced with AAV8-GFAP-Ascl1^{SA6}-mCherry or AAV8-GFAP-Ascl1-mCherry expressed neuronal markers within 14 days post-transduction, with Ascl1^{SA6} promoting the formation of more mature dendritic arbors compared to Ascl1. However, mCherry expression disappeared by 2-months post-transduction of the AAV8-GFAP-mCherry control-vector. To circumvent reporter issues, AAV-GFAP-iCre (control) and AAV-GFAP-Ascl1 (or Ascl1^{SA6})-iCre constructs were generated and injected into the cerebral cortex of Rosa reporter mice. In all comparisons of AAV capsids (AAV5 and AAV8), GFAP promoters (long and short), and reporter mice (Rosa-zsGreen and Rosa-tdtomato), Ascl1^{SA6} transduced cells more frequently expressed early- (Dcx) and late- (NeuN) neuronal markers. Furthermore, Ascl1^{SA6} repressed the expression of astrocytic markers Sox9 and GFAP more efficiently than Ascl1. Finally, we co-transduced an AAV expressing ChR2-(H134R)-YFP,

an optogenetic actuator. After channelrhodopsin photostimulation, we found that Ascl1^{SA6} co-transduced astrocytes exhibited a significantly faster decay of evoked potentials to baseline, a neuronal feature, when compared to iCre control cells. Taken together, our findings support an enhanced neuronal conversion efficiency of Ascl1^{SA6} vs. Ascl1, and position Ascl1^{SA6} as a critical transcription factor for future studies aimed at converting adult brain astrocytes to mature neurons to treat disease.

KEYWORDS

proneural bHLH transcription factors, phospho-site mutations, neuronal reprogramming, cerebral cortex, astrocytes, induced neuron, adeno-associated virus, glial fibrillary acidic protein

Introduction

Neurological diseases are most often associated with the loss or dysfunction of specific neuronal populations. Once lost, neurons are not replaced, except in rare circumstances and in restricted brain niches (Grade and Gotz, 2017; Barker et al., 2018). The lack of a regenerative response, combined with a paucity of neurotherapeutics, has prompted the exploration of various neuronal replacement strategies, including exogenous cell transplants and the stimulation of endogenous neural stem cells. However, these approaches have yet to result in sufficient neuronal integration for long-term functional recovery (Adams and Morshead, 2018; Ruddy and Morshead, 2018). Moreover, introducing exogenous human cells, especially fetal stem or progenitor cells, raises ethical concerns, and may be confounded by immune rejection, tumorigenicity, and supply constraints. Identifying an *endogenous* neuronal repair strategy in which new neurons functionally integrate into existing neural circuitry would be transformative as it would provide new therapeutic strategies to treat neurodegenerative disease.

We have begun to exploit the potential of direct neuronal reprogramming for endogenous neuronal replacement (Bocchi et al., 2021; Vasan et al., 2021). This feat exploits decades of research into the roles of lineage-specifying basic-helix-loop-helix (bHLH) transcription factors (TF) in driving subtype-specific neurogenesis in the embryonic brain (Grade and Gotz, 2017; Vasan et al., 2021). The proneural bHLH TFs, including Neurog2, Ascl1 and Neurod4, and downstream bHLH genes, such as Neurod1, have emerged as critical architects of neurogenesis in the embryonic brain (Oproescu et al., 2021) and are now being exploited to drive neuronal conversion of heterologous cell types (Bocchi et al., 2021; Vasan et al., 2021). During development, proneural bHLH TFs act at the top of transcriptional cascades, turning on other TFs, such as Neurod1, which function at later developmental stages to control neuronal differentiation. However, bHLH TFs are not active in all cellular contexts and can be inhibited by environmental signals. For example, in the embryonic cortex, Neurog2 is only sufficient (by gain-of-function; Li et al., 2012) and necessary (by loss-of-function; Fode et al., 2000; Schuurmans et al., 2004; Britz et al., 2006) to specify a glutamatergic neuronal fate between embryonic day (E) 11.5 to E14.5, despite continued expression at later stages during the neurogenic period, which ends at E17. Similarly, Ascl1, which specifies a GABAergic interneuron fate in the embryonic ventral telencephalon (Casarosa et al., 1999), can only induce ectopic GABAergic genes in dorsal telencephalic progenitors at early (E12.5) and not late (E14.5) embryonic stages (Fode et al., 2000; Schuurmans et al., 2004; Britz et al., 2006).

The cell context-dependent activities of the proneural genes extend to neuronal reprogramming where there is growing consensus that the conversion of somatic cells to an induced neuron (iNeuron) fate is more efficient when the starter cell is more similar in identity (i.e., neural lineage). Thus, to efficiently convert distantly related fibroblasts to iNeurons, Ascl1 is combined with other TFs, as in the initial "BAM" combination (Brn2/Pou3f2, Ascl1, and Myt1l) (Vierbuchen et al., 2010; Wapinski et al., 2013). In this context, Ascl1 plays a crucial role as a pioneer TF, opening chromatin associated with a specific trivalent signature (H3K4me1, H3K27ac, and H3K9me3), which is then accessed by Brn2 and other neurogenic TFs (Wapinski et al., 2013). Other studies have reported that Ascl1 can convert fibroblasts to iNeurons directly, but the maturation of these iNeurons is limited (Chanda et al., 2014). Similarly, Ascl1 can trigger human pericytes to transdifferentiate into iNeurons, but only when co-expressed with Sox2, which facilitates the transiting of cells through a neural stem/progenitor cell-like stage (i.e., conversion is not direct) (Karow et al., 2012, 2018). The ability of Ascl1 to induce neural progenitor cells to differentiate into neurons is in keeping with its developmental role (Oproescu et al., 2021), and has been recapitulated using progenitor cell lines (Raposo et al., 2015) or pluripotent stem cells *in vitro*, with Ascl1 acting as a pioneer TF (Chanda et al., 2014; Yang et al., 2017; Aydin et al., 2019).

Astrocytes are common target cells for neuronal conversion as their activated state in neurodegenerative diseases and in injuries such as stroke contributes to disease pathology (Bocchi et al., 2021; Vasan et al., 2021). *Ascl1* can convert cortical astrocytes to iNeurons *in vitro*, either when misexpressed alone (Berninger et al., 2007; Heinrich et al., 2010, 2012; Kempf et al., 2021) or together with other TFs, to make for instance, dopaminergic iNeurons (Rivetti di Val Cervo et al., 2017). Spinal cord astrocytes can also be reprogrammed to iNeurons but interestingly, a distinct V2 interneuron-like identity is achieved, rather than a cortical phenotype (Kempf et al., 2021). While there are reports that Ascl1 can convert adult midbrain astrocytes to iNeurons *in vivo* (Liu et al., 2015), most studies suggest Ascl1 has low conversion efficacy in the adult cortex and hippocampus *in vivo* (Jessberger et al., 2008; Grande et al., 2013). Thus, understanding how proneural genes such as Ascl1 are regulated (i.e., inhibited), especially *in vivo*, is key for their efficient use in regenerative medicine. Several approaches have been taken to enhance the neuronal conversion efficacy of Ascl1 and Neurog2. For instance, expressing Ascl1 together with other TFs, as recently shown with a CRISPR-based approach, can enhance neuronal conversion, with resultant iNeurons having therapeutic benefits in a Parkinson's disease model (Giehrl-Schwab et al., 2022). Similarly, *Neurog2* can be combined with other signals, such as Bcl2, to become a potent lineage converter, in part due to enhanced survival *in vivo* (Gascon et al., 2016). The knockdown of REST, a transcriptional repressor of neurogenic genes, also enhances neuronal lineage conversion (Masserdotti et al., 2015; Drouin-Ouellet et al., 2017). Finally, in another ground-breaking study, CRISPR-activation of mitochondrial genes enriched in neurons enhanced Neurog2 and Ascl1 reprogramming efficacy (Russo et al., 2021). Identifying and targeting the regulatory events that block bHLH TF activity is thus proving a fruitful strategy to improve neuronal reprogramming.

To address the challenge of lower neuronal conversion efficiency *in vivo* compared to *in vitro* (Vasan et al., 2021), we explored the importance of phosphorylation as a critical post-translational modification of Ascl1. It is now well accepted that when neurogenic bHLH TFs are expressed outside of their normal cellular context (Li et al., 2012, 2014), they are subject to phosphorylation-dependent inhibition that limits their neurogenic activity. Indeed, bHLH TF function is inhibited via phosphorylation by proline-directed serine threonine kinases (e.g., GSK3, ERK1/2, Cdks), which act in a "rheostat-like fashion;" the more serine-proline (SP) or threonine-proline (TP) sites phosphorylated, the less these TFs bind to DNA and transactivate their target genes to promote neuronal fate specification and differentiation (Ali et al., 2011; Hindley et al., 2012; Li et al., 2012, 2014). To keep bHLH TFs active, our group (Li et al., 2012, 2014) and others (Ali et al., 2011, 2020; Hindley et al., 2012; Azzarelli et al., 2015, 2022) have mutated serines (S) and threonines (T) in proline (P)-directed phospho-sites to alanines (A) (i.e., SP/TP to SA/TA mutations). These mutations prevent phosphorylation by inhibitory proline-directed kinases and increase the neurogenic potential of bHLH TFs in the embryonic mouse and frog nervous systems (Marcus et al., 1998; Ali et al., 2011, 2020; Hindley et al., 2012; Li et al., 2012, 2014; Azzarelli et al., 2015, 2022).

The goal of this study was to determine whether a mutated version of Ascl1, termed Ascl1^{SA6}, is more efficient at inducing neuronal conversion of cortical astrocytes in the adult brain *in vivo*. We initiated this study using AAV and GFAP promoters (Lee et al., 2008), a combination that has since been shown to be less astrocyte-specific than initially reported due to cis-effects of TF coding sequences on the GFAP promoter (Wang et al., 2021). Nevertheless, by directly comparing Ascl1 to Ascl1^{SA6} in all of our studies, we demonstrate that compared to Ascl1, Ascl1^{SA6} has a superior capacity to induce neuronal marker expression, promote the acquisition of more elaborate dendritic arbors, and to repress astrocytic genes in the adult cerebral cortex. The enhanced capacity of Ascl1^{SA6} to induce neuronal gene expression is in keeping with embryonic studies conducted previously, and suggests that further studies of the reprogramming capacity of Ascl1^{SA6} are warranted.

Materials and methods

Animals and genotyping

Animal procedures were approved by the Sunnybrook Research Institute (21-757) in compliance with the Guidelines of the Canadian Council of Animal Care. In all adult animal experiments, we used male C57BL/6 wild-type mice, Rosa-ZsGreen (JAX #007906) and Rosa-tdtomato (JAX #007914) transgenic mice (Madisen et al., 2010), maintained on a C57BL/6 background, and obtained from Jackson Laboratory. For the collection of the embryonic day (E) 14.5 dorsal (dTel) and ventral (vTel) telencephalon, CD1 outbred mice were crossed and the day of the vaginal plug was considered E0.5. Mice were housed under 12-h light/12-h dark cycles with free access to food and water. PCR primers and conditions for genotyping were conducted using Jackson Laboratory protocols: Rosa-ZsGreen: wild-type forward: 5′-CTG GCT TCT GAG GAC CG-3′; wild-type reverse: 5′-AAT CTG TGG GAA GTC TTG TCC-3′; mutant forward: 5′-ACC AGA AGT GGC ACC TGA C-3′; mutant reverse: 5′-CAA ATT TTG TAA TCC AGA GGT TGA-3′. Rosa-tdtomato: mutant reverse: 5′-GGC ATT AAA GCA GCG TAT CC-3′; mutant forward: 5′-CTG TTC CTG TAC GGC ATG G-3′. PCR cycles were as follows: 94°C 2 min, 10× (94°C 20 s, 65°C 15 s *–0.5c per cycle decrease, 68°C 10 s), 28× (94°C 15 s min, 60°C 15 s, 72°C 10s), 72°C 2 min.

Adeno-associated viruses cloning and packaging

pGFAP-mCherry-AAV (which we refer to as AAV8-GFAPlong-mCherry) and pGFAP-Mash1mCherry-AAV (which we refer to as AAV/8-GFAPlong-Ascl1-mCherry) were a gift from Leping Cheng (Liu et al., 2015) and include a 2.2 kb GFAP promoter (Zhuo et al., 1997; Liu et al., 2015). We replaced Ascl1 with Ascl1^{SA6} in AAV2/8-GFAPlong-Ascl1-mCherry. In Ascl1^{SA6}, serines in all six SP sites was mutated to alanines (as in Li et al., 2014). pAAV-GFAPshort-iCre was subcloned from pAAV-GFAP-mNeurod1-T2A-iCre, a kind gift of Dr. Maryam Faiz (Livingston et al., 2020), and includes a 681 bp (gfaABC(1)D) modified GFAP promoter (Lee et al., 2008). We outsourced to GenScript to clone Ascl1-t2a-iCre and Ascl1^{SA6}-t2a-iCre into AAV5-GFAPshort, and then to replace the GFAPshort promoter with the GFAPlong promoter in the AAVs from Leping Cheng (Liu et al., 2015). After cloning, all AAVs were packaged by VectorBuilder, Inc., either with AAV capsid 8 or 5. For optogenetic experiments, AAV5-EF1a-double floxed-hChR2(H134R)-EYFP-WPRE-HGFpA (catalog # 51502-AAV5) was purchased from Addgene (20298).

Intracranial injection of adeno-associated viruses

For intracranial injections, 16-week-old male C57BL/6 mice were anesthetized using isoflurane (2%, 1 L/min; Fresenius Kabi, CP0406V2) and injected subcutaneously with an analgesic, either buprenorphine (0.1 mg/kg; Vetergesic, 02342510) or Tramadol-HCL (20 mg/kg; Chiron, RxN704598), along with Baytril® (2.5 mg/kg; Bayer, 02249243), and saline (0.5 ml, Braun, L8001). A burr hole was drilled through the skull over the cortex and a stereotaxic instrument was used to identify bregma and lambda coordinates for injection. For all AAV injections, 4.8×10^9 genome copies (GC) in a 1 uL total volume were delivered into the motor cortex at 0.1 µl/min over a 10 min span using a 5 l Hamilton syringe with 33-gauge needle (Hamilton, 7803-07). A stereotax was used to target the motor cortex with the following coordinates (AP: + 2.15, L/M: ± 1.7, DV: −1.7). For AAV-GFAP-mCherry vectors, C57Bl/6 animals were used, while for AAV-GFAP-iCre vectors, injections were performed in Rosa-tdtomato or Rosa-zsGreen mice. Only for the Rosa-tdtomato mice was there a change in the injection paradigm - we injected 1×10^{12} GC/ml in a 1 uL total volume (or 1×10^9 GC total) with coordinates (AP: 2.2 LM: 0.6 DV:1.0).

Optogenetics and electrophysiology

Adeno-associated viruses-injected mice were anesthetized using 2% isoflurane and a 4 mm craniotomy was performed (from bregma: AP 1.7mm, ML + −2.15). After removal of the dura, a silicone-based polydimethylsiloxane (PDMS) window was placed over a thin layer of 1% agarose (in PBS) covering the cortical tissue. The mice were transferred to an FVMPE-RS multiphoton microscope (Olympus) and placed under a 25x/1.05NA objective lens (Olympus) while a tungsten electrode (0.255 mm Ø, A-M System) was inserted at a 30° angle, through the PDMS window, reaching a depth of 100 µm into the cortex. An Insight Ti:Sapphire laser (SpectraPhysics) tuned to 900 nm was used to excite the ZsGreen fluorescence, whose emission was then collected by a PMT aligned with a band-pass filter (485–540 nm). A second channel (575–630 nm) was also recorded simultaneously to better visualize the position of the Tungsten electrode's tip into the tissue. For simultaneous focused photostimulation (PS) of ChR2, a raster scanned visible wave-length laser (458 nm) with a separate galvanometer was used. The PS was presented over a circular area of 250 µm in diameter where Zs-green-positive cells were present. The PS was repeated ten times over the same area at 10 s intervals (PS off). The PS was delivered over the circular area at 4 Hz with a power of 4 mW/mm^2, and lasted for a total of 3 s. The low-impedance tungsten electrode was used to acquire voltage changes in the LFP band (1−300 Hz), recorded in current clamp mode by the Axon multiclamp 700B amplifier (Molecular devices). The analog signal was amplified 40 times (40 mV/mV) and digitized by the data acquisition system Digidata 1440A (Molecular devices). A two-phase decay model was used to describe the repolarization phase of the LFP signal, and the slower component was reported as the decay constant.

Tissue processing and sectioning

Mice were anesthetized with ketamine (75 mg/kg, Narketan, 0237499) and xylazine (10 mg/kg, Rompun, 02169592) prior to perfusion. Intracardial perfusion was performed with approximately 20x blood volume using a peristaltic pump at a flow rate of 10 ml/min with ice-cold saline (0.9% NaCl, Braun, L8001), followed by 4% paraformaldehyde (PFA, Electron Microscopy Sciences, 19208) in phosphate buffer saline (PBS, Wisent, 311-011-CL) for 5 mins. Brains were collected and post-fixed overnight in 4% PFA in PBS, cryoprotected at 4°C in 20% sucrose (Sigma, 84097)/1X PBS overnight. Coronal brain sections were cut at 10−30 µm on a Leica CM3050 cryostat (Leica Microsystems Canada Inc., Richmond Hill, ON, Canada) and collected on Fisherbrand™ Superfrost ™ Plus Microscope Slides (Thermo Fisher Scientific, 12-550-15).

Immunostaining

Slides were washed in 0.3% Triton X-100 in PBS, then blocked for 1 h at room temperature in 10% horse serum

(HS, Wisent, 065-150) and 0.1% Triton X-100 (Sigma, T8787) in PBS (PBST). Primary antibodies were diluted in blocking solution as follows: mouse anti-Ascl1 (1:100, BD Bioscience #556604), rat anti-BrdU (1:250, Abcam #ab6326), rabbit anti-Dcx (1:500, Abcam #ab18723), goat anti-GFAP (1:500, Novus #100-53809), guinea pig-anti MAP2 (1:1000, Synaptic Systems #188 004), mouse anti-NeuN (1:500, Millipore Sigma #MAB377), and rabbit anti-Sox9 (1:500, Millipore #AB5535). Slides were washed three times for 10 min each in 0.1% Triton-X-100 in PBS, and incubated with 1:500 dilutions of species-specific secondary antibodies all from Invitrogen Molecular Probes™ for 1 h at room-temperature. Secondary antibodies conjugated to Alexa568 included goat-anti-rat (A11077) and donkey-anti-rabbit (A10042), to Alexa488 included donkey-anti-rabbit (A21206), goat-anti-mouse (A11029) or donkey-anti-goat (A11055), and to Alexa647 included goat-anti-guinea pig (A11073). Slides were washed three times in PBS and counterstained with 4′,6-diamidino-2-phenylindole (DAPI, Invitrogen, D1306). Finally, the slides were washed three times in PBS and mounted in Aqua-polymount (Polysciences Inc.,18606-20).

RNA *in situ* hybridization

We performed colorimetric RNA-*in situ* hybridization (ISH) using a digoxygenin-labeled *Ascl1* riboprobe as previously described (Touahri et al., 2015). We performed fluorescent RNA-ISH using an RNAscope® Multiplex Fluorescent Detection Kit v2 (ACD #323110) and followed the manufacturer's instructions. Briefly, brain sections were post-fixed (4% PFA/1XPBS) for 15 min at 4°C, and then, at room-temperature, dehydrated in 50%, 70%, and 100% ethanol (Commercial Alcohols, P016EAAN) for 5 min each, and incubated in H_2O_2 solution for 10 min. Sections were then incubated in 1x target retrieval solution for 5 min at 95°C, washed in dH_2O, and then incubated in Protease Plus (ACD, 322331) for 15 min at 40°C before washing in washing buffer. We used a labeled RNA probe for Ascl1 (Mm-*Ascl1* #313291) and used the negative and positive control probes provided. Sections were incubated with the probes for 2 h at 40°C. Amplification and staining steps were completed following the manufacturer's instructions, using an Opal™ 570 (1:1500, Akoya #FP1488001KT) fluorophore.

Western blotting

C57/Bl6 motor cortices were transduced with AAV8-GFAPlong-mCherry, AAV8-GFAPlong-Ascl1-mCherry or AAV8-GFAPlong-Ascl1^{SA6}-mCherry viruses using the coordinates described above. After 7 dpi, left and right brain hemispheres were harvested, mCherry^{+} motor cortices were microdissected, and tissue was lysed in NP-40 lysis buffer (0.05 M Tris pH 7.5, 0.15 M NaCl, 1% NP-40, 1 mM EDTA, 50 mM NaF, 0.2 mM Na_3VO_4, 2 mM PMSF, 0.05 mM MG132, #M7449, Sigma), 1X complete protease inhibitor tablet (#04 693 116 001, Roche) for 30 min on ice. E14.5 CD1 telencephalons were collected and dissected into dorsal (dTel) and ventral (vTel) domains and similarly lysed in the same buffer. Brain lysates were centrifuged at 13,000g for 15 min and cleared supernatants were collected. Protein concentrations were quantified using a Bradford assay (#500-0006, Biorad) and a BSA protein standard. 10 μg of total protein was run on 10% SDS-PAGE gels at 70 V during stacking and 120 V while resolving. Separated proteins were transferred to PVDF membranes (#1620177, Biorad) in transfer buffer (25 mM Tris, 192 mM glycine, 20% methanol, pH 8.3) at 40 V overnight at 4°C. Membranes were blocked in TBST (10 mM Tris, 100 mM NaCl, pH 7.4, 0.1% Tween-20) with 5% (W/V) powdered milk for 1 h at room temperature and then incubated with primary antibodies diluted in the same blocking solution overnight at 4°C. Membranes were washed 3 × 10 min in TBST, and then incubated for 1 h at room temperature with 1/10,000 dilutions of horseradish peroxidase (HRP)-coupled secondary antibodies (Anti Rabbit IgG #7074S, Cell Signaling Technology, Anti Mouse IgG #Pierce 31430, Thermo Fisher Scientific) Membranes were washed 3 × 10 mins at room temperature and then processed with ECL Plus Western Blotting Reagent (#29018904, GE Healthcare) before developing with X-ray film (#1141J52, LabForce) and Biorad Chemidoc MP imaging system using Image Lab software. Primary antibodies included: 1/1000 rabbit mAb (#4695S) anti-p44/42 MAPK (Erk1/2) (137F5) (Cell Signaling Technology), 1/1000 rabbit mAb (#4370S) anti-phospho-p44/42 MAPK (Erk1/2) (Thr202/Tyr204) (D13.14.4E) XP® (Cell Signaling Technology), 1/1000 rabbit mAb (#12456S) anti-GSK-3β (C5C5Z) XP® (Cell Signaling Technology), 1/1000 rabbit pAb (#PA5-82086) anti-CDK1 (Thermo Fisher Scientific), 1/1000 rabbit pAb anti-β-actin (#ab8227, Abcam), 1/1000 mouse anti-ASCL1 (#556604, BD Biosciences), 1/1000 rabbit pAb (#ab74065, Abcam) anti-ASCL1and Rabbit mAb anti-phospho-Ascl1 (Li et al., 2014). Densitometry was assessed using Image J, and phospho-Ascl1 expression levels were normalized relative to Ascl1 and to β-actin.

Phos-tag™ western blots to detect phosphorylated Ascl1

Protein lysates collected for Western blotting were de-phosphorylated by incubating with 400 units of Lambda Protein Phosphatase, with 1X NEBuffer for Protein MetalloPhosphatases (PMP) and 1 mM Mncl2 (NEB, cat# P0753S) at 30°C for 30 min. 10 μg of untreated and phosphatase-treated protein was then run at 50 mA constant

current at 4°C on 10% acrylamide gels containing 20 μM Phos-tag ^{TM} reagent (#AAL-107, FUJIFILM Wako Chemicals, United States Corporation) and 40 μM $MnCl_2$ (Woods et al., 2022). Gels were washed 3 × 10 min in transfer buffer containing 10 mM EDTA followed by a final 10 min wash in transfer buffer without EDTA before transfer to PVDF membranes and Western blotting with 1/1000 rabbit pAb (#ab74065) anti-ASCL1.

Imaging, quantification, and statistics

All images were taken using a Leica DMi8 Inverted Microscope (Leica Microsystems CMS, 11889113) with the following exceptions. Images in **Figures 3D, 4B** were acquired using a Zeiss Z1 Observer/Yokogawa spinning disk (Carl Zeiss) microscope. Tiled images encompassing the entire motor cortex were acquired using 30 μm z-stacks with a 1 μm step-size with a 20X objective. In **Figures 3B,C**, whole section images were scanned with the Zeiss AxioScan Z1 unit (Carl Zeiss Canada) using a Plan-Apochromat 10X objective and acquired with a Hamamatsu CCD camera. Figures were created with Adobe Photoshop and schematics were created with a license to BioRender.com. Statistical analyses were conducted using GraphPad Prism 9.2.0 Software. Mean values and error bars representing the standard error of the mean (s.e.m.) are plotted. Quantification of immunostained cells was performed on three brains per condition and a minimum of three sections per brain. Comparisons were made using a One-Way ANOVA and Tukey multiple comparisons. Significance was defined as p-values less than 0.05 and denoted as follows: ns, not significant, $<0.05^{*}$, $<0.01^{**}$, $<0.001^{***}$.

Results

Ascl1 is phosphorylated by proline-directed serine/threonine kinases in the adult cortex *in vivo*

Phosphorylation of Ascl1 on six SP sites (S62, S88, S185, S189, S202, and S218) by proline-directed serine-threonine kinases (e.g., ERK, GSK3, and CDK1; **Figure 1A**) has so far only been demonstrated in transfected HEK293 (Li et al., 2014), neuroblastoma (Woods et al., 2022), and glioblastoma (Azzarelli et al., 2022) cells *in vitro*. To determine whether Ascl1 is phosphorylated when expressed in adult cortices *in vivo*, we transduced both motor cortex hemispheres of adult C57Bl/6 mice using a stereotax to guide viral delivery (AP: + 2.15, L/M: ± 1.7, DV: -1.7). We delivered a total of $4.8^{\wedge}10^{9}$ genome copies (GC) of adeno-associated virus (AAV) 8 carrying a 2.2 kb human GFAP promoter (Zhuo et al., 1997; Lee et al., 2008) (hereafter, GFAPlong, as in Lee et al., 2008; Liu et al., 2015) to drive the expression of mCherry (control), Ascl1-mCherry or Ascl1^{SA6}-mCherry fusion proteins (**Figure 1B**). Notably, this viral delivery system was previously used to express Ascl1 in adult midbrain astrocytes, leading to their successful conversion to iNeurons *in vivo* (Liu et al., 2015). After 7 days post-infection (dpi), left and right motor cortices were independently microdissected and analyzed for the expression of kinases that might phosphorylate Ascl1. ERK and its active pERK form (**Figure 1C**), as well as GSK3 and CDK1 (**Figure 1D**), were all expressed in the adult cortex and thus potentially available to phosphorylate Ascl1.

In the adult brain, Ascl1 is expressed in a limited number of cells, including active neural stem cells in the ventricular-subventricular zone (V-SVZ) and neuroblasts in the rostral migratory stream (RMS) (Jessberger et al., 2008; Urban et al., 2016), declining in these regions as animals age (Kaise et al., 2022). We confirmed that Ascl1 was indeed expressed in the V-SVZ and RMS by immunostaining coronal sections through the adult motor cortex (**Figure 1E**). To detect Ascl1 expression after viral transduction, and to assess its phosphorylation status, we performed western blotting using two polyclonal antibodies against total Ascl1 and a monoclonal antibody against Ascl1 phosphorylated on S185 (designated phospho-Ascl1) (Li et al., 2014). Ascl1-mCherry fusion proteins (~53 kDa) labeled with a BD Biosciences antibody were overexpressed 1.5- and 7.3-fold over background levels at 7 days post Ascl1- and Ascl1^{SA6}-transduction, respectively (**Supplementary Figures S1A,B**). A comparison of phospho-Ascl1/total-Ascl1 ratios revealed 2.1- and 10.3-fold decreases in relative Ascl1 phosphorylation after Ascl1 and Ascl1^{SA6} transduction vs. mCherry controls (i.e., endogenous Ascl1), respectively (**Supplementary Figures S1A,B**). These data support the contention that endogenous Ascl1 is phosphorylated on SP sites and suggest that overexpressed Ascl1^{SA6} is not phosphorylated, as we have previously shown in the embryonic cortex (Li et al., 2014).

As the phospho-Ascl1 antibody had previously only been validated *in vitro* (Li et al., 2014), to provide further support for Ascl1 phosphorylation in the adult brain *in vivo*, we subjected protein lysates to phosphatase treatment, and ran treated and untreated samples on a Phos-tag impregnated gel (Woods et al., 2022) (**Figure 1F**). Two prominent proteins between ~28 and 37 kDa were labeled with anti-Ascl1 (Abcam) in the adult brain, running just above the predicted MW of 25 kDa for Ascl1 (**Supplementary Figure S1D**), and matching the MW of labeled proteins in embryonic day (E) 14.5 ventral telencephalic lysates (positive control; **Supplementary Figure S1C**). In mCherry and Ascl1-mCherry transduced brains collected in two independent experiments, western blotting with anti-Ascl1 (Abcam) revealed both a faster migrating unphosphorylated Ascl1 band just above the 25 kDa marker and a slower migrating phosphorylated band of ~37 kDa that resolved upon phosphatase treatment

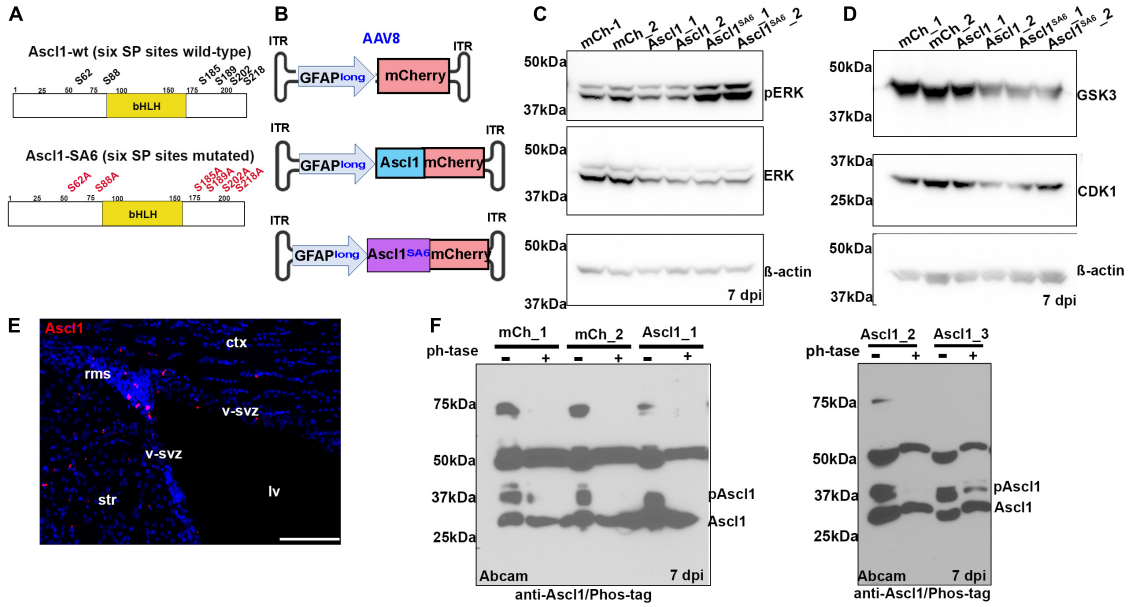

FIGURE 1
Ascl1 is phosphorylated by proline-directed serine-threonine kinases in the adult brain *in vivo*. **(A)** Schematic illustration of the sequence of wild-type (wt) Ascl1 with SP sites designated, and Ascl1^{SA6}, with SA mutations indicated. **(B)** Schematic illustration of AAV8-GFAPlong-mCherry vectors. **(C,D)** Western blot analysis of lysates from right (sample 1) and left (sample 2) cortical hemispheres transduced with AAV8-GFAPlong-mCherry (mCh), AAV8-GFAPlong-Ascl1-mCherry (Ascl1) or AAV8-GFAPlong-Ascl1^{SA6}-mCherry (Ascl1^{SA6}), analyzed for the expression of pERK, ERK, and β-actin **(C)**, or GSK3, CDK1, and β-actin **(D)**. **(E)** Ascl1 expression in the ventricular-subventricular zone (V-SVZ) in a coronal section of the adult cortex. **(F)** Phos-tag western blot of cortical lysates from left (sample 1); left (sample 2); and right (sample 3) cortical hemispheres transduced with mCherry or Ascl1-mCherry in two independent experiments shown in separate gels either treated or not with Lambda protein phosphatase (ph'tase) and blotted with anti-Ascl1 (Abcam). Scale bars in panel **E** = 100 μm. ct, cortex; lv, lateral ventricle; rms, rostral migratory stream; str, striatum; v-svz, ventricular-subventricular zone. Significance was defined as *p*-values less than 0.05 and denoted as follows: ns, not significant, <0.05 *, <0.01 **, <0.001 ***.

(Figure 1F). Taken together, these data support the contention that Ascl1 is indeed phosphorylated in the adult brain *in vivo*.

Ascl1^{SA6} has an enhanced ability to induce neuronal marker expression and a mature neuronal morphology compared to Ascl1

The main goal of our study was to determine whether serine-to-alanine mutations in the six SP sites in Ascl1 would enhance neuronal conversion efficacy. Notably, our group previously demonstrated that Ascl1^{SA6} was more efficient at neuronal conversion when introduced into E12.5 cortical progenitors (Li et al., 2014), but the question remained, would this modified bHLH transcription factor more effectively convert adult cortical astrocytes to iNeurons? To determine whether Ascl1 and Ascl1^{SA6} had different abilities to induce neuronal marker expression when misexpressed in adult cortical astrocytes *in vivo*, we transduced the same set of AAV8-GFAPlong constructs into the motor cortex of C57Bl/6 mice and harvested the brains at 14 dpi (Figure 2). Packaged AAVs (4.8×10^9 GC total in a 1 uL total volume) were stereotactically injected into the cortex of C57Bl/6 mice, using the same coordinates as in Figure 1 (AP: + 2.15, L/M: ± 1.7, DV: −1.7).

In control mCherry-transduced brains, the majority of mCherry$^+$ cells had an astrocytic morphology and 95.00 ± 1.03% co-expressed GFAP (Figures 2A,C). Conversely, when Ascl1-mCherry or Ascl1^{SA6}-mCherry were transduced, only 24.79 ± 0.52% and 16.31 ± 1.29% of the mCherry$^+$ cells co-expressed GFAP, respectively (Figures 2A,C). To determine whether the transduced cells instead acquired neuronal marker expression, we examined the expression of NeuN, a mature neuronal marker (Figure 2B). As expected, a minor portion of control mCherry-transduced cortical cells co-expressed NeuN (14.90 ± 1.40%), while both Ascl1 (58.36 ± 1.81%) and Ascl1^{SA6} (80.75 ± 0.82%) induced 3.9- and 5.4-fold increases in the number of mCherry cells co-expressing NeuN, respectively (Figures 2B,D).

The increase in NeuN expression suggested that Ascl1^{SA6} might have an enhanced capacity to induce neuronal differentiation compared to Ascl1, as shown in the embryonic cortex (Li et al., 2014) and in glioblastoma cells (Azzarelli et al., 2022). To examine the differentiation status of these cells more closely, we examined high magnification images and

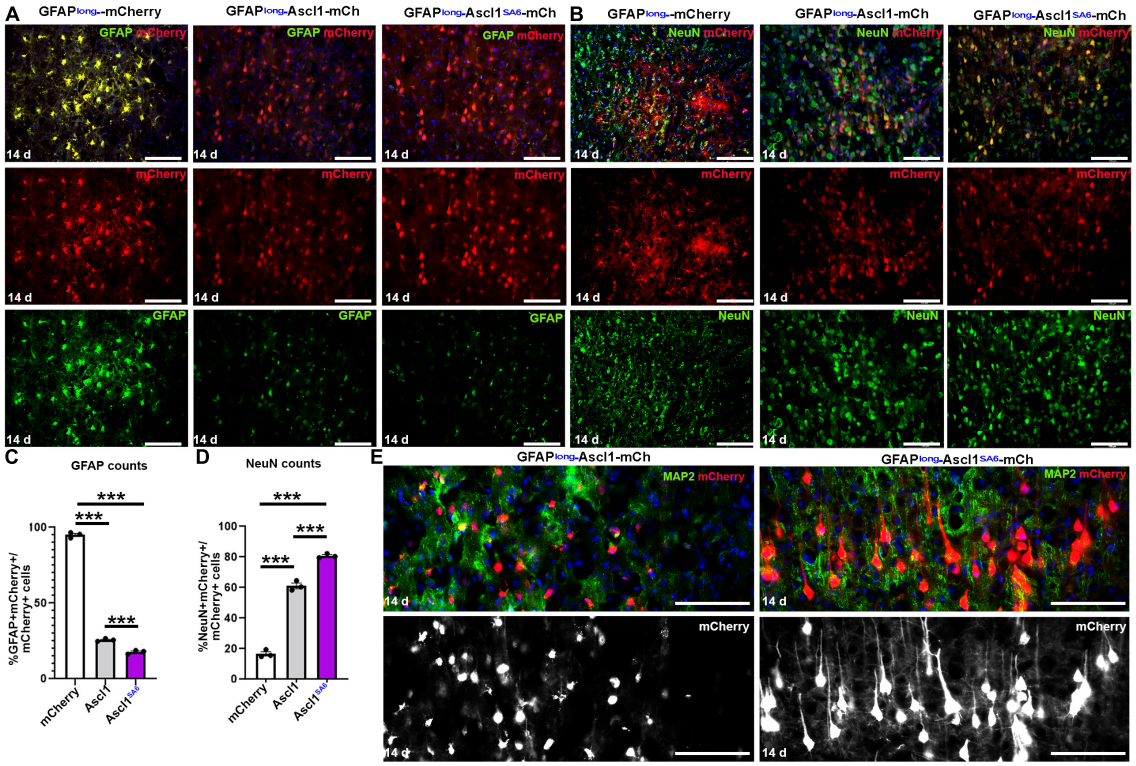

FIGURE 2
Ascl1 and Ascl1^{SA6} induce neuronal marker expression when expressed in cortical astrocytes *in vivo*. **(A,B)** mCherry co-expression with GFAP **(A)** or NeuN **(B)** 14 days post-transduction of AAV8-GFAPshort-mCherry, AAV8-GFAPshort-Ascl1-mCherry, or AAV8-GFAPshort-Ascl1^{SA6}-mCherry. Blue is DAPI counterstain. **(C,D)** Quantification of the percentage of mCherry^{+} transduced cells expressing GFAP **(C)** or NeuN **(D)** 14 days post-transduction. **(E)** High magnification images of mCherry^{+} cells co-stained with MAP2 at 14 days post-transduction of AAV8-GFAPshort-Ascl1-mCherry, or AAV8-GFAPshort-Ascl1^{SA6}-mCherry. Blue is DAPI counterstain. Scale bars = 100 μm. Significance was defined as *p*-values less than 0.05 and denoted as follows: ns, not significant, <0.05 *, <0.01 **, <0.001 ***.

co-expression with MAP2, a dendritic marker (Figure 2E). Strikingly, Ascl1^{SA6}-transduced cortical astrocytes developed elaborate dendritic arbors and mature neuronal morphologies, while Ascl1-transduced cells only developed short neurite-like projections, supporting the enhanced neuronal differentiation properties of Ascl1^{SA6} (Figure 2E).

To analyze neuronal maturation at later stages, we next tried to extend the timeline of analysis to 2 months post-transduction, but at this timepoint we no longer detected mCherry expression in any of the control mCherry-transduced brains (data not shown), precluding further analyses and prompting a change in the lineage tracing system we employed.

Adeno-associated viruses-glial fibrillary acidic protein-iCre can be used for long-term tracing of the fate of transduced cortical astrocytes *in vivo*

To circumvent the issues observed with mCherry reporter expression long-term, we turned to a Cre-based, permanent lineage tracing system. We used an AAV5-GFAPshort-iCre vector previously used in a neuronal reprogramming study to misexpress Neurod1 in cortical astrocytes (Livingston et al., 2020), replacing Neurod1 with Ascl1 or Ascl1^{SA6} to create AAV5-GFAPshort-Ascl1-t2a-iCre (abbreviated Ascl1-iCre) and AAV5-GFAPshort-Ascl1^{SA6}-t2a-iCre (abbreviated Ascl1^{SA6}-iCre) vectors (Figure 3A). Packaged AAVs (4.8×10^9 GC total in a 1 uL total volume) were stereotactically injected into the motor cortex of Rosa-zsGreen mice, using the same coordinates as in Figure 1 (AP: + 2.15, L/M: ± 1.7, DV: −1.7). The Rosa-zsGreen and Rosa-tdtomato alleles contain floxed STOP cassettes that prevent reporter expression except in the presence of Cre, which recombines the STOP cassette out. We observed robust zsGreen expression even 2 months after viral transduction, as shown with an exemplar Ascl1-iCre transduced brain (Figure 3B).

To confirm that with this iCre-based system we could induce *Ascl1* expression in cortical astrocytes, we first examined transcript distribution in Ascl1-iCre transduced brains at 2 months dpi using RNA *in situ* hybridization with a digoxygenin-labeled *Ascl1* riboprobe (Figure 3C).

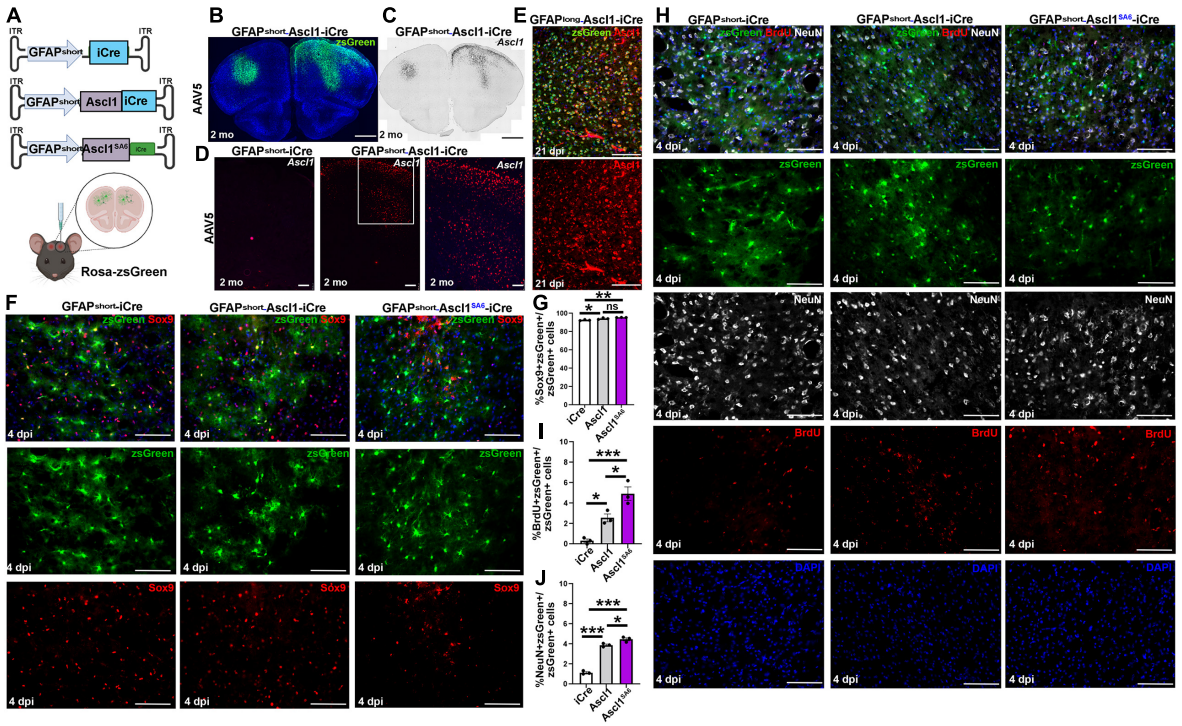

FIGURE 3
Establishing a Cre-based lineage tracing system to follow the fate of cortical astrocytes transduced *in vivo*. **(A)** Schematic illustration of AAV5-GFAPshort-iCre vectors and injection strategy into the cortex *in vivo*. **(B)** zsGreen expression in the cortex of Rosa-zsGreen mice injected with AAV5-GFAPshort-Ascl1-iCre at 2-months post-transduction. Blue is DAPI counterstain. **(C,D)** Colorimetric RNA *in situ* hybridization **(C)** and fluorescent RNAscope analysis **(D)** of Ascl1 transcript distribution in cortices transduced with AAV5-GFAPshort-iCre **(D)** or AAV5-GFAPshort-Ascl1-iCre **(C,D)** at 2-months post-transduction. The boxed area in D is magnified in the panel to the right. **(E)** Ascl1 immunostaining of motor cortex of Rosa-zsGreen animal transduced with AAV5-GFAPlong-Ascl1-iCre and harvested 21 dpi. **(F,G)** Rosa-zsGreen cortex transduced with AAV5-GFAPshort-iCre, AAV5-GFAPshort-Ascl1-t2a-iCre, and AAV5-GFAPshort-Ascl1^{SA6}-t2a-iCre at 4 dpi, showing zsGreen epifluorescence and Sox9 expression **(F)**. Quantification of the percentage of zsGreen^{+} cells that co-express GFAP **(G)**. **(H–J)** Rosa-zsGreen cortex transduced with AAV5-GFAPshort-iCre, AAV5-GFAPshort-Ascl1-t2a-iCre, and AAV5-GFAPshort-Ascl1^{SA6}-t2a-iCre at 4 dpi, showing zsGreen epifluorescence, NeuN (white), and Brdu (red) expression **(H)**. Blue is DAPI counterstain. Quantification of the percentage of zsGreen^{+} cells that co-express BrdU **(I)** and NeuN **(J)**. Scale bars in panels **B,C** = 200 μm, in panel **D** = 75 μm, and in panels **E,F,H** = 100 μm. Significance was defined as *p*-values less than 0.05 and denoted as follows: ns, not significant, <0.05 *, <0.01 **, <0.001 ***.

Final confirmation was performed using RNAscope, which definitively showed that while *Ascl1* transcripts were not detected in the parenchyma of the adult cortex transduced with iCre control vectors, robust *Ascl1* expression was detected in the Ascl1-iCre transduced brains 2 months post-transduction (Figure 3D). Finally, we confirmed that *Ascl1* transcripts were translated into protein by immunostaining Rosa-zsGreen brains transduced with an AAV5-GFAP-Ascl1-iCre vector, revealing nuclear Ascl1 expression in the zsGreen transduced cells at 21 dpi (Figure 3E).

Next, to test the specificity of our reporter system for astrocytic labeling, we performed short-term lineage tracing at 4 dpi. AAV5-GFAPshort vectors driving the expression of iCre, Ascl1-iCre and Ascl1^{SA6}-iCre were transduced into Rosa-zsGreen motor cortices and at 4 dpi, co-expression of zsGreen with Sox9, an astrocytic marker, was examined (Figure 3F). In the iCre control transduced brains, zsGreen^{+} cells had an astrocytic morphology, and the majority co-expressed Sox9 (92.6 ± 0.4%) (Figures 3F,G). Similarly, even though the astrocytic morphologies of zsGreen^{+} cells transduced with Ascl1 and Ascl1^{SA6} vectors were less pronounced, at 4 dpi, the majority of these cells expressed the astrocytic marker Sox9 (94.3 ± 0.5% and 95.5 ± 0.1%, respectively; Figures 3F,G). Notably, both Ascl1 and Ascl1^{SA6} induced small but significant 1.02- and 1.03-fold increases in Sox9 expression compared to control iCre transduction, consistent with Sox9 being an Ascl1 target gene in oligodendrocyte lineage development (Li et al., 2014). However, overall, we can conclude that for all three vectors, the majority of transduced cells are astrocytes, validating the specificity of our delivery system, at least at these early stages.

One of the questions in the field is whether astrocytes that are converted to iNeurons go through a proliferative

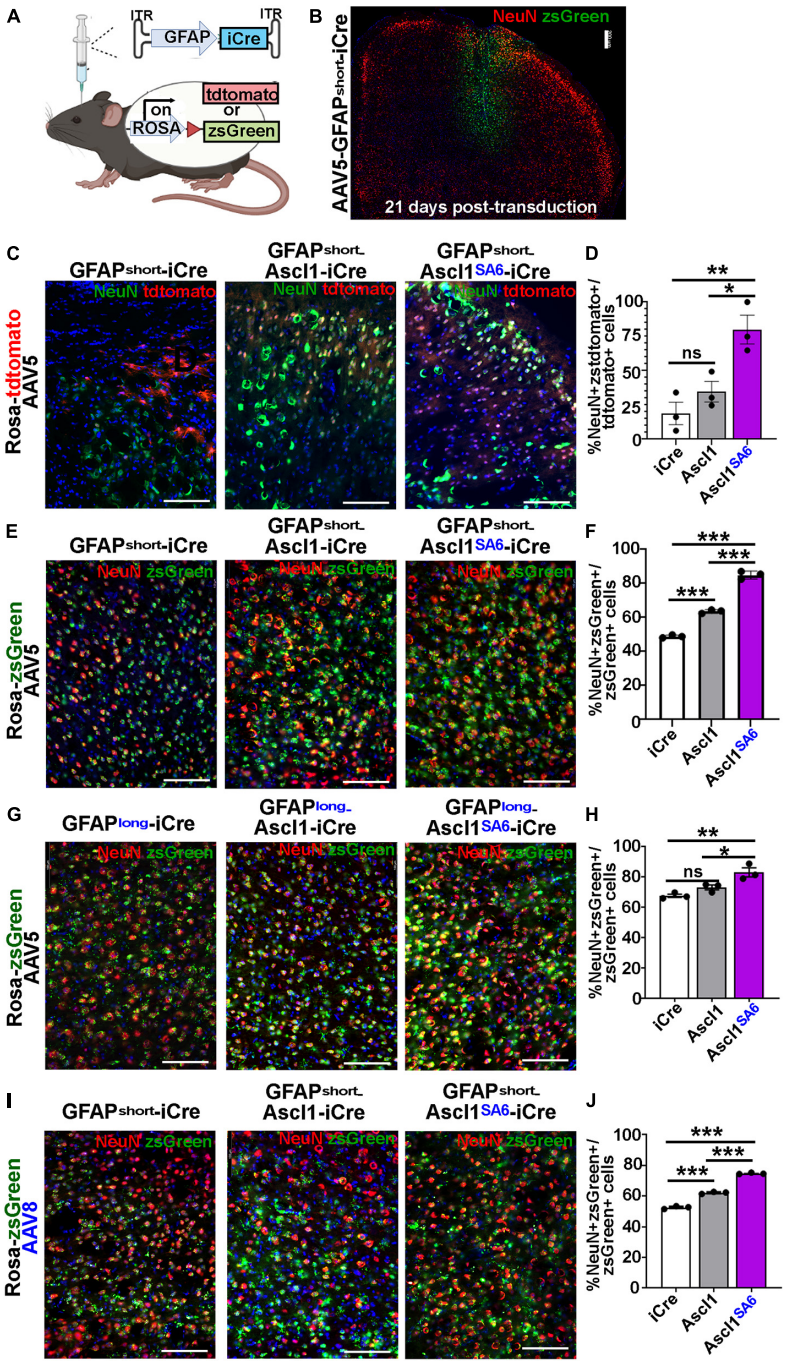

FIGURE 4
Ascl1^{SA6} induces more transduced cortical cells to express NeuN, a mature neuronal marker, than Ascl1. **(A)** Schematic illustration of Cre-based lineage tracing strategy, using AAV5-GFAPshort vectors and Rosa-tdtomato or Rosa-zsGreen transgenic animals. **(B)** Low magnification image of Rosa-zsGreen cortex transduced with AAV5-GFAPshort-iCre at 21 days post-transduction, showing zsGreen epifluorescence and NeuN expression. **(C)** Rosa-tdtomato cortex transduced with AAV5-GFAPshort-iCre, AAV5-GFAPshort-Ascl1-t2a-iCre, and AAV5-GFAPshort-Ascl1^{SA6}-t2a-iCre at 21 days post-transduction, showing tdtomato epifluorescence and NeuN expression. **(D)** Quantification of the percentage of tdtomato^{+} cells that co-express NeuN. **(E)** Rosa-zsGreen cortex transduced with AAV5-GFAPshort-iCre, AAV5-GFAPshort-Ascl1-t2a-iCre, and AAV5-GFAPshort-Ascl1^{SA6}-t2a-iCre at 21 days post-transduction, showing zsGreen epifluorescence and NeuN expression. **(F)** Quantification of the percentage of zsGreen^{+} cells that co-express NeuN. **(G)** Rosa-zsGreen cortex transduced with AAV5-GFAPlong-iCre, AAV5-GFAPlong-Ascl1-t2a-iCre, and AAV5-GFAPlong-Ascl1^{SA6}-t2a-iCre at 21 days post-transduction, showing zsGreen epifluorescence and NeuN expression. **(H)** Quantification of the percentage of zsGreen^{+} cells that co-express NeuN. **(I)** Rosa-zsGreen cortex transduced with AAV8-GFAPshort-iCre, AAV8-GFAPshort-Ascl1-t2a-iCre, and AAV8-GFAPshort-Ascl1^{SA6}-t2a-iCre at 21 days post-transduction, showing zsGreen epifluorescence and NeuN expression. **(J)** Quantification of the percentage of zsGreen^{+} cells that co-express NeuN. Scale bars in panel **B** = 200 μm, and panels **C,E,G,I** = 100 μm. Significance was defined as *p*-values less than 0.05 and denoted as follows: ns, not significant, <0.05 *, <0.01 **, <0.001 ***.

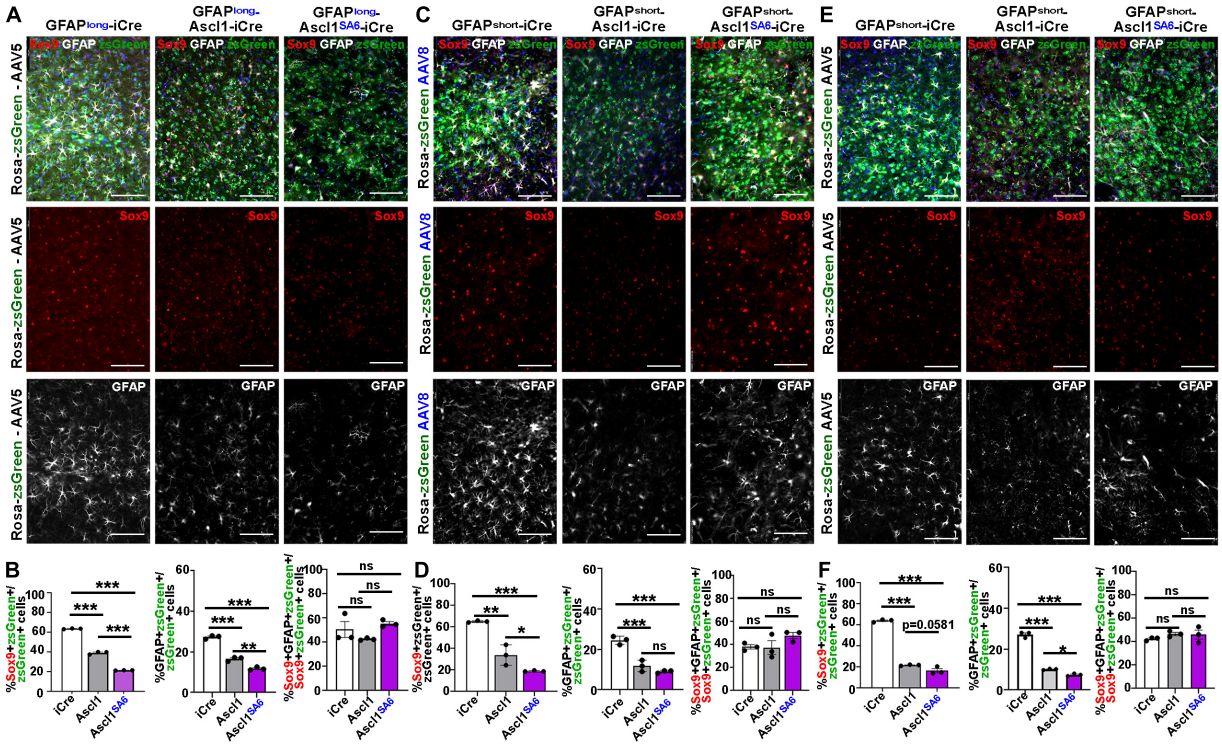

FIGURE 5

Ascl1^{SA6} more efficiently represses astrocytic markers Sox9 and GFAP in transduced cortical cells compared to Ascl1. **(A)** Rosa-zsGreen cortex transduced with AAV5-GFAPlong-iCre, AAV5-GFAPlong-Ascl1-t2a-iCre, and AAV5-GFAPlong-Ascl1^{SA6}-t2a-iCre at 21 days post-transduction, showing zsGreen epifluorescence, Sox9 (red) and GFAP (white) expression in merged and separate channels. Blue is a DAPI counterstain. **(B)** Quantification of the percentage of zsGreen^{+} cells that co-express Sox9 or GFAP, and the percentage of zsGreen^{+}Sox9^{+} cells that co-express GFAP. **(C)** Rosa-zsGreen cortex transduced with AAV5-GFAPshort-iCre, AAV5-GFAPshort-Ascl1-t2a-iCre, and AAV5-GFAPshort-Ascl1^{SA6}-t2a-iCre at 21 days post-transduction, showing zsGreen epifluorescence, Sox9 (red) and GFAP (white) expression in merged and separate channels. Blue is a DAPI counterstain. **(D)** Quantification of the percentage of zsGreen^{+} cells that co-express Sox9 or GFAP, and the percentage of zsGreen^{+}Sox9^{+} cells that co-express GFAP. **(E)** Rosa-zsGreen cortex transduced with AAV8-GFAPshort-iCre, AAV8-GFAPshort-Ascl1-t2a-iCre, and AAV8-GFAPshort-Ascl1^{SA6}-t2a-iCre at 21 days post-transduction, showing zsGreen epifluorescence, Sox9 (red) and GFAP (white) expression in merged and separate channels. Blue is a DAPI counterstain. **(F)** Quantification of the percentage of zsGreen^{+} cells that co-express Sox9 or GFAP, and the percentage of zsGreen^{+}Sox9^{+} cells that co-express GFAP. Scale bars = 100 μm. Significance was defined as *p*-values less than 0.05 and denoted as follows: ns, not significant, <0.05 *, <0.01 **, <0.001 ***.

stage. Given that Ascl1 can induce neural progenitor cells to proliferate in permissive environments in which Notch signaling is active (Castro et al., 2011; Li et al., 2014), we asked whether the overexpression of Ascl1 in adult astrocytes triggered re-entry into the cell cycle. Notably, we performed these studies only at 4 dpi given the recent demonstration that BrdU inhibits astrocyte to neuron conversion when administered for longer periods (Wang et al., 2022). Both Ascl1 (2.55 ± 0.38%) and Ascl1^{SA6} (4.93 ± 0.66%) induced 8.2-fold and 15.8-fold increases in BrdU incorporation in zsGreen^{+} transduced cells relative to the iCre control transduction (0.31 ± 0.18%), respectively (**Figures 3H,I**). Moreover, even after only 4 dpi, there were small but significant 3.4-fold and 3.9-fold increases in the ratio of zsGreen transduced cells expressing NeuN after transduction with Ascl1 (3.89 ± 0.09%) and Ascl1^{SA6} (4.47 ± 0.14%) compared to iCre controls (1.15 ± 0.10%), respectively (**Figures 3H,J**). However, the percentage of proliferating cells remains very low, less than 5%, in both instances, either because only a subset of cells are induced to proliferate, or because cells that incorporate BrdU undergo cell death (Wang et al., 2022).

In summary, the AAV-GFAP-iCre system that we employed can be used to express Ascl1 in cortical astrocytes, and to trigger Cre-dependent reporter expression, which in turn can be used to trace the fate of transduced cells in the adult cerebral cortex.

Mutating serine phospho-acceptor sites in *Ascl1* augments neuronal lineage conversion in the adult cortex

In vivo astrocyte-to-neuron lineage conversion has been reported using different AAVs (AAV5 or AAV8), which have

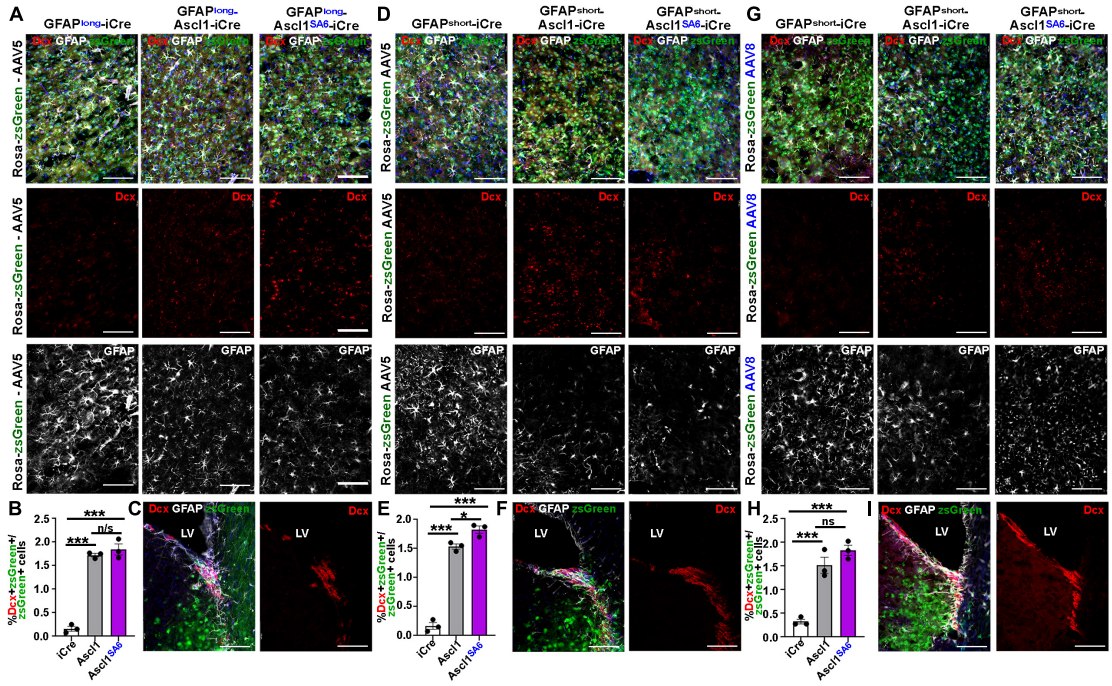

FIGURE 6
Limited induction of Dcx expression in GFAP^{+} transduced astrocytes by Ascl1 and Ascl1^{SA6}. **(A–C)** Rosa-zsGreen cortex transduced with AAV5-GFAPlong-iCre, AAV5-GFAPlong-Ascl1-t2a-iCre, and AAV5-GFAPlong-Ascl1^{SA6}-t2a-iCre at 21 days post-transduction, showing zsGreen epifluorescence, Dcx (red) and GFAP (white) expression in the parenchyma of the motor cortex **(A)** or in the ventricular-subventricular zone (V-SVZ) **(C)**. Blue is DAPI counterstain. **(B)** Quantification of the percentage of zsGreen^{+} cells that co-express Dcx. **(D–F)** Rosa-zsGreen cortex transduced with AAV5-GFAPshort-iCre, AAV5-GFAPshort-Ascl1-t2a-iCre, and AAV5-GFAPshort-Ascl1^{SA6}-t2a-iCre at 21 days post-transduction, showing zsGreen epifluorescence, Dcx (red) and GFAP (white) expression in the parenchyma of the motor cortex **(D)** or in the ventricular-subventricular zone (V-SVZ) **(F)**. Blue is DAPI counterstain. Quantification of the percentage of zsGreen^{+} cells that co-express Dcx **(E)**. **(G–I)** Rosa-zsGreen cortex transduced with AAV8-GFAPshort-iCre, AAV8-GFAPshort-Ascl1-t2a-iCre, and AAV8-GFAPshort-Ascl1^{SA6}-t2a-iCre at 21 days post-transduction, showing zsGreen epifluorescence, Dcx (red) and GFAP (white) expression in the parenchyma of the motor cortex **(G)** or in the ventricular-subventricular zone (V-SVZ) **(I)**. Blue is DAPI counterstain. Quantification of the percentage of zsGreen^{+} cells that co-express Dcx **(H)**. Scale bars = 100 μm. LV, lateral ventricle. Significance was defined as p-values less than 0.05 and denoted as follows: ns, not significant, <0.05 *, <0.01 **, <0.001 ***.

both been reported to transduce cortical astrocytes (Aschauer et al., 2013), and using a 681bp human gfaABC(1)D promoter (Lee et al., 2008; Livingston et al., 2020) (hereafter, GFAPshort) or the 2.2 kb GFAPlong promoter described above (Barker et al., 2018; Chen et al., 2020; Livingston et al., 2020; Puls et al., 2020). We thus questioned which promoter and AAV delivery system was optimal. Notably, the GFAPshort promoter shows similar astrocyte-specificity as a 2.2 kb GFAPlong promoter, but drives two-fold higher levels of gene expression (Lee et al., 2008). We thus compared AAV5 and AAV8 capsids containing GFAPlong and GFAPshort promoters (Lee et al., 2008), and transduced Rosa-zsGreen and Rosa-tdtomato reporter mice, two of the brightest fluorescent reporters (Madisen et al., 2010) (**Figure 4**). Each comparative group had a set of three genetic cargos: iCre alone (control), Ascl1-iCre, or Ascl1^{SA6}-iCre. Our three comparisons were AAV8 vs. AAV5 with the short GFAP promoter, GFAPshort vs. GFAPlong in AAV5, and Rosa-tdtomato vs. Rosa-zsGreen using AAV5-GFAP short constructs. As above, packaged AAVs (4.8×10^{9} GC total in a 1 uL total volume) were stereotactically injected into the motor cortex using the same coordinates (AP: + 2.15, L/M: ± 1.7, DV: −1.7).

We first compared the ability of AAV5-GFAPshort constructs to induce NeuN expression when injected into the cortex of Rosa-tdtomato mice (**Figures 4C,D**) and Rosa-zsGreen (**Figures 4E,F**) mice. In Rosa-tdtomato cortices analyzed at 21 dpi, statistically similar numbers of iCre (18.8 ± 8.1%) and Ascl1 (34.7 ± 7.5%) transduced tdtomato^{+} cells expressed NeuN, while Ascl1^{SA6} transduction induced a 4.3-fold increase in the number of NeuN expressing tdtomato^{+} cells (79.9 ± 10.5%) compared to iCre "baseline" levels (**Figures 4C,D**). We then compared the same AAV5-GFAPshort constructs transduced into motor cortices of Rosa-zsGreen mice. In Rosa-zsGreen cortices analyzed at 21 dpi, Ascl1 (63.6 ± 0.6%) and Ascl1^{SA6} (85.0 ± 1.3%) induced 1.3- and 1.7-fold increases, respectively, in the number of tdtomato^{+} cells expressing NeuN compared to iCre control levels (48.9 ± 0.5%) (**Figures 4E,F**). Thus, in both reporter mice, Ascl1^{SA6} was more efficient at inducing NeuN expression compared to

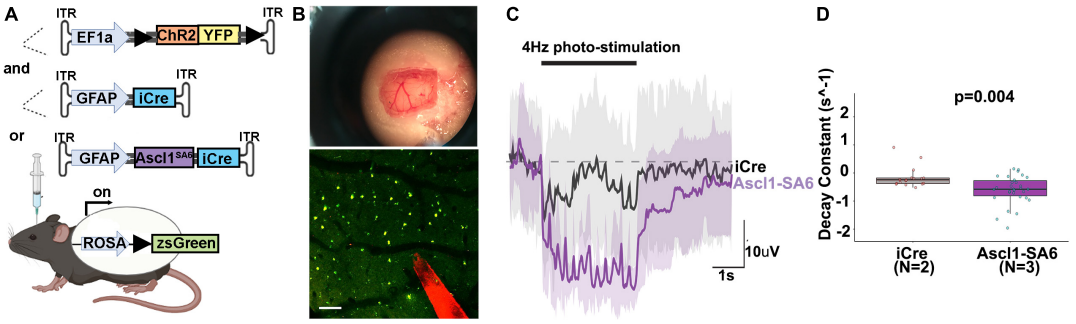

FIGURE 7
Optogenetic stimulation of ChR2 actuator reveals that Ascl1^{SA6} transduced cells have a shorter decay constant. **(A)** Schematic illustration of optogenetic experiment in which we injected AAVs carrying ChR2-(H134R)-YFP, an optogenetic actuator, and co-transduced AAV5-GFAPshort-iCre or AAV5-GFAPshort-Ascl1^{SA6}-iCre into the cortex of Rosa-zsGreen mice. A 4 weeks later, photostimulation experiments were performed. **(B)** Craniotomy and cortical window used for simultaneous photostimulation and electrophysiological recordings. Also shown is a two-photon z-stack projection of the cortical tissue showing zsGreen^{+} cells (green channel) and the tungsten electrode tip (red channel); the circular yellow area represents the site of stimulation near the electrode; scalebar = 100 μm. **(C)** Representative raw voltage traces showing the changes in the LFP band following 3 s of photostimulation at 4 Hz for both Ascl1^{SA6} (purple trace) and iCre (black trace) treatments. Shaded areas indicate the voltage standard deviation measured across different repetitions, within the same photostimulated area. **(D)** Measurement of the decay constant of photostimulated cells in iCre and Ascl1^{SA6} transduced brains. Dots in the boxplots indicate individual measures and "N" indicates the number of mice used in each group. Significance was defined as *p*-values less than 0.05 and denoted as follows: ns, not significant, <0.05 *, <0.01 **, <0.001 ***.

Ascl1, but given that zsGreen expression appeared more widespread than tdtomato, we used Rosa-zsGreen mice for the remainder of the study.

We next assessed neuronal marker expression induced by AAV5-GFAPlong constructs introduced into Rosa-zsGreen motor cortices (**Figures 4G,H**). At 21 dpi, 67.7 ± 1.1% of the iCre control transduced zsGreen^{+} cells expressed NeuN (**Figures 4G,H**). Compared to AAV5-GFAPshort-iCre constructs, the AAV5-GFAPlong-iCre vector induced a 1.4-fold increase in "background" reporter expression in neurons, suggesting that the long promoter is less astrocyte-specific. Nevertheless, when Ascl1^{SA6} was expressed from the GFAPlong promoter, 1.2-fold more zsGreen^{+} cells expressed NeuN (83.2 ± 2.9%) compared to iCre, whereas Ascl1 neuronal conversion rates (73.2 ± 1.6%) were not above iCre baseline (67.7 ± 1.1%) (**Figures 4G,H**).

Next, we compared the AAV8 capsid using the GFAPshort promoter. With this system, we also found that 52.6 ± 0.6% of iCre control transduced zsGreen^{+} cells expressed NeuN, but both Ascl1 (62.2 ± 0.4%), and more strikingly, Ascl1^{SA6} (74.8 ± 0.3%) induced significant 1.2- and 1.4-fold increases, respectively in the number of zsGreen^{+} cells expressing NeuN at 21 dpi (**Figures 4I,J**). From these studies, we conclude that Ascl1^{SA6} transduced cells more frequently express NeuN compared to Ascl1 transduced cells when delivered to the adult motor cortex using GFAP promoter elements. In addition, our study supports previous studies using transgenic mice that suggested that the GFAPshort promoter is more specific to cortical astrocytes than the GFAPlong promoter (Lee et al., 2008). Finally, compared to AAV8, the AAV5 capsid labels fewer cortical neurons when GFAP-iCre sequences are included, and may thus be better suited for initial astrocyte targeting and neuronal reprogramming *in vivo*.

Ascl1^{SA6} and to a lesser extent Ascl1 downregulates astrocytic marker expression

True lineage conversion requires that targeted cells, in our case astrocytes, not only turn on neuronal markers, but also extinguish the expression of glial markers. Indeed, in the embryonic cortex *in vivo* (Li et al., 2014) and in neuroblastoma (Woods et al., 2022) and glioblastoma (Azzarelli et al., 2022) cells *in vitro*, Ascl1^{SA6} is more efficient at turning on neuronal gene expression and less efficient at transactivating the Sox9 glial promoter compared to Ascl1 (Li et al., 2014). Here, we thus asked whether in the adult cortex, Ascl1^{SA6} could more efficiently downregulate Sox9 and GFAP expression in mature astrocytes. In this set of experiments, we compared the AAV5 vector carrying GFAPlong and GFAPshort promoters and the AAV8 vector with the GFAPshort promoter. As above, packaged AAVs (4.8×10^{9} GC total in a 1 uL total volume) were stereotactically injected into the motor cortex of Rosa-zsGreen animals using the same coordinates (AP: + 2.15, L/M: ± 1.7, DV: −1.7), and brains were harvested at 21 dpi.

As expected, the majority of iCre-transduced cells expressed Sox9, an astrocytic marker, after 21 dpi regardless of whether iCre was expressed with AAV5-GFAP-long (63.7 ± 0.2%) (**Figures 5A,B**), AAV8-GFAPshort (65.1 ± 0.5%) (**Figures 5C,D**), or AAV5-GFAPshort (64.0 ± 0.8%)

(Figures 5E,F) vectors, confirming astrocytic targeting of a large proportion of cells. However, the ratio of iCre control cells that co-expressed GFAP was lower than Sox9 for all vectors, including AAV5-GFAP-long (27.3 ± 0.5%) (Figures 5A,B), AAV8-GFAPshort (24.5 ± 1.2%) (Figures 5C,D) or AAV5-GFAPshort (27.2 ± 0.8%) (Figures 5E,F). One possibility is that astrocytes that initially expressed GFAP at the time of transduction turned off their GFAP expression within the 21 days before analysis, or alternatively, GFAP may be transcribed and not translated. Nevertheless, regardless of this discrepancy, based on Sox9 expression, we can conclude that over half of iCre control-transduced cells are astrocytes at 21 dpi.

We next assessed Sox9/zsGreen co-expression 21 days after transduction of Ascl1, revealing 1. 62-, 1.92- and 2.94-fold reductions, respectively, using AAV5-GFAP-long (39.3 ± 0.8%) (Figures 5A,B), AAV8-GFAPshort (34.0 ± 5.5%) (Figures 5C,D) or AAV5-GFAPshort (21.8 ± 0.3%) (Figures 5E,F) vectors. In all cases, Ascl1^{SA6} reduced Sox9/zsGreen co-expression levels even further, with 2. 95-, 3.43- and 4.65-fold reductions, respectively using AAV5-GFAP-long (21.6 ± 0.1%) (Figures 5A,B), AAV8-GFAPshort (19.0 ± 0.3%) (Figures 5C,D) or AAV5-GFAPshort (16.5 ± 2.0%) (Figures 5E,F) vectors.

Similarly, an analysis of GFAP/zsGreen co-expression at 21 dpi revealed 1. 65-, 2.08- and 2.68-fold reductions, respectively, using AAV5-GFAP-long (16.6 ± 0.6%) (Figures 5A,B), AAV8-GFAPshort (11.8 ± 1.6%) (Figures 5C,D) or AAV5-GFAPshort (10.1 ± 0.2%) (Figures 5E,F) vectors. More pronounced 2.32- and 3.66-fold reductions in GFAP/zsGreen co-expression were observed at 21 dpi using AAV5-GFAP-long (11.8 ± 0.4%) (Figures 5A,B) and AAV5-GFAP short (7.4 ± 0.3%) (Figures 5E,F) vectors, respectively, to express Ascl1^{SA6}. However, overexpression of Ascl1^{SA6} using AAV8-GFAPshort gave a similar 2.72-fold reduction in GFAP/zsGreen co-expression (9.0 ± 0.4%) as seen with Ascl1 (Figures 5C,D). Notably, the reduction in astrocytic marker was not due to changes in the ratio of Sox9^{+} cells that co-expressed GFAP, so both Sox9 single^{+} and Sox9/GFAP double^{+} cells were equally affected (Figures 5B,D,F). Taken together, these data support the contention that Ascl1 and Ascl1^{SA6} both suppress an astrocytic fate in the adult cortex, but Ascl1^{SA6} is more efficient at glial repression, similar to studies in the embryonic cortex (Li et al., 2014).

Few Ascl1 and Ascl1^{SA6} transduced cells go through a Dcx^{+} neuroblast stage

It has been suggested that neuronal lineage conversion *in vivo* should include a transitory, immature Dcx^{+} neuroblast stage, as has been shown *in vitro* (Bocchi et al., 2021). We thus examined Dcx expression following the overexpression of Ascl1 and Ascl1^{SA6} in motor cortex astrocytes, again comparing the AAV5 vector carrying GFAPlong and GFAPshort promoters and the AAV8 vector with the GFAPshort promoter using the same coordinates and dosage, and brains were harvested at 21 dpi.

As expected, very few iCre-transduced cells expressed Dcx after 21 dpi regardless of whether iCre was expressed with AAV5-GFAP-long (0.16 ± 0.05%) (Figures 6A,B), AAV8-GFAPshort (0.33 ± 0.05%) (Figures 6G,H), or AAV5-GFAPshort (0.17 ± 0.06%) (Figures 6D,E) vectors. After 21 dpi, there were 10. 9-, 4. 72-, and 9.20-fold increases in Dcx/zsGreen co-expression following the overexpression of Ascl1 using AAV5-GFAP-long (1.72 ± 0.04%) (Figures 6A,B), AAV8-GFAPshort (1.52 ± 0.17%) (Figures 6G,H) or AAV5-GFAPshort (1.53 ± 0.04%) (Figures 6D,E) vectors, respectively, reflecting a very small fraction of the total transduced cells. Similarly, Ascl1^{SA6} induced 11. 67-, 5. 64-, and 10.94-fold increases in Dcx/zsGreen co-expression when delivered to the motor cortex using AAV5-GFAP-long (1.84 ± 0.12%) (Figures 6A,B), AAV8-GFAPshort (1.83 ± 0.11%) (Figures 6G,H) or AAV5-GFAPshort (1.83 ± 0.06%) (Figures 6D,E) vectors, respectively. However, with the exception of AAV5-GFAPshort, Ascl1^{SA6} was not better than Ascl1 at inducing Dcx expression. Notably, we confirmed that Dcx antibody staining was correct, as strong expression was seen in the V-SVZ, where neuroblasts are generated (Figures 6C,F,I).

Taken together, these data suggest that most transduced cells do not undergo a Dcx neuroblast stage, or that this stage is very transitory.

Ascl1^{SA6} induces electrophysiological properties of iNeurons in targeted astrocytes

To promote functional recovery in pathological conditions, iNeurons must integrate into existing neural circuits by making synaptic connections with endogenous neurons and sending axons to appropriate neuronal targets. To test neural network integration of iNeurons *in vivo*, we co-transduced AAVs carrying GFAP-iCre or GFAP-Ascl1^{SA6} with FLEX-ChR2-(H134R)-YFP, a Cre-dependent optogenetic actuator that offers a sensitive way to photoactivate neurons and elicit large evoked potentials (Figure 7A). After 36 days, we made a cranial window and performed intracortical electrophysiological recordings to assess local field potentials, a measure of aggregate neuronal activity, in response to ChR2 photoactivation (20 Hz, 10 ms pulse length, 5s total) (Figure 7B). In a representative trace, and quantified for several sites, Ascl1^{SA6} iNeurons transduced cortices exhibited a faster decay of evoked potentials to baseline than did iCre transduced cortices (Figures 7C,D), a neuronal feature. This data thus supports the contention that Ascl1^{SA6} successfully converts transduced astrocytes into functional iNeurons.

Discussion

In this study, we performed a detailed comparison of the capacity of Ascl1 and Ascl1^{SA6} to induce neuronal markers and suppress glial markers when expressed in adult cortical astrocytes *in vivo*. We found that with each combination of AAV capsids, GFAP promoters and Rosa-reporter lines tested, a higher proportion of Ascl1^{SA6} transduced cells consistently expressed NeuN, a mature neuronal marker, and acquired complex dendritic arbors compared to cells transduced with Ascl1 or iCre controls. In contrast, an equivalent, low number of Ascl1 and Ascl1^{SA6} transduced cells had the signature of a transitory Dcx^{+} neuroblast stage, suggesting that either this stage is very transitory, or not induced by these TFs. In addition, both Ascl1 and Ascl1^{SA6} could suppress the expression of astrocytic markers (Sox9 and GFAP), although Ascl1^{SA6} was again superior in this regard. The enhanced neurogenic capacity of Ascl1^{SA6} vs. Ascl1 is in keeping with prior studies in embryonic cortical progenitor cells *in vivo* (Li et al., 2014). In addition, it was recently demonstrated that ASCL1^{SA5} (note that the human ASCL1 gene has 5 SP sites) can induce a glioblastoma stem cell line to undergo terminal differentiation and exit the cell cycle more effectively than native ASCL1, leading to growth suppression of this tumor cell line (Azzarelli et al., 2022). Taken together with our work in the current study, there is now cumulative support for the enhanced pro-neurogenic and anti-astrocytic capacity of Ascl1^{SA6} vs. Ascl1.

Even though our data shows clear differences between Ascl1 and Ascl1^{SA6} in regulating neuronal marker expression when expressed in the adult brain, with an abundance of caution, it is important to acknowledge a recent debate created by several high-profile 2021 and 2022 publications that questioned whether brain glia (astrocytes, microglia) can be converted to neurons *in vivo* (Rao et al., 2021; Wang et al., 2021). Notably, with each of our strategies, incorporating different AAV capsids and GFAP promoters, our intent was to preferentially target cortical astrocytes without any leaky expression in endogenous neurons. However, similar to others, we observed a significant level of reporter expression in endogenous neurons, using either mCherry or iCre control vectors. Thus, we were not able to achieve the astrocytic specificity that we desired. Moving forward, it is important to address these concerns by incorporating robust lineage tracing of the starter glial population, and by pre-labeling endogenous neurons, as outlined in a new position paper (Bocchi et al., 2021).

Notably, Wang et al. (2021) found that the TF coding sequences act in cis to alter the astrocyte specificity of the GFAP promoter, an experimental confound that is enhanced over time, as astrocytic-specificity is initially observed at 4 days post-transduction, even with a GFAP-Neurod1-mCherry vector (Wang et al., 2021). Presumably, the same cis-effects of the Ascl1 cargo are taking place in our system. In this regard, it is interesting that bHLH TFs suppress the GFAP promoter indirectly by sopping up glial cofactors, such as CBP-SMAD, and preventing STAT activation, all of which are required to transactivate the GFAP promoter (Sun et al., 2001). One possibility is that this indirect mode of suppression of glial gene expression may account for some of the reduced Sox9 and GFAP expression induced by Ascl1 and Ascl1^{SA6}. However, as Ascl1 and Ascl1^{SA6} differ in only six codons, it seems unlikely that the enhanced capacity of Ascl1^{SA6} to turn on neuronal genes and turn off glial genes is solely due to the cis-activity of these two genes being significantly different. For instance, in addition to sopping up glial cofactors, Ascl1 and Ascl1^{SA6} may suppress glial genes by inducing the expression of downstream transcriptional repressors, an indirect mode of action that was previously attributed to Neurog2 during cortical development (Kovach et al., 2013). Regardless of how Ascl1 and Ascl1^{SA6} function during neuronal reprogramming, astrocytic suppression by the proneural bHLH TFs Neurog2 and Ascl1 has been firmly established in the embryonic CNS (Oproescu et al., 2021). Indeed, embryonic cortical progenitors have a reduced propensity to differentiate into astrocytes, based on *in vitro* differentiation assays or *in vivo* lineage tracing (Han et al., 2021). We thus favor the model that Ascl1^{SA6} can both suppress astrocytic gene expression and transactivate neuronal genes more efficiently than Ascl1, as we showed definitively in the embryonic brain (Li et al., 2014).

The Rao et al. (2021) study highlights a different concern, as their manuscript contradicted an earlier claim that microglia could be converted to iNeurons *in vivo* (Matsuda et al., 2019). In a published response by the authors of the initial microglia-to-iNeuron conversion paper, the authors suggested that the lentiviral delivery strategy used by Rao et al. (2021) achieved Neurod1 expression at a magnitude lower than what is required for successful neuronal reprogramming (Matsuda and Nakashima, 2021). However, a recent report using glial lineage tracing similarly suggested that Neurod1 has a limited capacity to convert brain astrocytes to iNeurons (Leib et al., 2022). Nevertheless, the importance of achieving threshold levels of the bHLH TFs has similarly been shown in the embryonic brain, with Neurog2 not able to convert ventral telencephalic progenitors to a dorsal cortical fate in Ascl1^{Neurog2KI} mice (Parras et al., 2002), whereas high levels of Neurog2 expression achieved by *in utero* electroporation of the ventral telencephalon effectively induces a cortical fate in ventral domains (Kovach et al., 2013). Thus, levels of bHLH TF expression are indeed important to how these genes function and their capacity to turn on downstream genes.

As a final comment, even though the GFAP promoter may drive background labeling of endogenous neurons, it does not negate the capacity of glia to be converted to neurons, as shown definitively using retroviruses *in vivo*, and supported by hundreds of *in vitro* studies (Barker et al., 2018; Sharif et al., 2021; Vasan et al., 2021). In our study in the adult brain, it is possible that the astrocytes we targeted are resident cells in the brain parenchyma, or newly generated reactive astrocytes derived from V-SVZ neural stem cells, as shown

recently (Faiz et al., 2015). Lineage tracing of V-SVZ cells using nestin-Cre^{ERT2} (Faiz et al., 2015) and of resident astrocytes using Aldh1l1-Cre^{ERT2} (Srinivasan et al., 2016) could help to distinguish the source of new neurons. Indeed, in December 2021, a position paper listed important new obligatory controls for *in vivo* neuronal reprogramming, designed to address recent controversies in the field, including: lineage tracing (neuronal and glial), lineage trajectory analyses (single cell transcriptomic studies) and functional assessments of iNeuron activity (Bocchi et al., 2021).

As a final statement, in support of the therapeutic power of neuronal reprogramming, new studies demonstrating that the beneficial effects of neuronal reprogramming are lost upon chemogenetic silencing or ablation of new neurons in Parkinson's disease (Qian et al., 2020) and stroke (Irie et al., 2021) models, respectively, provide growing support for the potential therapeutic power of endogenous neuronal replacement.

Data availability statement

The raw data supporting the conclusions of this article will be made available by the authors, without undue reservation.

Ethics statement

The animal study was reviewed and approved by the Sunnybrook Research Institute Comparative Research Animal Care Committee (ACC).

Author contributions

HG and EP did the conceptualization, carried out the data curation and formal analysis, investigated, visualized, and validated the data, performed the methodology, wrote the original draft, and wrote, reviewed, and edited the manuscript. DZ carried out the formal analysis, investigated and validated the data, performed the methodology, and wrote, reviewed, and edited the manuscript. JaM, LV, and AT carried out the data curation and formal analysis, investigated and validated the data, performed the methodology, and wrote, reviewed, and edited the manuscript. FS, TF, and VC carried out the data curation, performed the methodology, validated the data, and wrote, reviewed, and edited the manuscript. ML investigated and validated the data, performed the methodology, and wrote, reviewed, and edited the manuscript. OP investigated the data, performed the methodology, and wrote, reviewed, and edited the manuscript. NK carried out the formal analysis and investigated the data. DK, MF, BS, and JM carried out the resources, supervised the data, and wrote, reviewed, and edited the manuscript. CS carried out the funding acquisition, project administration, and resources, did the conceptualization, supervised and validated the data, wrote the original draft, and wrote, reviewed, and edited the manuscript. All authors contributed to the article and approved the submitted version.

Funding

This research was funded by a Canadian Institutes of Health Research (CIHR) Project grant awarded to JM, CS, and BS (PJT 155983) and partially by the University of Toronto's Medicine by Design initiative, which receives funding from the Canada First Research Excellence Fund (CFREF). Medicine by Design Cycle 2 and Pivotal Experiment funding was awarded to CS and MF. EP was supported by a University of Toronto Fellowship and Ontario Graduate Scholarship. ML was supported by the CIHR Ph.D. fellowship.

Acknowledgments

We acknowledge and thank Petia Stefanova in the SRI Histology Facility for assistance with cryosectioning. We thank Tom Enbar and Daniela Lozano Casasbuenas in Maryam Faiz's laboratory, and Kelly Markham-Coultes in Isabelle Aubert's laboratory for technical assistance. We also thank Leping Cheng for reagents. JM holds the CRC Tier1 Chair in Alzheimer's disease supported by Canada Research Chairs Program. CS holds the Dixon Family Chair in Ophthalmology Research.

Conflict of interest

The authors hold a provisional patent 509459-US on method and compositions for neuronal reprogramming, submitted on June 9th, 2021. The conversion application was submitted June 9th, 2022.

Publisher's note

Supplementary material

The Supplementary Material for this article can be found online at: https://www.frontiersin.org/articles/10.3389/fnins.2022.917071/full#supplementary-material

References

Adams, K. V., and Morshead, C. M. (2018). Neural stem cell heterogeneity in the mammalian forebrain. *Prog. Neurobiol.* 170, 2–36.

Ali, F., Hindley, C., McDowell, G., Deibler, R., Jones, A., Kirschner, M., et al. (2011). Cell cycle-regulated multi-site phosphorylation of Neurogenin 2 coordinates cell cycling with differentiation during neurogenesis. *Development* 138, 4267–4277. doi: 10.1242/dev.067900

Ali, F. R., Marcos, D., Chernukhin, I., Woods, L. M., Parkinson, L. M., Wylie, L. A., et al. (2020). Dephosphorylation of the proneural transcription factor ASCL1 re-engages a latent post-mitotic differentiation program in neuroblastoma. *Mol. Cancer Res.* 18, 1759–1766.

Aschauer, D. F., Kreuz, S., and Rumpel, S. (2013). Analysis of transduction efficiency, tropism and axonal transport of AAV serotypes 1, 2, 5, 6, 8 and 9 in the mouse brain. *PLoS One* 8:e76310. doi: 10.1371/journal.pone.0076310

Aydin, B., Kakumanu, A., Rossillo, M., Moreno-Estelles, M., Garipler, G., Ringstad, N., et al. (2019). Proneural factors Ascl1 and Neurog2 contribute to neuronal subtype identities by establishing distinct chromatin landscapes. *Nat. Neurosci.* 22, 897–908. doi: 10.1038/s41593-019-0399-y

Azzarelli, R., Hardwick, L. J., and Philpott, A. (2015). Emergence of neuronal diversity from patterning of telencephalic progenitors. *Wiley Interdiscip. Rev. Dev. Biol.* 4, 197–214.

Azzarelli, R., McNally, A., Dell'Amico, C., Onorati, M., Simons, B., and Philpott, A. (2022). ASCL1 phosphorylation and ID2 upregulation are roadblocks to glioblastoma stem cell differentiation. *Sci. Rep.* 12:2341. doi: 10.1038/s41598-022-06248-x

Barker, R. A., Gotz, M., and Parmar, M. (2018). New approaches for brain repair-from rescue to reprogramming. *Nature* 557, 329–334. doi: 10.1038/s41586-018-0087-1

Berninger, B., Guillemot, F., and Gotz, M. (2007). Directing neurotransmitter identity of neurones derived from expanded adult neural stem cells. *Eur. J. Neurosci.* 25, 2581–2590. doi: 10.1111/j.1460-9568.2007.05509.x

Bocchi, R., Masserdotti, G., and Götz, M. (2021). Direct neuronal reprogramming: Fast forward from new concepts toward therapeutic approaches. *Neuron* 110, 366–393. doi: 10.1016/j.neuron.2021.11.023

Britz, O., Mattar, P., Nguyen, L., Langevin, L. M., Zimmer, C., Alam, S., et al. (2006). A role for proneural genes in the maturation of cortical progenitor cells. *Cereb. Cortex* 16, i138–i151.

Casarosa, S., Fode, C., and Guillemot, F. (1999). Mash1 regulates neurogenesis in the ventral telencephalon. *Development* 126, 525–534.

Castro, D. S., Martynoga, B., Parras, C., Ramesh, V., Pacary, E., Johnston, C., et al. (2011). A novel function of the proneural factor Ascl1 in progenitor proliferation identified by genome-wide characterization of its targets. *Genes Dev.* 25, 930–945. doi: 10.1101/gad.627811

Chanda, S., Ang, C. E., Davila, J., Pak, C., Mall, M., Lee, Q. Y., et al. (2014). Generation of induced neuronal cells by the single reprogramming factor ASCL1. *Stem Cell Rep.* 3, 282–296.

Chen, Y. C., Ma, N. X., Pei, Z. F., Wu, Z., Do-Monte, F. H., Keefe, S., et al. (2020). A NeuroD1 AAV-based gene therapy for functional brain repair after ischemic injury through in vivo astrocyte-to-neuron conversion. *Mol. Ther.* 28, 217–234. doi: 10.1016/j.ymthe.2019.09.003

Drouin-Ouellet, J., Lau, S., Brattas, P. L., Rylander Ottosson, D., Pircs, K., Grassi, D. A., et al. (2017). REST suppression mediates neural conversion of adult human fibroblasts via microRNA-dependent and -independent pathways. *EMBO Mol. Med.* 9, 1117–1131. doi: 10.15252/emmm.201607471

Faiz, M., Sachewsky, N., Gascon, S., Bang, K. W., Morshead, C. M., and Nagy, A. (2015). Adult neural stem cells from the subventricular zone give rise to reactive astrocytes in the cortex after stroke. *Cell Stem Cell* 17, 624–634. doi: 10.1016/j.stem.2015.08.002

Fode, C., Ma, Q., Casarosa, S., Ang, S. L., Anderson, D. J., and Guillemot, F. (2000). A role for neural determination genes in specifying the dorsoventral identity of telencephalic neurons. *Genes Dev.* 14, 67–80.

Gascon, S., Murenu, E., Masserdotti, G., Ortega, F., Russo, G. L., Petrik, D., et al. (2016). Identification and successful negotiation of a metabolic checkpoint in direct neuronal reprogramming. *Cell Stem Cell* 18, 396–409. doi: 10.1016/j.stem.2015.12.003

Giehrl-Schwab, J., Giesert, F., Rauser, B., Lao, C. L., Hembach, S., Lefort, S., et al. (2022). Parkinson's disease motor symptoms rescue by CRISPRa-reprogramming astrocytes into GABAergic neurons. *EMBO Mol. Med.* 14:e14797. doi: 10.15252/emmm.202114797

Grade, S., and Gotz, M. (2017). Neuronal replacement therapy: previous achievements and challenges ahead. *NPJ Regen. Med.* 2:29. doi: 10.1038/s41536-017-0033-0

Grande, A., Sumiyoshi, K., Lopez-Juarez, A., Howard, J., Sakthivel, B., Aronow, B., et al. (2013). Environmental impact on direct neuronal reprogramming in vivo in the adult brain. *Nat. Commun.* 4:2373.

Han, S., Okawa, S., Wilkinson, G. A., Ghazale, H., Adnani, L., Dixit, R., et al. (2021). Proneural genes define ground-state rules to regulate neurogenic patterning and cortical folding. *Neuron* 109:2847-2863.e11. doi: 10.1016/j.neuron.2021.07.007

Heinrich, C., Blum, R., Gascon, S., Masserdotti, G., Tripathi, P., Sanchez, R., et al. (2010). Directing astroglia from the cerebral cortex into subtype specific functional neurons. *PLoS Biol.* 8:e1000373. doi: 10.1371/journal.pbio.1000373

Heinrich, C., Gotz, M., and Berninger, B. (2012). Reprogramming of postnatal astroglia of the mouse neocortex into functional, synapse-forming neurons. *Methods Mol. Biol.* 814, 485–498. doi: 10.1007/978-1-61779-452-0_32

Hindley, C., Ali, F., McDowell, G., Cheng, K., Jones, A., Guillemot, F., et al. (2012). Post-translational modification of Ngn2 differentially affects transcription of distinct targets to regulate the balance between progenitor maintenance and differentiation. *Development* 139, 1718–1723. doi: 10.1242/dev.077552

Irie, T., Matsuda, T., Hayashi, Y., Kamiya, A., Kira, J.-I., and Nakashima, K. (2021). Direct neuronal conversion of microglia/macrophages reinstates neurological function after stroke. *bioRxiv [preprint]* doi: 10.1101/2021.09.26.461831

Jessberger, S., Toni, N., Clemenson, G. D. Jr., Ray, J., and Gage, F. H. (2008). Directed differentiation of hippocampal stem/progenitor cells in the adult brain. *Nat. Neurosci.* 11, 888–893.

Kaise, T., Fukui, M., Sueda, R., Piao, W., Yamada, M., Kobayashi, T., et al. (2022). Functional rejuvenation of aged neural stem cells by Plagl2 and anti-Dyrk1a activity. *Genes Dev.* 36, 23–37. doi: 10.1101/gad.349000.121

Karow, M., Camp, J. G., Falk, S., Gerber, T., Pataskar, A., Gac-Santel, M., et al. (2018). Direct pericyte-to-neuron reprogramming via unfolding of a neural stem cell-like program. *Nat. Neurosci.* 21, 932–940. doi: 10.1038/s41593-018-0168-3

Karow, M., Sanchez, R., Schichor, C., Masserdotti, G., Ortega, F., Heinrich, C., et al. (2012). Reprogramming of pericyte-derived cells of the adult human brain into induced neuronal cells. *Cell Stem Cell* 11, 471–476.

Kempf, J., Knelles, K., Hersbach, B. A., Petrik, D., Riedemann, T., Bednarova, V., et al. (2021). Heterogeneity of neurons reprogrammed from spinal cord astrocytes by the proneural factors Ascl1 and Neurogenin2. *Cell Rep.* 36:109409.

Kovach, C., Dixit, R., Li, S., Mattar, P., Wilkinson, G., Elsen, G. E., et al. (2013). Neurog2 simultaneously activates and represses alternative gene expression programs in the developing neocortex. *Cereb. Cortex* 23, 1884–1900. doi: 10.1093/cercor/bhs176

Lee, Y., Messing, A., Su, M., and Brenner, M. (2008). GFAP promoter elements required for region-specific and astrocyte-specific expression. *Glia* 56, 481–493. doi: 10.1002/glia.20622

Leib, D., Chen, Y. H., Monteys, A. M., and Davidson, B. L. (2022). Limited astrocyte-to-neuron conversion in the mouse brain using NeuroD1 overexpression. *Mol. Ther.* 30, 982–986. doi: 10.1016/j.ymthe.2022.01.028

Li, S., Mattar, P., Dixit, R., Lawn, S. O., Wilkinson, G., Kinch, C., et al. (2014). RAS/ERK signaling controls proneural genetic programs in cortical development and gliomagenesis. *J. Neurosci.* 34, 2169–2190. doi: 10.1523/JNEUROSCI.4077-13.2014

Li, S., Mattar, P., Zinyk, D., Singh, K., Chaturvedi, C. P., Kovach, C., et al. (2012). GSK3 temporally regulates neurogenin 2 proneural activity in the neocortex. *J. Neurosci.* 32, 7791–7805. doi: 10.1523/JNEUROSCI.1309-12.2012

Liu, Y., Miao, Q., Yuan, J., Han, S., Zhang, P., Li, S., et al. (2015). Ascl1 Converts Dorsal Midbrain Astrocytes into Functional Neurons In Vivo. *J. Neurosci.* 35, 9336–9355. doi: 10.1523/JNEUROSCI.3975-14.2015

Livingston, J., Lee, T., Daniele, E., Phillips, C., Krassikova, A., Enbar, T., et al. (2020). Direct reprogramming of astrocytes to neurons leads to functional recovery after stroke. *bioRxiv [preprint]* doi: 10.1101/2020.02.02.929091

Madisen, L., Zwingman, T. A., Sunkin, S. M., Oh, S. W., Zariwala, H. A., Gu, H., et al. (2010). A robust and high-throughput Cre reporting and characterization system for the whole mouse brain. *Nat. Neurosci.* 13, 133–140. doi: 10.1038/nn.2467

Marcus, E. A., Kintner, C., and Harris, W. (1998). The role of GSK3beta in regulating neuronal differentiation in Xenopus laevis. *Mol. Cell Neurosci.* 12, 269–280.

Masserdotti, G., Gillotin, S., Sutor, B., Drechsel, D., Irmler, M., Jorgensen, H. F., et al. (2015). Transcriptional Mechanisms of Proneural Factors and REST in Regulating Neuronal Reprogramming of Astrocytes. *Cell Stem Cell* 17, 74–88. doi: 10.1016/j.stem.2015.05.014

Matsuda, T., Irie, T., Katsurabayashi, S., Hayashi, Y., Nagai, T., Hamazaki, N., et al. (2019). Pioneer factor NeuroD1 rearranges transcriptional and epigenetic profiles to execute microglia-neuron conversion. *Neuron* 101, 472–485e7.

Matsuda, T., and Nakashima, K. (2021). Clarifying the ability of NeuroD1 to convert mouse microglia into neurons. *Neuron* 109, 3912–3913. doi: 10.1016/j.neuron.2021.11.012

Oproescu, A. M., Han, S., and Schuurmans, C. (2021). New insights into the intricacies of proneural gene regulation in the embryonic and adult cerebral cortex. *Front. Mol. Neurosci.* 14:642016. doi: 10.3389/fnmol.2021.642016

Parras, C. M., Schuurmans, C., Scardigli, R., Kim, J., Anderson, D. J., and Guillemot, F. (2002). Divergent functions of the proneural genes Mash1 and Ngn2 in the specification of neuronal subtype identity. *Genes Dev.* 16, 324–338. doi: 10.1101/gad.940902

Puls, B., Ding, Y., Zhang, F., Pan, M., Lei, Z., Pei, Z., et al. (2020). Regeneration of functional neurons after spinal cord injury via in situ NeuroD1-mediated astrocyte-to-neuron conversion. *Front. Cell Dev. Biol.* 8:591883. doi: 0.3389/fcell.2020.591883

Qian, H., Kang, X., Hu, J., Zhang, D., Liang, Z., Meng, F., et al. (2020). Reversing a model of Parkinson's disease with in situ converted nigral neurons. *Nature* 582, 550–556.

Rao, Y., Du, S., Yang, B., Wang, Y., Li, Y., Li, R., et al. (2021). NeuroD1 induces microglial apoptosis and cannot induce microglia-to-neuron cross-lineage reprogramming. *Neuron* 109, 4094-4108.e5. doi: 10.1016/j.neuron.2021.11.008

Raposo, A., Vasconcelos, F. F., Drechsel, D., Marie, C., Johnston, C., Dolle, D., et al. (2015). Ascl1 coordinately regulates gene expression and the chromatin landscape during neurogenesis. *Cell Rep.* 10, 1544–1556.

Rivetti di Val Cervo, P., Romanov, R. A., Spigolon, G., Masini, D., Martin-Montanez, E., Toledo, E. M., et al. (2017). Induction of functional dopamine neurons from human astrocytes in vitro and mouse astrocytes in a Parkinson's disease model. *Nat. Biotechnol.* 35, 444–452. doi: 10.1038/nbt.3835

Ruddy, R. M., and Morshead, C. M. (2018). Home sweet home: the neural stem cell niche throughout development and after injury. *Cell Tissue Res.* 371, 125–141. doi: 10.1007/s00441-017-2658-0

Russo, G. L., Sonsalla, G., Natarajan, P., Breunig, C. T., Bulli, G., Merl-Pham, J., et al. (2021). CRISPR-mediated induction of neuron-enriched mitochondrial proteins boosts direct glia-to-neuron conversion. *Cell Stem Cell* 28:524-534.e7.

Schuurmans, C., Armant, O., Nieto, M., Stenman, J. M., Britz, O., Klenin, N., et al. (2004). Sequential phases of cortical specification involve Neurogenin-dependent and -independent pathways. *Embo J.* 23, 2892–2902. doi: 10.1038/sj.emboj.7600278

Sharif, N., Calzolari, F., and Berninger, B. (2021). Direct In Vitro Reprogramming of Astrocytes into Induced Neurons. *Methods Mol. Biol.* 2352, 13–29.

Srinivasan, R., Lu, T. Y., Chai, H., Xu, J., Huang, B. S., Golshani, P., et al. (2016). New transgenic mouse lines for selectively targeting astrocytes and studying calcium signals in astrocyte processes in situ and in vivo. *Neuron* 92, 1181–1195. doi: 10.1016/j.neuron.2016.11.030

Sun, Y., Nadal-Vicens, M., Misono, S., Lin, M. Z., Zubiaga, A., Hua, X., et al. (2001). Neurogenin promotes neurogenesis and inhibits glial differentiation by independent mechanisms. *Cell* 104, 365–376. doi: 10.1016/s0092-8674(01)00224-0

Touahri, Y., Adnani, L., Mattar, P., Markham, K., Klenin, N., and Schuurmans, C. (2015). Non-isotopic RNA in situ hybridization on embryonic sections. *Curr. Protoc. Neurosci.* 70, 1221–12225.

Urban, N., van den Berg, D. L., Forget, A., Andersen, J., Demmers, J. A., Hunt, C., et al. (2016). Return to quiescence of mouse neural stem cells by degradation of a proactivation protein. *Science* 353, 292–295.

Vasan, L., Park, E., David, L. A., Fleming, T., and Schuurmans, C. (2021). Direct neuronal reprogramming: bridging the gap between basic science and clinical application. *Front. Cell Dev. Biol.* 9:681087. doi: 10.3389/fcell.2021.681087

Vierbuchen, T., Ostermeier, A., Pang, Z. P., Kokubu, Y., Sudhof, T. C., and Wernig, M. (2010). Direct conversion of fibroblasts to functional neurons by defined factors. *Nature* 463, 1035–1041.

Wang, L., Serrano, C., Zhong, X., Ma, S., Zou, Y., and Zhang, C. L. (2021). Revisiting astrocyte to neuron conversion with lineage tracing in vivo. *Cell* 184:5465-5481.e16. doi: 10.1016/j.cell.2021.09.005

Wang, T., Liao, J. C., Wang, X., Wang, Q. S., Wan, K. Y., Yang, Y. Y., et al. (2022). Unexpected BrdU inhibition on astrocyte-to-neuron conversion. *Neural Regen. Res.* 17, 1526–1534. doi: 10.4103/1673-5374.325747

Wapinski, O. L., Vierbuchen, T., Qu, K., Lee, Q. Y., Chanda, S., Fuentes, D. R., et al. (2013). Hierarchical mechanisms for direct reprogramming of fibroblasts to neurons. *Cell* 155, 621–635.

Woods, L. M., Ali, F. R., Gomez, R., Chernukhin, I., Marcos, D., Parkinson, L. M., et al. (2022). Elevated ASCL1 activity creates de novo regulatory elements associated with neuronal differentiation. *BMC Genom.* 23:255. doi: 10.1186/s12864-022-08495-8

Yang, N., Chanda, S., Marro, S., Ng, Y. H., Janas, J. A., Haag, D., et al. (2017). Generation of pure GABAergic neurons by transcription factor programming. *Nat. Methods* 14, 621–628. doi: 10.1038/nmeth.4291

Zhuo, L., Sun, B., Zhang, C. L., Fine, A., Chiu, S. Y., and Messing, A. (1997). Live astrocytes visualized by green fluorescent protein in transgenic mice. *Dev. Biol.* 187, 36–42.

frontiers | Frontiers in Neuroscience

TYPE Mini Review
PUBLISHED 13 September 2022
DOI 10.3389/fnins.2022.916055

OPEN ACCESS

EDITED BY
Filipe Pinto-Teixeira,
FR3743 Centre de Biologie Intégrative (CBI), France

REVIEWED BY
Laura López-Mascaraque,
Cajal Institute (CSIC), Spain
Katherine Long,
King's College London, United Kingdom
David Ohayon,
FR3743 Centre de Biologie Intégrative (CBI), France

*CORRESPONDENCE
Karine Loulier
karine.loulier@inserm.fr

†These authors have contributed equally to this work

SPECIALTY SECTION
This article was submitted to Neurogenesis, a section of the journal Frontiers in Neuroscience

RECEIVED 08 April 2022
ACCEPTED 19 July 2022
PUBLISHED 13 September 2022

CITATION
Clavreul S, Dumas L and Loulier K (2022) Astrocyte development in the cerebral cortex: Complexity of their origin, genesis, and maturation.
Front. Neurosci. 16:916055.
doi: 10.3389/fnins.2022.916055

Astrocyte development in the cerebral cortex: Complexity of their origin, genesis, and maturation

Solène Clavreul †, Laura Dumas † and Karine Loulier *

Institute for Neurosciences of Montpellier (INM), Univ Montpellier, INSERM, Montpellier, France

In the mammalian brain, astrocytes form a heterogeneous population at the morphological, molecular, functional, intra-, and inter-region levels. In the past, a few types of astrocytes have been first described based on their morphology and, thereafter, according to limited key molecular markers. With the advent of bulk and single-cell transcriptomics, the diversity of astrocytes is now progressively deciphered and its extent better appreciated. However, the origin of this diversity remains unresolved, even though many recent studies unraveled the specificities of astroglial development at both population and individual cell levels, particularly in the cerebral cortex. Despite the lack of specific markers for each astrocyte subtype, a better understanding of the cellular and molecular events underlying cortical astrocyte diversity is nevertheless within our reach thanks to the development of intersectional lineage tracing, microdissection, spatial mapping, and single-cell transcriptomic tools. Here we present a brief overview describing recent findings on the genesis and maturation of astrocytes and their key regulators during cerebral cortex development. All these studies have considerably advanced our knowledge of cortical astrogliogenesis, which relies on a more complex mode of development than their neuronal counterparts, that undeniably impact astrocyte diversity in the cerebral cortex.

KEYWORDS

astrocytes, cerebral cortex, gliogenesis, proliferation, maturation

Introduction

Astrocytes are key cellular partners of neurons and blood vessels in the central nervous system. The last two decades have seen an accumulation of new studies aiming at characterizing these cells initially considered as simple support cells for neurons. All these works have progressively revealed an unexpected diversity of these astrocytes in the brain where they constitute a heterogeneous population at the morphological, molecular, functional, inter-, and intra-region levels (Khakh and Deneen, 2019). Various

astrocyte subtypes have been first described based on their morphology and few key molecular markers such as GFAP for white matter fibrous and reactive astrocytes and S100ß for gray matter protoplasmic astrocytes. Nowadays, additional molecular markers for cortical astrocytes have been described, such as NFIA, GLAST, Sox9, or Aldh1l1, enabling the investigation of astrocyte physiology (Molofsky et al., 2012). Until now, the cellular and molecular mechanisms underlying the establishment of astrocyte diversity during development have remained difficult to explore due to the absence of specific markers for each astrocyte subtype. In recent years, refinements in cell lineage tracking techniques that have moved to multicolor to increase the number of clones that could be tracked simultaneously, reviewed in Dumas et al. (2022), and in high-throughput transcriptomics (Wagner and Klein, 2020) have elucidated key elements of cortical astrocyte development in the mammalian brain. In this minireview, we compile in synthetic form the latest findings on the development of cortical astrocytes from their multiple sources of production to the key factors regulating their generation and maturation which together highlight the complexity of the genesis of cortical astrocytes.

Origins of cortical astrocytes

Embryonic source

Radial glia

At the end of the neurogenic phase around the 16th embryonic day (E16) during mouse development, radial glial cells (RGC) lose their neurogenic potential and progressively acquire most of astrocyte features (Mori et al., 2005). This gliogenic switch is regulated by intrinsic and epigenetic factors (Adnani et al., 2018). Radial glia produces most of astrocyte precursors by E18, which subsequently migrate to the white or grey matter where they differentiate into fibrous and protoplasmic astrocytes, respectively (Tabata, 2015). Cell lineage studies have revealed the existence of bipotent progenitors successively producing neurons and astrocytes, as well as restricted progenitors generating only certain neuronal or glial subtypes (Kriegstein and Alvarez-Buylla, 2009). Mosaic Analysis with Double Markers (MADM) clonal analysis show that 1/6 of neurogenic radial glia cortical progenitors produce glia (Gao et al., 2014). Remaining RGC eventually differentiate directly into astrocytes (**Figure 1**). They undergo morphological changes, lose their apical contact, become unipolar and retract their radial fibers, before moving away their cell body from the ventricular zone and becoming multipolar, thus acquiring their astrocyte morphology (Kriegstein and Alvarez-Buylla, 2009). In addition to direct transformation into astrocyte precursors, RGC generate apical multipotent intermediate progenitors that express ASCL1 and EGFR as revealed by Li and collaborators using a combination of single-cell RNA-Seq with intersectional lineage analysis (Li et al., 2021). The colonization of the neocortical wall is achieved by a fraction of apical cortical progenitors which delaminate from the ventricular zone before birth (**Figure 1**). Multiplexed clonal analysis based on multicolor MAGIC Markers strategy reveal that astrocyte precursors disperse prenatally in a non-stereotyped way in the cortical parenchyma where they expand as scattered clonal units, which can result in a sparse distribution of sibling astrocytes at later stages (Clavreul et al., 2019; Ojalvo-Sanz and López-Mascaraque, 2021). Aside from RGC, cortical astrocytes arise from alternative embryonic sources that might contribute to their diversity. It includes oligodendrocyte progenitor cells, Olig2 progenitors and embryonic subpallial progenitors.

Oligodendrocyte progenitor cells

Oligodendrocyte progenitor cells (OPCs) are glial cells identified by their expression of NG2, Olig2, PDGFRα, or PLP markers. Cortical astrocyte subpopulations are generated from at least two regionally distinct sources of NG2-expressing OPCs: a ventral subset (Huang et al., 2014, 2019) and pallial progenitor derivatives (Sánchez-González et al., 2020; **Figure 1**). Their potential to differentiate into astrocytes is however transient from E12 (Huang et al., 2019) to neonatal stage (Huang et al., 2014; Sánchez-González et al., 2020). Unlike their multipotent dorsal counterpart, ventral OPCs appear to be monopotent glial progenitors (Zhu et al., 2011). In contrast, NG2-expressing OPCs deriving from pallial progenitors produce both protoplasmic and fibrous astrocytes (Sánchez-González et al., 2020). In the adult dorsal cortex, up to 1.6% of S100β + protoplasmic astrocytes arise from these two distinct sources of OPCs (Zhu et al., 2008). In addition to NG2-Cre (Zhu et al., 2008), NG2-Cre^{ERTM} BAC (Zhu et al., 2011), NG2-Cre^{ERT2} KI (Huang et al., 2014, 2019), the fate of OPC has been tracked using other mouse lines such as PLP-Cre^{ERT2} (Doerflinger et al., 2003; Guo et al., 2009, 2010), Olig2-Cre^{ERTM} (Takebayashi et al., 2002; Dimou et al., 2008), Pdgfrα-$^{Cre/ERT2}$ (Rivers et al., 2008; Kang et al., 2010). Protoplasmic astrocytes can be generated from early PLP-positive OPCs while no astrocytes are observed after adult induction of the Cre recombinase in PLP-Cre^{ERT2}; reporter mice confirming their transient potential to give astrocytes (Guo et al., 2009, 2010).

Olig2 progenitors

On the other hand, from 5 to 11% of reporter-positive astrocytes are found in the grey matter at 6 months after adult induction in Olig2Cre^{ERTM}; reporter mice (Dimou et al., 2008). However, Olig2 expression is not restricted to NG2 glia as some embryonic and even adult subventricular zone (SVZ) neural progenitor cells also express this marker. Olig2 is a bHLH transcription factor involved in cortical astrocyte development, from the specification to differentiation stages. Indeed, most, if not all, protoplasmic astrocytes issued from cortical progenitors

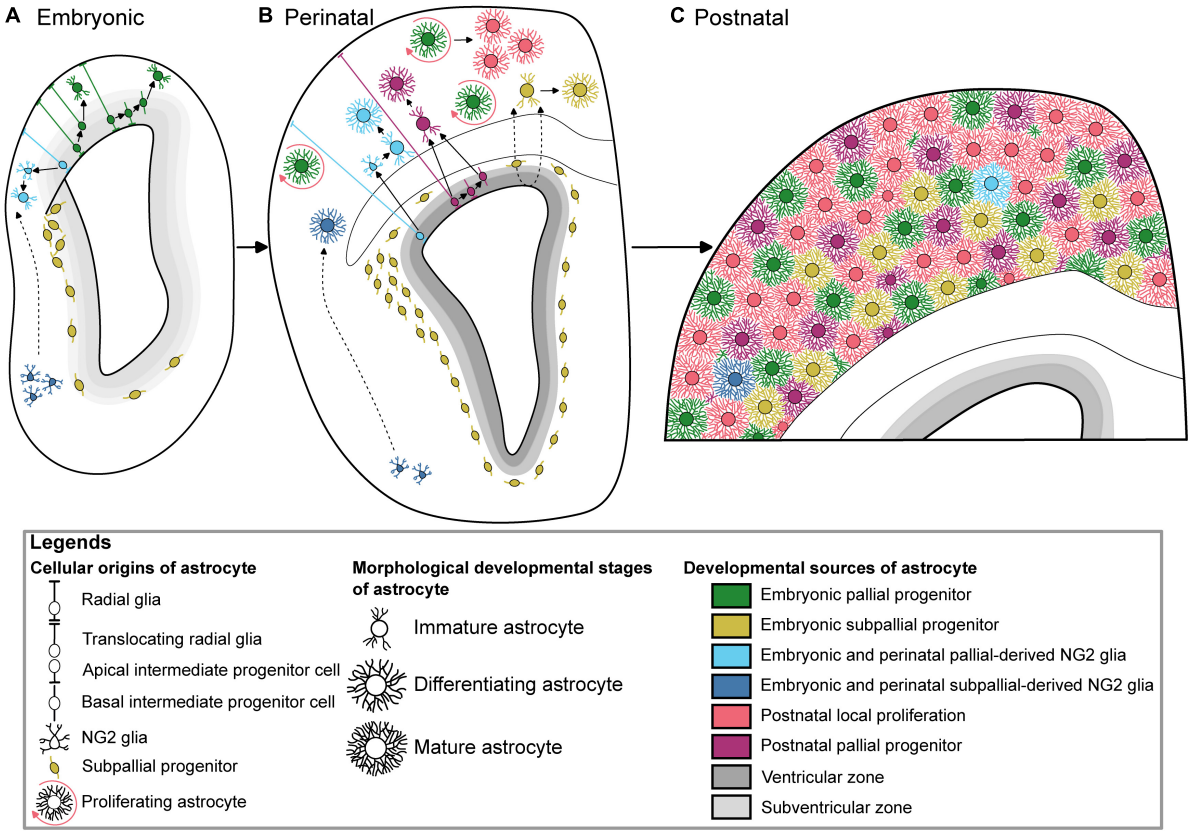

FIGURE 1
Multiple developmental origins underlying the generation of cortical astrocytes. **(A)** Embryonic astrogliogenesis relies on immature astrocytes deriving from translocating pallial radial glia, multipotent intermediate pallial progenitors, two independent oligodendrocyte progenitor cells sources, and subpallial progenitors. **(B)** New cortical perinatal astrocytes are generated from radial glia, local proliferation, intermediate progenitors, pallial and subpallial oligodendrocyte progenitor cells, and colonizing subpallial progenitors. **(C)** Color-coded protoplasmic astrocytes based on their respective developmental sources tiling the whole postnatal cortex. The postnatal local proliferation is mainly observed in the upper layers, while subpallial-derived astrocytes are GFAP-positive suggesting their lower layer localization. Of note, these subpallial-derived astrocytes have not been described after P10. The dotted arrows show hypothetic migration paths.

transitioned by the Olig2 lineage as clearly demonstrated by Olig2-Cre genetic fate mapping combined with multicolor reporters (Clavreul et al., 2019). It has been shown that Olig2 promotes macroglia identity by repressing the neuronal phenotype among certain neural progenitors arising from both the pallium and subpallium (Marshall et al., 2005). Moreover, Olig2 participates in the astrocyte differentiation in the dorsal pallium, but not in the basal forebrain (Ono et al., 2008). In the cerebral cortex, Olig2 is progressively downregulated as astrocytes mature (Cai et al., 2007; Zhu et al., 2012) while its expression is maintained in other regions. Indeed, Olig2 is a marker for more than 80% of the mature astrocytes located in the globus pallidus, olfactory bulb, midbrain, thalamus, medulla, and spinal cord (Tatsumi et al., 2018; Wang et al., 2021). In the spinal cord, Olig2 progenitors of the pMN domain give rise to motor neurons, OPCs as well as a subpopulation of Olig2+ astrocyte progenitors that retained Olig2 expression as they differentiate and mature until adulthood (Ohayon et al., 2019). Interestingly, Olig2+ and GFAP+ astrocytes occupy mutually exclusive areas in the adult brain (Tatsumi et al., 2018). In the globus pallidus, the Olig2-astrocyte subset tends to express GABA transporter-3 and/or SLC7A10 transporter of NAA (Tatsumi et al., 2018, 2021), suggesting that a molecularly and regionally distinct subpopulation of astrocytes may exert specific functions. In addition, Olig2-expressing astrocyte subtype is as well-found in the juvenile spinal cord and exhibits a unique gene expression signature that includes *inka2*, *kcnip3*, and *slc7a10* showing a first link between a developmental origin of an astrocyte subtype and its molecular identity that could influence synapse organization and activity (Ohayon et al., 2021). In contrast, cortical astrocytes derived from pallial and subpallial sources exhibit a perivascular shape that indicates common function between developmentally distinct populations (Marshall and Goldman, 2002). Adult astrocytes can act as quiescent neural stem cells. Indeed, mitotic and cell cycle control genes are expressed in a rare subpopulation of uniformly distributed putative astrocyte progenitors (AST5) and a specific hippocampal subset of neural stem cell (AST4) that

could proliferate in response to pathological stimulus in the mouse (Batiuk et al., 2020). Interestingly, in the striatum and somatosensory cortex, parenchymal astrocytes have recently been shown to be latent neural stem cells, capable to generate neuroblasts upon treatment with stroke-related and mitogen cues (Magnusson et al., 2020).

Subpallial origin

In the forebrain and in the spinal cord, astrocytes are born from RGC within the boundaries of their allocated territories delineated by their neuroepithelial progenitors (Hochstim et al., 2008; Tsai et al., 2012). Nonetheless, few studies hints that some cortical astrocytes may arise from outside the cerebral cortex. An overlooked source of cortical astrocytes comes from subpallial progenitors located in the ganglionic eminences (Marshall and Goldman, 2002; Nery et al., 2002; **Figure 1**). These progenitors belong to the Dlx2 lineage reflecting their ventral telencephalic origin and they emigrate dorsally toward the cortical parenchyma. They colonize the core of the dorsolateral corner of the perinatal SVZ by progressively displacing Aldolase C/Zebrin-II + pallial resident progenitors to the edge (Staugaitis et al., 2001; Marshall and Goldman, 2002). Enrolled into the late wave of an uncommon medial tangential migration stream (E14–E16), Dlx2 + subpallial progenitors migrate within the dorsal periventricular zone (Anderson et al., 2001). Two subpallial astrocyte progenitor subtypes expressing either Sparc or Sparcl1 have recently been identified in the perinatal cortex suggesting that molecularly divergent astrocytes derived from the subpallium might differently regulate neuronal synaptic formation (Liu et al., 2022). *Aldh1l1* gene and Sparc expression pattern is gradually increased along the dorsoventral axis of the adult brain (Morel et al., 2017). The regulation of synaptic activity has been shown to be region-selective. Indeed, subcortical astrocytes appear less competent at modulating the function of cortical neurons *in vitro* (Morel et al., 2017). Subpallial Dlx2-expressing progenitors develop notably into GFAP-positive astrocytes and oligodendrocytes in the juvenile cortex, white matter and striatum (Marshall and Goldman, 2002; Nery et al., 2002). Likewise, Dlx2 is a key factor used to reprogram both adult astrocyte (Heinrich et al., 2010) and OPC (Boshans et al., 2021) into GABAergic interneuron or tripotent neural progenitor cell (Zhang et al., 2022). Interestingly, astrocytes originating from both pallial and subpallial progenitors have been recently shown to converge to a similar postnatal transcriptional signature by combining STICR barcoding and scRNA-seq (Bandler et al., 2022). However, the extent of the contribution of this subpallial subset to the cortical astrocyte population is unknown. It is also unclear if these ventrally-derived astrocytes survive beyond the postnatal day (P) 10 (Marshall and Goldman, 2002) and if they play a specific function in the cerebral cortex.

Postnatal production

Postnatal subventricular zone progenitors

After birth, a loss of RGC occurs (Marshall et al., 2003). Astrocytes generated afterward are thought to be issued from SVZ progenitors, which are not, unlike RGC, attached to the pial surface (**Figure 1**). The postnatal contribution of SVZ progenitors to astrocyte production will continue until P14 (Levison and Goldman, 1993). While Nestin expression characterizes RGC, a study using Nestin-Cre^{ER} mice also showed proliferating Nestin + glial progenitors in the SVZ and detached from the pial surface, after tamoxifen injection at the end of embryogenesis (Burns et al., 2009). This confirms that perinatal gliogenesis occurs in both the VZ with a RGC origin, and the SVZ, where intermediate progenitors give birth to cells migrating to the white matter and to the cerebral cortex and differentiating into astrocytes and oligodendrocytes. However, the postnatal contribution of SVZ progenitors to astrocyte production has been challenged by a study using postnatal electroporation of episomal reporters to label postnatal SVZ progenitors which shows that only a few cortical astrocytes arise from these electroporated SVZ progenitors (Ge et al., 2012). Nonetheless, further postnatal electroporation and retroviral injection experiments show that postnatal SVZ progenitors can produce cortical astrocytes, even to a lesser extent compared to other postnatal source of astrogliogenesis (Ge et al., 2012; Wang et al., 2013; Stogsdill et al., 2017). This result was confirmed with different strategies based on the electroporation of integrative reporters (Clavreul et al., 2019; Figueres-Oñate et al., 2019), including one that showed that pial astrocytes, in addition to protoplasmic astrocytes, are also issued from rapidly dividing SVZ progenitors (Clavreul et al., 2019). Several studies have highlighted the importance of using integrative vs. episomal vectors which are diluted in highly proliferative cells and, therefore, may not recapitulate the whole progeny issued from labeled parent cells (Figueres-Oñate et al., 2015; Clavreul et al., 2019). The heterogeneity and positional identity of VZ/SVZ progenitors that differentially contribute to cortical astrocyte generation may contribute to the cortical astrocyte diversity. For instance, HOPX is a marker of a subpopulation of pallial neural progenitor cells, enriched at the dorso-medial subdomain of the postnatal SVZ that are set to become fibrous astrocyte in the corpus callosum (Zweifel et al., 2018). Finally, fate mapping of Gli1 + progenitor cells in the mouse postnatal cortex revealed a Gli1 + subpopulation of astrocyte progenitors in the SVZ which will eventually generate half of the total cortical astrocyte population (Gingrich et al., 2022). Gli1 being a transcriptional target of Shh signaling, these results indicate that a subpopulation of neonatal progenitors generating cortical astrocytes is defined by Shh signaling and that diversity of astrocyte lineages might contribute to their functional diversity.

Postnatal local proliferation

After birth, a major source of protoplasmic astrocytes is the local proliferation of pioneer astrocytes that settle in the cortex (**Figure 1**). In 1913, Ramón y Cajal first hypothesized that mature astrocytes could divide in the cortical parenchyma. He observed and drew astrocyte doublets connected by their somas. Mitotic figures of astrocytes and/or glia-like cells were later labeled after incorporating the BrdU analogue 3H-thymidine and observed with electron microscopy or with light microscope autoradiography (Fan and Agid, 2018). Later studies showed that local proliferation is already a source of astrocytes at embryonic stages using time-lapse imaging on E18 mouse brain slices in culture (Burns et al., 2009). In this experiment, glial cells expressing GFP after tamoxifen induction in E16 Nestin-CreER;EGFP mice undergo symmetric divisions in the cortical parenchyma every 12 h. The number of glial cells increases significantly during the first postnatal weeks (Bandeira et al., 2009) and local proliferation is a major source of astrocytes in the mouse cerebral cortex at these postnatal stages *via* symmetric divisions of differentiated astrocytes (Ge et al., 2012). The authors showed that 19% of cortical astrocytes are proliferating at P3, and only 1.5% are still dividing at P14. At least in the outer cortical layers, these proliferating astrocytes contribute to nearly half of the astrocyte population primarily through symmetric division. Unexpectedly, dividing parent astrocytes are already differentiated cells exhibiting electrophysiological properties, slightly distinct from the non-dividing astrocytes. Daughter astrocytes functionally incorporate the existing glial network by forming, for example, late perivascular end-feet at P20 (Ge et al., 2012). Strikingly, daughter astrocytes can spread away from their siblings and intermingle with neighboring non-related astrocytes (Clavreul et al., 2019). The proliferative phase is however brief as it essentially occurs before P10 to progressively decline by the end of the third postnatal week in the rat cortex (Moroni et al., 2018).

Astrogliogenesis

Astrocyte generation mechanisms at population and individual cell levels

Gliogenesis switch

Studying distinct stages of astrocyte development has so far been challenging due to similar markers between astrocyte and neural progenitors together with the lack of stage-specific markers of astrocyte lineage progression. Cortical astrocytes are generated from astrocyte precursor cells (APC), whose molecular identity was so far unknown. APC are generated in at least two temporally distinct waves, either directly or indirectly, from RGC in the developing cortex (Tabata, 2015). After neurogenesis, the first embryonic source of APC arises from the transformation of some translocating RGC. Around birth, the second and principal wave of APC production comes from basal multipotent intermediate progenitor cells that differentiate from their apical analogues previously generated by RGC (Li et al., 2021). Interestingly, both translocating RGC and basal multipotent intermediate progenitors share a common hallmark through the expression of *Ascl1*, *Egfr*, and *Olig2* (Li et al., 2021). In addition, at least some if not all basal multipotent intermediate precursors express Gsx2 after induction by the morphogen Shh that blocks GliR3 (Zhang et al., 2020). EGFR-positive progenitor cells have been also detected in the developing human cortex at the gliogenic switch (Fu et al., 2021). Two subgroups of EGFR + cells, called OAPC and APC, share molecular features with astrocytes and are mainly localized in the outer SVZ. OAPCs express part of astrocyte (SLC1A3, SPARCL1), oligodendrocyte (OLIG2), and outer RGC (HOPX) while APCs express a separate set of astrocyte (SLC1A3, ALDOC) and proliferative (MKI67) marker gene suggesting an immature stage (Fu et al., 2021). After several rounds of proliferation, these multipotent intermediate precursors generate cortical astrocytes and oligodendrocytes as well as a subset of olfactory bulb interneurons at least in mice (Zhang et al., 2020; Li et al., 2021).

Astrocyte clone size and composition

Astrocyte clones are highly heterogeneous in terms of size. E13 to E15 progenitors generate astrocyte clones of an average of 8–10 cells, with a high variability up to 40–50 cells (Clavreul et al., 2019; Ojalvo-Sanz and López-Mascaraque, 2021). This maximum size of astrocyte clones is low in the lower layers of the cerebral cortex, compared to its size toward the upper part of the cortex. In terms of astrocyte subtypes, the multicolor method StarTrack, with a GFAP promoter, showed subtype restricted clones, comprised of either protoplasmic or pial astrocytes (García-Marqués and López-Mascaraque, 2013). However, MAGIC markers strategy (Loulier et al., 2014) relying on the ubiquitous CAG promoter, unraveled the bipotency of cortical progenitors with more than 80% of pial astrocytes belonging to heterogenous clones. These heterogeneous clones included both astrocyte subtypes and astrocytes displaying intermediate morphologies encompassing the specific morphological characteristics of the pial and protoplasmic subtypes (Clavreul et al., 2019). Other multicolor clonal analysis of GFAP + cortical progenitors revealed a minority of clones containing sibling cells belonging to both astrocyte and oligodendrocyte lineage (Ojalvo-Sanz and López-Mascaraque, 2021). Therefore, some progenitors maintain the potential to generate different glial cell types. Thus, cortical progenitors are a heterogeneous cell population with respect to which astrocyte subtype they produce, as well as the clonal size and the dispersion of their cell descent. At the clonal level, cortical astrocyte network development appears non-stereotyped. This suggests that the

establishment of this network is based on plastic clonal units generated by astrocyte progenitors. These progenitors appear unspecified and capable of expanding and maturing heterogeneously, with their daughter cells probably acquiring their final characteristics through interactions with their cellular and molecular environment. Clonal analysis associated with molecular profiling of astrocyte sister cells should help to better understand the astroglial potential of cortical progenitors in the near future.

Molecular actors of astrogliogenesis

Among the numerous transcription factors involved in astrocyte generation described in the past years, such as Sox9 and NFIA (Adnani et al., 2018), Zbtb20 is a zinc finger and BTB domain-containing protein 20 transcription factor expressed by neural progenitor cells concomitantly to other family members during the astrogliogenesis phase (Nagao et al., 2016; Medeiros de Araújo et al., 2021). Cortical astrogenesis has been shown to be respectively promoted and reduced by the overexpression and knockdown of Zbtb20 after dorsal electroporation at E15. Astrogenesis is partly promoted by the cooperation between Zbtb20 and NFIA to inhibit the *Brn2* gene involved in neurogenesis (Nagao et al., 2016). The postnatal role of the Zbtb20 has been recently clarified (Medeiros de Araújo et al., 2021). Early conditional deletion of Zbtb20 leads to an increase in a particular subtype of GFAP + astrocytes across all cortical layers. The overexpression of a dominant-negative form of Zbtb20 associated with Primrose syndrome disrupts severely astrogenesis suggesting redundant function between Zbtb family members in astrocyte formation (Medeiros de Araújo et al., 2021). Ezh2 is a histone methyltransferase of the polycomb repressive complex 2 (PRC2) that maintains a transcriptional repressive state in cortical progenitors by methylating the histone H3 at the lysine 27 three times (H3K27me3) (Pereira et al., 2010). This polycomb epigenetic system controls the temporal narrowness of the neurogenic phase in dorsal progenitors and therefore their neural differentiated identity fate. After loss of the PRC2 function in Ezh2-null mice, the developmental timing is accelerated and premature differentiated astrocytes, defined by their GFAP immunoreactivity, are found in the cortical plate from E16 (Pereira et al., 2010). The transforming growth factor-β1 (TGF-β1) is a cytokine that induces premature astrogenesis in the dorsomedial cortex by affecting the polarity of a RGC subset (Stipursky et al., 2014). Released after cortical injuries, blood-derived fibrinogen triggers the differentiation of SVZ neural precursor cells into reactive astrocytes contributing to the scar formation *via* BMP receptor signaling (Pous et al., 2020).

Using comprehensive and integrated transcriptomic and epigenomic analyses to delineate gene regulatory programs from mouse embryonic stem cells toward astrocytes, Tiwari and colleagues pointed out astrocyte-specific genes that acquire priming only upon commitment to the astrocyte lineage and uncovered that epigenetic priming in regulatory elements precedes the stage-specific acquisition of active chromatin and transcriptional activation during astrogliogenesis (Tiwari et al., 2018). They showed *in vitro* that Nfia, Atf3, and Runx2 mediate gene expression programs underlying astrogliogenesis while Nfia and Atf3 promoted astrogliogenesis by suppressing neurogenesis and promoting cell-cycle exit of progenitors, respectively. In addition they demonstrated *in vivo* that Nfia, Atf3, and Runx2 overexpression using *in utero* electroporation of plasmid vectors at E15 steered neurogenic RGC away from generating neurons and promoted astrocyte generation at E18 (Tiwari et al., 2018).

Astrocyte maturation

The transition from astrocyte progenitor cell to mature astrocyte comes with drastic changes in their morphology (Stogsdill et al., 2017; Clavreul et al., 2019) and gene expression (Cahoy et al., 2008; Zhang et al., 2016).

Establishment of astrocyte spatial organization at cell and population levels

Morphological changes at the cellular level

Cortical astrocytes contact neuronal cell bodies, dendritic spines, nodes of Ranvier, blood vessels, and synapses within their arborization domain (Serwanski et al., 2017; Cohen-Salmon et al., 2021). Cajal already observed a complex arborization using Golgi's method (Ramón y Cajal, 1909; García-Marín et al., 2007). Recent works relying on endogenous sparse labeling techniques (Hösli et al., 2022) and digital reconstructions (Zisis et al., 2021) have revealed the complex three-dimensional structural details of astroglia processes at the vascular but also at the synaptic interfaces (Torres-Ceja and Olsen, 2022). Astrocyte arborization has been underestimated for a long time due to the lack of immunomarkers labeling not only main processes, as shown with GFAP, S100β, or Aldh1l1 staining, but also fine branches. Expression of fluorescent protein reporters using viral injections, transgenic mouse lines or plasmid electroporations, under the control of promoters, such as gfaABC1D (Stogsdill et al., 2017), GFAP (Halassa et al., 2007), Aldh1l1 (Cahoy et al., 2008), and S100β (Tong et al., 2013), made the visualization of both cell body and complex arborization possible. Expression of a GFAP-GFP reporter in mouse confirmed the existence of astrocyte territorial domains (Halassa et al., 2007; Stogsdill et al., 2017) and multicolor (Livet et al., 2007) or bicolor (Oberheim et al., 2008) lineage tracing studies revealed the territorial organization of astrocyte

domains in the rodent cerebral cortex. From P7 to P21, the complexity of cortical astrocyte arborization increases during development (Clavreul et al., 2019) and is concomitant with synaptogenesis and functions (Stogsdill et al., 2017). After the first postnatal week and a phase of proliferation and dispersion, astrocytes undergo a maturation phase where volume and morphological complexity keep increasing at the single cell level. Morphological differences such as cell orientation and arborization complexity are also found between cortical layers (Lanjakornsiripan et al., 2018; Abdeladim et al., 2019). This is particularly true between cortical astrocytes from layers II/III vs. layer VI. Layers II/III astrocytes are more vertically elongated, toward the pial surface while those from layer VI, where neuron morphology and synaptic/dendritic density differ, are more horizontally elongated and less complex (Lanjakornsiripan et al., 2018).

Dispersion and organization at the clonal level

With the radial unit hypothesis, Pasko Rakic proposed that the cerebral cortex develops as a cortical columns array, or "radial units," each originating from distinct RGC located in the VZ (Rakic, 1988). Glial progenitors migrate, similarly to neurons, along radial glia processes (Zerlin et al., 1995). Several strategies combining RGC monocolor sparse labeling and clonal analysis show that their astroglial descent form radial columns (Magavi et al., 2012; Tsai et al., 2012). Cortical columns are composed of both pyramidal neurons and astrocytes (Magavi et al., 2012; Gao et al., 2014). However, multicolor clonal analysis of astrocyte dispersion unraveled a so far underestimated highly heterogeneous dispersion in the mediolateral and anteroposterior axis (Clavreul et al., 2019; Ojalvo-Sanz and López-Mascaraque, 2021). Sibling astrocytes can be found sparsely distributed or forming columns in lower layers or in both lower and upper layers of the cerebral cortex. Astrocyte columns are formed by several disconnected groups or clusters of several siblings. Altogether, these data suggest a discontinuity of the astrocyte network at early stages, with a dispersion of the newly generated astrocytes from embryonic and postnatal progenitors, followed by local proliferation, resulting in intermixed neighboring clones. After this dynamic phase of proliferation and dispersion during the first postnatal week, the cortical astrocyte network organization and dispersion progressively settle down (Clavreul et al., 2019).

Molecular actors of astrocyte maturation

Astrocytes share a common molecular profile which includes the expression of *Aqp4*, *Dbx2*, *Sox9*, or even *Slc1a3* genes respectively involved in water transport, neural patterning, astrocyte specification, and glutamate uptake (Zeisel et al., 2018; Batiuk et al., 2020). Yet, several transcriptomically different subtypes of mature cortical astrocytes (ACTE1 and 2, AST1 to 3) have been identified in adults due to their unique molecular signature. Two subgroups of telencephalon astrocytes (ACTE1 and 2) have been initially described based on the expression of *Mfge8* and *Lhx2* genes, additionally split into protoplasmic and fibrous/pial astrocytes according to their differential expression of *Gfap* (Zeisel et al., 2018). The diversity of cortical astrocytes has been further examined by combining single-cell RNA sequencing and spatial mapping (Batiuk et al., 2020). Representing 36.5% of ASCA-2 + selected astrocytes, AST1 cells are astrocytes found in the pial layer of the cortex and expressing high levels of *Gfap* and *Agt* (Batiuk et al., 2020). AST2 subtype is evenly distributed between mid-cortical layers and expresses *Unc13c*. AST3 astrocytes are uniformly dispersed throughout the cortex but prevailed in the cortical layer VI and are distinct from the AST1 subtype because they do not express *Gfap*. Using a combination of reporter mice, RNA microarray and histological analyses, another 8.3 astroglia subset has been shown to be enriched in the cortical layer V and expresses GLT1 and LGR6 (Miller et al., 2019). The shared expression of Norrin, modulating local dendritic spines development, by AST 2, 3 and 8.3 subpopulations suggests that the 8.3 astroglia might be included in the AST 2 and 3 subgroups (Batiuk et al., 2020). Interestingly, both AST2 and AST3 cells are two types of non-laminar astrocytes respectively enriched in transcripts linked to glutamatergic and GABAergic neurotransmission suggesting the fine tuning of synaptic function across the different layers of the cortex (Batiuk et al., 2020; Bayraktar et al., 2020). In addition to non-laminar subtypes, some astrocyte subtypes define a new laminar organization of the cortex by expressing layer-specific genes (Bayraktar et al., 2020). Evident and stable from P14, this organization is divided into superficial, mid, and deep astrocyte laminae and differs from the six classical neuronal cortical layers. For example, *Chrdl1* is expressed by upper-layer astrocytes localized in neuronal layers II–IV, while *Il33* is enriched in deep-layer astrocytes in layers V–VI (Bayraktar et al., 2020). Moreover, the laminar astrocyte organization is specific to each cortical area and neuronal cues play an instructive role in the establishment of these laminar astrocytes (Bayraktar et al., 2020). Several subset of astrocytes express neuroactive genes such as *Chrdl1* in upper astrocytes (Bayraktar et al., 2020), *Norrin* in 8.3 astroglia (Miller et al., 2019), AST2 and AST3 astrocytes (Batiuk et al., 2020), or *Sparc/Sparcl1* in subpallial-derived astrocytes (Liu et al., 2022) that modulates synapse formation.

At the epigenetic level, a wide range of transcriptionally active open chromatin is shared between GFAP + cortical astrocytes and Bergman glia (Welle et al., 2021). Binding sites of the nuclear factor I (Nfi) family, known to promote astrocyte differentiation, are enriched in about 25% in these open chromatin regions. Cortical astrocytes execute well specific transcriptional programs centralized around Lhx2 and FoxG1 that are epigenetically controlled. Even in the young

adult mouse, astrocytes keep epigenetic marks from their region-restricted RGC specification (Welle et al., 2021). By modeling astrogliogenesis from mouse stem cell coupled to next-generation sequencing and computational approaches, Tiwari and colleagues described regulatory elements and transcriptional programs underlying astrocyte generation and maturation as well as stage- and lineage-specific transcriptomic and epigenetic signatures. More specifically, they demonstrated that Runx2 counteracts action of a reactive phenotype to promote astrocyte maturation *in vitro* (Tiwari et al., 2018). More recently, investigating changes in chromatin accessibility using transposase accessible chromatin using sequencing (ATAC-Seq) in astrocytes isolated from P4 and at 2-month old mouse cerebral cortex, Lattke and colleagues showed that ETS, HOX, ROR families directed chromatin remodeling event and contributed to transcriptional changes associated with astrocyte maturation. In addition, they showed that *in vitro* differentiation of NSC into astrocytes failed to recapitulate *in vivo* maturation as *in vitro* differentiated astrocytes failed to gain chromatin accessibility at many regulatory elements associated with mature astrocyte specific genes (Lattke et al., 2021). Finally, using 3D culture, Lattke and colleagues showed that extrinsic signals, such as FGF2, promoted the transcriptional and epigenetic maturation of astrocytes by making accessible the specific gene sites allowing the maturation of astrocytes. Interestingly, these sites are accessible in adult cortical astrocytes *in vivo*, but not in culture, highlighting the necessity to have the right combination of extrinsic signals and 3D environment to obtain fully matured cortical astrocytes.

Discussion

All this work in the mouse model sheds light on the complexity of astroglial development in the mammalian brain. This complexity is expected to be even greater in the human brain as many key morphologic and molecular features between rodent and primate/human cortical astrogliogenesis have been highlighted (Majo et al., 2020). For example, two additional categories of astrocytes are found specifically in the human cerebral cortex and absent in the rodent brain: the interlaminar astrocytes in layer I and varicose projection astrocytes in deep layers V–VI. However, the functional significance of this diversity remains elusive yet and the means to investigate *in vivo* these questions out of reach as human cortical astrogliogenesis time frame greatly overlaps with neurogenesis and occurs *in utero* to a large extent (Malik et al., 2013). Despite this challenge, recent progresses have been made in our understanding of the generation of cortical astrocyte diversity in the human brain. By combining analysis of published human cortical single-cell RNA-Seq datasets with immunostainings performed on human fetal brain samples collected around mid-gestation, Yang and collaborators showed that cortical astrocytes, along with oligodendrocytes and olfactory bulb interneurons, were born from basal multipotent intermediate progenitors (bMIPCs) expressing EGFR, ASCL1, OLIG2, and OLIG1 (Yang et al., 2022). Interestingly these bMIPCs are also found in the mouse brain (Li et al., 2021) and thus seems to be a common feature of cortical astrocyte development from these two species. More recently, a distinctive feature between mouse and human cortical astrogliogenesis has been uncovered by Allen and collaborators. By performing fate mapping of VZ and OSVZ niches using local delivery of GFP-expressing viral vectors on organotypic slices of primary human neocortex from gestational weeks 18–23, they showed that astroglial outputs from these two niches were different. While OSVZ progenitor cells generate white matter astrocytes, VZ progenitors give rise to more superficial grey matter astrocytes. This study provides a very good example of the link between the origin and diversity generation of distinct cortical astrocyte subtypes at the morphological and molecular levels in the human brain (Allen et al., 2022). Understanding the details of astrocyte diversity is all the more important as the involvement of astrocytes in human neurodevelopmental disorders is increasingly well-documented. For instance, analysis of the cell type-specific transcriptomic changes in the cerebral cortex of autism spectrum disorder (ASD) patients show early defects in the cellular state of microglia and protoplasmic astrocytes in addition to the disruption of the synaptic signaling of the upper-layer cortical circuitry (Velmeshev et al., 2019). A deeper investigation of alterations of early key steps of human astrocyte development is now within reach thanks to human iPSC-derived 3D cortical spheroids (Sloan et al., 2017). In this powerful *in vitro* model for human astrocyte development, distinct transcriptional profiles between early- and late-stage organoid-derived astrocytes, resembling to primary human fetal astrocytes and mature astrocytes respectively, can be found and recapitulate astrocyte maturation during *in vitro* differentiation. While more data will be needed to characterize the level of astrocyte morphological complexity and glial reactivity in these *in vitro* models, this represents an extremely promising methodology to efficiently model the development of human cortical astrocytes in physiological and pathological contexts. In addition to new models recapitulating astrocyte development, especially in human tissue, a comprehensive analysis of astrocyte morphology, localization, functions, and markers will be needed to better appreciate astrocyte diversity. The first comprehensive and systematic comparison of two regionally distinct astrocytes was recently made possible using a combination of integrated methods encompassing anatomy, electrophysiology, imaging techniques, transcriptomic, and proteomic (Chai et al., 2017). Striatal and hippocampal astrocytes have been shown to be functionally, morphologically, and molecularly distinct, suggesting the existence of neural circuit-specialized astrocytes (Chai et al., 2017). This approach has not yet been used for cortical astrocytes but will help to understand the relationship

between astrocyte diversity and function, an essential element to fully apprehend the contribution of astrocyte diversity and its proper generation to a functional brain. Although key features of cortical astrogliogenesis in rodents and primates/humans are progressively unraveled, the complexity of the generation of astrocyte diversity still keeps many of its secrets. Many challenges remain ahead of us. In particular, it will be critical to fully apprehend the similarities and differences between the generation of brain astrocytes in rodents and humans in order to determine the extent to which invaluable mouse genetic models for exploring neurodevelopmental pathologies *in vivo* can be exploited to elucidate the contribution of defective astrogliogenesis or aberrant astrocyte function to these pathologies. Human-specific features, such as the presence of distinctive astrocyte subtypes not found in other species or dedicated progenitors responsible for the generation of particular cortical astrocyte subtypes, remain to also be further challenged in dedicated models such as 3D organoids and in other species to understand how the complex choreography of cerebral cortex development can proceed smoothly despite the specificities of the generation of each distinct cell type. All these aspects will be key to unravel the yet poorly understood causes and course for neurodevelopmental disorders.

Author contributions

LD designed and realized the figure with the outputs of SC and KL. All authors had the idea for the article, performed the literature search and data analysis, drafted and critically revised the manuscript, and approved the submitted version.

Funding

This work was supported by INSERM and ATIP-Avenir program.

Conflict of interest

The authors declare that the research was conducted in the absence of any commercial or financial relationships that could be construed as a potential conflict of interest.

Publisher's note

All claims expressed in this article are solely those of the authors and do not necessarily represent those of their affiliated organizations, or those of the publisher, the editors and the reviewers. Any product that may be evaluated in this article, or claim that may be made by its manufacturer, is not guaranteed or endorsed by the publisher.

References

Abdeladim, L., Matho, K. S., Clavreul, S., Mahou, P., Sintes, J.-M., Solinas, X., et al. (2019). Multicolor multiscale brain imaging with chromatic multiphoton serial microscopy. *Nat. Commun.* 10:1662. doi: 10.1038/s41467-019-09552-9

Adnani, L., Han, S., Li, S., Mattar, P., and Schuurmans, C. (2018). "Mechanisms of Cortical Differentiation," in *International review of cell and molecular biology*, (Amsterdam: Elsevier), 223–320. doi: 10.1016/bs.ircmb.2017.07.005

Allen, D. E., Donohue, K. C., Cadwell, C. R., Shin, D., Keefe, M. G., Sohal, V. S., et al. (2022). Fate mapping of neural stem cell niches reveals distinct origins of human cortical astrocytes. *Science* 376, 1441–1446. doi: 10.1126/science.abm5224

Anderson, S. A., Marín, O., Horn, C., Jennings, K., and Rubenstein, J. L. (2001). Distinct cortical migrations from the medial and lateral ganglionic eminences. *Dev. Camb. Engl.* 128, 353–363.

Bandeira, F., Lent, R., and Herculano-Houzel, S. (2009). Changing numbers of neuronal and non-neuronal cells underlie postnatal brain growth in the rat. *Proc. Natl. Acad. Sci. U.S.A.* 106, 14108–14113. doi: 10.1073/pnas.0804650106

Bandler, R. C., Vitali, I., Delgado, R. N., Ho, M. C., Dvoretskova, E., Ibarra Molinas, J. S., et al. (2022). Single-cell delineation of lineage and genetic identity in the mouse brain. *Nature* 601, 404–409. doi: 10.1038/s41586-021-04237-0

Batiuk, M. Y., Martirosyan, A., Wahis, J., de Vin, F., Marneffe, C., Kusserow, C., et al. (2020). Identification of region-specific astrocyte subtypes at single cell resolution. *Nat. Commun.* 11:1220. doi: 10.1038/s41467-019-14198-8

Bayraktar, O. A., Bartels, T., Holmqvist, S., Kleshchevnikov, V., Martirosyan, A., Polioudakis, D., et al. (2020). Astrocyte layers in the mammalian cerebral cortex revealed by a single-cell in situ transcriptomic map. *Nat. Neurosci.* 23, 500–509. doi: 10.1038/s41593-020-0602-1

Boshans, L. L., Soh, H., Wood, W. M., Nolan, T. M., Mandoiu, I. I., Yanagawa, Y., et al. (2021). Direct reprogramming of oligodendrocyte precursor cells into GABAergic inhibitory neurons by a single homeodomain transcription factor Dlx2. *Sci. Rep.* 11:3552. doi: 10.1038/s41598-021-82931-9

Burns, K. A., Murphy, B., Danzer, S. C., and Kuan, C.-Y. (2009). Developmental and post-injury cortical gliogenesis: a genetic fate-mapping study with Nestin-CreER mice. *Glia* 57, 1115–1129. doi: 10.1002/glia.20835

Cahoy, J. D., Emery, B., Kaushal, A., Foo, L. C., Zamanian, J. L., Christopherson, K. S., et al. (2008). A transcriptome database for astrocytes, neurons, and oligodendrocytes: a new resource for understanding brain development and function. *J. Neurosci.* 28, 264–278. doi: 10.1523/JNEUROSCI.4178-07.2008

Cai, J., Chen, Y., Cai, W.-H., Hurlock, E. C., Wu, H., Kernie, S. G., et al. (2007). A crucial role for Olig2 in white matter astrocyte development. *Development* 134, 1887–1899. doi: 10.1242/dev.02847

Chai, H., Diaz-Castro, B., Shigetomi, E., Monte, E., Octeau, J. C., Yu, X., et al. (2017). Neural circuit-specialized astrocytes: Transcriptomic. proteomic, morphological, and functional evidence. *Neuron* 95, 531–549. doi: 10.1016/j.neuron.2017.06.029

Clavreul, S., Abdeladim, L., Hernández-Garzón, E., Niculescu, D., Durand, J., Ieng, S.-H., et al. (2019). Cortical astrocytes develop in a plastic manner at both clonal and cellular levels. *Nat. Commun.* 10:4884. doi: 10.1038/s41467-019-12791-5

Cohen-Salmon, M., Slaoui, L., Mazaré, N., Gilbert, A., Oudart, M., Alvear-Perez, R., et al. (2021). Astrocytes in the regulation of cerebrovascular functions. *Glia* 69, 817–841. doi: 10.1002/glia.23924

Dimou, L., Simon, C., Kirchhoff, F., Takebayashi, H., and Gotz, M. (2008). Progeny of Olig2-expressing progenitors in the gray and white matter of the adult

mouse cerebral cortex. *J. Neurosci.* 28, 10434–10442. doi: 10.1523/JNEUROSCI.2831-08.2008

Doerflinger, N. H., Macklin, W. B., and Popko, B. (2003). Inducible site-specific recombination in myelinating cells. *Genesis* 35, 63–72. doi: 10.1002/gene.10154

Dumas, L., Clavreul, S., Michon, F., and Loulier, K. (2022). Multicolor strategies for investigating clonal expansion and tissue plasticity. *Cell. Mol. Life Sci.* 79:141. doi: 10.1007/s00018-021-04077-1

Fan, X., and Agid, Y. (2018). At the origin of the history of glia. *Neuroscience* 385, 255–271. doi: 10.1016/j.neuroscience.2018.05.050

Figueres-Oñate, M., García-Marqués, J., Pedraza, M., De Carlos, J. A., and López-Mascaraque, L. (2015). Spatiotemporal analyses of neural lineages after embryonic and postnatal progenitor targeting combining different reporters. *Front. Neurosci.* 9:87. doi: 10.3389/fnins.2015.00087

Figueres-Oñate, M., Sánchez-Villalón, M., Sánchez-González, R., and López-Mascaraque, L. (2019). Lineage Tracing and Cell Potential of Postnatal Single Progenitor Cells In Vivo. *Stem Cell Rep.* 13, 700–712. doi: 10.1016/j.stemcr.2019.08.010

Fu, Y., Yang, M., Yu, H., Wang, Y., Wu, X., Yong, J., et al. (2021). Heterogeneity of glial progenitor cells during the neurogenesis-to-gliogenesis switch in the developing human cerebral cortex. *Cell Rep.* 34:108788. doi: 10.1016/j.celrep.2021.108788

Gao, P., Postiglione, M. P., Krieger, T. G., Hernandez, L., Wang, C., Han, Z., et al. (2014). Deterministic progenitor behavior and unitary production of neurons in the neocortex. *Cell* 159, 775–788. doi: 10.1016/j.cell.2014.10.027

García-Marín, V., García-López, P., and Freire, M. (2007). Cajal's contributions to glia research. *Trends Neurosci.* 30, 479–487. doi: 10.1016/j.tins.2007.06.008

García-Marqués, J., and López-Mascaraque, L. (2013). Clonal identity determines astrocyte cortical heterogeneity. *Cereb. Cortex* 23, 1463–1472. doi: 10.1093/cercor/bhs134

Ge, W.-P., Miyawaki, A., Gage, F. H., Jan, Y. N., and Jan, L. Y. (2012). Local generation of glia is a major astrocyte source in postnatal cortex. *Nature* 484, 376–380. doi: 10.1038/nature10959

Gingrich, E. C., Case, K., and Garcia, A. D. R. (2022). A subpopulation of astrocyte progenitors defined by Sonic hedgehog signaling. *Neural. Develop.* 17:2. doi: 10.1186/s13064-021-00158-w

Guo, F., Ma, J., McCauley, E., Bannerman, P., and Pleasure, D. (2009). Early postnatal proteolipid promoter-expressing progenitors produce multilineage cells in vivo. *J. Neurosci.* 29, 7256–7270. doi: 10.1523/JNEUROSCI.5653-08.2009

Guo, F., Maeda, Y., Ma, J., Xu, J., Horiuchi, M., Miers, L., et al. (2010). Pyramidal neurons are generated from oligodendroglial progenitor cells in adult piriform cortex. *J. Neurosci.* 30, 12036–12049. doi: 10.1523/JNEUROSCI.1360-10.2010

Halassa, M. M., Fellin, T., Takano, H., Dong, J.-H., and Haydon, P. G. (2007). Synaptic Islands defined by the territory of a single astrocyte. *J. Neurosci.* 27, 6473–6477. doi: 10.1523/JNEUROSCI.1419-07.2007

Heinrich, C., Blum, R., Gascón, S., Masserdotti, G., Tripathi, P., Sánchez, R., et al. (2010). Directing astroglia from the cerebral cortex into subtype specific functional neurons. *PLoS Biol.* 8:e1000373. doi: 10.1371/journal.pbio.1000373

Hochstim, C., Deneen, B., Lukaszewicz, A., Zhou, Q., and Anderson, D. J. (2008). Identification of positionally distinct astrocyte subtypes whose identities are specified by a homeodomain code. *Cell* 133, 510–522. doi: 10.1016/j.cell.2008.02.046

Hösli, L., Zuend, M., Bredell, G., Zanker, H. S., Porto, de Oliveira, C. E., et al. (2022). Direct vascular contact is a hallmark of cerebral astrocytes. *Cell Rep.* 39:110599. doi: 10.1016/j.celrep.2022.110599

Huang, W., Guo, Q., Bai, X., Scheller, A., and Kirchhoff, F. (2019). Early embryonic NG2 glia are exclusively gliogenic and do not generate neurons in the brain. *Glia* 67, 1094–1103. doi: 10.1002/glia.23590

Huang, W., Zhao, N., Bai, X., Karram, K., Trotter, J., Goebbels, S., et al. (2014). Novel NG2-CreERT2 knock-in mice demonstrate heterogeneous differentiation potential of NG2 glia during development. *Glia* 62, 896–913. doi: 10.1002/glia.22648

Kang, S. H., Fukaya, M., Yang, J. K., Rothstein, J. D., and Bergles, D. E. (2010). NG2+ CNS glial progenitors remain committed to the oligodendrocyte lineage in postnatal life and following neurodegeneration. *Neuron* 68, 668–681. doi: 10.1016/j.neuron.2010.09.009

Khakh, B. S., and Deneen, B. (2019). The emerging nature of astrocyte diversity. *Annu. Rev. Neurosci.* 42, 187–207. doi: 10.1146/annurev-neuro-070918-050443

Kriegstein, A., and Alvarez-Buylla, A. (2009). The glial nature of embryonic and adult neural stem cells. *Annu. Rev. Neurosci.* 32, 149–184. doi: 10.1146/annurev.neuro.051508.135600

Lanjakornsiripan, D., Pior, B.-J., Kawaguchi, D., Furutachi, S., Tahara, T., Katsuyama, Y., et al. (2018). Layer-specific morphological and molecular differences in neocortical astrocytes and their dependence on neuronal layers. *Nat. Commun.* 9:1623. doi: 10.1038/s41467-018-03940-3

Lattke, M., Goldstone, R., Ellis, J. K., Boeing, S., Jurado-Arjona, J., Marichal, N., et al. (2021). Extensive transcriptional and chromatin changes underlie astrocyte maturation in vivo and in culture. *Nat. Commun.* 12, 4335. doi: 10.1038/s41467-021-24624-5

Levison, S. W., and Goldman, J. E. (1993). Both oligodendrocytes and astrocytes develop from progenitors in the subventricular zone of postnatal rat forebrain. *Neuron* 10, 201–212. doi: 10.1016/0896-6273(93)90311-E

Li, X., Liu, G., Yang, L., Li, Z., Zhang, Z., Xu, Z., et al. (2021). Decoding cortical glial cell development. *Neurosci. Bull.* 37, 440–460. doi: 10.1007/s12264-021-00640-9

Liu, J., Wu, X., and Lu, Q. (2022). Molecular divergence of mammalian astrocyte progenitor cells at early gliogenesis. *Development* 149:dev199985. doi: 10.1242/dev.199985

Livet, J., Weissman, T. A., Kang, H., Draft, R. W., Lu, J., Bennis, R. A., et al. (2007). Transgenic strategies for combinatorial expression of fluorescent proteins in the nervous system. *Nature* 450, 56–62. doi: 10.1038/nature06293

Loulier, K., Barry, R., Mahou, P., Le Franc, Y., Supatto, W., Matho, K. S., et al. (2014). Multiplex cell and lineage tracking with combinatorial labels. *Neuron* 81, 505–520. doi: 10.1016/j.neuron.2013.12.016

Magavi, S., Friedmann, D., Banks, G., Stolfi, A., and Lois, C. (2012). Coincident generation of pyramidal neurons and protoplasmic astrocytes in neocortical columns. *J. Neurosci.* 32, 4762–4772. doi: 10.1523/JNEUROSCI.3560-11.2012

Magnusson, J. P., Zamboni, M., Santopolo, G., Mold, J. E., Barrientos-Somarribas, M., Talavera-Lopez, C., et al. (2020). Activation of a neural stem cell transcriptional program in parenchymal astrocytes. *Elife* 9:e59733. doi: 10.7554/eLife.59733

Majo, M., Koontz, M., Rowitch, D., and Ullian, E. M. (2020). An update on human astrocytes and their role in development and disease. *Glia* 68, 685–704. doi: 10.1002/glia.23771

Malik, S., Vinukonda, G., Vose, L. R., Diamond, D., Bhimavarapu, B. B. R., Hu, F., et al. (2013). Neurogenesis continues in the third trimester of pregnancy and is suppressed by premature birth. *J. Neurosci.* 33, 411–423. doi: 10.1523/JNEUROSCI.4445-12.2013

Marshall, C. A. G., and Goldman, J. E. (2002). Subpallial dlx2-expressing cells give rise to astrocytes and oligodendrocytes in the cerebral cortex and white matter. *J. Neurosci.* 22, 9821–9830. doi: 10.1523/JNEUROSCI.22-22-09821.2002

Marshall, C. A. G., Novitch, B. G., and Goldman, J. E. (2005). Olig2 directs astrocyte and oligodendrocyte formation in postnatal subventricular zone cells. *J. Neurosci.* 25, 7289–7298. doi: 10.1523/JNEUROSCI.1924-05.2005

Marshall, C. A. G., Suzuki, S. O., and Goldman, J. E. (2003). Gliogenic and neurogenic progenitors of the subventricular zone: Who are they, where did they come from, and where are they going? *Glia* 43, 52–61. doi: 10.1002/glia.10213

Medeiros de Araújo, J. A., Barão, S., Mateos-White, I., Espinosa, A., Costa, M. R., et al. (2021). ZBTB20 is crucial for the specification of a subset of callosal projection neurons and astrocytes in the mammalian neocortex. *Development* 148:dev196642. doi: 10.1242/dev.196642

Miller, S. J., Philips, T., Kim, N., Dastgheyb, R., Chen, Z., Hsieh, Y.-C., et al. (2019). Molecularly defined cortical astroglia subpopulation modulates neurons via secretion of Norrin. *Nat. Neurosci.* 22, 741–752. doi: 10.1038/s41593-019-0366-7

Molofsky, A. V., Krenick, R., Ullian, E., Tsai, H. -h, Deneen, B., Richardson, W. D., et al. (2012). Astrocytes and disease: a neurodevelopmental perspective. *Genes Dev.* 26, 891–907. doi: 10.1101/gad.188326.112

Morel, L., Chiang, M. S. R., Higashimori, H., Shoneye, T., Iyer, L. K., Yelick, J., et al. (2017). Molecular and functional properties of regional astrocytes in the adult brain. *J. Neurosci.* 37, 8706–8717. doi: 10.1523/JNEUROSCI.3956-16.2017

Mori, T., Buffo, A., and Götz, M. (2005). "The novel roles of glial cells revisited: the contribution of radial glia and astrocytes to neurogenesis," in *Current topics in developmental biology*, (Amsterdam: Elsevier), 67–99. doi: 10.1016/S0070-2153(05)69004-7

Moroni, R. F., Deleo, F., Regondi, M. C., Madaschi, L., Amadeo, A., and Frassoni, C. (2018). Proliferative cells in the rat developing neocortical grey matter: new insights into gliogenesis. *Brain Struct. Funct.* 223, 4053–4066. doi: 10.1007/s00429-018-1736-8

Nagao, M., Ogata, T., Sawada, Y., and Gotoh, Y. (2016). Zbtb20 promotes astrocytogenesis during neocortical development. *Nat. Commun.* 7:11102. doi: 10.1038/ncomms11102

Nery, S., Fishell, G., and Corbin, J. G. (2002). The caudal ganglionic eminence is a source of distinct cortical and subcortical cell populations. *Nat. Neurosci.* 5, 1279–1287. doi: 10.1038/nn971

Oberheim, N. A., Tian, G.-F., Han, X., Peng, W., Takano, T., Ransom, B., et al. (2008). Loss of astrocytic domain organization in the epileptic brain. *J. Neurosci.* 28, 3264–3276. doi: 10.1523/JNEUROSCI.4980-07.2008

Ohayon, D., Aguirrebengoa, M., Escalas, N., Jungas, T., and Soula, C. (2021). Transcriptome profiling of the Olig2-expressing astrocyte subtype reveals their unique molecular signature. *iScience* 24:102806. doi: 10.1016/j.isci.2021.102806

Ohayon, D., Escalas, N., Cochard, P., Glise, B., Danesin, C., and Soula, C. (2019). Sulfatase 2 promotes generation of a spinal cord astrocyte subtype that stands out through the expression of Olig2. *Glia* 67, 1478–1495. doi: 10.1002/glia.23621

Ojalvo-Sanz, A. C., and López-Mascaraque, L. (2021). Gliogenic potential of single pallial radial glial cells in lower cortical layers. *Cells* 10:3237. doi: 10.3390/cells10113237

Ono, K., Takebayashi, H., Ikeda, K., Furusho, M., Nishizawa, T., Watanabe, K., et al. (2008). Regional- and temporal-dependent changes in the differentiation of Olig2 progenitors in the forebrain, and the impact on astrocyte development in the dorsal pallium. *Dev. Biol.* 320, 456–468. doi: 10.1016/j.ydbio.2008.06.001

Pereira, J. D., Sansom, S. N., Smith, J., Dobenecker, M.-W., Tarakhovsky, A., and Livesey, F. J. (2010). Ezh2, the histone methyltransferase of PRC2, regulates the balance between self-renewal and differentiation in the cerebral cortex. *Proc. Natl. Acad. Sci. U.S.A.* 107, 15957–15962. doi: 10.1073/pnas.1002530107

Pous, L., Deshpande, S. S., Nath, S., Mezey, S., Malik, S. C., Schildge, S., et al. (2020). Fibrinogen induces neural stem cell differentiation into astrocytes in the subventricular zone via BMP signaling. *Nat. Commun.* 11:630. doi: 10.1038/s41467-020-14466-y

Rakic, P. (1988). Specification of cerebral cortical areas. *Science* 241, 170–176. doi: 10.1126/science.3291116

Ramón y Cajal, S. (1909). *Histologie du système nerveux de l'homme et des vertébrés*. Paris: Maloine.

Rivers, L. E., Young, K. M., Rizzi, M., Jamen, F., Psachoulia, K., Wade, A., et al. (2008). PDGFRA/NG2 glia generate myelinating oligodendrocytes and piriform projection neurons in adult mice. *Nat. Neurosci.* 11, 1392–1401. doi: 10.1038/nn.2220

Sánchez-González, R., Bribián, A., and López-Mascaraque, L. (2020). Cell fate potential of NG2 progenitors. *Sci. Rep.* 10:9876. doi: 10.1038/s41598-020-66753-9

Serwanski, D. R., Jukkola, P., and Nishiyama, A. (2017). Heterogeneity of astrocyte and NG2 cell insertion at the node of ranvier: Frequency of glial insertion at the node. *J. Comp. Neurol.* 525, 535–552. doi: 10.1002/cne.24083

Sloan, S. A., Darmanis, S., Huber, N., Khan, T. A., Birey, F., Caneda, C., et al. (2017). Human astrocyte maturation captured in 3d cerebral cortical spheroids derived from pluripotent stem cells. *Neuron* 95, 779.e–790.e. doi: 10.1016/j.neuron.2017.07.035

Staugaitis, S. M., Zerlin, M., Hawkes, R., Levine, J. M., and Goldman, J. E. (2001). Aldolase C/Zebrin II expression in the neonatal rat forebrain reveals cellular heterogeneity within the subventricular zone and early astrocyte differentiation. *J. Neurosci.* 21, 6195–6205. doi: 10.1523/JNEUROSCI.21-16-06195.2001

Stipursky, J., Francis, D., Dezonne, R. S., Bérgamo de Araújo, A. P., Souza, L., Moraes, C. A., et al. (2014). TGF-Î21 promotes cerebral cortex radial glia-astrocyte differentiation in vivo. *Front. Cell. Neurosci.* 8:393. doi: 10.3389/fncel.2014.00393

Stogsdill, J. A., Ramirez, J., Liu, D., Kim, Y. H., Baldwin, K. T., Enustun, E., et al. (2017). Astrocytic neuroligins control astrocyte morphogenesis and synaptogenesis. *Nature* 551, 192–197. doi: 10.1038/nature24638

Tabata, H. (2015). Diverse subtypes of astrocytes and their development during corticogenesis. *Front. Neurosci.* 9:114. doi: 10.3389/fnins.2015.00114

Takebayashi, H., Nabeshima, Y., Yoshida, S., Chisaka, O., Ikenaka, K., and Nabeshima, Y. (2002). The basic helix-loop-helix factor Olig2 is essential for the development of motoneuron and oligodendrocyte lineages. *Curr. Biol.* 12, 1157–1163. doi: 10.1016/S0960-9822(02)00926-0

Tatsumi, K., Isonishi, A., Yamasaki, M., Kawabe, Y., Morita-Takemura, S., Nakahara, K., et al. (2018). Olig2-Lineage Astrocytes: A distinct subtype of astrocytes that differs from gfap astrocytes. *Front. Neuroanat.* 12:8. doi: 10.3389/fnana.2018.00008

Tatsumi, K., Kinugawa, K., Isonishi, A., Kitabatake, M., Okuda, H., Takemura, S., et al. (2021). Olig2-astrocytes express neutral amino acid transporter SLC7A10 (Asc-1) in the adult brain. *Mol. Brain* 14:163. doi: 10.1186/s13041-021-00874-8

Tiwari, N., Pataskar, A., Péron, S., Thakurela, S., Sahu, S. K., Figueres-Oñate, M., et al. (2018). Stage-specific transcription factors drive astrogliogenesis by remodeling gene regulatory landscapes. *Cell Stem Cell* 23, 557.e–571.e. doi: 10.1016/j.stem.2018.09.008

Tong, X., Shigetomi, E., Looger, L. L., and Khakh, B. S. (2013). Genetically encoded calcium indicators and astrocyte calcium microdomains. *Neurosci.* 19, 274–291. doi: 10.1177/1073858412468794

Torres-Ceja, B., and Olsen, M. L. (2022). A closer look at astrocyte morphology: Development, heterogeneity, and plasticity at astrocyte leaflets. *Curr. Opin. Neurobiol.* 74:102550. doi: 10.1016/j.conb.2022.102550

Tsai, H.-H., Li, H., Fuentealba, L. C., Molofsky, A. V., Taveira-Marques, R., Zhuang, H., et al. (2012). Regional astrocyte allocation regulates CNS synaptogenesis and repair. *Science* 337, 358–362. doi: 10.1126/science.1222381

Velmeshev, D., Schirmer, L., Jung, D., Haeussler, M., Perez, Y., Mayer, S., et al. (2019). Single-cell genomics identifies cell type–specific molecular changes in autism. *Science* 364, 685–689. doi: 10.1126/science.aav8130

Wagner, D. E., and Klein, A. M. (2020). Lineage tracing meets single-cell omics: opportunities and challenges. *Nat. Rev. Genet.* 21, 410–427. doi: 10.1038/s41576-020-0223-2

Wang, H., Xu, L., Lai, C., Hou, K., Chen, J., Guo, Y., et al. (2021). Region-specific distribution of Olig2-expressing astrocytes in adult mouse brain and spinal cord. *Mol. Brain* 14:36. doi: 10.1186/s13041-021-00747-0

Wang, X., Chang, L., Guo, Z., Li, W., Liu, W., Cai, B., et al. (2013). Neonatal SVZ EGFP-labeled cells produce neurons in the olfactory bulb and astrocytes in the cerebral cortex by in-vivo electroporation. *Neuroreport* 24, 381–387. doi: 10.1097/WNR.0b013e328360f7ef

Welle, A., Kasakow, C. V., Jungmann, A. M., Gobbo, D., Stopper, L., Nordström, K., et al. (2021). Epigenetic control of region-specific transcriptional programs in mouse cerebellar and cortical astrocytes. *Glia* 69, 2160–2177. doi: 10.1002/glia.24016

Yang, L., Li, Z., Liu, G., Li, X., and Yang, Z. (2022). developmental origins of human cortical oligodendrocytes and astrocytes. *Neurosci. Bull.* 38, 47–68. doi: 10.1007/s12264-021-00759-9

Zeisel, A., Hochgerner, H., Lönnerberg, P., Johnsson, A., Memic, F., van der Zwan, J., et al. (2018). Molecular architecture of the mouse nervous system. *Cell* 174, 999.e–1014.e. doi: 10.1016/j.cell.2018.06.021

Zerlin, M., Levison, S., and Goldman, J. (1995). Early patterns of migration, morphogenesis, and intermediate filament expression of subventricular zone cells in the postnatal rat forebrain. *J. Neurosci.* 15, 7238–7249. doi: 10.1523/JNEUROSCI.15-11-07238.1995

Zhang, X., Mennicke, C. V., Xiao, G., Beattie, R., Haider, M. A., Hippenmeyer, S., et al. (2020). Clonal analysis of gliogenesis in the cerebral cortex reveals stochastic expansion of glia and cell autonomous responses to egfr dosage. *Cells* 9:2662. doi: 10.3390/cells9122662

Zhang, Y., Li, B., Cananzi, S., Han, C., Wang, L.-L., Zou, Y., et al. (2022). A single factor elicits multilineage reprogramming of astrocytes in the adult mouse striatum. *Proc. Natl. Acad. Sci. U.S.A.* 119, e2107339119. doi: 10.1073/pnas.2107339119

Zhang, Y., Sloan, S. A., Clarke, L. E., Caneda, C., Plaza, C. A., Blumenthal, P. D., et al. (2016). Purification and characterization of progenitor and mature human astrocytes reveals transcriptional and functional differences with mouse. *Neuron* 89, 37–53. doi: 10.1016/j.neuron.2015.11.013

Zhu, X., Bergles, D. E., and Nishiyama, A. (2008). NG2 cells generate both oligodendrocytes and gray matter astrocytes. *Development* 135, 145–157. doi: 10.1242/dev.004895

Zhu, X., Hill, R. A., Dietrich, D., Komitova, M., Suzuki, R., and Nishiyama, A. (2011). Age-dependent fate and lineage restriction of single NG2 cells. *Development* 138, 745–753. doi: 10.1242/dev.047951

Zhu, X., Zuo, H., Maher, B. J., Serwanski, D. R., LoTurco, J. J., Lu, Q. R., et al. (2012). Olig2-dependent developmental fate switch of NG2 cells. *Development* 139, 2299–2307. doi: 10.1242/dev.078873

Zisis, E., Keller, D., Kanari, L., Arnaudon, A., Gevaert, M., Delemontex, T., et al. (2021). Digital reconstruction of the neuro-glia-vascular architecture. *Cereb. Cortex* 31, 5686–5703. doi: 10.1093/cercor/bhab254

Zweifel, S., Marcy, G., Lo Guidice, Q., Li, D., Heinrich, C., Azim, K., et al. (2018). HOPX Defines heterogeneity of postnatal subventricular zone neural stem cells. *Stem Cell Rep.* 11, 770–783. doi: 10.1016/j.stemcr.2018.08.006

frontiers | Frontiers in Neuroscience

TYPE Original Research
PUBLISHED 02 December 2022
DOI 10.3389/fnins.2022.919462

OPEN ACCESS

EDITED BY
Simon Hippenmeyer,
Institute of Science and Technology Austria (IST Austria), Austria

REVIEWED BY
Roberta Azzarelli,
University of Cambridge, United Kingdom
Simona Lodato,
Humanitas University, Italy

*CORRESPONDENCE
Sophie Péron
sopperon@uni-mainz.de
Benedikt Berninger
benedikt.berninger@kcl.ac.uk

†These authors have contributed equally to this work

SPECIALTY SECTION
This article was submitted to Neurogenesis, a section of the journal Frontiers in Neuroscience

RECEIVED 13 April 2022
ACCEPTED 09 November 2022
PUBLISHED 02 December 2022

CITATION
Galante C, Marichal N, Scarante FF, Ghayad LM, Shi Y, Schuurmans C, Berninger B and Péron S (2022) Enhanced proliferation of oligodendrocyte progenitor cells following retrovirus mediated Achaete-scute complex-like 1 overexpression in the postnatal cerebral cortex *in vivo*. *Front. Neurosci.* 16:919462. doi: 10.3389/fnins.2022.919462

Enhanced proliferation of oligodendrocyte progenitor cells following retrovirus mediated Achaete-scute complex-like 1 overexpression in the postnatal cerebral cortex *in vivo*

Chiara Galante[1†], Nicolás Marichal[2†], Franciele Franco Scarante[2,3], Litsa Maria Ghayad[2], Youran Shi[2,4], Carol Schuurmans[5,6,7], Benedikt Berninger[1,2,4,8,9*] and Sophie Péron[1,2*]

[1]Institute of Physiological Chemistry, University Medical Center Johannes Gutenberg University, Mainz, Germany, [2]Centre for Developmental Neurobiology, Institute of Psychiatry, Psychology & Neuroscience, King's College London, London, United Kingdom, [3]Department of Pharmacology, Ribeirão Preto Medical School, University of São Paulo, São Paulo, Brazil, [4]The Francis Crick Institute, London, United Kingdom, [5]Biological Sciences Platform, Sunnybrook Research Institute, Toronto, ON, Canada, [6]Department of Biochemistry, University of Toronto, Toronto, ON, Canada, [7]Department of Laboratory Medicine and Pathobiology, University of Toronto, Toronto, ON, Canada, [8]MRC Centre for Neurodevelopmental Disorders, Institute of Psychiatry, Psychology & Neuroscience, King's College London, London, United Kingdom, [9]Focus Program Translational Neuroscience, Johannes Gutenberg University, Mainz, Germany

The proneural transcription factor Achaete-scute complex-like 1 (Ascl1) is a major regulator of neural fate decisions, implicated both in neurogenesis and oligodendrogliogenesis. Focusing on its neurogenic activity, Ascl1 has been widely used to reprogram non-neuronal cells into induced neurons. *In vitro*, Ascl1 induces efficient reprogramming of proliferative astroglia from the early postnatal cerebral cortex into interneuron-like cells. Here, we examined whether Ascl1 can similarly induce neuronal reprogramming of glia undergoing proliferation in the postnatal mouse cerebral cortex *in vivo*. Toward this goal, we targeted cortical glia during the peak of proliferative expansion (i.e., postnatal day 5) by injecting a retrovirus encoding for Ascl1 into the mouse cerebral cortex. In contrast to the efficient reprogramming observed *in vitro*, *in vivo* Ascl1-transduced glial cells were converted into doublecortin-immunoreactive neurons only with very low efficiency. However, we noted a drastic shift in the relative number of retrovirus-transduced Sox10-positive oligodendrocyte progenitor cells (OPCs) as compared to glial fibrillary acidic protein (GFAP)-positive astrocytes. Genetic fate mapping demonstrated that this increase in OPCs was not due to Ascl1-mediated astrocyte-to-OPC fate conversion. Rather, EdU incorporation

experiments revealed that Ascl1 caused a selective increase in proliferative activity of OPCs, but not astrocytes. Our data indicate that rather than inducing neuronal reprogramming of glia in the early postnatal cortex, Ascl1 is a selective enhancer of OPC proliferation.

KEYWORDS

astrocyte, gliogenesis, lineage reprogramming, neurogenesis, proliferation, proneural, Sox10, Ascl1

Introduction

The postnatal mammalian brain is largely devoid of persistent neurogenesis, except from specialized niches such as the subependymal zone of the lateral ventricle and the subgranular zone of the dentate gyrus (Denoth-Lippuner and Jessberger, 2021). In all other brain regions, neurons lost due to disease or injury cannot be replaced, resulting in irreversible circuit dysfunction and functional impairments. Harnessing the neurogenic potential of glia to produce new neurons by direct lineage reprogramming has emerged as an approach for potential repair of diseased circuits in non-neurogenic brain areas such as the cerebral cortex (Peron and Berninger, 2015).

The basic helix-loop-helix (bHLH) transcription factor Achaete-scute complex-like 1 (Ascl1) orchestrates multiple and in some respect opposing aspects of cortical development such as cellular proliferation and cell cycle exit, as well as neural fate choice (Castro et al., 2011; Guillemot and Hassan, 2017). It is generally believed that oscillating levels of Ascl1 expression promote progenitor proliferation while high and constant levels promote neuronal differentiation (Imayoshi et al., 2013).

In the ventral telencephalon, Ascl1 controls GABAergic neurogenesis by regulating expression of homeobox genes of the distal-less gene family (*Dlx* genes) in progenitors (Casarosa et al., 1999; Poitras et al., 2007). Leveraging its neurogenic activity, we previously demonstrated that expression of Ascl1 in mouse postnatal cortical astrocytes *in vitro* was sufficient to reprogram these into functional neurons endowed with GABAergic neuron properties (Berninger et al., 2007; Heinrich et al., 2010). Likewise, Ascl1 was found to reprogram cultured cells of human origin, including fibroblasts and pericytes, into neurons *in vitro* (Karow et al., 2012; Chanda et al., 2014). Finally, co-expression of Ascl1 and Dlx2 in reactive glia of the adult epileptic hippocampus resulted in the induction of neurons with neurochemical and electrophysiological hallmarks of hippocampal interneurons (Lentini et al., 2021). Beyond its important role in neurogenesis, Ascl1 also plays an important role in gliogenesis. For instance, deletion of Ascl1 was found to cause a decrease in neonatal oligodendrogliogenesis in the dorsal telencephalon, resulting in a relative increase in astrocytes among Ascl1 ablated cells (Nakatani et al., 2013). These studies raise the question whether Ascl1 induces glia-to-neuron conversion *in vivo*, or potentially regulates other aspects of gliogenesis such as proliferation.

Here we addressed this question by injecting Ascl1-encoding retrovirus into the mouse cerebral cortex at postnatal day 5 (P5), i.e., at a time when glial cell populations undergo massive expansion (Psachoulia et al., 2009; Ge et al., 2012). We found that Ascl1 induced only very limited glia-to-neuron reprogramming *in vivo*. In contrast, we observed a drastic increase in proliferative activity in oligodendrocyte progenitor cells (OPCs) but not in astrocytes. These data do not only reveal a rather restricted neuronal reprogramming capacity of Ascl1 when overexpressed in early postnatal astrocytes alone, but also unveils highly divergent responses of distinct glial cell types to this proneural gene.

Materials and methods

Cell culture

Postnatal cortical astrocytes were isolated from cortices of C57BL/6J mice between postnatal day 5–7 days (P5–7), which were obtained from the Translational Animal Research Center of the University Medical Center Mainz. P5–P7 astrocytes were cultured as previously described (Heinrich et al., 2011; Sharif et al., 2021). Briefly, after isolation, cells were expanded for 7–10 days in Astromedium: Dulbecco's Modified Eagles Medium, Nutrient Mixture F12 (DMEM/F12, Gibco, Carlsbad, CA, USA, 21331-020); 10% Fetal Bovine Serum (FBS, Invitrogen, 10270-106); 5% Horse Serum (Thermo Fisher Scientific, Waltham, MA, USA, 16050-130); 1× Penicillin/Streptomycin (Thermo Fisher Scientific, Waltham, MA, USA, 15140122); 1× L-GlutaMAX Supplement (Thermo Fisher Scientific, Waltham, MA, USA, 35050-0380); 1× B27 Supplement (Thermo Fisher Scientific, Waltham, MA, USA, 17504001); and supplemented with 10 ng/μl Epidermal Growth Factor (EGF; Peprotech, Cranbury, NJ, USA, AF-100-15) and 10 ng/μl basic-Fibroblast Growth Factor (FGF-2; Peprotech, Cranbury, NJ, USA, 100-18B). Cells were incubated at 37°C in 5% CO_2. When cells reached 70–80% confluency, cells were detached with 0.05% Trypsin

EDTA (Life Technologies, Carlsbad, CA, USA, 15400054) for 5 min at 37°C. Cells were subsequently seeded onto poly-D-lysine hydrobromide-coated (PDL; Sigma, Merck, Germany, P0899) glass coverslips (12 mm, Menzel-Gläser, Thermo Fisher Scientific, Waltham, MA, USA, 631-0713) in 24-well plates at a density of 50,000–80,000 cells/well in 500 µl Astromedium supplemented with 10 ng/µl EGF and 10 ng/µl FGF-2.

Plasmids and retroviruses

Moloney Murine Leukaemia Virus (MMLV)-based retroviral vectors (Heinrich et al., 2011) were used to express Ascl1 under control of the chicken β-actin promoter with a cytomegalovirus enhancer (pCAG). A green fluorescent protein (GFP) or DsRed reporter was cloned in behind an Internal Ribosome Entry Site (IRES). To generate the pCAG-Ascl1-IRES-DsRed/GFP retroviral constructs, a cassette containing the coding sequences flanked by attL recombination sites was generated through the excision of the coding sequences for Ascl1 from the pCIG2 parental vector (Li et al., 2014) *via* *Xho*I/*Sal*I double restriction. Isolated fragment was inserted into the pENTRY1A Dual Selection (Thermo Fisher Scientific, Waltham, MA, USA) intermediate vector linearized *via* *Sal*I. The final retroviral constructs were subsequently obtained via recombination catalyzed by the LR Clonase II (Thermo Fisher Scientific, Waltham, MA, USA, 11791020), which substituted the ccdB cassette in the destination vector pCAG-ccdB-IRES-DsRed or pCAG-ccdB-IRES-GFP with Ascl1 coding sequence. Transduction with MMLV-based retroviral vectors encoding only the fluorescent protein GFP or DsRed behind an IRES under control of pCAG promoter (pCAG-IRES-DsRed/pCAG-IRES-GFP) (Heinrich et al., 2011) was used for control experiments. Viral particles were produced using gpg helper free packaging cells to generate Vesicular Stomatitis Virus Glycoprotein (VSV-G)-pseudotyped retroviral particles (Ory et al., 1996). Viral stocks were titrated by transduction of HEK293 cultures. Viral titers used were in the range of 10^7 TU/ml.

Retroviral transduction

After seeding the cells and letting them attach for 4 h in the incubator, cells were transduced with 1 µl retrovirus/well and incubated at 37°C in 8% CO_2. One day later, treated medium was removed and substituted with 500 µl of B27 Differentiation Medium: DMEM/F12 (Gibco, Carlsbad, CA, USA, 21331-020); 1× Penicillin/Streptomycin (Thermo Fisher Scientific, Waltham, MA, USA, 15140122); 1× L-GlutaMAX Supplement (Thermo Fisher Scientific, Waltham, MA, USA, 35050-0380); 1× B27 Supplement (Thermo Fisher Scientific, Waltham, MA, USA, 17504001). Cells were treated again with 1 µl/well of retrovirus. One day later, the culture volume was brought to 1 ml/well with fresh B27 Differentiation Medium. Cells were kept in culture for a total of 7 days *in vitro* before fixation for immunocytochemical analyses.

Immunocytochemistry

Cells were fixed with 4% paraformaldehyde (PFA, Sigma, Merck, Germany, P6148) for 10–15 min and washed three times with 1× PBS (Gibco, Carlsbad, CA, USA, 70013-016) before storage at 4°C. Washed cells were first incubated for 1 h at room temperature (RT) with blocking solution [3% bovine serum albumin (BSA; Sigma, Merck, Germany, A7906) and 0.5% Triton X-100 (Sigma, Merck, Germany, X100) in 1× PBS] and then with primary antibodies diluted in blocking solution for 2–3 h at RT. After three washes with 1× PBS, cells were incubated with secondary antibodies for 1 h at RT. Cells were then counterstained with DAPI (Sigma, Merck, Germany, D8417) diluted 1:1,000 in blocking solution, then washed three time in 1× PBS before being mounted with Aqua Polymount (Polysciences, Warrington, PA, USA, 18606-20). The following primary antibodies were used: β-Tubulin III (Mouse IgG2b, 1:1,000; Sigma, Merck, Germany, T8660); Green Fluorescent Protein (GFP, Chicken, 1:300, AvesLab, Davies, CA, USA, GFP-1020); GFAP (rabbit, 1:1,000, Agilent, Santa Clara, CA, USA, Z0334); Red Fluorescent Protein (RFP, rat, 1:400, Proteintech Group Inc., Rosemont, IL, USA, 5F8). Secondary antibodies were diluted 1:1,000 in blocking solution and were conjugated to: A488 anti-chicken (donkey, Jackson Immunoresearch, Ely, UK, 703-545-155); Cy3 anti-mouse (goat, Dianova, Hamburg, Germany, 115-165-166); Cy3 anti-rat (goat, Dianova, Hamburg, Germany, 112-165-167); Cy5 anti-rabbit (goat, Dianova, Hamburg, Germany, 111-175-144).

Animals and animal procedures

The study was performed in accordance with the guidelines of the German Animal Welfare Act, the European Directive 2010/63/EU for the protection of animals used for scientific purposes and the Animal (Scientific Procedures) Act 1986 and was approved by local authorities (Rhineland-Palatinate State Authority, permit number 23 177 07-G15-1-031; ethical committee of King's College London and the UK Home Office, permits numbers PD025E9BC and PP8849003). Male and female C57BL/6J pups were purchased with their mother from Janvier Labs (Le Genest-Saint-Isle, France) or Charles River Laboratories (Walden, UK). Male and female transgenic mGFAP-Cre/EGFP mice used in this study for fate-mapping experiments were generated in house. For this, mice in which the expression of Cre recombinase is driven by mouse GFAP promoter [mGFAP-Cre; B6.Cg-Tg(Gfap-cre)77.6 Mvs/2J, JAX024098] (Gregorian et al., 2009) were crossed with an EGFP reporter mouse line [CAG-EGFP; Gt(ROSA)26Sortm1.1(CAG-EGFP)Fsh/Mmjax, JAX032037] (Sousa et al., 2009). Mice were kept in a 12:12 h light-dark cycle in Polycarbonate

Type II cages (350 cm^2). Animals were provided with food and water *ad libitum* and all efforts were made to reduce the number of animals and their suffering. Before the surgery, animals received a subcutaneous injection of Carprofen [Rimadyl® (Zoetis, Parsipanny, NJ, USA), 4 mg/kg of body weight, in 0.9% NaCl (Amresco, VWR International, Radnor, PA, USA)]. Anesthesia was induced by intraperitoneal (i.p.) injection of a solution of 0.5 mg/kg Medetomidin (Pfizer, New York, NY, USA), 5 mg/kg Midazolam (Hameln, Hameln-Germany) and 0.025 mg/kg Fentanyl (Albrecht GmbH, Aulendorf, Germany) in 0.9% NaCl. Viruses were injected in the cerebral cortex using glass capillaries (Hirschmann, Eberstadt, Germany, 9600105) pulled to obtain a 20 μm tip diameter. Briefly, a small incision was made on the skin with a surgical blade and the skull was carefully opened with a needle. Each pup received a volume of 0.5–1 μl of retroviral suspension targeted to the somatosensory and visual cortical areas. After injection, the wound was closed with surgical glue (3 M Vetbond, Thermo Fisher Scientific, Waltham, MA, USA, NC0304169) and anesthesia was terminated by i.p. injection of a solution of 2.5 mg/kg Atipamezol (Pfizer, New York, NY, USA), 0.5 mg/kg Flumazenil (Hameln, Hameln-Germany) and 0.1 mg/Kg Buprenorphin (RB Pharmaceutials, Richmond, VA, USA) in 0.9% NaCl. Pups were left to recover on a warm plate (37°C) before returning them to their mother. Recovery state was checked daily for a week after the surgery.

Tissue preparation and immunohistochemistry

Animals were lethally anesthetized with a solution of 120 mg/kg Ketamine (Zoetis, Parsipanny, NJ, USA) and 16 mg/kg Xylazine (Bayer, Leverkusen, Germany) (in 0.9% NaCl, i.p.) and transcardiacally perfused with pre-warmed 0.9% NaCl followed by ice-cold 4% paraformaldehyde (PFA, Sigma, Merck, Germany, P6148). The brains were harvested and post-fixed for 2 h to overnight in 4% PFA at 4°C. Then, 40 μm thick coronal sections were prepared using a vibratome (Microm HM650V, Thermo Scientific, Waltham, MA, USA) and stored at −20°C in a cryoprotective solution [20% glucose (Sigma, Merck, Germany, G8270), 40% ethylene glycol (Sigma, Merck, Germany, 324558), and 0.025% sodium azide (Sigma, Merck, Germany, S2202), in 0.5× phosphate buffer 15 mM $Na_2HPO_4{\cdot}12H_2O$ (Merck, Darmstadt, Germany, 10039-32-4); 16 mM $NaH_2PO_4{\cdot}2H_2O$ (Merck, Darmstadt, Germany, 13472-35-0); pH 7.4].

For immunohistochemistry, brain sections were washed three times for 15 min with 1× TBS [50 mM Tris (Thermo Fisher Scientific, Waltham, MA, USA, 15504-020); 150 mM NaCl (Amresco, VWR International, Radnor, PA, USA, 0241); pH7.6] and then incubated for 1.5 h in blocking solution: 5% Donkey Serum (Sigma, Merck, Germany, S30); 0.3% Triton X-100; 1× TBS. Slices were then incubated with primary antibodies diluted in blocking solution for 2–3 h at RT, followed by an overnight incubation at 4°C. After three washing steps with 1× TBS, slices were incubated with secondary antibodies diluted blocking solution for 1 h at RT. Slices were washed twice with 1× TBS, incubated with DAPI dissolved 1:1,000 in 1× TBS for 5 min at RT and washed three times with 1× TBS. For mounting, slices were washed two times with 1× Phosphate Buffer [30 mM $Na_2HPO_4{\cdot}12H_2O$ (Merck, Darmstadt, Germany, 10039-32-4); 33 mM $NaH_2PO_4{\cdot}2H_2O$ (Merck, Darmstadt, Germany, 13472-35-0); pH 7.4] and were dried on Superfrost (Thermo Fisher Scientific, Waltham, MA, USA) microscope slides. Sections were further dehydrated with toluene and covered with cover-glasses mounted with DPX mountant for histology (Sigma, Merck, Germany, 06522) or directly mounted with Prolong™Gold (Thermo Fisher Scientific, Waltham, MA, USA, P36930). The following primary antibodies were used: Achaete-scute complex-like 1 (Ascl1, mouse IgG1, 1:400, BD Pharmingen, Franklin Lakes, NJ, USA, 556604); Doublecortin (DCX, goat, 1:250, Santa Cruz Biotechnology, Dallas, TX, USA, sc-8066); Green Fluorescent Protein (GFP, chicken, 1:1,000, AvesLab, Davies, CA, USA, GFP-1020); Glial Fibrillary Acidic Protein (GFAP, rabbit, 1:300, Agilent, Santa Clara, CA, USA, Z0334); Ionized calcium-binding adapter molecule 1 (Iba1, rabbit, 1:800, Agilent, Santa Clara, CA, USA, 16A11); mCherry (chicken, 1:300, EnCor Biotechnology, Gainsville, FL, USA, CPCA-mCherry); Red Fluorescent Protein (RFP, rabbit, 1:500, Biomol, Hamburg, Germany, 600401379S); and SRY-Box 10 (Sox10, goat, 1:100, Santa Cruz Biotechnology, Dallas, TX, USA, sc-17342). Secondary antibodies were made in donkey and conjugated with: A488 (anti-chicken, 1:200, Jackson Immunoresearch, Ely, UK, 703-545-155); A488 (anti-rabbit, 1:200, Thermo Fisher Scientific, Waltham, MA, USA, A21206); A647 (anti-rabbit, 1:500, Thermo Fisher Scientific, Waltham, MA, USA, A31573); A488 (anti-mouse, 1:200, Thermo Fisher Scientific, Waltham, MA, USA, A21202); A647 (anti-mouse, 1:500, Thermo Fisher Scientific, Waltham, MA, USA, A31571); Cy3 (anti-chicken, 1:500, Dianova, Hamburg, Germany, 703-165-155); Cy3 (anti-goat, 1:500, Dianova, Hamburg, Germany, 705-165-147); Cy3 (anti-mouse, 1:500, Thermo Fisher Scientific, Waltham, MA, USA, A10037); Cy3 (anti-rabbit, 1:500, Dianova, Hamburg, Germany, 711-165-152); and Cy5 (anti-goat, 1:500, Dianova, Hamburg, Germany, 705-175-147).

5-Ethynyl-2′-deoxyuridine incorporation assay

Animals received a single injection of 50 mg/kg (in 0.9% NaCl and 0.25% DMSO, i.p.) 5-Ethynyl-2′-deoxyuridine (EdU, Sigma, Merck, Germany, 900584) 3 h prior to perfusion at 12 days post-injection. The immunohistochemistry protocol

was modified as follows for combinatorial detection of EdU: brain sections were washed three times with TBS and then incubated for 2 h in blocking solution [2.5% Donkey Serum, 2.5% Goat Serum (when no staining for Sox10; Sigma, Merck, Germany, G9023), 0.3% Triton X100 in TBS] at RT. Sections were incubated with primary antibodies diluted in blocking solution for 2 h at RT followed by an overnight incubation at 4°C (when no staining for Sox10), or 72 h at 4°C (when staining for Sox10). After three washes with TBS, the sections were incubated for 30 min at RT with the Click-iT EdU Imaging Kit Reaction Cocktail (for 500 µl: 430 µl of 1× Click iT EdU Reaction buffer, 20 µl of $CuSO_4$, 1.2 µl Alexa Fluor Azide 647, 50 µl Click iT EdU buffer additive; Thermo Fisher Scientific, Waltham, MA, USA, C10340). Finally, the sections were washed three times with TBS, incubated for 5 min at RT with DAPI (5 µM in PBS) and washed again three times with TBS before being mounted using Mowiol (Cat# 17951-500, Polysciences, Warrington, PA, USA) supplemented with DABCO (Cat# 15154-500, Polysciences, Warrington, PA, USA). The following primary antibodies were used: Red Fluorescent Protein (RFP, rabbit, 1:500, Biomol, Hamburg, Germany, 600401379S); SRY-Box 10 (Sox10, goat, 1:300, R&D Systems, Minneapolins, MN, USA, AF2864). The following secondary antibodies were used: goat Anti-Rabbit A568 (1:1,000; Thermo Fisher, Waltham, MA, USA, A-11011), Donkey anti-Rabbit Cy3 (1:1,1000, Jackson Immunoresearch, Ely, UK, 711-165-152) and Donkey anti-Goat A647 (1:1,000; Thermo Fisher Scientific, Waltham, MA, USA, AB2535864) (A647, 1:1,000).

Imaging and data analysis

Confocal images were acquired using a TCS SP5 (Leica Microsystems, Wetzlar, Germany) confocal microscope (Institute of Molecular Biology, Mainz, Germany) equipped with four PMTs, four lasers (405 Diode, Argon, HeNe 543, HeNe 633) and a fast-resonant scanner using a 20× dry objective (NA 0.7) or a 40× oil objective (NA 1.3), or with a Zeiss LSM 800 confocal microscope (Carl Zeiss Microscopy, Jena, Germany) equipped with four solid-state lasers (405, 488, 561, and 633 nm) at a 20× objective (NA 0.8) (Centre for Developmental Neurobiology, King's College London). Alternatively, images were acquired with a Zeiss Axio Imager.M2 fluorescent microscope equipped with an ApoTome (Carl Zeiss Microscopy, Jena, Germany) at a 20× dry objective (NA 0.7) or a 63× oil objective (NA 1.25). For imaging of brain sections, serial Z-stacks spaced at 0.3–2.13 µm distance were acquired to image the whole thickness of the section.

For *in vitro* experiments, biological replicates (n) were obtained from independent cultures prepared from different animals. For each *n*, the value corresponds to the mean value of two technical replicates (i.e., two coverslips). Cell quantifications were performed on 4 × 4 tile scans (individual tile size: 624.70 µm × 501.22 µm). For *in vivo* experiments, *n* corresponds to the number of animals. Quantifications were performed on equally spaced sections (240 or 480 µm) covering the whole area with transduced cells. For fate-mapping experiments in mGFAP-Cre/EGFP mice, cells were quantified in 3–5 sections per animal.

For images used for illustration, the color balance of each channel was uniformly adjusted in Photoshop (Adobe, Mountain View, CA, USA). If necessary, Lookup Tables were changed to maintain uniformity of color coding within figures. When appropriate, a median filter (despeckle) was applied in Fiji (Fiji.sc) to pictures presenting salt-and-pepper noise, and noise was filtered via removal of outlier pixels.

Statistical analysis

The number of independent experiments (*n*) and number of cells analyzed are reported in the main text or figure legends. Data are represented as means ± SD. Statistical analysis was performed in SPSS Statistics 23 V5 (IBM, Armonk, NY, USA). Normality of distribution was assessed using Shapiro–Wilk test and the significance of the differences between control and Ascl1 groups was analyzed by *t*-test for independent samples or Mann–Whitney *U* test (for normally and non-normally distributed data, respectively). *P*-values are indicated in the figures. Graphs were prepared in GraphPad Prism 5 (GraphPad, San Diego, CA, USA).

Results

Achaete-scute complex-like 1 converts postnatal cortical glia into neurons with very low efficiency *in vivo*

Our earlier work showed that Ascl1 can reprogram cultured postnatal astroglia into neurons (Berninger et al., 2007; Heinrich et al., 2010; Gascon et al., 2016). Here, we investigated whether Ascl1 can reprogram proliferative cortical glia toward a neuronal fate *in vivo*. Cortical glia massively expands during the first postnatal week by local proliferation and can be targeted by retroviral vectors (Ge et al., 2012; Clavreul et al., 2019). Thus, retroviruses may serve as suitable vectors to test the hypothesis that forced expression of Ascl1 can induce neuronal reprogramming. To validate the approach, we first injected a control virus encoding only a reporter gene (pCAG-IRES-DsRed) into the mouse cerebral cortex at P5 and assessed the identity of the transduced cells by immunohistochemical analysis at 3 days post injection (3 dpi) (**Figure 1A**). We found that virtually all transduced cells were immunopositive

for glial markers (Figure 1B). The majority of transduced cells were immunoreactive for the astroglial marker GFAP (67.0 ± 8.9%, 753 transduced cells analyzed, *n* = 3 mice; Figures 1B,C), and the remaining were oligodendroglial cells immunoreactive for Sox10 (29.6 ± 6.1%, 753 transduced cells analyzed, *n* = 3 mice; Figures 1B,C). Rarely, we found transduced cells immunoreactive for the microglial marker Iba1 (0.9 ± 1.0%, 578 transduced cells analyzed, *n* = 3 mice; Figures 1B,D). Importantly, none of the control-transduced cells expressed the immature neuronal marker DCX (0.0 ± 0.0%, 578 transduced cells analyzed, *n* = 3 mice; Figures 1B,D). These results indicate that retroviruses injected in the P5 mouse cerebral cortex *in vivo* specifically transduce astroglial and oligodendroglial lineage cells.

To examine the consequences of forced expression of Ascl1, we next injected control (pCAG-DsRed) or Ascl1-encoding (pCAG-Ascl1-DsRed or pCAG-Ascl1-GFP) retrovirus and investigated whether the proneural factor could reprogram P5 proliferative glia into neurons using immunohistochemistry (Figure 2A). Analysis was performed at 12 dpi, based on previous evidence of retrovirus-mediated glia-to-neuron reprogramming within 7–14 days *in vivo* (Heinrich et al., 2014; Gascon et al., 2016; Herrero-Navarro et al., 2021). Many reporter-positive cells were found at the site of retrovirus injection (Figure 2B), and Ascl1 was effectively expressed in cells transduced with Ascl1, while it was absent from control-transduced cells (Figure 2C). Control-transduced cells lacked DCX expression (0.0 ± 0.0%, 2,157 transduced cells analyzed, *n* = 3 mice; Figures 2D,E), confirming that the control vector did not induce a cell fate switch. Surprisingly, Ascl1-transduced cells also largely remained immunonegative for DCX (Figures 2D,E), with only a small, albeit statistically significant number of transduced cells exhibiting an immature neuron-like morphology and expressing DCX (Ascl1: 4.6 ± 1.6%, 720 transduced cells analyzed, *n* = 3 mice) (Figures 2D,E). To confirm the biological activity of our Ascl1-encoding retrovirus, we transduced cultures of cortical astrocytes with control (pCAG-DsRed or pCAG-GFP) or Ascl1-encoding (pCAG-Ascl1-DsRed) retrovirus (Supplementary Figure 1A). Following transduction with control virus, virtually no β-Tubulin III-immunoreactive cells were found (0.1 ± 0.2%, 1,398 transduced cells analyzed, *n* = 3 biological replicates; Supplementary Figures 1B,C). In contrast, astrocytes transduced with Ascl1-encoding retrovirus acquired neuron-like morphology and expressed β-Tubulin III (27.3 ± 3.8%, 3,061 transduced cells analyzed, *n* = 4 biological replicates; Supplementary Figures 1B,C). Together, our results indicate that despite the neurogenic potential of Ascl1 *in vitro*, *in vivo* reprogramming by Ascl1 by and large fails.

Achaete-scute complex-like 1 expression in postnatal cortical glia increases the relative number of cells expressing oligodendroglial markers

Given that only a few Ascl1-transduced cells were converted into neurons, we examined whether the remainder of the transduced cells nevertheless had responded to Ascl1 with downregulation of glial markers. We therefore analyzed the expression of the pan-oligodendroglial marker Sox10 and the astroglial marker GFAP in Ascl1-transduced cells (Figures 3A–C). Consistent with our analysis at 3 dpi (Figure 1), control-transduced cells at 12 dpi were glial cells, with two thirds of the cells expressing the astroglial marker GFAP (63.3 ± 12.1%, 1,885 transduced cells analyzed, *n* = 3 mice) while the other third expressed Sox10 (35.6 ± 11.3%, 1,885 transduced cells analyzed, *n* = 3 mice; Figures 3A,C). As expected, the expression of GFAP and Sox10 was mutually exclusive in control-transduced cells (0.3 ± 0.6% of GFAP/Sox10-positive cells, 1,885 transduced cells analyzed, *n* = 3 mice; Figures 3B,C and Supplementary Movie 1). Following transduction with Ascl1-encoding virus, we observed a marked alteration in the relative expression of glial markers. Strikingly, only one fifth of transduced cells exclusively expressed GFAP (Ascl1, 18.7 ± 3.1%, 848 transduced cells analyzed, *n* = 4 mice), a three folds reduction compared to control transductions. Interestingly, the reduction in GFAP expression was concomitant with a two folds increase in the relative number of Sox10-only expressing cells (70.0 ± 7.7%, 848 transduced cells analyzed, *n* = 4 mice; Figure 3C). Moreover, a modest but significant increase in the relative number of cells co-expressing Sox10 and GFAP was observed in Ascl1-transduced cells (Figures 3B,C and Supplementary Movie 2). The detection of GFAP/Sox10-immunopositive cells following transduction with Ascl1-encoding virus (4.5 ± 2.6%, 848 transduced cells analyzed, *n* = 4 mice, Figures 3B,C and Supplementary Movie 2) may capture cells in a "mixed" glial state. Together, these results indicate that although largely failing to redirect proliferative glial cells toward neurogenesis, these cells appear to be responsive to Ascl1 overexpression. Changes in the relative numbers of Sox10- vs. GFAP-positive cells could be accounted for either by: (i) conversion of the astroglial lineage toward the oligodendroglial lineage; (ii) glial cell type-specific changes in the rates of proliferation (and/or death) of cells of the oligodendroglial or astroglial lineage, respectively.

10.3389/fnins.2022.919462

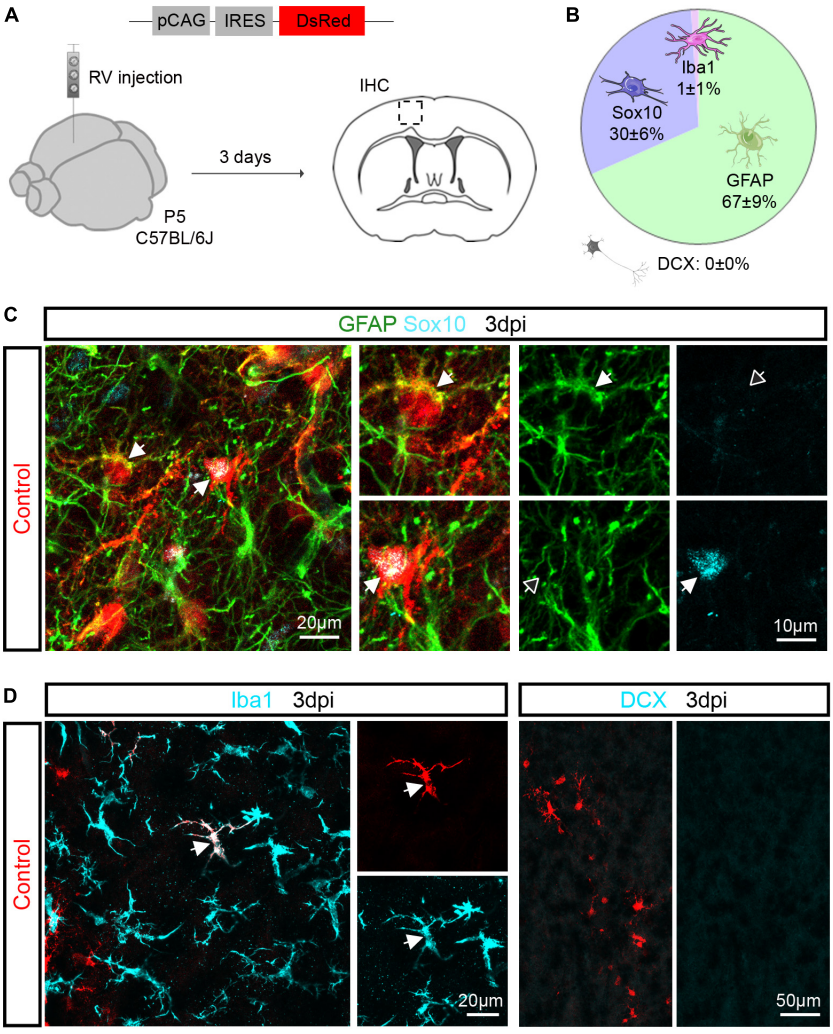

FIGURE 1
Retroviruses injected in the postnatal cerebral cortex selectively transduce glial cells. **(A)** Experimental scheme. A control retrovirus pCAG-IRES-DsRed was injected in the cerebral cortex of P5 mice and immunohistochemical analysis was performed 3 days later. **(B)** Pie chart showing the relative number of oligodendroglial (Sox10-positive), astroglial (GFAP-positive), microglial (Iba1-positive) and neuronal (DCX-positive) cells among transduced cells. **(C)** Confocal images depicting control-transduced cells (in red, arrows) co-expressing GFAP (in green, upper insets) or Sox10 (in cyan, lower insets). **(D)** Confocal images depicting control-transduced cell (in red) co-expressing Iba1 (in cyan) (left panel). No control-transduced cells expressing DCX were found (in cyan) (right panel). Empty arrows indicate marker-negative cells. IHC, immunohistochemistry; RV, retrovirus; dpi, days post injection.

Genetic fate mapping argues against massive astrocyte-to-oligodendrocyte progenitor cell conversion following Achaete-scute complex-like 1 overexpression

Intrigued by this finding, we performed genetic fate mapping experiments to follow the fate of transduced astroglia employing mGFAP-Cre/EGFP mice, in which permanent green-fluorescent labeling was specifically achieved in cells with an active mGFAP promoter (i.e., astrocytes) by Cre-mediated removal of the loxP-flanked STOP cassette upstream of EGFP. We injected control (pCAG-DsRed) or Ascl1-encoding (pCAG-Ascl1-DsRed) retrovirus in the cortex of P5 mGFAP-Cre/EGFP mice and quantified at 12 dpi the relative proportion of cells expressing EGFP and/or Sox10 among RFP-positive transduced cells (Figure 4). In line with our immunohistochemical analysis (Figure 3), most cells transduced with control retrovirus were EGFP-positive (585 transduced cells analyzed, $n = 3$ mice, Figure 4B, upper pie chart, yellow and white pie chart sectors), indicative of astroglial identity. While we previously had not observed cells co-expressing GFAP and Sox10 in control transductions (Figure 3), we recorded here a minor proportion of control transduced cells co-expressing EGFP and

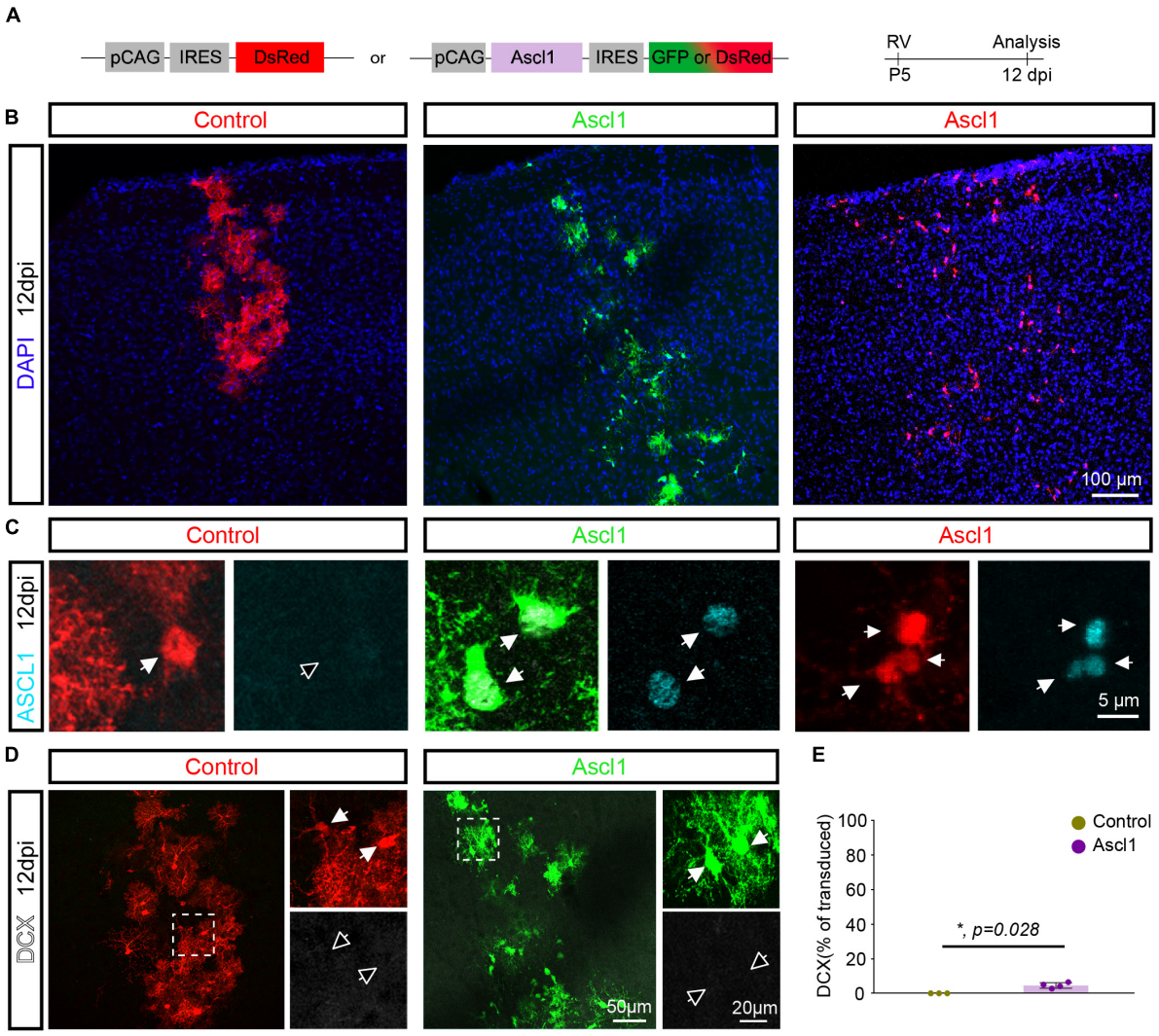

FIGURE 2
Achaete-scute complex-like 1 (Ascl1) converts postnatal glia into neurons with low efficiency *in vivo*. **(A)** Experimental scheme. A control (pCAG-IRES-DsRed) or Ascl1-encoding (pCAG-Ascl1-GFP or pCAG-Ascl1-DsRed) retrovirus was injected in the cerebral cortex of P5 mice and immunohistochemical analysis was performed 12 days later. **(B)** Low-magnification confocal images depicting transduced cells at cortical site of injection. **(C)** Immunohistochemistry confirmed the lack of expression of Ascl1 in control-transduced postnatal cortical glia and efficient Ascl1 induction (in cyan) by Ascl1-encoding retroviruses. **(D)** Confocal images depicting the maintenance of a glial morphology and lack of DCX induction (in white) in control or Ascl1-transduced cells. Empty arrows indicate marker-negative cells. **(E)** Quantification of the percentage of transduced cells expressing DCX at 12dpi indicates that Ascl1 induces neurogenesis from postnatal cortical glia with low efficiency. Mean ± SD, Mann–Whitney *U* test. RV, retrovirus; dpi, days post injection.

Sox10. The remainder of the transduced cells were not fate-mapped (EGFP-negative) and, as expected, partly composed of Sox10-positive oligodendroglial cells (Figure 4B, upper pie chart, pink pie chart sector). In accordance with our immunohistochemical analysis (Figure 3), we noted a very different relative distribution following transduction with Ascl1 (878 transduced cells analyzed, n = 3 mice, Figure 4B, lower pie chart). Similar to our earlier analysis, we found that a larger proportion of Ascl1-transduced cells were Sox10-positive (Figure 4B, lower pie chart, white and pink pie chart sector), as compared with control. Sox10-positive cells were also detected among the EGFP-positive cells (Figure 4B, lower pie chart, white pie chart sector), in line with the observation that some Ascl1 transduced cells expressed both GFAP and Sox10. Most importantly, however, our analysis showed that the vast majority of Sox10-positive cells were still EGFP-negative (Figures 4A,B, lower pie chart, pink pie chart sector). Taken together, these data indicate that the observed increase in the relative proportion of Sox10-expressing oligodendroglia among Ascl1-retrovirus transduced cells is by and large not attributable to direct lineage conversion of astrocytes into oligodendroglial cells.

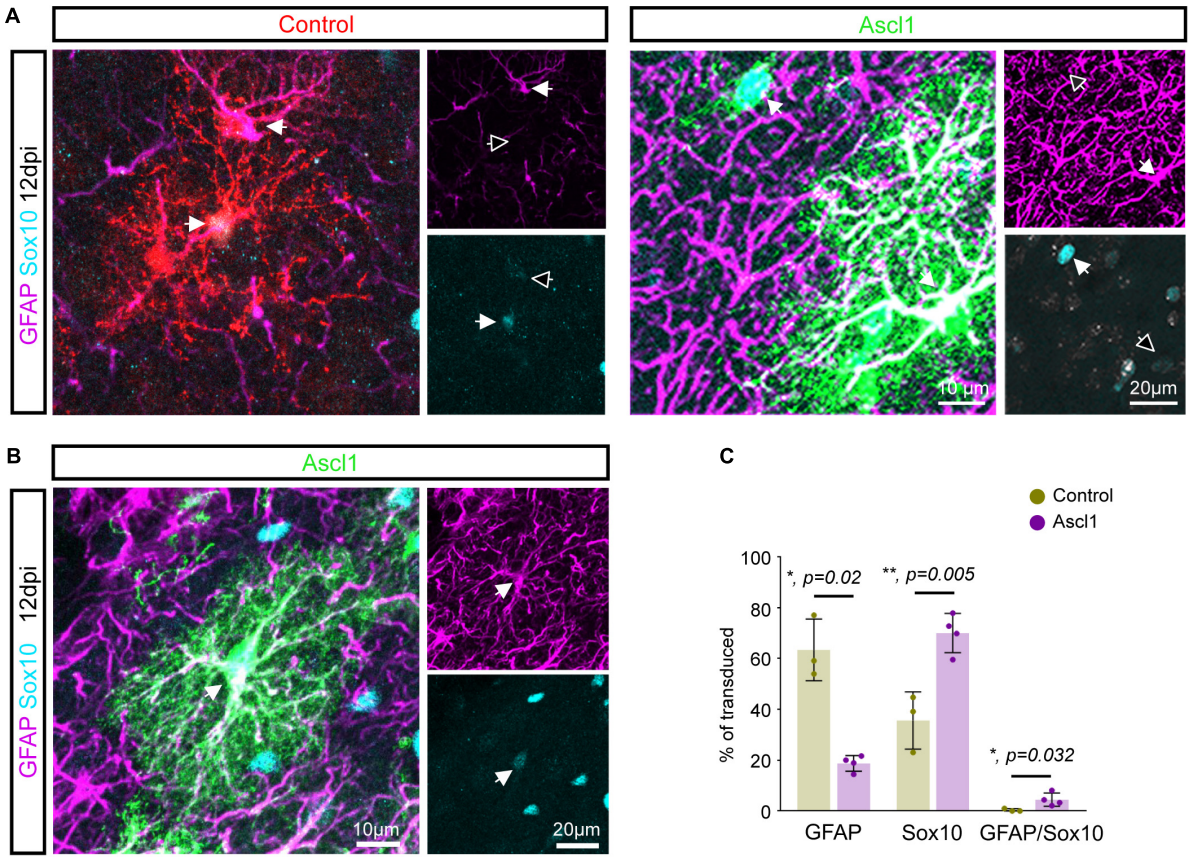

FIGURE 3
Achaete-scute complex-like 1 (Ascl1) induces an increase in the number of Sox10 expressing cells. **(A)** Confocal images depicting control and Ascl1-transduced cells expressing either GFAP (in magenta) or Sox10 (in cyan). **(B)** Confocal images depicting Ascl1-transduced cells co-expressing GFAP (in magenta) and Sox10 (in cyan). **(C)** Quantification of the percentage of transduced cells expressing GFAP, Sox10 or both markers at 12 dpi indicates a concomitant reduction in the relative number of cells expressing an astroglial marker and increase in the relative number of cells expressing an oligodendroglial marker upon transduction with Ascl1. Empty arrows indicate marker-negative cells. Mean ± SD, *t*-test for independent samples (for GFAP and Sox10) and Mann–Whitney *U* test (for GFAP/Sox10).

Achaete-scute complex-like 1 induces proliferation in Sox10-positive oligodendrocyte progenitor cells

To examine the alternative possibility that Ascl1 promoted a higher proliferation rate in OPCs vs. astrocytes, we pulse-labeled proliferating cells by systemic injection of the thymidine analogue EdU 3 h prior to sacrifice at 12 dpi (**Figures 5A,B**). Expansion of cortical glia rapidly declines after the first two postnatal weeks (Psachoulia et al., 2009; Ge et al., 2012; Clavreul et al., 2019). Accordingly, we found that none of the control-transduced cells had incorporated EdU (0.0 ± 0.0%, 218 transduced cells analyzed, $n = 3$ mice; **Figures 5A,C**). Strikingly, the 3 h EdU pulse resulted in labeling of a significant proportion of Ascl1-transduced cells (14.1 ± 4.7%, 177 transduced cells analyzed, $n = 3$ mice; **Figures 5A,C**). Analysis of the identity of the EdU-positive Ascl1-transduced cells showed that virtually all expressed Sox10 (96.7 ± 5.8%, 56 EdU-positive Ascl1-transduced cells analyzed, $n = 3$ mice; **Figure 5D**), indicative of a specific effect on the proliferative status of the oligodendroglial lineage. Together, our data indicates that Ascl1 promotes cell cycle activity selectively in cells of the oligodendroglial and not the astroglial lineage, thereby accounting for the change in the relative numbers of these two lineages following Ascl1 overexpression *in vivo*.

Discussion

In the present study, we assessed the effect of Ascl1 overexpression in glia during their proliferative expansion phase in the early postnatal cerebral cortex. In contrast to earlier findings *in vitro* (Berninger et al., 2007; Heinrich et al., 2010; Gascon et al., 2016)—which we confirmed herein—we found that glia-to-neuron conversion by Ascl1 was very

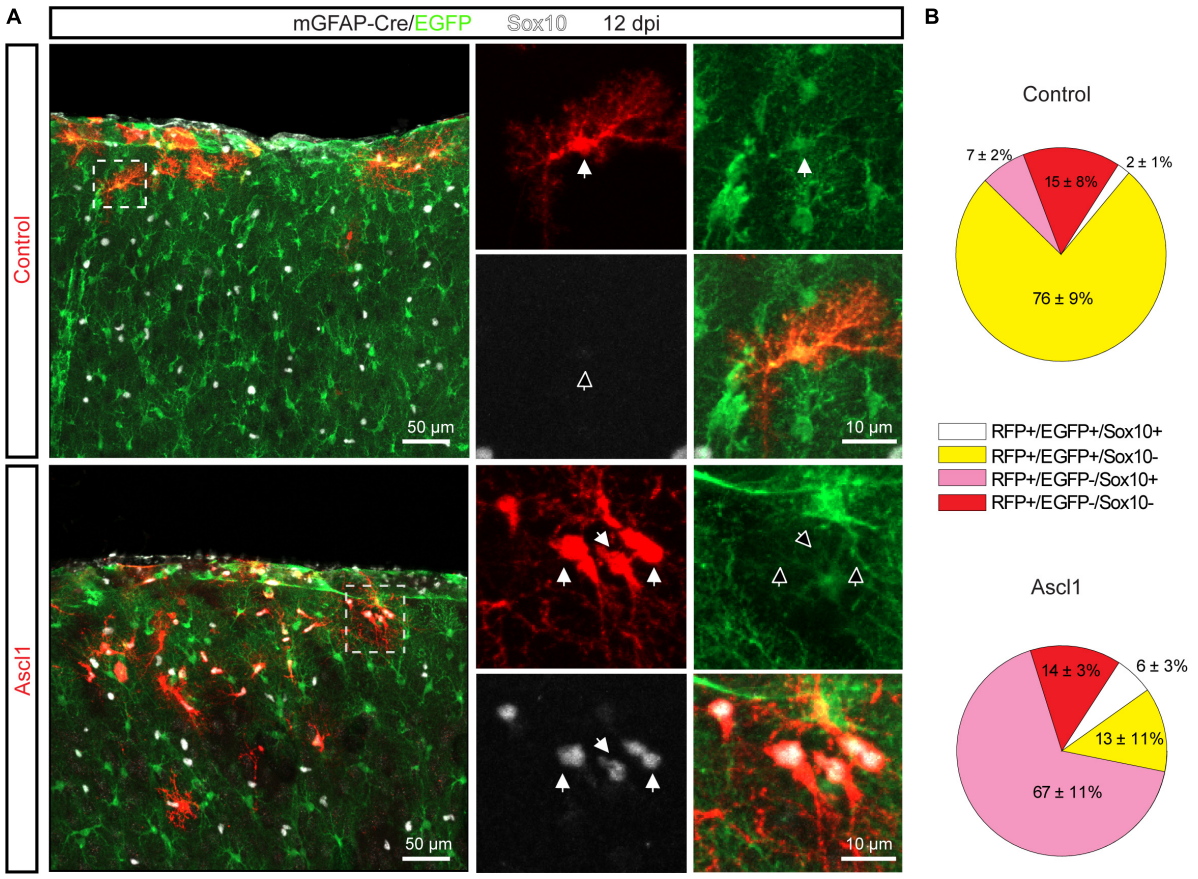

FIGURE 4
The increase in the relative proportion of Sox10-expressing cells is not due to Achaete-scute complex-like 1 (Ascl1) mediated conversion of astrocytes into OPCs. **(A)** Confocal images depicting control- and Ascl1-transduced cells (in red) in mGFAP-Cre/EGFP mice at 12 dpi. Empty arrows indicate marker-negative cells. **(B)** Pie charts showing the relative number of transduced cells co-expressing EGFP and/or Sox10 at 12 days following transduction with control (upper pie chart) or Ascl1 (lower pie chart) retrovirus. Mean ± SD. Dpi, days post injection.

inefficient in the early postnatal cortex *in vivo*. However, Ascl1 overexpression shifted the number of Sox10-positive OPCs vs. GFAP-positive astrocytes among transduced cells. While a minor contribution of astrocyte-to-OPC conversion might have occurred, this effect could be attributed by and large to increased cell cycle activity in OPCs as shown by genetic fate mapping and EdU incorporation experiments. Overall, these data indicate that Ascl1 differentially affects cell cycle activity in distinct glial cell types, highlighting the importance of cellular context for the consequences of Ascl1 overexpression.

The low rate of glia-to-neuron conversion triggered by Ascl1 *in vivo* is in agreement with previous studies reporting inefficient neuronal reprogramming following retrovirus- or lentivirus-mediated expression of Ascl1 alone in reactive glia in the adult lesioned cortex (Heinrich et al., 2014), adult striatum (Niu et al., 2015), and adult lesioned spinal cord (Su et al., 2014). In contrast to these studies, another study reported very efficient reprogramming of astrocytes into mature neurons following adeno-associated virus (AAV)-mediated expression of Ascl1 in the dorsal midbrain, striatum and somatosensory cortex (Liu et al., 2015). However, misidentification of endogenous neurons as glia-derived neurons was recently reported following AAV-mediated expression of Neurod1, possibly due to transgene sequence-specific effects acting *in cis* (Wang et al., 2021). Thus, one possible explanation for the apparent discrepancy in reprogramming efficiency *in vivo* is that, similarly to Neurod1, AAV-mediated expression of Ascl1 resulted in labeling of endogenous neurons. Future studies combining AAV-mediated expression of reprogramming factors such as Ascl1 with genetic lineage tracing are required to clarify the origin of seemingly induced neurons (Wang et al., 2021; Leaman et al., 2022).

The apparent difference in reprogramming potency of Ascl1 *in vitro* and *in vivo* could be attributed to various factors: (i) Enhanced cellular plasticity of cultured astrocytes as compared to astrocytes *in vivo* despite both being of similar age and in a similar proliferative state. The protocol employed here to culture and reprogram astrocytes may enhance their competence to undergo cell fate conversion. Indeed, a previous

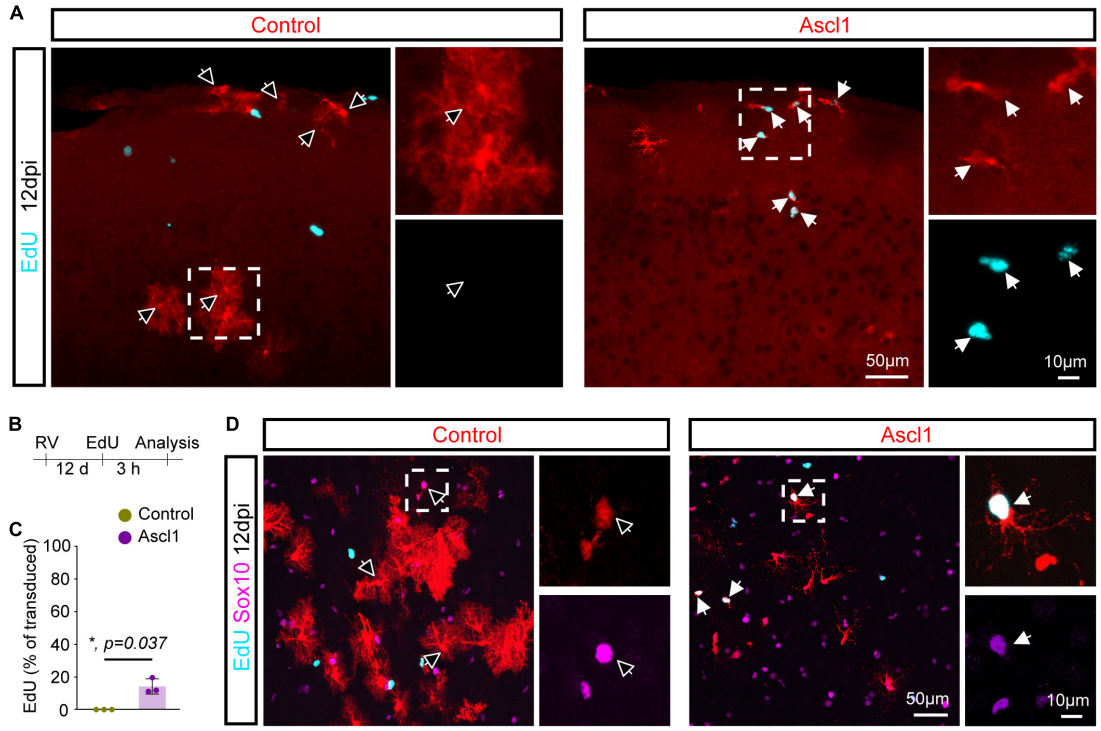

FIGURE 5
Achaete-scute complex-like 1 (Ascl1)-overexpresion increases proliferative activity of Sox10-possitive cells. **(A)** Confocal images depicting incorporation of EdU by transduced cells. **(B)** Experimental scheme. EdU was injected to the mice 3 h prior to sacrifice 12 days after retrovirus injection. **(C)** Quantification of the percentage of transduced cells that have incorporated EdU indicates that, in contrast to control cells, some Ascl1-transduced cells are maintained in a proliferative state. Mean ± SD, Mann–Whitney *U* test. **(D)** Confocal images depicting Sox10 expression in EdU-positive transduced cells. Empty arrows indicate EdU-negative cells. RV, retrovirus; dpi, days post injection.

study showed that allowing astrocytes to mature *in vitro* for few days prior to proneural factor activation resulted in a drastic decrease in reprogramming rate, an effect that could be attributed to activation of the REST/coREST repressor complex and accompanying epigenetic maturation (Masserdotti et al., 2015). *In vivo*, REST/coREST complex activity may be already higher, thereby safeguarding astrocyte identity against Ascl1-induced neurogenic reprogramming. (ii) Another important difference is the obviously more complex local environment *in vivo*. Nearly nothing is known about the influence that other cell types exert on cells that undergo reprogramming. However, *in vitro* studies have shown that human pericytes undergoing reprogramming by Ascl1 and Sox2 pass through a neural stem cell-like stage during which they become responsive to several intercellular signaling pathways including Notch signaling (Karow et al., 2018). Thus, it is conceivable that signaling molecules as well as extracellular matrix components secreted by cells within the local environment could impinge on early and perhaps more vulnerable reprogramming stages, thereby curtailing progression toward neurogenesis. The overall very low conversion efficiency suggests that glial cells possess effective safeguarding mechanisms that protect them against acquiring a neurogenic fate. In fact, these safeguarding mechanisms are effective even when confronted with a powerful transcription factor with pioneer factor activity, such as Ascl1 (Wapinski et al., 2013; Raposo et al., 2015; Park et al., 2017).

While Ascl1 did not induce neurogenic conversion in cells of the astroglial and oligodendroglial lineages, we observed a significant shift in the ratio of virus-transduced astroglial to oligodendroglial cells. This shift can be accounted for primarily by increased proliferation of Sox10-positive OPCs following Ascl1 overexpression, whereas astroglia-to-OPC conversion may have contributed only marginally. The fact that approximately 15% of the Ascl1-expressing OPCs incorporated EdU during a 3 h time window may indicate that this population proliferated homogenously and at a drastically shortened cell cycle length as compared to OPCs under control conditions (Psachoulia et al., 2009). EdU saturation experiments would help to determine the growth fraction of cells actively engaged in cell cycle among all Ascl1-expressing OPCs. Furthermore, it would be of great interest to learn whether Ascl1-overexpressing OPCs eventually exit the cell cycle and differentiate into oligodendrocytes. If so, Ascl1-induced expansion of the OPC pool could be a strategy for regenerating oligodendrocytes in demyelinating diseases. Ascl1-induced OPC cell cycle activity observed here is consistent

with earlier findings reporting a physiological role of Ascl1 in regulating OPC proliferation in the adult spinal cord (Kelenis et al., 2018).

Intriguingly, studies in the adult hippocampus have previously reported that similar retroviral expression of Ascl1 in neural stem cells promoted oligodendrogliogenesis instead of GABAergic neurogenesis (Jessberger et al., 2008; Braun et al., 2015). While these data were interpreted as an Ascl1-induced change in cell fate of adult neural stem cells, our data may open the alternative possibility that Ascl1 overexpression enhanced the local proliferation of retrovirus-targeted OPCs, or potentially even a combination of both effects.

Previous work has highlighted the proliferation-promoting role of Ascl1. While critical for neuronal differentiation of ventral telencephalic progenitors, Ascl1 also regulates genes involved in cell cycle regulation, and Ascl1 deletion results in reduced progenitor proliferation (Castro et al., 2011). Moreover, Ascl1 overexpression in embryonic cortical progenitors induces proliferation and the expression of Sox9, a glioblast marker (Li et al., 2014). Likewise, Ascl1 plays a key role in neural stem cell activation in the adult hippocampus (Andersen et al., 2014) while its downregulation promotes return to quiescence (Urban et al., 2016). Furthermore, Ascl1 induction also takes part in the reactivation of a neurogenic program in astrocytes in response to injury or silencing of Notch signaling in the adult striatum or cortex, a process which involves transient proliferation of Ascl1-expressing astrocytes (Magnusson et al., 2014; Nato et al., 2015; Zamboni et al., 2020). Against this context, it is intriguing that we found that the proliferation-promoting effect of Ascl1 is restricted to OPCs when overexpressed at P5, and astrocytes did not enter cell cycle. One speculative possibility is that the differential response of OPCs and astrocytes to Ascl1 depends on temporal expression dynamics. In our experimental conditions, Ascl1 expression is likely to be relatively constant. In contrast, previous studies found that in proliferating neural stem cells, which molecularly are more akin to astrocytes than OPCs, Ascl1 expression undergoes oscillations that are out-of-phase with oscillating effectors downstream of Notch signaling (Imayoshi et al., 2013). Our data provide the first example of proliferation induced by constant and likely high levels of Ascl1 and warrant future studies into the cell type specific sensitivity to Ascl1 expression dynamics.

Data availability statement

The raw data supporting the conclusions of this article are openly available from the King's College London research data repository, KORDS, at doi: 10.5061/dryad.6gb90. Any reagents that this study generated will be shared by the corresponding authors upon reasonable request. All other study data are included in the article and/or **Supplementary material**.

Ethics statement

The animal study was reviewed and approved by the Rhineland-Palatinate State Authority and the Ethical Committee of King's College London and the UK Home Office.

Author contributions

CG, NM, FS, LG, YS, and SP: methodology, investigation, and formal analysis. CS: resources. CG, NM, and SP: writing—original draft. CS, BB, and SP: funding acquisition, conceptualization, visualization, and writing—review and editing. All authors contributed to the article and approved the submitted version.

Funding

This research was funded in part by the Wellcome Trust (206410/Z/17/Z). For the purpose of open access, the author has applied a CC BY public copyright license to any author accepted manuscript version arising from this submission. This study was also supported by funding from the European Research Council (ERC) under the European Union's Horizon 2020 Research and Innovation Programme (grant agreement No. 101021560, IMAGINE), the German Research Foundation (BE 4182/11-1 project number 357058359; CRC1080, project No. 221828878), and the research initiative of Rheinland-Pfalz at the Johannes Gutenberg University Mainz (ReALity) to BB, by the Inneruniversitäre Forschungsförderung Stufe I of the Johannes Gutenberg University Mainz to SP, and by core funding to the Francis Crick Institute from Cancer Research United Kingdom, The Medical Research Council, and the Wellcome Trust (FC001002). NM was supported by a fellowship from the Human Frontiers Science Program (HFSP Long-Term Fellowship, LT000646/2015). FS was supported by a fellowship from São Paulo Research Foundation (FAPESP) process No. 2021/13515-5.

Acknowledgments

We are grateful to the members of the Berninger laboratory for their helpful comments and critical feedback over the course of this study. We are grateful to B. Rico (King's College London) for her support throughout the project. We acknowledge support from the Microscopy Core Facility of the Institute of Molecular Biology (IMB) Mainz. The data published in this work are partially included in the doctoral thesis of CG published by the Johannes Gutenberg-Universität Mainz (Galante, 2019) and in a preprint server (Galante et al., 2020; doi: 10.1101/2022.04.13.488173).

Conflict of interest

The authors declare that the research was conducted in the absence of any commercial or financial relationships that could be construed as a potential conflict of interest.

Publisher's note

All claims expressed in this article are solely those of the authors and do not necessarily represent those of their affiliated organizations, or those of the publisher, the editors and the reviewers. Any product that may be evaluated in this article, or claim that may be made by its manufacturer, is not guaranteed or endorsed by the publisher.

Supplementary material

The Supplementary Material for this article can be found online at: https://www.frontiersin.org/articles/10.3389/fnins.2022.919462/full#supplementary-material

References

Andersen, J., Urban, N., Achimastou, A., Ito, A., Simic, M., Ullom, K., et al. (2014). A transcriptional mechanism integrating inputs from extracellular signals to activate hippocampal stem cells. *Neuron* 83, 1085–1097. doi: 10.1016/j.neuron.2014.08.004

Berninger, B., Costa, M. R., Koch, U., Schroeder, T., Sutor, B., Grothe, B., et al. (2007). Functional properties of neurons derived from in vitro reprogrammed postnatal astroglia. *J. Neurosci.* 27, 8654–8664. doi: 10.1523/JNEUROSCI.1615-07.2007

Braun, S. M., Pilz, G. A., Machado, R. A., Moss, J., Becher, B., Toni, N., et al. (2015). Programming hippocampal neural stem/progenitor cells into oligodendrocytes enhances remyelination in the adult brain after injury. *Cell Rep.* 11, 1679–1685. doi: 10.1016/j.celrep.2015.05.024

Casarosa, S., Fode, C., and Guillemot, F. (1999). Mash1 regulates neurogenesis in the ventral telencephalon. *Development* 126, 525–534.

Castro, D. S., Martynoga, B., Parras, C., Ramesh, V., Pacary, E., Johnston, C., et al. (2011). A novel function of the proneural factor Ascl1 in progenitor proliferation identified by genome-wide characterization of its targets. *Genes Dev.* 25, 930–945. doi: 10.1101/gad.627811

Chanda, S., Ang, C. E., Davila, J., Pak, C., Mall, M., Lee, Q. Y., et al. (2014). Generation of induced neuronal cells by the single reprogramming factor ASCL1. *Stem Cell Rep.* 3, 282–296. doi: 10.1016/j.stemcr.2014.05.020

Clavreul, S., Abdeladim, L., Hernandez-Garzon, E., Niculescu, D., Durand, J., Ieng, S. H., et al. (2019). Cortical astrocytes develop in a plastic manner at both clonal and cellular levels. *Nat. Commun.* 10:4884. doi: 10.1038/s41467-019-12791-5

Denoth-Lippuner, A., and Jessberger, S. (2021). Formation and integration of new neurons in the adult hippocampus. *Nat. Rev. Neurosci.* 22, 223–236. doi: 10.1038/s41583-021-00433-z

Galante, C. (2019). Factors determining competence for *in vivo* glia-to-neuron conversion. *Johannes Gutenberg-Universität Mainz* doi: 10.25358/openscience-2366

Galante, C., Marichal, N., Schuurmans, C., berninger, B., and Peron, S. (2022). Low-efficiency conversion of proliferative glia into induced neurons by Ascl1 in the postnatal mouse cerebral cortex *in vivo*. bioRxiv. doi: 10.1101/2022.04.13.488173

Gascon, S., Murenu, E., Masserdotti, G., Ortega, F., Russo, G. L., Petrik, D., et al. (2016). Identification and successful negotiation of a metabolic checkpoint in direct neuronal reprogramming. *Cell Stem Cell* 18, 396–409. doi: 10.1016/j.stem.2015.12.003

Ge, W. P., Miyawaki, A., Gage, F. H., Jan, Y. N., and Jan, L. Y. (2012). Local generation of glia is a major astrocyte source in postnatal cortex. *Nature* 484, 376–380. doi: 10.1038/nature10959

Gregorian, C., Nakashima, J., Le Belle, J., Ohab, J., Kim, R., Liu, A., et al. (2009). Pten deletion in adult neural stem/progenitor cells enhances constitutive neurogenesis. *J. Neurosci.* 29, 1874–1886. doi: 10.1523/JNEUROSCI.3095-08.2009

Guillemot, F., and Hassan, B. A. (2017). Beyond proneural: Emerging functions and regulations of proneural proteins. *Curr. Opin. Neurobiol.* 42, 93–101. doi: 10.1016/j.conb.2016.11.011

Heinrich, C., Bergami, M., Gascon, S., Lepier, A., Vigano, F., Dimou, L., et al. (2014). Sox2-mediated conversion of NG2 glia into induced neurons in the injured adult cerebral cortex. *Stem Cell Rep.* 3, 1000–1014. doi: 10.1016/j.stemcr.2014.10.007

Heinrich, C., Blum, R., Gascon, S., Masserdotti, G., Tripathi, P., Sanchez, R., et al. (2010). Directing astroglia from the cerebral cortex into subtype specific functional neurons. *PLoS Biol.* 8:e1000373. doi: 10.1371/journal.pbio.1000373

Heinrich, C., Gascon, S., Masserdotti, G., Lepier, A., Sanchez, R., Simon-Ebert, T., et al. (2011). Generation of subtype-specific neurons from postnatal astroglia of the mouse cerebral cortex. *Nat. Protoc.* 6, 214–228. doi: 10.1038/nprot.2010.188

Herrero-Navarro, A., Puche-Aroca, L., Moreno-Juan, V., Sempere-Ferrandez, A., Espinosa, A., Susin, R., et al. (2021). Astrocytes and neurons share region-specific transcriptional signatures that confer regional identity to neuronal reprogramming. *Sci. Adv.* 7:eabe8978. doi: 10.1126/sciadv.abe8978

Imayoshi, I., Isomura, A., Harima, Y., Kawaguchi, K., Kori, H., Miyachi, H., et al. (2013). Oscillatory control of factors determining multipotency and fate in mouse neural progenitors. *Science* 342, 1203–1208. doi: 10.1126/science.1242366

Jessberger, S., Toni, N., Clemenson, G. D. Jr., Ray, J., and Gage, F. H. (2008). Directed differentiation of hippocampal stem/progenitor cells in the adult brain. *Nat. Neurosci.* 11, 888–893. doi: 10.1038/nn.2148

Karow, M., Camp, J. G., Falk, S., Gerber, T., Pataskar, A., Gac-Santel, M., et al. (2018). Direct pericyte-to-neuron reprogramming via unfolding of a neural stem cell-like program. *Nat. Neurosci.* 21, 932–940. doi: 10.1038/s41593-018-0168-3

Karow, M., Sanchez, R., Schichor, C., Masserdotti, G., Ortega, F., Heinrich, C., et al. (2012). Reprogramming of pericyte-derived cells of the adult human brain into induced neuronal cells. *Cell Stem Cell* 11, 471–476. doi: 10.1016/j.stem.2012.07.007

Kelenis, D. P., Hart, E., Edwards-Fligner, M., Johnson, J. E., and Vue, T. Y. (2018). ASCL1 regulates proliferation of NG2-glia in the embryonic and adult spinal cord. *Glia* 66, 1862–1880. doi: 10.1002/glia.23344

Leaman, S., Marichal, N., and Berninger, B. (2022). Reprogramming cellular identity in vivo. *Development* 149:dev200433. doi: 10.1242/dev.200433

Lentini, C., d'Orange, M., Marichal, N., Trottmann, M. M., Vignoles, R., Foucault, L., et al. (2021). Reprogramming reactive glia into interneurons reduces chronic seizure activity in a mouse model of mesial temporal lobe epilepsy. *Cell Stem Cell* 28, 2104–2121. doi: 10.1016/j.stem.2021.09.002

Li, S., Mattar, P., Dixit, R., Lawn, S. O., Wilkinson, G., Kinch, C., et al. (2014). RAS/ERK signaling controls proneural genetic programs in cortical development and gliomagenesis. *J. Neurosci.* 34, 2169–2190. doi: 10.1523/JNEUROSCI.4077-13.2014

Liu, Y., Miao, Q., Yuan, J., Han, S., Zhang, P., Li, S., et al. (2015). Ascl1 converts dorsal midbrain astrocytes into functional neurons in vivo. *J. Neurosci.* 35, 9336–9355. doi: 10.1523/JNEUROSCI.3975-14.2015

Magnusson, J. P., Goritz, C., Tatarishvili, J., Dias, D. O., Smith, E. M., Lindvall, O., et al. (2014). A latent neurogenic program in astrocytes regulated by Notch signaling in the mouse. *Science* 346, 237–241. doi: 10.1126/science.346.6206.237

Masserdotti, G., Gillotin, S., Sutor, B., Drechsel, D., Irmler, M., Jorgensen, H. F., et al. (2015). Transcriptional mechanisms of proneural factors and rest in regulating neuronal reprogramming of astrocytes. *Cell Stem Cell* 17, 74–88. doi: 10.1016/j.stem.2015.05.014

Nakatani, H., Martin, E., Hassani, H., Clavairoly, A., Maire, C. L., Viadieu, A., et al. (2013). Ascl1/Mash1 promotes brain oligodendrogenesis during myelination and remyelination. *J. Neurosci.* 33, 9752–9768. doi: 10.1523/JNEUROSCI.0805-13.2013

Nato, G., Caramello, A., Trova, S., Avataneo, V., Rolando, C., Taylor, V., et al. (2015). Striatal astrocytes produce neuroblasts in an excitotoxic model of Huntington's disease. *Development* 142, 840–845. doi: 10.1242/dev.116657

Niu, W., Zang, T., Smith, D. K., Vue, T. Y., Zou, Y., Bachoo, R., et al. (2015). SOX2 reprograms resident astrocytes into neural progenitors in the adult brain. *Stem Cell Rep.* 4, 780–794. doi: 10.1016/j.stemcr.2015.03.006

Ory, D. S., Neugeboren, B. A., and Mulligan, R. C. (1996). A stable human-derived packaging cell line for production of high titer retrovirus/vesicular stomatitis virus G pseudotypes. *Proc. Natl. Acad. Sci. U.S.A.* 93, 11400–11406. doi: 10.1073/pnas.93.21.11400

Park, N. I., Guilhamon, P., Desai, K., McAdam, R. F., Langille, E., O'Connor, M., et al. (2017). ASCL1 reorganizes chromatin to direct neuronal fate and suppress tumorigenicity of glioblastoma stem cells. *Cell Stem Cell* 21, 411. doi: 10.1016/j.stem.2017.08.008

Peron, S., and Berninger, B. (2015). Reawakening the sleeping beauty in the adult brain: Neurogenesis from parenchymal glia. *Curr. Opin. Genet. Dev.* 34, 46–53. doi: 10.1016/j.gde.2015.07.004

Poitras, L., Ghanem, N., Hatch, G., and Ekker, M. (2007). The proneural determinant MASH1 regulates forebrain Dlx1/2 expression through the I12b intergenic enhancer. *Development* 134, 1755–1765. doi: 10.1242/dev.02845

Psachoulia, K., Jamen, F., Young, K. M., and Richardson, W. D. (2009). Cell cycle dynamics of NG2 cells in the postnatal and ageing brain. *Neuron Glia Biol.* 5, 57–67. doi: 10.1017/S1740925X09990354

Raposo, A., Vasconcelos, F. F., Drechsel, D., Marie, C., Johnston, C., Dolle, D., et al. (2015). Ascl1 Coordinately regulates gene expression and the chromatin landscape during neurogenesis. *Cell Rep.* 10, 1544–1556. doi: 10.1016/j.celrep.2015.02.025

Sharif, N., Calzolari, F., and Berninger, B. (2021). Direct in vitro reprogramming of astrocytes into induced neurons. *Methods Mol. Biol.* 2352, 13–29. doi: 10.1007/978-1-0716-1601-7_2

Sousa, V. H., Miyoshi, G., Hjerling-Leffler, J., Karayannis, T., and Fishell, G. (2009). Characterization of Nkx6-2-derived neocortical interneuron lineages. *Cereb. Cortex* 19(Suppl 1), i1–i10. doi: 10.1093/cercor/bhp038

Su, Z., Niu, W., Liu, M. L., Zou, Y., and Zhang, C. L. (2014). In vivo conversion of astrocytes to neurons in the injured adult spinal cord. *Nat. Commun.* 5:3338. doi: 10.1038/ncomms4338

Urban, N., van den Berg, D. L., Forget, A., Andersen, J., Demmers, J. A., Hunt, C., et al. (2016). Return to quiescence of mouse neural stem cells by degradation of a proactivation protein. *Science* 353, 292–295. doi: 10.1126/science.aaf4802

Wang, L. L., Serrano, C., Zhong, X., Ma, S., Zou, Y., and Zhang, C. L. (2021). Revisiting astrocyte to neuron conversion with lineage tracing in vivo. *Cell* 184, 5465–5481.e16. doi: 10.1016/j.cell.2021.09.005

Wapinski, O. L., Vierbuchen, T., Qu, K., Lee, Q. Y., Chanda, S., Fuentes, D. R., et al. (2013). Hierarchical mechanisms for direct reprogramming of fibroblasts to neurons. *Cell* 155, 621–635. doi: 10.1016/j.cell.2013.09.028

Zamboni, M., Llorens-Bobadilla, E., Magnusson, J. P., and Frisen, J. (2020). A widespread neurogenic potential of neocortical astrocytes is induced by injury. *Cell Stem Cell* 27, 605–617.e5. doi: 10.1016/j.stem.2020.07.006

Frontiers in Neuroscience

Provides a holistic understanding of brain function from genes to behavior

Part of the most cited neuroscience journal series which explores the brain - from the new eras of causation and anatomical neurosciences to neuroeconomics and neuroenergetics.

Discover the latest Research Topics

See more →

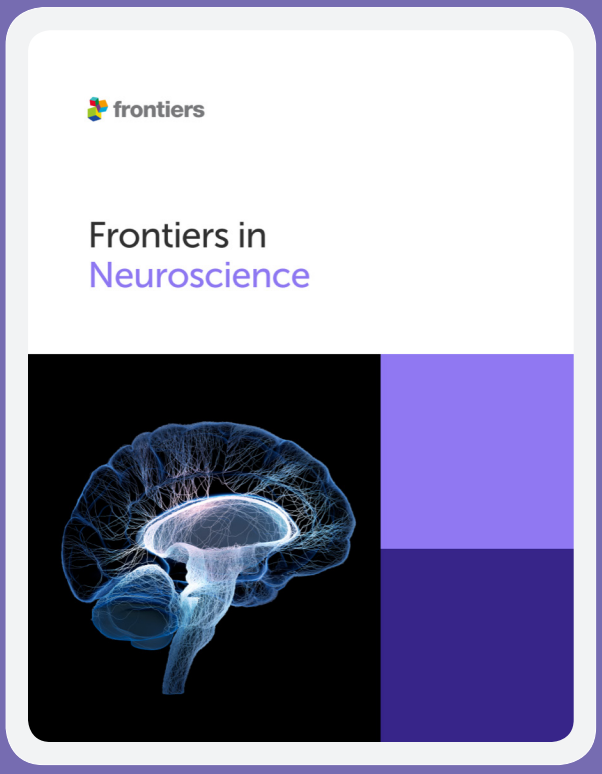

Frontiers

Avenue du Tribunal-Fédéral 34
1005 Lausanne, Switzerland
frontiersin.org

Contact us

+41 (0)21 510 17 00
frontiersin.org/about/contact